Evaluation of Novel Epoxy-Tigliane Compounds as Modulators of Dermal Fibroblast-Myofibroblast Differentiation, Scar Tissue Resolution and Fibrosis; and Elucidation of Their Underlying Mechanisms of Action

Jordanna Dally, BSc MRes

Thesis presented for the degree of *Philosophiae Doctor* (Doctor of Philosophy)

Regenerative Biology Group, Oral and Biomedical Sciences, School of Dentistry, Cardiff University

2018

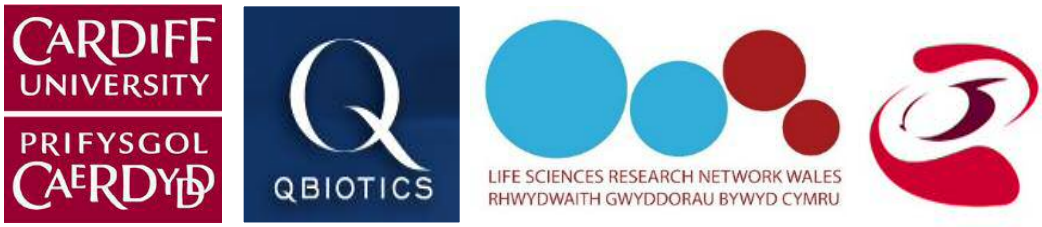

Dedication

To Grampy Fred… it's a little bit more than colouring in the lines, Gramp - but this is for you. I miss you every day.

"Twenty years from now, you'll be more disappointed by the things that you didn't do than by the ones you did do. So throw off the bowlines. Sail away from the safe harbour. Catch the trade winds in your sails. Explore. Dream. Discover." - H. Jackson Brown Jr.

Acknowledgements

First and foremost, I would like to express my sincere gratitude and appreciation to both of my supervisors, Dr Ryan Moseley and Dr Robert (Bob) Steadman. I couldn't have asked for better supervisors than the ones I've found in you. You've supported and encouraged me throughout this process and always made me feel like help was never far away. To Ryan, thank you for providing so much positivity and enthusiasm on a daily basis and to Bob, thank you for being my sounding board and giving much needed interjections of witty banter whenever things were getting a bit too serious! I'm truly grateful to you both for your advice and guidance over the last four years - as well as your patience during our seemingly chaotic group meetings! Lastly, thank you for taking a punt and seeing some potential in me when I was just a fresh-faced MRes student. Your belief in my ability to undertake a PhD and to make the most of this project has been priceless. I'll never forget it.

In addition, I would like to thank my funders - the QBiotics Group and Life Sciences Research Network Wales. Thank you to Dr Paul Reddell and Dr Victoria Gordon for giving me the chance to undertake such an amazing research project; and to LSRNW, who have provided a platform for me to talk about my research/get drunk each year at their awesome conferences! I am also grateful for the funding received by CITER, enabling my conference travel to Brussels and allowing me to present in the Young Investigator Category. It was a wonderful opportunity to present alongside several excellent early-career researchers and I felt privileged to be amongst them. I would also like to express my sincerest gratitude to Dr Rae Moses; for not only helping me in the lab when needed, but performing the Microarray analysis at the Queensland Institute of Medical Research, allowing me to obtain essential data.

I am hugely grateful to everyone who has provided support, and more importantly, friendship, within both of my departments. Firstly, thanks to the technical team at the School of Dentistry; who contribute significantly to the successful running of the department, as well as providing equipment expertise/knowledge. Particular thanks go to Dr Adam Midgley; who has not only been a font of wisdom over the last four years, providing much needed support and guidance in the lab, but has also been a great friend. Thank you for listening to my woes (over a pint), always taking the mick out of me, and for mentoring me since my Master's degree. You're one of the best scientists I know and I'm a better scientist for being around you.

So many thanks to all of my colleagues and friends at the School of Dentistry and the Institute of Nephrology; particularly my office buddies, Dan, Rob, Ruth, Nadia, Rich, Katrina, Emma BD and Meg; and my Nephro pals, Kate, Lucy, Amy, Jerry, Charlie and Lex. Together you've made my PhD life a joy; filled with wit, humour and unlimited support. It really has meant the world to me.

Here go the big ones… to Dan, it's been a crazy whirlwind since I decided you were the one to talk to at that first CITER conference. Thanks for checking in on me during all those hours in the darkroom, for listening to me when I was constantly worrying, and for all the care packages delivered over the last 6 months (I might've starved to death otherwise!). You've had an almost blind faith in me the entire time, and it's always been appreciated (even if I haven't said it aloud).

To Emma, my work mam... you may not think it, but you've been a rock to me over the last few years. I've loved sharing a lab bench with you (no matter how untidy!) and getting song lyrics into each conversation (we tried our best and we succeeded). Thank you for always being so giving with your time and immense knowledge (blots, blots, Western blots). It's been invaluable to me.

To my work wife, Elen… these last 5 years of post-grad have been a long old slog and I'm so glad it was you I got to spend the days with. Thank you for putting up with my seemingly constant moaning by shoving coffees, crosswords (and the occasional fig) at me. Your biting sarcasm and wit has been a daily tonic and I'm so glad I have you in my life.

To my main bae, Anna… I don't think I can put into words how much your presence in my life has meant to me over the last 4 years. Thank you for making my home life such a dream, for harmonising on every song, for getting me up in the morning (well, trying!), laughing at my jokes and just generally putting up with me. You're a wizard, Dr Barrett, and there's not one aspect of my life that doesn't feel better with you in it. You've made me smile and laugh every day; and I couldn't have done this without you.

Last, but by no means least, I'd like to thank my wonderful family - Mam, Dad, Greg and Nanny. Your unwavering support and love means everything to me. Thank you for always encouraging me to "just do your best, that's all you can do". It's allowed me to be brave and take on this PhD, in spite of all my fears. Love you millions.

Thesis Summary

EBC-46 and EBC-211 are novel epoxy-tiglianes found to occur naturally within seeds of the Fontain's Blushwood Tree, indigenous to the Queensland tropical rainforest in Australia. The Australian biotechnology company, QBiotics Group, has demonstrated that EBC-46 stimulates enhanced dermal wound healing responses *in vivo*, following cancer treatment and tumour destruction in domesticated animals. Consequently, QBiotics is developing EBC-46 as both a human and veterinary anti-cancer therapy. However, little is known on how the epoxy-tiglianes induce their exceptional healing effects; manifested as rapid wound re-epithelialisation, wound contraction/closure and minimal scarring.

This study aimed to determine how EBC-46 and EBC-211 mediate these exceptional wound healing effects *in vitro*, via analysis of dermal fibroblast (DF)/myofibroblast genotypic and phenotypic responses; following epoxy-tigliane treatment (0.001 - 10 μg/mL). A number of wound healing responses were assessed, such as transforming growth factor-β_1 (TGF-β_1)-driven DF-myofibroblast differentiation, extracellular matrix (ECM) synthesis/turnover, global gene expression and underlying signalling pathways.

Studies exhibited that EBC-46 and EBC-211 significantly inhibited α-smooth muscle actin (αSMA) expression, stress fibre formation and myofibroblast formation at 0.1 μg/mL and 10 μg/mL, respectively. Such concentrations were also shown to reduce type I/III collagen; and up-regulate matrix metalloproteinase-1 (MMP-1) gene and protein levels. The epoxy-tiglianes also increased elastin, hyaluronan and pericellular coat synthesis, via up-regulated hyaluronan synthase (HAS) expression. Microarray analysis and protein level validation identified numerous differentially expressed genes in epoxy-tigliane-treated DFs. Up-regulated genes included proteinases and other 'anti-fibrotic' genes; while down-regulated genes included protease inhibitors, myofibroblast- and cytoskeletal-related genes; as well as other 'pro-fibrotic' genes. Inhibitory effects upon TGF-β_1-driven, DF-myofibroblast differentiation were shown to be protein kinase C (PKC)-dependent.

This study has provided evidence to explain the reduced scarring responses observed in epoxy-tigliane-treated skin; highlighting the potential of epoxy-tiglianes as novel therapeutics for excessive scarring situations.

Publications and Presentations

Publications

Dally, J., Khan, J.S., Voisey, A., Charalambous, C., John, H.L., Woods, E.L., Steadman, R., Moseley, R. and Midgley, A.C. 2017. Hepatocyte Growth Factor Mediates Enhanced Wound Healing Responses and Resistance to Transforming Growth Factor-β_1-Driven Myofibroblast Differentiation in Oral Mucosal Fibroblasts. *International Journal of Molecular Sciences* 18(9). DOI: 10.3390/ijms18091843.

Presentations

Dally, J., Moses, R.L., Midgley, A.C., Reddell, P.W., Steadman, R. and Moseley, R. Pharmaceutical Evaluation of Novel Tigliane Compounds as Modulators of Dermal Fibroblast-Myofibroblast Differentiation, Scar Tissue Resolution and Fibrosis. 1st Annual Life Sciences Research Network Wales (Sêr Cymru) Scientific Meeting, Cardiff, UK, 2014 (Poster).

Dally, J., Moses, R.L., Midgley, A.C., Reddell, P.W., Steadman, R. and Moseley, R. Wound Healing Properties of Australian Rainforest Compounds. 13th Annual Speaking of Science Conference, Cardiff, UK, 2015 (Poster; **Prize Awarded**).

Dally, J., Moses, R.L., Midgley, A.C., Howard-Jones, R.A., Errington, R.J., Reddell, P.W., Steadman, R. and Moseley, R. Modulatory Effects of Novel Epoxy-Tigliane Pharmaceuticals on Dermal Fibroblast-Myofibroblast Wound Healing Responses Mediate Enhanced Anti-Scarring Properties. 3rd South West Regional Regenerative Medicine Meeting, Bristol, UK, 2015 (Poster).

Dally, J., Moses, R.L., Midgley, A.C., Howard-Jones, R.A., Errington, R.J., Reddell, P.W., Steadman, R. and Moseley, R. Modulatory Effects of Novel Epoxy-Tigliane Pharmaceuticals on Dermal Fibroblast-Myofibroblast Wound Healing Responses Mediate Enhanced Anti-Scarring Properties. 7th Joint Meeting of European Tissue Repair Society and Wound Healing Society, Copenhagen, Denmark, 2015 (Poster).

Dally, J., Moses, R.L., Midgley, A.C., Howard-Jones, R.A., Errington, R.J., Reddell, P.W., Steadman, R. and Moseley, R. Modulatory Effects of Novel Epoxy-Tigliane Pharmaceuticals on Dermal Fibroblast-Myofibroblast Wound Healing Responses Mediate Enhanced Anti-Scarring Properties. British Society for Oral and Dental Research Annual Meeting, Cardiff, UK, 2015 (Poster).

Dally, J., Moses, R.L., Midgley, A.C., Reddell, P.W., Steadman, R. and Moseley, R. Modulatory Effects of Novel Epoxy-Tiglianes on Dermal Fibroblast-Myofibroblast

Differentiation Mediate Their Anti-Scarring Properties. 30th Annual Medicine and Dentistry Postgraduate Research Day, Cardiff, UK, 2015 (Poster; **Prize Awarded**).

Dally, J., Moses, R.L., Midgley, A.C., Reddell, P.W., Steadman, R. and Moseley, R. Modulatory Effects of Novel Epoxy-Tigliane Pharmaceuticals on Dermal Fibroblast-Myofibroblast Differentiation Mediate Their Enhanced Anti-Scarring Properties. 2nd Annual Life Sciences Research Network Wales (Sêr Cymru) Scientific Meeting, Cardiff, UK, 2015 (Oral; **Prize Awarded**).

Dally, J., Moses, R.L., Midgley, A.C., Reddell, P.W., Steadman, R. and Moseley, R. Modulatory Effects of Novel Epoxy-Tigliane Pharmaceuticals on Dermal Fibroblast-Myofibroblast Differentiation Mediate Their Enhanced Anti-Scarring Properties. 1st Wales Kidney Research Unit Annual Meeting, Cardiff, UK, 2015 (Poster).

Dally, J., Moses, R.L., Midgley, A.C., Reddell, P.W., Steadman, R. and Moseley, R. Modulatory Effects of Novel Epoxy-Tiglianes on Dermal Fibroblast-Myofibroblast Wound Healing Responses. Sêr Cymru Postgraduate Conference, Swansea, UK, 2016 (Poster).

Dally, J., Moses, R.L., Midgley, A.C., Reddell, P.W., Steadman, R. and Moseley, R. Modulatory Effects of Novel Epoxy-Tiglianes on Dermal Fibroblast-Myofibroblast Differentiation via Classical Protein Kinase C Activation. 31st Annual Medicine and Dentistry Postgraduate Research Day, Cardiff, UK, 2017 (Oral).

Dally, J., Moses, R.L., Midgley, A.C., Boyle, G.M., Reddell, P.W., Steadman, R. and Moseley, R. Modulatory Effects of Novel Epoxy-Tiglianes on Dermal Fibroblast-Myofibroblast Differentiation via Classical Protein Kinase C Activation. European Tissue Repair Society '(T)issues of War and Peace' Conference, Brussels, Belgium, 2017 (Oral; Young Investigator Prize Session).

Dally, J., Moses, R.L., Midgley, A.C., Boyle, G.M., Reddell, P.W., Steadman, R. and Moseley, R. Modulatory Effects of Novel Epoxy-Tiglianes on Dermal Fibroblast-Myofibroblast Differentiation via Classical Protein Kinase C Activation. Cardiff Institute of Tissue Engineering and Repair Annual Scientific Meeting, Cardiff, UK, 2017 (Oral).

Dally, J., Moses, R.L., Midgley, A.C., Boyle, G.M., Reddell, P.W., Steadman, R. and Moseley, R. Modulatory Effects of Novel Epoxy-Tiglianes upon Dermal Fibroblast-Myofibroblast Differentiation via Classical Protein Kinase C (PKC) Activation. 3rd Annual Life Sciences Research Network Wales (Sêr Cymru) Scientific Meeting, Cardiff, UK, 2017 (Oral).

Glossary of Abbreviations and Nomenclature

3D	Three-Dimensional
ACTA2	Actin α_2
ACTC1	Actin α
ADAMTS	A Disintegrin/Metalloproteinase with Thrombospondin Motif
AFAP1	Actin Filament Associated Protein 1
ANOVA	Analysis of Variance
APMA	4-Aminophenylmercuric Acetate
ARHGEF2	Rho/Rac Guanine Nucleotide Exchange Factor 2
ARHGAP22	Rho GTPase Activating Protein 22
αSMA	α-Smooth Muscle Actin
BAMBI	BMP and Activin Membrane-Bound Inhibitor
BCA	Bicinchoninic Acid
BIM-1	Bisindolylmaleimide-1
BMP	Bone Morphogenetic Protein
BSA	Bovine Serum Albumin
C5ORF13	Chromosome 5, Open Reading Frame 13
CALD1	Caldesmon 1
CAMKII	Calmodulin Kinase II
CASE	Compound *Astragalus* and *Salvia miltiorrhiza* extract
CD44	Cluster of Differentiation 44
CDH2	Cadherin-2
CDKN2B	Cyclin-Dependent Kinase Inhibitor 2B
cDNA	Complementary Deoxyribonucleic Acid
cRNA	Complementary Ribonucleic Acid
CT	Cycle Threshold
CTGF	Connective Tissue Growth Factor
CTSK	Cathepsin K
COL	Collagen
COL1α_1	Type I Collagen, α_1 Chain
COL3α_1	Type III Collagen, α_1 Chain

COMP	Cartilage Oligomeric Matrix Protein
CXCL	C-X-C Motif Chemokine Ligand
CYR61	Cysteine-Rich, Angiogenic Inducer 61
DAG	Diacylglycerol
dCT	Delta Cycle Threshold/Difference in Cycle Threshold
dd-H_2O	Double-Distilled Water
DF	Dermal Fibroblasts
DMEM	Dulbecco's Modified Eagle Medium
DMSO	Dimethyl Sulphoxide
DNA	Deoxyribonucleic Acid
DNase	Deoxyribonuclease
dNTPs	Deoxyribonucleotide Triphosphates
DPT	Dermatopontin
EBC-46	12-tigloyl-13-(2-methylbutanoyl)-6,7-epoxy-4,5,9,12,13,20-hexahydroxy-1-tiglian-3-one
EBC-211	12-tigloyl-13-(2-methylbutanoyl)-5,6-epoxy-4,5,9,12,13,20-hexahydroxy-1-tiglian-3-one
ECL	Enhanced Chemiluminescence
ECM	Extracellular Matrix
EDA-FN	Extra Domain-A-Fibronectin
EDTA	Ethylenediaminetetraacetic Acid
EFEMP1	EGF-Containing Fibulin-Like ECM Protein 1
EGF	Epidermal Growth Factor
EGFR	Epidermal Growth Factor Receptor
EHBP1	EH Domain Binding Protein 1
ELISA	Enzyme-Linked Immunosorbent Assay
ELN	Elastin
ENC1	Ectodermal-Neural Cortex
ERK	Extracellular Signal-Regulated Kinase
5-FU	Fluorouracil
FA	Focal Adhesion
F-Actin	Filamentous Actin

FAK	Focal Adhesion Kinase
FAM	Fluorescein Amidite
FAT1	FAT Tumour Suppressor Homolog 1
FBLN	Fibulin
FBN	Fibrillin
FCS	Foetal Calf Serum
FGF	Fibroblast Growth Factor
FITC	Fluorescein Isothiocyanate
FKBP1A	FK506 Binding Protein 1A
FLN	Filamin
FN	Fibronectin
FRET	Fluorescence Resonance Energy Transfer
FS-CM	Fibroblast Serum-Containing Medium
FSTL1	Follistatin-like 1
G-actin	Globular Actin
GAG	Glycosaminoglycans
GAL	Galanin Propeptide
GAPDH	Glyceraldehyde 3-Phosphate Dehydrogenase
GAS6	Growth Arrest-Specific 6
gDNA	Genomic Deoxyribonucleic Acid
GDP	Guanosine Diphosphate
GEF	Guanine Nucleotide Exchange Factor
GLIPR2	GLI Pathogenesis-Related 2
GLS	Glutaminase
Gö6976	5,6,7,13-tetrahydro-13-methyl-5-oxo-12H-indolo(2,3-a)pyrrolo(3,4-c)carbazole-12-propanenitrile
GREM	Gremlin
GTP	Guanosine Triphosphate
HA	Hyaluronan
HABP	Hyaluronic Acid Binding Protein
HaCaT	Normal Human Keratinocyte Cell Line of Skin Origin
HAS	Hyaluronan Synthase

HRP	Horseradish Peroxidase
HYAL	Hyaluronidase
ICC	Immunocytochemistry
IFN	Interferon
IGF	Insulin-Like Growth Factor
IGFBP3	Insulin-Like Growth Factor Binding Protein 3
IgG	Immunoglobulin G
IL	Interleukin
IPA	Ingenuity Pathway Analysis
ITGA2	Integrin α_2
ITGA11	Integrin α_{11}
ITGBL1	Integrin β-like$_1$
IVT	*In vitro* Transcription
JAK	Janus-Activated Kinase
JNK	C-Jun N-Terminal Kinase
kB	Kilobase
kDa	Kilodalton
KLF4	Krüppel-Like Factor 4
LAP	Latency Associated Protein
LIMA1	LIM Domain and Actin Binding 1
LOX	Lysyl Oxidase
LPXN	Leupaxin
MACF1	Microtubule-Actin Cross-Linking Factor 1
MAPK	Mitogen Activated Protein Kinase
MEG3	Maternally Expressed 3
MGB-NFQ	Minor Groove Binder Non-Fluorescent Quencher
MMP	Matrix Metalloproteinase
mRNA	Messenger Ribonucleic Acid
MYLK	Myosin Light Chain Kinase
OA	Oleanolic Acid
OD	Optical Density
OMF	Oral Mucosal Fibroblast

OMT	Oxymatrine
PAI	Plasminogen Activator Inhibitor
PBS	Phosphate Buffered Saline
PCR	Polymerase Chain Reaction
PDGF	Platelet-Derived Growth Factor
PDL	Pulsed Dye Laser
PDPN	Podoplanin
PG	Proteoglycan
PI16	Peptidase Inhibitor 16
PI3K	Phosphatidylinositide 3-Kinase
PKC	Protein Kinase C
PLAU	Urokinase-Type Plasminogen Activator
PLOD2	Pro-Collagen-Lysine 2-Oxoglutarate 5-Dioxygenase 2
PMN	Polymorphonuclear
PVDF	Polyvinylidene Difluoride
QIMR	Berghofer Queensland Institute of Medical Research
qPCR	Real-Time Quantitative Polymerase Chain Reaction
RAC	Ras-related C3 Botulinum Toxin Substrate
RFU	Relative Fluorescence Unit
RHO	Ras Homolog Gene Family Member
RHOBTB	RHOB and Rho-related BTB Domain Containing 3
RIPA	Radio-Immunoprecipitation Assay
RNA	Ribonucleic Acid
RNase	Ribonuclease
ROCK	Rho-associated Kinase
ROS	Reactive Oxygen Species
RQ	Relative Quantification
rRNA	Ribosomal Ribonucleic Acid
R-SMAD	Receptor-Associated SMAD
RT	Reverse Transcription
RT-qPCR	Reverse Transcription-Quantitative Polymerase Chain Reaction

S100A4	S100 Calcium Binding Protein A4
SARA	SMAD Anchor for Receptor Activation
SD	Standard Deviation
SDS-PAGE	Sodium Dodecyl Sulphate-Polyacrylamide Gel Electrophoresis
SEM	Standard Error of the Mean
SERPIN	Serpin Peptidase Inhibitor
S-FM	Serum-Free Medium
SHRM	Shroom
SHROOM3	Shroom Family Member 3
SLC3A2	Solute Carrier Family 3, Member 2
SLRPs	Small Leucine-Rich Proteoglycans
SPHK1	Sphingosine Kinase 1, Transcript Variant 1
SPP1	Osteopontin
STAT	Signal Transducer and Activator of Transcription
SYBR	N',N'-dimethyl-N-[4-[(E)-(3-methyl-1,3-benzothiazol-2-ylidene)methyl]-1-phenylquinolin-1-ium-2-yl]-N-propylpropane-1,3diamine
SYNC1	Syncoilin
TAMRA	5-carboxytetramethylrhodamine
TAE	Tris/Acetate/Ethylenediaminetetraacetic Acid
TBE	Tris/Borate/Ethylenediaminetetraacetic Acid
TBS	Tris Buffered Saline
TFPI2	Tissue Factor Pathway Inhibitor 2
TGF-β	Transforming Growth Factor-β
TGF-βR	Transforming Growth Factor-β Receptor
TGM2	Transglutaminase 2
TIMP	Tissue Inhibitor of Metalloproteinase
TNC	Tenascin C
TNF	Tumour Necrosis Factor
TPM1	Tropomyosin α_1
TRAF3IP2	TRAF3 Interacting Protein 2, Transcript Variant 2
TRIB3	Tribbles Homolog 3

TSG-6	TNF-Stimulated Gene-6
TUBB2A	Tubulin β_2A
TUBB2B	Tubulin β_2B
UNG	Uracil-N Glycoslyase
uPA	Urokinase-Type Plasminogen Activator
UV	Ultraviolet
VCAN	Versican
VEGF	Vascular Endothelial Growth Factor
VIC	2'-chloro-7'phenyl-1,4-dichloro-6-carboxy-fluorescein
vWF	Von Willebrand Factor
ΔΔCT	Comparative Cycle Threshold

Table of Contents

Chapter 1

General Introduction

Chapter 1 - General Introduction

1.1 Overview

Cutaneous wound healing encompasses a dynamic, naturally orchestrated series of events, by which the skin repairs itself following physical injury or trauma. When the skin's protective barrier is compromised and equilibrium is lost, an intricate cycle of biochemical, molecular and cellular processes are initiated in an attempt to restore dermal functionality (Enoch and Leaper, 2005; Krafts, 2010; Reinke and Sorg, 2012). However, effective wound resolution requires the co-ordinated effort and timing of a plethora of cell types, growth factors and extracellular matrix (ECM) components. Combined with the need for rapid wound closure, cutaneous repair often results in scar formation. If this fails to resolve or terminate in a timely manner, persistent and pathological tissue fibrosis can occur (Sarrazy *et al*. 2011; Reinke and Sorg, 2012). As a common, albeit undesirable, consequence of wound healing, scarring significantly contributes to the global healthcare burden. In the developed world, approximately 100 million patients develop scars annually through elective surgery and operations following trauma. Many of these are the outcome of excessive, unregulated dermal repair; including an estimated 4 million burn scars and 11 million keloid scars (Sund, 2000; Bayat *et al*. 2003). People with dermal scarring may suffer physical, aesthetic, psychological and social consequences that are also linked with significant financial and emotional costs (Dorfmüller, 1995; Taal and Faber, 1998; Robert *et al*. 1999). At present, however, the majority of existing therapeutic approaches are clinically sub-standard; likely due to an incomplete understanding of the molecular basis of repair. Furthermore, there are a lack of animal models that adequately recapitulate human conditions, mechanisms underlying pathological scarring remain elusive and clinical research in the field is hampered by a multi-morbid patient population (Eming *et al*. 2014; Kaplani *et al*. 2018). Ultimately, such issues have contributed to the paucity of large-scale, high-quality 'efficacy of use' clinical trials for both existing and emerging therapies; as well as a deficiency of efficacious treatments for pathological scarring (Reish and Eriksson, 2008; Eming *et al*. 2014). Hence, there is an unmet clinical need

to develop novel wound healing agents, ideally enhancing normal wound repair or promoting tissue regeneration (Sen *et al*. 2009).

EBC-46 and EBC-211 are novel epoxy-tiglianes found to occur naturally within seeds of the Fontain's Blushwood Tree, indigenous to the Queensland tropical rainforest in Australia (Reddell and Gordon, 2007). Sourced for its potential bioactivity, EBC-46 is currently under development by the QBiotics Group as an anti-cancer treatment; as it has been shown to exhibit tumouricidal properties through palliative treatment of solid tumours in over 300 exploratory case studies with companion animals and 110 canine clinical trials (Reddell *et al*. 2014; Barnett *et al*. 2018). Furthermore, following tumour ablation, exceptional wound repair responses and enhanced cosmesis have been observed at treatment sites, manifested as rapid re-epithelialisation, closure and minimal scarring. In light of such beneficial effects and proof-of-concept data on the drug's efficacy and safety in both mouse and companion animal models, QBiotics Group are developing EBC-46 as an anti-cancer pharmaceutical for both veterinary and human use; with EBC-46 having recently completed Phase I human clinical trials (Boyle *et al*. 2014; Reddell *et al*. 2014; Campbell *et al*. 2017; Barnett *et al*. 2018).

Due to the observed preferential healing responses in treated skin and with limited information regarding how EBC-46 induces such effects, this PhD study has focused on elucidating the effects of EBC-46 and a less active derivative, EBC-211, on dermal fibroblasts (DFs). Established as key mediators of acute dermal wound healing/scar formation, normal primary human DFs were used throughout this project. A number of *in vitro* studies were performed to assess the effects of EBC-46 and EBC-211 upon key DF responses; such as DF-myofibroblast differentiation, ECM synthesis/turnover, global gene expression and signalling pathways. Comparisons were drawn between EBC-46 and EBC-211 across a range of concentrations (0 - 10 µg/mL), in the absence or presence of transforming growth factor-β_1 (TGF-β_1). This aimed to determine the optimal dose range *in vitro*, whilst observing the effects of the epoxy-tiglianes upon standard genotypic and phenotypic DF responses. DFs and myofibroblasts represent

feasible targets for the modulatory actions and anti-fibrotic properties of the epoxy-tiglianes, as observed *in vivo* (Reddell *et al*. 2014; Campbell *et al*. 2017).

1.2 Skin Structure and Function

The skin is a dynamic, self-renewing organ that covers the surface of the body; acting as a continuous barrier, serving to separate the human body's internal environment from the outside world. As the body's largest structure, the integumentary system is crucial in ensuring an organism's protection against external stressors. The skin itself performs a diverse array of physiological functions, including prevention of pathogen invasion and ultraviolet (UV) damage. It also shields its host against mechanical and chemical insults, as well as free radicals; decreasing the chance of oxidative damage occurring (Menon, 2002; Lee *et al*. 2006; Proksch *et al*. 2008; Darlenski *et al*. 2011; D'Orazio *et al.* 2013). In addition, the skin provides somatosensory information with regards to temperature, touch and pain; while in response to sunlight, it synthesises vitamin D (Holick *et al*. 1987; Menon, 2002). The skin is also predominantly involved in homeostasis, aiding in maintenance of thermoregulation, fluid balance, insulation and water/solute loss. Without such a pliable, yet resistant defensive layer, the body would swiftly fall prey to bacterial attack and desiccation. However, discrete regions of the skin exist to prevent these adverse events from occurring (Baroni *et al*. 2012; Sotiropoulou and Blanpain, 2012; Figure 1.1).

With regards to human anatomy, the skin is the first line of defence and its ability to continuously maintain, renew and restore confers a selective advantage (Reinke and Sorg, 2012). As a protective interface between the external environment and deeper muscular and skeletal layers, the skin comprises three structural compartments: the outer epidermis, inner dermis and underlying hypodermis (Baroni *et al*. 2012; Figure 1.1). Each layer's function directly relates to its composition and the cell populations within these areas are characteristically distinct. In order to maintain the skin's form and function, there is constant turnover of several cell types via processes including proliferation, differentiation and apoptosis (Song *et al*. 1997; Böttcher-Haberzeth *et al*. 2010). Overall, these events collectively maintain the skin's protective properties

and if these homeostatic mechanisms become irregular, pathology may occur. Loss or disruption of skin integrity often occurs due to injury or trauma, which can result in failure of cutaneous function. Re-establishing or preserving both skin integrity and function is imperative and therefore, initiation of wound healing begins immediately post-tissue damage (Singer and Clark, 1999; Kondo and Ishida, 2010). As mentioned previously, wound repair plays a crucial role in restoring integumentary equilibrium (Section 1.1). However, effective wound resolution requires the synchronised effort of a variety of cell types, cytokines and structural components present in the layers of the skin (Krafts, 2010; Reinke and Sorg, 2012).

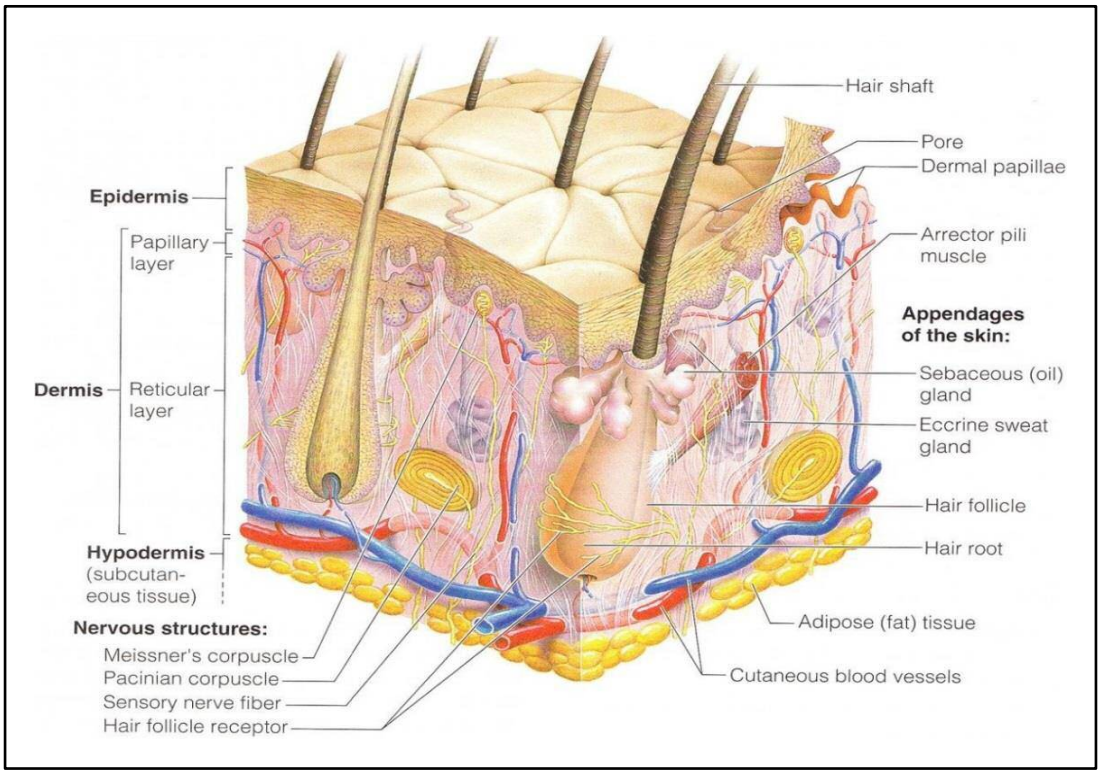

Figure 1.1. A three-dimensional (3D) view of the structure of the skin, including the epidermis, dermis and hypodermis. Primary sub-cutaneous tissue, skin appendages and nerve structures are also demonstrated (Marieb and Hoehn, 2010).

1.2.1 The Epidermis

As the outermost layer of the skin, the epidermis is a tough, compartmentalised and highly keratinised structure; predominantly functioning to provide protection for the underlying layers. In order to continually defend the body against hazardous stimuli, the epidermis comprises a composite system of continuously renewing cells (Proksch *et al*. 2008; Baroni *et al*. 2012; Figure 1.2). Under normal conditions, a balance exists between the processes of proliferation and desquamation, resulting in complete cell turnover every 28 days (Webb *et al*. 2004; Baroni *et al*. 2012). This cycle of continual replacement maintains epidermal integrity and the importance of this equilibrium is emphasised by specific skin disorders, arising from abnormalities in these processes; including ichthyoses and psoriasis (Pullmann *et al*. 1977; Deo and Deshmukh, 2018; Zaki and Choate, 2018). Therefore, it is clear that the epidermis is both a mechanical barrier and metabolically active tissue; preserving stability and providing protection against environmental insults, whilst allowing cells to respond to various stimuli and aid in repair (Fuchs and Raghavan, 2002; Simpson *et al*. 2011).

As a consequence of undergoing continuous desquamation, the epidermis requires constant renewal, which is facilitated by the layer's primary cell type. Accounting for around 80 - 95 % of epidermal cells, keratinocytes are squamous epithelial cells that mature, differentiate and migrate to replace dead cells that are lost from the body's surface (Milstone, 2004; Candi *et al*. 2005; Lorencini *et al*. 2014). Named due to their production of filamentous keratin proteins, keratinocytes both produce and respond to growth factors and cytokines, in order to stimulate or inhibit cell proliferation and migration (Suter *et al*. 2009; Baroni *et al*. 2012). In the epidermis, they are organised in a way which permits progression away from the underlying basement membrane; possessing phenotypic differences corresponding to function, at different epidermal depths. Consequently, this results in a stratified epidermal arrangement, comprising strata representing different stages of keratinocyte differentiation/maturation (Song *et al*. 1997; Balasubramani *et al*. 2001; Brohem *et al*. 2011; Simpson *et al*. 2011). The epidermis contains the *stratum basale*, *stratum spinosum*, *stratum granulosum* and *stratum corneum*; with the former three layers comprising the viable epidermis and

the latter forming the non-viable region (Figure 1.2). Keratinocyte maturation begins in the inner *stratum basale*, which consists of a stem cell monolayer responsible for continuous renewal of the epidermis (Blanpain and Fuchs, 2006; Baroni *et al*. 2012; van Smeden *et al*. 2014). Attached firmly to the underlying basal lamina, these cells are mitotically active and are able to proliferate rapidly into differentiated progeny, when necessary. Keratinocyte stem cells represent only approximately 2 - 7 % of the basal layer cells and are typically quiescent. However, upon wounding, surrounding stem cells are recruited to proliferate (Alonso and Fuchs, 2003; Blanpain and Fuchs, 2006; Fu and Sun, 2009; Simpson *et al*. 2011).

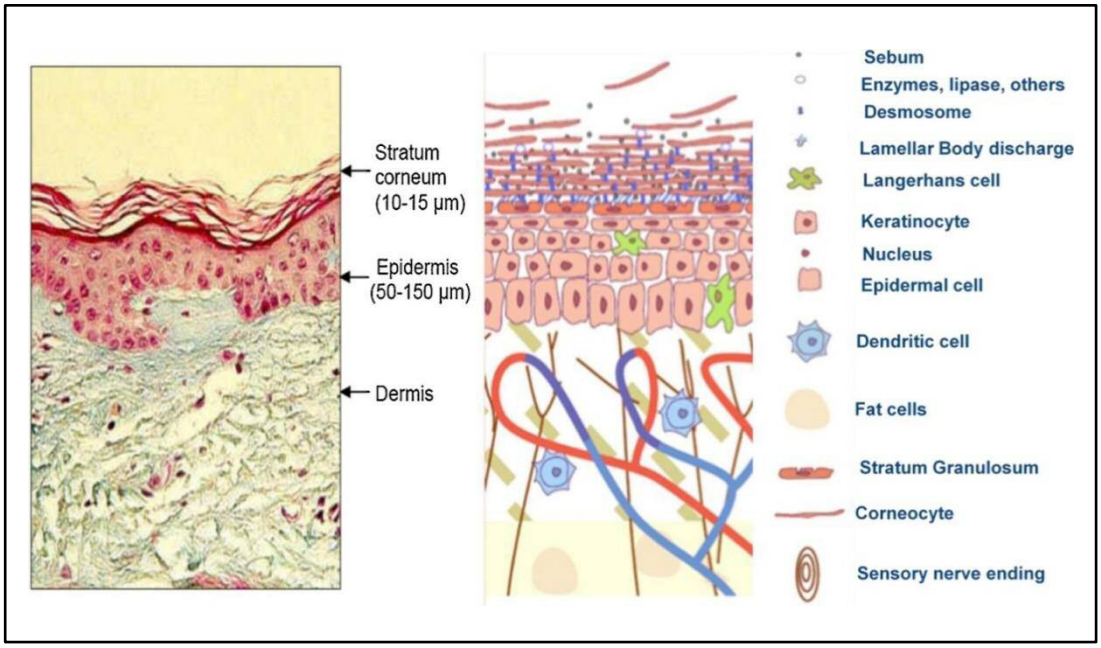

Figure 1.2. Diagram showing the skin's *stratum corneum*, epidermis and dermis; and cellular distribution within these layers. Sequential distribution of differing cell types is displayed and the approximate thickness of each layer is shown (Menon, 2002).

Approximately 40 % of cells in the *stratum basale* are daughter transient amplifying cells, which replicate at a higher frequency than the keratinocyte stem cells, but are capable of far fewer population doublings (Jones and Watt, 1993; Fu and Sun, 2009). These cells undergo a limited number of mitotic divisions before differentiating and detaching from the basement membrane. Subsequently, they feed upwards through the suprabasal layers towards the skin surface (Fu and Sun, 2009). The second most abundant epidermal cells also reside in the *stratum basale*, contributing to the skin's photoprotective properties. Originating from the neural crest, melanocytes are cells responsible for synthesising melanin; the pigment involved in protection against UV radiation (Cichorek *et al*. 2013; D'Orazio *et al.* 2013; Natarajan *et al*. 2014). In order to transfer synthesised melanin, dendritic processes of the melanocytes contact the keratinocytes and allow granules to accumulate over the keratinocyte nuclei (Klaus, 1969; Tsatmali *et al.* 2002; Boissy, 2003). These 'supranuclear caps' protect the basal cells at the earliest point in the differentiation process, preventing cellular mutation at the *stratum basale* and subsequent movement of abnormal cells to the surface of the skin (Plonka *et al.* 2009; Cichorek *et al*. 2013).

After the daughter keratinocytes leave the *stratum basale*, they migrate towards the apical *stratum spinosum*. In this cell-dense layer, keratinocytes grow larger, establish robust intercellular connections and commit to terminal differentiation via cell cycle exit (Brohem *et al*. 2011; Simpson *et al*. 2011). As keratinocytes continue to progress towards the interface with the environment, their cell morphology alters drastically. Within the granular layer, the cells flatten and organelles disintegrate post-exposure to lysosomal enzymes; they also accumulate lipid granules, which are critical for the maintenance of the water barrier (Candi *et al*. 2005; Brohem *et al*. 2011; Simpson *et al*. 2011). Subsequently, keratinocytes are more resistant to destruction before their ascension into the outermost layer. As displayed in Figure 1.2, the *stratum corneum* represents the final stage of keratinocyte differentiation, with cells now referred to as 'corneocytes'. These are flat, anuclear, keratin-filled cells that form several layers and are surrounded by a lipid-protein matrix, preventing water loss and establishing an effective barrier against most micro-organisms, chemicals and fluids. Ultimately,

corneocytes readily desquamate and slough from the skin surface; to be replaced by inner layers of cells progressing outward (Milstone, 2004; Fu and Sun, 2009; Brohem *et al*. 2011; Eckhart *et al*. 2013; Lorencini *et al*. 2014; van Smeden *et al*. 2014).

As well as keratinocytes and melanocytes, other cells of the epidermis contribute to epidermal homeostasis. Langerhans cells are dendritic, antigen-presenting cells that migrate to local lymph nodes to initiate an immune response. Encompassing 2 - 4 % of the epidermal cell population, they are predominantly located within the *stratum spinosum* (Sparber, 2014; Atmatzidis *et al*. 2017). In contrast, Merkel cells are found to reside within the *stratum basale* and are closely associated with hair follicles and nerve fibres; functioning as the skin's mechanoreceptors and transmitting the touch sensation (Moll *et al*. 2005; Boulais and Misery, 2008). In order to provide structural integrity, cells throughout the epidermis are connected adjacently via desmosomes; whilst basal epithelial cells are connected to the basal lamina via hemi-desmosomes. However, in order for the skin to perform its diverse array of physiological functions efficiently, dermal-epidermal cross-talk must occur (Fuchs, 2007; Fu and Hsu, 2013; Bassino *et al*. 2017).

1.2.2 The Dermis

Epidermal development during embryogenesis, the processes of wound healing and normal homeostatic mechanisms all depend on the interactions between the dermis and epidermis (Balasubramani *et al*. 2001; Brohem *et al*. 2011). These exchanges are modulated by the well-characterised basement membrane, which anchors the loose dermal connective tissue to the overlying epidermis. The basement membrane acts as both a dynamic and steady junction between the two layers, stabilising the above epidermis mechanically through hemi-desmosomes, whilst controlling movement of bioactive molecules in either direction (McMillan *et al*. 2003; Yurchenco *et al*. 2004; LeBleu *et al*. 2007; Breitkreutz *et al*. 2013). Regarding composition, the constituents of the basement membrane mainly consist of type IV collagen, proteoglycans (PGs), glycosaminoglycans (GAGs) and laminin; as well as growth factors/cytokines. Thus, the basement membrane represents a reservoir for controlled release during wound

repair processes and physiological remodelling (Iozzo, 2005; Brohem *et al*. 2011).

Situated below the basement membrane, the dermis consists of a connective tissue layer that confers considerable tensile strength and flexibility to the skin. The dermis is characterised by a highly vascularised network of fibrous proteins, predominantly comprising collagen and elastic fibres; surrounded by a ground substance consisting of PGs, GAGs and glycoproteins (Braverman and Fonferko, 1982; Balasubramani *et al*. 2001; Kielty *et al*. 2002; Brohem *et al*. 2011; Figure 1.2). Together, this meshwork constitutes the ECM and its contents allow the region to bear mechanical load, while providing epidermal nutrition and insulation (Krieg and Aumailley, 2011; Breitkreutz *et al*. 2013). In addition to ECM, the dermis also hosts specialised structures, such as nerves and hair follicles; as well as sweat and sebaceous glands. The presence of the above components reflect the primary dermal functions, which consist of protection from injury, pressure detection and thermoregulation (Baroni *et al*. 2012; Arda *et al*. 2014).

Although much less cell-dense than the epidermis, numerous cell types are present within the dermis; including DFs and immune cells. However, it is chiefly populated by mesodermally-derived DFs, which are responsible for synthesising and depositing ECM components (Frantz *et al*. 2010; Baroni *et al*. 2012). DFs also possess protective roles, readily differentiating into myofibroblasts following dermal injury, in order to contract and pull the wound edges together. Therefore, they are particularly critical to the dermal wound healing process, due to their abilities in repairing the defective injury site and restoring dermal homeostasis through the synthesis and remodelling of ECM components (Clark, 1993; Gabbiani, 2003; Schultz and Wysocki, 2009). They also support keratinocyte re-epithelialisation, via autocrine and paracrine interaction with these cells at the wound site (Werner *et al*. 2007; Brohem *et al*. 2011). Further, minor cell populations also reside within the dermis and facilitate its protective role. Neutrophils and macrophages act as a vanguard of defence, migrating to the wound site and identifying/eliminating any foreign invaders which have progressed beyond the epithelial barrier. Macrophages are also involved in clearance of cell debris and

apoptotic cells (Singer and Clark, 1999; Eming *et al*. 2007; Murray and Wynn, 2011). Thus, as found in the epidermis, it is clear that the cells present in the dermal layer reflect its primary functions. Similarly to its role in supporting the above epidermis, the dermis is likewise supported by the underlying hypodermis.

1.2.3 The Hypodermis

Also known as the sub-cutaneous layer or subcutis, the hypodermis is the innermost skin region and is found directly above the muscle layer. It contains loose connective tissue abundant in both collagen and adipocyte cells, allowing the skin to slide over the deep fascia easily, whilst offering protection from mechanical shock (Song *et al*. 1997; Baroni *et al*. 2012; Arda *et al*. 2014). Furthermore, the adipose tissue present provides thermal insulation and contributes to energy storage and metabolism. The hypodermis is populated by DFs and macrophages, whilst an extensive vascular network supplies nutrients and removes waste products (Baroni *et al*. 2012; Arda *et al*. 2014). Together, the dermis and hypodermis are the most effective skin barriers regarding traumatic and thermal insults (Baroni *et al*. 2012). Nevertheless, the body is frequently subjected to hazardous environmental stimuli and often suffers tissue damage. As a result, the skin has developed a fundamental repair strategy (Eming *et al*. 2014).

1.3 Acute Dermal Wound Healing

As the organ most challenged by external stressors, the integumentary system often endures cell and tissue damage; compromising its protective function. Consequently, the skin has evolved a set of complex mechanisms, which aim to restore integrity of the barrier following injury or trauma (Reinke and Sorg, 2012; Eming *et al*. 2014). If the skin is damaged and equilibrium is lost, the acute dermal wound healing process is initiated. Encompassing a dynamic, highly-coordinated series of events, cutaneous healing comprises several histologically and functionally distinct phases. Each of the phases are characterised by a variety of chemical, molecular and cellular processes; typically culminating in wound repair (Enoch and Leaper, 2005; Krafts, 2010; Reinke and Sorg, 2012; Pang *et al*. 2017). However, efficacious wound resolution requires a

rapid, yet well-orchestrated, response from a plethora of cell types, growth factors, cytokines and ECM components. Moreover, the aforementioned phases are not only intricate, but overlapping; all contributing to restore tissue functionality (Enoch and Leaper, 2005; Gurtner *et al*. 2008; Reinke and Sorg, 2012; Eming *et al*. 2014). Acute wound healing is broadly divided into three phases: inflammation, proliferation and remodelling (Figure 1.3; Singer and Clark, 1999; Reinke and Sorg, 2012).

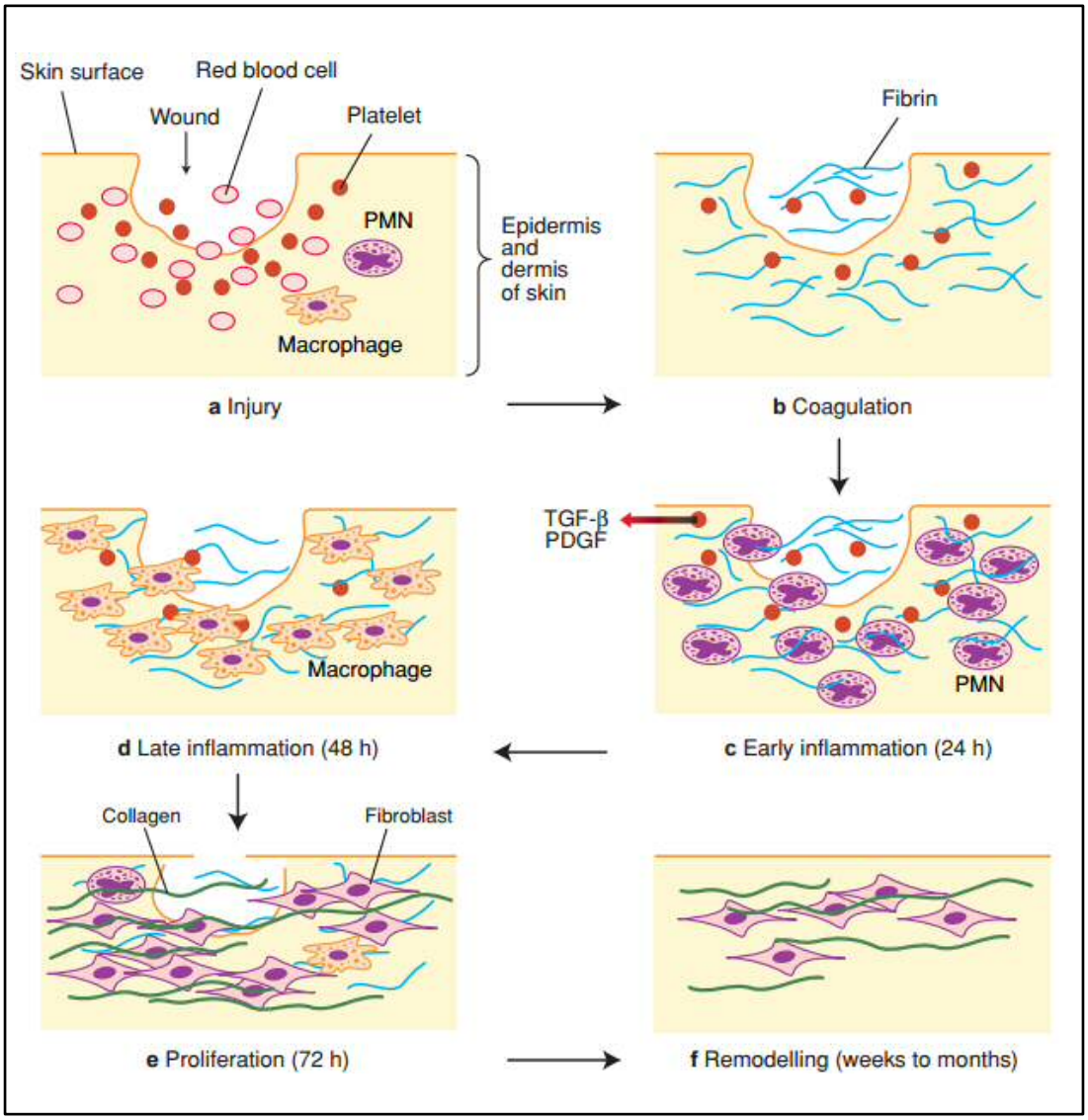

Figure 1.3. Diagram demonstrating the overlapping phases of wound repair and the cellular constituents involved, beginning with the initial injury (A); and followed by haemostasis (B), early and late inflammation (C and D, respectively), proliferation (E) and remodelling/maturation (F; Beanes *et al*. 2003).

1.3.1 The Inflammatory Phase

Beginning immediately after injury, the inflammatory phase is characterised by the initiation of haemostasis and influx of immune cells into the wound site (Figure 1.3). Haemostasis is a rapid process, aiming to minimise blood loss from the trauma site. and consists of two major processes: fibrin clot development and coagulation. Upon injury, vasoconstriction occurs in blood vessels adjacent to those that have ruptured, in order to staunch further blood loss (Beanes *et al*. 2003; Li *et al*. 2007; Reinke and Sorg, 2012). Damaged endothelial cells release thromboxanes, which act to constrict the blood vessels and assist platelet aggregation, promoting the coagulation cascade (Broughton *et al*. 2006). The coagulation cascade is an essential step for continuation of the wound repair process, as the formation of a fibrin clot represents an alternate protective barrier from the environment after loss of dermal integrity. The clot also acts as a provisional matrix, where cells needed for debris clearance from the wound site and ECM remodelling are able bind to this temporary scaffold (Clark *et al*. 1982; Broughton *et al*. 2006; Li *et al*. 2007; Reinke and Sorg, 2012).

Platelets are the first subset of cells to enter the wound site and clot homeostasis is dependent on their adhesion and aggregation. Following wounding, collagen binds to the plasma glycoprotein, von Willebrand factor (vWF), after its exposure through endothelial cell damage (Nurden, 2011; Pakyari *et al*. 2013). Activated platelets are attracted and attach to the collagen-vWF complexes, signifying thrombus formation. First forming a mass, aggregated platelets subsequently start secreting inflammatory factors and various clotting factors; stimulating the chemotaxis of necessary cells to the injured site. High concentrations of such factors initiate the inflammatory phase and blood plasma proteins, including thrombin, lead to the conversion of fibrinogen to fibrin (Hoffman and Monroe, 2005; Li *et al*. 2007; Nurden, 2011; Reinke and Sorg, 2012; Eming *et al*. 2014). Fibrin then cross-links with fibronectin (FN), forming a clot that is insoluble and structurally stable. Along with preventing excessive protein and blood loss, the fibrin-FN mass is the main structural support during the early stages of wound healing and provides the basic architecture for further cell adherence and recruitment (Corbett *et al*. 1997; Enoch and Leaper, 2005; Eming *et al*. 2014). Other

glycoproteins found in the fibrin-FN plug are vitronectin and thrombospondin. These are involved in cell-ECM and ECM-ECM interactions, which regulate cell proliferation, adhesion and migration. Also, platelets in the clot and those arriving at the injury site release their α-granules and secrete growth factors and cytokines, including vascular endothelial growth factor (VEGF), platelet-derived growth factor (PDGF), epidermal growth factor (EGF) and TGF-β_1 (Beanes *et al*. 2003; Enoch and Leaper, 2005; Guo and Dipietro, 2010; Reinke and Sorg, 2012; Pakyari *et al*. 2013). Such factors persist and promote later characteristics of wound repair, including cell proliferation, ECM deposition and wound contraction (Li *et al*. 2007).

Shortly after the aforementioned vasoconstriction, the aggregated platelets release histamine and serotonin, that results in vasodilation and an accompanying increase in local capillary permeability. This allows a greater number of inflammatory cells to infiltrate the wound (Beanes *et al*. 2003; Enoch and Leaper, 2005). Migration occurs by chemotaxis and promotes the inflammatory phase, which is characterised by the sequential infiltration of neutrophils, macrophages and lymphocytes (Broughton *et al*. 2006; Guo and Dipietro, 2010). Overlapping with the late haemostatic phase, the inflammatory phase commences within an hour of wounding and can be divided into early and late stages, based on the type of inflammatory cell involved (Figure 1.3). In the first instance, neutrophils are drawn to the injury site by chemoattractants, such as complement components, TGF-β_1 and bacterial peptides (Mutsaers *et al.* 1997; Li *et al*. 2007; Reinke and Sorg, 2012). Neutrophils are initially present in high numbers and are responsible for the innate anti-microbial removal of bacteria and cell debris. They also secrete proteases and produce reactive oxygen species (ROS), which break down damaged tissue and aid in eliminating bacteria. Non-wounded skin around the injury site is protected from proteolysis by the presence of protease inhibitors (Yager and Nwomeh, 1999; Guo and Dipietro, 2010; Pakyari *et al*. 2013; Wilgus *et al*. 2013). Digestion of bacteria and debris is achieved by phagocytosis and after 48 - 72 hours, the late inflammatory phase begins (Figure 1.3; Beanes *et al*. 2003).

During the late inflammatory phase, monocytes are attracted to the wound site and

undergo differentiation into macrophages. They are initially drawn to the injury site by many of the same chemoattractants that recruit the neutrophils and are essential to the continuation of wound repair (Mutsaers *et al.* 1997; Enoch and Leaper, 2005). Macrophages are responsible for clearing any apoptotic cells (including neutrophils) and phagocytosing any bacteria and/or cell debris; such actions pave the way for the resolution of inflammation. Macrophages later undergo a phenotypic transition to a reparative state, during which the cells are capable of stimulating angiogenesis, DFs and keratinocytes; in order to encourage tissue regeneration (Li *et al*. 2007; Mosser and Edwards, 2008; Guo and Dipietro, 2010; Reinke and Sorg, 2012). Macrophages stimulate these cells via the production of cytokines and growth factors, such as EGF, PDGF, TGF-β, fibroblast growth factor (FGF) and insulin-like growth factor (IGF-1). In turn, these factors promote cell proliferation, ECM synthesis and granulation tissue formation. Therefore, macrophages promote transition into the proliferative phase of wound healing (Beanes *et al*. 2003; Martin and Leibovich, 2005; Reinke and Sorg, 2012; Pakyari *et al*. 2013).

1.3.2 The Proliferative Phase

As the inflammation resolves, the proliferative stage overlaps and it is characterised by angiogenesis, collagen synthesis/deposition, granulation tissue formation and re-epithelialisation (Figure 1.3). Commencing within a few days following injury, it lasts for approximately 2 weeks and during this phase, the focus is mainly reparative. The key aspects of the proliferative phase are restoration of the vasculature, creation of a more permanent barrier to cover the denuded site and synthesis of a new ECM. As such, it is necessary to produce large numbers of DFs and keratinocytes required for the formation of the ECM and epidermis, respectively. Similarly to the other phases of wound repair, several processes occur in parallel to one another. With regards to the proliferative stage, angiogenesis and fibroplasia occur simultaneously (Enoch and Leaper, 2005; Li *et al*. 2007; Guo and Dipietro, 2010; Reinke and Sorg, 2012; Pakyari *et al*. 2013).

During angiogenesis, capillaries adjacent to the wound site allow vascular endothelial

cells to migrate to the wound site. As the activities of DFs and keratinocytes require oxygen and nutrients, angiogenesis is imperative to the other stages of wound repair (Lamalice *et al*. 2007; Li *et al*. 2007). Subsequently, DF and keratinocyte proliferation and migration help maintain neovascularisation, as the newly-formed ECM acts as a scaffold through which endothelial cells can migrate. Endothelial cells are attracted to the area by FN and angiogenic factors released by other cells, such as angiogenin, VEGF, FGF and TGF-β (Broughton *et al*. 2006; Lamalice *et al*. 2007; Li *et al*. 2007). The clot formed in the haemostatic phase also plays a vital role in angiogenesis, acting as a reservoir of these aforementioned growth factors, that are released upon platelet degranulation. Plasminogen activators and secreted collagenases are also integral to this process as plasmin activation is required for clot degradation to take place. For capillary sprouting to occur, matrix metalloproteinases (MMPs) must proteolytically degrade the basement membrane of the parent vessel, which allows endothelial cell migration and proliferation (Sang, 1998; Pepper, 2001; Enoch and Leaper, 2005; Li *et al*. 2007; Newman *et al*. 2011; Reinke and Sorg, 2012). Once formed, the new vessels participate in granulation tissue formation and provide nutrients to growing tissues. Ultimately, once the wound bed achieves adequate perfusion, the proliferation and migration of endothelial cells gradually ceases (Broughton *et al*. 2006; Li *et al*. 2007).

Approximately 48 - 72 hours following wounding, DFs migrate to the wound site and proliferate. DF accumulation begins as the inflammatory phase ends and at 1 week post-injury, DFs are the most abundant cell type in the wound (Beanes *et al*. 2003). Chemotactically attracted to the wound by TGF-β_1 and PDGF, DFs initially utilise the established platelet-fibrin-FN clot to migrate over the wound area (Knox *et al*. 1986; Corbett *et al*. 1997; Beanes *et al*. 2003). Once in the wound, DFs begin to synthesise new ECM, the bulk of which consists of collagen, hyaluronan (HA), FN, elastin, GAGs and PGs (Chapter 1.5). As such, by 3 - 5 days following injury, initial fibrin/FN matrix is replaced by newly formed granulation tissue consisting of new blood vessels, DFs, myofibroblasts, inflammatory cells and endothelial cells; and newly synthesised ECM components (Clark *et al*. 1982; Badylak, 2002; Eckes *et al*. 2010; Reinke and Sorg, 2012). Once deposited, collagen synthesis can occur with greater vigour, as ground

substance is crucial to successful aggregation of collagen fibres. Collagen deposition increases the wound's tensile strength, providing further resistance to any potential future injury. DF synthesis and subsequent FN and type III collagen deposition allow replacement of the provisional clot and are the dominant tensile proteins present in the wound bed, until the maturation phase begins (Kurkinen *et al*. 1980; Mutsaers *et al.* 1997; Bainbridge, 2013). Once the ECM components and granulation tissue have been established, DFs begin to apoptose; converting the tissue composition from a largely cellular environment to collagen-rich tissue. This transition signifies the onset of the later maturation/remodelling phase (Madden and Peacock, 1971; Reinke and Sorg, 2012).

During the latter stages of granulation tissue formation, completion of epidermal re-epithelialisation occurs; during which keratinocytes proliferate and migrate over the wound bed, providing coverage and protection against the external environment for the new tissue (Woodley *et al*. 1985; Yamaguchi and Yoshikawa, 2001; Broughton *et al*. 2006). Stimulated by a lack of contact inhibition, wound-edge basal keratinocytes migrate across the upper layers of the granulation tissue-filled wound. Like the DFs, migrating keratinocytes use the fibrin-FN clot created during the inflammatory stage as an attachment site. In order to progress, the keratinocytes must dissolve the clot, debris and certain ECM components (Enoch and Leaper, 2005; Li *et al*. 2007; Reinke and Sorg, 2012). This digestion is mediated by MMPs, of which MMP-1 and MMP-9 are synthesised by the keratinocytes. These are responsible for collagen degradation and liberation of keratinocytes from their anchorage to the basal lamina, respectively (Saarialho-Kere *et al*. 1992; Parks, 1999; Pepper, 2001; Li *et al*. 2007). Keratinocytes also secrete plasminogen activators, which convert plasminogen into plasmin, thus allowing fibrin degradation (Morioka *et al*. 1987; Yamaguchi and Yoshikawa, 2001). Keratinocytes continue migrating across from either side of the wound site, until the advancing epithelial cells meet. At this stage, further movement is halted by contact inhibition and keratinocytes secrete proteins to form the new basement membrane. Subsequently, cells revert to their static form via reversal of morphological changes they underwent to migrate; and further keratinocyte growth and differentiation re-

establishes the stratified epithelium of the epidermis. Such events signal progression into the maturation/remodelling phase of wound healing (Enoch and Leaper, 2005; Broughton *et al*. 2006; Li *et al*. 2007; Eckes *et al*. 2010).

1.3.3 The Maturation/Remodelling Phase

Following the proliferative phase (Section 1.3.2), the wound repair process enters its concluding maturation/remodelling phase (Figure 1.3). Enduring for approximately 6 - 24 months post-wounding, the tissue maturation stage is characterised by vascular regression, wound contraction, granulation tissue remodelling and the conclusion of re-epithelialisation (Pakyari *et al*. 2013; Guo and Dipietro, 2010). Remodelling assists in the development of wounded tissue, to approach that of normal tissue. However, a period of contraction preludes this and reaches its peak at approximately 2 weeks post-injury (Li *et al*. 2007). During wound contraction, the surface area of the injury site is reduced, promoting eventual closure of the wound. Contraction begins during granulation tissue formation with DF activity, but is more effectively carried out after DFs have differentiated into myofibroblasts (Chapter 1.4). After exposure to TGF-β_1, a proportion of the wound DFs undergo differentiation and express α-smooth muscle actin (αSMA). Undifferentiated DFs express β-actin and γ-actin isoforms alone; thus, the myofibroblasts represent a specialised contractile cell type (Gabbiani *et al*. 1971; Darby *et al*. 1990; Stadelmann *et al*. 1998; Gabbiani, 2003; Li *et al*. 2007; Pakyari *et al*. 2013). Myofibroblasts predominately modulate wound contraction and contain the same actin type also found in smooth muscle cells. Attracted by FN and growth factors, the cells migrate across the provisional clot and ECM, in order to reach the wound edges. Via the extension of pseudopodia, connections are formed between the myofibroblasts and other myofibroblasts, the ECM and desmosomes along the wound edges (Darby *et al*. 1990; Stadelmann *et al*. 1998; Yamaguchi and Yoshikawa, 2001; Gabbiani, 2003; Li *et al*. 2007). Additonally, at the fibronexus, myofibroblastic actin is linked across the cell membrane to ECM proteins, including collagen, FN and HA (Eyden, 1993). Due to the formation of these extensive adhesions, contraction of the entire granulating bed is possible; decreasing the wound size effectively. As the myofibroblasts contract and close the wound, DFs reinforce the wound bed through

collagen deposition (Rudolph, 1979; Stadelmann *et al*. 1998; Broughton *et al*. 2006). Once closure is complete, the cells stop contracting and begin to undergo apoptosis. Simultaneous breakdown of the provisional matrix leads to a decrease in HA and an increase in GAGs, which gradually trigger DFs and myofibroblasts to cease migrating and proliferating. Consequently, this signifies progression into the tissue maturation /remodelling phase (Desmoulière *et al*. 1995; Stadelmann *et al*. 1998; Hinz, 2006).

Remodelling is the last stage of wound repair, in which numerous structural changes take place that allow the area to regain functionality over time. As the wound bed's vascular density normalises, the type III collagen found within the granulation tissue is replaced by newly synthesised type I collagen. Type I collagen fibres have a higher tensile strength than type III and thus, confer greater resistance to future injuries (Li *et al*. 2007; Guo and Dipietro, 2010; Reinke and Sorg, 2012; Pakyari *et al*. 2013). Any disorganised fibres are rearranged, cross-linked and aligned along tension lines. This gradual collagen synthesis and turnover is modulated by MMPs and tissue inhibitors of MMPs (TIMPs; Chapter 1.5.6). Around 3 weeks post-injury, collagen synthesis and breakdown reach a state of equilibrium (Beanes *et al.* 2003; Visse and Nagase, 2003; Li *et al*. 2007; Reinke and Sorg, 2012). As the stage progresses, the tensile strength of the wound increases and the architecture approaches that of uninjured tissue. Upon wound resolution, an organised, avascular, collagenous scar remains; lacking dermal appendages and a tensile strength of up to 70 % of that demonstrated by uninjured tissue (Enoch and Leaper, 2005; Li *et al*. 2007; Reinke and Sorg, 2012).

1.4 Cellular Components of Wound Healing

As highlighted previously (Chapter 1.3), wound repair is a finely balanced process and the wide range of cell types involved reflects its complexity. However, in the settings of excessive tissue fibrosis, DFs and the differentiated counterparts, myofibroblasts, play vital roles in pathological outcome. Largely contributing to the efficiency of the normal wound healing process, the cells have fundamental roles in determining the extent of wound contraction, closure, resolution and scar tissue formation.

1.4.1 Dermal Fibroblasts

DFs are connective tissue cells possessing elongated, spindle-shaped morphologies; with multiple processes originating from the cell body. DFs are of mesodermal origin and therefore, express vimentin. However, to date, no exclusively expressed markers to identify DFs have been identified and thus, their characterisation relies primarily on morphological, proliferative and phenotypical features (Chang *et al*. 2002; Schultz and Wysocki, 2009; Bainbridge, 2013; Sudo *et al*. 2013). Generally, fibroblasts are a heterogeneous cell population, demonstrating plasticity with regards to phenotype and exhibiting differences based upon anatomical location; as well as across sites of the same organ. This has been evidenced in fibroblasts from different skin sites that have displayed positional memory, as well as distinct gene expression profiles (Fries *et al*. 1994; Chang *et al*. 2002; Kendall and Feghali-Bostwick, 2014). DFs have various functions within the dermis, such as the synthesis of ECM proteins (Chapter 1.5) and biochemical mediators (e.g. proteases and growth factors); and wound contraction through differentiation into myofibroblasts (Chapter 1.4.2). DFs also support wound re-epithelialisation through autocrine and paracrine interaction with keratinocytes. Thus, DFs are essential to acute wound repair and tissue restoration; playing critical roles in synthesis, degradation and ECM remodelling (Chapter 1.3; Maas-Szabowski *et al*. 1999; Gabbiani, 2003; Desmoulière *et al*. 2005; Sarrazy *et al*. 2011; Bainbridge, 2013; Darby *et al*. 2014).

Due to their essential roles in ECM synthesis and remodelling, dysfunction in DFs or conversion to a senescent phenotype impacts on ECM architecture; which can lead to impaired healing. DFs regulate ECM turnover by controlling the expression of the MMPs and TIMPs (Chapter 1.5.6; Wall *et al*. 2008; Schultz and Wysocki, 2009; Eckes *et al*. 2010; Wells *et al*. 2016). The presence of TGF-β_1 reduces ECM degradation via decreasing MMP expression and increasing TIMP expression. However, if synthesis of ECM components is higher than their degradation, this can lead to excessive scar formation, due to continuous ECM deposition. Therefore, if DFs and myofibroblasts persist at the wound site for longer than is necessary, pathological fibrosis can occur (Chapter 1.7; Overall *et al*. 1989; Li *et al*. 2007; Eckes *et al*. 2010; Jumper *et al*. 2015).

Therefore, it is clear that the timely production and breakdown of ECM components, orchestrated by DFs, is pivotal to successful wound resolution. In normal conditions, production of ECM proteins is rapid as DFs proliferate to fill the wound space (Eckes *et al*. 2010; Reinke and Sorg, 2012). Specific ECM components, such as collagen, HA and FN, are responsible for facilitating the adhesion and migration of a variety of cell types and help support tissue integrity (Sottile and Hocking, 2002). Also, secretion of growth factors (e.g. FGF, VEGF, TGF-β), self-stimulate DFs and activate nearby cells; signalling gene expression alterations and maintaining cell viability, whilst attracting new cells to the wound space (Bennett and Schultz, 1993; Broughton *et al*. 2006).

To migrate to the wound site, DFs employ cytoskeletal remodelling and actomyosin interactions to re-organise and contract parts of their cytoplasm. The locomotion of DFs involves structural membrane extensions called filopodia and lamellipodia. The areas where these extensions meet the surface for adherence, focal adhesions (FAs) assemble. The integrin-mediated cell-ECM adhesions, or focal complexes, assemble to form a 'bridge' between the cell's actin cytoskeleton and exterior components of the ECM (Badley *et al*. 1980; Schwartz and Horwitz, 2006; Kopecki and Cowin, 2016). The extensive structure of actin found in the DF cytoskeleton provides a framework that both supports the plasma membrane and controls cell morphology through the assembly or disassembly of actin filaments. Radially oriented actin filament bundles are present at the migrating cell's leading edge; while axial bundles, known as stress fibres, underlie the cell body (Pellegrin and Mellor, 2007; Sandbo and Dulin, 2011; Carlier *et al*. 2015; Kopecki and Cowin, 2016). In addition, FAs also contain signalling proteins that aid in regulating cytoskeletal dynamics, conveying a responsive sensory aspect to the cells (Bershadsky *et al*. 2006). Therefore, DFs are anchored to the ECM via their cortical cytoskeleton of actin filaments, through which sensory information, such as mechanical stress or tension, can be mechanotransduced from the adhesive surface into the cytoplasm through FA anchor points (Wang *et al*. 2001; Langevin *et al*. 2011). Mechanical stress or force-induced deformations in the surrounding ECM can lead to a cellular response, causing the synthesis and release of excess cytokines, resulting in the DFs altering their morphology to adapt to their surroundings. When

mechanical stress is encountered, it is common for DFs to upregulate pro-fibrogenic genes involved in DF-myofibroblast differentiation and ECM component production (Grinnell, 2000; Tomasek *et al*. 2002; Sandbo and Dulin, 2011). These mechanically-stimulated DFs are referred to as 'proto-myofibroblasts', classed as an intermediate between DFs and their fully differentiated form, the myofibroblast (Figure 1.4). They contain bundles of actin fibres, but lack αSMA, and produce weak contractile forces. Additionally, maintenance of the proto-myofibroblast phenotype is dependent upon tension applied to a non-compliant sub-stratum. Nevertheless, the main contractile force is generated once differentiated myofibroblasts are induced, by a combination of mechanical tension, extra domain-A-fibronectin (EDA-FN) and TGF-β_1 (Desmoulière *et al*. 1993, 2005; Hinz *et al*. 2001; Tomasek *et al*. 2002; Hinz, 2006).

1.4.2 Myofibroblasts

Upon tissue injury, a population of DFs present at the wound site are stimulated to differentiate into myofibroblasts. As aforementioned (Chapter 1.4.1), this is induced via a combination of occurrences: mechanical stress imposed upon the tissue, TGF-β_1 stimulation and the presence of the FN splice variant, EDA-FN (Serini *et al*. 1998; Tomasek *et al*. 2002; Gabbiani, 2003; Desmoulière *et al*. 2005). As demonstrated in Figure 1.4, DF-myofibroblast differentiation occurs over a two-step process; with the formation of proto-myofibroblasts as an intermediate stage (Chapter 1.4.1). Though non-differentiated DFs have vital roles in wound healing, myofibroblast formation is essential for wound contraction and closure (Tomasek *et al*. 2002; Gabbiani, 2003; Sarrazy *et al*. 2011). Rarely found in healthy human physiology, myofibroblasts apply large contractile forces to the microenvironment, pulling the wound edges together (Kendall and Feghali-Bostwick, 2014).

The differences between stages of the differentiation process are discerned by the presence of differing forms of smooth muscle actin (Figure 1.5). At the intermediate step, proto-myofibroblasts express β- and γ-actin isoforms; whereas myofibroblasts express the α-form (Tomasek *et al*. 2002; Gabbiani, 2003; Desmoulière *et al*. 2005). Vital to the myofibroblast's contractile apparatus, αSMA is the characteristic marker

of these cells and its expression is required for their contractile activities (Serini and Gabbiani, 1999; Darby *et al*. 2014). Additionally, myofibroblasts are morphologically different to their undifferentiated counterparts; possessing larger, wider, polygonal shapes (Figure 1.4; Gabbiani, 2003). Upon stimulation by the aforementioned factors (Figure 1.4), morphological changes and phenotypic transitions occur in DFs, leading to actin cytoskeleton reorganisation. This characterised by an increase in the number and thickness of αSMA stress fibres, which are incorporated into large microfilament bundles; running parallel with the long axis of the cell and terminating at the cellular periphery (Figure 1.4).

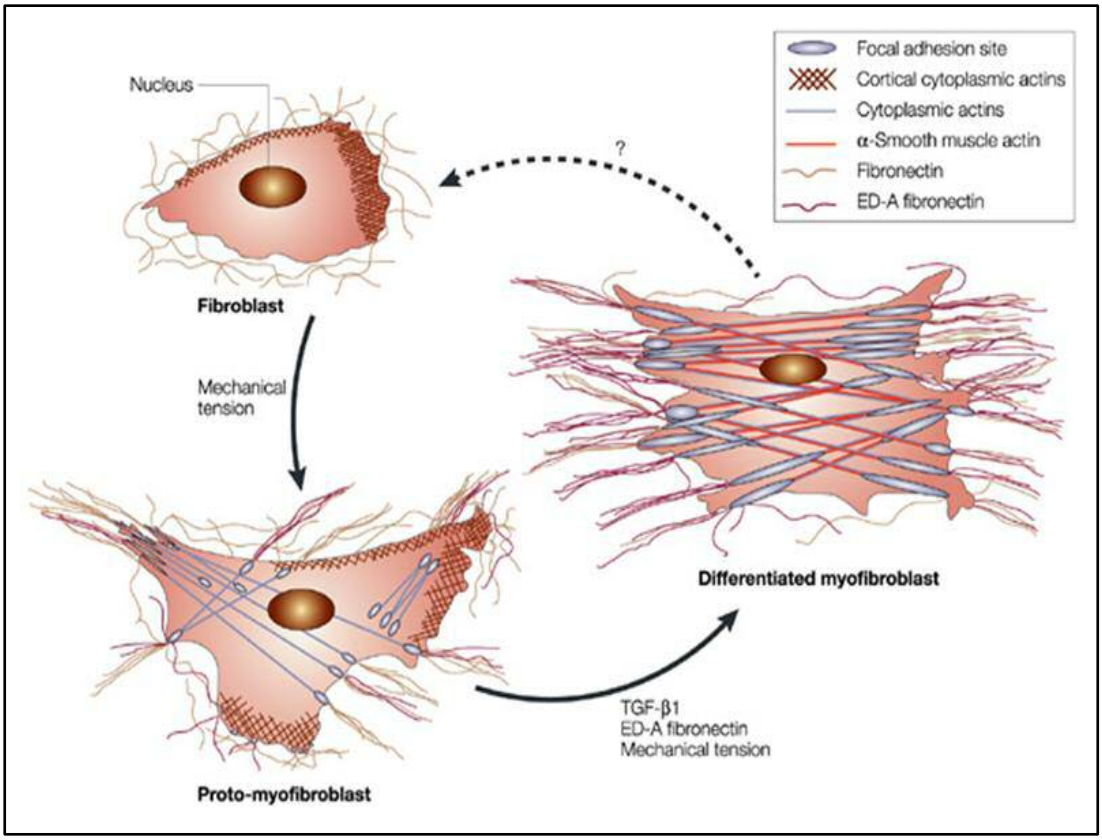

Figure 1.4. Diagram detailing the transition from fibroblast to an intermediate proto-myofibroblast, prior to terminal differentiation into its final form, the myofibroblast. Pro-fibrotic factors involved in promoting differentiation are also shown: mechanical tension, EDA-FN and TGF-β_1 (Gabbiani, 2003).

Moreover, immature FA complexes and mature FAs of DFs and proto-myofibroblasts, respectively; switch to super-mature FAs (Figure 1.5). These larger structures convey significantly higher resistance to extracellular strain and the transmission of greater intracellular contractile forces to the ECM (Dugina *et al*. 2001; Hinz *et al*. 2003; Goffin *et al*. 2006; Hinz, 2006; Sandbo and Dulin, 2011; Darby *et al*. 2014; Bochaton-Piallat *et al*. 2016). Via TGF-β_1-stimulated increases in pro-fibrogenic genes, myofibroblasts synthesise excessive amounts of ECM proteins to increase stability of the granulation tissue. Additionally, the gain of contractility and super-mature FA formation provide cells with the ability to anchor to the wound edges and pull the wound closed.

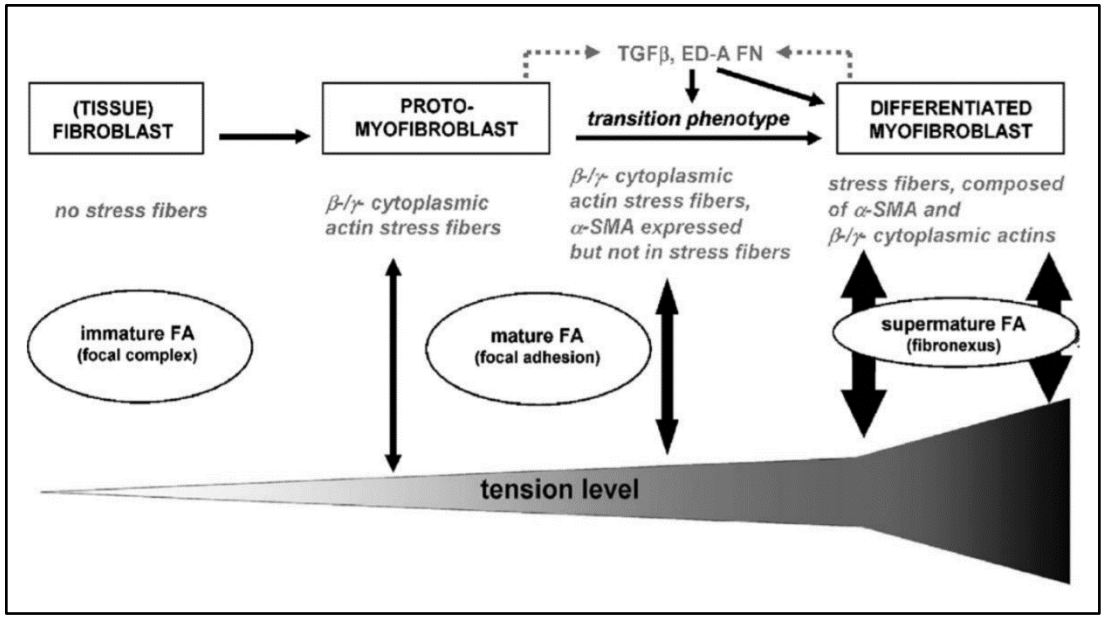

Figure 1.5. Diagram demonstrating the feedback relations between matrix stiffness, FA maturation and DF-myofibroblast differentiation. Factors contributing to the DF-myofibroblast differentiation mechanism are shown, in addition to the actin isoform expression profiles of each cell type (Hinz, 2006).

In normal conditions, upon completion of wound contraction/closure, myofibroblast apoptosis is promoted. However, it is possible that aberrations in wound contraction can prevent efficient wound closure or cause excessive scar formation (Chapter 1.7). In conclusion, the mechanisms underlying wound closure must be tightly regulated, as too little or too much can have severe implications on healing outcome (Tomasek *et al*. 2002; Gabbiani, 2003; Eckes *et al*. 2010; Darby *et al*. 2014; Eming *et al*. 2014).

With regards to the mechanisms underlying DF-myofibroblast differentiation, TGF-β_1 is considered the most potent stimulator of DF-myofibroblast differentiation. TGF-β_1 induces its response on DFs through signal transduction, from the cell membrane to nucleus, via binding to serine/threonine TGF-β receptors (TGF-βRs) and activating downstream intracellular signalling molecules (Leask and Abraham, 2004; Schiller *et al*. 2004; Feng and Derynck, 2005; Sandbo and Dulin, 2011). Such regulators are part of the SMAD protein family (Figure 1.6). The signalling cascade initiates upon TGF-β_1 binding to TGF-βRII, which subsequently recruits TGF-βRI to a complex. This complex phosphorylates and activates the intracellular, receptor-associated SMAD (R-SMAD) proteins (Wrana *et al*. 1992; Piek *et al*. 1999; Schiller *et al*. 2004; Massagué *et al*. 2005). R-SMADs, SMAD2 and SMAD3, are phosphorylated by the TGF-βRs; the SMAD anchor for receptor activation (SARA) interacts directly with SMAD2 and SMAD3; and this facilitates their recruitment to the activated TGF-βR complex (Tsukazaki *et al*. 1998; Schiller *et al*. 2004). Once the R-SMADs are phosphorylated, co-SMAD4 forms a heterodimeric complex with phosphorylated R-SMADs (Figure 1.6). This complex is subsequently translocated to the nucleus, where it acts as a transcription regulator; binding target sites upon gene promoters and either enhancing or suppressing gene transcription (Heldin *et al*. 1997; Massagué and Wotton, 2000; Inman *et al*. 2002; Schiller *et al*. 2004).

In addition to the TGF-β_1/SMAD signalling pathway, HA, a GAG found in the ECM, has also been found to be involved in TGF-β_1-driven DF-myofibroblast differentiation. In a co-operating pathway (Figure 1.6), HA associates with cluster of differentiation 44 (CD44); inducing its co-localisation with epidermal growth factor receptor (EGFR). A

phosphorylation of EGFR then occurs, resulting in downstream activation of ERK1/2 (Webber *et al*. 2009b; Meran *et al*. 2007, 2011; Midgley *et al*. 2013). Calmodulin kinase II (CAMKII) is then phosphorylated in a similarly biphasic manner to upstream ERK1/2 (Midgley *et al*. 2013). Dysregulation of CD44, EGFR or hyaluronan synthase 2 (HAS2) expression leads to loss of downstream ERK1/2 and CAMKII phosphorylation; and subsequent loss of αSMA induction (Midgley *et al*. 2013). In addition, formation of a HA pericellular coat is involved in maintaining the myofibroblast phenotype; as pericellular coat formation was shown to be absent after inhibition of HA synthesis, which resulted in inhibition of DF-myofibroblast differentiation (Webber *et al*. 2009a, 2009b). The hyaladherin, TSG6, is also involved in TGF-β_1-induced DF-myofibroblast differentiation, by virtue of its association with HA (Figure 1.6).

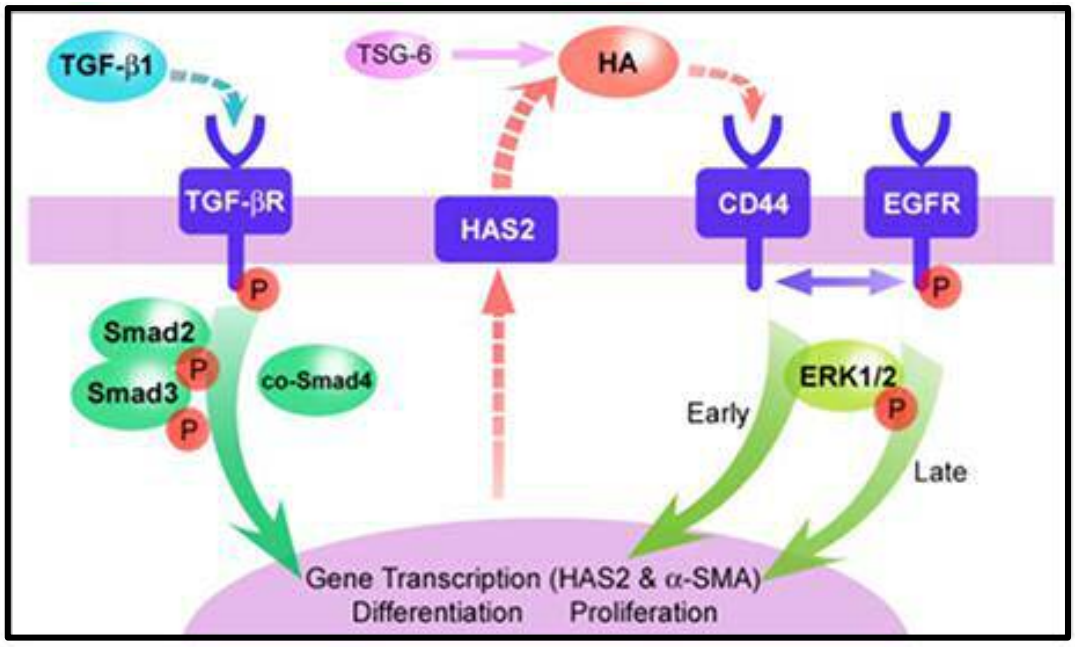

Figure 1.6. Diagram showing the TGF-β_1/SMAD and HA-mediated signalling pathways underpinning DF-myofibroblast differentiation. When DFs are stimulated by TGF-β_1, TGF-βR is phosphorylated (P); signalling through SMAD2/3 and co-SMAD4. The HA-mediated CD44 and EGFR signalling is through ERK1/2. When both pathways signal in parallel, the cell undergoes differentiation into a myofibroblast (image adapted from Simpson *et al*. 2010 and Meran *et al*. 2011).

TSG6 is involved in cross-linking of HA and post-TGF-β_1 stimulation, TSG6 expression increases. In contrast, loss of the myofibroblast phenotype is linked to the inhibition of TSG6 expression (Webber *et al*. 2009a, 2009b; Martin *et al.* 2016). As such, it has been demonstrated that pro-fibrotic cytokine, TGF-β_1, modulates DF-myofibroblast differentiation via continuous activation of the SMAD pathway, while simultaneously stimulating the HA-mediated CD44/EGFR pathway; both of which are needed for DFs to differentiate into myofibroblasts (Figure 1.6; Simpson *et al*. 2010; Meran *et al*. 2011).

1.5 The Extracellular Matrix

Present in all mammalian organs, the ECM is the non-cellular, structural component of the tissues; providing both the crucial physical scaffolding for cellular constituents and interacting with these to orchestrate an array of biochemical and biomechanical signals. Such interactions are required for tissue homeostasis and morphogenesis, as well as cell migration, proliferation, differentiation, adhesion and survival (Daley *et al*. 2008; Järveläinen *et al*. 2009; Frantz *et al*. 2010). The ECM was initially thought to be an inert, space-filling material that imparted only mechanical strength. However, it is now known that the ECM forms a complex, highly dynamic 3D network which is constantly undergoing remodelling, either enzymatically or non-enzymatically (Daley *et al*. 2008; Järveläinen *et al*. 2009; Frantz *et al*. 2010). Often referred to as 'gel-like', the ECM is fundamentally composed of water, proteins and polysaccharides, as well as collagens, elastin, structural glycoproteins, PGs (including HA) and GAGs. Specific tissues have ECMs with unique compositions, however, which are generated through tissue development and altered to suit their organ's functionality (Daley *et al*. 2008; Järveläinen *et al*. 2009; Frantz *et al*. 2010). With regards to the skin, synthesis of the ECM and its turnover/remodelling are essential to both cutaneous homeostasis and wound repair post-injury or trauma; with ECM composition contributing significantly to healing outcome. An understanding of how the various constituents contribute to the repair process may provide valuable insights into the pathological or preferential mechanisms underlying fibrosis or scarless healing/regeneration, respectively (Daley *et al*. 2008; Järveläinen *et al*. 2009).

1.5.1 Collagens

Collagens are the most abundant protein family in the human body, comprising 30 % of the total protein content. They are the primary structural components of the ECM, providing strength and integrity; and have crucial roles in a broad range of functions, including tissue scaffolding/morphogenesis, angiogenesis, wound repair and cellular adhesion and migration. Tissues vary in the type, size, distribution and alignment of their constituent collagens, depending upon the functional properties of said tissue (van der Rest and Garrone, 1991; Gelse *et al*. 2003; Ricard-Blum *et al*. 2018). Despite these variances, the molecular structure of the collagen molecules are always either homo or hetero-trimers made up of one, two or three different α-chains, containing at least one triple-helical domain. These structural units are known as tropocollagen (Brodsky and Persikov, 2005; Gordon and Hahn, 2010; Ricard-Blum *et al*. 2018). To date, 28 types of collagen have been identified and these have been broadly divided into two groups: fibrillar and non-fibrillar. The fibrillar collagens (e.g. I, III and V) are characterised by their ability to assemble into their highly orientated supramolecular aggregates (fibres); whereas the non-fibrillar collagens (e.g. IV) can be found within the body's basement membranes (van der Rest *et al*. 1991; Bella and Hulmes, 2017; Nyström and Bruckner-Tuderman, 2018). Throughout the skin in particular, 20 types of collagen have been reported to be present during development and/or adulthood. Type I and III fibrillar collagens are the most abundant in the dermis. Type I collagen is the most common type, while type III collagen comprises approximately one third of the dermal fibril content (Gelse *et al*. 2003; Bella and Hulmes, 2017; Nyström and Bruckner-Tuderman, 2018). Depending on their location, dermal collagen fibrils vary greatly in their diameters; the papillary dermis containing mostly thinner fibrils and the reticular layer robust, thicker fibrils (Nyström and Bruckner-Tuderman, 2018).

Types I and III are also the major collagens involved in wound repair, synthesised by both DFs and keratinocytes. Post-injury, type III collagen is most rapidly synthesised by DFs, providing a temporary structure for other ECM molecules to develop around (Mutsaers *et al.* 1997; Bainbridge, 2013). Approximately 40 % of collagen present in granulation tissue is type III, compared to only 25 % found in unwounded tissue. As

the wound heals, gradual turnover of collagen occurs as type III collagen undergoes degradation (Chapter 1.5.6); and the ECM matures from being rich in type III to rich in type I collagen (Mutsaers *et al.* 1997; Li *et al*. 2007; Bainbridge, 2013). Ultimately, this culminates in avascular scar tissue formation with an increased tensile strength. This strength originates from the organised fibre formation and cross-links between collagen fibres. Although type I collagen is associated with greater tensile strength, it also has a degree of stiffness; whereas the presence of type III collagen is linked with more elastic tissues (Birk and Trelstad, 1986; Beanes *et al.* 2003; Moseley *et al.* 2004; Li *et al*. 2007; Bainbridge, 2013). Thus, the higher amounts of type III collagen found in early-gestational wound healing may result in a less rigid wound site, contributing to the scarless healing response found in foetal repair (Chapter 1.6.1). In contrast, if type I and/or type III collagen production by DFs and myofibroblasts is dysregulated, excessive fibrosis can occur (Chapter 1.7). Therefore, the balance between collagen production, degradation and turnover is imperative to normal wound healing; while collagen expression levels, distribution and alignment can impact healing outcomes (Gelse *et al*. 2003; Slemp and Kirschner, 2006; Li *et al*. 2007; Gauglitz *et al.* 2011).

1.5.2 Elastin

Elastin is a fibre-forming connective tissue protein that confers elasticity to the skin. In association with collagen, elastin fibres are responsible for both the resilience and elastic recoil of the dermal matrix; permitting resumption of the skin's original form following stretching or contraction (Rosenbloom *et al*. 1993; Debelle and Tamburro, 1999; Midwood and Schwarzbauer, 2002; Frantz *et al*. 2010). The relaxed network of elastin and collagen fibres allow the tissue to resist tensile stresses, whilst providing structural support and flexibility. Also, elastin stretch is crucially limited by the tight association with collagen fibres, which reduce the degree that the elastin fibres can extend (Frantz *et al*. 2010; Muiznieks and Keeley, 2013). Elastogenesis initiates upon tropoelastin molecule secretion from fibroblasts and smooth muscle cells. Tethered to the cell surface, these soluble precursors assemble into fibres and become highly cross-linked to each other through adjacent lysine residues (Rosenbloom *et al*. 1993; Debelle and Tamburro, 1999; Wise and Weiss, 2009; Frantz *et al*. 2010). Members of

the lysyl oxidase (LOX) family modulate this process, allowing the development of an insoluble elastic meshwork (Lucero and Kagan, 2006; Frantz *et al*. 2010). In addition, elastic fibres also contain glycoprotein microfibrils, primarily fibrillins, which are vital to the fibre's integrity (Midwood and Schwarzbauer, 2002; Wagenseil and Mecham, 2007). Following deposition, tropoelastin synthesis is markedly reduced and there is little turnover of mature elastin, which is an extremely stable, insoluble polymer. In the majority of mammalian tissues, the bulk of elastogenesis takes place during late-foetal and in early-neonatal periods (Swee *et al*. 1995; Debelle and Tamburro, 1999; Wise and Weiss, 2009). After wounding, elastic fibres are not detected in the newly-deposited granulation tissue; contributing to the rigidity and inelasticity of the ECM found in scar tissue (Zheng *et al*. 2006; Eckes *et al*. 2010).

1.5.3 Glycoproteins

Non-collagenous glycoproteins are structural, high molecular weight proteins which function as ECM adhesion molecules. Secreted by many cell types, including DFs and keratinocytes, the most prominent glycoproteins within the skin include FN, laminin, tenascin, vitronectin and thrombospondin. Such glycoproteins mediate cell-cell and cell-ECM interactions, which dictate cell functions including adhesion and migration (Kwiatkowska and Kwiatkowska-Korczak, 1999; Halper and Kjaer, 2014). Particularly, the most abundant and well-characterised is FN, which influences diverse processes including inflammation and wound repair. FN has a broad distribution in the dermis, particularly in the basement membrane region; and exists in both tissue and plasma forms (Romberger, 1997; Eckes *et al*. 2010). Regarding wound repair, only tissue FN is vital to the healing process, whereas plasma FN is dispensable (Sakai *et al*. 2001). Together with fibrin, FN forms the provisional matrix in dermal wounds, permitting inflammatory cells and DFs to infiltrate the wound site; and providing a network for keratinocytes to migrate across during re-epithelialisation (Clark *et al*. 1982; Schultz and Wysocki, 2009; Eckes *et al*. 2010). Furthermore, FN is also able to act as a link or 'bridge' between cells and the ECM, co-ordinating their interactions. Consequently, FN is able to regulate cellular activities, including migration, adhesion, proliferation, ECM synthesis and differentiation (Romberger, 1997; Schultz and Wysocki, 2009). FN

modulates these processes through its binding domains and ability to attach to cell-surface integrins; which act as receptors, allowing the cells to adhere to various ECM constituents. During wound repair, the association between integrin α4β7 and EDA-FN mediates DF-myofibroblast differentiation. As previously described (Chapter 1.4), EDA-FN expression is up-regulated in DFs exposed to the pro-fibrotic cytokine, TGF-β_1, and is necessary for αSMA up-regulation; therefore, rendering it a marker for DF-myofibroblast differentiation (Clark, 1990; Muro *et al*. 2003; Kohan *et al*. 2010; Sandbo and Dulin, 2011).

1.5.4 Proteoglycans and Glycosaminoglycans

As well as the structural proteins and adhesive glycoproteins, the ECM also contains various PGs and GAGs. These surround, or are deposited or co-polymerised around other ECM proteins; such as collagen and elastin (Schultz and Wysocki, 2009; Eckes *et al*. 2010). The PGs are negatively charged proteins, which are comprised of a core protein backbone, with polysaccharide (GAG) chains covalently attached. The poly-diverse PG superfamily contains over 30 different glycoproteins that are both heavily glycosylated and hydrophilic; endowing them with high water-binding capacities and the capability to absorb up to 1000 times their volume (Ruoslahti, 1988; Järveläinen *et al*. 2009; Eckes *et al*. 2010; Schaefer and Schaefer, 2010). This provides hydration for the dermis and contributes to the ECM's 'gel-like' ground substance. PGs can be found in the skin's basement membrane, upon cells and in the matrices surrounding mesenchymal cells; performing a wide range of functions, such as ECM organisation, modulation of growth factor activity and regulation of collagen fibrillogenesis (Iozzo, 1998; Schultz and Wysocki, 2009; Eckes *et al*. 2010).

With regards to composition, protein core variation is responsible for the synthesis of PGs with differing molecular constructions and thus, functions. Furthermore, the attached GAGs also offer unique roles to each PG. As such, there is a vast structural diversity existing in the PG family, arising from differences in the size and amino acid sequence of the protein core, as well as the size, number and sulphation patterns of attached GAGs (Iozzo, 1998; Frantz *et al*. 2010; Schaefer and Schaefer, 2010). Due to

this heterogeneity, PGs have been classified into three sub-families: cell-surface PGs, modular PGs and small leucine-rich PGs (SLRPs). Based on their GAG chains, PGs can be further divided into two main categories: chondroitin sulphate PGs and heparan sulphate PGs (Frantz *et al*. 2010; Schaefer and Schaefer, 2010). Chondroitin sulphate PGs include versican and the SLRPs, decorin and biglycan; whereas heparan sulphate PGs include perlecan and syndecan (Ruoslahti, 1988; Schaefer and Iozzo, 2008). The predominant PG species within the dermis is decorin, which comprises over 95% of the total PG content, with biglycan mostly expressed by keratinocytes and found in the dermis in smaller quantities (Moseley *et al*. 2004). Within the skin, decorin plays a key role in collagen fibrillogenesis regulation and the binding and sequestration of growth factors, particularly TGF-β_1 (Neame *et al*. 2000; Kresse and Schönherr, 2001; Moseley *et al*. 2004). Also, post-dermal injury, both decorin and biglycan have been suggested to hold regulatory roles in the inflammatory response (Oksala *et al*. 1995; Moseley *et al*. 2004). Versican has also been demonstrated to be up-regulated post-wounding, participating in various processes including cell migration, adhesion and proliferation (Wang *et al*. 2000; Moseley *et al*. 2004). With regards to the heparan sulphate PGs, perlecan has roles in modulating FGF2, VEGF and PDGF and thus, their subsequent wound repair functions; including cell migration, adhesion, proliferation and angiogenesis. Its importance in growth factor regulation has been demonstrated using perlecan-deficient mice, which showed poor wound tissue vascularisation and delayed wound healing, as a result of decreased FGF2-mediated angiogenesis (Zhou *et al*. 2004; Knox and Whitelock, 2006; Eckes *et al*. 2010).

1.5.5 Hyaluronan

Established as the skin's most prevalent GAG, HA is a high molecular weight ($1x10^4$ - $1x10^7$ Da), non-sulphated, multi-functional polysaccharide distributed ubiquitously throughout connective and epithelial tissues (Laurent *et al*. 1996; Stern and Maibach, 2008; Albeiroti *et al*. 2015). A negatively-charged polymer, HA's molecular structure consists of alternating disaccharide units of N-acetylglucosamine and D-glucuronic acid, linked by β(1 - 4) and β(1 - 3) glycosidic bonds. Unlike other GAGs, HA does not exist as a structural constituent of PGs and therefore, is the only GAG not covalently

linked to a core protein or synthesised by the Golgi (Laurent *et al*. 1996; Fraser *et al*. 1997; Stern and Maibach, 2008; Albeiroti *et al*. 2015). HA synthesis occurs within the plasma membrane and is catalysed by the membrane-bound, hyaluronan synthases (HASs), which polymerise HA chains before they translocate through the membrane into the ECM (Prehm, 1984; Weigel and DeAngelis, 2007; Stern and Maibach, 2008). Three mammalian HAS genes have been isolated and characterised: HAS1, HAS2 and HAS3 (Spicer and McDonald, 1998). These synthesise HA of differing molecular sizes, with HAS1 and HAS2-derived HA possessing molecular weights of 2×10^5 - 2×10^6 Da; and HAS3-derived HA possessing a molecular weight of 1×10^5 - 1×10^6 Da. It has also been shown that HAS1 and HAS3 produce HA with broad molecular size distribution (2×10^5 - 2×10^6 Da), whereas HAS2 synthesises HA with a broad, but extremely large molecular size (>2×10^6 Da; Itano *et al*. 1999).

Despite the simplicity of its structure, HA exhibits substantial functional diversity. As well having roles in ECM stability and tissue hydration, HA influences many biological processes, including embryogenesis, malignant transformation, wound healing and fibrosis (Fraser *et al*. 1997; Toole, 2002; Stern and Maibach, 2008). After its synthesis and release, HA undergoes re-organisation and assembly by hyaladherins and these alterations significantly contribute to HA's functional diversity. Hyaladherins interact with and bind HA in order to modulate its function and several types exist, either as cell receptors or extracellular hyaladherins (Toole, 1990; Day and Prestwich, 2002). These include CD44, TSG6 and versican; all of which are members of the link domain family and bind HA via this link region (Kohda *et al*. 1996; Milner and Day, 2003). As aforementioned, CD44 and TSG6 play vital roles in TGF-β_1-driven DF-myofibroblast differentiation via their association with HA (Chapter 1.4.2). They are also involved in modulating cellular migration, ECM stability and inflammation (Meran *et al*. 2007; Webber *et al*. 2009a, 2009b; Martin *et al*. 2016).

In addition to its crucial roles in TGF-β_1-driven DF-myofibroblast differentiation and maintenance of the myofibroblastic phenotype (Chapter 1.4.2), HA performs various additional roles in wound repair. During the inflammatory phase, HA accumulates at

the wound site, either by DF secretion or via the vasculature. Its primary function is the modulation of DF and inflammatory cell activities, including cellular proliferation, adhesion and migration; and pro-inflammatory cytokine synthesis and phagocytosis of invading microbes, respectively (Weigel *et al*. 1986; Chen and Abatangelo, 1999; Stern and Maibach, 2008). Levels of HA synthesised are elevated during granulation tissue maturation and re-epithelialisation. However, eventually, HA synthesis ceases and the existing HA is de-polymerised by hyaluronidases (HYALs). CD44 also plays a key role in HA catabolism by assisting HYAL1 and HYAL2, the only somatically active HA-degrading enzymes in humans (Csoka *et al*. 2001; Harada and Takahashi, 2007). Furthermore, HA polymers can be degraded by reactive oxygen species (ROS). In the skin, HA catabolism results in formation of lower molecular weight fragments, which have been found to stimulate inflammatory gene expression in macrophages; as well as promoting wound site neovascularisation (Deed *et al*. 1997; Jiang *et al*. 2006; Gao *et al*. 2010; Monzon *et al*. 2010). However, an increased presence of lower molecular weight HA fragments can also lead to fibrosis, as they promote cellular proliferation, synthesis of type I collagen and TGF-β_1 expression, as well as being pro-inflammatory and pro-migratory (David-Raoudi *et al*. 2008; Tolg *et al*. 2014a, 2014b). As such, the efficient clearance of HA degradation products from the wound site is important to minimise the potential for excessive fibrosis.

1.5.6 Extracellular Matrix Turnover and Remodelling

As new ECM is continually being synthesised, homeostasis is maintained by a tightly-regulated production of proteinases and their inhibitors. These modulate synthesis/ turnover of all ECM constituents and are secreted by DFs, keratinocytes, neutrophils and macrophages. Such ECM regulation and controlled degradation is key to normal tissue remodelling and wound repair, during each stage of the healing process. ECM remodelling occurs via the actions of four different families of proteinases: cysteine proteinases, aspartic proteinases, serine proteinases and matrix metalloproteinases (MMPs). These are responsible for ECM protein catabolism and are classified based on the structures of their active sites and catalytic mechanisms. However, the latter

two families are believed to be of greater importance to dermal remodelling (Kähäri and Saarialho-Kere, 1997; Barrick *et al*. 1999; Parks, 1999; Caley *et al*. 2015).

The MMPs are a family of structurally-related, zinc and calcium-dependent enzymes, which can collectively degrade the majority of ECM components. Furthermore, they are also capable of cleaving other substrates, including other proteinases, cytokines and growth factors (Kähäri and Saarialho-Kere, 1997; Parks, 1999; Caley *et al*. 2015). Currently, 23 MMP genes have been identified in humans and the MMPs themselves can be divided into seven groups, based on their substrate specificity and structural organisation. These are the collagenases, gelatinases, stromelysins, membrane-type MMPs, metalloelastases, matrilysins and other MMPs (Visse and Nagase, 2003; Itoh, 2015; Caley *et al*. 2015). MMP production and activation is regulated by a number of factors, including the expression of pro-inflammatory cytokines and growth factors; and the ECM's mechanical properties, as well as the actin cytoskeleton of cells, such as DFs (Ries and Petrides, 1995; Tomasek *et al*. 1997; Dasu *et al*. 2003). Upon tissue injury and following their activation, MMPs function in regulating the inflammatory response, cell migration, re-epithelialisation and scar tissue remodelling. Thus, they represent key mediators of dermal wound resolution; particularly, because they are not constitutively expressed in the skin, but are temporarily induced in response to exogenous signals post-injury (Kähäri and Saarialho-Kere, 1997; Parks, 1999; Xue *et al*. 2006; Schultz and Wysocki, 2009).

Overall, MMPs allow new ECM constituents to be synthesised without any damaged components being incorporated into the new tissue. However, if their expression or activity is chronically elevated, pathological breakdown of the ECM can occur; which is associated with impaired wound repair (Wysocki *et al*. 1993; Schultz and Wysocki, 2009; Caley *et al*. 2015). During normal wound healing, MMP activities are regulated by endogenous tissue inhibitors of MMPs (TIMPs); of which TIMP-1 and TIMP-2 can inhibit the vast majority of MMPs. The equilibrium between active MMPs and TIMPs controls the rate of ECM turnover. If this balance is disturbed, it can result in chronic wound development or excessive dermal fibrosis, depending upon whether there is

excess MMP or TIMP activity, respectively (Vaalamo *et al*. 1996; Muller *et al*. 2008; Caley *et al*. 2015).

1.6 Scarless Wound Repair

1.6.1 Foetal Wound Repair

Prior to the end of the second trimester of gestation, there is evidence that scarless healing occurs following foetal injury, producing normal skin architecture at the site of the wound. In contrast, foetal injuries that occur after this point heal in the same manner as adult wounds (Lorenz *et al*. 1992; Lorenz and Adzick, 1993; Larson *et al*. 2010). It was originally thought that the sterile intrauterine environment permitted scarless repair. However, early studies showed this environment is neither necessary nor sufficient for scar-free healing. It was subsequently shown that it may be due to intrinsic differences between foetal and adult tissue (Lorenz *et al*. 1992; Longaker *et al*. 1994; Larson *et al*. 2010). Early-gestational wounds undergo similar wound repair phases to adult wounds. However, repair occurs more rapidly in foetal wounds, with the wound healing stages progressing more rapidly compared to those in the adult. Furthermore, differences have been established between the respective cell types; in particular the fibroblasts (Lorenz and Adzick, 1993; Lee and Eun, 1999; Nauta *et al*. 2011; Yagi *et al.* 2016).

Foetal wounds have less inflammatory cell infiltrate and reduced cytokine expression than their adult counterparts, yet they heal more rapidly. This could be explained by the intrinsic variations between foetal and adult fibroblasts (Larson *et al*. 2010). The two demonstrate differences in collagen and HA synthesis, in addition to other ECM constituents. Whereas type I collagen is the predominant form in human skin, early-gestational wounds are characterised by an ECM rich in type III collagen (Lovvorn *et al*. 1999; Moore *et al*. 2018). *In vitro* studies have not only demonstrated that foetal fibroblasts synthesise more collagen altogether than adult DFs, but that they express greater levels of type III in particular (Merkel *et al*. 1988; Larson *et al*. 2010). Type III collagen accounts for 10 - 20 % total collagen in post-natal skin, in comparison to 30 - 60 % in foetal skin. This is rapidly deposited in foetal wounds, presenting as a finer

reticular network, indistinguishable from the surrounding uninjured skin (Smith *et al.* 1986; Beanes *et al*. 2002; Yagi *et al*. 2016). Increased prolyl hydroxylase activity also correlates with the greater collagen synthesis induced in foetal wounds, acting as an important rate-limiter in its production. Thus, as well as differing collagen synthesis, altered enzymatic regulation of collagen production is displayed by foetal fibroblasts (Lorenz and Adzick, 1993; Larson *et al*. 2010; Li *et al.* 2017). Cross-linking of collagen has also been found to increase with gestational age, concurrent with the transition to a fibrotic phenotype. While cross-links increase matrix rigidity and are associated with scar maturation, it is thought that an unlinked collagen environment coincides with a more flexible, elastic ECM; therefore contributing to scarless healing (Yagi *et al*. 2016; Moore *et al*. 2018). Additionally, lysyl oxidase has been found expressed at lower levels in early-gestational versus late-gestational murine wounds. As a catalyst of collagen cross-linking, this demonstrates the importance of collagen organisation on healing outcome (Smith-Mungo and Kagan, 1998; Colwell *et al*. 2006).

HA is also differentially expressed in scarless healing situations, versus normal acute wound environments. Elevated and more persistent HA synthesis has been shown in early-gestational foetal wounds; due to increased HAS expression and lesser activity of the HA-degrading enzyme, HYALs (Longaker *et al*. 1989; Mast *et al*. 1995; West *et al*. 1997). Moreover, foetal fibroblasts have been found to express increased surface receptors for HA, enhancing their migratory abilities (Chen *et al.* 1989; Alaish *et al*. 1994). Generally, the HA content of the ECM is increased more rapidly than in adult wounds. Such deposition is assisted by the lack of pro-inflammatory cytokines found in foetal wounds, which would usually down-regulate HA expression (Kennedy *et al*. 2000; Larson *et al*. 2010). HAS1 expression is not found in foetal fibroblasts, which is linked with scarless healing and resistance to TGF-β_1 differentiation. In contrast, DF differentiation is associated with HAS1/2 up-regulation (Yamada *et al*. 2004; Meran *et al.* 2007). HAS2 is also recognised as essential to embryonic and early-gestational development, albeit an environment in which fibroblasts are resistant to developing fibrotic phenotypes. In this setting, HAS2 stimulates cell migration and invasiveness in a complementary manner (Camenisch *et al*. 2000). Some studies have highlighted

that high HA concentration in the extracellular space, found during the first phases of wound repair or early-gestational development, would limit the ECM deposition; collagen in particular (Iocono *et al*. 1998; Croce *et al*. 2001). Higher molecular weight HA has been shown to induce type III collagen synthesis and TGF-β_3 expression; both of which are associated with scarless healing. Thus, increased presence of native HA may contribute to the scarless healing phenotype associated with early-gestational wound repair (David-Raoudi *et al.* 2008; Li *et al.* 2017).

With regards to ECM turnover, in scarless healing situations, there is a greater MMP activity than TIMP activity; favouring earlier remodelling and faster collagen turnover (Dang *et al*. 2003; Yagi *et al*. 2016; Moore *et al.* 2018). Inductions in MMP-1, -9 and -14 expression have been exhibited in foetal wounds, occurring more rapidly and at greater levels than in scarring wounds; whereas increased TIMP-1 and -3 expression has been found in scarring wounds alone (Dang *et al*. 2003). As such, these findings demonstrate that differential proteinase and inhibitor expression profiles contribute to preferential healing outcomes.

1.6.2 Oral Mucosal Wound Repair

Oral mucosal wound repair exhibits dramatically reduced scar formation. However, it is not believed to be completely scarless, as is observed with early-gestational foetal wound repair. Oral mucosal wounds undergo similar wound healing phases as adult dermal wounds; although, the time period that each phase lasts varies and there are intrinsic differences between DFs and oral mucosal fibroblasts (OMFs), in particular (Szpaderska *et al*. 2003; Mak *et al*. 2009; Nauta *et al*. 2011; Glim *et al*. 2013). Thus, OMFs represent a cell population that are genotypically and phenotypically distinct from DFs. Regarding their phenotypic differences, OMFs have been found to possess 'younger' phenotypes, in comparison to patient-matched DFs. Such phenotypes are similar to those of foetal fibroblasts and therefore, may be responsible for the rapid, minimal scar formation observed in oral mucosal wounds (Enoch *et al*. 2009, 2010). Furthermore, OMFs have been demonstrated to senesce much later than DFs, after undergoing a longer proliferative lifespan and more population doublings. Also, the

proliferation of OMFs has been reported to occur at a quicker rate, in comparison to DFs. It has been shown that the delayed senescence that takes place in OMFs is due to their ability to retain their telomere length for a prolonged period of time, versus population doubling-matched DFs (Enoch *et al*. 2009, 2010; Peake *et al*. 2014).

In terms of migration, OMFs are capable of migrating to the wound site more rapidly than their dermal counterparts; ultimately resulting in a quicker re-population of the denuded area and thus, faster ECM synthesis (al-Khateeb *et al*. 1997; Shannon *et al*. 2006; Enoch *et al*. 2009, 2010). In comparison to the ECM synthesised by DFs, there are also differences in the ECM constituents produced by OMFs. Within oral wounds, increased levels of chondroitin sulphate and FN have been reported. Another study showed that there is a less prolonged expression of EDA-FN found in oral, compared to dermal wounds. Furthermore, despite demonstrating a more elastic phenotype, elastin expression was found to be lower in oral wounds. However, this could be due to the increased presence of other elastic fibres, such as elaunin and oxytalan (Wong *et al*. 2009; Glim *et al*. 2013, 2014). OMFs also exhibit greater re-organisation of the ECM, compared to DFs. MMP-2 synthesis and expression has been demonstrated as increased by OMFs. This may be the result of a decreased expression of both TIMP-1 and TIMP-2, decreasing their inhibitory actions on the MMPs (Stephens *et al*. 2001; Shannon *et al*. 2006; Chen *et al*. 2010; Enoch *et al*. 2010; Glim *et al*. 2013, 2014). In contrast, various other MMPs were observed to have a reduced presence, compared to the levels found in dermal wounds; including MMP-1, -8, -9, -10 and -13 (Chen *et al*. 2010).

In contrast to DFs, OMFs have also been shown to be resistant to differentiation, in response to TGF-β_1 stimulation. This was shown through a lack of αSMA expression and stress fibre formation (Shannon *et al*. 2006; Meran *et al*. 2007; Dally *et al*. 2017). Such resistance has been shown to be associated with a failure to induce HAS1 and HAS2 transcription and thus, failure to assemble HA pericellular coats (Meran *et al*. 2007). Recently, hepatocyte growth factor (HGF) has been shown to be involved in OMF resistance to TGF-β_1-driven differentiation. HGF is a pleiotropic growth factor

which exhibits potent mitogenic, morphogenic, motogenic, angiogenic, anti-fibrotic and anti-inflammatory properties in a number of different cell types (Conway *et al*. 2006; Nakamura *et al*. 2011; Dally *et al*. 2017). Consequently, HGF possesses roles in normal tissue development during embryogenesis; and in promoting tissue repair in tissues, such as the skin and oral mucosa (Glim *et al*. 2013; Dally *et al*. 2017). OMFs have been shown to express significantly elevated HGF levels, in comparison to DFs (Stephens *et al*. 2001; Shannon *et al*. 2006). Knockdown of HGF expression has been demonstrated to inhibit OMF migratory and proliferative responses. In addition, HGF knockdown abrogated the resistance, demonstrated by OMFs, to TGF-β_1-driven DF-myofibroblast differentiation; as evidenced through increased αSMA expression and stress fibre formation. Such resistance to differentiation is likely to play a significant role in the minimal scarring outcomes observed in oral mucosal wounds (Dally *et al*. 2017).

1.7 Pathological Dermal Scarring

As previously mentioned (Chapter 1.3), the wound repair process is tightly regulated and this is required for efficacious wound resolution to occur. Scar development is a normal hallmark of acute dermal wound healing. Occasionally however, pathological fibrosis can occur (Eming *et al*. 2014; Do and Eming, 2016). Excessive scars form due to aberrations in the normal physiological wound repair processes and may develop following any insults to the dermis. These can include abrasions, lacerations, surgical incisions, burn injuries, vaccinations and piercings. In humans, two primary types of pathological fibrosis are recognised: hypertrophic scars and keloids (Bran *et al*. 2009; Gauglitz *et al*. 2011; Eming *et al*. 2014).

Overall, scarring significantly contributes to the global healthcare burden and in the developed world alone. Approximately 100 million people develop scars annually via 25 million operations post-trauma and 55 million after elective surgery (Sund, 2000; Gauglitz *et al*. 2011). Many of these scars are a consequence of dysregulated dermal repair, including an estimated 4 million burn scars and 11 million keloid scars (Sund, 2000; Bayat *et al*. 2003). People with dermal scarring may suffer physical, aesthetic,

psychological and social consequences, that are also linked with significant financial and emotional costs (Dorfmüller, 1995; Taal and Faber, 1998; Robert *et al*. 1999). In particular, patients suffering with hypertrophic/keloid scars may have a significantly impaired quality of life; as they may be subjected to pain, contractures and pruritus. For burn survivors, excessive scarring represents the first cause of morbidity and the prevalence of hypertrophic scarring post-burn is approximately 67 % (Bombaro *et al*. 2003; Gauglitz *et al*. 2011; Arno *et al*. 2014). Traditionally, the clinical discrimination between hypertrophic scars and keloids has been problematic, which has resulted in unsuitable decisions being made, with regards to management and treatment. First discerned over 50 years ago, both scar types were defined as rising above skin level (Mancini and Quaife, 1962; Peacock *et al*. 1970; Gauglitz *et al*. 2011). However, it is now known that various epidemiological and histological differences exist between the two; and these aid differential clinical diagnosis (Table 1.1; Slemp and Kirschner, 2006; Atiyeh, 2007; Gauglitz *et al*. 2011).

1.7.1 Hypertrophic Scarring

Most commonly observed after burn injuries (Table 1.1), hypertrophic scars typically develop within 4 - 8 weeks of the initial wounding (Gauglitz *et al*. 2011). Developing as raised tissue possessing a red hue (Figure 1.7), hypertrophic scars undergo a rapid growth phase for up to approximately 6 months; before a static phase begins which subsequently and spontaneously leads to a regression period (Alster and Tanzi, 2003; Slemp and Kirschner, 2006; Bran *et al*. 2009). Although hypertrophic scars are raised due to excessive scar formation, unlike keloids, the scarring does not extend beyond the confines of the initial wound margins. Thus, the boundaries of the original lesion are preserved before regression and tissue flattening over time (Peacock *et al*. 1970; Bayat *et al*. 2003). Regarding incidence, hypertrophic scars are more prevalent than keloids as they usually occur as result of aggravated acute dermal healing, following trauma or surgery. Unlike keloid scarring, they do not have a higher incidence in any particular population or predilection towards forming in any precise anatomical area (Table 1.1; Burd and Huang, 2005; Gauglitz *et al*. 2011; Arno *et al*. 2014). However, they tend to develop in locations subjected to high tension, such as the neck, ankles,

Table 1.1. Characteristics of hypertrophic and keloid scars. Epidemiological, clinical and histological differences between hypertrophic and keloid scars (adapted from Gauglitz *et al*. 2011 and Arno *et al*. 2014).

Hypertrophic Scars	Keloid Scars
Remain confined to borders of the original wound	Grow beyond the borders of the original wound margins
Rarely painful and less pruritic	Extremely painful and pruritic
Develop post-trauma, within 4 - 8 weeks following wounding	Can develop either post-trauma or spontaneously; tend to develop later
Regress spontaneously, often within 1 year	No spontaneous regression; there is continuous growth indefinitely
No predominant anatomical sites, but commonly found in high tension areas	Predilection sites include earlobes, cheeks, shoulders, chest and knees
40 - 70 % incidence following surgery, and up to 91 % incidence following burn injuries	6 - 16 % incidence in the African population. More common in those with darker skin types
Associated with contractures	Not associated with contractures
Less genetic predisposition	Genetic predisposition
Low recurrence rates post-surgical excision of the original scar	High recurrence rates post-surgical excision of the original scar
Contain primarily fine, well-organised, wavy, type III collagen bundles found parallel to the epidermal surface	Contain primarily large, thick and disorganised type I and III collagen bundles
Presence of myofibroblasts and αSMA	Lack of myofibroblasts and αSMA

shoulders and knees. Contractures, or the pathological shortening of scar tissue, are also associated with hypertrophic scars, which can severely impact functionality of the tissue (Muir, 1990; Tredget *et al*. 1997; Goel and Shrivastava, 2010; Gauglitz *et al*. 2011).

Histologically, hypertrophic and keloid scarring is quite different, despite both types containing excessive collagen levels (Table 1.1). Hypertrophic scars primarily contain type III collagen, well-organised into bundles and oriented parallel to the epidermal surface (Slemp and Kirschner, 2006; Bran *et al*. 2009; Verhagen *et al*. 2009; Gauglitz *et al*. 2011). Abundant myofibroblast-containing nodules are also found throughout the tissue and in post-burn hypertrophic scarring, myofibroblast apoptosis has been found to occur much later than during normal acute dermal repair. Furthermore, DF and myofibroblast numbers are generally increased in hypertrophic scars, compared to normal scars or normal skin (Nedelec *et al*. 2001; Bran *et al*. 2009; Gauglitz *et al*. 2011; Sarrazy *et al*. 2011). In addition to delayed apoptosis and greater DF densities, strong and persistent expression of TGF-β and its receptors have also been shown in hypertrophic scar fibroblasts, following burn injuries. Differential expression of TGF-β isoforms and receptors have been shown for both hypertrophic- and keloid-derived fibroblasts and thus, these differences may have a crucial role in the development of both scar types; rather than the mere absence or presence of TGF-β itself (Schmid *et al*. 1998; Bock *et al*. 2005; Lu *et al*. 2005; Gauglitz *et al*. 2011). Consequently, greater densities of DFs and the persistent myofibroblast presence at the wound site results in excessive collagen-rich ECM synthesis/deposition and wound contraction. It is the excessive contractile activity that ultimately causes pathological contractures, which are not associated with keloids, due to a lack of myofibroblasts (Ehrlich *et al*. 1994; van der Veer *et al*. 2009; Gauglitz *et al*. 2011; Sarrazy *et al*. 2011).

Other factors that may exacerbate hypertrophic scar development include increased wound tension, affected haemostasis, insufficient debridement/pathogen clearance, amplified neo-vascularisation, exaggerated inflammation, atypical ECM remodelling and delayed re-epithelialisation (Mustoe *et al*. 2002; Mutalik, 2005; van der Veer *et*

al. 2009). Despite these risk factors, when hypertrophic scars do develop, they tend to regress within a few years. In contrast, keloids do not follow the same pattern of evolution, stabilisation and involution (Bran *et al*. 2009; Gauglitz *et al*. 2011).

1.7.2 Keloid Scarring

In contrast to hypertrophic scars (Chapter 1.7.1), keloid scars can develop for up to several years following injury or trauma and may even form spontaneously, in the absence of any known injury (Murray, 1994; Gauglitz *et al*. 2011). Keloids appear as pink/purple bosselated tumours which are firm, yet mildly tender (Figure 1.7). They are locally aggressive and continue to grow beyond the borders of the initial wound margins, typically invading the surrounding tissue. Consequently, the scars persist as benign, irregularly-shaped tumours with well-demarcated edges that do not regress over time (Muir, 1990; Murray, 1994; Bayat *et al*. 2003; Bran *et al*. 2009; Gauglitz *et al*. 2011). Furthermore, although both scar types can be pruritic, keloids may be the source of significant pruritus, pain, disfigurement, functional loss and psychological turmoil due to their proliferative quality (Murray, 1994; Gauglitz *et al*. 2011; Eming *et al*. 2014). Keloids have a predilection towards developing on the earlobes, cheeks, chest, upper arms and shoulders. However, unlike with hypertrophic scars, there is a high chance of recurrence post-surgical excision (Muir, 1990; Murray, 1994; Niessen *et al*. 1999; Burd and Huang, 2005; Verhagen *et al*. 2009). With regards to incidence, keloid scar formation is quite rare and although hypertrophic scarring is much more common (Table 1.1), both scar types possess equal sex distribution with the greatest occurrences taking place in the second and third decades (Murray, 1994; Gauglitz *et al*. 2011; Jumper *et al*. 2015). In contrast to hypertrophic scarring, the susceptibility to keloid development appears to have a genetic basis. Although seen in individuals of all races (except albinos), dark-skinned people have been found to be genetically predisposed; with an incidence of 6 - 16 % reported in African populations. Patients with keloid scars often confirm a positive family history, unlike those suffering from hypertrophic scarring (Murray, 1994; Niessen *et al*. 1999; Bayat *et al*. 2005; Shih and Bayat, 2010; Gauglitz *et al*. 2011).

Histologically, keloid tissue is primarily composed of disorganised, hypocellular type I and III collagen bundles (Table 1.1). In contrast to hypertrophic tissue, keloid scars do not contain nodules or excess myofibroblasts and their collagen fibres are thicker (Clore *et al*. 1979; Slemp and Kirschner, 2006; Bran *et al*. 2009; Gauglitz *et al*. 2011). However, both pathologies demonstrate excessive production of fibroblast proteins, suggesting either a failure in the appropriate down-regulation of wound repair cells or a pathological persistence in wound site signalling (Bran *et al*. 2009; Gauglitz *et al*. 2011). With regards to keloid development, the exact aetiology and pathogenesis is not well-understood. However, current research seems to suggest that keloid scars develop through a dysregulated, multi-factorial wound healing response, mounted by genetically susceptible individuals in response to trauma or injury; resulting in an excessive ECM deposition and expansion into surrounding areas of normal skin (Chin *et al*. 2001; Brown and Bayat, 2009; Gauglitz *et al*. 2011). Evidence to date suggests a prolonged inflammatory phase, with a greater presence of mast cells, lymphocytes and macrophages. Pro-inflammatory cytokines and growth factors are also found to be up-regulated in keloids, versus the levels found in normal wound repair; including interferon (IFN)-β, tumour necrosis factor (TNF)-α, interleukin (IL)-6, TGF-β_1 and -β_2 (McCauley *et al*. 1992; Boyce *et al*. 2001; Shih *et al*. 2010; Bagabir *et al*. 2012). These prolonged and exaggerated responses lead to greater cell recruitment to the wound site, resulting in excessive proliferation. In particular, greater fibroblast proliferation contributes to the more sustained and aggressive fibrotic response shown in keloids, in comparison to normal and hypertrophic situations (Shih *et al*. 2010; Gauglitz *et al*. 2011).

Keloid-derived fibroblasts possess altered phenotypes compared to normal DFs and hypertrophic fibroblasts, behaving and responding differently to growth factors and cytokines. As well as undergoing more rapid migration and proliferation than normal DFs, they display lower rates of apoptosis through down-regulation of related genes, such as p53 (Bettinger *et al*. 1996; Calderon *et al*. 1996; Sayah *et al*. 1999; Funayama *et al*. 2003; De Felice *et al*. 2007). In addition, they exhibit higher numbers of growth factor receptors and respond faster to such growth factors, including PDGF and TGF-

β_1, compared to normal DFs; which may act to up-regulate these cells from the very beginning of wound healing (Haisa *et al*. 1994; Slemp and Kirschner, 2006; Bran *et al*. 2009; Gauglitz *et al*. 2011). Also, the fibroblasts themselves express greater levels of specific growth factors, including VEGF, PDGF, TGF-β_1 and -β_2 (Marneros and Krieg, 2004; Chike-Obi *et al*. 2009; Shih *et al*. 2010). Overall, these characteristics serve to increase the numbers of fibroblasts in the wound, leading to greater ECM synthesis. ECM production/deposition is exacerbated by keloid-derived fibroblasts, as they are capable of producing 2 - 3 times more collagen than DFs (Uitto *et al*. 1985; Friedman *et al*. 1993; Huang *et al*. 2013). In addition, it is thought that there is decreased ECM turnover in keloid scars, contributing to their expansion beyond the wound margins. MMP-9 levels were found to be low, while MMP-2 levels were found to be increased in keloid tissue (Neely *et al*. 1999; Shih *et al*. 2010; Gauglitz *et al*. 2011). There is also altered HA expression between keloids and normal wounds; with HA typically found within the papillary dermis in normal wounds, but observed between the epidermal layers in keloid scars (Bertheim and Hellström, 1994; Meyer *et al*. 2000; Huang *et al*. 2013; Jumper *et al*. 2015).

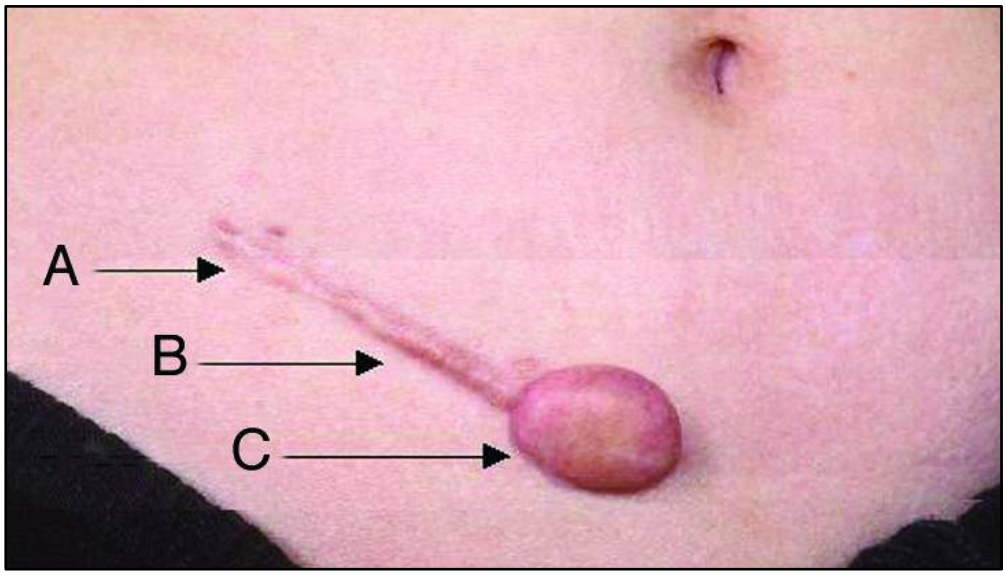

Figure 1.7. Clinical photograph highlighting the occurrence of multiple scar types at the same anatomical site; (A) widespread (B) hypertrophic and (C) keloid scars seen on a Caucasian female, following surgical intervention (Bayat *et al*. 2003).

1.8 Current Therapies for Excessive Scarring

Despite the significant aforementioned physiological and psychological burdens that may affect patients suffering with pathologically excessive scarring (Chapter 1.7), no optimal treatment regimens have been identified to date for either hypertrophic or keloid scarring. Indeed, most of the currently used therapeutic approaches are being employed for both scar types (Chike-Obi *et al*. 2009; Gauglitz, 2013). Multiple studies on hypertrophic and keloid scar formation have resulted in a plethora of therapeutic strategies intended to prevent, attenuate or improve both scar types. However, the general consensus of recent reviews evaluating the efficacy of current hypertrophic and keloid therapies, is that high-quality research into the effects on both scar types is still lacking, with more well-designed, controlled trials needed to provide a sound evidence base and reliably inform clinical decision-making (Durani and Bayat, 2008; Gauglitz *et al*. 2011; Gauglitz, 2013; Arno *et al*. 2014). Nevertheless, there are many management options available, which have previously exhibited varying degrees of clinical success (Durani and Bayat, 2008; Chike-Obi *et al*. 2009).

In patients prone to pathological scar formation, there are a number of factors that can increase the risk of development. Delayed epithelialisation beyond 10 - 14 days, wounds subjected to tension, lack of adequate debridement, poor haemostasis and infection all increase the incidence of pathological scarring dramatically (Mustoe *et al*. 2002; Mutalik, 2005; Slemp and Kirschner, 2006). Thus, rapid closure of wounds, under little to no tension, that have been adequately and appropriately debrided is essential (Slemp and Kirschner, 2006; Gauglitz *et al*. 2011). Preventative treatments include pressure therapy, silicone gel sheeting and flavonoids; with pressure therapy representing the preferred prophylactic option for both hypertrophic and keloid scar treatment, since the 1970s (Macintyre and Baird, 2006; Atiyeh, 2007; Gauglitz *et al*. 2011; Gauglitz, 2013). To date, pressure garments are primarily utilised for post-burn hypertrophic scar prevention, despite there being little scientific evidence to support their use. The recommendations for the amount and duration of pressure are based on empirical observations; and it has been reported that pressure should be applied for a minimum 23 hours a day, for 6 - 24 months (Macintyre and Baird, 2006; Atiyeh,

2007; Gauglitz, 2013; Arno *et al*. 2014). Pressure therapy can also cause discomfort, which results in reduced patient compliance to therapy (Macintyre and Baird, 2006). Furthermore, their underlying mechanism of action remains poorly understood. It is thought that mechanical compression decreases collagen synthesis and increases its degradation by limiting the blood, oxygen and nutrient supplies to the scar tissue; as well as increasing DF apoptosis rates (Renò *et al*. 2001; Gauglitz *et al*. 2011; Gauglitz, 2013; Arno *et al*. 2014). Topical silicone gel sheeting is another recognised therapy in scar management and current opinion suggests that its beneficial response is due to occlusion and hydration; rather than the silicone possessing an inherent anti-fibrotic effect (de Oliveira *et al*. 2001; Mustoe, 2008; Gauglitz, 2013; Arno *et al*. 2014). Its use is favoured for areas of consistent movement and although the mechanism of action is unclear, it is thought that maintained hydration of the *stratum corneum* positively affects cytokine-mediated signalling between keratinocytes and DFs (Mustoe, 2008; Gauglitz *et al*. 2011). However, a recent Cochrane meta-analysis, evaluating silicone gel efficacy for use in the treatment of hypertrophic and keloid scars, concluded that any positive effects reported in the studies analysed were obscured by poor-quality research. As such, the effectiveness of silicone gel sheeting remains unclear (O'Brien and Pandit, 2006; Durani and Bayat, 2008; Gauglitz, 2013; O'Brien and Jones, 2013; Arno *et al*. 2014). Lastly, flavonoids are found in topical scar creams and are thought to possess anti-fibrotic properties; including inhibition of the proliferation, collagen synthesis and contraction of hypertrophic and keloid-derived DFs. However, efficacy studies performed on these scar creams have yielded controversial data (Phan *et al*. 2003; Gauglitz *et al*. 2011).

Regarding mature scars, current treatment strategies include surgical excision, intra-lesional corticosteroid delivery, cryotherapy, radiotherapy and laser therapy (Slemp and Kirschner, 2006; Atiyeh, 2007; Gauglitz *et al*. 2011; Arno *et al*. 2014). The surgical excision of hypertrophic and keloid scars remains a traditional approach, with many clinicians recommending surgery as first-line treatment if disabling contractures are present (Slemp and Kirschner, 2006; Ogawa *et al*. 2011; Arno *et al*. 2014). However, it is imperative to differentiate between scar types before surgical manipulation, as

excision may not be necessary. In the case of keloids, this option should be avoided unless adjuvant therapy is provided post-surgery, as reoccurrence rates are high (45 - 100 %). Consequently, keloid excision may lead to the development of a larger scar around the original wound area (Mustoe *et al*. 2002; Poochareon and Berman, 2003; Mutalik, 2005; Chike-Obi *et al*. 2009; Gauglitz, 2013). Concerning hypertrophic scars, timing of treatment is an important pre-operative consideration; as they can regress over time and thus, removal may not be needed. Nevertheless, post-excisional rates of recurrence are normally low for hypertrophic scars (Gauglitz *et al*. 2011; Gauglitz, 2013). Since the mid-1960s, intra-lesional corticosteroid injections have been widely used, often in combination with surgery or cryotherapy. This approach is considered a first-line therapy with regards to keloid attenuation, whereas it remains a second-choice treatment modality for hypertrophic scars (Yosipovitch *et al*. 2001; Mustoe *et al*. 2002; Boutli-Kasapidou *et al*. 2005; Jalali and Bayat, 2007; Gauglitz *et al*. 2011). It is thought that corticosteroids primarily act through suppression of the inflammatory response; and secondly, via inhibition of DF proliferation and ECM synthesis, as well as increased collagen degradation (Cruz and Korchin, 1994; Atiyeh, 2007; Reish and Eriksson, 2008; Gauglitz, 2013; Arno *et al*. 2014). However, several applications are typically required and response rates to these injections are highly variable, ranging from 50 - 100 %. Recurrence rates also vary from 9 - 50 % and the longer the course of steroidal treatment, the greater the risk of inducing side-effects; including dermal atrophy, hypopigmentation and telangiectasia (Niessen *et al*. 1999; Alster and Tanzi, 2003; Reish and Eriksson, 2008; Chike-Obi *et al*. 2009; Gauglitz *et al*. 2011; Gauglitz, 2013). As a mono-therapy, the usefulness of cryotherapy is limited to the treatment of small scars and is believed to induce vascular damage, leading to anoxia and thus, tissue necrosis (Rusciani *et al*. 1993; Layton *et al*. 1994; Niessen *et al*. 1999; Durani and Bayat, 2008; Gauglitz, 2013). Sessions every 3 - 4 weeks are recommended and success rates following two sessions of contact or spray cryosurgery range between 30 - 75 %; with better outcomes when utilised upon hypertrophic scars, rather than keloids (Rusciani *et al*. 1993; Mustoe *et al*. 2002; Barara *et al*. 2012; Arno *et al*. 2014). However, the newer intra-lesional cryoneedle method has shown greater efficacy in comparison to the contact and spray approaches; with regards to treatment of both

keloids and hypertrophic scars (Har-Shai *et al*. 2003; Love and Kundu, 2013; Arno *et al*. 2014). For keloid scars in particular, radiotherapy has been used as an adjunct to surgical excision. This combined therapeutic approach is most efficacious for severe cases of keloid scarring; and is most commonly initiated within 48 hours of surgical removal (Sällström *et al*. 1989; Escarmant *et al*. 1993; Guix *et al*. 2001; Ragoowansi *et al*. 2003; Chike-Obi *et al*. 2009; Arno *et al*. 2014). Irradiation is thought to inhibit the proliferation of keloid-derived DFs and neovascular buds, resulting in decreased collagen deposition. However, this treatment modality not only confers similar risks to those of corticosteroid treatment and cryotherapy, but also increases the risk of carcinogenesis (Mustoe *et al*. 2002; Atiyeh, 2007; Reish and Eriksson, 2008; Gauglitz, 2013). Finally, laser therapy has been utilised in the treatment of both hypertrophic scars and keloids. The most encouraging results have been demonstrated using the pulsed dye laser (PDL) and it is thought that the PDL induces thermal damage to the scar microvasculature; causing local ischemia, reducing DF proliferation and leading to altered collagen production (Alster and Williams, 1995; Reiken *et al*. 1997; Alster and Handrick, 2000; Reish and Eriksson, 2008). Nevertheless, laser therapy remains an emerging technology and further research is needed to provide a sound evidence base for its safety, efficacy, dosage/timing regimens and long-term outcomes (Khatri *et al*. 2007; Arno *et al*. 2014).

In addition to the aforementioned prophylactic and mature scar therapies, there are several more recently established therapies available for the treatment of excessive scars, including fluorouracil (5-FU), interferon (IFN) and bleomycin. Utilised with PDL and corticosteroids, 5-FU currently appears to be the most promising treatment for both hypertrophic and keloid scarring (Fitzpatrick, 1999; Asilian *et al*. 2006; Arno *et al*. 2014). 5-FU is a pyrimidine analogue and has been shown to interfere with TGF-β signalling and inhibit type I collagen gene expression by DFs *in vitro* (Wendling *et al*. 2003). However, the underlying mechanism of action of 5-FU has not yet been fully elucidated and furthermore, common side-effects of the therapy include ulceration at the injection site, hyper-pigmentation, burning sensations and pain (Chike-Obi *et al*. 2009; Gauglitz, 2013; Arno *et al*. 2014). IFN sub-dermal injections have also been

reported to be more efficacious than corticosteroids in averting post-surgical keloid recurrence. IFN has been shown to reduce DF type I and III collagen synthesis, while IFN-α2b is thought to have anti-proliferative properties (Jimenez *et al*. 1984; Berman and Duncan, 1989; Gauglitz, 2013; Arno *et al*. 2014). However, not only is IFN therapy expensive, the injections are painful enough to warrant regional anaesthesia and flu -like symptoms are common post-exposure (Mustoe *et al*. 2002; Gauglitz *et al*. 2011; Arno *et al*. 2014). Finally, the anti-cancer agent, bleomycin sulphate, may represent a promising future treatment for both hypertrophic and keloid scars. It is thought to induce apoptosis and inhibit DF collagen synthesis via decreased TGF-β_1 stimulation. However, in order for bleomycin to be included in clinical treatment protocols more frequently, further efficacy and toxicity trials are necessary (España *et al*. 2001; Reish and Eriksson, 2008; Gauglitz, 2013; Arno *et al*. 2014).

Thus, despite the varied range of current and emerging prophylactic and therapeutic treatments available, it is apparent that the majority of current therapies for keloid and hypertrophic scars remain clinically unsatisfactory. This is likely due to a number of reasons, including an incomplete understanding of the molecular basis of normal healing and pathological scarring situations (Eming *et al*. 2014; Kaplani *et al*. 2018). Also, there is a paucity of large-scale, high-quality clinical trials for both existing and emerging therapies. As such, there is an unmet clinical need to develop novel wound healing agents; supported by a sound evidence base, proving efficacy and safety for assured clinical use (Reish and Eriksson, 2008; Sen *et al*. 2009; Eming *et al*. 2014).

1.9 Epoxy-Tiglianes, EBC-46 and EBC-211

Implemented by biotechnology company, QBiotics Group (Yungaburra, Australia), a large library of novel epoxy-tigliane compounds were discovered through the use of EcoLogic™ Technology (Reddell and Gordon, 2007). EcoLogic™ Technology integrates knowledge of the distribution, habitats and ecological interactions of plants, animals and microbes of Australia's tropical rainforests; with a mechanistic understanding of the stress response chemistry, signalling and host defence of endemic plant species. This approach has allowed specific plants, which have demonstrated the potential to

produce chemicals with highly desirable properties, to be identified and selected for further screening (Reddell and Gordon, 2007; QBiotics Group). Via these screening studies, the naturally-derived epoxy-tigliane, EBC-46 (12-tigloyl-13-(2-methylbutanoyl)-6,7-epoxy-4,5,9,12,13,20-hexahydroxy-1-tiglian-3-one) was discovered to possess potent bioactivity. Subsequently, the compound was chosen as a lead candidate for pharmaceutical optimisation and development by the QBiotics Group (Reddell and Gordon, 2007).

EBC-46 is found to occur within seeds of the Fountain's Blushwood Tree (*Fontainea picrosperma*), indigenous to the Queensland tropical rainforest (Lamont *et al*. 2016). Within the plant, EBC-46 plays a biological role in host defence, acting as a chemical deterrent against predation by native mammalian herbivores. It is believed that the compound dissuades marsupials in the surrounding area, initiating an inflammatory response on ingestion (Reddell and Gordon, 2007; QBiotics Group). The 'less active' analogue, EBC-211 (12-tigloyl-13-(2-methylbutanoyl)-5,6-epoxy-4,5,9,12,13,20-hexahydroxy-1-tiglian-3-one) is an EBC-46 derivative, with approximately 100-fold lesser activity. Both of these compounds are complex, small molecules that are not readily amenable to laboratory synthesis. Still, they are relatively easy to harvest, purify and isolate from kernels of the tree's fruit. Furthermore, growth of large-scale *Fontainea picrosperma* plantations have been found to be feasible, with regards to commercial production (Boyle *et al*. 2014; Lamont *et al*. 2016). Along with the other EBC family members, EBC-46 and EBC-211 chemical structures (Figure 1.8A and B, respectively), have now been elucidated (Reddell and Gordon, 2007; Dong *et al*. 2008; Dong *et al*. 2009; QBiotics Group).

1.9.1 Epoxy-Tigliane Anti-Cancer Properties

Selected for its potential bioactivity, EBC-46 has since been shown to possess potent tumouricidal properties and is currently under drug development by QBiotics Group as a novel anti-cancer agent. To date, exploratory case studies have been performed on over 300 client-owned companion animals (dogs, cats and horses), with solid sub-cutaneous and cutaneous tumours. Also, veterinary clinical trials containing 110 dogs

with mast cell tumours or soft tissue sarcomas have also been performed (Campbell *et al*. 2017; Barnett *et al*. 2018; QBiotics Group). In each of these cases, participants were treated with EBC-46 as part of their palliative care, which was administered by intra-lesional injection. Overall, trials have been carried out upon numerous types of tumour including melanomas, sarcomas, carcinomas, sarcoids, spindle cell and mast cell tumours. Such studies have demonstrated the potent anti-cancer effects of EBC-46, culminating in the rapid ablation of tumours previously deemed inoperable. The majority of tumours were eradicated without recurrence (measured at 12 months); and the drug appeared well-tolerated, revealing no long-term side-effects (Campbell *et al*. 2017; Barnett *et al*. 2018; QBiotics Group). Examples of the efficacy of EBC-46 against sarcoids can be seen in Figures 1.9 and 1.10. In light of the obvious beneficial tumouricidal properties and compelling proof-of-concept data on the drug's efficacy and safety in tumour-bearing mouse models and other animals, QBiotics Group are currently developing EBC-46 as a pharmaceutical therapy for human and veterinary use. At time of writing, EBC-46 has completed Phase I human clinical trials, within a palliative head/neck cancer patient cohort (Boyle *et al*. 2014; Campbell *et al*. 2017; Barnett *et al*. 2018; QBiotics Group).

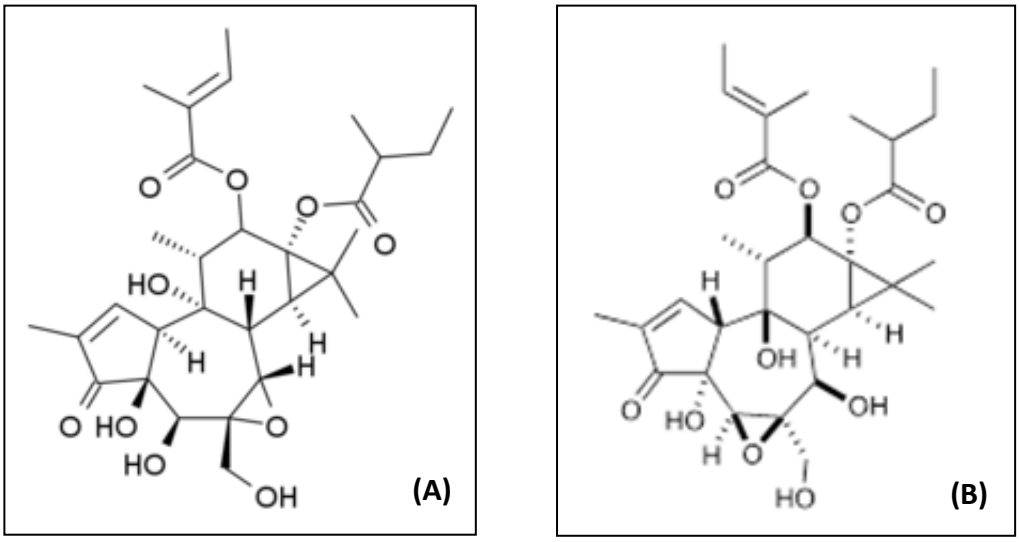

Figure 1.8. The chemical structure of EBC-46 (A) and its 'less active' derivative, EBC-211 (B) found in seeds of the Fountain's Blushwood tree, endemic to Queensland's tropical rainforest (QBiotics Group, Yungaburra, Australia).

As aforementioned, intra-lesional treatment of tumour-bearing mouse models using EBC-46 was also performed, in order to provide pre-clinical data supporting the use of the compound as a topical injection and contribute to the proof-of-concept data, regarding the drug's efficacy and safety (Boyle *et al*. 2014). Via these studies, EBC-46 has been established as a signalling, rather than cytotoxic molecule; inducing rapid haemorrhagic necrosis of treated tumours. The compound is thought to achieve this through a combination of actions: disruption of tumour vasculature and initiation of an acute, highly localised pro-inflammatory response. Boyle *et al*. (2014) found that EBC-46 induces permeability of endothelial cell monolayers *in vitro*, as well as blood vessel disruption and vascular swelling *in vivo*. Furthermore, after administration of EBC-46, erythema and oedema were found to be significantly higher in mice bearing tumours, versus those with normal skin. These results suggest that vascular damage is specific to tumour sites, with minimal impact upon healthy tissue; resulting in anti-cancer efficacy. Thus, it is hypothesised that EBC-46 remains at the tumour site, with the vascular disruption preventing EBC-46 from entering systemic circulation (Boyle *et al*. 2014). Ultimately, EBC-46 treatment was shown to stimulate eschar formation and subsequent tumour slough. Such rapid tumour ablation is seemingly long-term, demonstrated by a lack of relapse within 12 months post-treatment, in over 70 % of cases; suggesting that EBC-46 treatment may lead to enduring inhibition of tumour cell growth *in vivo* (Boyle *et al*. 2014).

With regards to the underlying epoxy-tigliane mechanism of action, EBC-46 has been found to act through the activation of classical protein kinase C (PKC) isoforms (PKC-βI, -βII, -α, and -γ), with particular specificity for the β-isoforms. EBC-46 co-injection with pan-PKC inhibitor, bisindolylmaleimide-1 (BIM-1), resulted in loss of efficacy *in vivo* (Boyle *et al*. 2014). However, the full mechanism of action and any downstream signalling pathways activated have not yet been determined. Thus, further research is being undertaken to elucidate the pathways underlying these potent tumouricidal responses (QBiotics Group).

Figure 1.9. Intra-tumoural injection of a large equine sarcoid with EBC-46. Left-hand image: prior to treatment. Right-hand image: 22 h post-treatment, showing marked reduction in volume and the apparent ablation of tumour mass (Reddell *et al*. 2014; QBiotics Group).

Figure 1.10. Intra-tumoural injection of an equine sarcoid with EBC-46. Left image: 6 days post-injection of 0.75 mg EBC-46. Right image: Day 10, following final injection of 1.5 mg EBC-46; with almost complete sarcoid loss and wound resolution (Reddell *et al*. 2014; QBiotics Group).

1.9.2 Epoxy-Tigliane Effects on Wound Healing

Following the tumour ablation induced during the exploratory studies and veterinary clinical trials into EBC-46's anti-cancer effects, unexpected enhanced dermal wound healing responses were observed (Campbell *et al*. 2014, 2017; Reddell *et al*. 2014). Following tumour slough and without any management or intervention, the wounds displayed rapid granulation tissue development, accelerated wound closure and re-epithelialisation, reduced scarring and skin appendage reformation (Campbell *et al*. 2014, 2017; Reddell *et al*. 2014). After observations, veterinary wound healing trials were initiated and these have demonstrated similar improvements in wound healing outcomes. Many cases included in these trials were wounds previously unresponsive to months of treatment, in line with current care strategies (Reddell *et al*. 2014). For example, the case study presented in Figure 1.11 displays a deep, necrotising facial wound that was unresponsive to 3 months of previous treatment. Following EBC-46 administration, complete wound resolution occurred in 3.5 months and exceptional dermal cosmesis was evidenced by minimal scarring and hair re-growth (Figure 1.11; Reddell *et al*. 2014; QBiotics Group). Restoration of normal dermal pigmentation and fur re-growth was also observed following topical gel EBC-46 treatment of epidermal viral plaques in a Hungarian Vizsla dog, accompanied by near complete elimination of the exophytic lesions (Hansen *et al*. 2018). Throughout the veterinary trials upon wounds, the drug has been well-tolerated with no evidence of significant adverse effects after EBC-46 treatment (Reddell *et al*. 2014; QBiotics Group).

Despite the preferential wound healing effects previously observed, little is known on how epoxy-tiglianes exert these responses (Reddell *et al*. 2014; QBiotics Group). Recently, *in vitro* studies to assess the effects of both EBC-46 and EBC-211 on wound healing responses were performed, using DFs and a normal human keratinocyte cell line of skin origin (HaCaTs; Moses, 2016). Both epoxy-tiglianes were found to retard DF proliferation and delay DF cell cycle transitions, but exerted no significant effects on their migratory responses. Regarding their effects on HaCaTs, the epoxy-tiglianes were exhibited to stimulate HaCaT proliferation and accelerate cell cycle transitions, along with HaCaT scratch wound re-population/migration (Moses, 2016). As shown

with EBC-46's anti-cancer effects, the enhanced HaCaT responses stimulated by both epoxy-tiglianes *in vitro* were modulated via PKC activation; specifically the classical PKC isoforms. Pharmacological inhibition of PKC phosphorylation utilising BIM-1 and Gö6976 (pan- and α-/βI-PKC inhibitors, respectively), have been shown to abrogate the effects of EBC-46 and EBC-211 upon HaCaT proliferation and migration (*currently*

Figure 1.11. Effects of both topical gel application and intra-lesional injection (0.5 mg /mL) of EBC-46 on a deep non-healing necrotising facial wound. (A) Before the initial treatment, (B) 3 days after treatment began, (C) 28 days post-topical gel treatment, just before administering a single dose injection of EBC-46 into multiple sites around the wound area, (D) 104 days after initial treatment and 76 days following injectable treatment (Reddell *et al*. 2014; QBiotics Group).

unpublished data). Overall, these findings suggest that epoxy-tigliane PKC activation stimulates enhanced keratinocyte responses, which may explain the rapid wound re-epithelialisation observed in compound-treated skin *in vivo* (Campbell *et al*. 2014, 2017; Reddell *et al*. 2014).

As well as rapid wound re-epithelialisation, accelerated granulation tissue formation and minimal scarring represent key responses of interest observed following epoxy-tigliane treatment *in vivo* (Campbell *et al*. 2014, 2017; Reddell *et al*. 2014). As TGF-β_1-driven, DF-myofibroblast differentiation is vital to normal dermal wound closure/ contraction and scarring, the epoxy-tigliane effects on DFs, and their differentiated myofibroblast counterparts, are of great interest. In addition, as detailed previously (Chapter 1.7), pathological myofibroblast persistence is a significant driver of fibrosis and altered DF phenotypes are central to the formation of hypertrophic and keloid scar tissue (Gauglitz *et al*. 2011). Consequently, DFs and myofibroblasts represent viable pharmaceutical targets to explain the minimal scarring observed post-epoxy-tigliane treatment *in vivo* (Campbell *et al*. 2014, 2017; Reddell *et al*. 2014).

1.10 Study Aims and Objectives

Despite the significant beneficial wound repair effects previously observed (Chapter 1.9.2), little is known on how novel epoxy-tiglianes exert such responses, regarding DFs and myofibroblasts particularly. Therefore, the present study aimed to elucidate how these exceptional wound healing responses are stimulated, by determining the effects of EBC-46 and its 'less active' derivative, EBC-211, on DFs and myofibroblasts *in vitro*. Additionally, the study also aimed to ascertain whether PKC activation is the underlying mechanism of action responsible for the anti-scarring responses observed in epoxy-tigliane-treated skin. As DFs and myofibroblasts are key mediators of ECM synthesis and turnover, wound closure and contraction and scarring, they represent viable targets for explanation of the minimal scarring observed *in vivo*. Specifically, the present study aimed to:

- Assess whether EBC-46 and EBC-211 modulate TGF-β_1-driven DF-myofibroblast differentiation, in the absence and presence of TGF-β_1.

- Examine the effects of EBC-46 and EBC-211 upon ECM component synthesis and turnover by DFs, in the presence of TGF-β_1.
- Determine the effects of EBC-46 and EBC-211 on global gene expression in DFs; and validate any key differentially expressed genes, in the presence of TGF-β_1.
- Identify whether EBC-46 and EBC-211 modulate their effects via PKC activation, particularly the classical isoforms, in the presence of TGF-β_1.

The hypothesis of this project is that the novel epoxy-tiglianes, EBC-46 and EBC-211, may induce a more regenerative healing response, compared to the normal dermal reparative process, which culminates in scar formation. By undertaking such studies, it is envisaged that a more comprehensive understanding of DF responses to epoxy-tiglianes would be gained, along with insight into potential mechanism(s) of action. This could provide further justification for the pharmaceutical development of these compounds as novel wound healing agents; for the clinical treatment of pathological and excessive dermal scarring situations.

Chapter 2

Materials and Methods

Chapter 2 - Materials and Methods

2.1 General Cell Treatments

2.1.1 Epoxy-Tigliane Preparation and Treatments

Epoxy-tiglianes, EBC-46 and EBC-211, were supplied by QBiotics Group (Yungaburra, Australia). Before use, the compounds were solubilised in dimethyl sulfoxide (DMSO, >99.7 %; Sigma-Aldrich, Gillingham, UK), under sterile laboratory conditions (Section 2.2). Powdered batches of EBC-46 and EBC-211 were solubilised in order to produce stock concentrations at 100 mg/mL and 10 mg/mL, respectively. The stock aliquots (10 µL) were stored at -20 °C to minimise freeze-thaw effects and to ensure stability for several months. These aliquots were used to yield EBC-46 and EBC-211 dilutions at the following concentrations: 10 mg/mL, 1 mg/mL, 0.1 mg/mL, 0.01 mg/mL and 0.001 mg/mL. DMSO was utilised as a diluent and aliquots (10 µL) were stored at -20 °C. On requirement, these were thawed at room temperature. Prior to experimental use, final concentrations were prepared in serum-free medium (S-FM; Section 2.2.1) as follows: 10 µg/mL, 1 µg/mL, 0.1 µg/mL, 0.01 µg/mL and 0.001 µg/mL. Solutions were prepared as required, and remained stable at 4 °C for a time period of 1 week. Compound-free controls were also prepared, containing 1 % DMSO, to account for the presence of DMSO in compound-containing media dilutions. In all experimental cell cultures, cells were exposed to a maximum of 1 % DMSO. Experiment-specific compound treatments and treatment periods, are detailed in the following Sections and Chapters.

2.1.2 Transforming Growth Factor-Beta$_1$ Preparation and Treatments

Recombinant human transforming growth factor-beta$_1$ (TGF-β_1; PeproTech, London, UK), was reconstituted to 100 µg/mL in 10 mM citric acid buffer (pH 3), under sterile conditions (Section 2.2). Once solubilised, stock aliquots (10 µL) were kept at -20 °C to minimise any freeze-thaw effects and ensure stability for up to 12 months. When required, stock aliquots were thawed at room temperature and final experimental

concentrations of 10 ng/mL were used in S-FM dilutions (Section 2.2.1). Compound-free controls were also prepared, containing both 1 % DMSO and TGF-β_1 (10 ng/mL), to account for DMSO's presence in the compound-containing medium dilutions and to confirm normal dermal fibroblast (DF)-myofibroblast differentiation upon TGF-β_1 treatment. Experiment-specific TGF-β_1 treatment periods are detailed in the ensuing Sections and Chapters.

2.2 General Cell Culture

To ensure sterility and cleanliness of the working environment, tissue culture safety cabinets and any equipment housed within the cabinets were disinfected with 70 % ethanol, before commencing cell culture. Each of the cabinets and water baths were sterilised weekly; incubators underwent the same treatment monthly, following an added heat decontamination step (180 °C overnight). Equipment specific to the Cell Culture Suite remained as such while any glass or plasticware, double-distilled water (dd-H_2O) or phosphate buffered saline (PBS) required for culturing, were sterilised by autoclaving (123 °C at 15 lb/m^2, for 15 min). Any purchased, sterilised consumables were not autoclaved. Before their use, fibroblast serum-containing medium (FS-CM), serum-free medium (S-FM; containing the same components as FS-CM, except 10 % foetal calf serum; FCS), 0.05 % (w/v) trypsin/0.53 mM ethylenediaminetetraacetic acid (trypsin-EDTA) and FCS were warmed to 37 °C within a Fisherbrand™ Isotemp GPD 20 water bath (all purchased from Thermo Fisher Scientific, Loughborough, UK).

2.2.1 Dermal Fibroblast Culture

All experiments were carried out using primary human DFs. Cells were derived from biopsies (6 mm) obtained from uninjured skin of healthy patients undergoing routine oral surgery at the Cardiff University Dental Hospital, Cardiff, UK (*n = 4*, 2 male and 2 female, patient age range: 48 - 77 years; Enoch *et al.* 2009, 2010). Skin biopsies were taken after obtaining Local Research Ethical Committee approval and informed patient consent. DF cultures were established upon enzymatic degradation of the tissue and single-cell suspension, as previously detailed (Stephens *et al.* 1996; Enoch *et al.* 2009, 2010). DFs were seeded into 75 cm^2 cell culture flasks (Sarstedt, Leicester, UK), in 10

mL FS-CM, comprising Dulbecco's Modified Eagle's Medium (DMEM), 1 % L-glutamine (2 mM) and 1 % antibiotics (100 U/mL penicillin G sodium, 0.25 µg/mL amphotericin B and 100 µg/mL streptomycin sulphate) and 10 % FCS (all purchased from Thermo Fisher Scientific). The cells were cultured within a 37 °C humidified incubator in 5 % CO_2/95 % air atmosphere; with FS-CM replaced every 48 - 72 h. Once confluent cell monolayers were achieved, cells were either sub-cultured into fresh flasks (1:3 split), or seeded into experiments following determination of cell density (Section 2.2.2). Experimental procedure consisted of a 48 h DF growth period, 48 h serum-starvation period and treatment period (0 - 72 h). DFs were seeded at approximately equivalent numbers between passages 9 - 17 and starved using S-FM. S-FM allowed cell-cycle synchronisation via growth arrest at G_o stage. Unless stated otherwise, cell treatments and stimulations were performed in S-FM to avoid any potential influences of serum factors upon gene expression or wound healing responses (Section 2.1).

2.2.2 Sub-Culture and Cell Counting

On reaching optimal confluence (Section 2.2.1), DFs were sub-cultured at a 1:3 ratio, in order to maintain appropriate cell density levels. The following reagent amounts were used for 75 cm^2 culture flasks and were scaled up or down with the use of 175 cm^2 or 25 cm^2 flasks, respectively. In order to passage DFs, FS-CM was removed and cells were briefly washed in PBS to remove any residual traces of medium. DFs were then evenly covered with 3 mL of trypsin-EDTA and incubated for 5 min at 37 °C, to ensure detachment from the flask base. Following incubation and flask agitation, DFs were examined using an Eclipse™ TS100® Inverted Microscope (Nikon, Kingston, UK) to ensure detachment. DFs were treated with equal volumes of FS-CM to neutralise protease activity and the total volumes transferred to 20 mL tubes and centrifuged, for 5 min at 377 xg. Residual supernatants were removed, before re-suspending the remaining pellets in 30 mL FS-CM and seeding into new cell culture flasks (10 mL/75 cm^2).

Prior to experimentation, cell density and viability were assessed in order to ensure that equal cell numbers were seeded into each experimental well or flask. If the DFs

required counting, cell pellets were re-suspended in volumes of FS-CM conducive to exact counting (volume used dependent on pellet size). Single-cell suspensions were achieved via agitation and 10 µL aliquots were taken and mixed using equal volumes of Trypan Blue (0.4 %; Sigma-Aldrich). Once homogenised, 10 µL of the mixture was pipetted into a Neubauer Improved Haemocytometer (Sigma-Aldrich). Cell number and viability were assessed via Trypan Blue Exclusion Assay (Mishell and Shiigi, 1980); and visualised by light microscopy, using an Eclipse™ TS100 Inverted Microscope at x100 magnification. Viable cells with intact membranes do not take up Trypan Blue dye and therefore, non-viable stained cells were excluded from cell counts. Once DF densities were established, cells were seeded as needed; any experiment-specific DF seeding densities are detailed in the following Sections and Chapters.

2.2.3 Cryopreservation, Storage and Revival

Excess cells obtained via the serial passaging of DFs were routinely stored at varying numbers and passages. For cryopreservation, cell pellets produced via sub-culturing (Section 2.2.2), were re-suspended in a freezing solution, consisting of 90 % FCS and 10 % DMSO. Suspensions were subsequently transferred into cryovials (Greiner Bio-One, Stonehouse, UK; 1 mL/cryovial), which were slow-cooled at a 1 °C/min rate via the use of isopropanol-containing freezing vessels (Sigma-Aldrich). Following gradual freezing for 24 h at -80 °C, cryovials were transferred to liquid nitrogen (196 °C), for long-term storage. When needed, cryopreserved DFs were retrieved and revived by rapidly thawing cryovials at 37 °C for 3 min. Cells were then washed via the addition of 9 mL FS-CM to 1 mL of cell suspension and centrifuged at 377 xg for 5 min. After removal of residual supernatants, the remaining DF pellets were re-suspended in 30 mL FS-CM, before seeding into new cell culture flasks (10 mL/75 cm^2), as previously described (Section 2.2.2).

2.2.4 Mycoplasma Contamination Screening

Post-revival and before experimentation, DFs were routinely tested to screen for the presence of Mycoplasma contamination. This procedure was performed by Dr Maria Stack (School of Dentistry, Cardiff, UK), through use of the Venor®GeM Classic Kit for

Mycoplasma detection (Minerva Biolabs, Berlin, Germany). To determine the status of infection, 200 µL samples of culture media were taken once DFs reached 90 - 100 % confluence. Samples were stored at -20 °C pending analysis. Once thawed on ice, the samples were incubated for 5 min at 95 °C and any cell debris was subsequently removed by centrifugation for 15 s at 10,000 xg. A polymerase chain reaction (PCR) master mix was prepared using primer/nucleotide mix (1.25 µL), nuclease-free H_2O (5.9 µL), GoTaq® polymerase (0.1 µL), internal control (1.25 µL), 25 mM magnesium chloride (1 mM final concentration; 0.5 µL), and 5 X GoTaq® Flexi buffer (2.5 µL; all purchased from Promega, Chilworth, UK). The samples (1 µL supernatant), as well as the positive and negative controls (1 µL DNA template and 1 µL nuclease-free H_2O, respectively), were added to 0.2 mL PCR tubes containing PCR master mix (11.5 µL). These were cycled as follows: 1 cycle at 94 °C for 2 min, followed by 39 cycles at 94 °C for 30 s, 55 °C for 30 s and 72 °C for 30 s.

During PCR cycling, agarose gels (2 %) were cast using 1.4 g of agarose in 70 mL 0.5 X Tris/borate/EDTA buffer (TBE; 5.4 g Tris base, 2.75 g boric acid, 2 mL 0.5 M EDTA; pH 8; all bought from Sigma-Aldrich). SafeView Nucleic Acid Stain (7 µL; NBS Biologicals, Huntingdon, UK), was added to gels to visualise PCR products. Post-PCR, 2 µL Loading Dye (6 X; Promega) was added to samples. Subsequently, 10 µL samples and 10 µL of 100 bp DNA Reference Ladder (Promega), were loaded onto the gels. Samples were then run at 100 V for 20 min using a Mini-Horizontal Electrophoresis Unit (Jencons-PLS, Leighton Buzzard, UK). Positive contamination was evidenced by detection of a strong band at 270 bp, whereas negative contamination was demonstrated by band production at 191 bp. The internal control produced a band at 191 bp, representing a successful reaction, unless strong Mycoplasma contamination was found; in which case, the band was not visible. Any cultures identified as Mycoplasma-positive were discarded.

2.3 Immunocytochemistry

Indirect immunofluorescent visualisation of α-smooth muscle actin (αSMA) was utilised to assess the effects of EBC-46 and EBC-211 treatment (Section 2.1), on DF-

myofibroblast differentiation; while direct visualisation of filamentous actin (F-actin) was used to assess their effects on cytoskeletal rearrangement. Confluent DFs were trypsinised, counted and seeded (Sections 2.2.1 and 2.2.2), into Nunc™ Lab-Tek™ 8-well chamber slides (Thermo Fisher Scientific). Cells were seeded in FS-CM (250 µL/well) at a cell density of $2.5x10^4$ cells/mL and were maintained in a 37 °C humidified incubator in 5 % CO_2/95 % air atmosphere, for the duration of the experiment. After 48 h, DFs were growth-arrested via culturing in S-FM (250 µL/well; Section 2.2.1) for a further 48 h. After growth arrest, S-FM was replaced with S-FM containing EBC-46 or EBC-211 at the following concentrations: 0 µg/mL, 0.001 µg/mL, 0.01 µg/mL, 0.1 µg/mL, 1 µg/mL or 10 µg/mL (3 wells/concentration); in the presence or absence of TGF-β_1 (10 ng/mL; Section 2.1). Cells were maintained in treated S-FM (250 µL/well) for 24 h, 48 h or 72 h.

Following the appropriate treatment period, media was removed from the cells and wells were washed briefly with PBS (x1). DFs were fixed with 4 % paraformaldehyde (150 µL/well; Santa Cruz Biotechnology, Dallas, USA), for 10 min and washed briefly with PBS (x1). Cells were subsequently permeabilised using 0.1 % Triton X-100 (250 µL/well; Sigma-Aldrich) for 5 min and washed briefly with PBS (x1). Any non-specific binding was blocked using 1 % (w/v) bovine serum albumin (BSA; Sigma-Aldrich) in PBS (herein referred to as BSA-PBS; 250 µL/well), for 1 h at room temperature. Cells were then washed briefly with 0.1 % (w/v) BSA-PBS (x3). For αSMA visualisation, DFs were incubated with mouse monoclonal anti-αSMA primary antibody (2 mg/mL; Sigma-Aldrich), diluted in 0.1 % (w/v) BSA-PBS (1:100; 250 µL/well) overnight at 4 °C. To ensure that any observed staining was due to primary antibody-antigen binding, isotype immunoglobulin G (IgG) controls were also included. DFs were incubated with naïve IgG (2 mg/mL; Dako, Glostrup, Denmark), diluted in 0.1 % (w/v) BSA-PBS (1:100; 250 µL/well) at 4 °C overnight, instead of primary antibody. For F-actin visualisation, cells were incubated in phalloidin-fluorescein isothiocyanate (FITC)-conjugated antibody (0.5 mg/mL; Sigma-Aldrich), diluted in 0.1 % (w/v) BSA-PBS (1:100; 250 µL/well), for 45 min at room temperature.

Following all aforementioned antibody incubations, cells were washed briefly in 0.1 % (w/v) BSA-PBS (x3), then re-washed with 0.1 % (w/v) BSA-PBS for 5 min (x3). In the case of phalloidin-FITC treated wells, wash steps were doubled and incubation with secondary antibody was not required. All other wells were subsequently incubated in goat polyclonal anti-mouse IgG Alexa Fluor® 488-conjugated secondary antibody (2 mg/mL; Thermo Fisher Scientific), diluted in 0.1 % (w/v) BSA-PBS (1:1000; 250 µL/well); for 1 h, at room temperature, under darkness. Cells were washed briefly in 0.1 % (w/v) BSA-PBS (x3) and re-washed with 0.1 % (w/v) BSA-PBS for 5 min (x3). Subsequently, nuclei were stained using Hoechst solution (1 mg/mL; Sigma-Aldrich), diluted in 0.1 % (w/v) BSA-PBS (1:2000; 250 µL/well) at room temperature, for 30 min, under darkness. Cells were washed briefly in 0.1 % (w/v) BSA-PBS (x3) and re-washed in 0.1 % (w/v) BSA-PBS for 5 min (x3). Following the final wash step, chambers were removed from wells and slides were mounted with Gerhard Menzel coverslips (Thermo Fisher Scientific), using FluorSave™ reagent (Merck Millipore, Darmstadt, Germany). Slides were set for 10 min under darkness and examined by fluorescent microscopy, via a Leica® Dialux™ 20 Microscope (Leica Microsystems, Milton Keynes, UK). Images were taken at x400 magnification with HCImage acquisition software (Hamamatsu Corporation, Sewickley, USA); and processed via Adobe Photoshop software (Adobe Systems, San Jose, USA). Each experiment was performed at *n = 3*.

2.4 Reverse Transcription-Quantitative Polymerase Chain Reaction

Combined techniques of reverse transcription (RT) and complementary DNA (cDNA) synthesis, followed by amplification via the real-time quantitative polymerase chain reaction (qPCR), were used to assess the effects of epoxy-tigliane treatment (Section 2.1), on the gene expression of differentiation and extracellular matrix (ECM)-related genes (Tables 2.1 and 2.2). Confluent DFs were trypsinised, counted and seeded into sterile 6-well culture plates (Sarstedt; Sections 2.2.1 and 2.2.2). Cells were seeded in FS-CM (2 mL/well), at a cell density of $2.5x10^4$ cells/mL and were maintained at 37 °C in 5 % CO_2/95 % air atmosphere, for the duration of the experiment. After 48 h, cells were growth-arrested via culturing in S-FM (2 mL/well; Section 2.2.1), for 48 h. Post-growth arrest, S-FM was replaced with S-FM containing either EBC-46 or EBC-211 at

the following concentrations: 0 µg/mL, 0.001 µg/mL, 0.01 µg/mL, 0.1 µg/mL, 1 µg/mL or 10 µg/mL (3 wells/concentration); in the absence/presence of TGF-β_1 (10 ng/mL; Section 2.1). Cells were maintained in treated S-FM (2 mL/well) for 24 h, 48 h or 72 h. Following the appropriate treatment period, medium was removed from cells and wells were washed briefly with PBS (x1). Following wash removal, the samples were harvested (Section 2.4.1). During subsequent steps, Ambion™ ribonuclease (RNase)-free/deoxyribonuclease (DNase)-free tubes (Thermo Fisher Scientific), were used to minimise contamination.

2.4.1 RNA Extraction and Purification

Total RNA was extracted using Qiagen RNeasy Mini Kits (Qiagen Ltd., Manchester, UK), according to manufacturer's instructions; with all buffers utilised provided in the Kit. Post-wash removal (Section 2.4), cells were lysed via the addition of Buffer RLT (350 µL/well) and to maximise RNA yield, DF monolayers were further disrupted by well scraping. Cell suspensions were subsequently transferred into sterile tubes (1.5 mL); and vortexed for 15 s to ensure homogeneity. One volume of 70 % ethanol (350 µL), was added to each sample tube in order to promote selective binding to RNeasy membranes. Post-homogenisation via re-pipetting, samples were transferred to the RNeasy Mini spin columns pre-placed in collection tubes (In Kit). Spin columns were centrifuged at 10,000 xg for 30 s and flow-through was discarded. Buffer RW1 (350 µL/column) was then added to aid the removal of contaminants through washing and centrifugation, as above. Flow-through was discarded as previously described and purification of RNA by DNA eradication was initiated.

Additional on-column DNA digestion and removal was performed using RNase-free DNase Kits (Qiagen), according to manufacturer's instructions. All reagents utilised were provided in the Kit and prior to use, DNase I stock was reconstituted in 550 µL RNase-free water. Upon immediate requirement, DNase I master mix was prepared comprising 10 µL DNase I stock solution and 70 µL Buffer RDD (80 µL/sample). After mixing gently, the mix was centrifuged briefly at 10,000 xg and added directly to the column membranes (80 µL/sample) at room temperature, for 15 min. Following the

incubation, Buffer RW1 was added (350 µL/column) to wash away remaining DNase I and the columns were centrifuged at 10,000 xg for 30 s; with flow-eluate discarded, as before. Diluted Buffer RPE (concentrated Buffer RPE, plus four volumes of 100 % ethanol), was subsequently added (500 µL/column), to wash the RNeasy membranes further and centrifugation was performed, as before. Flow-through was discarded and an identical volume of Buffer RPE was added; spin columns were then centrifuged at 10,000 xg for 2 min, drying the membranes. Columns were transferred to fresh 2 mL collection tubes and centrifuged at 10,000 xg for 1 min, ensuring the elimination of ethanol/Buffer RPE carryover into the RNA elution stage. Finally, the columns were transferred to fresh 1.5 mL collection tubes (In Kit); and 30 µL RNase-free water was added to each RNeasy membrane. Following 1 min incubations at room temperature, the spin columns in their collection tubes were centrifuged at 10,000 xg for 1 min, to elute RNA from the membranes.

Concentrations and purities of RNA samples were assessed using a NanoDrop™ 2000 Spectrophotometer (Thermo Fisher Scientific). RNA concentrations were quantified through measuring each sample's absorbance at 260 nm (ng/µL), whilst RNA purity was determined using the 260/280 nm ratio (assessment of protein contamination). Samples were used if their 260/280 nm ratios were >1.8, indicating sufficient purity for downstream applications and further analysis.

2.4.2 Reverse Transcription and Complementary DNA Synthesis

Extracted, purified RNA samples (Section 2.4.1) were converted to complementary DNA (cDNA), with Applied Biosystems™ High Capacity cDNA RT Kits (Thermo Fisher Scientific), according to manufacturer's instructions. All reagents used were provided within the Kit. All stages were performed on ice to preserve RNA integrity; and the random primer method was utilised. RT master mix was prepared containing, per sample: 10 X RT buffer (2 µL), nuclease-free water (3.7 µL), 10 X RT random primers (2 µL), RNase inhibitor (0.5 µL), 25 X deoxyribonucleotide triphosphates (dNTP) Mix (100 mM; 0.8 µL); and Multiscribe™ Reverse Transcriptase (1 µL). After gentle mixing, RT master mix was pipetted into fresh Thermal Cycler tubes (10 µL/sample), along

with the RNA samples (volumes calculated according to RNA concentration). RNase-free water was subsequently added to each tube, to a final volume of 20 µL, and mixed gently. Negative control RTs were performed for each experiment, using RNase-free water as a substitute for RNA sample, to account for any contaminants. Reaction tubes were briefly centrifuged and placed into the PTC-225 Peltier Thermal Cycler (Bio-Rad Laboratories, Watford, UK), before programming the cycle conditions as follows: 25 °C for 10 min, 37 °C for 2 h, 85 °C for 5 min and held at 4 °C. The first stage permitted the random primers to anneal to the RNA and was followed by an 'extension stage', which allowed the reverse transcriptase to attach to dNTPs. A final dissociation stage resulted in the separation of the RNA template/newly synthesised cDNA complex, denaturing the reverse transcriptase simultaneously. The resulting cDNA was stored at -20 °C until required.

2.4.3 Real-Time Quantitative Polymerase Chain Reaction

Amplification of cDNA via qPCR was performed using the Applied Biosystems™ ViiA™ 7 Real-Time PCR System (Thermo Fisher Scientific), via use of Applied Biosystems™ TaqMan® primer probes (Table 2.1) or SYBR™ Green dyes (Table 2.2; all purchased from Thermo Fisher Scientific); according to manufacturer's protocols. Post-thermal cycling (Section 2.4.2), qPCR was carried out in MicroAmp™ Optical 96-Well Reaction Plates (Thermo Fisher Scientific), with 20 µL/well final volumes. For TaqMan®-based reactions, master mix was prepared containing: TaqMan® Fast Universal PCR Master Mix (2 X) no AmpErase® UNG (10 µL), RNase-free water (4 µL), TaqMan® expression assay primer/probe mix (FAM™ reporter/MGB-NFQ quencher; 1 µL); and eukaryotic 18S ribosomal RNA (rRNA) endogenous control (VIC® reporter/TAMRA™ quencher; 1 µL). The TaqMan® target and reference gene expression assay mixes (Table 2.1), contained forward and reverse PCR primers and TaqMan® probes. For SYBR™-based reactions, master mix was prepared containing: Power SYBR™ Green PCR Master Mix (10 µL), RNase-free water (4.8 µL); and forward and reverse primers (10 µM; 0.6 µL/primer). For any SYBR™-based runs, qPCR was performed simultaneously using glyceraldehyde 3-phosphate dehydrogenase (GAPDH) as the reference gene; with custom-designed primer sequences utilised (Table 2.2).

Table 2.1. Applied Biosystems™ TaqMan® gene expression assay mixes. Catalogue and assay IDs are provided *in lieu* of primer sequences, as Applied Biosystems™ do not supply this information.

Gene Target	TaqMan® Gene Expression Assay
18S rRNA	4310893E
αSMA (ACTA2)	Hs00426835_g1
CD44	Hs01075861_m1
EGFR	Hs01076078_m1
TSG6 (TNFAIP6)	Hs00200180_m1
COL3 (COL3α_1)	Hs00943809_m1
ELN	Hs00355783_m1
MMP-1	Hs00899658_m1
HAS1	Hs00758053_m1
HAS2	Hs00193435_m1
HAS3	Hs00193436_m1

Table 2.2. Applied Biosystems™ SYBR™ Green gene expression assay primers. On delivery, primer efficiencies were optimised by group members through use of a 10-fold dilution series (90 - 100 % efficiency accepted).

Gene Target	Custom-Designed Primer Sequences
GAPDH	**Forward:** 5'-CCTCTGATTCAACAGCGACAG-'3 **Reverse:** 5'-TGTCATACCAGGAAATGAGCTTGA-'3
EDA-FN	**Forward:** 5'GCTCAGAATCCAAGCGGAGA'3 **Reverse:** 5'-CCAGTCCTTTAGGGCGATCA-'3
COL1 (COL1α_1)	**Forward:** 5'-TGTTCAGCTTTGTGGACCTCCG-'3 **Reverse:** 5'-CGCAGGTGATTGGTGGGATGTCT-'3

Each reaction mixture was mixed gently and briefly centrifuged, prior to 16 µL being added to each well. Respective cDNA samples (4 µL) were subsequently added to the wells. Negative control reactions were also included for each plate, with RNase-free water substituting the cDNA samples, to account for any reagent contamination and undesirable signal. Reaction plates were then covered and sealed with MicroAmp™ Optical Adhesive Film (Thermo Fisher Scientific), limiting the possibility of well cross-contamination. After a 30 s centrifugation step, the reaction plates were transferred to the PCR system.

2.4.4 Relative Quantification

Following completion of qPCR runs, the comparative cycle threshold (ΔΔCT) method was used to calculate the relative quantification (RQ) of gene expression. CT values, where amplification is within the curve's linear range, were used in this process. CTs of the standard reference gene (rRNA or GAPDH) were subtracted from target gene CT values to obtain delta CT (dCT) values (known as the cycle threshold differences). The mean dCT value for the experimental control group samples was calculated and subsequently, expression of the target gene in experimental samples relative to the mean control group expression was determined using the following equation:

$$2^{-(dCT(\text{Experimental Target}) - dCT(\text{Mean Control Group}))}$$

Resulting RQ values for every sample group/experimental condition were averaged and standard error of the mean (SEM) values were calculated. Each experiment was performed independently at $n = 3$.

2.5 Western Blotting

Western blotting was performed to elucidate the effects of epoxy-tigliane treatment (Section 2.1), upon DF/myofibroblast synthesis of ECM components. Western blot analyses of protein levels were performed for type I and type III collagens, peptidase inhibitor 16 (PI16) and elastin. Following trypsinisation, DFs were counted and seeded into separate 75 cm^2 cell culture flasks (Sections 2.2.1 and 2.2.2). Cells were seeded

in FS-CM (10 mL/flask) at a cell density of 9 x 10^4 cells/mL and were cultured in a 37 °C humidified incubator, within 5 % CO_2/95 % air atmosphere, for the duration of the experiment. After 48 h, cells were growth-arrested through culturing in S-FM (10 mL/flask; Section 2.2.1) for 48 h. Post-growth arrest, S-FM was replaced with S-FM, containing either EBC-46 or EBC-211 at the following concentrations: 0 µg/mL, 0.001 µg/mL, 0.01 µg/mL, 0.1 µg/mL, 1 µg/mL or 10 µg/mL (1 flask/concentration); in the presence of TGF-β_1 (10 ng/mL; Section 2.1). Cells were cultured in treated S-FM (10 mL/flask), for 24 h or 72 h. Following the appropriate treatment period, medium was removed from the cells and flasks were washed briefly in ice-cold PBS (x1). Post-wash removal, the flasks were harvested for total protein extraction (Section 2.5.1). During ensuing steps, sterile Eppendorf® tubes (1.5 mL; Eppendorf Ltd., Stevenage, UK), were used to minimise contamination. Comprehensive buffer (Table 2.3) and primary antibody (Table 2.4) lists are included.

2.5.1 Protein Extraction and Quantification

Total protein was extracted via use of the Pierce® Radio-Immunoprecipitation Assay (RIPA) extraction buffer (Thermo Fisher Scientific), according to the manufacturer's instructions. Prior to use, one cOmplete™ Protease Inhibitor Cocktail tablet (Roche Ltd., Welwyn Garden City, UK), was added to 25 mL of ice-cold RIPA buffer (Table 2.3) and vortexed to dissolve. Post-wash removal (Section 2.5), DFs were lysed by addition of RIPA/inhibitor buffer (400 µL/flask). Cell/ECM lysates were obtained by scraping the flask contents into the buffer before transfer into pre-chilled tubes. To maximise protein yield, samples were sonicated using a Digital SLPe™ Cell Disruptor (Branson Ultrasonics, Slough, UK); and vortexed briefly before centrifuging at 10,000 xg for 15 min, at 4 °C. Resulting supernatants were subsequently transferred into fresh, pre-chilled 1.5 mL tubes and samples were stored at -80 °C, until required.

In order to determine protein concentration, extracted supernatants were quantified via the Pierce® Bicinchoninic Acid (BCA) Protein Assay Kit (Thermo Fisher Scientific); according to manufacturer's protocol. A standard BSA series was prepared between a range of 125 - 2000 µg/mL as a concentration reference. Standards and samples

were vortexed briefly and centrifuged at 8000 xg for 30 s, at 4 °C. Both standards and extracted supernatants were then added to a 96-well plate (10 µL/well; in duplicate) and Pierce® Working Reagent (200 µL/well) was added. Plates were then shaken for 30 s and incubated at 37 °C for 30 min. Following incubation, protein quantification was performed through measuring endpoint absorbance at 562 nm via a FLUOstar® Omega Plate Reader (BMG Labtech, Aylesbury, UK); and the combined analysis software, MARS™. Values calculated were standard curve-dependent and the mean absorbance measurements of blank replicates were subtracted from the readings of all of the other standards and samples. Final protein concentrations were expressed as µg/mL.

2.5.2 Protein Separation, Transfer and Membrane Blocking

Following extraction and quantification, protein separation and identification was performed using sodium dodecyl sulphate-polyacrylamide gel electrophoresis (SDS-PAGE)/Western blotting analysis. Sample protein supernatants (10 µg) were pipetted into sterile Eppendorf® PCR tubes (0.2 mL; Eppendorf Ltd.) and reducing buffer (Bio-Rad Laboratories; Table 2.3) was added (3 parts sample:1 part reducing buffer). The tubes were then vortexed briefly, centrifuged for 30 s and incubated at 95 ^{o}C for 5 min. Following incubation, tubes were centrifuged for 30 s and left to cool on ice. Subsequently, total sample volumes were loaded into 4-15 % Mini-PROTEAN® TGX™ pre-cast gradient gels (15-wells, holding 15 µL/well; Bio-Rad Laboratories). Each sample set was run with 8 µL of pre-stained Precision Plus Protein™ Kaleidoscope™ ladder (Bio-Rad Laboratories), through the Mini-Protean® Tetra Cell system (Bio-Rad Laboratories). The tank was filled with 1X running buffer (Table 2.3) and the samples underwent SDS-PAGE separation for 80 min at 100 V.

During the electrophoretic period, Hybond™-P 0.45 polyvinylidene difluoride (PVDF) blotting membranes (GE Healthcare, Amersham, UK), were prepared by soaking in methanol, dd-H_2O and transfer buffer (Table 2.3), consecutively for 5 min each. Post-separation, gels were detached from casts and assembled into a transfer 'sandwich' comprising a transfer cassette (x1), sponges (x4), gradient gel (x1), PVDF membrane

Table 2.3. Buffers for SDS-PAGE/Western blotting techniques. List of buffers used during protein extraction, quantification, separation, transfer and blot probing.

Buffer	Contents
Pierce® RIPA/cOmplete™ inhibitor lysis and extraction buffer (25 mL)	25 mM Tris-HCl (pH 7.6), 150 mM NaCl, 1 % NP-40, 1 % sodium deoxycholate, 0.1 % SDS, 1 cOmplete™ Protease Inhibitor Cocktail tablet (Roche Ltd.).
Reducing buffer (1 mL)	β-mercaptoethanol (100 µL), 4X Laemmli Sample Buffer (Bio-Rad Laboratories, 900 µL).
Running buffer (1 L)	For 10X: 30 g Tris/Trizma®, 144 g glycine, 10 g SDS, top up to 1 L with dd-H_2O (all purchased from Sigma-Aldrich). For 1X: 100 mL running buffer (10X), 900 mL dd-H_2O.
Transfer buffer (1 L)	For 10X: 30 g Tris/Trizma®, 144 g glycine, top up to 1 L with dd-H_2O. For 1X: 100 mL transfer buffer (10X), 200 mL methanol (Sigma-Aldrich), 700 mL dd-H_2O.
Tris-buffered saline (TBS; 1 L)	For 10X: 24.2 g Tris/Trizma®, 80 g sodium chloride (Sigma-Aldrich), made up to 1 L with dd-H_2O (pH 7.4). For 1X: 100 mL TBS (10X), 900 mL dd-H_2O.
1 % TBS-Tween (1 L)	1 mL Tween® 20 (Sigma-Aldrich) in 1 L TBS (1X).
Blocking buffer (50 mL)	5 % (w/v) powdered skimmed milk (2.5 g), made up to 50 mL with 1 % (v/v) TBS-Tween.

(x1); and extra thick filter paper (x2; all purchased from Bio-Rad Laboratories). All components were pre-soaked in transfer buffer and on assembly, a Mini Trans-Blot® Cell System (Bio-Rad Laboratories), was filled with cold 1X transfer buffer. When the transfer cassette and ice block were placed within the cell system, the proteins were transferred to the PVDF membrane at 100 V for 1 h. Protein transfer efficiency was determined by membrane exposure to Ponceau S solution (Sigma-Aldrich), for 5 min at room temperature, upon the plate rocker. Once effective transfer was confirmed, the stain was removed through 10 min washes with dd-H_2O (x3) on the plate rocker. Membranes were subsequently incubated with 5 % milk blocking buffer (Table 2.3), for 1 h on the plate rocker, at room temperature, to prevent non-specific binding.

2.5.3 Membrane Probing and Visualisation

Post-blocking, blots were rinsed for 1 min with 1 % tris-buffered saline (TBS)-Tween (x1; Table 2.3), on the plate rocker at room temperature. Blots were then incubated with the chosen primary antibody (Table 2.4), diluted in blocking buffer (Table 2.3). All primary antibodies used, along with their dilutions and incubation conditions, are detailed in Table 2.4 (all purchased from Abcam, Cambridge, UK). Protein loading levels were confirmed upon each blot, utilising β-actin as a loading control (Abcam). Following primary antibody incubation, blots were washed for 5 min with 1 % TBS-Tween (x3), on the plate rocker, at room temperature. Swine polyclonal anti-rabbit horseradish peroxidase (HRP)-conjugated secondary antibody (0.26 g/L; Dako), diluted within blocking buffer (1:5000), was utilised to incubate the membranes; for 1 h, at room temperature, on the plate rocker. Post-secondary exposure, blots were washed again for 5 min with 1 % TBS-Tween (x3), at room temperature, on the plate rocker; which was followed by a final wash in TBS alone, in order to ensure removal of background (Table 2.3).

Proteins were visualised using the enhanced chemiluminescence (ECL) method. This was performed through exposure to ECL™ Prime Detection Reagent (GE Healthcare). To ensure full coverage and reactivity, membranes were incubated for 3 min, under darkness, at room temperature; before placing in a Hypercassette™ (GE Healthcare).

Hyperfilm™-ECL™ (GE Healthcare), was placed on the membranes and left to expose for the appropriate time period, according to manufacturer's instructions. Film was subsequently developed through the use of a Curix-60 Developer (AGFA Healthcare, Greenville, USA). Immunoblot images were scanned using a Gel Doc™ EZ System and Image Lab™ Software (Bio-Rad Laboratories). Each experiment was performed independently at *n = 3*.

Table 2.4. Western blot primary antibodies. Summary list of the primary antibodies used during Western blot analysis; including their expected molecular weights, host animals, clonal type, concentrations, selected dilutions and preferred incubation conditions (Abcam, Cambridge, UK).

Primary Antibody	Type and Host	Concentration	Dilution	Expected Molecular Weight	Incubation Conditions
β-actin	Polyclonal - Rabbit	0.9 mg/mL	1:20,000	42 kDa	1 h at RT
Type I Collagen	Polyclonal - Rabbit	0.9 mg/mL	1:5000	130 kDa	4 °C overnight
Type III Collagen	Polyclonal - Rabbit	2 mg/mL	1:1000	138 kDa	4 °C overnight
Elastin	Polyclonal - Rabbit	0.9 mg/mL	1:1000	68 kDa	4 °C overnight
PI16	Polyclonal - Rabbit	1 mg/mL	1:1000	100 kDa	4 °C overnight

2.6 Hyaluronan Enzyme-Linked Immunosorbent Assays

To assess the effects of epoxy-tigliane treatment (Section 2.1), on DF/myofibroblast synthesis and release of hyaluronan (HA), HA enzyme-linked immunosorbent assays (ELISAs) were performed to quantify soluble HA released into the media. Following trypsinisation, confluent cells were counted and seeded into sterile 6-well plates (Sections 2.2.1 and 2.2.2). DFs were seeded in FS-CM (2 mL/well) at a cell density of $2.5x10^4$ cells/mL and were maintained at 37 °C, in a 5 % CO_2/95 % air atmosphere, for the duration of the experiment. Following 48 h, cells were growth-arrested through culturing in S-FM (2 mL/well; Section 2.2.1), for 48 h. After growth arrest, S-FM was replaced with S-FM, containing either EBC-46 or EBC-211 (0 µg/mL, 0.001 µg/mL, 0.01 µg/mL, 0.1 µg/mL, 1 µg/mL or 10 µg/mL; 3 wells/concentration), in the absence or presence of TGF-β_1 (10 ng/mL; Section 2.1). Cells were maintained in treated S-FM (2 mL/well) for 72 h. After 72 h treatment, conditioned media samples were collected into sterile Eppendorf® tubes (1.5 mL); and stored at -80 °C until required. HA concentrations were assessed using HA ELISA Test Kits (Corgenix, Broomfield, USA), according to manufacturer's instructions. All of the reagents, buffers, controls and reference solutions were provided (In Kit), which were warmed to room temperature before use. Immediately before use, wash buffer was prepared using 33X concentrate PBS wash (30 mL; In Kit), made up to 1 L with dd-H_2O (0.01 M final concentration, pH 7.35).

Once at room temperature, all HA reference solutions, HA controls and conditioned media samples were briefly vortexed and centrifuged for 30 s. Each of these was subsequently diluted in fresh 1.5 mL tubes by adding 10 parts reaction buffer:1 part solution/control/sample. All dilutions were vortexed and centrifuged as before, and 100 µL of each were added to the appropriate wells of a HA binding protein (HABP)-coated 96-well plate. Reagent blanks (100 µL reaction buffer) were also included to represent the 0 ng/mL reference solution, giving an overall plate reference range of 0 - 800 ng/mL. The assay was then incubated for 1 h at room temperature, to allow the HA present in the samples to bind the immobilised HABP. Post-incubation, wells were emptied carefully to avoid cross-contamination and washed using wash buffer

(x4) to remove non-bound molecules. Wells were inverted between each wash and any excess buffer was removed by blotting plates on absorbent paper. After residue removal, HRP-conjugated HABP solution was added (100 µL/well) and incubated for 30 min at room temperature; allowing complex formation with bound HA. The wells were then emptied and washed, as previously described. One-component substrate solution (100 µL/well) was subsequently added for 30 min, under darkness, at room temperature; allowing a chromogenic reaction to occur. Lastly, 100 µL stop solution (0.36 N sulphuric acid), was added to each well to end the enzymatic reaction.

HA concentration was determined spectrophotometrically by measuring the optical density (OD) of every well at 450 nm using the FLUOstar® Omega Plate Reader; and its incorporated analysis software, MARS™. Values calculated were standard curve-dependent, which were plotted from the mean ODs of reagent blanks and reference solutions of known concentration (assayed in duplicate). Mean concentrations of HA (ng/mL) and the SEM values were calculated for each condition/sample group. Each of the experiments were performed independently, at *n = 3*.

2.7 Hyaluronan Particle Exclusion Assays

To assess the effects of epoxy-tigliane treatment (Section 2.1), on the formation of HA pericellular coats by DFs/myofibroblasts, erythrocyte particle exclusion assays were performed in order to visualise HA accumulation in DF pericellular regions; as previously described (Meran *et al.* 2007, 2008). Following trypsinisation, confluent DFs were counted and seeded into sterile 6-well culture plates (Sections 2.2.1 and 2.2.2). Cells were seeded in FS-CM (2 mL/well), at a density of $2.5x10^4$ cells/mL and were cultured in a 37 °C humidified incubator, in 5 % CO_2/95 % air atmosphere, for the duration of the experiment. Following 48 h, DFs were growth-arrested through culturing in S-FM (2 mL/well; Section 2.2.1), for a further 48 h. After growth arrest, S-FM was replaced with S-FM containing either EBC-46 or EBC-211 (0 µg/mL, 0.001 µg/mL, 0.01 µg/mL, 0.1 µg/mL, 1 µg/mL or 10 µg/mL; 3 wells/concentration), in the absence or presence of TGF-β_1 (10 ng/mL; Section 2.1). Cells were maintained in treated S-FM (2 mL/well) for 72 h and after treatment, medium was removed from

the DFs. Pericellular coat/region visualisation was performed by incubating cells with formalised horse erythrocytes, which were extracted from defibrinated horse blood (TCS Biosciences, Buckingham, UK). In advance of experimentation, blood samples (3 mL) were washed consecutively with PBS (20 mL); and centrifuged at 1000 xg for 7 min at 4 °C, until the supernatant was clear. Following the final wash, erythrocyte pellets were resuspended in 1 mL of S-FM. Upon removal of conditioned medium, DF monolayers were treated with erythrocytes suspended in S-FM (50 µL erythrocyte resuspension in 1 mL S-FM/well). Plates were gently agitated to evenly distribute the erythrocytes; prior to incubation at 37 °C, for 10 - 30 min, in 5 % CO_2/95 % air atmosphere. Erythrocyte confluence was optimised and observed during incubation to assess the wells for optimal resolution. Through HA's molecular size and its polyanionic nature, erythrocytes are repelled from the DF cell membranes; resulting in the formation of 'exclusion zones' representing pericellular coat regions. Zones were visualised under light microscopy, using an Axiovert™ 135 Inverted Microscope (Zeiss, Oberkochen, Germany) with a C5985™ CCD camera (Hamamatsu Corporation, Sewickley, USA). Digital images were taken at x100 magnification using OpenLab™ 3.0.8 Software (Improvision Ltd., Coventry, UK). Each experiment was performed independently at *n = 3*.

2.8 Global Gene Expression Analysis by Microarray

Microarray analysis was performed to assess any gene expression changes occurring in DFs/myofibroblasts, in response to a range of epoxy-tigliane treatments. Following trypsinisation, DFs (derived from four patient sources; Section 2.2.1) were counted and seeded into separate sterile 175 cm^2 tissue culture flasks (Sarstedt; Sections 2.2.1 and 2.2.2); at a density of 9 x 10^4 cells/mL (20 mL FS-CM/flask). DFs were maintained at 37 °C, in 5 % CO_2/95 % air atmosphere, for the duration of the experiment. Post-48 h culture, cells were growth-arrested via culturing in S-FM (20 mL/flask; Section 2.2.1), for 48 h. Subsequently, S-FM was replaced with S-FM containing either EBC-46 (0.01 µg/mL or 0.1 µg/mL) or EBC-211 (1 µg/mL or 10 µg/mL); in the presence of TGF-β_1 (10 ng/mL; Section 2.1). Compound-free controls were also included, in the presence of TGF-β_1 (10 ng/mL; Section 2.1). Cells were cultured in treated S-FM (20

mL/flask) for either 24 or 72 h (Table 2.5). In total, 12 flasks/patient were established for *n = 4* independent experiments (Table 2.5). Following the appropriate treatment period, all medium was removed from the cells; this was immediately replaced with a mixture of RNAprotect® Cell Reagent (5 mL; Qiagen Ltd.) and the respective culture media (1 mL) at a 5:1 ratio/flask. After gentle agitation, the cell suspensions were transferred to sterile Falcon™ tubes (15 mL; Sigma-Aldrich) and stored at 4 °C for later shipment to the QIMR Berghofer Medical Research Institute (QIMR; Brisbane, Australia). Further experimental work and sample analysis was performed by Dr Rachael Moses (School of Dentistry, Cardiff, UK), at QIMR.

2.8.1 RNA Extraction, Purification and Quantification

Total RNA was extracted from samples (Section 2.8), using Qiagen RNeasy Plus Mini Kits (Qiagen Ltd., Chadstone, Australia), according to the manufacturer's instructions. All buffers and tubes used were provided in the Kit. Cell/RNAprotect® suspensions (650 µL/sample), were transferred to RNase-free tubes and centrifuged at 10,000 xg for 1 min at room temperature. Resulting supernatants were discarded and the remaining cell pellets were resuspended in Buffer RLT Plus (350 µL/sample), containing 0.1 % β-mercaptoethanol. Resuspended lysates were then homogenised via vortexing, prior to transfer to genomic DNA (gDNA) eliminator spin columns, pre-placed in collection tubes. The spin columns were centrifuged at 10,000 xg for 30 s at room temperature and resulting flow-through was kept. Spin columns were then discarded, eliminating any gDNA contamination. One volume of 70 % ethanol (350 µL/sample), was added to collected flow-throughs, in order to promote selective binding of RNA to RNeasy membranes. After homogenisation via pipetting, samples were transferred to their respective RNeasy spin columns, pre-placed in collection tubes. Spin columns were centrifuged as prior and flow-through was discarded, in advance of Buffer RW1 (700 µL/column) addition. To aid removal of contaminants by washing, centrifugation was performed and flow-through was discarded, as prior. Diluted Buffer RPE (Buffer RPE, plus four volumes of 100 % ethanol), was then added (500 µL/column; x2) to wash the RNeasy membranes further. The first centrifugation step was performed as before, whereas the second was extended to 2 min to dry the

Table 2.5. Microarray cell culture conditions. Summary of the ten culture conditions established/patient source for each HumanHT-12v4 BeadChip (Illumina®, Scoresby, Australia). A total of 40 samples underwent microarray gene analysis (*n = 4* individual experiments), to obtain a global expression profile of changes occurring in DFs/ myofibroblasts, in response to EBC-46 and EBC-211 treatment.

Treatment Number	Epoxy-Tigliane Concentration (µg/mL)	TGF-β_1 Concentration (ng/mL)	Treatment Incubation Time (h)
1	0 (1 % DMSO)	10	24
2	0 (1 % DMSO)	10	72
3	0.01 EBC-46	10	24
4	0.01 EBC-46	10	72
5	0.1 EBC-46	10	24
6	0.1 EBC-46	10	72
7	1 EBC-211	10	24
8	1 EBC-211	10	72
9	10 EBC-211	10	24
10	10 EBC-211	10	72

membranes. The spin columns were transferred to fresh 2 mL collection tubes and centrifuged at 10,000 xg for 1 min at room temperature, to ensure the elimination of ethanol and Buffer RPE carry-over into the RNA elution stages. Spin columns were subsequently transferred to new collection tubes (1.5 mL) and nuclease-free water (50 µL/column) was added directly to the RNeasy membranes. Following a 1 min incubation at room temperature, the spin columns/collection tubes were centrifuged at 10,000 xg for 1 min, at room temperature; to elute the RNA.

RNA concentration and purity of samples was determined using the NanoDrop® Lite (Thermo Fisher Scientific, Scoresby, Australia). Sample purities were assessed using 260/280 nm absorbance ratios (assessment of protein contamination); purities >1.8 were considered satisfactory for downstream applications and further analysis. RNA integrity was evaluated via agarose gel electrophoresis; a 2:1 ratio of 28S rRNA:18S rRNA confirmed sample integrity. Agarose gels (1 %) were prepared using SeaKem® LE agarose (Lonza, Mount Waverley, Australia) and 1X Tris/Acetate/EDTA (TAE) buffer (Thermo Fisher Scientific; Merck Millipore, Bayswater, Australia; Univar Ltd., Ingleburn, Australia, respectively). The agarose was dissolved via heating and mixed thoroughly before cooling; and addition of 10 mg/mL ethidium bromide (8 µL; Sigma-Aldrich, Castle Hill, Australia). The mixture was homogenised, poured into an RNase-free gel casting mould and set at room temperature for 30 min. RNA samples (10 µL) were subsequently loaded into the gel wells and run alongside 1 kB DNA marker (10 µL; Thermo Fisher Scientific). Electrophoresis was applied to loaded gels at 90 V for 30 min in 1X TAE running buffer; upon run completion, gels were viewed and images were taken under 312 nm ultraviolet (UV) light using the Vilber Lourmat® UV imager (Thermo Fisher Scientific). The DNA marker served as a guide for molecular size.

2.8.2 Complementary RNA Synthesis and Purification

Extracted RNA samples (Section 2.8.1) were prepared for microarray analysis via use of Illumina® TotalPrep™ RNA Amplification Kits (Thermo Fisher Scientific); according to manufacturer's instructions. All the buffers, reagents and cartridges utilised were provided in the Kit. To amplify and generate biotinylated complementary RNA (cRNA)

before hybridisation (Section 2.8.3), total RNA (500 ng/sample) was transferred into Ambion™ RNase-free microtubes (Thermo Fisher Scientific). The samples were then adjusted to final 11 µL volumes using nuclease-free water. To synthesise first strand cDNA, RT master mix was prepared comprising, per sample: 10 X First Strand Buffer (2 µL), RNase Inhibitor (1 µL), Array Script™ Reverse Transcriptase (1 µL), dNTP Mix (4 µL) and T7 Oligo(dT) Primer (1 µL). Master Mix (9 µL/sample) was then added to the tubes, mixed thoroughly and centrifuged at 10,000 xg at room temperature, for 15 s. Samples were subsequently placed in the GeneAmp™ 2400 PCR system (Perkin Elmer, Melbourne, Australia); and incubated at 42 °C for 2 h. Post-cycle, the samples were centrifuged at 10,000 xg for 15 s at 4 °C; and stored upon ice.

In order to create a double-stranded cDNA template, second strand cDNA synthesis was begun by preparation of master mix containing, per sample: 10X Second Strand Buffer (10 µL), dNTP Mix (4 µL), RNase H (1 µL), DNA Polymerase (2 µL); and nuclease-free water (63 µL). Master mix (80 µL/sample) was subsequently added to samples, mixed thoroughly and centrifuged at 10,000 xg for 15 s, at 4 °C. Tubes were placed in the GeneAmp™ 2400 PCR System and incubated at 16 °C for 2 h. Following the cycle, second strand cDNA samples were purified through addition of cDNA binding buffer (250 µL/sample). Tubes were mixed thoroughly and centrifuged at 10,000 xg for 15 s at 4 °C before samples were transferred to filter cartridges, pre-placed in collection tubes (In Kit). Filter cartridges were then centrifuged at 10,000 xg for 1 min at room temperature and flow-through was discarded. Wash buffer (500 µL/cartridge) was added to aid contaminant removal and centrifugation was performed as prior, with flow-eluate discarded as before. Cartridges were re-spun to ensure the full removal of wash buffer before their transfer to cDNA elution tubes (In Kit). Lastly, cDNA was eluted using nuclease-free water, pre-warmed to 55 °C (20 µL/cartridge); following 2 min incubation and centrifugation at 10,000 xg for 1.5 min, both performed at room temperature.

Post-cDNA elution, biotin-labelled cRNA was synthesised using *in vitro* transcription (IVT). Master mix was prepared according to manufacturer's instructions, containing

per sample: T7 10 X Reaction Buffer (2.5 µL), T7 Enzyme Mix (2.5 µL) and Biotin-NTP mix (2.5 µL). Master mix (7.5 µL/sample) was subsequently added to samples, mixed thoroughly and centrifuged at 10,000 xg for 15 s at 4 °C. Tubes were then placed in a 37 °C Thermal Cycler for 16 h. Post-incubation, enzymatic reactions were terminated by nuclease-free water addition (75 µL/sample); and mixed by gentle vortexing. After labelled cRNA synthesis, cRNA purification was performed to remove enzymes, salts and unincorporated nucleotides. cRNA Binding Buffer (350 µL) and 100 % ACS grade ethanol (250 µL; Sigma-Aldrich) were added to each sample, mixed thoroughly by re-pipetting and solutions were immediately transferred to cRNA filter cartridges, pre-placed in collection tubes (In Kit). Filter cartridges were centrifuged at 10,000 xg for 1 min at room temperature and flow-eluate was discarded, before wash buffer (650 µL/cartridge) was added. Centrifugation and flow-through removal were performed, as prior. Cartridges were re-spun to ensure full removal of trace wash buffer, before transfer to new cRNA collection tubes (In Kit). Lastly, cRNA was eluted by addition of nuclease-free water, pre-warmed to 55 °C (100 µL/cartridge). After 2 min incubation at room temperature, the filter cartridges were centrifuged at 10,000 xg for 2 min at room temperature, to elute purified cRNA. Sample concentrations and cRNA purities were assessed, as detailed previously (Section 2.8.1).

2.8.3 Illumina® Complementary RNA Hybridisation

Direct hybridisation of cRNA samples to the complementary gene-specific sequence HumanHT-12v4 BeadChips (Illumina®), was performed through the Whole-Genome Gene Expression Assay System (Illumina®); according to manufacturer's instructions. All reagents, tubes and BeadChips used were provided in the Kit and the latter were warmed to room temperature, prior to use. Furthermore, HYB and HCB tubes were incubated at 58 °C and mixed thoroughly for 10 min, before use. cRNA samples (750 ng) were aliquoted into separate hybridisation tubes and volumes were made up to 5 µL/sample with RNase-free water. Tubes were subsequently heated at 65 °C for 5 min, briefly centrifuged and cooled to room temperature. HYB Mix (10 µL) was then added to each sample.

In preparation for cRNA loading, hybridisation chambers were assembled and HCB Buffer (200 µL) was decanted into eight humidifying buffer reservoirs (x4 inserts for x4 chips). The cRNA samples (15 µL) were subsequently loaded onto HumanHT-12v4 BeadChips (Illumina®) and these were placed into the chambers, securely sealed and incubated on a rocker; at 58 °C for 16 h. After incubation, BeadChips were removed from the hybridisation chambers and a number of wash stages were carried out; as described below, and according to the manufacturer's instructions. On removal, the BeadChips were submerged in Wash E1BC Solution (comprising 6 mL E1BC Buffer in 2 L RNase-free water) and cover-seals were detached. BeadChips were then placed within the slide racks, submerged in Wash E1BC Solution (250 mL/rack); which were transferred to an Illumina® Hybex® Waterbath immersed in high-temperature Wash Buffer (250 mL; lllumina®). Following 10 min incubation, the slide racks were rinsed sequentially with fresh Wash E1BC Solution (x10; 250 mL/rack); before transferring to an orbital shaker for 5 min at room temperature (for all forthcoming shake steps, the orbital shaker was set to medium-low). Slide racks were washed successively in 100 % ethanol (250 mL/rack) as before, and shaken for 10 min at room temperature. Slide racks were washed again with new Wash E1BC Solution (x10; 250 mL/rack) and shaken for 2 min at room temperature. BeadChips were subsequently transferred to their respective wash trays and Block E1 Buffer was added (4 mL/tray), for 10 min at room temperature upon a plate rocker (for all rock steps, speed was set at medium). Block E1 Buffer was removed and replaced with new Buffer containing Streptavidin-Cy3 (1:1000; 2 mL/tray), which binds biotinylated cRNA; trays were rocked as prior. BeadChips were subsequently transferred to their slide racks, washed consecutively in Wash E1BC Solution (x5; 250 mL/rack) and shaken for 5 min at room temperature. Finally, slide racks containing BeadChips were dried via centrifugation at 1000 xg for 4 min, at room temperature.

2.8.4 Data Acquisition and Gene Expression Analysis

BeadChips were scanned with the iScan™ System on an Agilent™ GS2565 Microarray Scanner (Agilent Technologies, Mulgrave, Australia) according to the manufacturer's instructions. The system used a laser to excite the fluor of the single-base extension

product on the beads, with the subsequent light emissions recorded and analysed. BeadChips were scanned according to the Whole-Genome Gene Expression Direct Hybridisation Assay Guide (Illumina®); decoded data input into the iScan™ system corresponded to specific BeadChips.

The aforementioned BeadChips cover >47,000 transcripts and known splice variants across the human transcriptome; providing a genome-wide transcriptional coverage of >25,000 characterised genes, gene candidates and splice variants. Raw data files were filtered, normalised and extracted via BeadStudio™ Gene Expression Module and BeadScan™ Software (Illumina®). Data was then imported into the GeneSpring™ GX v12.5 Expression Analysis Software (Agilent Technologies), for normalisation and detection score-based filtering, heatmap clustering and visualisation; and statistical analysis. Expression values were normalised via quantile normalisation with default settings; entities were filtered based upon detection score calculated using Genome Studio™ Software (Illumina®), where $p = <0.05$ was considered significant. Data from each treatment group ($n = 4$ independent experiments) were grouped for combined analyses through Ingenuity® Pathway Analysis (IPA®) Software (Qiagen Ltd.). Further analysis of the microarray data with IPA® Software used Ingenuity® Knowledge Base (Qiagen Ltd.) to visualise gene pathways and aid microarray dataset interpretation.

Various databases were utilised to identify characteristics and functions of genes of interest, in addition to information obtained with GeneSpring™ GX v12.5 Expression Analysis Software and IPA® Software. The databases utilised included GeneCards (*www.genecards.org*), PubMed (*www.ncbi.nlm.nih.gov/gene*) and Uniprot (*www.uniprot.org*).

2.9 Matrix Metalloproteinase Activity Assays

Matrix metalloproteinase (MMP) activity assays were undertaken to assess changes in MMP activity levels; post-DF treatment with EBC-46 and EBC-211 (0 µg/mL, 0.001 µg/mL, 0.01 µg/mL, 0.1 µg/mL, 1 µg/mL or 10 µg/mL), in the presence of TGF-β_1 (10 ng/mL; Section 2.1), at 24 h and 72 h. Following trypsinisation, cells were counted,

seeded, growth-arrested and treated, as previously described (Section 2.5). After the appropriate treatment period, conditioned media samples were collected into sterile Eppendorf® tubes (1.5 mL); and maintained at -80 °C until required. MMP-1 activities were quantified via SensoLyte® Plus 520 MMP-1 Assay Kits, while MMP-3/-10/-12 activity levels were quantified using SensoLyte® 520 MMP-3/-10/-12 Assay Kits, respectively (all purchased from AnaSpec, Liège, Belgium). Assays were performed according to the manufacturer's instructions; with all of the buffers, substrates, reference standards and reagents provided in each Kit, which were thawed to room temperature before use. When required, media samples were thawed on ice, briefly vortexed and centrifuged for 30 s.

Total MMP-1 was isolated by addition of media samples and MMP-1 standards (100 µL/well) to appropriate wells of a monoclonal anti-human MMP-1 antibody-coated 96-well plate. Reagent blanks (dilution buffer) were also included to represent the 0 ng/mL reference solution, giving an overall plate reference range of 0 - 200 ng/mL. Plates were sealed with adhesive film (In Kit), to prevent evaporation and incubated for 2 h at room temperature on a plate rocker, allowing any MMP-1 present within samples to bind to the immobilised antibodies. Post-incubation, wells were emptied carefully to avoid any cross-contamination and rinsed using 1X wash buffer (200 µL/ well; x4), to remove non-bound molecules. Wells were inverted between each wash and any residual solution was removed by blotting plates on absorbent paper. After excess buffer removal, pro-MMP-1 was activated through sample incubation with 1 mM 4-aminophenylmercuric acetate (APMA; 100 µL/well; In Kit). Plates were sealed using adhesive film and incubated for 3 h at 37 °C, before wells were emptied and washed as previously described. After excess buffer removal, MMP-1 substrate (100 µL) was added to each well and plates were sealed prior to incubation at room temperature for 1 h, under darkness. MMP-1 activity is measured through the substrate's 5-FAM/QXL™ 520 fluorescence resonance energy transfer (FRET) peptide, which upon cleavage, releases the fluorophore from its quencher. Fluorescence intensity was quantified at 490 nm/520 nm excitation/emission using the FLUOstar® Omega Plate Reader; and its incorporated analysis software, MARS™. The values

calculated were standard curve-dependent, which was plotted from mean readings of the reagent blanks and six reference standards of known concentration (tested in duplicate). The average value gained for reagent blanks represented background fluorescence and was subtracted from all of the other well readings. Mean relative fluorescence unit (RFU) values and their SEM values were calculated for each condition/sample group. Each experiment was performed independently at *n = 3*.

MMP-3/-10/-12 activity levels were quantified using SensoLyte® 520 MMP-3/-10/-12 Assay Kits, respectively. Before adding samples to black flat-bottomed 96-well plates (Thermo Fisher Scientific), pro-MMPs were activated by incubation of culture media samples with 1 mM APMA; this was performed in sterile Eppendorf® tubes (0.5 mL; Eppendorf Ltd.). Samples undergoing analysis for MMP-3 and MMP-10 activity levels were activated for 24 h at 37 °C, whilst those undergoing analysis for MMP-12 were activated for 2 h at 37 °C. Following the appropriate incubation periods, tubes were maintained upon ice to stop further pro-MMP activation. Samples and fluorescence reference standards were then added to their respective wells (50 µL/well); reagent blanks (assay buffer) were included to represent 0 µM reference standard, giving an overall plate reference range of 0 - 2.5 µM. MMP-3/-10/-12 substrate solutions (1X) were added to their respective sample/control wells (50 µL/well); and mixed well by gently shaking the plate for 30 s. To initiate enzymatic reactions, plates were sealed and incubated at 37 °C for 1 h, under darkness. Using the same method as MMP-1, fluorescence intensity was quantified at 490 nm/520 nm excitation/emission using the FLUOstar® Omega Plate Reader and its incorporated analysis software, MARS™. Values obtained were standard curve-dependent, which was plotted from the mean readings of reagent blanks and six 5-FAM-Pro-Leu-OH reference standards of known concentration (tested in duplicate). The average value gained for the reagent blanks represented background fluorescence, which was subsequently subtracted from all other well readings. Mean RFU values and their SEM values were calculated for each condition/sample group. Each experiment was performed upon *n = 3* sample sets for each MMP analysed.

2.10 Protein Kinase C in Dermal Fibroblast-Myofibroblast Differentiation

2.10.1 Protein Kinase C Inhibitor Preparation and Treatments

Protein kinase C (PKC) inhibitors, bisindolylmaleimide-1 (BIM-1) and Gö6976 (Merck), were reconstituted to 1 mg/mL with DMSO, under sterile conditions (Section 2.2). Once solubilised, stock aliquots (10 µL) were kept at -20 °C to minimise any freeze-thaw effects and ensure stability for up to 4 months. When required, stock aliquots were thawed at room temperature and final experimental concentrations of 1 µM were used in the S-FM dilutions (Section 2.2.1). TGF-β_1-negative and TGF-β_1-positive (10 ng/mL; Sections 2.1.1 and 2.1.2, respectively) compound-free controls, containing 1 % DMSO and BIM-1 or Gö6976 (1 µM), were also prepared; to account for the presence of DMSO in the compound-containing media dilutions and any PKC inhibitor effects on normal DF-myofibroblast responses. Experiment-specific BIM-1 or Gö6976 treatment periods are detailed in the following Sections and Chapters.

2.10.2 Immunocytochemistry

Indirect immunofluorescent αSMA visualisation was used to assess whether epoxy-tigliane-stimulated effects upon stress fibre formation and thus, DF-myofibroblast differentiation, were modulated via PKC isoforms and their downstream signalling pathways. DFs were counted, seeded and growth-arrested; as described in Section 2.3. Following growth-arrest, S-FM was replaced with S-FM containing EBC-46 or EBC-211 (0.001 µg/mL, 0.01 µg/mL, 0.1 µg/mL, 1 µg/mL or 10 µg/mL); in the presence of TGF-β_1 (10 ng/mL; Section 2.1) and BIM-1 or Gö6976 at 1 µM (pan and α-/βI-PKC inhibitors, respectively; Section 2.10.1). TGF-β_1-negative and TGF-β_1-positive non-compound controls (Sections 2.1.1 and 2.1.2, respectively), in the absence/presence of BIM-1 or Gö6976 (Section 2.10.1), were also included. Cells were maintained in treated S-FM (250 µL/well) for 72 h (3 wells/concentration).

Following the 72 h treatment period, medium was removed from the cells and wells were washed briefly with PBS (x1). Chamber slides were processed and mounted, as described previously in Section 2.3. Images were captured at x400 magnification and each experiment was performed independently at *n = 3*.

2.10.3 Reverse Transcription-Quantitative Polymerase Chain Reaction

Combined techniques of RT and cDNA synthesis, followed by amplification via qPCR, were utilised to elucidate whether epoxy-tigliane-stimulated effects on αSMA gene expression, were modulated via PKC isoform activation. Cells were counted, seeded and growth-arrested; as detailed in Section 2.4. Following growth-arrest, S-FM was replaced with S-FM containing EBC-46 (0.01 µg/mL or 0.1 µg/mL) or EBC-211 (1 µg/mL or 10 µg/mL) with TGF-β_1 (10 ng/mL; Section 2.1); and in the absence or presence of BIM-1 or Gö6976 (1 µM; Section 2.10.1). TGF-β_1-negative and TGF-β_1-positive compound-free controls (Sections 2.1.1 and 2.1.2, respectively), in the absence or presence of BIM-1 or Gö6976 (Section 2.10.1), were also included. Cells were maintained in treated S-FM (2 mL/well) for 72 h (3 wells/concentration).

Following the 72 h treatment period, medium was removed from the cells and wells were washed briefly with PBS (x1). Post-wash removal, RNA was extracted from the samples (Section 2.4.1), reverse transcribed (Section 2.4.2), amplified (Section 2.4.3) and quantified (Section 2.4.4); as detailed prior. Each experiment was performed independently at $n = 3$.

2.11 Statistical Analyses

Statistical analyses were performed via use of GraphPad Prism Software (GraphPad Software Inc., La Jolla, USA). Graphical data for each experimental condition/sample group are exhibited as average ± SEM. To determine statistical significance, one-way ANOVAs with post-hoc Tukey tests were used, with $p = <0.05$ considered significant. Regarding the Microarray data (Section 2.8.4), statistical analysis was performed on the differences in gene expression by an unpaired t-test, with Benjamini-Hochberg, multiple testing correction; with $p = <0.05$ considered significant. Data from each of the experiment groups ($n = 4$) were combined for analysis, with hierarchical clustering analysis performed for the comparison between treated samples and compound-free controls. Fold-changes in gene expression for each treatment group were identified; and compared to the compound-free control for each time-point, respectively.

Chapter 3

Epoxy-Tigliane Effects on Dermal Fibroblast-Myofibroblast Differentiation *in vitro*

Chapter 3 - Epoxy-Tigliane Effects on Dermal Fibroblast-Myofibroblast Differentiation *in vitro*

3.1 Introduction

Cutaneous wound healing encompasses a complex, dynamic and well-orchestrated series of events, during which the body attempts to restore tissue functionality and integrity (Enoch and Leaper, 2005; Reinke and Sorg, 2012). Following dermal insult, homeostatic mechanisms are halted and reparative responses are initiated. Wound repair processes are evolutionary conserved between species and meet the need to maintain the skin's fundamental functions. However, though efficient, wound repair is not functionally perfect and can be unfavourable (Seifert *et al*. 2012; Takeo *et al*. 2015; Erickson and Echeverri, 2018). Cutaneous scar formation is the physiological endpoint of the wound healing cascade and whether natural or pathological, leads to accumulated deposition of extracellular matrix (ECM) components; resulting in altered architecture and compromised skin function (Reinke and Sorg, 2012; Eming *et al*. 2014; Do and Eming, 2016).

As previously described (Chapter 1), during the maturation and remodelling phase of wound healing, fibroblasts differentiate into myofibroblasts under the influences of transforming growth factor-β_1 (TGF-β_1) and extra domain-A-fibronectin (EDA-FN); as well as mechanical tension (Desmoulière *et al*. 1993; Serini *et al*. 1998; Hinz *et al*. 2001a; Tomasek *et al*. 2002). Myofibroblasts express α-smooth muscle actin (αSMA) which is incorporated into stress fibres, providing a contractile apparatus that allows wound contraction, ECM synthesis and remodelling (Darby *et al*. 1990; Desmoulière *et al*. 2005). Contrastingly, *in vivo* quiescent dermal fibroblasts (DFs) are functionally and morphologically distinct to the myofibroblasts; featuring cytoplasmic actins, but lacking the αSMA-positive contractile phenotypes (Tomasek *et al*. 2002; Desmoulière *et al*. 2005). On wounding, changes in the connective tissue microenvironment occur and myofibroblastic modulation begins, resulting in proto-myofibroblast formation. These are characterised by cytoplasmic actin-containing stress fibres (β and γ) and

possess the ability to express and organise cellular fibronectin (Tomasek *et al*. 2002; Gabbiani, 2003). Acquisition of the myofibroblast phenotype is further promoted by the combined actions of EDA-FN, tension and primary differentiation inducer, TGF-β_1 (Desmoulière *et al*. 1993; Serini *et al*. 1998). Together, they promote synthesis of αSMA and 'super-mature' focal adhesion (FA) development, which upregulate cell contractility and ECM secretion (Hinz *et al*. 2001b; Malmström *et al.* 2004; Goffin *et al.* 2006). Therefore, expression of αSMA and stress fibre visualisation are regarded as the most reliable phenotypic markers of TGF-β_1-driven differentiation (Darby *et al*. 1990; Gabbiani, 2003).

Fibroblasts and proto-myofibroblasts play essential roles in mediating acute wound healing responses, including initial cellular migration, fibroplasia and stimulation of cytokine/growth factor production (Clark, 1993; Werner and Grose, 2003). However, myofibroblasts are regarded as the 'effector cells' of wound repair, existing in acute healing scenarios for a finite period and forming a dynamic, reciprocal network with the microenvironment (Tomasek *et al*. 2002; Darby *et al.* 2014). Upon restoration of tissue integrity in normal physiological settings, myofibroblast numbers are reduced drastically following a prominent apoptotic wave; producing a markedly less cellular and mechanically coherent scar (Desmoulière *et al*. 1995; Darby *et al.* 2014). Under pro-fibrotic stressors, however, myofibroblasts fail to undergo apoptosis and persist at the wound site. This can result in pathological dermal fibrosis, a dysregulated and detrimental condition characterised by aberrant, excessive ECM production (Aarabi *et al.* 2007; van der Veer *et al.* 2009). As described prior (Chapter 1), dermal fibrosis can be classed as either hypertrophic or keloid in nature; both types rise above the skin level, but differing pathologies suggest distinct mechanisms are responsible for their developments (Mancini and Quaife, 1962; Ehrlich *et al.* 1994; van der Veer *et al.* 2009). Though both possess an overabundance of dermal collagen, hypertrophic scars contain αSMA-positive myofibroblasts within nodular structures while keloids do not (Ehrlich *et al.* 1994; Gauglitz *et al.* 2011). Despite the lack of myofibroblasts, keloid tissue still demonstrates abnormal characteristics that promote aberrant scar formation. Keloid fibroblasts possess a marked increase in TGF-β_1 sensitivity, which

is abundantly expressed during the proliferative phase of wound repair; potentially resulting in upregulated fibroblast proliferation early in the healing process (Younai *et al.* 1994; Slemp and Kirschner, 2006). Strong and persistent expression of TGF-β_1 and its associated receptors has also been observed in the fibroblasts of post-burn hypertrophic scars (Schmid *et al.* 1998). Thus, both scar forms exhibit exacerbation of their DF phenotypes, contributing to persistent positive feedback loops resulting in ECM overproduction/dysregulation and subsequent fibrosis; suggesting failure in appropriate cellular downregulation or the pathological activation of normal acute signals (Schmid *et al.* 1998; Gauglitz *et al.* 2011).

In contrast to the aforementioned wound repair disorders, there are also situations which promote enhanced preferential or privileged healing responses. In adults, oral mucosal and dermal wounds progress through similar phases, including proliferation and remodelling (Sciubba *et al.* 1978; Szpaderska *et al.* 2003). The former represents a regenerative healing model, however; clinically distinguished from dermal healing with regards to both its rapidity of resolution and lack of scar formation (Szpaderska *et al.* 2003; Moore *et al.* 2018). These preferential characteristics are consequences of phenotypic variations between oral and dermal wound cell populations, with oral mucosal fibroblasts (OMFs) exhibiting enhanced proliferative, replicative, migratory and reorganisational capacities, compared to their patient-matched DF counterparts (Stephens *et al.* 1996; Enoch *et al.* 2009, 2010). Furthermore, OMFs possess lower TGF-β_1 expression and exhibit resistance to TGF-β_1-driven fibroblast-myofibroblast differentiation; allowing the OMFs to retain a 'non-scarring' phenotype (Meran *et al.* 2007; Schrementi *et al.* 2008). The intrinsic ability to heal scar-free is also observed in foetal skin, which shares many similarities with oral mucosal wound repair. Prior to 24 weeks gestation, foetal wounds heal rapidly with a lack of scar formation due to a fibroblast population exhibiting heightened migratory and proliferative abilities (Lorenz *et al.* 1993; Larson *et al.* 2010). As within the oral mucosa, low TGF-β_1 levels are present; however, unlike OMF responses to exogenous TGF-β_1 addition, fibrotic responses have been induced in foetal wound models following exposure to TGF-β_1 (Krummel *et al.* 1988; Whitby and Ferguson, 1991). The theory that myofibroblasts

may exist in foetal wounds is controversial. Nonetheless, though some studies have postulated that foetal fibroblasts respond to TGF-β_1, it is currently recognised that myofibroblasts are either negligibly present or absent in foetal wounds (Larson *et al.* 2010). The relative expression of TGF-β isoforms in both scarless healing scenarios suggest crucial roles in their preferential outcomes. Moreover, their tissue-intrinsic properties independent of their surrounding environments indicate that treatments directly targeting fibroblasts for modulation could be effective in manipulating post-natal healing to be more foetal-like (Longaker *et al.* 1994; Walmsley *et al.* 2015).

As previously described, similar beneficial healing responses to those exhibited by foetal skin and the oral mucosa have also been observed in veterinary case studies post-EBC-46 treatment (Campbell *et al.* 2017; Hansen *et al.* 2018). EBC-46 and EBC-211 are naturally derived epoxy-tiglianes found in seeds of the Fontain's Blushwood tree, indigenous to Queensland's tropical rainforest (Reddell and Gordon, 2007). As the lead epoxy-tigliane prototype of interest, EBC-46 was applied to dermal tumours determined by veterinarians as unresponsive to current treatment methods. These exploratory case studies and clinical trials (>300 and 110, respectively) have shown recurring observations of exceptional wound healing responses post-tumour slough (Reddell *et al.* 2014; Barnett *et al.* 2018). These include minimal scar formation, swift granulation tissue development and rapid wound closure, as well as reformation of skin appendages (Reddell *et al.* 2014). Despite these observations, little was known on how the epoxy-tiglianes exert such responses in treated skin; given the apparent 'enhancing' of processes in which DFs/myofibroblasts are heavily involved, greater understanding of the compound effects upon these cells was necessary, in order to pursue the epoxy-tiglianes as novel wound healing agents.

3.2 Chapter Aims

As previously detailed, TGF-β_1-driven DF-myofibroblast differentiation is an integral process in the acute wound healing cascade. Myofibroblasts possess essential roles in wound contraction, closure and scar formation; mediating wound resolution and outcome. The importance of maintaining the intricate balance between fibroblasts

and myofibroblasts is highlighted by the prevalence of aberrant fibrotic pathologies, as described previously. Contrastingly, genotypic and phenotypic cellular alterations may also have the capability to modify healing mechanisms favourably; resulting in scarless healing or regenerative responses. Compounds of the epoxy-tigliane family have demonstrated an induction of exceptional dermal wound healing responses *in vivo*. However, little was known on how the epoxy-tiglianes mediate their apparent anti-scarring characteristics. Therefore, the aim of this Chapter was to assess effects of EBC-46 or EBC-211 on DF-myofibroblast differentiation; specifically investigating whether the compounds mediate this process through modulation of the fibroblast-myofibroblast genotype and/or phenotype *in vitro*. Given that the epoxy-tiglianes promote reduced scarring responses in treated skin, DFs/myofibroblasts appear to be likely cellular targets for epoxy-tiglianes to induce such desirable wound healing responses.

3.3 Materials and Methods

DFs were sourced, cultured and counted, as previously described (Sections 2.2.1 and 2.2.2). Following determination of cell density and viability (Section 2.2.2), DFs were seeded into 8-well chamber slides for immunocytochemical analysis (Section 2.3) or 6-well plates for quantitative polymerase chain reaction (qPCR) analysis (Section 2.4) at $2.5x10^4$ cells/mL. Seeding, serum-starvation and treatment volumes were 250 µL and 2 mL for chamber slides and 6-well plates, respectively. DFs were kept in a 37 °C humidified incubator with 5 % CO_2/95 % air atmosphere for the duration of all of the experiments, as previously detailed (Section 2.2.1). Following growth arrest (Section 2.2.1), cells were treated with EBC-46 or EBC-211 at the following concentrations: 0 µg/mL, 0.001 µg/mL, 0.01 µg/mL, 0.1 µg/mL, 1 µg/mL or 10 µg/mL (Section 2.1.1) in the presence or absence of TGF-β_1 (Section 2.1.2). This range was deemed optimal, following a study in which 100 µg/mL epoxy-tigliane concentrations were shown to be cytotoxic to DFs (Moses, 2016). Following 24 h, 48 h or 72 h treatment periods, immunocytochemistry (ICC) was utilised to visualise αSMA or filamentous actin (F-actin) protein expression/stress fibre formation (Section 2.3); and qPCR was used to analyse αSMA, EDA-FN, cluster of differentiation 44 (CD44), epidermal growth factor

receptor (EGFR) and TNF-stimulated gene-6 (TSG6) gene expression (Section 2.4). Statistical analyses were performed, as previously described (Section 2.11).

3.4 Results

3.4.1 Effects of EBC-46 and EBC-211 on αSMA Stress Fibre Formation

To assess the effects of EBC-46 and EBC-211 on phenotypic changes associated with DF-myofibroblast differentiation, αSMA stress fibre formation was visualised by ICC. Analysis was performed on DFs cultured with either EBC-46 or EBC-211 at all of the aforementioned concentrations (Section 3.3) with/without TGF-β_1 (10 ng/mL) over 72 h culture. Representative images obtained are shown in Figures 3.1, 3.2, 3.3 and 3.4. Compound-free controls were also included for comparison purposes (Figures 3.1A and 3.1B, 3.2A and 3.2B, 3.3A and 3.3B, 3.4A and 3.4B). Primary antibody-free controls were also included to confirm the absence of non-specific binding (Figures 3.1H, 3.2H, 3.3H and 3.4H). As reported previously, TGF-β_1-stimulated differentiation was evidenced via positive αSMA staining and stress fibre formation; coupled with polygonal cell morphologies (Jenkins *et al.* 2004; Meran *et al.* 2007; Webber *et al.* 2009). Such characteristics were observed following TGF-β_1 treatment (Figures 3.1B, 3.2B, 3.3B and 3.4B); whereas TGF-β_1-negative control DFs demonstrated elongated, spindle-shaped morphologies with lack of stress fibre formation (Figures 3.1A, 3.2A, 3.3A and 3.4A).

Cells cultured with EBC-46 (0.001 - 10 μg/mL) in the presence of TGF-β_1 (10 ng/mL; Figure 3.1C - G) showed contrasting responses, compared to controls (Figure 3.1A and B). Lower concentrations of EBC-46 (0.001 - 0.01 μg/mL) displayed comparable αSMA expression and stress fibre formation to the TGF-β_1-positive controls (Figure 3.1B). However, larger polygonal morphologies were exhibited by cells treated with these concentrations, demonstrating more prominent αSMA stress fibre formation and cytoskeletal rearrangement than TGF-β_1-positive controls. Noticeable changes in morphology were also observed at 0.1 μg/mL (Figure 3.1E); despite the presence of αSMA expression localised to the DF perinuclear regions, there was a distinct lack of αSMA stress fibre formation observed. Therefore, 0.1 μg/mL-treated DFs showed

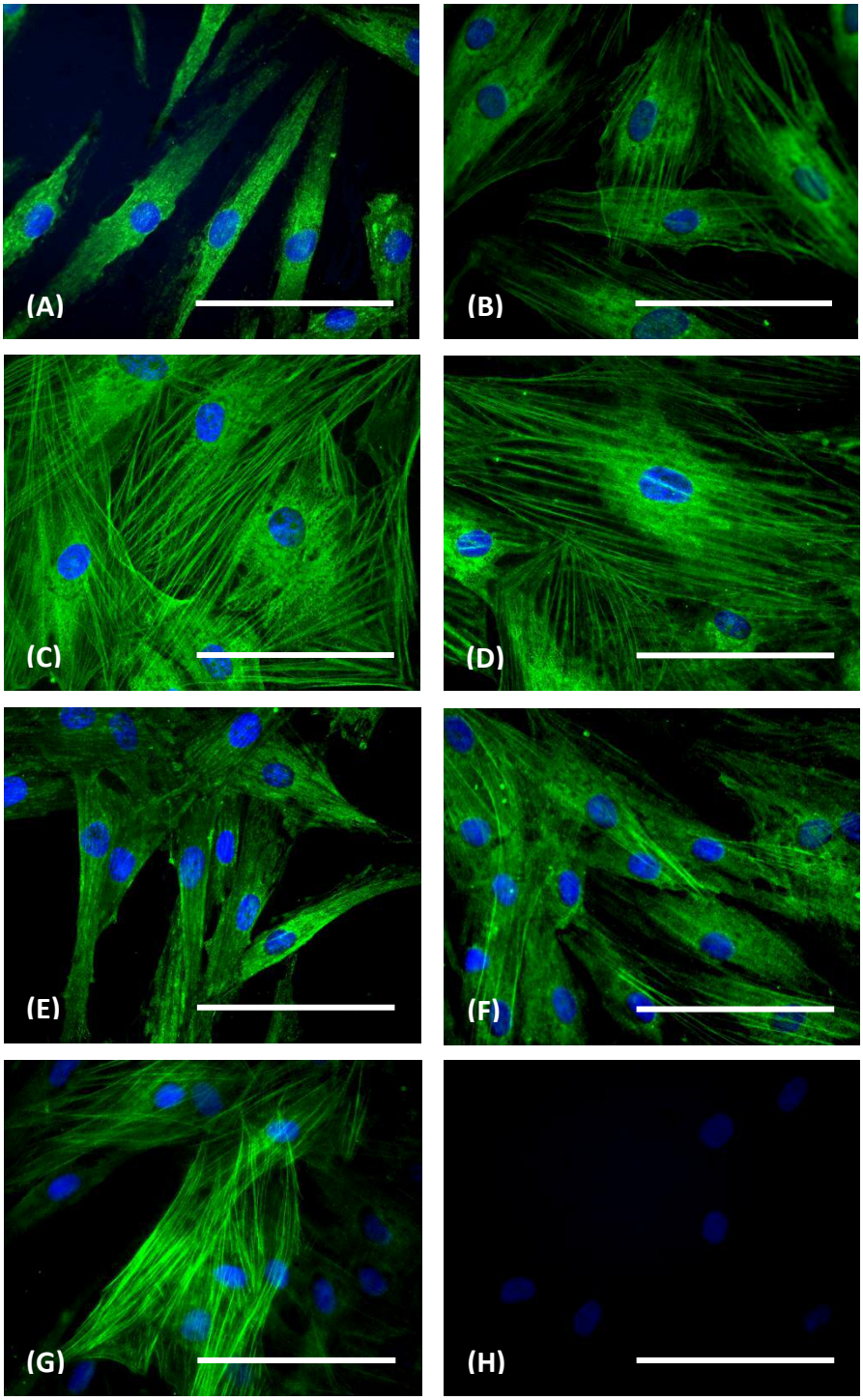

Figure 3.1. ICC analysis of DF-myofibroblast differentiation via visualisation of αSMA localisation and stress fibre formation (green), post-treatment with (B) 0 µg/mL, (C) 0.001 µg/mL, (D) 0.01 µg/mL, (E) 0.1 µg/mL, (F) 1 µg/mL, (G) 10 µg/mL of EBC-46 in the presence of TGF-β_1 (10 ng/mL) for 72 h. Both EBC-46 (0 µg/mL) - TGF-β_1 controls (A) and primary antibody-free controls (H) were included and nuclei were visualised by Hoechst stain (blue). Images displayed represent *n = 3* independent experiments captured at x400 magnification (scale bar = 100 µm).

elongated, spindle-shaped morphologies comparable to DF morphologies observed in TGF-β_1-negative controls (Figure 3.1A). At higher concentrations of EBC-46 (1 - 10 μg/mL), αSMA staining and stress fibre formation were again observed. Conversely to the typical myofibroblast morphology found at the lower EBC-46 concentrations (Figure 3.1C and D), however, stress fibre formation appeared to be less prominent and less uniformly arranged (Figure 3.1F and G).

Similar results were found when DFs were cultured with EBC-211 (0.001 - 10 μg/mL) in the presence of TGF-β_1 (Figure 3.2C - G). Most concentrations of EBC-211 (0.001 - 1 μg/mL) displayed comparable αSMA localisation and stress fibre formation to the TGF-β_1-positive controls (Figure 3.2B). Larger polygonal morphology was exhibited by cells treated with 0.001 and 0.01 μg/mL EBC-211 (Figure 3.2C and D), displaying more prominent stress fibre organisation and cytoskeletal rearrangement than the TGF-β_1-positive controls. At 0.1 - 1 μg/mL EBC-211 (Figure 3.2E and F), cells showed slightly altered morphology to the TGF-β_1-positive controls. Stress fibre organisation was more variable and less uniform than morphology seen at lower concentrations of EBC-211. However, the most notable change in phenotype was found at 10 μg/mL of EBC-211 (Figure 3.2G). Despite αSMA localisation around the perinuclear regions, a lack of stress fibre formation was observed, as previously seen at 0.1 μg/mL EBC-46. DFs treated with 10 μg/mL of EBC-211 demonstrated elongated, spindle-shaped morphologies comparable to the cellular morphologies observed in TGF-β_1-negative controls (Figure 3.2A); as was also apparent at 0.1 μg/mL EBC-46.

These studies were repeated for EBC-46 (0.001 - 10 μg/mL) in the absence of TGF-β_1 (Figure 3.3C - G). No major differences were observed in αSMA localisation or cellular morphology at 0.001 μg/mL and 0.1 μg/mL EBC-46 (Figure 3.3C and E), compared to TGF-β_1-negative controls (Figure 3.3A). However, at all other EBC-46 concentrations (Figure 3.3D, F and G), cells showed greater variability of form, with more polygonal and less elongated morphologies; but not to the same extent as seen previously, in the presence of TGF-β_1 (Figure 3.1). Stress fibre development was minimal, with cells showing more intermediate phenotypes, versus both positive and negative controls

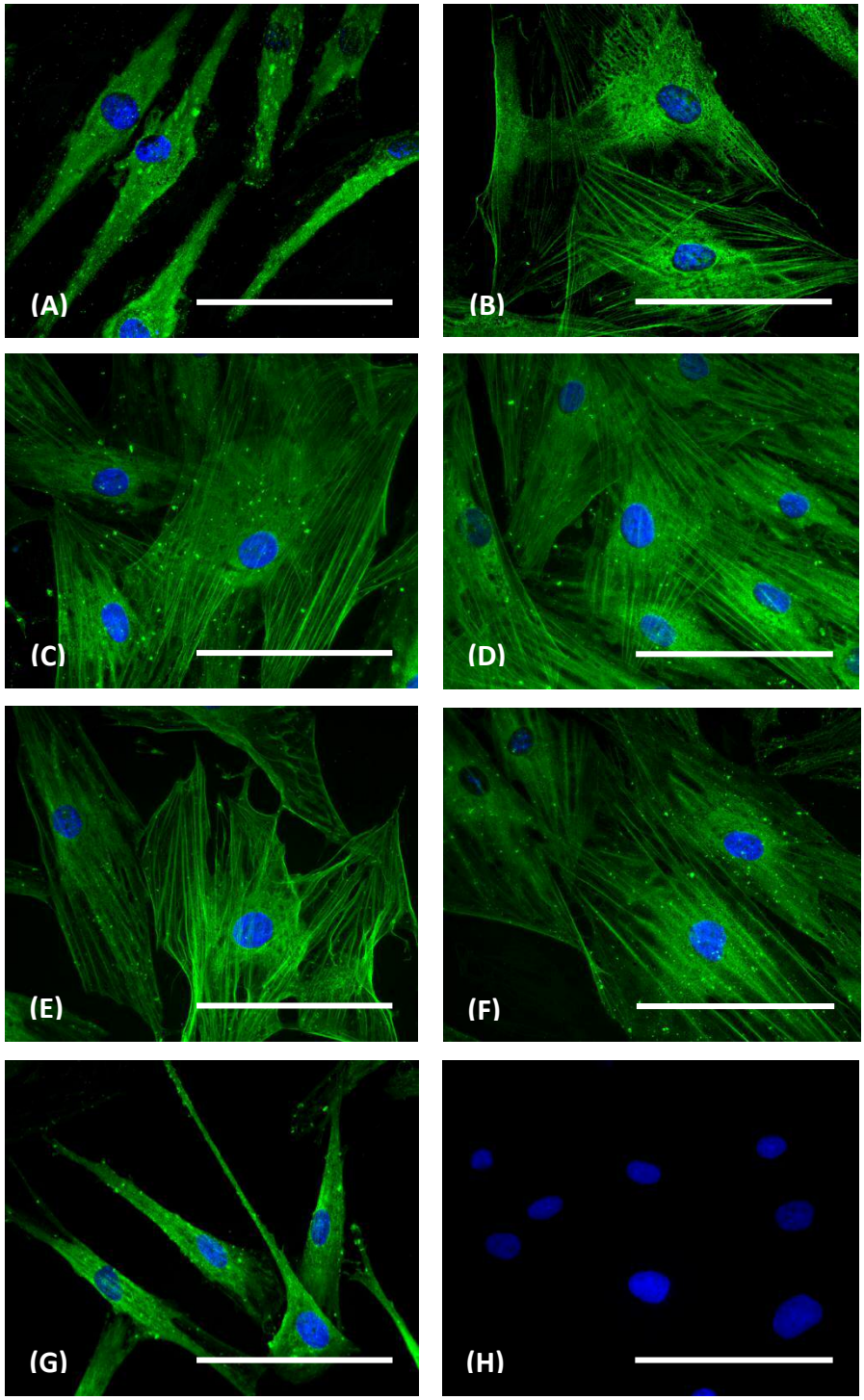

Figure 3.2. ICC analysis of DF-myofibroblast differentiation via visualisation of αSMA localisation and stress fibre formation (green), post-treatment with (B) 0 µg/mL, (C) 0.001 µg/mL, (D) 0.01 µg/mL, (E) 0.1 µg/mL, (F) 1 µg/mL and (G) 10 µg/mL EBC-211 in the presence of TGF-β_1 (10 ng/mL) for 72 h. EBC-211 (0 µg/mL) - TGF-β_1 controls (A) and primary antibody-free controls (H) were included and nuclei were visualised by Hoechst stain (blue). Images displayed represent *n = 3* independent experiments captured at x400 magnification (scale bar = 100 µm).

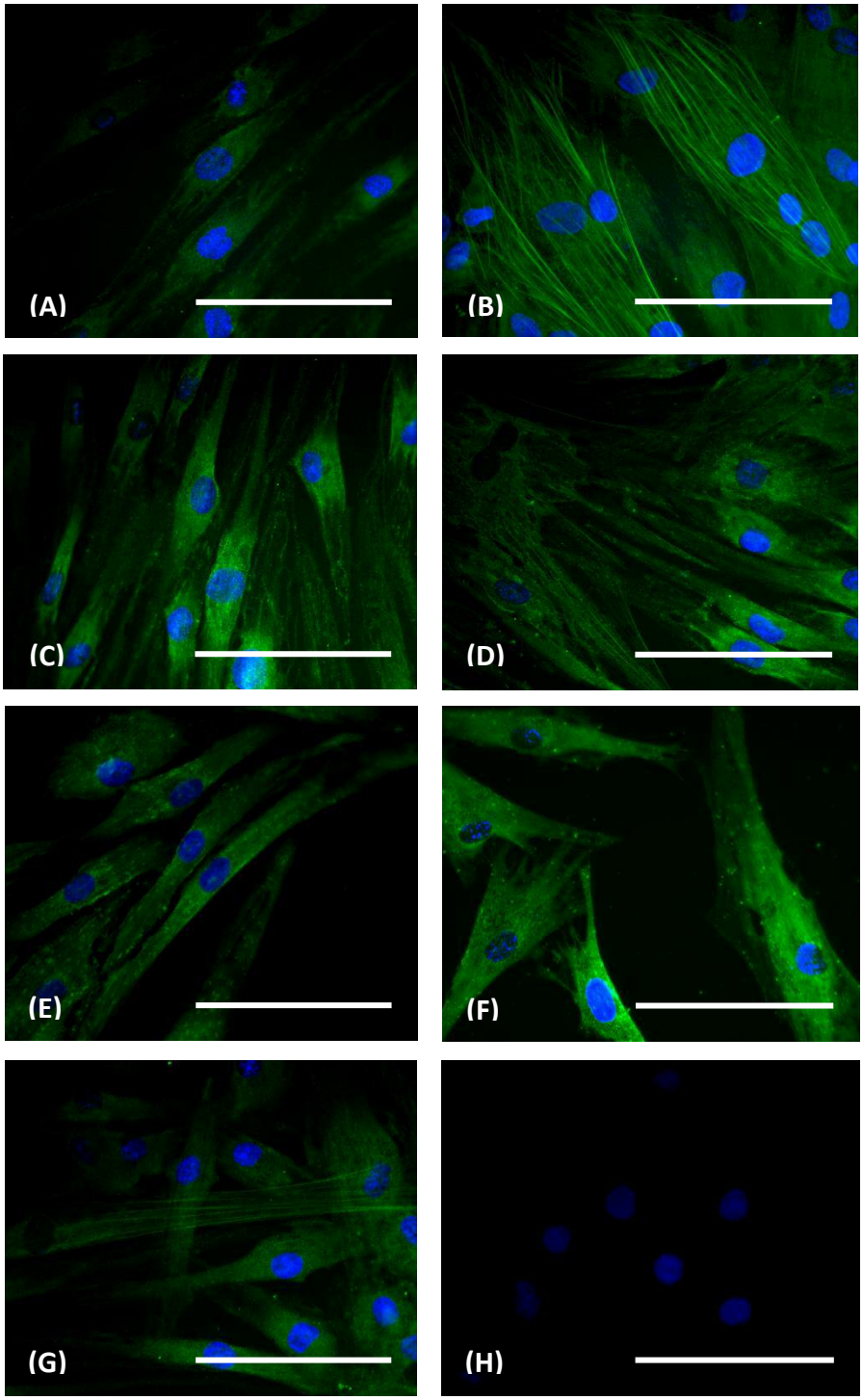

Figure 3.3. ICC analysis of DF-myofibroblast differentiation via visualisation of αSMA localisation and stress fibre formation (green), post-treatment with (A) 0 µg/mL, (C) 0.001 µg/mL, (D) 0.01 µg/mL, (E) 0.1 µg/mL, (F) 1 µg/mL and (G) 10 µg/mL EBC-46 in the absence of TGF-β_1 for 72 h. Both EBC-46 (0 µg/mL) + TGF-β_1 (10 ng/mL) controls (B) and primary antibody-free controls (H) were included and nuclei were visualised by Hoechst stain (blue). Images displayed represent *n = 3* independent experiments captured at x400 magnification (scale bar = 100 µm).

(Figure 3.3A and B). When exposed to EBC-211 (0.001 - 10 µg/mL) in the absence of TGF-β_1 (Figure 3.4C - 3.4G), no major differences in αSMA localisation or morphology were observed at 0.001 µg/mL or 0.01 µg/mL EBC-211 (Figure 3.4C and 3.4D), versus TGF-β_1-negative controls (Figure 3.4A); however, at all other EBC-211 concentrations (Figure 3.4E - G), DFs demonstrated a mixture of both spindle-shaped and polygonal morphologies. Stress fibre formation was minimal and immature in formation, unlike phenotypes observed in DFs treated with EBC-211 in the presence of TGF-β_1 (Figure 3.2).

3.4.2 Effects of EBC-46 and EBC-211 on αSMA Gene Expression

Following ICC studies (Section 3.4.1), qPCR analysis was performed to determine the effects upon αSMA gene expression levels. Quantification was performed upon cells cultured with EBC-46 or EBC-211 at all aforementioned concentrations (Section 3.3), with/without TGF-β_1 (10 ng/mL; Figures 3.5 and 3.6). Compound-free controls with/ without TGF-β_1 were further included to confirm normal DF-myofibroblast responses and for comparative purposes. As reported previously, TGF-β_1-driven differentiation was genotypically indicated via an up-regulation of αSMA gene expression, peaking between 48 - 72 h in culture (Meran *et al.* 2007; Webber *et al.* 2009). Findings were consistent with the previous studies, as approximately 15-fold and 21-fold increases in αSMA gene expression were seen following TGF-β_1 treatment (Figure 3.5 and 3.6, respectively); versus the TGF-β_1-negative controls.

Cells cultured with EBC-46 (0.001 - 10 µg/mL), in the presence of TGF-β_1 (10 ng/mL), exhibited varying differences in αSMA expression, compared to the TGF-β_1-positive control (Figure 3.5A). Lower concentrations of EBC-46 (0.001 - 0.01 µg/mL) showed significant increases in αSMA expression versus the TGF-β_1-positive control (2.2-fold and 1.9-fold, respectively; $p = <0.001$). This reflected the previous ICC data, in which lower concentrations of EBC-46 (Figure 3.1 C - D) displayed comparable, if not more extensive, αSMA stress fibre formation to TGF-β_1-positive controls (Figure 3.1B). In contrast, higher EBC-46 concentrations (1 - 10 µg/mL) did not show significant αSMA up-regulation, versus TGF-β_1-positive controls ($p = >0.05$). This also reflected the ICC

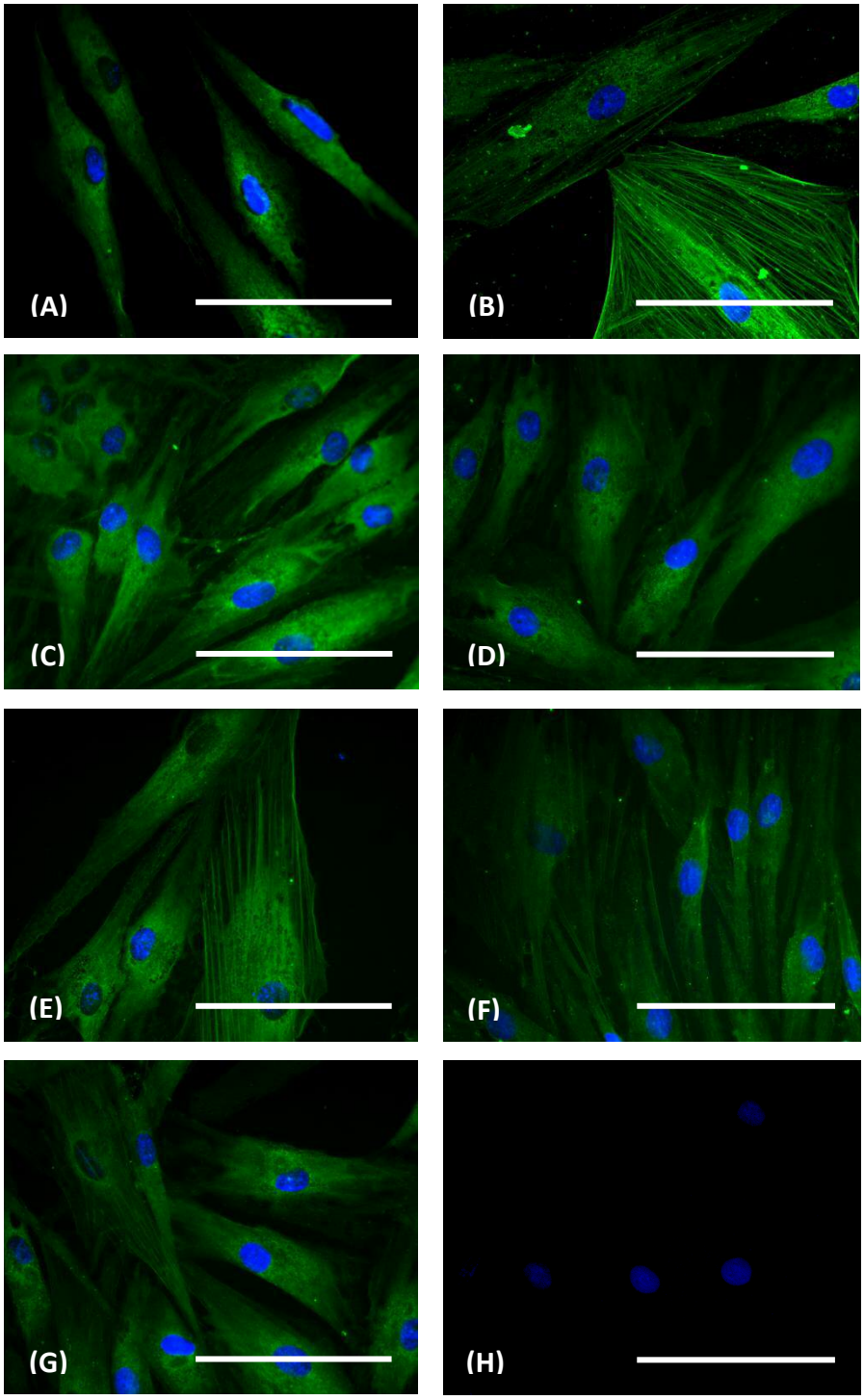

Figure 3.4. ICC analysis of DF-myofibroblast differentiation via visualisation of αSMA localisation and stress fibre formation (green), post-treatment with (A) 0 µg/mL, (C) 0.001 µg/mL, (D) 0.01 µg/mL, (E) 0.1 µg/mL, (F) 1 µg/mL and (G) 10 µg/mL EBC-211 in the absence of TGF-β_1 for 72 h. EBC-211 (0 µg/mL) + TGF-β_1 (10 ng/mL) controls (B) and primary antibody-free controls (H) were included and nuclei were visualised by Hoechst stain (blue). Images displayed represent *n = 3* independent experiments captured at x400 magnification (scale bar = 100 µm).

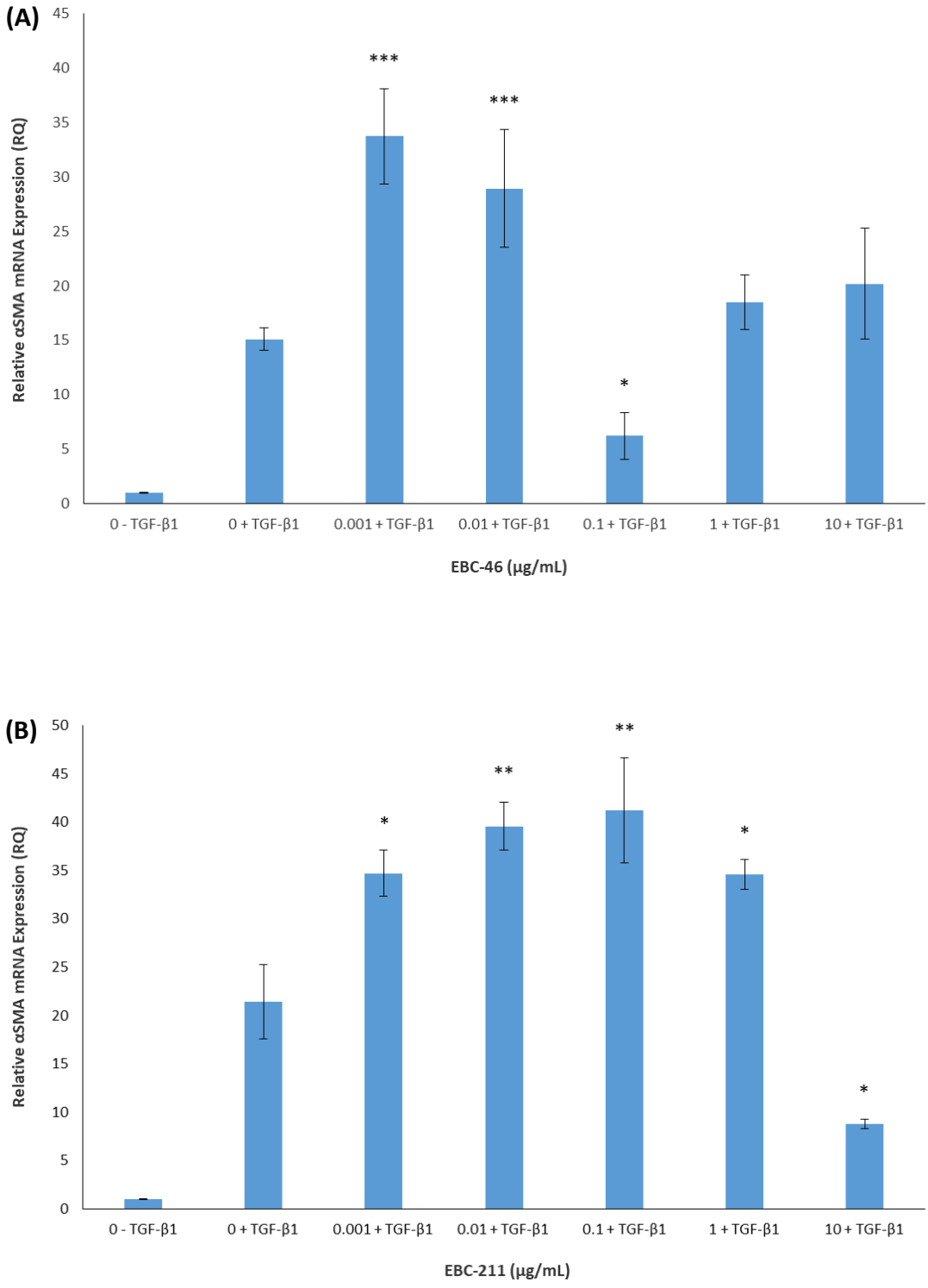

Figure 3.5. Analysis of DF-myofibroblast differentiation via quantification of αSMA gene expression by qPCR; post-treatment with (A) EBC-46 and (B) EBC-211 (0.001 µg/mL, 0.01 µg/mL, 0.1 µg/mL, 1 µg/mL and 10 µg/mL), in the presence of TGF-β_1 for 72 h. Compound-free controls ± TGF-β_1 (10 ng/mL) were included (*n = 3*, mean± SEM; *p = *<0.05, **<0.01, ***<0.001* versus TGF-β_1-positive controls).

data, in which cells at these concentrations demonstrated less prominent stress fibre development and more intermediate phenotypes (Figure 3.1F - G), versus the lower concentrations and TGF-β_1-positive controls (Figure 3.1 C - D and 3.1B, respectively). At 0.1 µg/mL EBC-46, however, a significant 2.4-fold down-regulation of αSMA gene expression was demonstrated; compared to TGF-β_1-positive controls (*p = <0.05*). This specific decrease reflected the lack of stress fibre formation and unique morphology observed by ICC (Figure 3.1E). Interestingly, despite down-regulation of αSMA at 0.1 µg/mL of EBC-46, expression was still approximately 6.2-fold higher than the TGF-β_1-negative control (Figure 3.5A). This indicated that αSMA gene expression remains to be induced in cells after 0.1 µg/mL EBC-46 treatment, but not to the same extent as TGF-β_1-stimulated DFs.

Comparable results to those induced by EBC-46 were demonstrated when DFs were cultured with EBC-211 (0.001 - 10 µg/mL), in the presence of TGF-β_1 (Figure 3.5B). Most EBC-211 concentrations (0.001 - 1 µg/mL) demonstrated significant increases in αSMA gene expression, in comparison to TGF-β_1-positive controls (1.6 - 1.9-fold; *p = <0.05* at 0.001 and 1 µg/mL, *p = <0.01* at 0.01 and 0.1 µg/mL). This corroborated the previously detailed ICC data, in which most EBC-211 concentrations (0.001 - 1 µg/mL; Figure 3.2 C - F) demonstrated comparable, if not more extensive, αSMA stress fibre formation versus TGF-β_1-positive controls (Figure 3.2B). However, at 10 µg/mL EBC-211, a significant 2.4-fold down-regulation of αSMA expression was found, compared to TGF-β_1-positive controls (*p = <0.05*). This specific reduction corroborated the lack of stress fibre formation and unique morphology observed via ICC (Figure 3.2G); as also evident with 0.1 µg/mL EBC-46. Interestingly, as similarly found with 0.1 µg/mL EBC-46 (Figure 3.5A), αSMA expression was still approximately 8.7-fold greater than the TGF-β_1-negative control (Figure 3.5B). This indicates that αSMA expression is still induced in DFs on 10 µg/mL EBC-211 treatment, but not to the same extent as TGF-β_1-stimulated DFs.

These studies were repeated for DFs cultured with EBC-46 (0.001 - 10 µg/mL) in the absence of TGF-β_1 (Figure 3.6A). However, in contrast to the TGF-β_1-positive studies

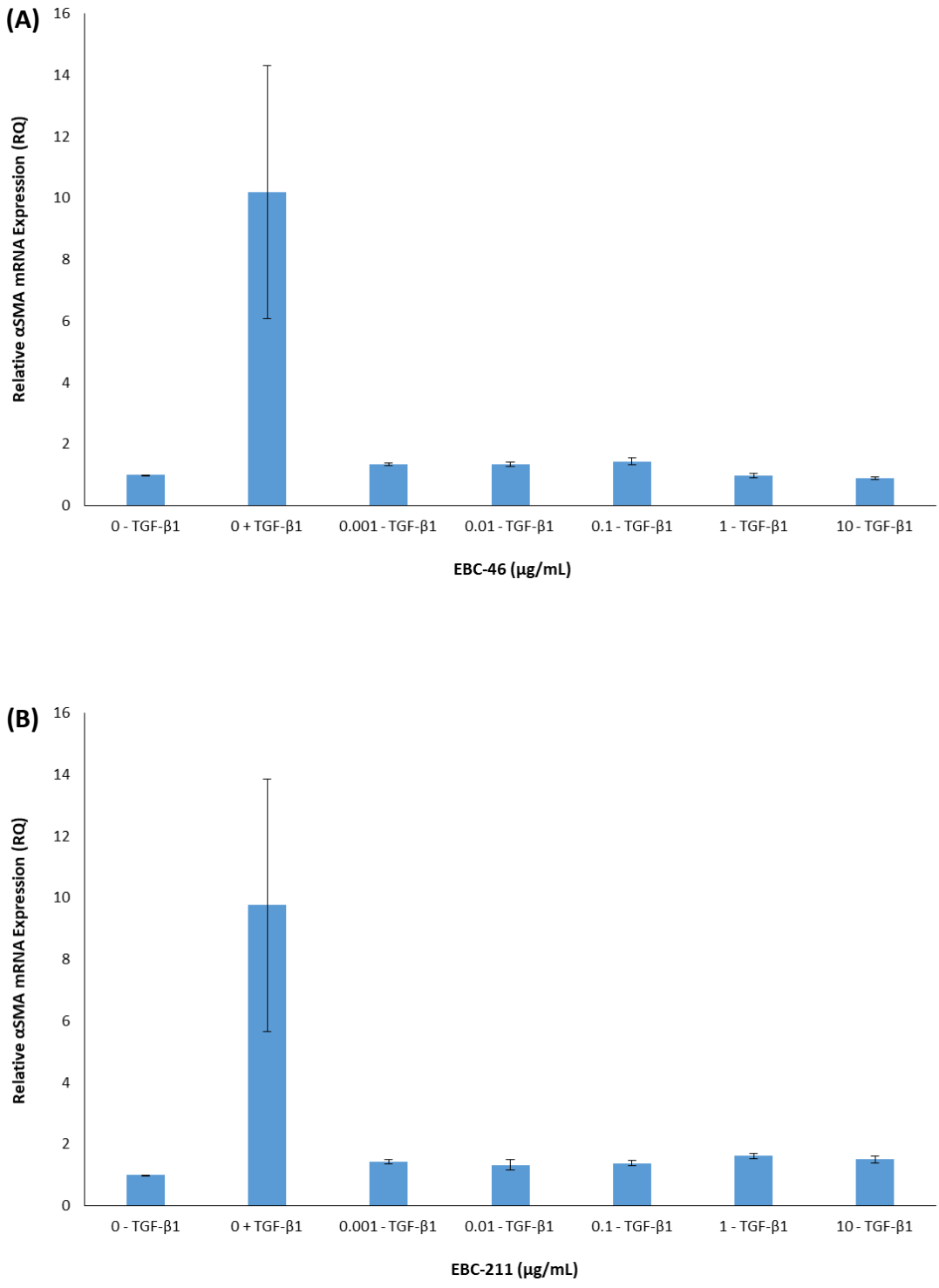

Figure 3.6. Analysis of DF-myofibroblast differentiation via quantification of αSMA gene expression by qPCR; post-treatment with (A) EBC-46 and (B) EBC-211 (0.001 µg/mL, 0.01 µg/mL, 0.1 µg/mL, 1 µg/mL and 10 µg/mL), in the absence of TGF-β_1 for 72 h. Compound-free controls ± TGF-β_1 (10 ng/mL) were also included (*n = 3*, mean ±SEM; *p = >0.05* for all concentrations versus TGF-β_1-negative controls).

(Figure 3.5A), no significant differences in αSMA expression were induced across all EBC-46 concentrations; versus the TGF-β_1-negative control (Figure 3.6A; *p = >0.05*). The RQs were approximately 7 - 11-fold decreased, compared to the TGF-β_1-positive control, corroborating the minimal/lack of stress fibre formation observed in the ICC studies (Figure 3.3C - G). Treatment with EBC-211 (0.001 - 10 µg/mL) in the absence of TGF-β_1, yielded similar responses to those induced following EBC-46 treatment. In contrast to the corresponding TGF-β_1-positive studies (Figure 3.5B), no significant differences in αSMA gene expression were induced across all concentrations; versus the TGF-β_1-negative control (Figure 3.6B; *p = >0.05*). RQs were approximately 6 - 7-fold decreased, compared to the TGF-β_1-positive control, corroborating the minimal stress fibre formation observed in corresponding ICC studies (Figure 3.4C - G).

3.4.3 Effects of EBC-46 and EBC-211 on Filamentous Actin Reorganisation

To assess the effects of EBC-46 and EBC-211 on phenotypic changes associated with DF-myofibroblast differentiation, the localisation and cytoskeletal reorganisation of F-actin was visualised using phalloidin-fluorescein isothiocyanate (FITC) staining and ICC. Analysis was performed upon DFs cultured with either EBC-46 or EBC-211 at all concentrations (Section 3.3) with or without TGF-β_1 (10 ng/mL) post-72 h treatment. Images representing all conditions are exhibited in Figures 3.7, 3.8, 3.9 and 3.10 and compound-free controls, in the absence and presence of TGF-β_1, were included for comparison purposes (Figures 3.7A - B, 3.8A - B, 3.9A - B and 3.10A - B). As reported previously, cytoskeletal reorganisation of DFs in response to TGF-β_1 was indicated by bundling of prominent F-actin fibres and polygonal cell morphologies across 72 h in culture (Meran *et al.* 2007). Such characteristics were found after TGF-β_1 treatment (Figures 3.7B, 3.8B, 3.9B and 3.10B); whereas TGF-β_1-negative control DFs exhibited small spindle-shaped morphologies, with F-actin localised around the cell periphery (Figures 3.7A, 3.8A, 3.9A and 3.10A).

Cells cultured with EBC-46 (0.001 - 10 µg/mL) in the presence of TGF-β_1 (Figure 3.7C - G) displayed varying results, compared to TGF-β_1 controls (Figure 3.7A - B). At both lower concentrations (0.001 - 0.01 µg/mL; Figure 3.7C - D) and higher concentrations

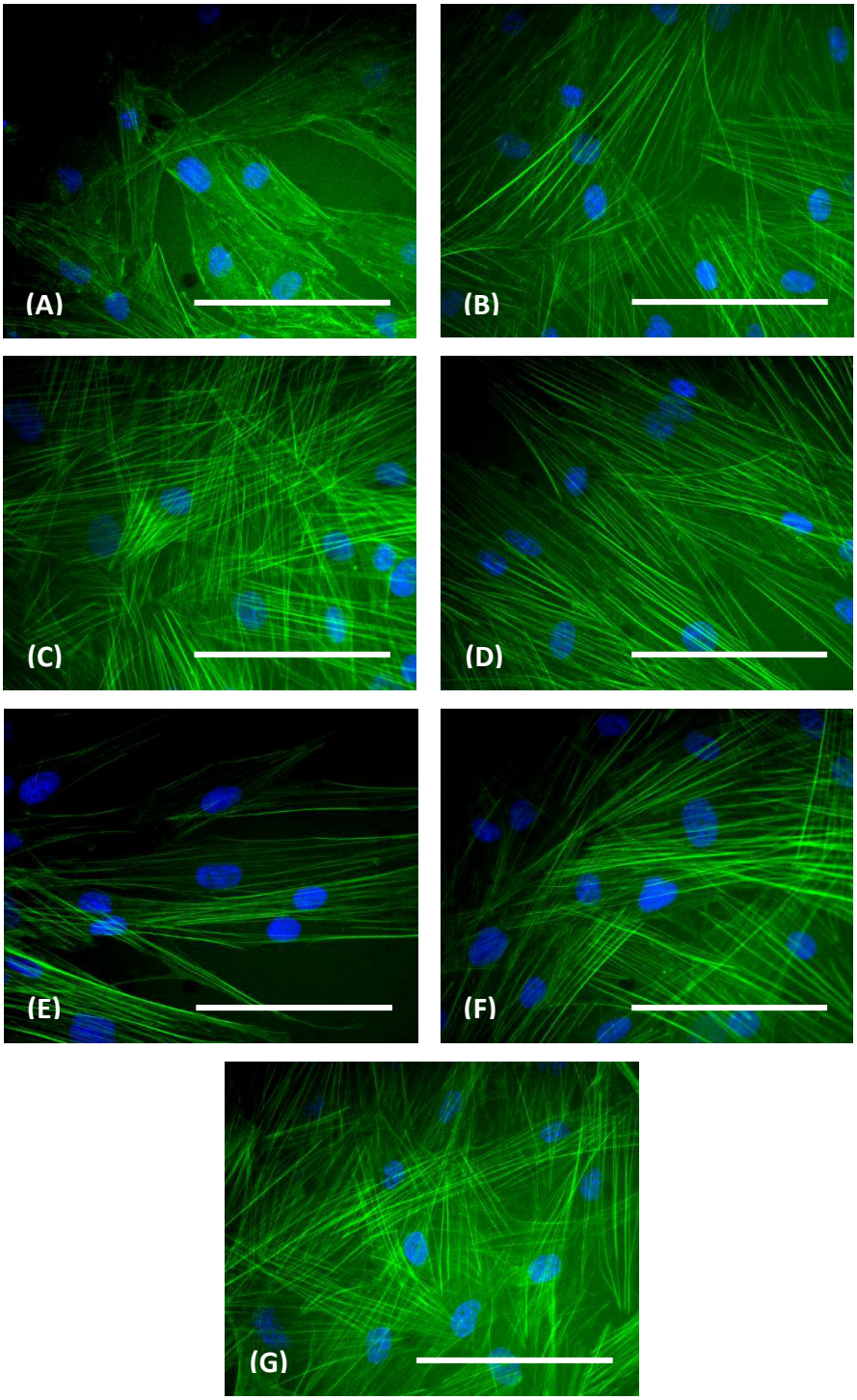

Figure 3.7. ICC analysis of DF-myofibroblast differentiation via the visualisation of F-actin localisation, arrangement and stress fibre formation (green), post-treatment with (B) 0 µg/mL, (C) 0.001 µg/mL, (D) 0.01 µg/mL, (E) 0.1 µg/mL, (F) 1 µg/mL, (G) 10 µg/mL of EBC-46 in the presence of TGF-β_1 (10 ng/mL) for 72 h. EBC-46 (0 µg/mL) - TGF-β_1 controls (A) were also included and nuclei were visualised by Hoechst stain (blue). Images displayed represent *n = 3* independent experiments captured at x400 magnification (scale bar = 100 µm).

(1 - 10 µg/mL; Figure 3.7F - G) of EBC-46, cells displayed similar F-actin localisation, stress fibre formation and cytoskeletal rearrangement to TGF-β_1-positive controls (Figure 3.7B). Cells were larger and polygonal in morphology, exhibiting prominent cytoskeletal reorganisation with F-actin filaments coalescing to form thick, uniform bundles extending from end to end within these cells. However, the most notable changes in phenotype were observed at 0.1 µg/mL EBC-46 (Figure 3.7E). Cytoskeletal reorganisation was less prominent, with the DFs retaining elongated, spindle-shaped morphologies intermediate between those shown by the controls, with/without TGF-β_1 supplementation (Figure 3.7A - B). F-actin fibres were less pronounced and poorly developed with a greater prominence around the cell periphery, comparable to the localisation found in TGF-β_1-negative controls (Figure 3.7A).

Similar results were found when DFs were cultured with EBC-211 (0.001 - 10 µg/mL), in the presence of TGF-β_1 (Figure 3.8C - G). Most concentrations of EBC-211 (0.001 - 1 µg/mL) demonstrated comparable F-actin distribution, stress fibre formation and cytoskeletal rearrangement to the TGF-β_1-positive controls (Figure 3.8B). Cells were larger and polygonal in appearance, showing prominent cytoskeletal reorganisation with F-actin filaments coalescing to form thick, uniform bundles extending from end to end within cells. The most notable changes in phenotype were shown at 10 µg/mL EBC-211 (Figure 3.8G). As previously observed at 0.1 µg/mL of EBC-46 (Figure 3.7E), cytoskeletal reorganisation was less prominent, with the cells possessing elongated, spindle-shaped morphologies intermediate between those exhibited by the controls, with/without TGF-β_1 supplementation (Figure 3.8A - B). The F-actin fibres were less pronounced and poorly developed at 10 µg/mL; with a greater prominence around the cell periphery, akin to localisation found in TGF-β_1-negative control cells (Figure 3.8A). This was also found at 0.1 µg/mL EBC-46 (Figure 3.7E).

These studies were repeated for EBC-46 (0.001 - 10 µg/mL), in the absence of TGF-β_1 (Figure 3.9C - G), over 72 h. At every concentrations, no major differences in F-actin localisation, stress fibre formation or cytoskeletal rearrangement were observed, in comparison to TGF-β_1-negative controls (Figure 3.9A). Cells demonstrated elongated

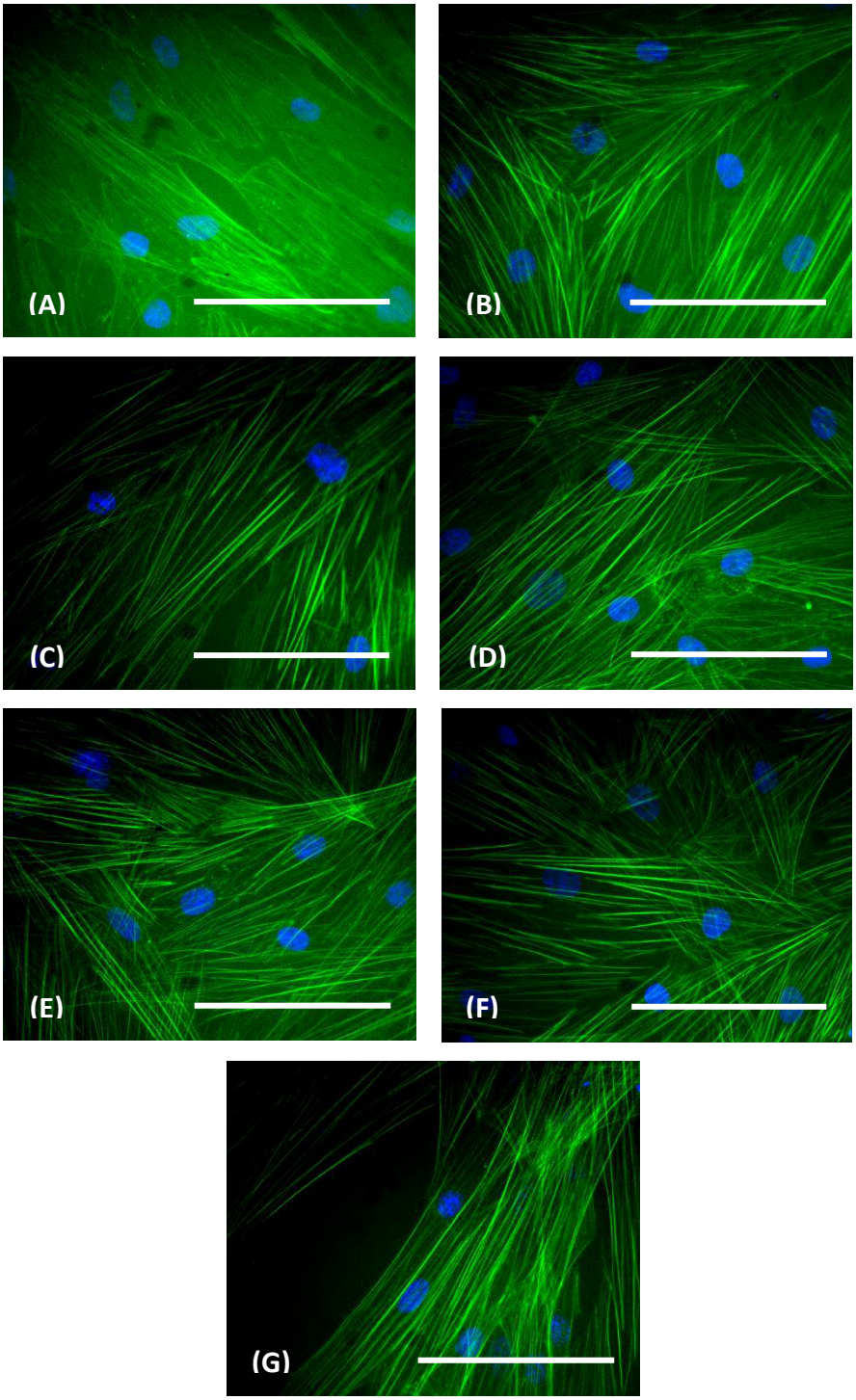

Figure 3.8. ICC analysis of DF-myofibroblast differentiation via the visualisation of F-actin localisation, rearrangement and stress fibre formation (green), post-treatment with (B) 0 µg/mL, (C) 0.001 µg/mL, (D) 0.01 µg/mL, (E) 0.1 µg/mL, (F) 1 µg/mL, (G) 10 µg/mL EBC-211 in the presence of TGF-β_1 (10 ng/mL) for 72 h. EBC-211 (0 µg/mL) - TGF-β_1 controls (A) were also included and nuclei were visualised by Hoechst stain (blue). Images displayed represent *n = 3* independent experiments captured at x400 magnification (scale bar = 100 µm).

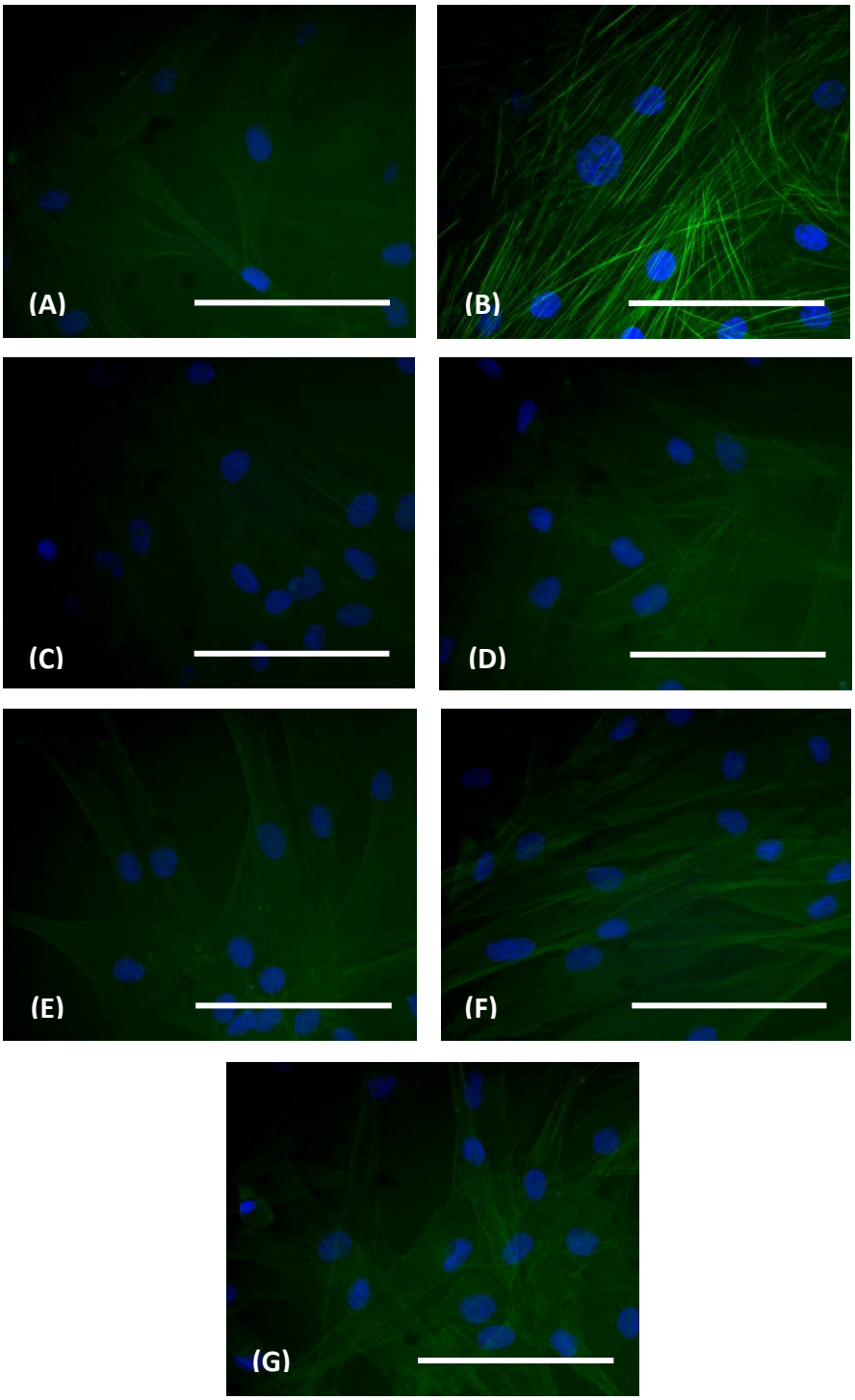

Figure 3.9. ICC analysis of DF-myofibroblast differentiation via the visualisation of F-actin localisation, rearrangement and stress fibre formation (green), post-treatment with (A) 0 µg/mL, (C) 0.001 µg/mL, (D) 0.01 µg/mL, (E) 0.1 µg/mL, (F) 1 µg/mL and (G) 10 µg/mL EBC-46 in the absence of TGF-β_1 for 72 h. EBC-46 (0 µg/mL) + TGF-β_1 (10 ng/mL) controls (B) were also included and nuclei were visualised using Hoechst stain (blue). Images displayed represent *n = 3* independent experiments captured at x400 magnification (scale bar = 100 µm).

spindle-shaped appearances at all concentrations and F-actin localisation was found around the cell periphery (Figure 3.9C - G). Following treatment with EBC-211 (0.001 - 10 µg/mL), in the absence of TGF-β_1 (Figure 3.10C - G), no major differences in the F-actin localisation, stress fibre formation or cytoskeletal arrangement were shown, compared TGF-β_1-negative controls (Figure 3.10A). As found at all concentrations of EBC-46, EBC-211-treated cells showed elongated, spindle-shaped morphologies and F-actin was particularly localised around the cell periphery (Figure 3.10C - G).

3.4.4 Effects of EBC-46 and EBC-211 on Myofibroblast Formation

Based on the inhibitory effects of EBC-46 (0.1 µg/mL) and EBC-211 (10 µg/mL) at 72 h, the effects of EBC-46 and EBC-211 on myofibroblast formation were assessed; to determine whether the epoxy-tiglianes were completely inhibiting differentiation or reversing the myofibroblast phenotype. αSMA stress fibre formation was visualised by ICC and analysis was performed on DFs cultured with either EBC-46 or EBC-211 at all of the aforementioned concentrations (Section 3.3), in the presence of TGF-β_1 (10 ng/mL), following 24 h and 48 h culture. Representative images obtained are shown in Figures 3.11, 3.12, 3.13 and 3.14. Compound-free controls with or without TGF-β_1 were also included for comparison purposes (Figures 3.11A - B, 3.12A - B, 3.13A - B and 3.14A - B). Primary antibody-free controls were further included to confirm the absence of non-specific binding (Figures 3.11H, 3.12H, 3.13H and 3.14H). As detailed previously (Section 3.4.1), DF-myofibroblast differentiation was indicated by positive αSMA staining and stress fibre formation, as well as polygonal morphology.

DFs cultured with EBC-46 (0.001 - 10 µg/mL) in the presence of TGF-β_1 (Figure 3.11C - G) for 24 h, showed varying results compared to the controls (Figure 3.11A and B). Lower EBC-46 concentrations (0.001 - 0.01 µg/mL; Figure 3.11C - D) displayed similar αSMA localisation and stress fibre formation to the TGF-β_1-positive controls (Figure 3.11B). The cells exhibited transitional morphologies, with poorly defined stress fibre formation and intermediate cytoskeletal rearrangement. However, at all of the other concentrations (0.1 - 10 µg/mL; Figure 3.11E - G), there was a distinct lack of stress fibre formation observed versus TGF-β_1-positive controls (Figure 3.11B). DFs showed

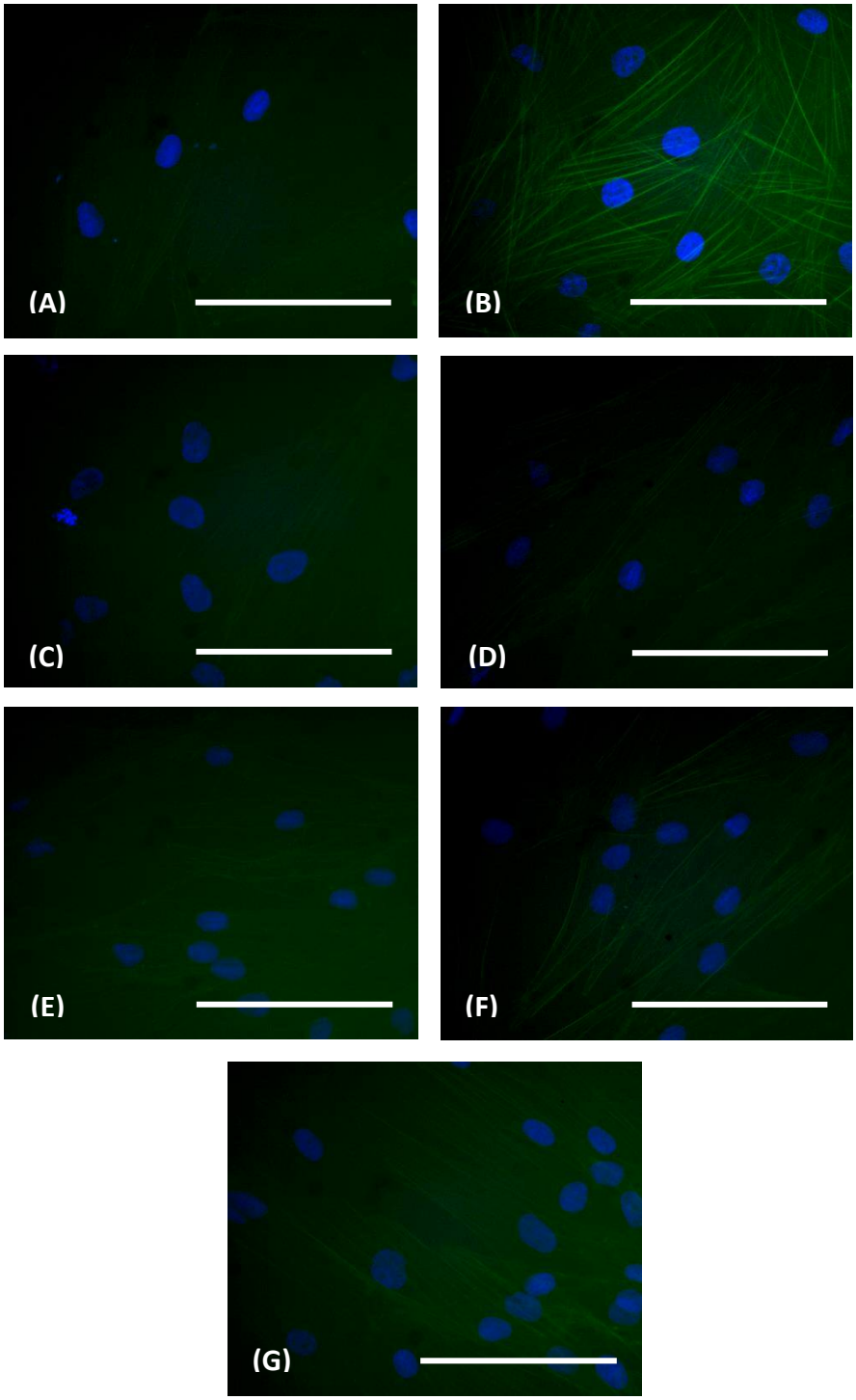

Figure 3.10. ICC analysis of DF-myofibroblast differentiation via visualisation of F-actin localisation, rearrangement and stress fibre formation (green), post-treatment with (A) 0 µg/mL, (C) 0.001 µg/mL, (D) 0.01 µg/mL, (E) 0.1 µg/mL, (F) 1 µg/mL and (G) 10 µg/mL EBC-211 in the absence of TGF-β_1 for 72 h. EBC-211 (0 µg/mL) + TGF-β_1 (10 ng/mL) controls (B) were also included and nuclei were visualised by Hoechst stain (blue). Images displayed represent *n = 3* independent experiments captured at x400 magnification (scale bar = 100 µm).

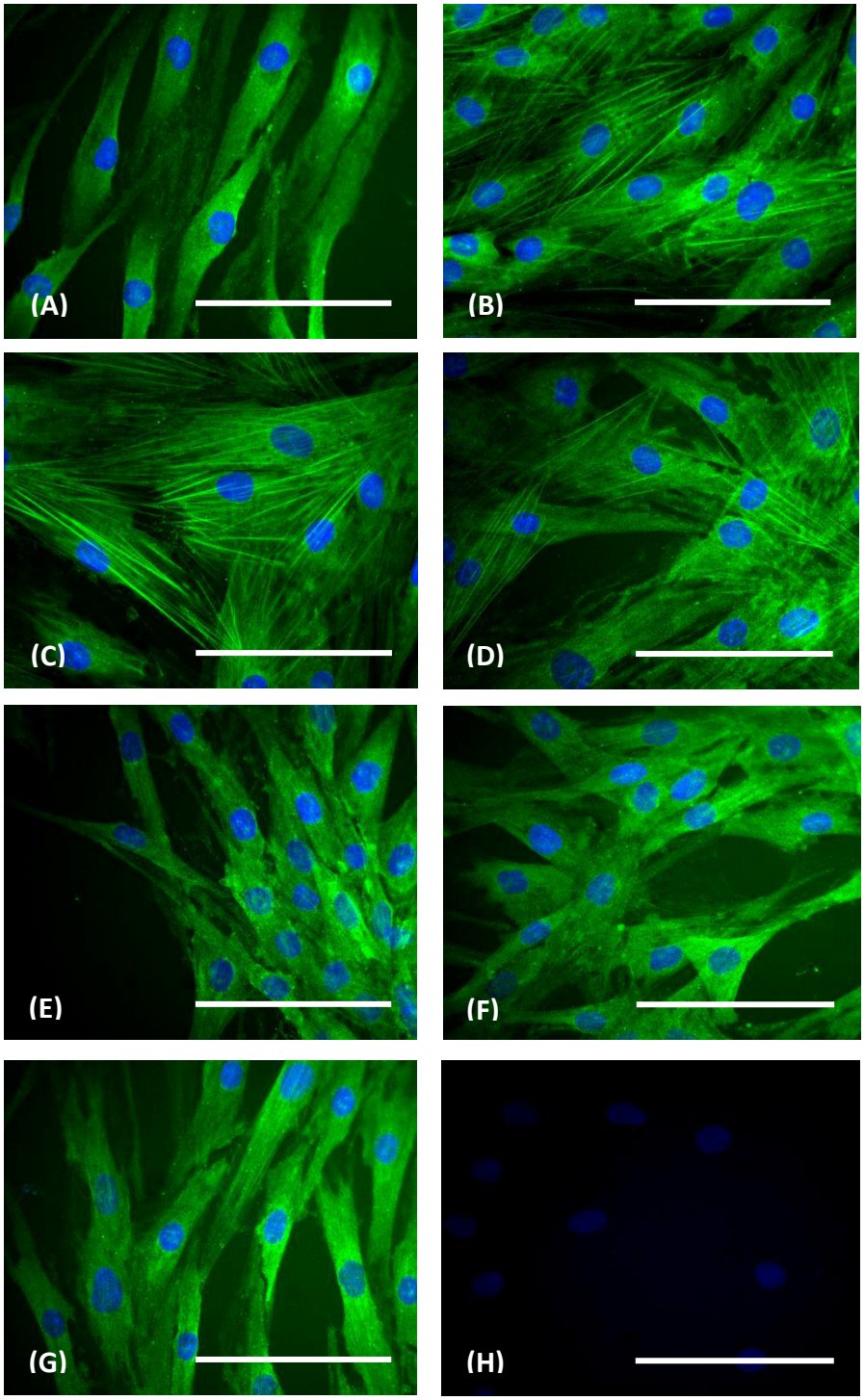

Figure 3.11. ICC analysis of DF-myofibroblast differentiation through visualisation of αSMA localisation and stress fibre formation (green), following treatment with (B) 0 µg/mL, (C) 0.001 µg/mL, (D) 0.01 µg/mL, (E) 0.1 µg/mL, (F) 1 µg/mL, (G) 10 µg/mL of EBC-46 in the presence of TGF-β_1 (10 ng/mL) for 24 h. Both EBC-46 (0 µg/mL) - TGF-β_1 controls (A) and primary antibody-free controls (H) were also included and nuclei were visualised by Hoechst stain (blue). Images displayed represent *n = 3* individual experiments captured at x400 magnification (scale bar = 100 µm).

αSMA localisation and elongated, spindle-shaped appearances, comparable to those observed in TGF-β_1-negative controls (Figure 3.11A). Moreover, at 0.1 µg/mL EBC-46 (Figure 3.11E), cellular aggregation was apparent, which was not seen in positive or negative controls (Figure 3.11A - B). After 48 h treatment with EBC-46 (Figure 3.12C - G), cells exhibited varying phenotypes compared to controls (Figure 3.12A and B). Lower EBC-46 concentrations (0.001 - 0.01 µg/mL; Figure 3.12C - D), showed similar αSMA localisation and stress fibre formation to the TGF-β_1-positive controls (Figure 3.12B). However, cells also demonstrated more mature myofibroblast morphologies than their TGF-β_1-positive counterparts, expressing more prominent stress fibres and uniformly polygonal forms. As found post-24 h treatment with 0.1 µg/mL of EBC-46, cells demonstrated a distinct lack of stress fibre formation following 48 h treatment (Figure 3.12E). The DFs also appeared spindle-shaped and elongated, similar to those observed in TGF-β_1-negative controls (Figure 3.12A). Moreover, the cell aggregation detected at this concentration after 24 h treatment, was retained at 48 h; although again, this was not found in controls (Figure 3.12A - B). These characteristics, shown following 0.1 µg/mL EBC-46 treatment, were also retained at 72 h; in line with prior findings (Figure 3.1E). At higher EBC-46 concentrations (1 - 10 µg/mL; Figure 3.12F - G), αSMA localisation and incorporation into stress fibres were observed. However, once again, in contrast to the typical myofibroblastic morphology observed at lower concentrations (Figure 3.12C - D), fibre formation appeared less prominent and less uniformly arranged (Figure 3.12F - G). Cells demonstrated transitional phenotypes, intermediate to those observed in positive and negative controls (Figure 3.12A - B); similar to morphologies seen at 72 h (Figure 3.1F - G).

Similar results were found when DFs were cultured with EBC-211 (0.001 - 10 µg/mL) in the presence of TGF-β_1 for 24 h and 48h (Figures 3.13C - G and 3.14C - G). Varying results were found versus TGF-β_1 positive and negative controls at 24 h (Figure 3.13A and B), with DFs at lower EBC-211 concentrations (0.001 - 0.1 µg/mL; Figure 3.13C - E) displaying similar αSMA expression and fibre formation to TGF-β_1-positive controls (Figure 3.13B). Cells displayed transitional morphologies, with poorly defined stress fibre formation and intermediate cytoskeletal rearrangement (Figure 3.13C - E). At 1

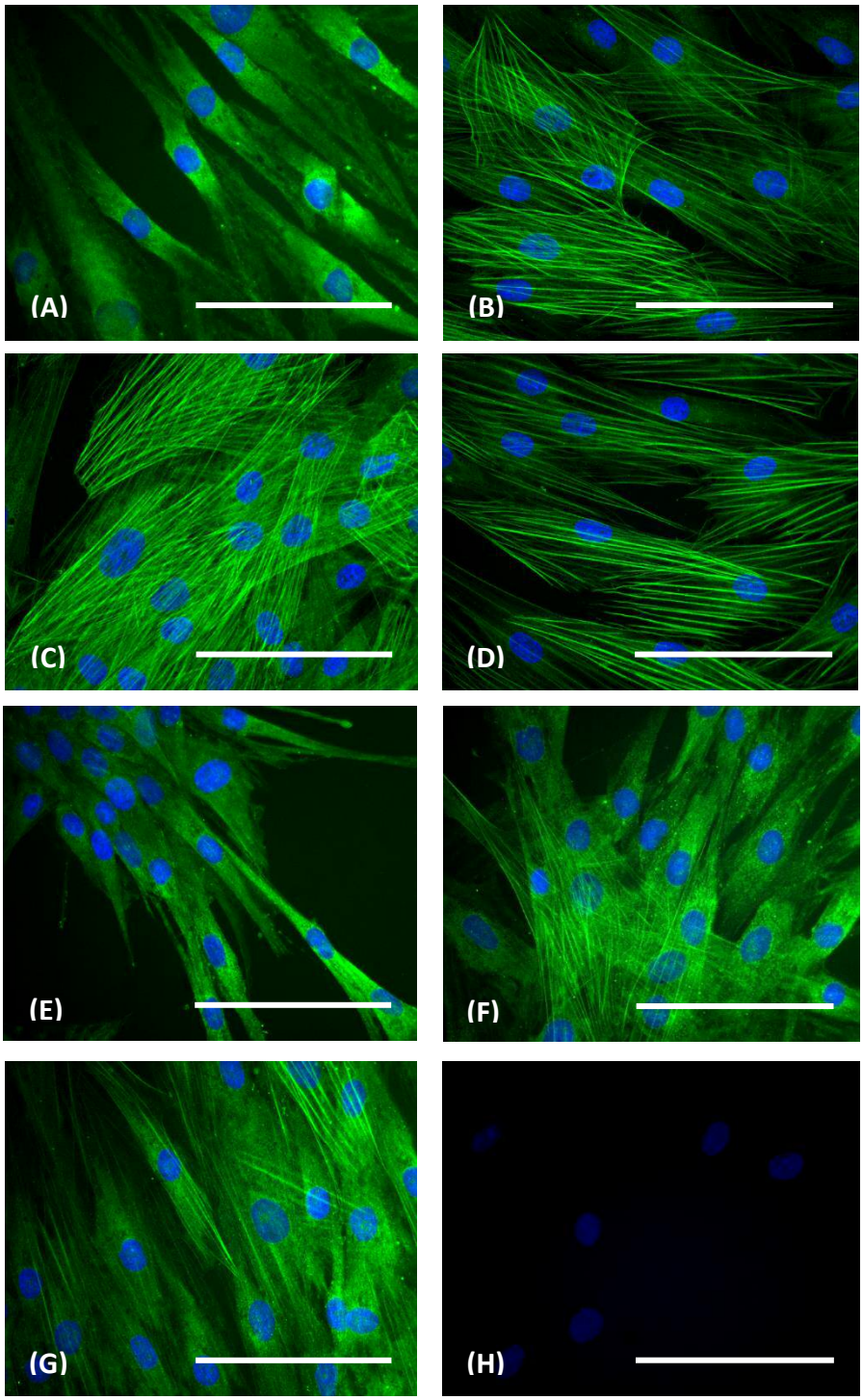

Figure 3.12. ICC analysis of DF-myofibroblast differentiation through visualisation of αSMA localisation and stress fibre formation (green), following treatment with (B) 0 µg/mL, (C) 0.001 µg/mL, (D) 0.01 µg/mL, (E) 0.1 µg/mL, (F) 1 µg/mL, (G) 10 µg/mL of EBC-46 in the presence of TGF-β_1 (10 ng/mL) for 48 h. Both EBC-46 (0 µg/mL) - TGF-β_1 controls (A) and primary antibody-free controls (H) were also included and nuclei were visualised by Hoechst stain (blue). Images displayed represent *n = 3* individual experiments captured at x400 magnification (scale bar = 100 µm).

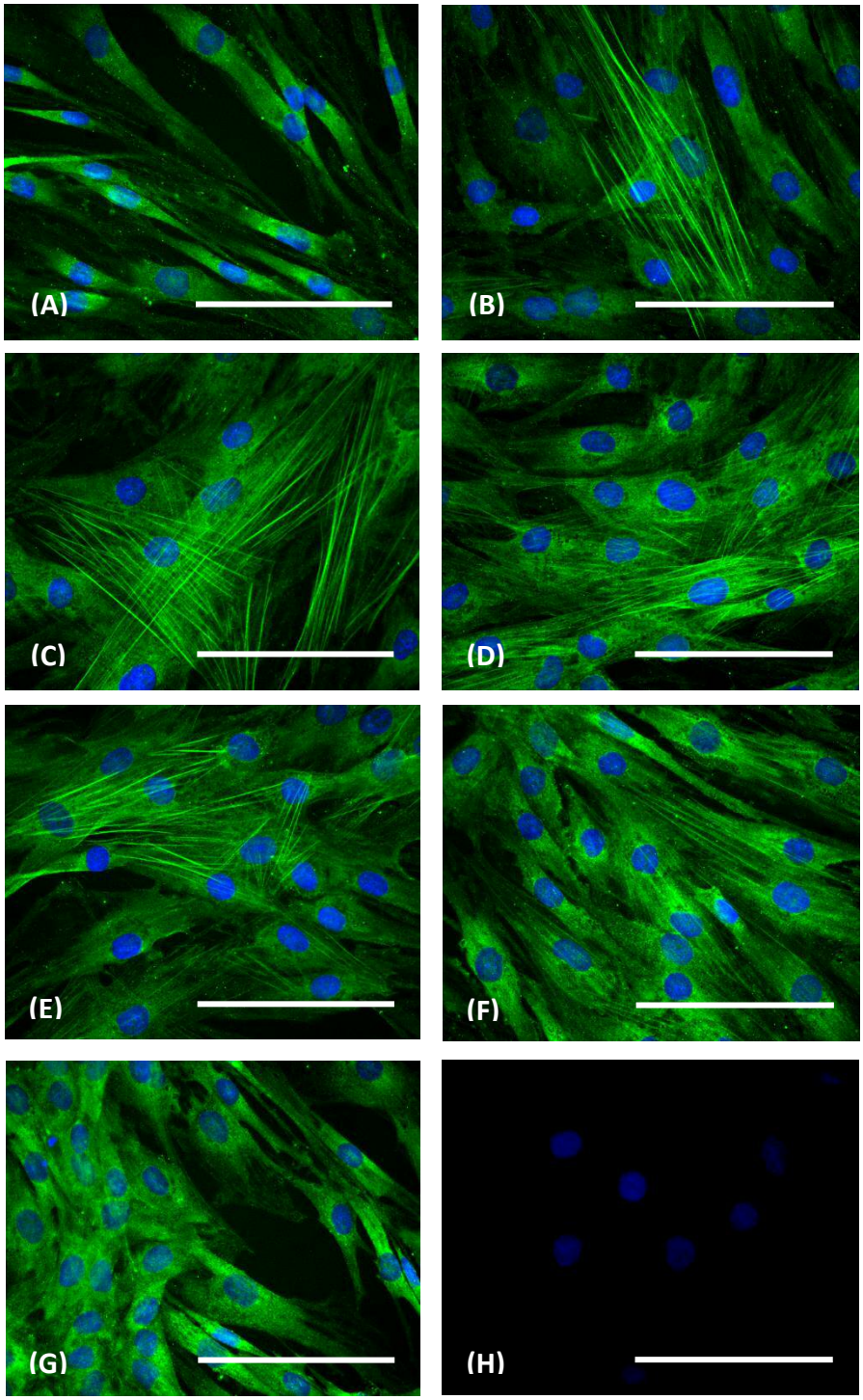

Figure 3.13. ICC analysis of DF-myofibroblast differentiation through visualisation of αSMA localisation and stress fibre formation (green), following treatment with (B) 0 µg/mL, (C) 0.001 µg/mL, (D) 0.01 µg/mL, (E) 0.1 µg/mL, (F) 1 µg/mL, (G) 10 µg/mL of EBC-211 in the presence of TGF-β_1 (10 ng/mL) for 24 h. EBC-211 (0 µg/mL) - TGF-β_1 controls (A) and primary antibody-free controls (H) were also included and nuclei were visualised by Hoechst stain (blue). Images displayed represent *n = 3* individual experiments captured at x400 magnification (scale bar = 100 µm).

μg/mL EBC-211, less stress fibre formation was observed in comparison to the lower EBC-211 concentrations, with cells possessing elongated phenotypes comparable to the TGF-β_1-negative controls (Figure 3.13A). However, at 10 μg/mL EBC-211 (Figure 3.13G), DFs showed a lack of stress fibre formation and displayed elongated, spindle-shaped morphologies, most comparable to TGF-β_1-negative controls (Figure 3.13A). Furthermore, cellular aggregation was observed at 10 μg/mL, which was not shown in controls (Figure 3.13A - B). These characteristics observed at 10 μg/mL were also present post-24 h treatment with 0.1 μg/mL EBC-46. Following 48 h treatment with EBC-211 in the presence of TGF-β_1 (Figure 3.14C - G), most concentrations (0.001 - 1 μg/mL) showed comparable αSMA expression and stress fibre development to TGF-β_1-positive controls (Figure 3.14B). At these concentrations, mature myofibroblastic morphologies were demonstrated by cells; characterised by prominent cytoskeletal arrangement, uniform stress fibre formation and large polyclonal phenotypes (Figure 3.14C - F). However, at 10 μg/mL of EBC-211 (Figure 3.14G), a distinct lack of stress fibre formation was observed; cells appeared spindle-shaped and elongated, similar in morphology to those found in the TGF-β_1-negative controls (Figure 3.14A). Cellular aggregation was also observed at this concentration, which was not shown in either control (Figure 3.14A - B). Therefore, both the absence of stress fibre formation and the presence of cell aggregation observed after 24 h treatment with 10 μg/mL EBC-211 (Figure 3.13G) were retained at 48 h (Figure 3.14G). These characteristics were also retained at 72 h (Figure 3.2G), as was also the case post-treatment with EBC-46 at 0.1 μg/mL.

3.4.5 Effects of EBC-46 and EBC-211 on DF-Myofibroblast Transition

Following the time-course ICC studies (Section 3.4.4), qPCR analysis was performed to assess the effects of EBC-46 and EBC-211 on genes involved in DF-myofibroblast transition. Quantification was performed upon cells cultured with either EBC-46 at 0.01 - 0.1 μg/mL or EBC-211 at 1 - 10 μg/mL, respectively; in the presence of TGF-β_1 (10 ng/mL), over 24 h, 48 h and 72 h in culture (Figures 3.15 and 3.16). Compound-free controls with/without TGF-β_1 were also included at each time-point to confirm normal DF-myofibroblast responses and for comparative purposes. As was previously

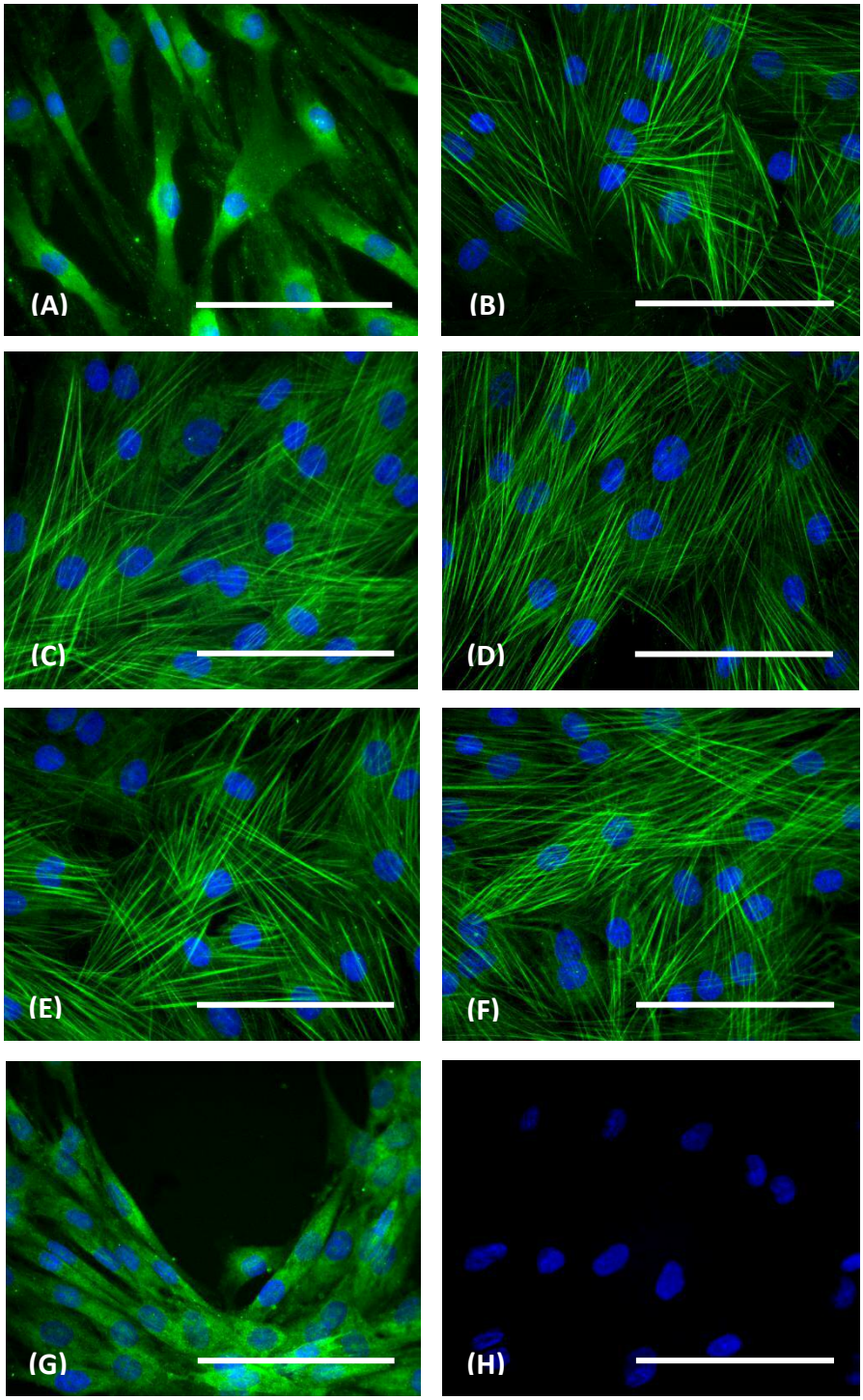

Figure 3.14. ICC analysis of DF-myofibroblast differentiation through visualisation of αSMA localisation and stress fibre formation (green), following treatment with (B) 0 µg/mL, (C) 0.001 µg/mL, (D) 0.01 µg/mL, (E) 0.1 µg/mL, (F) 1 µg/mL, (G) 10 µg/mL of EBC-211 in the presence of TGF-β_1 (10 ng/mL) for 48 h. EBC-211 (0 µg/mL) - TGF-β_1 controls (A) and primary antibody-free controls (H) were also included and nuclei were visualised by Hoechst stain (blue). Images displayed represent *n = 3* individual experiments captured at x400 magnification (scale bar = 100 µm).

described, TGF-β_1-stimulated differentiation was confirmed by the induction and up-regulation of myofibroblast markers, αSMA (Meran *et al.* 2007; Webber *et al.* 2009) and EDA-FN (Borsi *et al.* 1990; Midgley, 2014; Woods, 2016).

Regarding effects upon αSMA gene expression, cells cultured with EBC-46 (0.01 - 0.1 µg/mL) in the presence of TGF-β_1 (Figure 3.15A) showed a time-dependent induction of αSMA, peaking between 48 - 72 h. Following 24 h treatment, 0.01 µg/mL EBC-46 displayed a significant 1.6-fold up-regulation in αSMA expression, compared to the TGF-β_1-positive controls (*p = <0.05*). However, at 0.1 µg/mL EBC-46, a significant 5.4-fold down-regulation in αSMA expression was shown, compared to TGF-β_1-positive controls (*p = <0.01*; Figure 3.15A). This corroborated the 24 h ICC data, in which DFs showed a lack of stress fibre formation following 0.1 µg/mL EBC-46 treatment (Figure 3.11E). Post-48 h treatment, 0.01 µg/mL EBC-46 displayed an increase in expression versus the TGF-β_1-positive controls; although this was not statistically significant (*p = >0.05*). Similarly to the 24 h data, post-48 h 0.1 µg/mL EBC-46 treatment, significant 3-fold reduction of αSMA expression was identified; versus TGF-β_1-positive controls (*p = <0.001*; Figure 3.15A). This corroborated the 48 h ICC data, in which 0.01 µg/mL EBC-46 (Figure 3.12D), showed comparable αSMA expression/stress fibre formation to the TGF-β_1-positive controls and 0.1 µg/mL-treated cells exhibited a lack of stress fibre formation (Figure 3.12E). Following 72 h treatment and as observed previously (Figure 3.5A), a significant 1.6-fold increase in αSMA expression was found at 0.01 µg/mL EBC-46 with a 1.8-fold down-regulation at 0.1 µg/mL, versus TGF-β_1-positive controls (*p = <0.01*; Figure 3.15A). This further corroborated the 72 h ICC and qPCR data described prior (Figures 3.1D - E and 3.5A, respectively). Interestingly, despite being down-regulated at each time-point examined versus TGF-β_1-positive controls, αSMA expression following 0.1 µg/mL treatment was approximately 3.4-, 12.9- and 13.7-fold higher at 24 h, 48 h and 72 h, respectively; compared to TGF-β_1-negative controls. This indicated that αSMA expression is still induced in DFs at this EBC-46 concentration, but not to the same extent as TGF-β_1-stimulated DFs.

Similar studies with EBC-211 (1 - 10 µg/mL; Figure 3.15B), demonstrated comparable

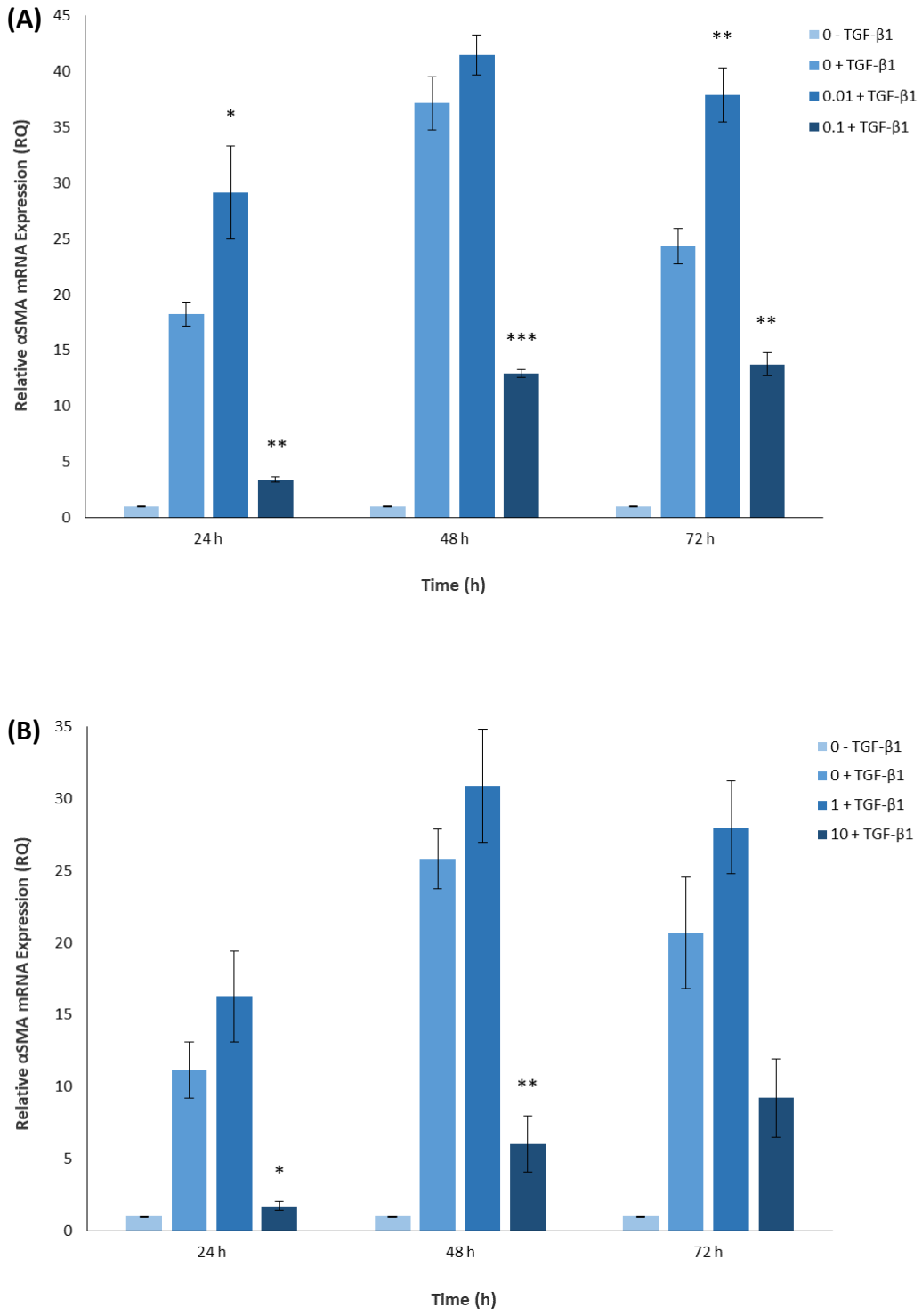

Figure 3.15. Analysis of DF-myofibroblast differentiation via quantification of αSMA gene expression by qPCR; following treatment with (A) EBC-46 (0.01 µg/mL and 0.1 µg/mL) and (B) EBC-211 (1 µg/mL and 10 µg/mL), in the presence of TGF-β_1 over 24, 48 and 72 h. Compound-free controls ± TGF-β_1 were included (*n = 3*, mean±SEM; *p = *<0.05, **<0.01, ***<0.001* versus TGF-β_1-positive controls).

responses to those induced by EBC-46. Cells cultured with EBC-211, in the presence of TGF-β_1, exhibited a time-dependent induction of αSMA gene expression, peaking between 48 - 72 h. Following 24 h treatment, 1 µg/mL EBC-211 displayed increased αSMA expression versus the TGF-β_1-positive control. However, this was not deemed statistically significant (*p = >0.05*). In contrast, a significant 6.5-fold down-regulation in αSMA expression was shown following 10 µg/mL of EBC-211 treatment, compared to TGF-β_1-positive controls (*p = <0.05*; Figure 3.15B). This corroborated the 24 h ICC data, in which cells at 1 µg/mL EBC-211 (Figure 13.3F) displayed comparable αSMA expression and stress fibre formation to TGF-β_1-positive controls; whilst 10 µg/mL-treated DFs exhibited no stress fibre formation (Figure 3.13G). Similarly to the 24 h data, following 48 h 1 µg/mL EBC-211 treatment, DFs exhibited an increase in αSMA expression versus TGF-β_1-positive controls. As with the 24 h data, however, this was deemed statistically significant (*p = >0.05*). In contrast, a significant 4.3-fold decrease in αSMA expression was found with 10 µg/mL EBC-211 treatment at 48 h; compared to TGF-β_1-positive controls (*p = <0.01*; Figure 3.15B). These results corroborated the 48 h ICC data, in which DFs demonstrated comparable αSMA expression, stress fibre development and morphology to the TGF-β_1-positive control cells following 1 µg/mL EBC-211 treatment (Figure 3.14F); DFs at 10 µg/mL EBC-211 demonstrated a lack of stress fibre formation (Figure 3.14G). Lastly, following 72 h treatment, cells showed an increase in αSMA expression at 1 µg/mL EBC-211, versus TGF-β_1-positive controls (Figure 3.15B). As was also found at 24 h and 48 h, however, this was not statistically significant (*p = >0.05*). Although a similar down-regulation in αSMA gene expression was shown at 10 µg/mL of EBC-211 at 72 h, as observed at previous time-points, this was not deemed statistically significant (*p = >0.05*). Despite this, these trends further corroborate 72 h ICC and qPCR data described previously (Figures 3.2F - G and 3.5B, respectively). Interestingly, as exhibited at 0.1 µg/mL of EBC-46, despite being down-regulated at each time-point examined, versus TGF-β_1-positive controls, αSMA gene expression following 10 µg/mL of EBC-211 treatment was still approximately 1.7-, 6- and 9.2-fold higher at 24 h, 48 h and 72 h, respectively; versus the TGF-β_1-negative controls. This indicated that αSMA expression is still induced in DFs at this EBC-211 concentration, but not to the same extent as TGF-β_1-stimulated DFs.

With regards to EDA-FN gene expression, as reported previously, it is increased post-TGF-β_1 treatment (Balza *et al*. 1988; Borsi *et al*. 1990; Kohan *et al*. 2010). The results were consistent with the reported studies, as consistent increases expression were demonstrated at each time-point; versus TGF-β_1-negative controls (Figure 3.16A and B). However, EDA-FN expression did not seem to increase as time progressed, in TGF-β_1-positive control cells. DFs cultured with EBC-46 (0.01 - 0.1 µg/mL) in the presence of TGF-β_1 (Figure 3.16A), showed up-regulation at both concentrations over time; in comparison to TGF-β_1-positive controls. At 24 h, 0.01 µg/mL EBC-46 demonstrated a significant 2-fold increase in EDA-FN expression (Figure 3.16A; *p = <0.01*). In contrast, 0.1 µg/mL of EBC-46 did not induce a statistically significant increase in EDA-FN gene expression versus TGF-β_1-positive controls (*p = >0.05*). Peak EDA-FN expression was observed following 48 h treatment with 0.01 µg/mL EBC-46, which induced 3.3-fold increase in expression (Figure 3.16A; *p = <0.001*). A significant 2.2-fold up-regulation was also found with 0.1 µg/mL EBC-46 at 48 h, versus the TGF-β_1-positive controls (*p = <0.01*). By 72 h, 0.01 and 0.1 µg/mL EBC-46 yielded 3.5-fold and 2.8-fold increases in EDA-FN expression, respectively; compared to TGF-β_1-positive controls. However, only the former was statistically significant (*p = <0.05*).

Similar studies with EBC-211 (1 - 10 µg/mL; Figure 3.16B) demonstrated comparable responses to those induced by EBC-46. At 24 h, 1 µg/mL EBC-211 showed significant 2-fold up-regulation in EDA-FN expression (Figure 3.16B; *p = <0.01*). In contrast, 10 µg/mL EBC-211 did not induce a significant change in expression, compared to TGF-β_1-positive controls (*p = >0.05*). After 48 h, 1 µg/mL EBC-211 induced a 3.2-fold up-regulation in EDA-FN expression (*p = <0.001*), whereas 0.1 µg/mL induced around 2-fold increase in expression (*p = <0.01*), versus TGF-β_1-positive controls (Figure 3.16B). Peak EDA-FN expression was observed following 72 h treatment with 1 µg/mL EBC-211, which induced an approximate 3.4-fold up-regulation in expression (*p = <0.01*). However, unlike 0.1 µg/mL of EBC-46 at 72 h (Figure 3.16A), a statistically significant 2.4-fold up-regulation in EDA-FN expression was also found at 10 µg/mL of EBC-211, versus TGF-β_1-positive controls (Figure 3.16B; *p = <0.05*).

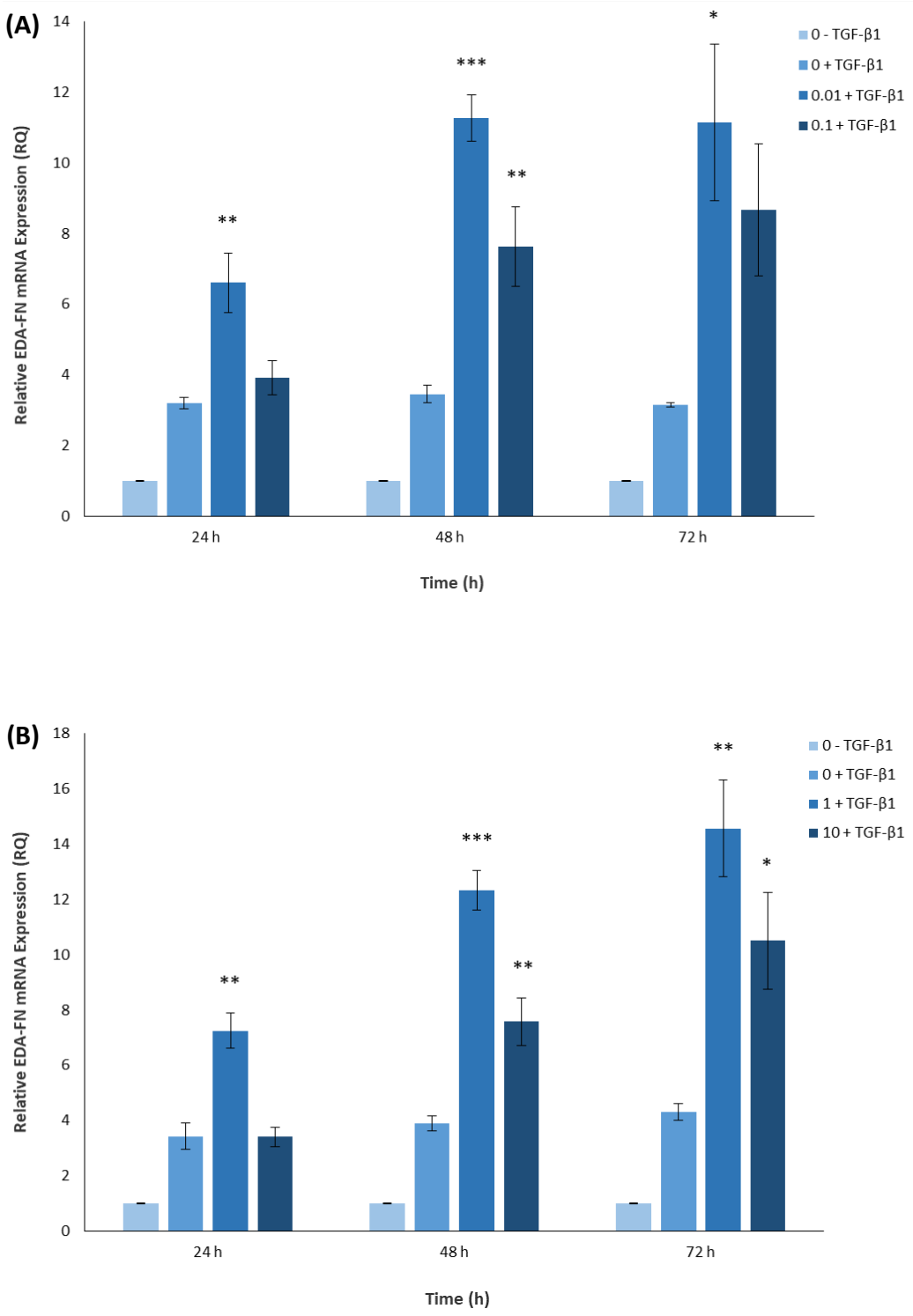

Figure 3.16. Analysis of DF-myofibroblast differentiation via quantification of EDA-FN gene expression by qPCR; following treatment with (A) EBC-46 (0.01 µg/mL and 0.1 µg/mL) and (B) EBC-211 (1 µg/mL and 10 µg/mL), in the presence of TGF-β_1 over 24 h, 48 h and 72 h. Compound-free controls ± TGF-β_1 were also included (*n = 3*, mean± SEM; *p = *<0.05, **<0.01, ***<0.001* versus TGF-β_1-positive controls).

3.4.6 Effects of EBC-46 and EBC-211 on Differentiation-Related Genes

To assess the effects of EBC-46 and EBC-211 on other genotypic changes associated with TGF-β_1-driven, DF-myofibroblast differentiation, qPCR analysis was performed to determine CD44, EGFR and TSG6 gene expression levels. Analysis was performed on DFs cultured with either EBC-46 or EBC-211 at all aforementioned concentrations (Section 3.3), in the presence of TGF-β_1 (10 ng/mL) over 72 h in culture (Figures 3.17 - 3.19). Compound-free controls with/without TGF-β_1 were also included to confirm normal DF-myofibroblast responses and for comparative purposes. Reported prior, TGF-β_1 treatment has been found to decrease CD44 and EGFR gene expression after 72 h culture (Midgley, 2014; Woods, 2016). In contrast, TGF-β_1-stimulated DFs show up-regulations in TSG6 expression at 72 h (Webber *et al*. 2009b; Martin *et al*. 2016). Findings detailed hereafter are consistent with these reported studies, as around 2-fold decreases in CD44 and EGFR gene expression were observed in TGF-β_1-positive DFs following 72 h treatment (Figures 3.17 and 3.18, respectively); versus the TGF-β_1-negative controls. TSG6 gene expression was approximately 4.5-fold up-regulated in TGF-β_1-positive DFs post-72 h treatment (Figure 3.19A and B); versus the TGF-β_1-negative controls.

With CD44 gene expression, DFs cultured with EBC-46 (0.001 - 10 µg/mL), within the presence of TGF-β_1 (Figure 3.17A), displayed a down-regulatory trend across all EBC-46 concentrations. However, no significant differences in CD44 gene expression were found; compared to the TGF-β_1-positive controls (Figure 3.17A; *p = >0.05*). RQs were approximately 2.7 - 3.7-fold decreased versus the TGF-β_1-negative controls, with the smallest down-regulation shown at 0.1 µg/mL EBC-46. Similar studies with EBC-211 at the same concentrations (Figure 3.17B), displayed comparable responses to those induced by EBC-46. However, statistically significant down-regulations were seen at all EBC-211 concentrations (*p = <0.05* at 0.01 µg/mL, *p = <0.01* at 0.001 µg/mL and 1 µg/mL and *p = <0.001* at 0.1 µg/mL), except 10 µg/mL (*p = >0.05*), versus the TGF-β_1-positive controls (Figure 3.17B).

In relation to EGFR expression, cells cultured with EBC-46 (0.001 - 10 µg/mL) in the

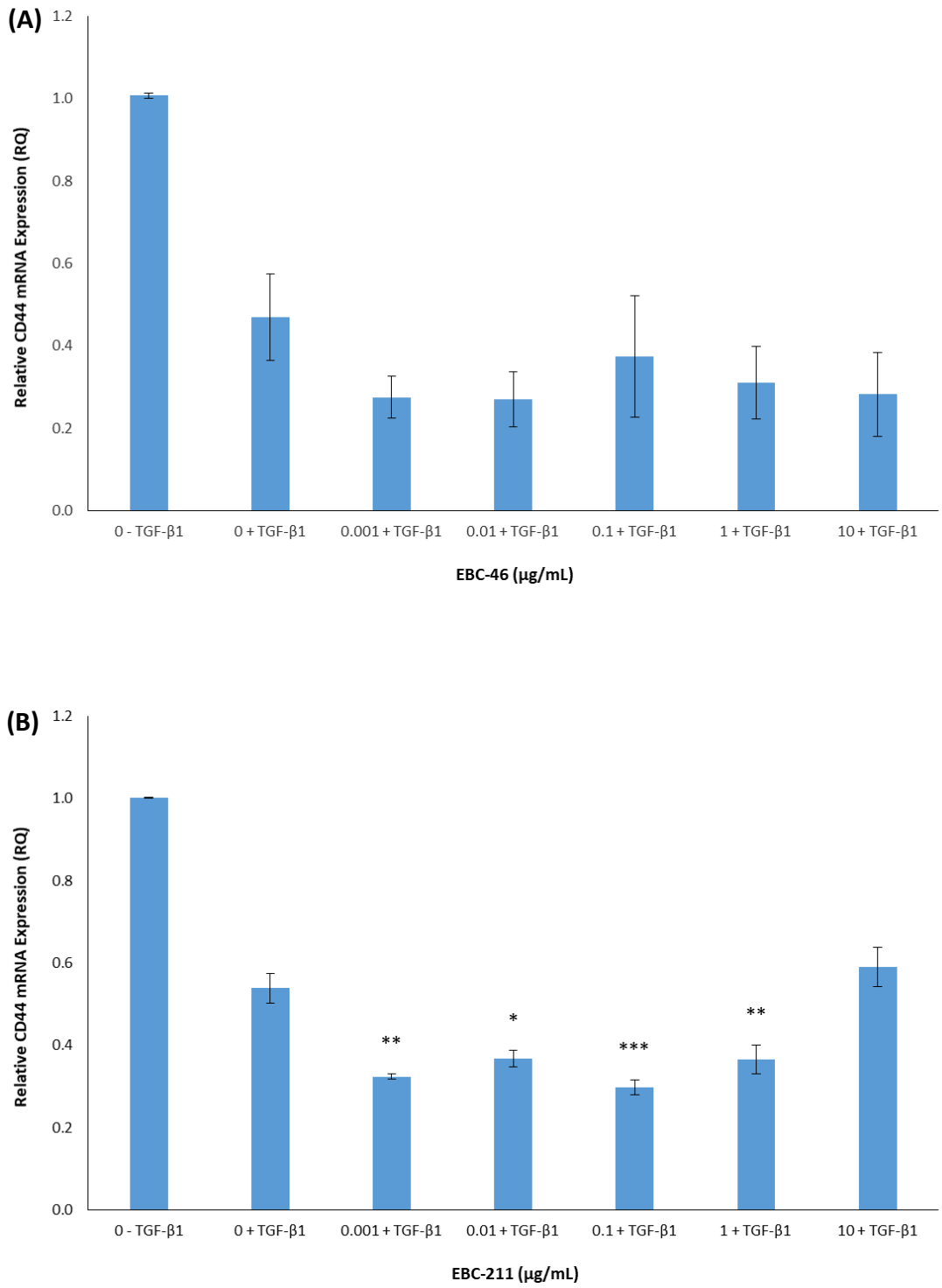

Figure 3.17. Analysis of DF-myofibroblast differentiation via quantification of CD44 gene expression by qPCR; post-treatment with (A) EBC-46 and (B) EBC-211 (0.001 µg/mL, 0.01 µg/mL, 0.1 µg/mL, 1 µg/mL and 10 µg/mL), in the presence of TGF-β_1, for 72 h. Compound-free controls ± TGF-β_1 were also included (*n = 3*, mean±SEM; *p = *<0.05, **<0.01, ***<0.001* versus TGF-β_1-positive controls).

presence of TGF-β_1 (Figure 3.18A), demonstrated a down-regulatory trend across all concentrations. However, no significant differences in EGFR expression were found; versus TGF-β_1-positive controls (Figure 3.18A; *p = >0.05*). RQs were approximately 3 - 4-fold down-regulated, compared to TGF-β_1-negative controls, similar to the trend in CD44 expression after EBC-46 treatment (Figure 3.17A). Studies using EBC-211 at the same concentrations (0.001 - 10 µg/mL; Figure 3.18B), yielded similar responses to those induced by EBC-46. Though EGFR expression was significantly decreased at 1 µg/mL (*p = <0.05*), no significant differences in EGFR expression were induced at all other concentrations; versus TGF-β_1-positive controls (Figure 3.18B; *p = >0.05*). Gene expression levels were approximately 2 - 3-fold decreased across all concentrations, compared to TGF-β_1-negative controls; similar to the trend in CD44 expression found following EBC-211 treatment (Figure 3.17B).

With regards to TSG6 expression, DFs cultured with EBC-46 (0.001 - 10 µg/mL) in the presence of TGF-β_1 (Figure 3.19A), showed down-regulation at all concentrations; in comparison to the TGF-β_1-positive controls. Statistically significant decreases in TSG6 expression were displayed at lower concentrations of EBC-46 (0.001 - 0.1 µg/mL; *p = <0.01*), producing 3.2 - 3.4-fold down-regulations (Figure 3.19A). The higher EBC-46 concentrations displayed even greater down-regulations (1 - 10 µg/mL; *p = <0.001*), demonstrating approximately 10-fold decreases in TSG6 expression versus TGF-β_1-positive controls. Similar studies using EBC-211 at the same concentrations (Figure 3.19B), demonstrated comparable genotypic responses to those induced by EBC-46. Statistically significant TSG6 down-regulation was found at all concentrations of EBC-211 versus TGF-β_1-positive controls (0.001 - 10 µg/mL; *p = <0.001*). As demonstrated with EBC-46, higher EBC-211 concentrations exhibited greater down-regulation (0.1 - 10 µg/mL; 2.2 - 3.4-fold) than at lower concentrations (0.001 - 0.01 µg/mL; 1.8 - 2-fold).

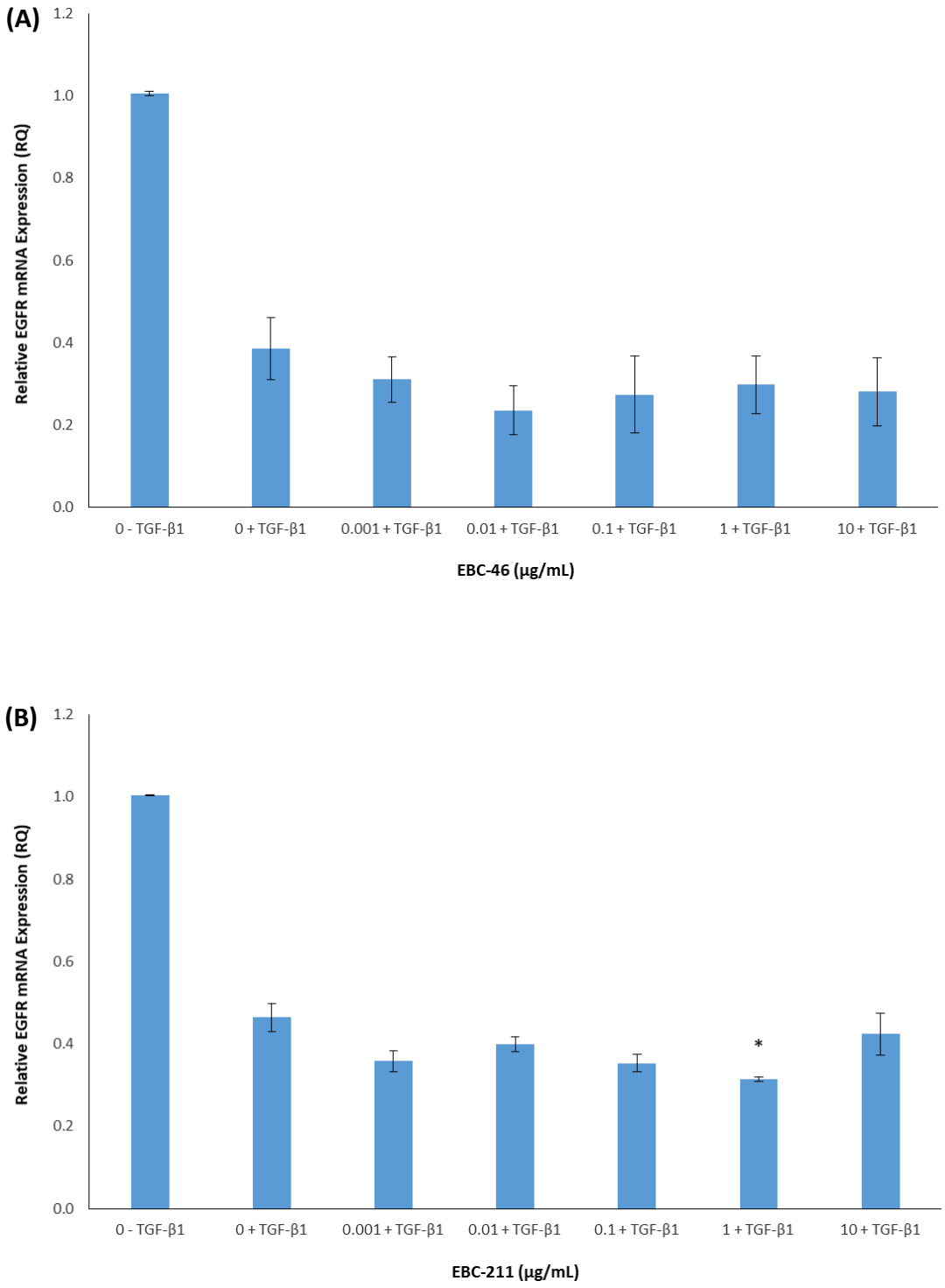

Figure 3.18. Analysis of DF-myofibroblast differentiation via quantification of EGFR gene expression by qPCR; post-treatment with (A) EBC-46 and (B) EBC-211 (0.001 µg/mL, 0.01 µg/mL, 0.1 µg/mL, 1 µg/mL and 10 µg/mL), in the presence of TGF-β_1, for 72 h. Compound-free controls ± TGF-β_1 were also included (*n = 3*, mean±SEM; *p = *<0.05* versus TGF-β_1-positive controls).

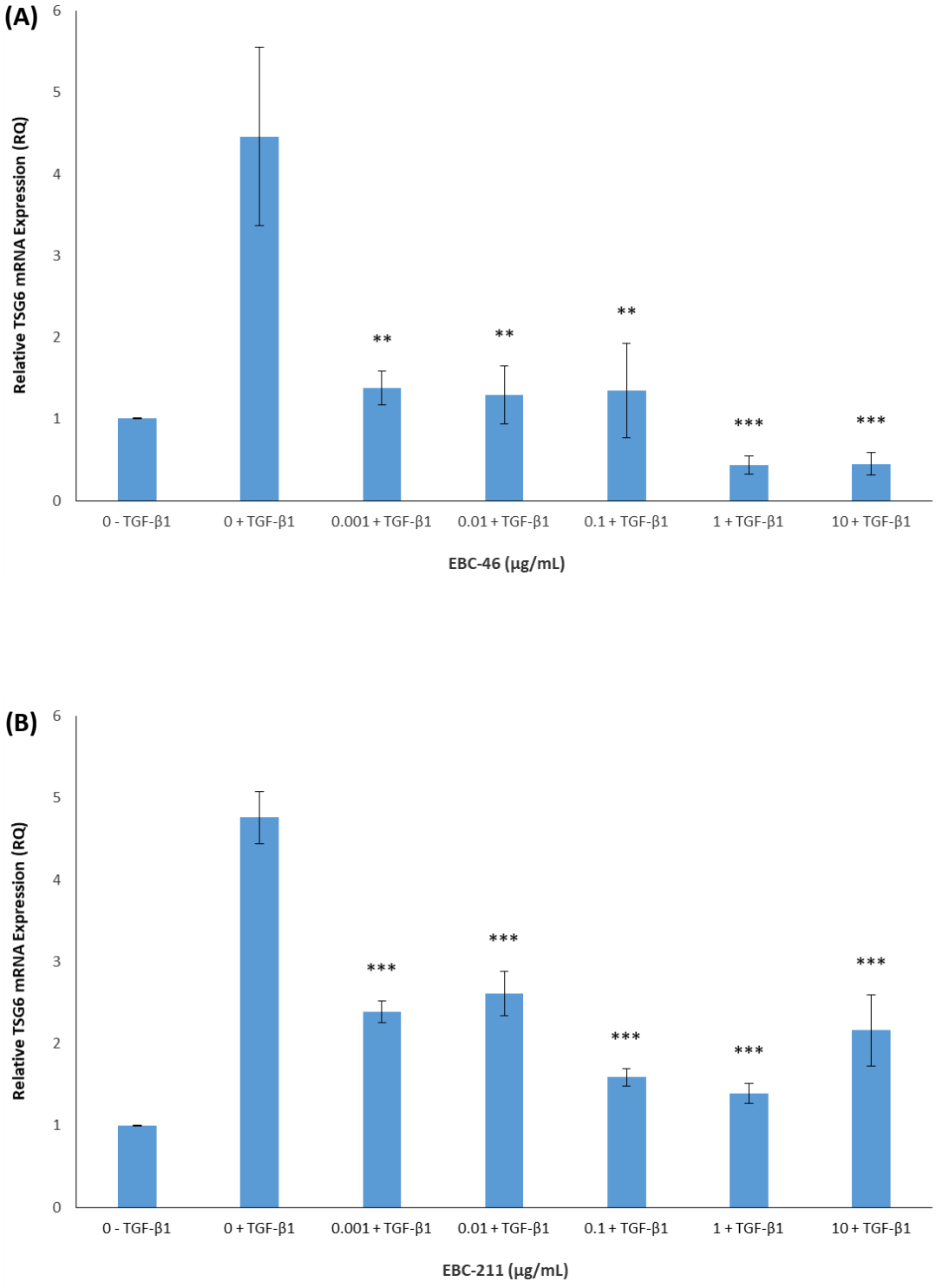

Figure 3.19. Analysis of DF-myofibroblast differentiation via quantification of TSG6 gene expression by qPCR; post-treatment with (A) EBC-46 and (B) EBC-211 (0.001 µg/mL, 0.01 µg/mL, 0.1 µg/mL, 1 µg/mL and 10 µg/mL), in the presence of TGF-β_1, for 72 h. Compound-free controls ± TGF-β_1 were also included (*n = 3*, mean±SEM; *p = **<0.01, ***<0.001* versus TGF-β_1-positive controls).

3.5 Discussion

The present Chapter focused on assessing the effects of novel epoxy-tiglianes, EBC-46 and EBC-211, on DF-myofibroblast differentiation and whether these compounds modulated DF/myofibroblast genotype and/or phenotype *in vitro*; to illicit minimal scarring responses *in vivo*. Palliative animal studies, carried out by veterinarians in collaboration with QBiotics Group, have previously demonstrated the preferential effects of epoxy-tiglianes on wound repair *in vivo* (Reddell *et al.* 2014; Campbell *et al.* 2017; Hansen *et al.* 2018). As detailed previously (Chapter 3.1), these anti-cancer animal studies and trials have indirectly led to recurrent observations of exceptional wound healing responses post-tumour slough. After these observations, veterinary wound healing trials were initiated and these demonstrated similar improvements in healing outcomes; including rapid granulation tissue formation, accelerated wound closure and re-epithelialisation, reduced scarring and appendage reformation. Many of the cases included in these trials were wounds that were previously unresponsive to months of treatment (Campbell *et al*. 2014, 2017; Reddell *et al*. 2014). In order to progress towards human clinical trials using epoxy-tiglianes as novel wound healing and anti-scarring agents, however; it is necessary to understand these modulatory actions at a cellular level.

The delicate equilibrium between successful and impaired wound healing outcomes has been well-documented, with even slight changes in the fibroblast-myofibroblast gene expression profiles or functions/phenotypes, impacting wound resolution and clinical outcome. The importance of maintaining this balance is highlighted through the prevalence of aberrant fibrotic pathologies, such as chronic wound development or during the excessive scar tissue development, observed during hypertrophic and keloid scarring. In contrast, however, it may be possible to induce more regenerative dermal responses in order to permit adult wounds to heal preferentially (Reinke and Sorg, 2012; Erickson and Echeverri, 2018). Such modification could potentially result in healing processes akin to those found in early-gestational and oral mucosal wound healing; as described previously (Chapter 3.1). The above-mentioned animal studies undertaken by the QBiotics Group indicated an induction of similar beneficial repair

responses to those exhibited during oral mucosal and foetal wound repair, post-EBC-46 treatment (Campbell *et al.* 2017; Hansen *et al.* 2018). One key observation after wound closure was a distinct lack of visible scarring in treated skin, implicating EBC-46 and related epoxy-tiglianes in the potential modulation of DFs and myofibroblasts (Reddell *et al.* 2014). As detailed prior (Chapter 3.1), DFs are significant mediators of acute wound healing events; readily undergoing TGF-β_1-stimulated differentiation to acquire a specialised phenotype responsible for scar formation, wound contraction/ and closure (Desmoulière *et al*. 1993; Clark, 1993; Hinz *et al*. 2001a). Given the vital importance of DFs and myofibroblasts to the wound healing process, modulation of the mechanisms involved in DF-myofibroblast transition may explain the favourable responses observed following epoxy-tigliane treatment.

DFs undergo differentiation to myofibroblasts via TGF-β_1-induced differentiation. As the primary stimulator, TGF-β_1 promotes αSMA synthesis and its incorporation into stress fibres, resulting in DFs acquiring mature contractile phenotypes (Desmoulière *et al*. 1993; Gabbiani, 2003; Malmström *et al.* 2004). Myofibroblasts possess distinct morphologies and gene expression profiles to their undifferentiated counterparts; in particular, they express greater αSMA levels, develop prominent αSMA stress fibres and undergo extensive polygonal, cytoskeletal rearrangement (Sappino *et al.* 1990; Desmoulière *et al*. 2005). As is well-established in the field, a combination of these factors indicates the presence of 'true' myofibroblasts. As αSMA is the actin isoform expressed by such cells, rather than quiescent fibroblasts, it is regarded as the gold-standard phenotypic marker of TGF-β_1-driven differentiation (Skalli *et al.* 1986; Darby *et al*. 1990; Hinz *et al*. 2001b; Gabbiani, 2003). Thus, initial studies assessed whether EBC-46 and EBC-211 were able to modulate αSMA gene expression and formation of stress fibres; thereby altering DF-myofibroblast genotype/phenotype.

At 0.1 µg/mL EBC-46 and 10 µg/mL EBC-211, in the presence of TGF-β_1, inhibition of stress fibre formation was apparent at 72 h. Despite expressing αSMA, cells at these concentrations lacked bundles of parallel stress fibre microfilaments and polygonal morphologies typically observed post-TGF-β_1 stimulation. Rather, the DFs displayed

characteristics akin to quiescent fibroblast morphologies, possessing elongated and spindle-shaped appearances (Gabbiani *et al.* 1971; Sandbo and Dulin, 2011). These studies were repeated in the absence of TGF-β_1, and no major differences in αSMA expression or morphology were found at most concentrations of EBC-46 or EBC-211, in comparison to the TGF-β_1-negative controls. Some concentrations showed greater variability, with either intermediate cell phenotypes or a mixture of spindle-shaped and polygonal morphologies; however, stress fibre development was minimal, if not completely lacking. The aforementioned observations were validated through qPCR studies, which showed significant reductions in αSMA expression at both 0.1 µg/mL EBC-46 and 10 µg/mL EBC-211 in the presence of TGF-β_1, versus the TGF-β_1-positive controls. Although expression was still notably higher than TGF-β_1-negative controls, such findings imply that specific epoxy-tigliane concentrations inhibit myofibroblast formation. In contrast, no significant differences in αSMA expression were found at any EBC-46 and EBC-211 concentrations in the absence of TGF-β_1, compared to TGF-β_1-negative controls. Together, these studies suggest that EBC-46 and EBC-211 have dose-dependent inhibitory effects upon myofibroblast differentiation; however, do not seem to significantly alter DF morphology/gene expression alone. Furthermore, these findings support research performed previously by Qbiotics Group, confirming EBC-211 as a lesser active analogue of EBC-46; as a 100-fold greater concentration is required to induce similar effects to those observed following treatment with EBC-46 (Moses, 2016).

In support of the previous studies and in order to elucidate whether epoxy-tiglianes were responsible for a phenotypic reversal or a complete inhibition of myofibroblast formation, further studies were performed at earlier time-points. At 0.1 µg/mL EBC-46 and 10 µg/mL EBC-211, in the presence of TGF-β_1, inhibition of αSMA stress fibre formation was also apparent at 24 h and 48 h. As shown at 72 h, despite expressing αSMA, cells at these concentrations lacked the characteristic stress fibre formation and polygonal morphology usually observed after TGF-β_1 stimulation (Sappino *et al.* 1990; Desmoulière *et al*. 2005). Furthermore, cells at these concentrations showed no intermediate or transitional morphologies over time; displaying features akin to

quiescent DFs, with narrow, elongated spindle-shapes (Gabbiani *et al.* 1971; Sandbo and Dulin, 2011). Pockets of DF aggregation were also apparent at 0.1 µg/mL EBC-46 and 10 µg/mL EBC-211 over time, forming a mesh-like cell monolayer. This could be due to the lack of myofibroblast phenotypes found at these concentrations, as TGF-β_1-driven differentiation inhibits migration *in vitro* (Ellis and Schor, 1996; Larson *et al.* 2010). However, this is not found in unstimulated fibroblasts, indicating that this cell migration and aggregation is due to epoxy-tigliane treatment; currently, it is not known how the compounds stimulate such responses. It has been hypothesised that motogenic effects, and TGF-β_1 antagonism towards these effects, can be modulated by alterations in hyaluronan (HA) synthesis. Indeed, foetal fibroblasts possess more surface receptors for HA, which enhance their migratory abilities; they also express low levels of TGF-β_1 (Ellis *et al*. 1992; Larson *et al.* 2010). Thus, further investigations focusing on compound effects on HA synthesis would aid in clarification of potential underlying mechanisms of these responses.

Aforementioned timecourse observations were validated using qPCR studies, which showed significant reductions in αSMA expression at both 0.1 µg/mL EBC-46 and 10 µg/mL EBC-211, in the presence of TGF-β_1, at 24 and 48 h. Although expression was still notably higher than that of unstimulated DFs, these findings imply that specific epoxy-tigliane concentrations inhibit myofibroblast formation from initial exposure to TGF-β_1; rather than reversing proto-myofibroblast/myofibroblast phenotypes. As a potential anti-scarring therapy, consideration must be given regarding the degree to which DF activity is impeded, as some is required for wound contraction to occur (Parekh and Hebda, 2017). However, foetal fibroblasts have been found to facilitate collagen gel reorganisation to the same extent as adult DFs, despite their differences in αSMA expression and contractile ability. This suggests that cellular forces exerted by undifferentiated fibroblasts are sufficient for ECM remodelling and subsequent wound resolution (Parekh and Hebda, 2017). Similar responses have been reported with OMFs, inducing accelerated contraction of collagen gels, while expressing lower αSMA levels (Shannon *et al.* 2006). These findings imply that reduced myofibroblast presence allows scarless/minimal scarring healing to occur, not an overall reduction

in wound contraction. Therefore, reduced expression of αSMA post-treatment with certain EBC-46 and EBC-211 concentrations; and the resulting lack of myofibroblast formation, may lead to minimal scarring responses following injury. This theory fits in with *in vivo* animal studies performed by the QBiotics group, exhibiting a reduced fibrotic response following treatment with the novel epoxy-tiglianes (Reddell *et al.* 2014; Campbell *et al.* 2017; Hansen *et al.* 2018). However, it is not yet understood why these inhibitory responses only occur at 0.1 µg/mL EBC-46 and 10 µg/mL EBC-211, but not at other concentrations. Such differences in response are hypothesised as being due to contrasting activation, distribution and localisation of PKC isoforms (Boyle *et al*. 2014).

To further assess the apparent modulatory effects of EBC-46 and EBC-211 upon the actin cytoskeleton, additional studies were performed examining their influence on cytoskeletal reorganisation. As previously mentioned (Chapter 1), upon wounding, actin polymerisation is initiated and globular actin (G-actin) subunits assemble into long polymerised F-actin fibres (Kopecki and Cowin, 2016). Under resting conditions, DFs display spindle-shaped appearances and actin expression is localised at the cell periphery. Post-TGF-β_1 stimulation, the cells become larger and polygonal in shape, demonstrating prominent cytoskeletal rearrangement, with F-actin microfilaments coalescing to form uniformly parallel bundles extending across the cell axis (Meran *et al.* 2007). Such modifications in the actin cytoskeleton regulate several functions during myofibroblast differentiation including FA formation, wound contraction and ECM remodelling, while simultaneously regulating transcription of associated genes. Therefore, the cytoskeleton plays an important role in augmenting signals leading to differentiation (Kopecki and Cowin, 2016). At 0.1 µg/mL EBC-46 and 10 µg/mL EBC-211, in the presence of TGF-β_1, cytoskeletal reorganisation was less prominent than typically observed post-TGF-β_1 stimulation. Despite the presence of polymerised F-actin, cells retained elongated, spindle-shaped appearances with less evident fibres localised more prominently around the cell periphery. Such responses are similar to those demonstrated by OMFs post-TGF-β_1 stimulation; these cells possess inherent resistance to TGF-β_1-driven differentiation, allowing them to maintain non-scarring

phenotypes which contribute to the regenerative healing ability of the oral mucosa (Meran *et al.* 2007; Dally *et al.* 2017). Changes in expression profiles of cytoskeletal-related proteins are indicative of discrepancies between fibrotic and scarless repair. Wounding has a differential effect on proteins associated with actin dynamics both in adult and foetal skin (Cowin *et al.* 2003; Kopecki and Cowin, 2016). Foetal wounds have been found to predominantly express epidermal F-actin, whereas adult wounds predominantly express dermal F-actin. This developmental switch may be important in foetal wound contraction and scarless repair, highlighting the potential for novel therapies capable of regulating the actin cytoskeleton (Cowin, 2005). Cell migration, motility, morphology, adhesion and differentiation can all be modulated, in part, by cytoskeletal assembly and disassembly. Thus, it would be beneficial to elucidate any preferentially expressed cytoskeletal genes occurring post-epoxy-tigliane treatment, such as via Microarray global gene analysis. Similar studies performed, in absence of TGF-β_1, indicated no significant differences in F-actin polymerisation or organisation at all epoxy-tigliane concentrations, versus TGF-β_1-negative controls. Therefore, the studies further suggest that the epoxy-tiglianes possess dose-dependent effects on the myofibroblast cytoskeleton. However, this does not seem to be the case in the absence of TGF-β_1, as also evidenced by the previous αSMA ICC and qPCR data.

Following on from the apparent effects on αSMA expression, stress fibre formation and F-actin reorganisation, potential epoxy-tigliane modulation of other associated genes involved in the DF-myofibroblast transition were explored. As aforementioned (Chapter 1 and 3.1), TGF-β_1 increases total fibronectin (FN) levels via preferentially promoting the accumulation of the EDA isoform (Balza *et al.* 1988; Borsi *et al.* 1990). In turn, EDA-FN facilitates and promotes TGF-β_1-driven myofibroblast differentiation and its expression is necessary for induction of the myofibroblastic phenotype (Serini *et al*. 1998). At 0.1 µg/mL and 10 µg/mL EBC-46 and EBC-211, respectively, increases in EDA-FN gene expression were shown following 48 - 72 h treatment, versus TGF-β_1-positive controls. This may contribute to explaining why αSMA expression was higher than the unstimulated DF controls at these concentrations; despite demonstrating significant decreases versus TGF-β_1-positive control. The presence of functional EDA

-FN is required for αSMA induction and inhibiting interactions between EDA-FN, the cell surface and TGF-β_1 can impair this. However, without TGF-β_1's presence, EDA-FN cannot induce αSMA alone; it is necessary, but not sufficient alone, to stimulate DF-myofibroblast differentiation and as such, exerts a permissive effect on TGF-β_1 (Serini *et al*. 1998; Tomasek *et al*. 2002). Foetal skin wounds have enhanced abilities to up-regulate ECM adhesion proteins, including FN. They express FN more rapidly than in adult wounds, facilitating rapid wound repair, cell anchoring and attachment (Larson *et al.* 2010). Thus, increases in EDA-FN expression at 0.1 μg/mL and 10 μg/mL EBC-46 and EBC-211, respectively, across time, with lack of αSMA stress fibre development, may partly explain the cellular aggregation also observed at these concentrations; as FN links cell surface integrins and adhesion molecules to ECM proteins, assisting cell attachment and migration.

As described previously (Chapter 1), HA has been shown to be a major modulator of TGF-β_1-driven DF-myofibroblast differentiation and previous studies have shown HA inhibition to antagonise the myofibroblast phenotype (Webber *et al.* 2009a). The HA -mediated co-localisation of CD44 with EGFR in lipid rafts has been established as a distinct, but cooperating pathway to the classical TGF-β/SMAD pathway; with both signalling in parallel to drive acquisition of the myofibroblast phenotype (Midgley *et al.* 2013). Pharmacological inhibition of EGFR has also been shown to attenuate TGF-β_1-stimulated induction of αSMA and aging fibroblasts have demonstrated a lack of EGFR expression, resulting in resistance to TGF-β_1-driven differentiation (Shiraha *et al*. 2000; Simpson *et al*. 2010). Therefore, potential effects of the epoxy-tiglianes on CD44 and EGFR gene expression were investigated. At all concentrations of EBC-46 and EBC-211 (barring at 1 μg/mL EBC-211), in the presence of TGF-β_1, no significant differences in EGFR expression were demonstrated. Still, down-regulatory trends in EGFR expression were observed versus the TGF-β_1-positive controls, that were also found in CD44 expression at all concentrations of EBC-46. Regarding EBC-211, CD44 expression, however, significant down-regulations were found at all concentrations, barring 10 μg/mL. These results are consistent with the previous findings, which have shown that post-TGF-β_1 stimulation, DFs demonstrate decreased expression of CD44

and EGFR after 72 h (Midgley, 2014; Woods, 2016). However, it is currently unknown why CD44/EGFR expression in myofibroblasts is attenuated. It may be that HA/CD44 interactions alter in myofibroblasts. In the fibroblasts, CD44 is diffuse throughout the plasma membrane; upon induction of differentiation, CD44 is moved into clusters by HA, resulting in the formation of a pericellular coat (Webber *et al.* 2009; Midgley *et al.* 2013). After TGF-β_1 stimulation, EGFR remains static, whilst the ability of CD44 to diffuse freely is attenuated as it colocalises with EGFR. Therefore, as fibroblast and myofibroblast functions differ, this reduction in expression may alter the signalling pathways mediating myofibroblast functions (Midgley *et al.* 2013; Woods, 2016).

As well as increased HA synthesis and pericellular coat formation, persistence of the myofibroblast phenotype is also associated with the expression of TSG6 (Webber *et al.* 2009a). As described in Chapter 1, TSG6 is a hyaladherin with key roles in HA coat formation and remodelling. HA interactions with the hyaladherins, such as TSG6, are essential in allowing TGF-β_1-driven differentiation to occur, as TSG6 is involved in HA cross-linking. As such, previous studies have shown that on TGF-β_1 stimulation, TSG6 expression is significantly higher in myofibroblasts. In contrast, loss of the phenotype is linked with inhibition of TSG6 expression (Webber *et al.* 2009a, 2009b; Martin *et al.* 2016). Thus, potential effects of the epoxy-tiglianes upon TSG6 gene expression were investigated. As found in previous studies, TGF-β_1-stimulated DFs exhibited an up-regulation in TSG6 expression at 72 h; whilst at all concentrations of EBC-46 and EBC-211, significant reductions in expression were shown. Interestingly, as detailed previously, differentiation was observed at all epoxy-tigliane concentrations, barring 0.1 µg/mL and 10 µg/mL EBC-46 and EBC-211, respectively. This contradicts the link between inhibition of TSG6 expression and the loss of the myofibroblast phenotype. However, most of the expression levels observed following epoxy-tigliane treatment were not as low as those found in unstimulated DFs, so positive contribution to the phenotype may still be present. Further studies at earlier timepoints would provide clearer indications of the relationship between TSG6 and epoxy-tigliane mechanisms of action. Furthermore, other studies have suggested that changes in the balance of hyaladherins determine whether the HA is assembled into coats or cables (Meran *et*

al. 2007). Therefore, further studies into epoxy-tigliane effects on HA synthesis and pericellular coat assembly would be helpful in determining the mechanism by which the epoxy-tiglianes inhibit myofibroblast differentiation at specific concentrations, but seemingly not at others.

Overall, there are prominent effects on TGF-β_1-driven myofibroblast differentiation following EBC-46 and EBC-211 treatment at specific concentrations; including αSMA and F-actin stress fibre modulation, inhibition (rather than reversal) of myofibroblast phenotype; and the modulation of differentiation-related gene expression. However, no significant modulations of the DF cytoskeleton were observed with epoxy-tigliane treatment alone. Thus, it was decided that only TGF-β_1-stimulated studies would be taken forward into further investigations. Findings from this Chapter corroborate the preferential healing outcomes that have been observed during the *in vivo* veterinary trials with EBC-46, during which wounds healed rapidly with minimal scarring. These characteristics are found in early-gestational and oral mucosal healing scenarios also, indicating the potential of analogous responses following epoxy-tigliane treatment. However, at time of writing, no studies have yet been performed to observe dermal histology after EBC-46 or EBC-211 treatment, with the aim of determining the ECM composition of wound sites. Such studies would be beneficial in elucidating whether myofibroblasts are present, if there is granulation tissue present and the ratio of type I collagen to type III collagen; amongst other factors. These exemplify characteristics of wound repair that differ in early-gestational and oral mucosal healing, compared to normal dermal wound healing. Further research is, thus, required to understand not only mechanisms by which these inhibitory effects occur, but also how they may impact typical myofibroblast functions; stimulating what resembles a scarless or a potentially regenerative healing outcome.

In addition to wound contraction, myofibroblasts are responsible for ECM synthesis, remodelling and scar tissue formation. Thus, based upon prior clinical reports of EBC-46 inducing rapid granulation tissue development and re-growth of appendages, as well as minimal scarring (Campbell *et al.* 2017; Hansen *et al.* 2018), it is hypothesised

that epoxy-tiglianes may modulate ECM synthesis and/or the proteolytic turnover of ECM components, such as type I collagen. Thus, the potential effects of EBC-46 and EBC-211 upon key components of the ECM were investigated; as detailed in Chapter 4.

Chapter 4

Epoxy-Tigliane Modulation of Dermal Extracellular Matrix Composition *in vitro*

Chapter 4 - Epoxy-Tigliane Modulation of Extracellular Matrix Composition *in vitro*

4.1 Introduction

As detailed previously (Chapter 1), during the remodelling phase of wound healing, the human body attempts to restore the functionality and maximal tensile strength of damaged dermal tissues through the degradation, synthesis and reorganisation of the extracellular matrix (ECM). The ECM is a dynamic scaffolding, anchoring cells and modifying function, via molecular and mechanical modulation (Gonzalez *et al.* 2016; Tracy *et al.* 2016). The majority of ECM components are produced by the fibroblasts, which regulate and modify their function in an autocrine manner; culminating in the remodelling of granulation tissue, wound contraction/closure and the formation of scar tissue (Bainbridge, 2013). Following acute wounding, the ECM of normal dermal wounds matures from one rich in type III collagen, hyaluronan (HA) and fibronectin (FN) to one rich in type I collagen; leading to avascular scar formation with increased tensile strength (Birk and Trelstad, 1986; Moseley *et al.* 2004; Bainbridge, 2013). The importance of ECM composition and its turnover in scar development has been well-documented, concerning the balance of glycosaminoglycans (GAGs; such as HA) and fibrous proteins (such as elastin and the collagens), dictating cellular phenotype and function; as well as extent of fibrosis induced (Halper and Kjaer, 2014; Ricard-Blum *et al.* 2018). During skin homeostasis, ECM synthesis/degradation are in equilibrium. However, both processes can be transiently shifted during wound repair and if their tight regulatory mechanisms are disturbed, pathology can take place (Do and Eming, 2016).

Excessive dermal fibrosis represents an aberrant state, characterised by excessive accumulation of ECM components, including FN and collagen (Ehrlich *et al.* 1994; Gauglitz *et al.* 2011). Keloid and hypertrophic scars both exhibit exacerbations of normal dermal fibroblast (DF) phenotypes, involving a persistence and/or an over-expression of transforming growth factor-β_1 (TGF-β_1) and TGF-β_2 signalling; which

subsequently results in excessive synthesis of collagen (Schmid *et al.* 1998; Lee *et al.* 1999). However, the two differ histologically, as keloid scars are primarily composed of disorganised type I and III collagen bundles that are thick, large and hypocellular; whilst hypertrophic tissue largely contains well-organised type III collagen bundles, characterised as wavy and fine. Furthermore, the latter are orientated parallel to the epidermis, with abundant nodules containing myofibroblasts (Ehrlich *et al.* 1994; Slemp and Kirschner, 2006; Gauglitz *et al.* 2011). Type I and III collagen accumulation is thought to arise from any imbalances in their expression and a lack of degradation by collagenases, including matrix metalloproteinase-1 (MMP-1; Fineschi *et al*. 2006; Giménez *et al*. 2017). *In vitro* studies have supported this hypothesis, demonstrating that TGF-β_1 triggers a DF transcriptional programme favouring collagen deposition by up-regulating type I collagen α_1 chain (COL1α_1) gene expression and reducing MMP-1 expression (Fineschi *et al*. 2006; Bujor *et al.* 2008; Goffin *et al.* 2010). Hypertrophic DFs have been shown to reduce MMP-1 expression and exhibit a lack of response to cytokines typically found to stimulate MMP-1 expression (Ghahary *et al.* 1996; Dasu *et al.* 2004; Eto *et al.* 2012); this was deemed true of keloid-derived DFs also (Uchida *et al.* 2003; Kuo *et al*. 2005; Smith *et al.* 2008). This suggests that decreased MMP expression potentiates collagen accumulation in fibrotic situations.

It has also been demonstrated that the expression of other key ECM components is down-regulated in pathological scarring scenarios, such as HA. The current research indicates that a lack of HA may exacerbate scar formation; with a number of studies hypothesising that altered HA distribution, organisation and turnover contributes to differences in the clinical characteristics of normal, hypertrophic and keloid scars, in comparison to normal skin architecture (Bertheim and Hellström, 1994; Meyer *et al*. 2000; Huang *et al.* 2009; Tan *et al.* 2011; Sidgwick *et al.* 2013). Elastin has also been shown to be differentially expressed between scar types, with enhanced expression and locational differences highlighted in several studies. Within keloid scars, elastin deposition has been detected in the deep dermis, rather than the superficial; and at higher densities compared to normal skin, as well as normal and hypertrophic scars (Amadeu *et al.* 2004; Chen *et al.* 2011). In addition, studies have revealed disturbed

elastin organisation to be more prominent in keloid and hypertrophic scar tissue, in comparison to normal scar tissue; with the deep dermis of keloids exhibiting unique distribution of elastin (Costa *et al.* 1999; Amadeu *et al.* 2004; Chen *et al.* 2011). Such changes in elastin content and organisation likely contribute to alterations observed in the mechanical properties of both keloid and hypertrophic scars, influencing their respective pathologies (Amadeu *et al.* 2004; Jumper *et al.* 2015).

Contrasting differences in ECM composition and turnover also contribute to scarless healing environments. While type I collagen is the predominant form in human skin, early-gestational wounds are characterised by an ECM abundant in type III collagen (Lovvorn *et al*. 1999; Moore *et al*. 2018). *In vitro* studies have not only demonstrated that foetal fibroblasts synthesise more total collagen than their adult counterparts, but that they specifically express higher levels of type III collagen (Merkel *et al*. 1988; Larson *et al*. 2010). Type III collagen accounts for 10 - 20 % of total collagen in post-natal skin, versus 30 - 60 % in foetal skin. This is rapidly deposited in foetal wounds, presenting as a fine reticular network indistinguishable from surrounding uninjured dermis (Smith *et al.* 1986; Beanes *et al*. 2002; Yagi *et al*. 2016). With regards to oral mucosal wounds, cells positive for type I pro-collagen were found to be significantly decreased compared to those in dermal wounds; indicating a potentially analogous ECM composition in oral mucosal and foetal wounds (Wong *et al*. 2009; Glim *et al*. 2013). Increased prolyl hydroxylase activity also correlates with a greater synthesis of collagen induced in foetal wounds, acting as an important rate-limiter in collagen production. Furthermore, distinct to the adult dermis, prolyl hydroxylase is regulated by polyadenosine diphosphate-ribose synthetase; an enzyme linked to cell repair. As such, as well as differing collagen synthesis, altered enzymatic regulation of collagen production is displayed by foetal fibroblasts (Lorenz and Adzick, 1993; Larson *et al*. 2010; Li *et al.* 2017). Cross-linking of collagen has also been shown to increase with gestational age, concurrent with transition to a scarring phenotype. Whereas cross-linking increases matrix rigidity and is associated with scar maturation, it is thought that an environment of unlinked collagen coincides with a more flexible ECM; thus, contributing to scarless repair (Yagi *et al*. 2016; Moore *et al*. 2018). In addition, lysyl

oxidase has been found to be expressed at relatively lower levels in early-gestational compared to late-gestational murine wounds. As a catalyst of collagen cross-linking, this further indicates the importance of collagen architecture and its organisation on repair outcomes (Smith-Mungo and Kagan, 1998; Colwell *et al*. 2006).

As found in pathological scenarios, HA is also differentially expressed in preferential healing environments versus normal acute wounding scenarios. In early-gestational foetal wounds, elevated and more persistent HA synthesis has been demonstrated; as a result of increased hyaluronan synthase (HAS) expression and reduced activity of the HA-degrading enzyme, hyaluronidase (Longaker *et al*. 1989; Mast *et al*. 1995; West *et al*. 1997). Foetal fibroblasts also express more surface receptors for HA and this enhances cell migration (Chen *et al.* 1989; Alaish *et al*. 1994). Furthermore, the ECM HA content is increased more rapidly than in adult wounds; such deposition is assisted by the lack of pro-inflammatory cytokines present in foetal wounds, which would usually down-regulate HA synthesis (Kennedy *et al*. 2000; Larson *et al*. 2010). In addition, higher molecular weight HA has been found to stimulate type III collagen synthesis and TGF-β_3 expression in DFs; with each HA form increasing MMP-1 gene expression. Such preferential responses further demonstrate HA's role in stimulating environments that favour scar-free healing (David-Raoudi *et al.* 2008; Li *et al.* 2017). Differential HAS isoform expression is also found in oral mucosal fibroblasts (OMFs), compared to DFs; with OMFs highly expressing HAS3, but not HAS1. In contrast, the converse is true for DFs; TGF-β_1 stimulation can induce HAS1 expression in DFs, but not OMFs (Yamada *et al*. 2004; Meran *et al*. 2007). Regarding HAS2, its expression is found in both cell populations; however, TGF-β_1 stimulation increases its expression in DFs, while reducing it in OMFs (Glim *et al*. 2013). This highlights the complexity of the differing gene profiles expressed in the fibroblasts that contribute to preferential healing scenarios and those involved in dermal repair/fibrosis; and the involvement of HA and HAS isoforms in these contrasting outcomes.

As well as ECM synthesis, ECM degradation is also necessary to promote healing. As detailed previously (Chapter 1), ECM remodelling during acute dermal wound repair

is primarily mediated by MMPs, such as MMP-1. In addition to the contrasting ECM compositions between the aforementioned tissues, differences in ECM degradation and remodelling have also been widely reported. In scarless healing scenarios, there is a greater proportion of MMP activity than tissue inhibitor of MMP (TIMP) activity; favouring earlier remodelling and faster collagen turnover (Dang *et al*. 2003; Yagi *et al*. 2016; Moore *et al.* 2018). Inductions in MMP-1, -9 and -14 expression have been exhibited in foetal wounds, occurring more rapidly and at higher levels than scarring wounds; whereas increased TIMP-1 and -3 expression has been displayed in scarring wounds alone (Dang *et al*. 2003). In addition to changes upon wounding, expression patterns of MMPs before wounding have also been hypothesised as contributors to preferential healing outcomes. OMFs display higher expression levels of MMP-2/-3 and decreased TIMP-1/-2 expression; versus DFs (Stephens *et al.* 2001; McKeown *et al.* 2007; Glim *et al*. 2013). Therefore, these findings demonstrate that differential proteinase/inhibitor expression profiles contribute to healing outcomes, whether pathological or preferential.

4.2 Chapter Aims

Previous studies (Chapter 3) have shown that the epoxy-tiglianes, such as EBC-46 and EBC-211, possess inhibitory effects upon TGF-β_1-driven myofibroblast differentiation and modulate the contractile phenotype and genotype of myofibroblasts at certain concentrations. Therefore, the findings indicated that epoxy-tiglianes may modulate other myofibroblast functions, such as ECM synthesis/turnover, facilitating minimal scarring outcomes; as evident *in vivo*. As ECM composition can regulate and modify cell phenotype and function, as well as the extent of scarring observed, the current Chapter investigated whether EBC-46 and EBC-211 could directly modulate synthesis and expression of key ECM components. Collagens, HA, elastin and MMPs are well-established as being differentially expressed in scenarios of fibrosis and preferential healing, versus normal acute healing. Thus, these studies were performed to provide further clarification of the repair outcomes observed *in vivo* following epoxy-tigliane treatment; such as wound healing with minimal scar formation (Reddell *et al.* 2014; Campbell *et al.* 2017; Hansen *et al.* 2018).

4.3 Materials and Methods

DFs were sourced, cultured and counted, as previously described (Chapters 2.2.1 and 2.2.2). Following determination of cell density and viability (Chapter 2.2.2), DFs were seeded into 6-well plates for quantitative polymerase chain reaction (qPCR) analysis and erythrocyte particle exclusion assays (Chapters 2.4 and 2.7, respectively) at 2.5 x 10^4 cells/mL. For Western blot analysis, cells were seeded at 9 x 10^4 cells/mL into 75 cm^2 culture flasks (Chapter 2.5). Seeding, serum-starvation and treatment volumes were 2 mL and 10 mL for 6-well plates and 75 cm^2 culture flasks, respectively. Cells were kept in a 37 °C humidified incubator with 5 % CO_2/95 % air atmosphere for the duration of experiments, as previously described (Chapter 2.2.1). Post-growth arrest (Chapter 2.2.1), cells were treated with EBC-46 or EBC-211 at either of the following concentrations: 0 µg/mL, 0.001 µg/mL, 0.01 µg/mL, 0.1 µg/mL, 1 µg/mL or 10 µg/mL (Chapter 2.1.1), in presence/absence of TGF-β_1 (Chapter 2.1.2). Following either 24 h, 48 h or 72 h treatment periods, qPCR was used to analyse COL1α_1, type III collagen, α_1 chain (COL3α_1), elastin (ELN), MMP-1 and HAS1, 2 and 3 gene expression (Chapter 2.4). Post-24 and 72 h treatment, Western blots were utilised to analyse type I and III collagens and elastin protein levels and turnover (Chapter 2.5). Post-72 h treatment, collected treatment media samples were used in HA enzyme-linked immunosorbent assays (ELISAs) to quantify soluble HA levels (Chapter 2.6); while erythrocyte particle exclusion assays were undertaken in order to visualise extent of HA pericellular coat formation (Chapter 2.7). Statistical analyses were performed, as previously described (Chapter 2.11).

4.4 Results

4.4.1 Effects of EBC-46 and EBC-211 on Type I Collagen Expression

To investigate the potential modulatory effects of EBC-46 and EBC-211 on key ECM components, qPCR analysis was performed to determine the effects upon the gene expression levels of COL1α_1. Relative quantification (RQ) was performed upon cells cultured with either EBC-46 or EBC-211 (Section 4.3), in the presence of TGF-β_1 (10 ng/mL), post-72 h treatment (Figure 4.1). Western blots were performed in order to

validate genotypic changes; with DFs cultured at the same conditions, at 24 h and 72 h (Figure 4.2). Compound-free controls, in the absence or presence of TGF-β_1, were further included to confirm normal DF-myofibroblast responses and for comparative purposes. As reported prior, TGF-β_1-induced up-regulation of COL1α_1 expression and subsequent type I collagen protein production are key indicators of myofibroblastic formation (Bujor *et al.* 2008; Fineschi *et al*. 2006; Goffin *et al.* 2010). Findings were consistent with the previous studies, as approximately 7.5-fold increases in COL1α_1 gene expression were found following TGF-β_1 treatment (Figure 4.1); versus TGF-β_1-negative controls.

Cells cultured with EBC-46 (0.001 - 10 µg/mL), in the presence of TGF-β_1 (10 ng/mL), exhibited varying COL1α_1 gene expression levels, versus the TGF-β_1-positive controls (Figure 4.1A). Lower concentrations of EBC-46 (0.001 - 0.01 µg/mL) demonstrated no significant up-regulations in COL1α_1 gene expression, ($p = >0.05$), while at the higher concentrations (1 - 10 µg/mL), significant up-regulation was identified versus TGF-β_1-positive controls (1.5 and 1.7-fold at $p = <0.05$ and $p = <0.01$, respectively). However, at 0.1 µg/mL EBC-46, 2-fold down-regulation of COL1α_1 gene expression was found; versus TGF-β_1-positive controls ($p = <0.05$). Interestingly, despite this decrease at 0.1 µg/mL EBC-46, COL1α_1 gene expression was still approximately 3.8-fold higher than the TGF-β_1-negative control (Figure 4.1A); indicating that COL1α_1 expression remains induced in DFs after 0.1 µg/mL EBC-46 treatment, but not to the same extent as that of TGF-β_1-stimulated DFs. Regarding protein levels, COL1 Western blots post-EBC-46 treatment appeared to indicate comparable levels of expression at all concentrations at 24 h; compared to TGF-β_1-positive controls. Similar findings were observed at 72 h, apart from at 0.1 µg/mL EBC-46, which decreased COL1 protein detection (Figure 4.2A).

Comparable results to those induced by EBC-46 were demonstrated when DFs were cultured with EBC-211 (0.001 - 10 µg/mL), in the presence of TGF-β_1 (Figure 4.1B). In response to 72 h treatment, most EBC-211 concentrations (0.001 - 1 µg/mL) showed up-regulations in COL1α_1 gene expression, compared to the TGF-β_1-positive controls.

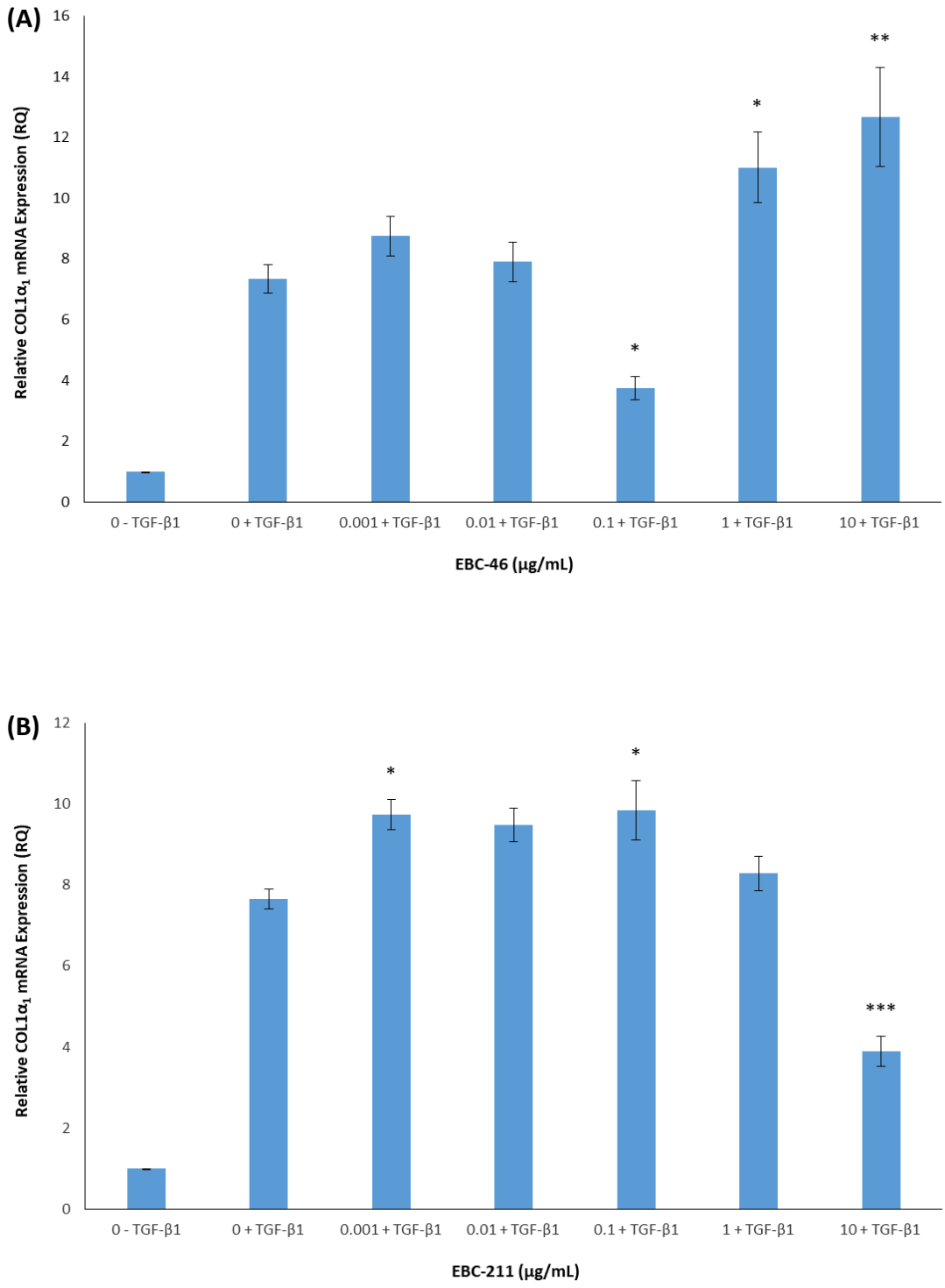

Figure 4.1. Type I collagen ($COL1\alpha_1$) gene expression in DFs, cultured in the presence of (A) EBC-46 and (B) EBC-211 at 0.001 µg/mL, 0.01 µg/mL, 0.1 µg/mL, 1 µg/mL and 10 µg/mL, in the presence of TGF-β_1, for 72 h. Compound-free controls ± TGF-β_1 (10 ng/mL) were also included (*n = 3*, mean±SEM; *p = *<0.05, **<0.01, ***<0.001* versus TGF-β_1-positive controls).

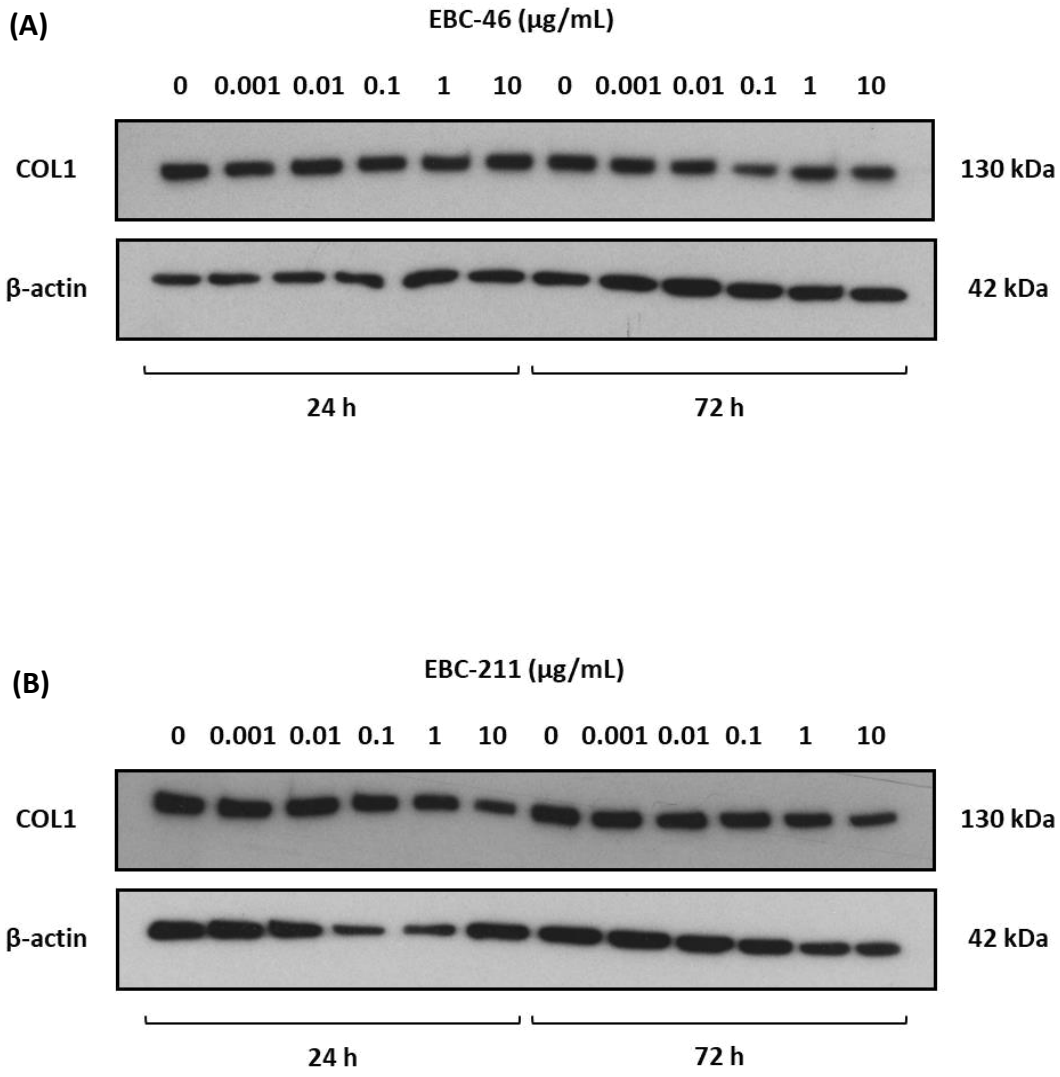

Figure 4.2. Western blot analyses of type I collagen (COL1) protein levels in DFs; cultured with either EBC-46 (A) or EBC-211 (B) at 0.001 µg/mL, 0.01 µg/mL, 0.1 µg/mL, 1 µg/mL and 10 µg/mL, in the presence of TGF-β_1 (10 ng/mL), for 24 and 72 h. TGF-β_1-positive, non-compound controls were also included at each time-point (*n = 3*).

However, only 0.001 and 0.1 µg/mL EBC-211 showed significant increases in COL1α_1 expression (both approximately 1.3-fold greater; *p = <0.05*). Similar to findings with 0.1 µg/mL EBC-46, 2-fold down-regulation of COL1α_1 gene expression was exhibited following 10 µg/mL EBC-211 treatment; versus TGF-β_1-positive controls (*p = <0.001*). Despite this decrease, COL1α_1 expression was still approximately 3.9-fold higher than TGF-β_1-negative controls (Figure 4.1B); indicating COL1α_1 expression is still induced in DFs following 10 µg/mL EBC-211 treatment, but not to the same extent as TGF-β_1-stimulated DFs. Regarding protein levels, Western blots for COL1 following EBC-211 treatment indicated comparable or higher levels of detection at most concentrations (0.001 - 1 µg/mL) at both time-points; compared to TGF-β_1-positive controls (Figure 4.2B). However, at 10 µg/mL EBC-211, decreased COL1 protein detection was found at both time-points; in comparison to the TGF-β_1-positive controls (Figure 4.2B). This resembled the gene expression profile observed following 72 h treatment with EBC-211 (Figure 4.1B).

4.4.2 Effects of EBC-46 and EBC-211 on Type III Collagen Expression

To investigate the potential modulatory effects of EBC-46 and EBC-211 on key ECM components, qPCR analysis was performed to determine the effects upon the gene expression levels of COL3α_1. RQ was performed upon DFs cultured with either EBC-46 or EBC-211 at all aforementioned concentrations (Chapter 4.3), in the presence of TGF-β_1 (10 ng/mL), following 72 h treatment (Figure 4.3). Western blots were also performed to validate genotypic changes; with DFs cultured at the same conditions, at 24 h and 72 h (Figure 4.4). Compound-free controls, in the absence or presence of TGF-β_1, were further included to confirm normal DF-myofibroblast responses and for comparative purposes.

Cells cultured with EBC-46 (0.001 - 10 µg/mL), in the presence of TGF-β_1 (10 ng/mL), exhibited concentration-specific differences in COL3α_1 gene expression, versus TGF-β_1-positive controls (Figure 4.3A). The higher EBC-46 concentrations (1 - 10 µg/mL) showed no significant increases in COL3α_1 expression, in comparison to the positive controls (*p = >0.05*). However, the lowest concentration (0.001 µg/mL) significantly

up-regulated COL3α_1 expression (1.7-fold up-regulation; *p = <0.05*). At 0.01 and 0.1 µg/mL, reductions in expression were observed; however, these were not found to be statistically significant (*p = >0.05*). Interestingly, the greatest down-regulation was found at 0.1 µg/mL EBC-46 (1.5-fold) versus TGF-β_1-positive controls; which was also the case with COL1α_1 gene expression (Figure 4.1A). However, in contrast to COL1α_1, COL3α_1 gene expression at 0.1 µg/mL EBC-46 was lower than expression in the TGF-β_1-negative controls (Figure 4.3A); indicating a potential down-regulatory synergy at this concentration. Overall, trends in COL3α_1 expression over EBC-46 concentrations were similar to those responses observed with COL1α_1; but to a lesser extent. With regards to COL3 protein levels, Western blots for COL3 following EBC-46 treatment exhibited similar trends in protein detection to the aforementioned gene expression profiles. After 24 h, comparable or increased COL3 protein levels were seen at lower EBC-46 concentrations (0.001 - 0.01 µg/mL); while lesser detection was found at the higher concentrations (1 - 10 µg/mL), versus TGF-β_1-positive controls (Figure 4.4A). However, the greatest COL3 reduction at this time-point was observed at 0.1 µg/mL EBC-46; versus the positive controls (Figure 4.4A). Similar findings were observed at 72 h; though expression of COL3 at the higher EBC-46 concentrations (1 - 10 µg/mL) appeared comparable to TGF-β_1-positive controls, unlike the lower levels shown at 24 h (Figure 4.4A).

Similar studies were performed using DFs cultured with EBC-211 (0.001 - 10 µg/mL), in the presence of TGF-β_1 (Figure 4.3B). In response to 72 h treatment, DFs exposed to lower EBC-211 concentrations (0.001 - 0.01 µg/mL) displayed approximately 1.3-fold increases in COL3α_1 gene expression; compared to the TGF-β_1-positive control. However, a down-regulatory trend was seen with increasing EBC-211 concentration (0.1 - 10 µg/mL); with 10 µg/mL demonstrating the greatest decrease in COL3α_1 gene expression (1.6-fold), as observed at 0.1 µg/mL EBC-46. A similar decrease was also shown in COL1α_1 expression after treatment at this concentration (Figure 4.1B). In contrast, however, the COL3α_1 expression at 10 µg/mL EBC-211 was lower than that of TGF-β_1-negative controls (Figure 4.3B); as also observed following 0.1 µg/mL EBC-46 treatment (Figure 4.3A). However, despite the aforementioned changes in gene

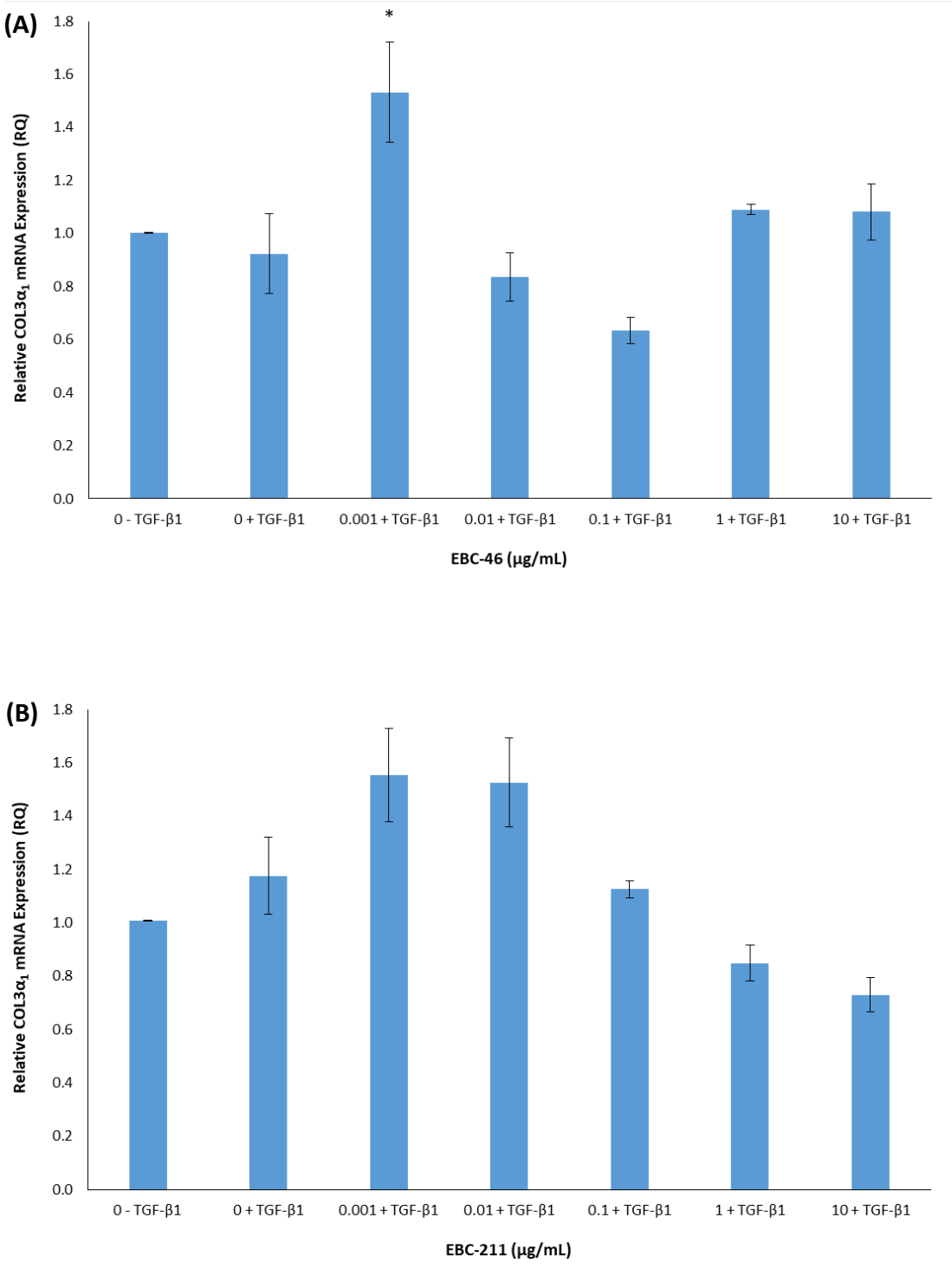

Figure 4.3. Type III collagen ($COL3\alpha_1$) gene expression in DFs, cultured with (A) EBC-46 and (B) EBC-211 at 0.001 µg/mL, 0.01 µg/mL, 0.1 µg/mL, 1 µg/mL and 10 µg/mL, in the presence of TGF-β_1 (10 ng/mL), for 72 h. Compound-free controls ± TGF-β_1 were also included (*n = 3*, mean±SEM; *p = *<0.05* compared to the TGF-β_1-positive controls).

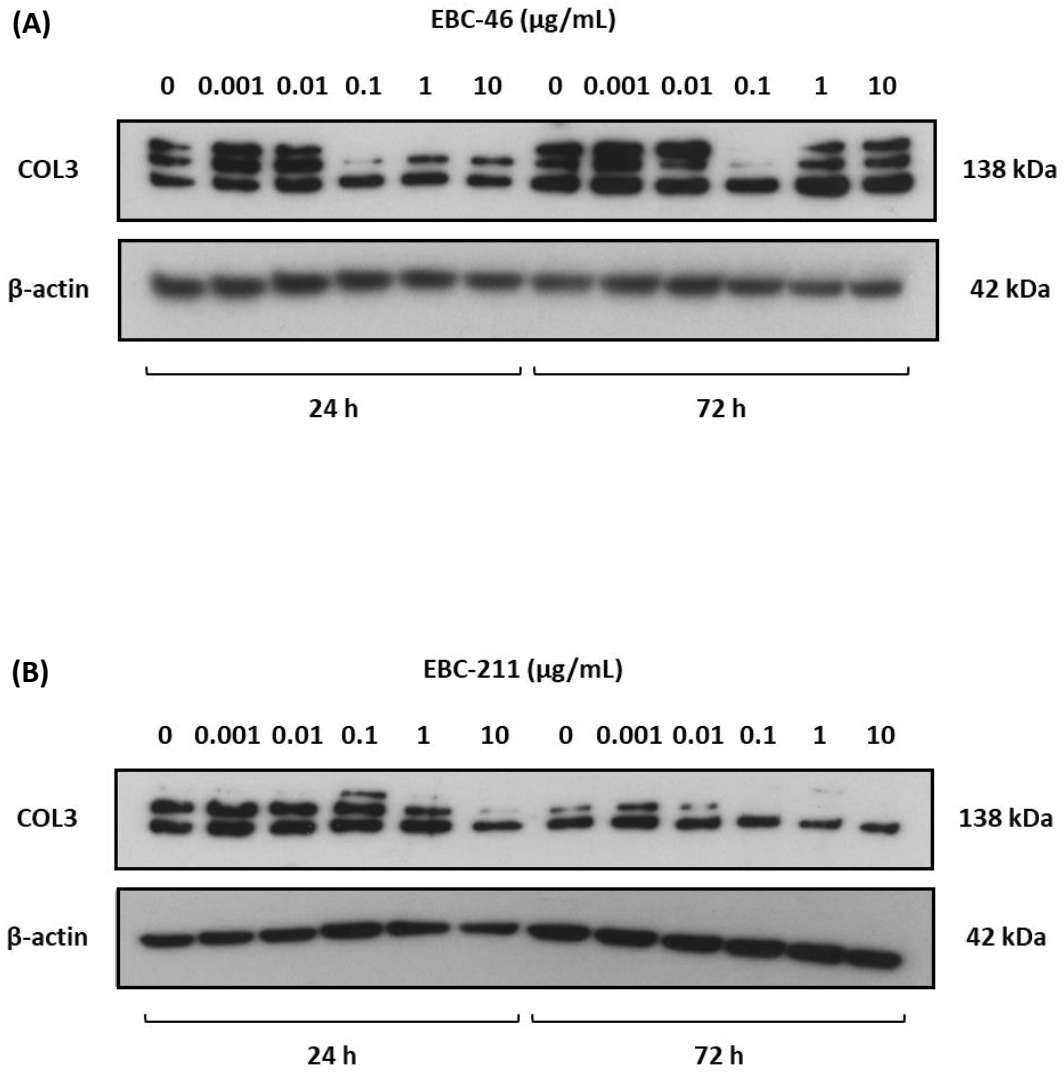

Figure 4.4. Western blot analyses of type III collagen (COL1) protein levels in DFs; cultured with either EBC-46 (A) or EBC-211 (B) at 0.001 µg/mL, 0.01 µg/mL, 0.1 µg/mL, 1 µg/mL and 10 µg/mL, in the presence of TGF-β_1 (10 ng/mL), for 24 and 72 h. TGF-β_1-positive, compound-free controls were also included at each time-point (*n = 3*).

expression, these were not found to be statistically significant (*p = >0.05*). Western blots for COL3 following EBC-211 treatment indicated comparable or higher levels of protein detection at most concentrations (0.001 - 1 µg/mL) after 24 h; with the same trend shown at 72 h with 0.001 - 0.01 µg/mL EBC-211, compared to TGF-β_1-positive controls (Figure 4.4B). However, decreased protein levels for COL3 were observed at 10 µg/mL EBC-211 at 24 h and at 0.1 - 10 µg/mL EBC-211 at 72 h; compared to TGF-β_1-positive controls (Figure 4.4B). Such COL3 protein detection profiles were similar to those expressed at the gene level (Figure 4.3B).

4.4.3 Effects of EBC-46 and EBC-211 on Elastin Expression

To investigate the potential modulatory effects of EBC-46 and EBC-211 on key ECM components, qPCR analysis was performed to determine the effects upon the gene expression levels of ELN. RQ was performed upon DFs cultured with either EBC-46 or EBC-211 at all aforementioned concentrations (Chapter 4.3), in the presence of TGF-β_1 (10 ng/mL), following 72 h treatment (Figure 4.5). Western blots were also carried out to validate genotypic changes; with DFs cultured at the same conditions, at 24 h and 72 h (Figure 4.6). Compound-free controls, in the absence or presence of TGF-β_1, were included to confirm normal DF-myofibroblast responses and for comparative purposes. As found in prior studies, TGF-β_1 stimulates increases in the ELN gene and protein expression (Liu and Davidson, 1988; Kähäri *et al.* 1992). The following results were consistent with the previous studies, as approximately 31-fold and 38-fold up-regulations in ELN gene expression were found after TGF-β_1 treatment (Figure 4.5A and B, respectively); versus TGF-β_1-negative controls.

Cells cultured with EBC-46 (0.001 - 10 µg/mL), in the presence of TGF-β_1 (10 ng/mL), showed varying degrees of up-regulation of ELN gene expression, versus the TGF-β_1-positive controls (Figure 4.5A). Lower EBC-46 concentrations (0.001 and 0.01 µg/mL) showed significant up-regulations in ELN expression (13.8 and 14.1-fold at *p = <0.01*, respectively); whereas the higher concentrations (1 and 10 µg/mL) displayed lesser inductions (8.7 and 7.4-fold at *p = >0.05*, respectively). However, at 0.1 µg/mL EBC-46, only an approximate 2.1-fold increase in ELN expression was exhibited; the least

prominent up-regulation of each concentration investigated, versus TGF-β_1-positive controls. As with 1 and 10 µg/mL of EBC-46, this up-regulation was not shown to be significant (*p = >0.05*). Interestingly, however, the aforementioned induction was still approximately 65.9-fold greater than TGF-β_1-negative controls (Figure 4.5A). At the protein level, Western blots for ELN following EBC-46 treatment did not discern any obvious differential responses between EBC cultures and controls at each time-point (Figure 4.6A); in contrast to the clear differences in ELN expression demonstrated at the gene level (Figure 4.5A).

Comparable results to those induced by EBC-46 were demonstrated when DFs were cultured with EBC-211 (0.001 - 10 µg/mL), in the presence of TGF-β_1 (Figure 4.5B). In response to 72 h treatment, all EBC-211 concentrations produced varying increases in ELN gene expression, versus the TGF-β_1-positive control. Lower concentrations of EBC-211 (0.001 - 0.01 µg/mL) displayed significant increases in ELN gene expression (7.3 - 7.9-fold at *p = <0.001*, respectively), whereas even greater up-regulation was shown at 0.1 and 1 µg/mL (13.4 and 12.6-fold at *p = <0.001*, respectively). However, similarly to the findings at 0.1 µg/mL EBC-46, only an approximate 2-fold increase in ELN gene expression was exhibited post-10 µg/mL EBC-211 treatment; compared to TGF-β_1-positive controls (*p = >0.05*). Interestingly, however, the aforementioned up-regulation was still demonstrated to be approximately 74.9-fold greater than TGF-β_1-negative controls (Figure 4.5B). Regarding ELN protein detection, Western blots for ELN after EBC-211 treatment indicated comparable levels of detection at most EBC-211 concentrations (0.001 - 0.1 µg/mL) after 24 h; with decreased levels shown at 1 - 10 µg/mL of EBC-211, versus TGF-β_1-positive controls (Figure 4.6B). Post-72 h, ELN protein detection appeared varied across concentrations, suggesting an inconsistent response upon EBC-211 treatment (Figure 4.6B).

4.4.4 Effects of EBC-46 and EBC-211 on Matrix Metalloproteinase-1

To investigate the modulatory effects of EBC-46 and EBC-211 upon ECM proteolytic turnover, qPCR analysis was performed to determine the gene expression levels of MMP-1. RQ was performed upon DFs cultured with either EBC-46 or EBC-211 at each

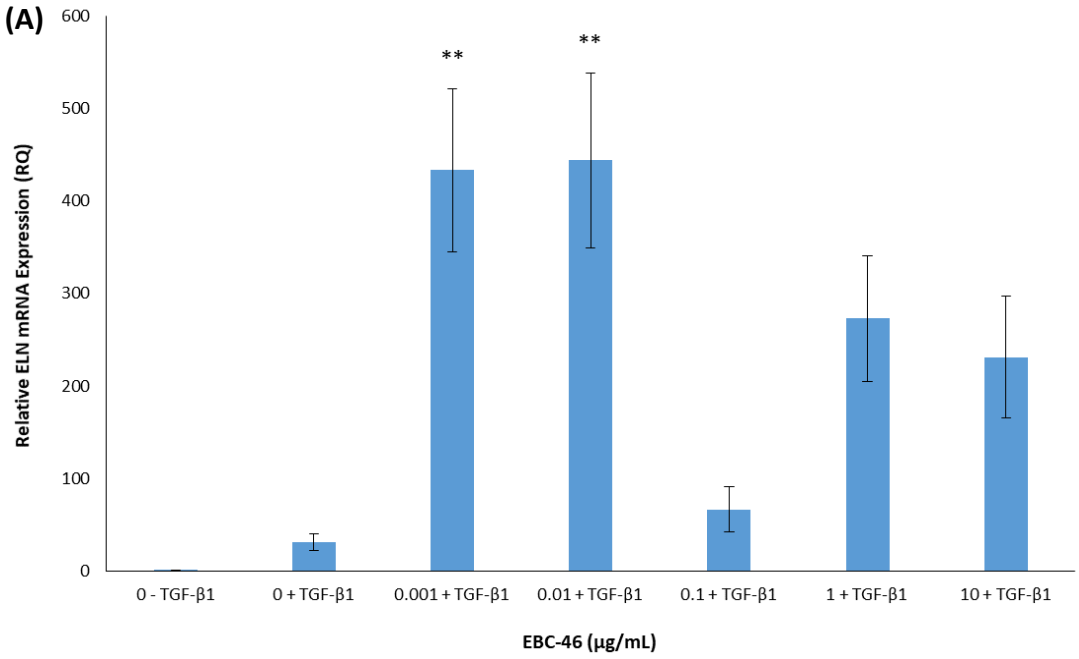

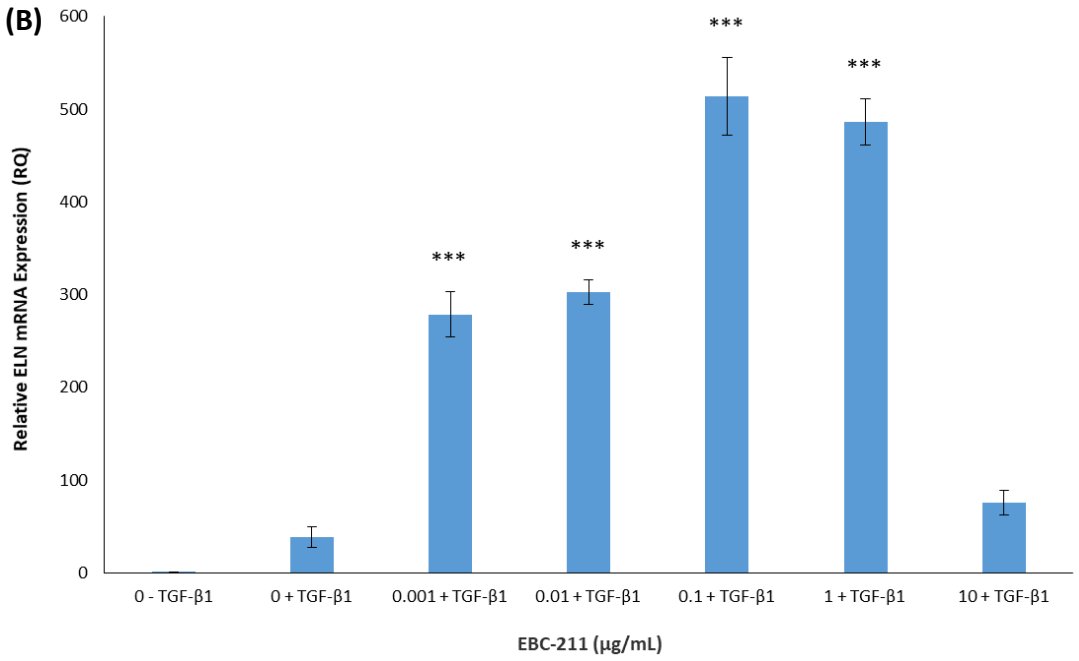

Figure 4.5. Elastin (ELN) gene expression in DFs, cultured with (A) EBC-46 and (B) EBC-211 at 0.001 µg/mL, 0.01 µg/mL, 0.1 µg/mL, 1 µg/mL and 10 µg/mL, in the presence of TGF-β_1, for 72 h. Compound-free controls ± TGF-β_1 (10 ng/mL) were also included (*n = 3*, mean±SEM; *p = **<0.01, ***<0.001* compared to the TGF-β_1-positive controls).

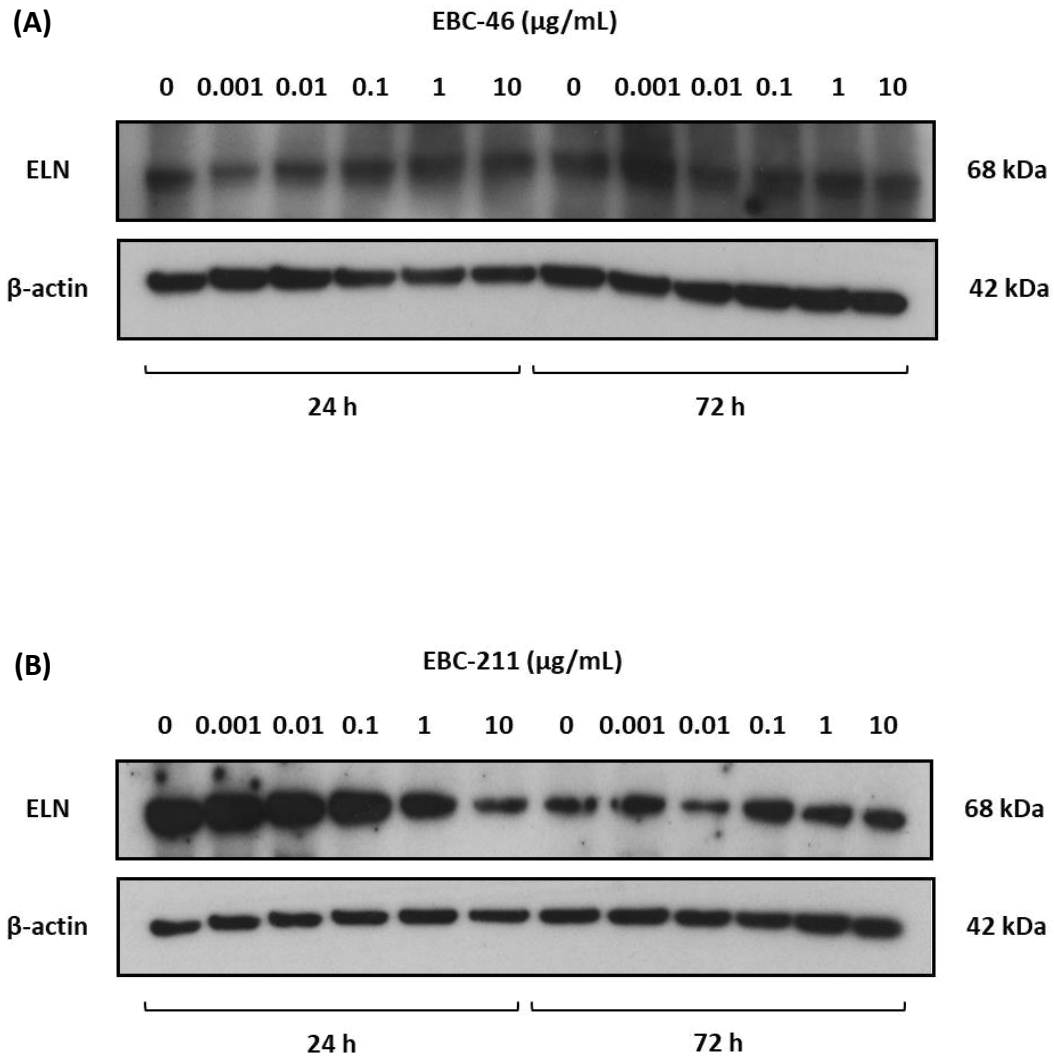

Figure 4.6. Western blot analyses of elastin (ELN) protein levels in DFs; cultured with either EBC-46 (A) or EBC-211 (B) at 0.001 µg/mL, 0.01 µg/mL, 0.1 µg/mL, 1 µg/mL and 10 µg/mL, in the presence of TGF-β_1 (10 ng/mL), for 24 h and 72 h. TGF-β_1-positive, compound-free controls were also included at each time-point (*n = 3*).

aforementioned concentration (Chapter 4.3), in the presence of TGF-β_1 (10 ng/mL), after 72 h treatment (Figure 4.7). Compound-free controls, with or without TGF-β_1, were also included to confirm normal myofibroblast responses and for comparative purposes. As reported in previous studies, TGF-β_1-driven down-regulation of MMP-1 gene expression is a key indicator of myofibroblast differentiation (Bujor *et al.* 2008; Fineschi *et al*. 2006; Goffin *et al.* 2010). Findings were consistent with the previous studies, as approximately 2-fold and 1.3-fold decreases in MMP-1 gene expression were found following TGF-β_1 treatment (Figure 4.7A and B, respectively); versus TGF-β_1-negative controls.

Cells cultured with EBC-46 (0.001 - 10 µg/mL), in the presence of TGF-β_1 (10 ng/mL), demonstrated varying degrees of up-regulation regarding MMP-1 gene expression, compared to the TGF-β_1-positive control cells (Figure 4.7A). Lower concentrations of EBC-46 (0.001 - 0.01 µg/mL) displayed up-regulated MMP-1 expression (3.4 and 9.8-fold, respectively); which were also found at greater levels at higher concentrations of EBC-46 (1 - 10 µg/mL; 28.8 and 11.6-fold, respectively). Nonetheless, such changes were not found to be statistically significant (*p = >0.05*). However, at 0.1 µg/mL EBC-46, an approximate 155-fold increase in MMP-1 gene expression was shown; versus the TGF-β_1-positive controls (*p = <0.001*). This up-regulation was also approximately 77.7-fold greater than the TGF-β_1-negative controls (Figure 4.7A).

Comparable results to those induced by EBC-46 were demonstrated when DFs were cultured with EBC-211 (0.001 - 10 µg/mL), in the presence of TGF-β_1 (Figure 4.7B). In response to 72 h treatment, all EBC-211 concentrations induced varying increases in MMP-1 expression, versus TGF-β_1-positive controls. At 0.001 - 1 µg/mL of EBC-211, increases in MMP-1 expression were between approximately 2.5 - 9.6-fold; but these were not statistically significant (*p = >0.05*). However, similarly to the findings at 0.1 µg/mL EBC-46, an approximate 254-fold increase in MMP-1 expression was exhibited after 10 µg/mL EBC-211 treatment; versus the TGF-β_1-positive controls (*p = <0.001*). Moreover, this increase in expression was also approximately 200-fold greater than TGF-β_1-negative controls (Figure 4.7B).

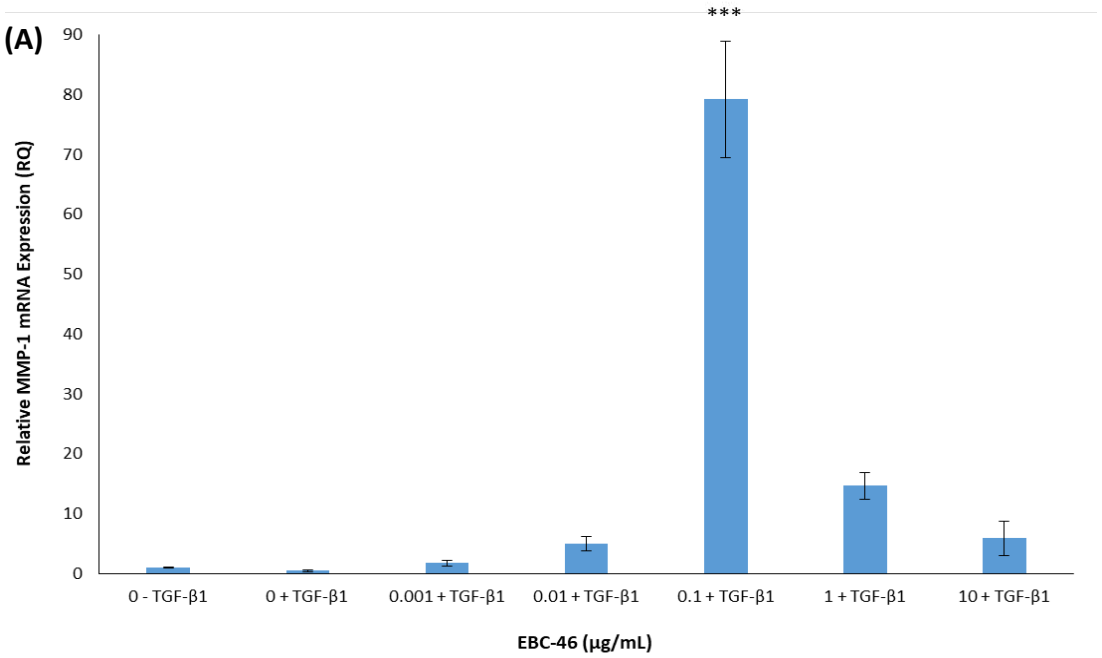

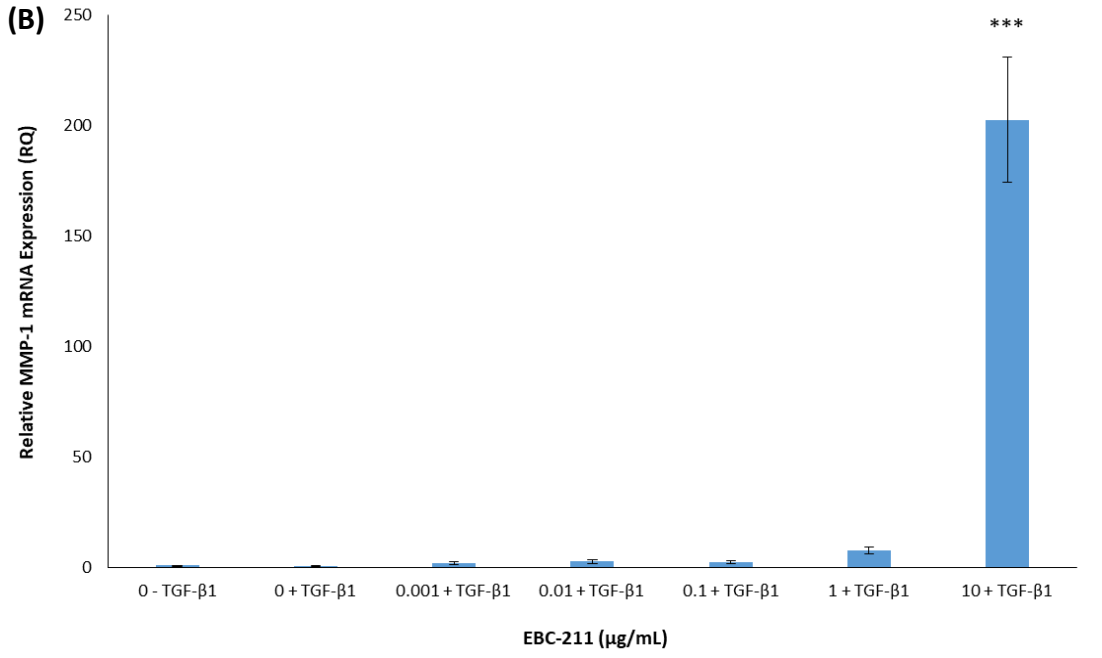

Figure 4.7. Matrix metalloproteinase-1 (MMP-1) gene expression in DFs, cultured with (A) EBC-46 and (B) EBC-211 at 0.001 µg/mL, 0.01 µg/mL, 0.1 µg/mL, 1 µg/mL and 10 µg/mL, in the presence of TGF-β_1, for 72 h. Compound-free controls ± TGF-β_1 (10 ng/mL) were also included (*n = 3*, mean±SEM; *p = ***<0.001* compared to TGF-β_1-positive controls).

4.4.5 Effects of EBC-46 and EBC-211 on Hyaluronan Synthase Expression

To investigate the modulatory effects of EBC-46 and EBC-211 on HA synthesis, qPCR analysis was performed to determine the gene expression of the three HA isoforms: HAS1, HAS2 and HAS3. RQ was performed upon DFs cultured with either EBC-46 at 0.01 - 0.1 μg/mL or EBC-211 at 1 - 10 μg/mL, respectively; in the presence of TGF-β_1 (10 ng/mL) following 24 h, 48 h and 72 h treatment (Section 4.3; Figures 4.8 - 4.10). Compound-free controls were also included at every time-point, in order to confirm normal DF-myofibroblast responses and for comparative purposes. As found in prior studies, TGF-β_1 stimulates differential responses in HA isoforms; with differentiation associated with HAS1 and HAS2 up-regulation in DFs (Meran *et al.* 2007).

Regarding effects on HAS1 expression, cells cultured with EBC-46 (0.01 - 0.1 μg/mL) in the presence of TGF-β_1 (Figure 4.8A), showed similar trends in expression across 72 h. Peak HAS1 gene expression for each condition was demonstrated at 24 h, with 0.01 and 0.1 μg/mL EBC-46 showing 6.1 and 9.3-fold decreases, respectively; versus TGF-β_1-positive controls (*p = >0.05*). Post-48 h exposure, both EBC-46 concentrations exhibited increases in HAS1 expression, compared to TGF-β_1-positive controls; due to the expression level in the TGF-β_1-positive control declining approximately 21.9-fold between 24 and 48 h. However, up-regulated HAS1 expression was not found to be statistically significant (3.1 and 1.4-fold at 0.01 and 0.1 μg/mL EBC-46, respectively; *p = >0.05*). Following 72 h treatment, HAS1 expression profiles were similar to those found at 48 h; with 0.01 and 0.1 μg/mL EBC-46 displaying 4.1 and 1.4-fold increases, respectively; versus TGF-β_1-positive controls. The former was found to be significant (*p = <0.05*; Figure 4.8A). Studies using EBC-211 (1 - 10 μg/mL; Figure 4.8B) displayed similar gene expression profiles at each time-point; with down-regulations in HAS1 expression evident at both EBC-211 concentrations, versus TGF-β_1-positive controls. Following 24 h treatment, the greatest down-regulation in HAS1 was shown at 1 and 10 μg/mL EBC-211, significantly reducing the gene expression by 7.6 and 17.8-fold, respectively (both *p = <0.001*). After 48 h, approximately 2.2 and 7.3-fold reductions were exhibited following 1 and 10 μg/mL EBC-211 treatment (both *p = <0.001*), while post-72 h treatment, 1.6 and 4.4-fold reductions in HAS1 expression were observed

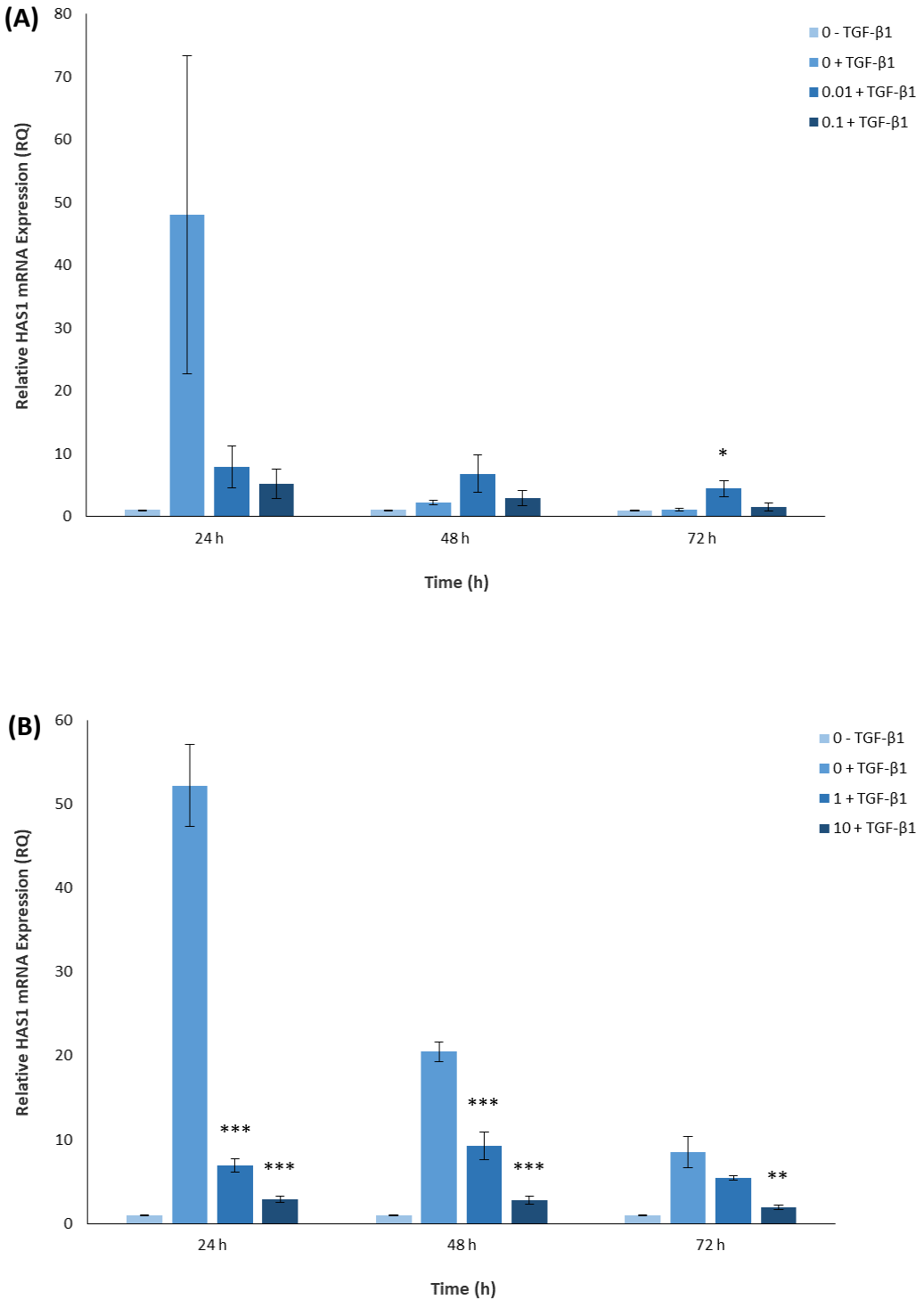

Figure 4.8. Hyaluronan synthase-1 (HAS1) gene expression in DFs, cultured with (A) EBC-46 (0.01 µg/mL and 0.1 µg/mL) and (B) EBC-211 (1 µg/mL and 10 µg/mL), in the presence of TGF-β_1, over 24 h, 48 h and 72 h in culture. Compound-free controls ± TGF-β_1 (10 ng/mL) were included (*n = 3*, mean±SEM; *p = *<0.05, **<0.01, ***<0.001* versus TGF-β_1-positive controls).

with 1 and 10 µg/mL of EBC-211 (*p = >0.05* and *p = <0.01*, respectively). Interestingly, however, despite such decreases in HAS1 expression at both EBC-211 concentrations over time, versus the TGF-β_1-positive controls; HAS1 expression was still greater than that of TGF-β_1-negative controls (Figure 4.8B); indicating that HAS1 expression is still induced after EBC-211 treatment, but not to the same extent as TGF-β_1-stimulated DFs.

Regarding HAS2 expression, DFs cultured with EBC-46 (0.01 - 0.1 µg/mL) and TGF-β_1 (Figure 4.9A), showed similar trends in expression over time; with increases in HAS2 expression evident at both EBC-46 concentrations at all time-points, versus TGF-β_1-positive controls. After 24 h treatment, 4 and 8.1-fold increases in HAS2 expression were exhibited by 0.01 and 0.1 µg/mL of EBC-46, respectively; the latter considered statistically significant (*p = <0.01*). Post-48 h treatment, approximately 8.8 and 11.3-fold increases were shown following 0.01 and 0.1 µg/mL EBC-46 exposure (*p = <0.01* and *p = <0.001*, respectively). Peak HAS2 gene expression for all concentrations was found at 72 h, with 0.01 and 0.1 µg/mL EBC-46 showing 8.3 and 11.9-fold increases, respectively; in comparison to TGF-β_1-positive controls. However, only the latter was found to be statistically significant (*p = <0.01*; Figure 4.9A). Comparable studies using 1 - 10 µg/mL EBC-211 displayed increases in HAS2 expression at both concentrations over time. After 24 h exposure, 6.9 and 13.6-fold up-regulations were exhibited by 1 and 10 µg/mL EBC-211, respectively; in comparison to TGF-β_1-positive controls. The latter increase was deemed statistically significant (*p = <0.01*). After 48 h treatment, approximately 8.3 and 12.7-fold increases in HAS2 expression were demonstrated at 1 and 10 µg/mL of EBC-211, respectively (both *p = <0.001*). At the final time-point (72 h), peak fold-changes in HAS2 expression were demonstrated, with 8.5 and 20.1-fold increases at 1 and 10 µg/mL EBC-211, respectively (both *p = <0.001*; Figure 4.9B).

Finally, regarding the effects upon HAS3 expression, cells cultured with EBC-46 (0.01 - 0.1 µg/mL), in the presence of TGF-β_1 (Figure 4.10A), showed differential responses between concentrations at every time-point. Following 24 h treatment, a significant 7.2-fold increase in HAS3 expression was observed at 0.01 µg/mL EBC-46 (*p = <0.05*), while 0.1 µg/mL induced a 3.3-fold down-regulation (*p = >0.05*); compared to TGF-β_1

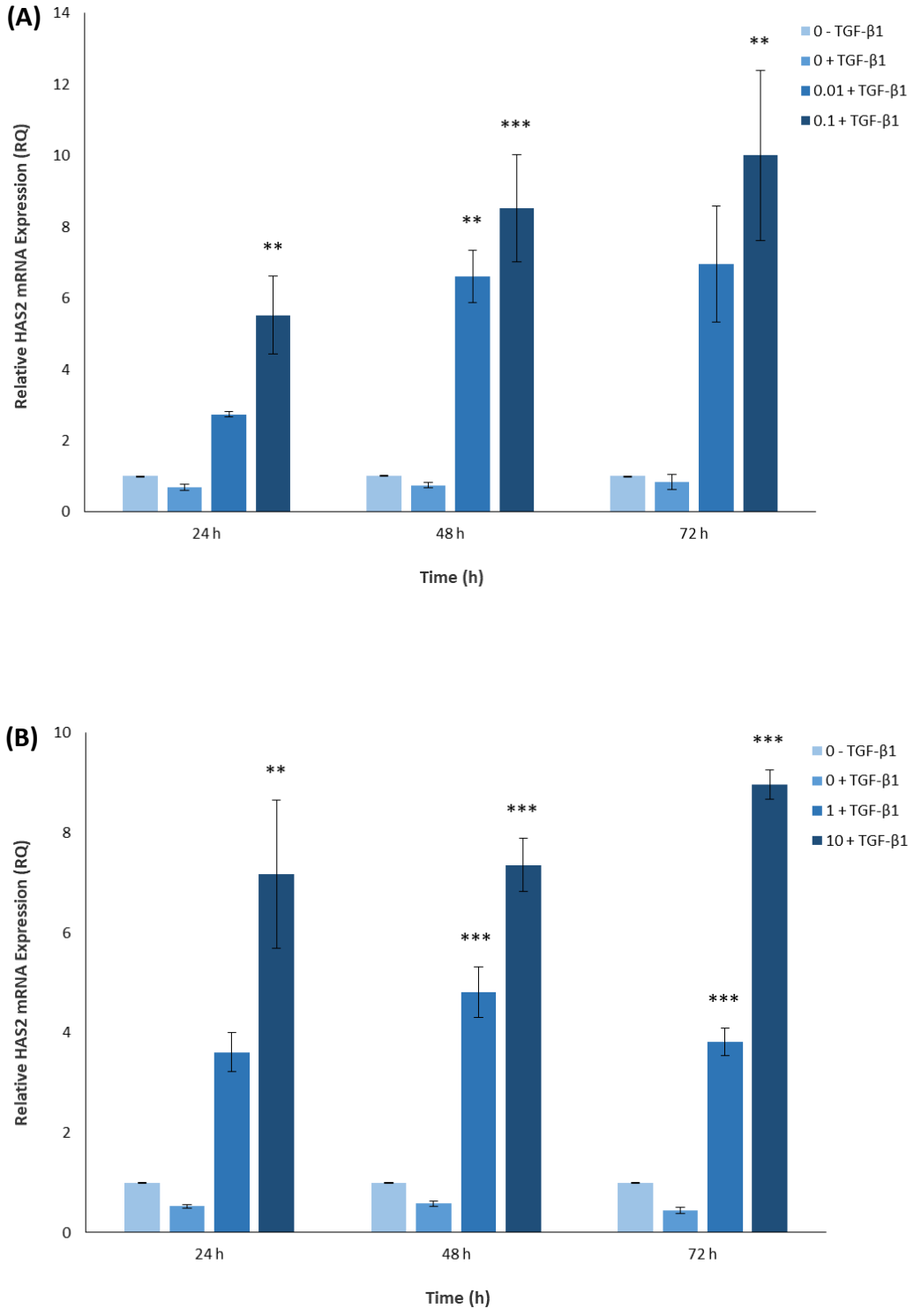

Figure 4.9. Hyaluronan synthase-2 (HAS2) gene expression in DFs, cultured with (A) EBC-46 (0.01 µg/mL and 0.1 µg/mL) and (B) EBC-211 (1 µg/mL and 10 µg/mL), in the presence of TGF-β_1; over 24 h, 48 h and 72 h in culture. Compound-free controls ± TGF-β_1 (10 ng/mL) were also included (*n = 3*, mean±SEM; *p = **<0.01, ***<0.001* compared to TGF-β_1-positive controls).

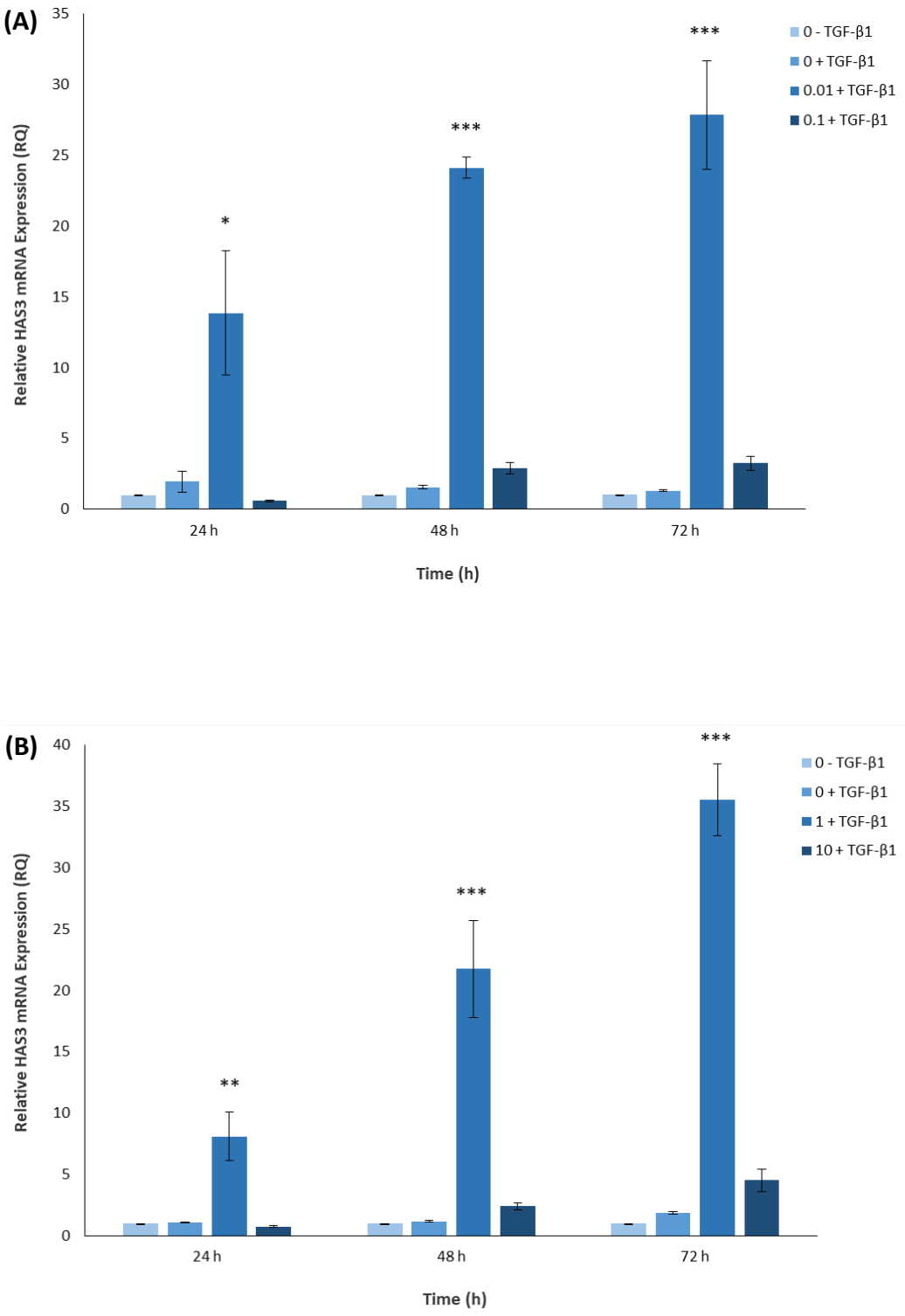

Figure 4.10. Hyaluronan synthase-3 (HAS3) gene expression in DFs, cultured with (A) EBC-46 (0.01 µg/mL and 0.1 µg/mL) and (B) EBC-211 (1 µg/mL and 10 µg/mL), in the presence of TGF-β_1, over 24 h, 48 h and 72 h in culture. Compound-free controls ± TGF-β_1 (10 ng/mL) were included (*n = 3*, mean±SEM; *p = *<0.05, **<0.01, ***<0.001* versus TGF-β_1-positive controls).

-positive controls. At 48 h, both concentrations exhibited increases in the expression of HAS3, with 0.01 and 0.1 µg/mL EBC-46 exhibiting approximately 15.6 and 1.9-fold up-regulations, respectively. However, only 0.01 µg/mL was found to be statistically significant (*p = <0.001*). Lastly, following 72 h treatment, peak increases in HAS3 gene expression were observed at both concentrations; with 0.01 and 0.1 µg/mL EBC-46 inducing approximately 21.2 and 2.5-fold increases, respectively. As found post-48 h treatment, however, only 0.01 µg/mL was found to be significant (*p = <0.001*; Figure 4.10A). Similar investigations with EBC-211 (1 - 10 µg/mL) demonstrated comparable findings, confirming the differential responses stimulated between concentrations of the epoxy-tiglianes, regarding HAS3 expression. Post-24 h exposure, a significant 7.5-fold up-regulation in expression was exhibited at 1 µg/mL EBC-211 (*p = <0.01*; Figure 4.10B), while 10 µg/mL inhibited HAS3 expression 1.4-fold (*p = >0.05*); versus TGF-β_1-positive controls. As displayed at 48 h with EBC-46, both concentrations of EBC-211 exhibited increased HAS3 expression; with 1 and 10 µg/mL inducing approximately 18.2 and 2-fold up-regulations, respectively. However, only 1 µg/mL was found to be statistically significant (*p = <0.001*). Additionally, as shown after 72 h treatment with EBC-46, peak increases in HAS3 expression were observed at both concentrations of EBC-211 after 72 h; with 1 and 10 µg/mL stimulating 19 and 2.4-fold up-regulations, respectively. As found following 48 h treatment, only the fold-change at 1 µg/mL was found to be significant (*p = <0.001*; Figure 4.10B).

4.4.6 Effects of EBC-46 and EBC-211 on Hyaluronan Levels

To assess the modulatory effects of EBC-46 and EBC-211 upon synthesis and release of extracellular HA, ELISA quantification was performed. HA concentration analyses were undertaken upon cells cultured with EBC-46 or EBC-211 at all aforementioned concentrations (Section 4.3), under the influence of TGF-β_1 (10 ng/mL), following 72 h treatment (Figure 4.11). Compound-free controls, with/without TGF-β_1, were also included as confirmation of normal DF-myofibroblast responses and for comparative purposes. As reported in previous studies, TGF-β_1 stimulates HAS expression and the accumulation of intracellular and extracellular HA in DFs (Meran *et al.* 2007).

Cells cultured with EBC-46 (0.001 - 10 µg/mL), in the presence of TGF-β_1 (10 ng/mL), showed varying degrees of up-regulation regarding HA synthesis and release; versus TGF-β_1-positive controls (Figure 4.11A). Lower concentrations of EBC-46 (0.001 - 0.01 µg/mL), demonstrated increases in HA synthesis (6.9 and 10-fold, respectively); that were found at even greater levels at higher concentrations of EBC-46 (1 - 10 µg/mL; 16.9 and 13.2-fold, respectively). Nevertheless, these changes were not found to be statistically significant (*p = >0.05*). However, at 0.1 µg/mL of EBC-46, approximately 29-fold greater HA production was identified, versus the TGF-β_1-positive controls (*p = <0.01*). Similar studies with EBC-211 (0.001 - 10 µg/mL) yielded comparable results to those obtained with EBC-46 (Figure 4.11B). All EBC-211 concentrations produced varying increases in HA levels, in comparison to TGF-β_1-positive controls. Lower EBC-211 concentrations (0.001 - 0.1 µg/mL) induced between 2.9 and 4-fold increases in total HA, although these were not exhibited to be statistically significant (*p = >0.05*). However, higher EBC-211 concentrations (1 and 10 µg/mL) stimulated even greater increases in HA levels (10.4 and 30.8-fold, respectively). Such changes were found to be statistically significant (*p = <0.01* and *p = <0.001*, respectively).

4.4.7 Effects of EBC-46 and EBC-211 on Hyaluronan Pericellular Coat Formation

Following the HA qPCR and ELISA findings (Sections 4.4.5 and 4.4.6, respectively), to assess the potential modulatory effects of EBC-46 and EBC-211 upon pericellular HA accumulation, erythrocyte exclusion assays were performed. Analysis of pericellular coat formation was carried out on DFs cultured with either EBC-46 or EBC-211 at all aforementioned concentrations (Section 4.3), in the presence of TGF-β_1 (10 ng/mL), following 72 h treatment (Figures 4.12 and 4.13). Compound-free controls, with or without TGF-β_1, were also included as a confirmation of normal DF-myofibroblast responses and for comparative purposes. As detailed in previous studies with TGF-β_1 stimulated DFs, cells develop notable pericellular HA coats; which along with HAS induction, are associated with DF-myofibroblast differentiation (Meran *et al.* 2007).

Cells cultured with EBC-46 (0.001 - 10 µg/mL), in the presence of TGF-β_1 (10 ng/mL; Figure 4.12C - G), demonstrated varying morphologies and HA coat assembly versus

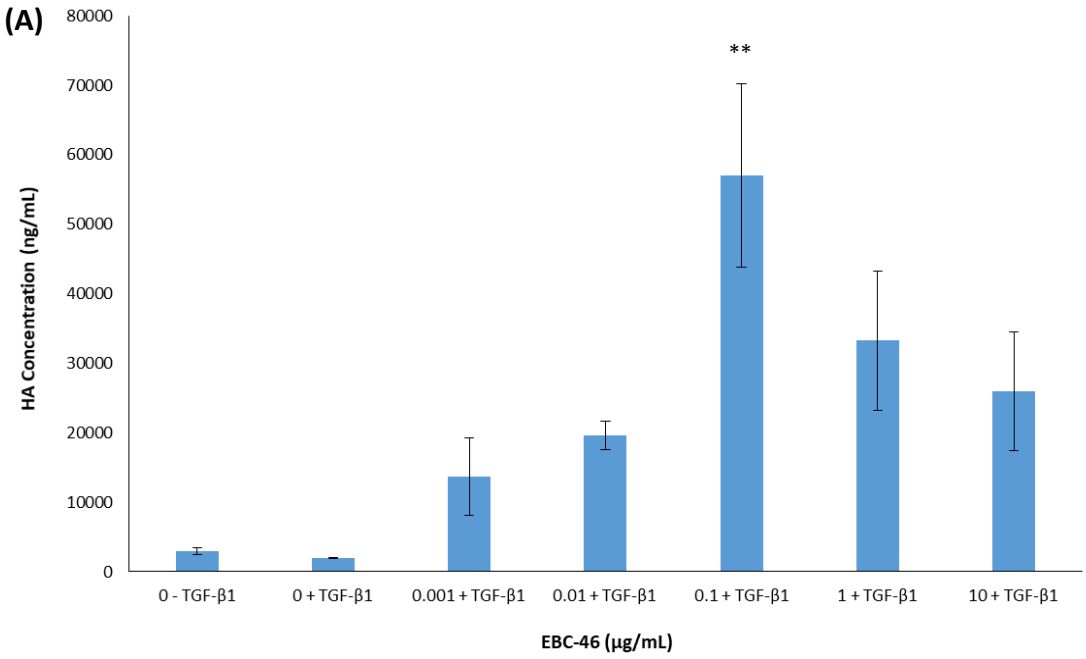

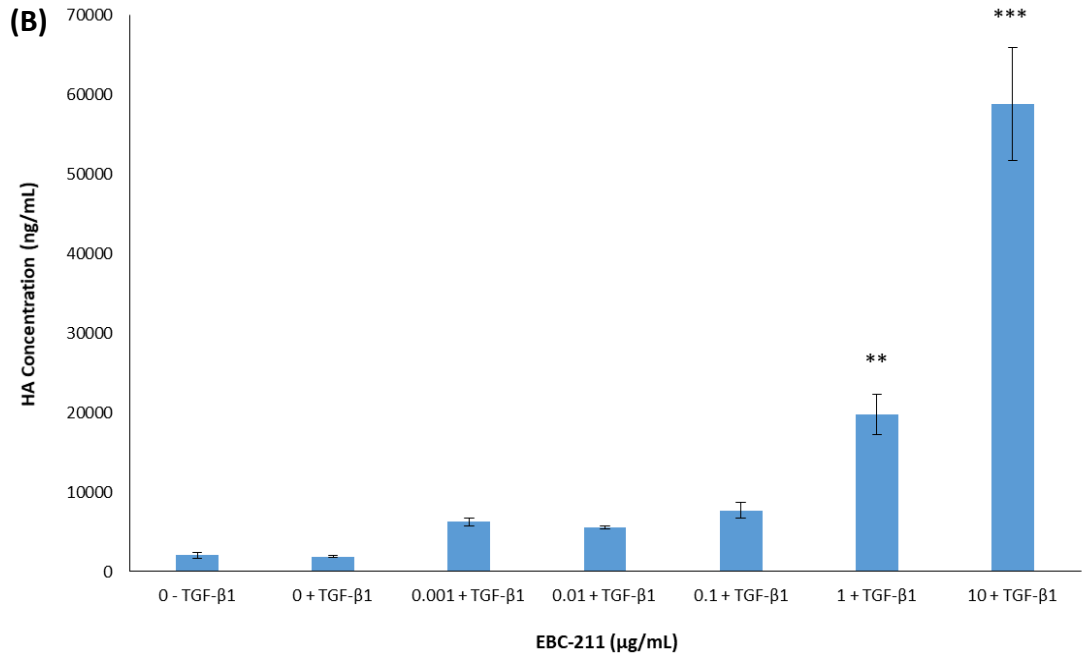

Figure 4.11. Hyaluronan (HA) production by DFs, cultured in the presence of (A) EBC-46 and (B) EBC-211 at 0.001 µg/mL, 0.01 µg/mL, 0.1 µg/mL, 1 µg/mL and 10 µg/mL, in the presence of TGF-β_1 (10 ng/mL), for 72 h. Compound-free controls ± TGF-β_1 were also included (*n = 3*, mean±SEM; *p = **<0.01, ***<0.001* compared to TGF-β_1-positive controls).

the controls (Figure 4.12A - B). Under resting conditions, DFs showed small spindle-shaped morphologies, with the erythrocytes gathering immediately adjacent to the DF membranes, due to the lack of significant HA coat assembly (Figure 4.12A). Upon TGF-β_1 stimulation, the DFs showed morphological changes consistent with those of myofibroblasts, as previously validated (Chapter 3). TGF-β_1-induced differentiation in DFs is associated with the assembly and formation of notable HA pericellular coats, which are seen under microscopy as exclusion zones of erythrocytes surrounding the cells. DFs at lower concentrations of EBC-46 (0.001 - 0.01 µg/mL), as shown in Figure 3.1, exhibited larger polygonal morphologies with evident stress fibre formation and cytoskeletal rearrangement. As shown prior, differentiation-associated morphology changes at such concentrations appeared more prominent than those shown by the TGF-β_1-positive controls; highlighting a potential synergy between TGF-β_1 and these concentrations. Regarding HA assembly, DFs at 0.001 and 0.01 µg/mL EBC-46 (Figure 4.12C - D, arrowed), appeared to possess greater HA coat sizes than those formed by TGF-β_1-positive control cells (Figure 4.12B, arrowed). Cells at higher concentrations of EBC-46 (1 - 10 µg/mL), as found in Figure 3.1 also, exhibited apparent stress fibre formation; however, in contrast to the lower concentrations, stress fibres appeared less prominent and morphologies were more elongated than polygonal. Concerning HA coat formation, cells at 1 and 10 µg/mL of EBC-46 (Figure 4.12F - G, arrowed) still possessed greater HA coat sizes than those synthesised by TGF-β_1-positive controls (Figure 4.12B, arrowed). However, the most notable morphological differences were shown at 0.1 µg/mL EBC-46. As found previously (Figure 3.1), cells showed a distinct lack of stress fibre development with elongated spindle-shaped morphologies; more comparable to resting DFs than their TGF-β_1-stimulated counterparts. Unlike TGF-β_1-negative control DFs, however, 0.1 µg/mL-treated cells showed pericellular HA coat formation; suggesting the presence of cells with intermediate phenotypes between DFs and myofibroblasts, or a differing cell type altogether.

Comparable findings to those stimulated by EBC-46 were displayed when cells were cultured using EBC-211 (0.001 - 10 µg/mL), in the presence of TGF-β_1 (Figure 4.13C - G). DFs demonstrated varying morphologies and pericellular coat formation, versus

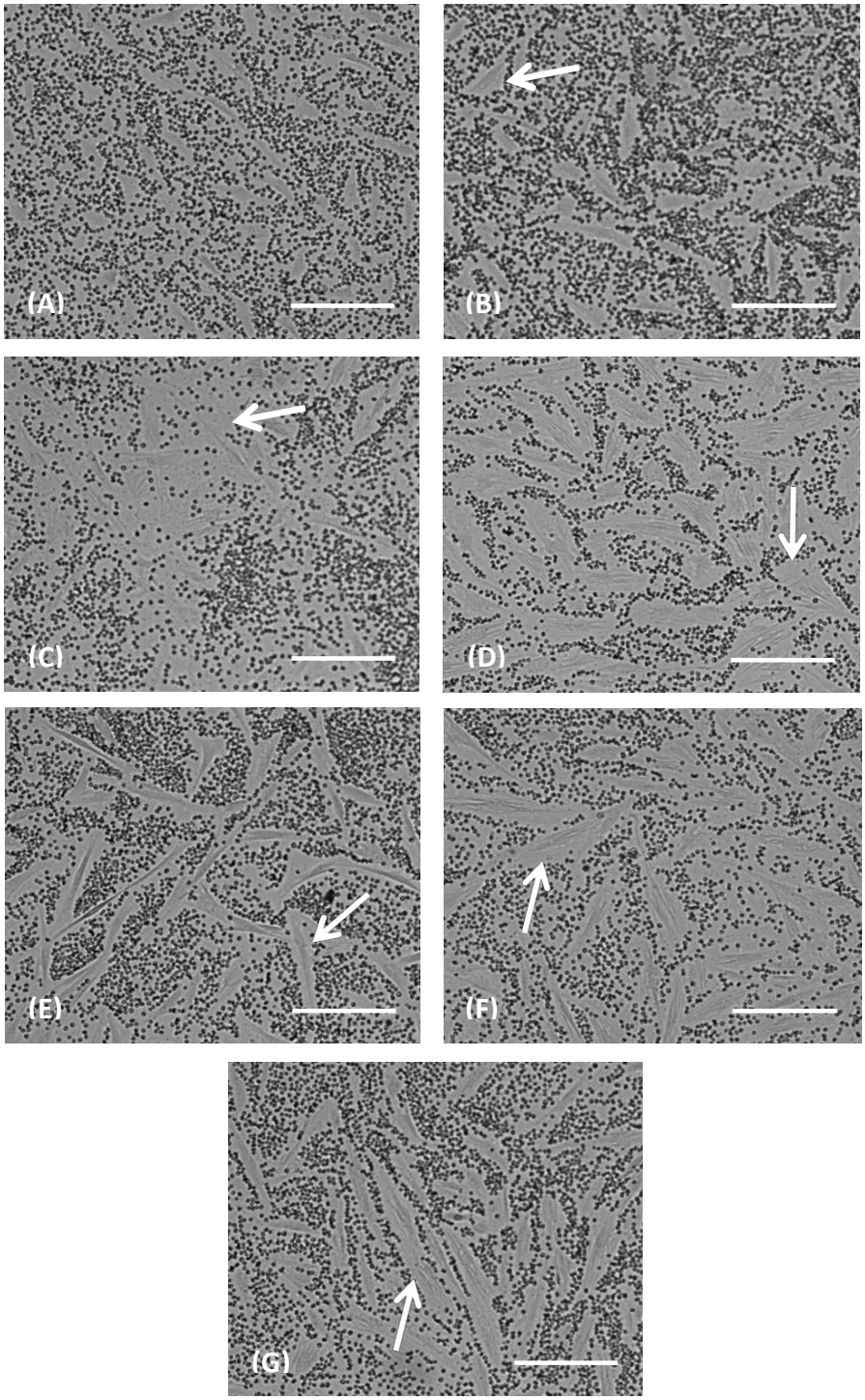

Figure 4.12. Erythrocyte exclusion assay analysis of DF-myofibroblast differentiation via visualisation of pericellular hyaluronan (HA) coat formation/assembly (arrowed), post-treatment with (B) 0 µg/mL, (C) 0.001 µg/mL, (D) 0.01 µg/mL, (E) 0.1 µg/mL, (F) 1 µg/mL and (G) 10 µg/mL of EBC-46, in the presence of TGF-β_1 (10 ng/mL), for 72 h. Compound-free, TGF-β_1-negative controls (A) were also included. Images displayed represent *n = 3* independent experiments captured at x100 magnification (scale bar = 25 µm).

controls (Figure 4.13A - B). Following 72 h treatment, cells at most concentrations of EBC-211 (0.001 - 1 µg/mL), exhibited comparable stress fibre development to TGF-β_1-positive control cells, but with more definitive phenotypes; as also exhibited in Figure 3.2. Out of all of the EBC-211 concentrations, cells treated with 0.001 µg/mL (Figure 4.13C), demonstrated morphologies and coat formation most comparable to TGF-β_1-positive control DFs. Stress fibres were shown, with more polygonal cell appearances not observed in the TGF-β_1-negative control (Figure 4.13A); indicating the occurrence of differentiation. Between 0.01 - 1 µg/mL EBC-211 (Figure 4.13D - F), DFs exhibited large, polygonal morphologies with apparent stress fibre formation and cytoskeletal rearrangement. DF-myofibroblast differentiation-associated morphology changes at these concentrations appeared more prominent than those observed in the TGF-β_1-positive control cells (Figure 4.13B); highlighting a potential synergy between these concentrations and TGF-β_1. With regards to HA assembly, pericellular coats at 0.01 - 1 µg/mL EBC-211 (Figure 4.13D - F, arrowed) appeared larger than those developed by TGF-β_1-positive control cells (Figure 4.13B, arrowed). However, as also seen at 0.1 µg/mL EBC-46, most notable morphological differences were observed at 10 µg/mL EBC-211. As found previously (Figure 3.2), DFs showed lacking stress fibre formation with elongated spindle-shaped appearances; more similar to resting fibroblasts than their TGF-β_1-stimulated counterparts. Unlike the TGF-β_1-negative DFs, however, DFs treated with 10 µg/mL EBC-211 displayed evident pericellular HA coat formation. As also found with 0.1 µg/mL EBC-46, this indicates that certain concentrations of both compounds influence cell phenotype and HA pericellular coat development.

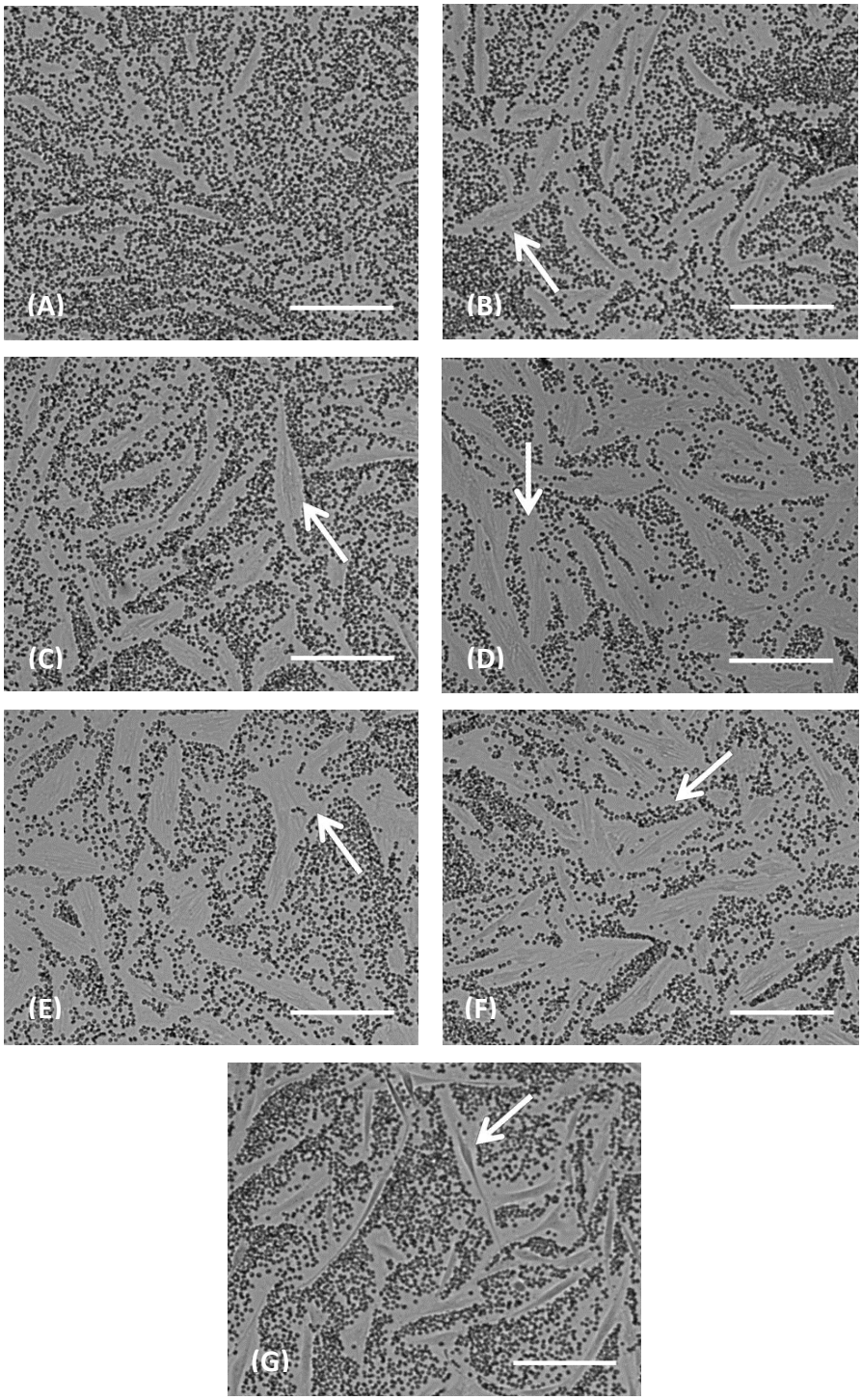

Figure 4.13. Erythrocyte exclusion assay analysis of DF-myofibroblast differentiation via visualisation of pericellular hyaluronan (HA) coat formation/assembly (arrowed), post-treatment with (B) 0 µg/mL, (C) 0.001 µg/mL, (D) 0.01 µg/mL, (E) 0.1 µg/mL, (F) 1 µg/mL and (G) 10 µg/mL EBC-211, in the presence of TGF-β_1 (10 ng/mL), for 72 h. Compound-free, TGF-β_1-negative controls (A) were also included. Images displayed represent *n = 3* independent experiments captured at x100 magnification (scale bar = 25 µm).

4.5 Discussion

Following on from Chapter 3, which highlighted the abilities of EBC-46 and EBC-211 in modulating TGF-β_1-driven differentiation and myofibroblast genotype/phenotype, the present Chapter aimed to investigate whether the effects of these novel epoxy-tiglianes extended to ECM modulation *in vitro*. Fibroblasts and myofibroblasts have fundamental roles in maintaining skin homeostasis and upon dermal wounding, the resting balance of ECM synthesis/turnover shifts; with both cell types responding in a manner which allows the restoration of equilibrium and ideally, skin functionality (Do and Eming, 2016). DFs and their differentiated counterparts are vital mediators of ECM synthesis, remodelling and proteolytic turnover; with key ECM components such as collagen, MMPs and HA produced by fibroblasts (Soo *et al.* 2000; Bainbridge, 2013). Consequently, the importance of ECM composition in scarring has been well-reported; with the above-mentioned components established as being differentially expressed in scenarios of both fibrosis and preferential healing, versus normal acute healing; as detailed prior (Section 4.1). Therefore, this Chapter focused on assessing whether EBC-46 and EBC-211 could directly modulate the synthesis and turnover of collagen, elastin, MMP-1 and HA *in vitro*; in the presence of TGF-β_1. As these factors are key in determining the extent of scar formation and fibrosis observed in various clinical scenarios, any effects stimulated by EBC-46 and EBC-211 may provide further clarification of the preferential wound healing outcomes observed *in vivo* post-EBC-46 treatment (Reddell *et al.* 2014; Campbell *et al.* 2017; Hansen *et al.* 2018).

Collagen is the most abundant fibre-forming protein in the skin; bestowing the ECM with structure, rigidity and tensile strength (Weinstein and Boucek, 1960; Tracy *et al.* 2016). Type I and III collagen compose approximately 85 - 90 % and 10 - 20 % of total collagen, respectively present in adult skin; indicating their importance in cutaneous architecture (Smith *et al.* 1986; Yagi *et al*. 2016). During wound repair, the presence, absence and/or ratio of specific collagen types contribute to the roles of the ECM in determining the extent of dermal fibrosis; these can also affect DF function. Thus, it is pertinent to consider the differences in collagen type, ratio, synthesis/turnover in normal healing, excessive scarring and scarless healing environments. As synthesis of

collagen is mainly induced by TGF-β signalling, initial studies undertaken within this Chapter focussed on evaluating whether EBC-46 and EBC-211 were able to modulate type I and III collagen expression; under the influence of TGF-β_1 (Varga *et al*. 1987).

At 0.1 μg/mL EBC-46 and 10 μg/mL EBC-211, significant down-regulation of COL1α_1 gene expression were observed; versus TGF-β_1-positive controls. In contrast, COL1α_1 expression at all other concentrations of both compounds showed an up-regulatory trend; with significant increases demonstrated at 1 and 10 μg/mL EBC-46 and 0.001 and 0.1 μg/mL EBC-211. Western blots were performed to validate gene responses observed. Post-EBC-46 treatment, no obvious differences in COL1 protein detection were perceived at 24 h, versus TGF-β_1-positive controls. At 72 h, however, decreased COL1 protein detection was observed at 0.1 μg/mL EBC-46; while comparable levels were observed at all other concentrations, versus TGF-β_1-positive controls. Following EBC-211 treatment, trends in protein detection at 24 h and 72 h reflected those seen at the genotypic level; indicating comparable or higher COL1 detection levels at most concentrations (0.001 - 1 μg/mL), except 10 μg/mL, where reduced protein detection was shown.

Regarding type III collagen expression, the only significant increase in COL3α_1 gene expression was found at the lowest EBC-46 concentration; despite up-regulations at higher concentrations of EBC-46 (1 - 10 μg/mL) and lower concentrations of EBC-211 (0.001 - 0.01 μg/mL). In contrast, down-regulatory trends were observed at 0.01 - 0.1 μg/mL and 0.1 - 10 μg/mL EBC-46 and EBC-211, respectively. As observed with type I collagen gene expression, the greatest decreases were exhibited at 0.1 and 10 μg/mL EBC-46 and EBC-211, respectively. Following qPCR studies, as performed with COL1, Western blots were performed. Following EBC-46 treatment, similar trends in COL3 protein detection were observed at both time-points, to the above-mentioned COL3 gene expression profile. However, the protein detection levels for 1 - 10 μg/mL EBC-46 were more comparable to the TGF-β_1-positive control at 72 h than at 24 h. After EBC-211 treatment, COL3 protein indicated comparable or higher levels of detection at most concentrations (0.001 - 1 μg/mL) at 24 h; with the same trend shown at 72 h

after 0.001 - 0.01 µg/mL treatment, versus their respective TGF-β_1-positive controls. However, as seen after 0.1 µg/mL EBC-46 treatment, decreased COL3 protein levels were observed at 10 µg/mL of EBC-211 at 24 h and 0.1 - 10 µg/mL of EBC-211 at 72 h. As such, the COL3 protein detection profile at 72 h was most similar to the trend expressed at the genotypic level.

Together, the aforementioned studies suggest that EBC-46 and EBC-211 have dose-dependent inhibitory effects upon collagen expression and synthesis. Although type I collagen gene expression was still found to be notably higher than that of the TGF-β_1-negative control cells at 0.1 and 10 µg/mL of EBC-46 and EBC-211, respectively; a comparable trend in α-smooth muscle actin (αSMA) gene expression was highlighted in Chapter 3. Therefore, these findings corroborate prior conclusions, which indicate that specific epoxy-tigliane concentrations inhibit myofibroblast formation. Previous *in vitro* studies support this hypothesis as normally, TGF-β_1 triggers a transcriptional programme that favours collagen deposition via up-regulation of COL1α_1 expression and a down-regulation of MMP-1 expression (Fineschi *et al*. 2006; Bujor *et al.* 2008; Goffin *et al.* 2010). Similarly to the effects on type I collagen, COL3 gene and protein expression were inhibited at these concentrations. However, unlike with the COL1α_1 findings, COL3α_1 gene expression at these concentrations was lower than that of the TGF-β_1-negative control; signifying potential down-regulatory synergy between TGF-β_1 and specific compound concentrations. Together, such findings imply that EBC-46 and EBC-211 may reduce collagen synthesis by DFs and/or induce MMP expression, potentially resulting in greater proteolytic ECM remodelling and/or faster collagen degradation/turnover; promoting an anti-fibrotic wound environment. Other plant-derived compounds have also demonstrated efficacy in inhibiting collagen synthesis in fibroblasts; including Compound *Astragalus* and *Salvia miltiorrhiza* extract (CASE), resveratrol, oleanolic acid (OA), shikonin and oxymatrine (OMT) (Fan *et al*. 2012; He *et al*. 2012; Mehta *et al*. 2016). In particular, resveratrol, shikonin and OMT were all found to decrease the gene and protein levels of type I and III collagens; the former compounds in hypertrophic scar-derived fibroblasts and the latter in keloid-derived fibroblasts (Fan *et al*. 2012; Zeng *et al*. 2013; Fan *et al*. 2015; Mehta *et al*. 2016). As

such, this may indicate potential therapeutic applications for the epoxy-tiglianes, in pathologically excessive scarring scenarios. Further histological studies post-epoxy-tigliane treatment would provide greater insights into the effect of the compounds upon wound site ECM composition *in vivo*; particularly the ratio of type I:III collagen present; and whether its arrangement is akin to that of scarless and/or regenerative environments. Additionally, the above-mentioned studies with OMT concluded that the alkaloid exerts its anti-fibrotic effects via the inhibition of SMAD3 production, its nuclear translocation and phosphorylation (Fan *et al*. 2012). Similar modulation was shown post-CASE treatment; SMAD2/3 phosphorylation was reduced and formation of complexes were blocked, along with nuclear translocation (He *et al*. 2012). These studies suggest, along with previous findings (Chapter 3) and those presented in the current Chapter, that epoxy-tigliane effects may be controlled via the TGF-β_1/SMAD pathway. As such, further studies are necessary in order to elucidate the underlying mechanisms by which these anti-fibrotic effects are induced.

In support of the aforementioned findings, further investigations were performed to assess whether type I collagen could also undergo increased degradation post-epoxy-tigliane treatment. As detailed previously (Chapter 1), ECM turnover and remodelling during dermal wound repair is primarily mediated by MMPs, including MMP-1. The latter protease is an important ECM modulator and has critical roles in the cleavage and degradation of type I and III collagens (Beanes *et al*. 2002; Do and Eming, 2016). Indeed, collagen accumulation is thought to arise from imbalances in their synthesis and lack of degradation by collagenases, including MMP-1; which can subsequently lead to excessive scar development (Fineschi *et al*. 2006; Giménez *et al*. 2017). Due to *in vivo* observations of minimal scar formation and rapid wound closure following epoxy-tigliane treatment (Reddell *et al.* 2014), along with the modulations of type I and III collagen demonstrated, potential effects upon MMP-1 gene expression were investigated.

Through qPCR studies, MMP-1 expression was shown to be up-regulated at all EBC-46 and EBC-211 concentrations following 72 h treatment; in the presence of TGF-β_1.

However, significant increases were only found at 0.1 and 10 µg/mL of EBC-46 and EBC-211, respectively. Such increases in gene expression were not only significantly greater than their respective controls, but also to all other concentrations of epoxy-tiglianes. These findings corroborate dose-dependent effects shown throughout, as well as those discovered previously (Moses, 2016). Results indicated that the epoxy-tiglianes concentrations may induce a transcriptional programme opposing that of TGF-β_1; favouring an anti-fibrotic DF phenotype capable of greater, faster turnover of collagen through the inhibition of collagen synthesis and stimulation of proteolytic remodelling/degradation (Bujor *et al.* 2008; Goffin *et al.* 2010). Increased MMP-1 in DFs may also facilitate keratinocyte migration into the wound bed and subsequent re-epithelialisation. High-affinity binding to type I collagen inhibits the keratinocytes mobility whereas collagen cleavage by MMP-1 aids in dissociating the keratinocytes from their integrin-mediated attachment to the ECM, and facilitates their migration (Parks, 1999; Tandara and Mustoe, 2011; Moses, 2016). Therefore, such stimulated responses may further contribute to the rapid re-epithelialisation and resolution of wounds shown *in vivo* after epoxy-tigliane treatment (Reddell *et al.* 2014; Campbell *et al.* 2017; Hansen *et al.* 2018). As detailed previously (Chapter 4.1), it has been well-documented that during scarless wound healing, there is greater MMP activity than TIMP activity; favouring earlier remodelling and faster collagen turnover (Dang *et al*. 2003; Yagi *et al*. 2016; Moore *et al.* 2018). Thus, further studies into MMP and TIMP activities would be beneficial in elucidating whether differential responses shown at the gene level are translated into proteolytic effects. Furthermore, due to the dose-dependent differences among compound concentrations, it would be advantageous to understand how these contrasting modulations manifest globally, via Microarray analyses.

In addition to collagen, elastin is another key fibrous protein of the ECM involved in ECM homeostasis; providing structural integrity, tissue resilience and absorption of mechanical overload (Klingberg *et al*. 2013). As described previously (Chapter 1), it is generally understood that elastin production by DFs is low post-injury, which partly accounts for the rigidity, reduced elasticity and the breaking strength of scar tissue;

compared with intact connective tissue (Schultz and Wysocki, 2009; Klingberg *et al*. 2013). However, several studies have demonstrated that elastin production by DFs is elevated following damage to tissue, in response to stimuli including TGF-β_1 (Liu and Davidson, 1988; Kähäri *et al.* 1992; Kucich *et al.* 1997). Regardless, it is believed that restoration of a dermal ECM mimicking unwounded skin structure and function may improve subsequent wound resolution. In theory, regarding elastin, the consequent tensile strength and elastic recoil would be akin to that of the intact dermis (Schultz and Wysocki, 2009; Klingberg *et al*. 2013). Thus, the potential effects of EBC-46 and EBC-211 upon elastin synthesis, in the presence of TGF-β_1, were of interest.

Using qPCR studies, ELN gene expression was found to be up-regulated at all EBC-46 and EBC-211 concentrations following 72 h treatment. These were significant at the lower concentrations of EBC-46 (0.001 - 0.01 μg/mL) and all EBC-211 concentrations, barring 10 μg/mL. In line with the aforementioned studies, it was found that TGF-β_1 alone stimulated ELN gene expression in DFs; however on epoxy-tigliane treatment, synergistic effects were apparent. Compared to the control, the lowest increases in ELN expression were shown at 0.1 and 10 μg/mL EBC-46 and EBC-211, respectively. Western blot analyses were performed as validation however, no obvious responses were discerned post-EBC-46 treatment and no obvious differences were exhibited at either time-point. Regarding EBC-211, comparable levels of protein detection were shown at most concentrations (0.001 - 0.1 μg/mL) after 24 h, with reduced amounts observed at 1 - 10 μg/mL EBC-211; versus the TGF-β_1-positive controls. Following 72 h treatment, ELN protein detection appeared inconsistent across concentrations. As a result of the unreliable nature of such antibody detection, further studies into ELN quantification would be pertinent to fully elucidate whether the responses observed at the gene level are translated to the phenotypic level. Elastin ELISAs would provide a more sensitive, accurate quantitative approach; whilst *ex vivo* immunolocalisation of post-treatment biopsied tissue for ELN, as well as the collagens and MMPs, would provide greater insight into the architecture of the ECM and protein orientation. As at specific concentrations, inhibition of collagen synthesis and induction of MMP-1 expression are observed, in combination with moderate elastin expression (0.1 and

10 µg/mL EBC-46 and EBC-211, respectively); greater investigation into MMP activity would be beneficial as several MMPs possess the ability to cleave and degrade ELN (Duca *et al*. 2004). Therefore, this may explain why findings at the protein level were inconsistent, compared to the expression induced at the genotypic level. Global gene expression analysis would also offer a more comprehensive view on whether certain up or down-regulations may be affecting elastin degradation, or its cross-linking. As detailed prior (Chapter 4.1), clarification of epoxy-tigliane effects would determine whether they confer preferential changes in organisation, deposition or distribution of elastin; compared to the characteristics attributed to normal acute, hypertrophic and keloid scarring (Amadeu *et al.* 2004; Venkataraman and Ramamurthi, 2011).

As well as the structural ECM constituents, glycosaminoglycans (GAGs) are also vital components of the wound healing response and are implicated in tissue fibrosis. HA is a ubiquitous GAG synthesised at greater levels in remodelling tissues; contributing not only to hydration of the ECM, but mediating cellular differentiation, proliferation and migration, amongst other processes (Vigetti *et al*. 2014). Synthesised at the cell membrane's inner surface by HAS enzymes, HA has been found to be predominantly produced by the HAS2 isoform and can be arranged into coats or cables (Spicer and McDonald, 1998; Albeiroti *et al*. 2015). Interestingly though, gene expression of HAS differs depending upon the cells and the surrounding environment; with OMFs highly expressing HAS3, but not HAS1. Additionally, upon TGF-β_1 exposure, HAS1 and HAS2 have been shown to be induced in DFs, but not in OMFs (Yamada *et al*. 2004; Meran *et al*. 2007; Glim *et al*. 2013). Indeed, along with the levels and types synthesised, HA organisation/turnover are hypothesised as being contributors to variations in clinical presentations of varying scar types; and those of normal skin and scarless situations (Bertheim and Hellström, 1994; Meyer *et al*. 2000; Tan *et al.* 2011; Sidgwick *et al.* 2013). Therefore, the effects of EBC-46 and EBC-211 upon HAS gene expression, HA synthesis and assembly were of significant interest.

HAS1 gene expression was found to be down-regulated after 24 h EBC-46 treatment at both concentrations (0.01 - 0.1 µg/mL) while after 48 h and 72 h treatment, small

increases were found at both. With regards to EBC-211, significant decreases in HAS1 expression were evident at every time-point for both concentrations (1 - 10 μg/mL); barring at 1 μg/mL. Interestingly, the high concentrations of both compounds always induced less HAS1 expression than their 10-fold lesser concentrated counterparts. Regarding HAS2 expression, EBC-46 (0.01 - 0.1 μg/mL) and EBC-211 (1 - 10 μg/mL) at both concentrations and time-points increased HAS2 expression. However, increases induced by the lower concentration of EBC-46 at 24 h and 72 h were not significant; also true for 1 μg/mL EBC-211 at 24 h. Lastly, HAS3 gene expression was significantly up-regulated by 0.01 and 1 μg/mL EBC-46 and EBC-211, respectively; at every time-point. Overall, the most significant increases by compounds at both concentrations were with HAS2 expression; whilst HAS1 was mostly down-regulated or unaffected and HAS3 up-regulation was concentration-dependent. Though HAS2 is the primary isoform expressed by DFs (Meran *et al.* 2007; Albeiroti *et al*. 2015), its increased and persistent expression by the epoxy-tiglianes is notable; in compared to the other HAS isoforms. HAS1 gene expression is absent in early-gestational fibroblasts and OMFs, associated with scarless healing and resistance to TGF-β_1 differentiation (Yamada *et al*. 2004; Meran *et al.* 2007). In contrast, TGF-β_1-driven myofibroblast differentiation is associated with HAS1/2 up-regulation (Meran *et al*. 2007). Interestingly, the HAS2 expression at 0.1 and 10 μg/mL EBC-46 and EBC-211, respectively; was highest at all of the time-points and increased across time. In normal DFs, this would be indicative of a pro-fibrotic phenotype; however, preceding work has shown (Chapters 3 and 4) that at such concentrations, there is an inhibition of myofibroblast formation. HAS2 is also recognised as essential to embryonic and early-gestational development, an environment in which DFs are resistant to developing scarring phenotypes. As such, in this setting, HAS2 stimulates cell migration and invasiveness in a complementary manner (Camenisch *et al*. 2000). Lastly, the significant up-regulation of HAS3 at 0.01 and 1 μg/mL EBC-46 and EBC-211, respectively; complements the previous findings. Myofibroblast formation was observed at these concentrations and HAS3 produces low-molecular weight HA; associated with more pro-fibrotic repair responses (David-Raoudi *et al.* 2008; Huang *et al.* 2009).

Following the qPCR studies, HA ELISAs and erythrocyte exclusion assays were carried out to validate the aforementioned genotypic responses and determine the effects of the compounds upon HA pericellular coat assembly, respectively; in the presence of TGF-β_1. Total HA protein production was found to be up-regulated following both EBC-46 and EBC-211 treatment at all concentrations (0.001 - 10 µg/mL), following 72 h treatment versus the TGF-β_1-positive controls. However, such increases were only significant at 0.1 µg/mL EBC-46 and 1 - 10 µg/mL EBC-211. With regards to HA coat assembly and cellular appearances, cells demonstrated morphologies that reflected those observed in ICC studies (Chapter 3). Following EBC-46 treatment, cells treated at all EBC-46 concentrations, except 0.1 µg/mL, appeared to possess larger HA coats than those synthesised by TGF-β_1-positive controls. This was also the case following EBC-211 treatment, barring at 10 µg/mL. Despite their cell morphologies resembling those of TGF-β_1-negative control cells (as observed in Chapter 3 also), at 0.1 and 10 µg/mL EBC-46 and EBC-211, cells displayed HA coat formation; unlike the lack of HA coat formation observed in TGF-β_1-negative DFs. This suggests the presence of cells with intermediate phenotypes between DFs and myofibroblasts. Some studies have highlighted that a high HA concentration in the extracellular space, found during the first phases of wound repair or early-gestational development, would limit the ECM deposition; collagen in particular (Iocono *et al*. 1998; Croce *et al*. 2001). This theory complements findings of this Chapter, as at 0.1 and 10 µg/mL EBC-46 and EBC-211, respectively; total HA synthesis was much greater than all the other concentrations, coinciding with inhibition of type I collagen synthesis and MMP-1 induction. Similar findings were reported by Croce *et al*. 2001, demonstrating that a high HA presence reduces the amount of proteins (especially collagen) present in the medium of DFs. This would suggest a role for HA in delaying cell differentiation and preventing scar formation.

Evident after the HAS2 and HA synthesis investigations, synergistic effects between epoxy-tiglianes and TGF-β_1 in pericellular coat promotion were seemingly identified. The genotypic data suggested that HAS2 is chiefly responsible for the amount of HA synthesised; though the data indicates HAS3 involvement at the more 'pro-fibrotic'

concentrations. As detailed prior (Chapter 4.1), elevated and persistent HA synthesis has been found in early-gestational foetal wounds, due to increased HAS expression and reduced activity of hyaluronidase (Longaker *et al*. 1989; Mast *et al*. 1995; West *et al*. 1997). Thus, it would be beneficial to investigate the amounts of HA-degrading enzyme present following epoxy-tigliane treatment. Foetal fibroblasts have also been shown to express more surface receptors for HA; enhancing their migratory abilities (Chen *et al.* 1989; Alaish *et al*. 1994). HA receptor prevalence studies would provide greater insight into whether cellular migration and aggregation, observed at certain concentrations in Chapter 3, is HA-modulated; as currently, it is not known how the compounds stimulate these responses. Taking these findings overall, epoxy-tigliane-induced collagen inhibition and MMP-1 induction, coupled with elevated synthesis of endogenous HA and pericellular coat assembly; would favour an ECM modulation akin to those of scarless environments, such as early-gestational tissue (Longaker *et al*. 1989; Mast *et al*. 1995; West *et al*. 1997; Iocono *et al*. 1998; Croce *et al*. 2001; Dang *et al*. 2003; Yagi *et al*. 2016). Therefore, these modulations may collectively contribute to explaining the healing outcomes exhibited *in vivo* post-epoxy-tigliane treatment; including wound resolution and minimal scar development (Reddell *et al.* 2014; Campbell *et al.* 2017; Hansen *et al.* 2018).

Previous studies (Chapters 3 and 4) have indicated that both EBC-46 and EBC-211 are capable of inducing beneficial responses in DFs; highlighting their potential usage as anti-fibrotic therapeutics in excessive scarring scenarios. However, little is known on how the epoxy-tiglianes exert their effects *in vivo* and what pathways are affected to encourage a more tissue regenerative outcome, as documented prior (Reddell *et al.* 2014; Campbell *et al.* 2017; Hansen *et al.* 2018). Therefore, in order to validate the aforementioned findings thus far, and to potentially identify more novel modes of action, Microarray analyses of global gene expression were undertaken to elucidate the overall effects of the epoxy-tiglianes on DF/myofibroblast behaviour; as detailed in Chapter 5.

Chapter 5

Epoxy-Tigliane Effects on Dermal Fibroblast/Myofibroblast Global Gene Expression, and Response Validation

Chapter 5 - Epoxy-Tigliane Effects on Dermal Fibroblast/Myofibroblast Global Gene Expression, and Response Validation

5.1 Introduction

As detailed previously (Chapter 1), normal acute wound repair encompasses a tightly regulated series of events, requiring the temporal regulation of numerous genes. In order for successful wound resolution to occur, thousands of genes may be actively involved in the transcriptional response to dermal injury and wound healing. Timely and co-ordinated processes, from messenger RNA (mRNA) transcription to resultant protein synthesis, are required to provide orchestration of the complex mechanisms and varied cell types that contribute to normal acute wound repair (Cole *et al*. 2001; Blumenberg and Tomic-Canic, 2007; Charles *et al*. 2008; Eming *et al*. 2010 and 2014; Pang *et al*. 2017). Identifying genes that may be activated (up-regulated) or silenced (down-regulated) during wound healing encourages a greater understanding of the mechanisms underlying successful wound closure; which may be of particular use in elucidating aetiologies of pathological conditions, such as chronic wound formation or excessive dermal fibrosis. Gene expression changes and effects upon the resulting protein synthesis can have significant effects on healing outcome, be it pathological or preferential (Sayah *et al*. 1999; Seifert *et al*. 2008; Hahn *et al*. 2013; Huang *et al*. 2015; Tan *et al*. 2015).

Regarding preferential wound healing responses, it has been reported that there are numerous differentially expressed genes associated with both the oral mucosal and early-gestational, foetal wound healing processes; versus normal post-natal healing (Colwell *et al*. 2008; Chen *et al*. 2010; Hu *et al*. 2014; Turabelidze *et al*. 2014). These differences have been observed in genes involved in cellular proliferation, migration and adhesion; in addition to genes related to growth factor and cytokine expression, extracellular matrix (ECM) synthesis and degradation, amongst others (Colwell *et al*. 2008; Helmo *et al*. 2013). Changes in these functional families, in combination or in

isolation, may also contribute to *in vitro* phenotypic differences observed after EBC-46 and EBC-211 treatment of dermal fibroblasts (DFs) and their transforming growth factor-β_1 (TGF-β_1)-induced myofibroblast counterparts (Chapter 3 and 4). Ultimately, these induced differences in the cells that modulate wound repair, contraction and closure, may significantly contribute to the clinical outcomes observed *in vivo*; such as accelerated granulation tissue development and minimal scarring (Campbell *et al*. 2014, 2017; Reddell *et al*. 2014). Therefore, global gene transcription profiling can be considered extremely useful in identifying the potential differences between normal responses and those following physiological or experimental alterations.

Since the advent of robust DNA Microarray technology, the method has been widely used in the context of wound repair and regeneration research; allowing researchers to obtain global pictures of transcriptional activity. This technique not only provides 'gene signatures' of the cell types investigated at certain time-points, but also allows target gene identification for further, more in-depth study (e.g. at the protein level). With regards to human DFs, various studies have investigated their gene expression profiles using Microarrays; compared to fibroblasts from anatomically discrete sites, including the oral mucosa (Chang *et al*. 2002; Enoch *et al*. 2009, 2010; Peake *et al*. 2014). Comparison to normal human DFs has also been performed using fibroblasts from pathological non-healing wounds (Brem *et al*. 2007; Wall *et al*. 2008; Peake *et al*. 2014); as well as those derived from regions of pathologically excessive scarring (Tsou *et al*. 2000; Satish *et al*. 2006; Smith *et al*. 2008; Russell *et al*. 2010). Insights into the differential responses between early- and late-gestational fibroblasts have also been gained via the use of murine models (Wulff *et al*. 2013; Hu *et al*. 2014). In light of the outlined benefits of Microarray technology, analyses were performed to elucidate the differential responses between normal DFs/myofibroblasts and those treated with the novel epoxy-tiglianes, EBC-46 and EBC-211.

5.2 Chapter Aims

Previous studies (Chapters 3 and 4), have shown that EBC-46 and EBC-211 appear to induce preferential wound repair responses in primary human DFs; as evidenced by

the inhibition of DF-myofibroblast differentiation and preferential modulation of key ECM components at specific epoxy-tigliane concentrations *in vitro*. Findings indicate that the epoxy-tiglianes encourage the inhibition and degradation of type I collagen through matrix metalloproteinase-1 (MMP-1) stimulation, coupled with the elevated synthesis of endogenous hyaluronan (HA) and pericellular coat assembly/formation. Such conclusions would favour establishment of an ECM environment akin to those of scarless healing tissues, including the oral mucosa and early-gestational, foetal skin (Longaker *et al*. 1989; Iocono *et al*. 1998; Croce *et al*. 2001; Dang *et al*. 2003; Yagi *et al*. 2016). As these responses may indicate the underlying mechanisms of action, with regards to the *in vivo* responses induced by epoxy-tiglianes, global gene expression analyses were performed via Microarray studies. This Chapter aimed to elaborate on the previous findings and to elucidate further genes differentially expressed in DFs/ myofibroblasts following epoxy-tigliane treatment. Protein validation studies were further performed on key differentially expressed genes, to determine whether these changes also occurred at the protein level. Overall, the Chapter aimed to elucidate whether gene changes reflected the healing outcomes observed *in vivo* post-epoxy-tigliane treatment, such as rapid granulation tissue formation/wound resolution and reduced scarring; and whether these were associated with the preferential healing responses observed in foetal and oral mucosal healing (Campbell *et al*. 2014, 2017; Reddell *et al*. 2014).

5.3 Materials and Methods

DFs were sourced, cultured and counted, as previously described (Chapters 2.2.1 and 2.2.2). Following determination of cell density and viability (Chapter 2.2.2), DFs were seeded into 175 cm^2 and 75 cm^2 culture flasks for Microarray analyses and Western blot/MMP activity assay analyses (Chapters 2.8 and 2.5/2.9, respectively); at 9 x 10^4 cells/mL. Cell seeding, serum-starvation and treatment volumes were 20 mL and 10 mL for 175 cm^2 and 75 cm^2 culture flasks, respectively. Cells were maintained at 37 °C, in 5 % CO_2/95 % air atmosphere, for the duration of experiments (Chapter 2.2.1). Following growth arrest (Chapter 2.2.1), DFs were treated with EBC-46 or EBC-211 at either of the ensuing concentrations: 0 µg/mL, 0.001 µg/mL, 0.01 µg/mL, 0.1 µg/mL,

1 µg/mL or 10 µg/mL (Chapter 2.1.1), in the presence of TGF-β_1 (Chapter 2.1.2). Post-24 h or 72 h treatment periods, Microarray analysis was utilised to determine DF/ myofibroblast global gene expression (Chapter 2.8), with Western blotting utilised to analyse peptidase inhibitor 16 (PI16) protein expression (Chapter 2.5). Conditioned media samples collected from 75 cm^2 flasks were also used in MMP activity assays, to assess changes in MMP-1, -3, -10 and -12 activity levels (Chapter 2.9). Statistical analyses were performed, as described previously (Chapter 2.11).

5.4 Results

5.4.1 Effects of EBC-46 and EBC-211 on Global Gene Expression

The Microarray analyses identified numerous genes differentially expressed by DFs, following EBC-46 (0.01 µg/mL and 0.1 µg/mL) and EBC-211 (1 µg/mL and 10 µg/mL) treatment, in the presence of TGF-β_1 (10 ng/mL), at 24 h and 72 h; in comparison to TGF-β_1-positive, non-compound controls at each time-point. Given the large number of genes analysed, only those differentially expressed ≥ 2-fold were focused upon.

Hierarchal clustering was performed using GeneSpring™ technology (Chapter 2.8.4), producing heatmaps and organising the gene expression data into sections of genes that were up or down-regulated. Heatmaps obtained for genes ≥ 2-fold differentially expressed following EBC-46 and EBC-211 treatment, at both 24 and 72 h, are shown in Figures 5.1 and 5.2, respectively; versus their respective compound-free controls. Such heatmaps permitted comparison of the differential responses between epoxy-tigliane-treated cells and the TGF-β_1-positive, compound-free controls; in addition to comparison between the different epoxy-tigliane concentrations at each time-point. Overall, larger differences were induced between epoxy-tigliane concentrations (i.e. between 0.01 and 0.1 µg/mL of EBC-46 and 1 and 10 µg/mL of EBC-211, respectively), in comparison to the differences induced between the two epoxy-tigliane analogues themselves; which appear more similar with regards to the gene expression profiles overall (Figures 5.1 and 5.2).

Tables 5.1 and 5.2 display the number of genes differentially expressed ≥ 2-fold, ≥ 3-

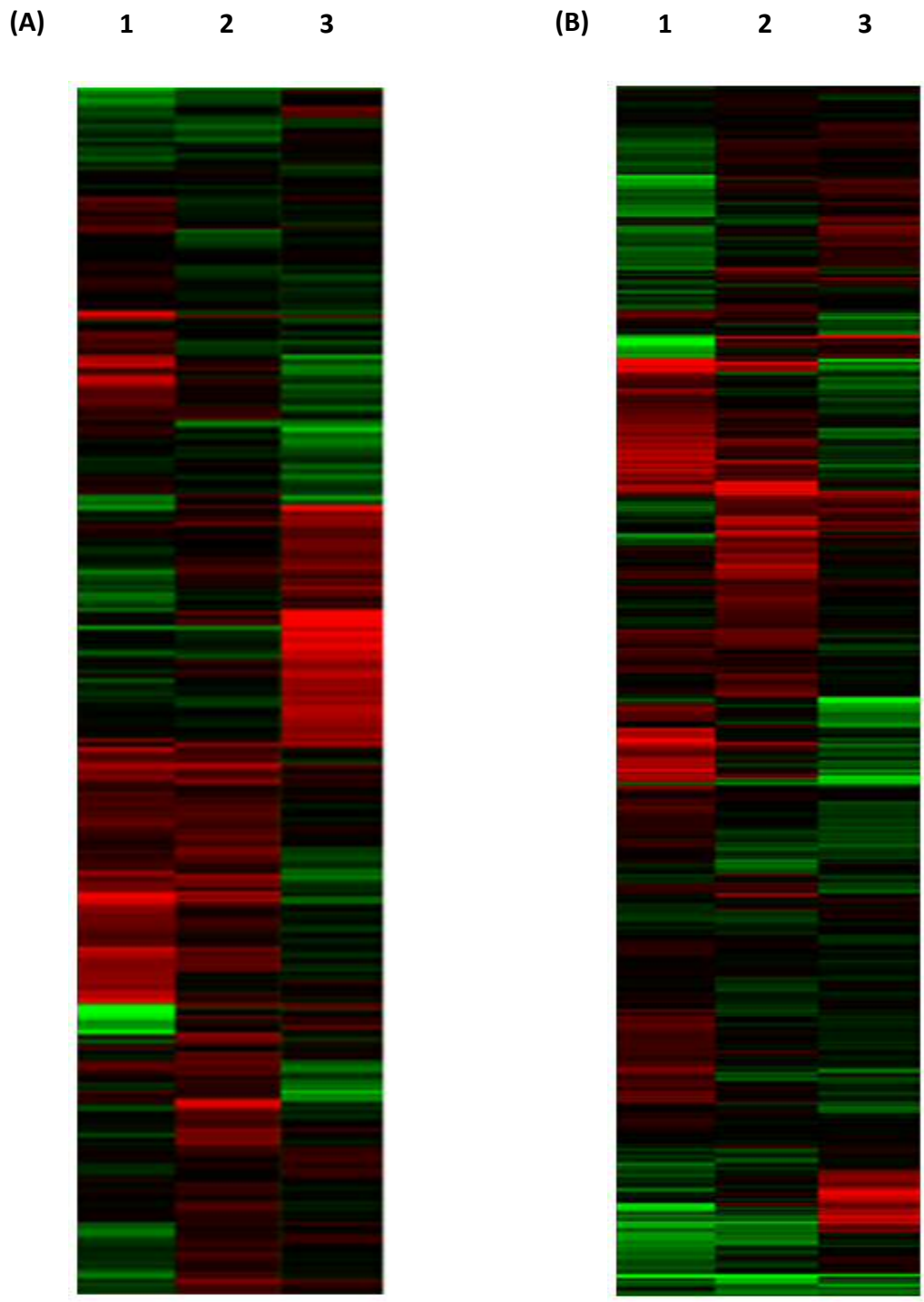

Figure 5.1. Heatmap visualisation through hierarchical clustering of genes ≥ 2-fold differentially expressed by DFs/myofibroblasts (*n = 4* patient sources), cultured with either 0.01 µg/mL or 0.1 µg/mL EBC-46, in the presence of TGF-β_1 (10 ng/mL), for 24 h (A) and 72 h (B); compared to TGF-β_1-positive, compound-free controls at each time-point. For both time-points, Lane 1 = control; Lane 2 = 0.01 µg/mL EBC-46; Lane 3 = 0.1 µg/mL EBC-46. **Red** = up-regulated, **Green** = down-regulated.

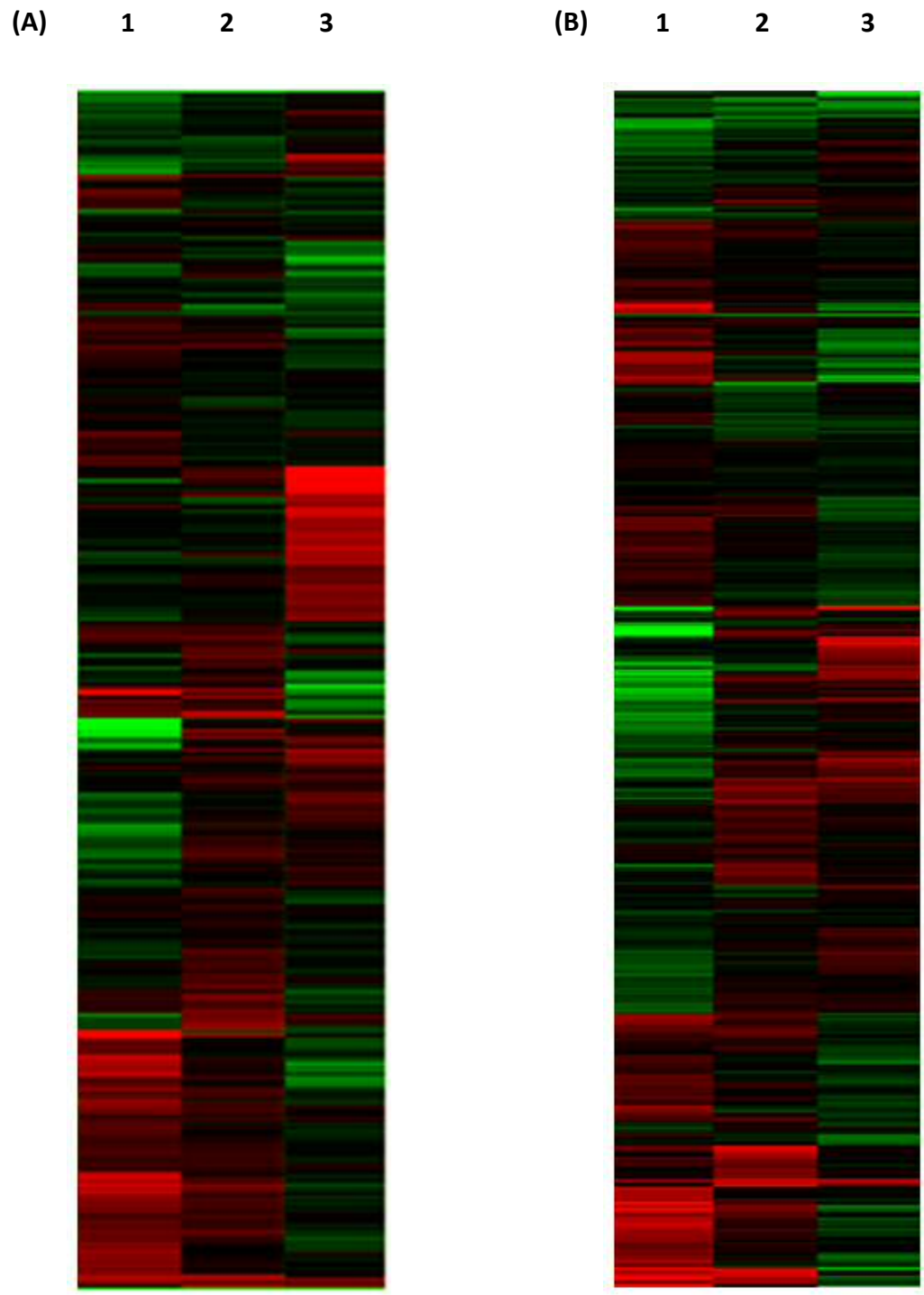

Figure 5.2. Heatmap visualisation through hierarchical clustering of genes ≥ 2-fold differentially expressed by DFs/myofibroblasts (*n = 4* patient sources), cultured with either 1 µg/mL or 10 µg/mL EBC-211, in the presence of TGF-β_1 (10 ng/mL), for 24 h (A) and 72 h (B); compared to TGF-β_1-positive, compound-free controls at each time-point. For both time-points, Lane 1 = control; Lane 2 = 1 µg/mL EBC-211; Lane 3 = 10 µg/mL EBC-211. **Red** = up-regulated, **Green** = down-regulated.

Table 5.1. Number of genes differentially expressed ≥ 2-fold, ≥ 3-fold, ≥ 5-fold and ≥ 10-fold in DFs/myofibroblasts, cultured with EBC-46 at 0.01 µg/mL or 0.1 µg/mL, in the presence of TGF-β_1 (10 ng/mL), for 24 h or 72 h; compared to TGF-β_1-positive, compound-free controls. **Red** = up-regulated, **Green** = down-regulated.

	24 h				72 h			
	0.01 µg/mL		0.1 µg/mL		0.01 µg/mL		0.1 µg/mL	
≥ 2-fold	96	69	350	278	118	101	251	284
≥ 3-fold	31	12	93	68	33	19	65	94
≥ 5-fold	9	6	26	20	8	2	20	22
≥ 10-fold	0	2	5	4	1	1	3	5

Table 5.2. Number of genes differentially expressed ≥ 2-fold, ≥ 3-fold, ≥ 5-fold and ≥ 10-fold in DFs/myofibroblasts, cultured with EBC-211 at 1 µg/mL or 10 µg/mL, in the presence of TGF-β_1 (10 ng/mL), for 24 h or 72 h; compared to TGF-β_1-positive, compound-free controls. **Red** = up-regulated, **Green** = down-regulated.

	24 h				72 h			
	1 µg/mL		10 µg/mL		1 µg/mL		10 µg/mL	
≥ 2-fold	92	75	328	297	118	102	221	266
≥ 3-fold	33	14	93	79	32	18	53	82
≥ 5-fold	10	6	26	19	12	4	18	22
≥ 10-fold	0	2	6	5	2	1	3	5

fold, ≥ 5-fold and ≥ 10-fold, compared to the respective TGF-β_1-positive, compound-free control at each time-point for EBC-46 and EBC-211, respectively. Fold-changes in gene expression were determined via the use of GeneSpring™ GX11, a statistical tool for Microarray data analyses (Chapter 2.8.4). Tables 5.1 and 5.2 exhibit that the greatest number of genes differentially expressed occurred at higher concentrations of EBC-46 and EBC-211 at both time-points (0.1 µg/mL and 10 µg/mL, respectively). Furthermore, the highest fold-changes (≥ 5-fold and ≥ 10-fold) were generally shown at 24 h, rather than 72 h. Due to the large number of genes identified as differentially expressed by Microarray analyses, the raw data displaying all genes differentially expressed is included for both EBC-46 and EBC-211 within the Supplementary Data (see Memory Stick enclosed).

Genes ≥ 2-fold differentially expressed were allocated into categories, based on their functional roles (Supplementary Data Tables); although many of the genes identified belonged to multiple categories, due to their other known functions. In addition, as displayed in the Supplementary Data Tables, certain genes were present more than once on each BeadChip; with separate probe IDs/Entrez Gene IDs. This resulted in more than one value produced for some differentially expressed genes, compared to the compound-free controls. Consequently, this offered additional validation of the gene expression changes. Categories of differentially expressed genes included myofibroblast formation-related genes, cytoskeletal-related genes, growth factor-related genes, cell signalling-related genes, cell adhesion/migration-related genes, ECM-related genes and proteases/protease inhibitor-related genes (Supplementary Data Tables). Key genes of interest were subsequently validated at the protein level, to determine whether the genotypic differences observed following epoxy-tigliane treatment were reflected at this level and therefore, likely to result in a phenotypic response (Chapters 5.4.2 and 5.4.3).

5.4.2 Validation of Peptidase Inhibitor 16 Gene Expression Changes

Western blot analyses were performed, in order to validate one of the greatest down-regulated genes identified during the Microarray studies: PI16. With regards to gene

expression, PI16 was found to be down-regulated at all concentrations analysed for both EBC-46 and EBC-211 at both 24 h and 72 h; with the greatest down-regulation observed at higher concentrations of both EBC-46 and EBC-211 (0.1 μg/mL and 10 μg/mL, respectively), particularly at 24 h (Proteinases/Proteinase Inhibitor-Related Genes, Supplementary Data Tables). PI16 Western blots are displayed in Figure 5.3A and 5.3B for EBC-46 and EBC-211, respectively; with β-actin used as a loading control for each blot.

The Western blots for PI16 following EBC-46 treatment appeared to indicate similar protein levels, at both 24 h and 72 h, at the 0.001 μg/mL concentration; versus their respective TGF-β_1-positive, compound-free controls (Figure 5.3A). In contrast, at all other EBC-46 concentrations at both time-points, protein levels displayed profound reductions in detectable PI16; in comparison to their respective TGF-β_1-positive, compound-free controls (Figure 5.3A). Post-EBC-211 treatment, the Western blots demonstrated higher PI16 protein levels at lower concentrations (0.001 - 0.01 μg/mL) at both time-points; compared to their respective TGF-β_1-positive, compound-free controls (Figure 5.3B). Furthermore, at 0.1 μg/mL EBC-211, similar protein detection levels were displayed to those shown by the controls, at both time-points (Figure 5.3B). However, at the higher concentrations of EBC-211 (1 - 10 μg/mL), there were profound reductions in detectable PI16 protein levels at both 24 h and 72 h; versus their respective TGF-β_1-positive, compound-free controls (Figure 5.3B). Thus, these findings reflect the differences observed at the gene level, in which PI16 was shown to be significantly down-regulated at 0.01 - 0.1 μg/mL and 1 - 10 μg/mL EBC-46 and EBC-211, respectively; at both 24 and 72 h (Proteinases/Proteinase Inhibitor-Related Genes, Supplementary Data Tables).

5.4.3 Validation of Matrix Metalloproteinase Gene Expression Changes

MMP activity assays were performed for MMP-1, -3, -10 and -12, as these MMPs were identified as being significantly up-regulated by EBC-46 and EBC-211 in DFs/ myofibroblasts, during Microarray studies (Proteinases/Proteinase Inhibitor-Related Genes, Supplementary Data Tables). The findings of MMP-1, -3, -10 and -12 activity

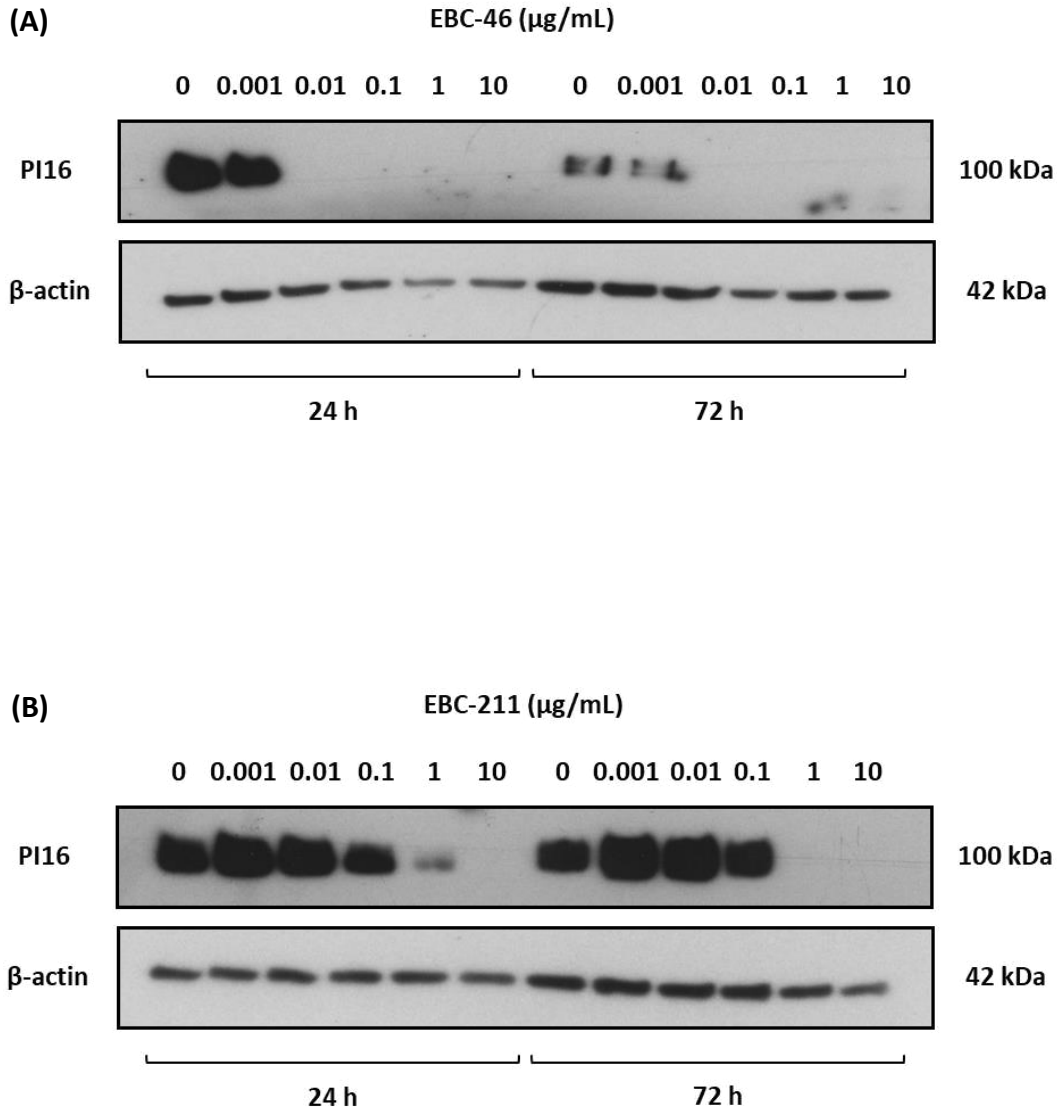

Figure 5.3. Western blot analysis of PI16 protein levels in DFs; cultured with either EBC-46 (A) or EBC-211 (B), at 0.001 µg/mL, 0.01 µg/mL, 0.1 µg/mL, 1 µg/mL and 10 µg/mL, in the presence of TGF-β_1 (10 ng/mL), for 24 and 72 h. TGF-β_1-positive, non-compound controls were also included at each time-point (*n = 3*).

assays are displayed in Figures 5.4, 5.5, 5.6 and 5.7, respectively. Regarding MMP-1 activity, no significant differences were found at lower EBC-46 concentrations (0.001 - 0.01 µg/mL) at both 24 h and 72 h; compared to their respective TGF-β_1-positive, compound-free controls (*p = >0.05*; Figure 5.4A). However, at higher concentrations of EBC-46 (0.1 - 10 µg/mL), MMP-1 activity was found to be significantly increased at both 24 h and 72 h (all *p = <0.001*; Figure 5.4A). In contrast, no significant differences were found at most EBC-211 concentrations (0.001 - 1 µg/mL) at both time-points; compared to their respective TGF-β_1-positive, compound-free controls (*p = >0.05*; Figure 5.4B). At 10 µg/mL of EBC-211, however, MMP-1 activity was exhibited to be significantly increased at both 24 h and 72 h (*p = <0.001*; Figure 5.4B). Such results reflect the differential expression found at the genotypic level, shown through both the Microarray analyses and quantitative polymerase chain reaction (qPCR) studies (Chapter 4). The former exhibited MMP-1 to be up-regulated at all concentrations analysed for both EBC-46 and EBC-211 following 24 h and 72 h treatment; with the greatest up-regulations observed at higher concentrations, particularly at 24 h (0.1 µg/mL and 10 µg/mL, respectively; Proteinases/Proteinase Inhibitor-Related Genes, Supplementary Data Tables). Such changes were also reflected in the qPCR studies, which demonstrated that 0.1 µg/mL and 10 µg/mL EBC-46 and EBC-211, respectively; significantly up-regulated MMP-1 gene expression in DFs, following 72 h treatment (Chapter 4).

Regarding MMP-3 activity, no significant differences were found post-EBC-46 or EBC-211 treatment at any concentrations analysed at 24 h; versus the respective TGF-β_1-positive, compound-free controls (all *p = >0.05*; Figure 5.5A and 5.5B, respectively). This was also found to be the case at 72 h, barring at 0.1 µg/mL and 10 µg/mL EBC-46 and EBC-211, respectively; which demonstrated significant increases in MMP-3 activity, versus the respective TGF-β_1-positive, compound-free controls (*p = <0.01* and *p = <0.001* in Figure 5.5A and 5.5B, respectively). The Microarray studies showed that MMP-3 gene expression was much higher at these concentrations than at 0.01 µg/mL and 1 µg/mL EBC-46 and EBC-211, respectively; particularly at 24 h. This suggested that there may be a delay between up-regulated expression and translation, leading

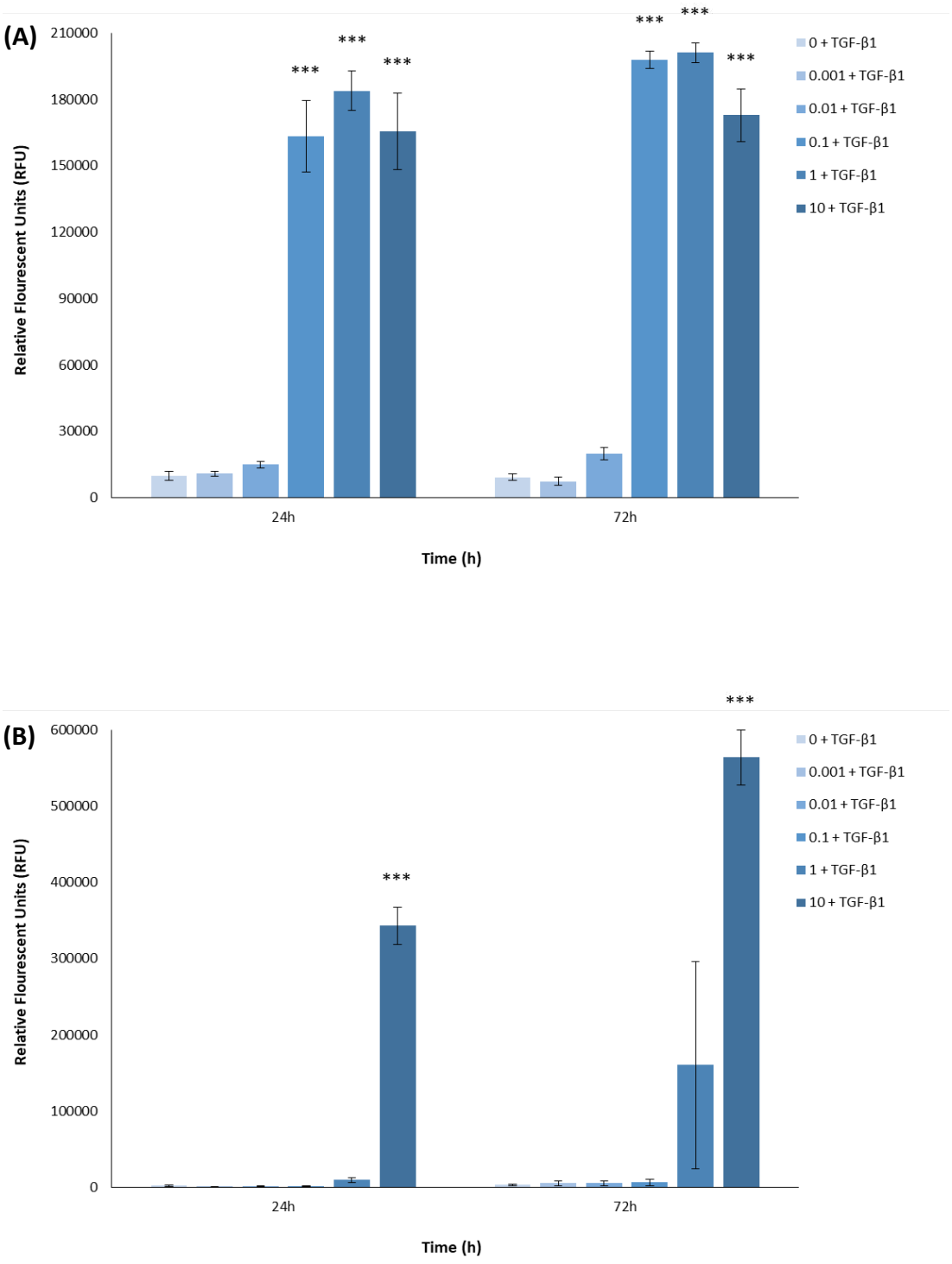

Figure 5.4. MMP-1 activity levels in DFs, cultured with either EBC-46 (A) or EBC-211 (B), at 0.001 µg/mL, 0.01 µg/mL, 0.1 µg/mL, 1 µg/mL and 10 µg/mL, in the presence of TGF-β_1 (10 ng/mL); for 24 and 72 h. TGF-β_1-positive, non-compound controls were also included at each time-point (*n = 3*, mean±SEM; *p = ***<0.001* versus TGF-β_1-positive controls).

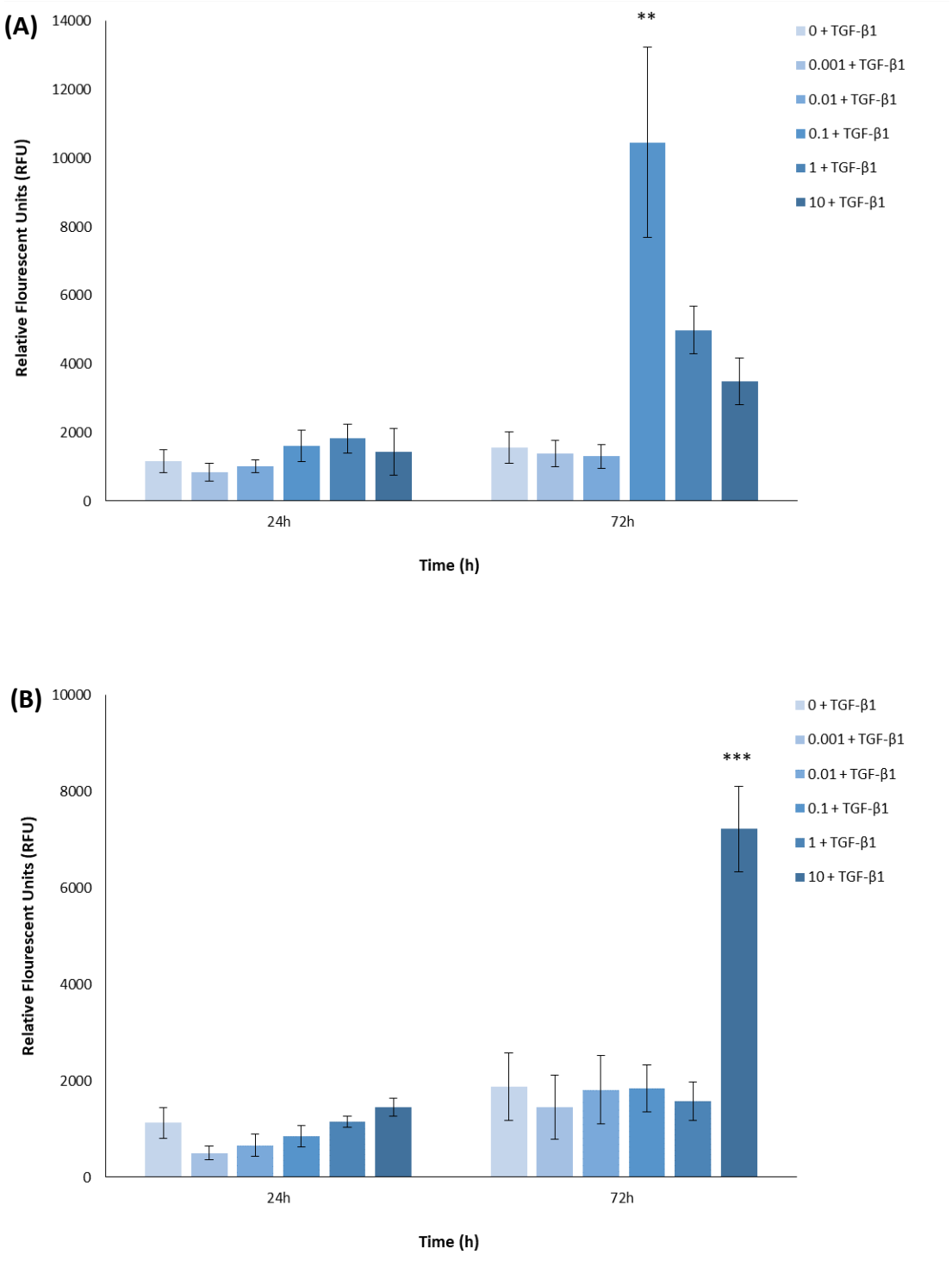

Figure 5.5. MMP-3 activity levels in DFs, cultured with either EBC-46 (A) or EBC-211 (B), at 0.001 µg/mL, 0.01 µg/mL, 0.1 µg/mL, 1 µg/mL and 10 µg/mL, in the presence of TGF-β_1 (10 ng/mL); for 24 and 72 h. TGF-β_1-positive, non-compound controls were also included at each time-point (*n = 3*, mean±SEM; *p = **<0.01, ***<0.001* versus TGF-β_1-positive controls).

to increased MMP3 activity.

MMP-10 gene expression was only shown to be increased at 0.1 µg/mL and 10 µg/mL EBC-46 and EBC-211, respectively, at 24 h (Proteinases/Proteinase Inhibitor-Related Genes, Supplementary Data Tables). Increases in MMP-10 activity were exhibited after 0.1 - 10 µg/mL EBC-46 treatment at both 24 h and 72 h; versus their respective TGF-β_1-positive, compound-free controls (Figure 5.6A). However, only increases at 1 µg/mL and 10 µg/mL were deemed statistically significant at 24 h (both *p = <0.01*); whereas, the elevations at 0.1 and 1 µg/mL were deemed statistically significant at 72 h (*p = <0.001* and *p = <0.05*, respectively; Figure 5.6A). In contrast, no significant differences in MMP-10 activity were shown at most EBC-211 concentrations (0.001 - 1 µg/mL), at both 24 h and 72 h; versus their respective TGF-β_1-positive, compound-free controls (*p = >0.05*; Figure 5.6B). At 10 µg/mL of EBC-211, however, MMP-10 activity was demonstrated to be significantly increased, post-24 h and 72 h treatment (*p = <0.01* and *p = <0.001*, respectively; Figure 5.6B). With greater gene expression demonstrated at 24 h, but higher activity at 72 h, this again suggests that there may be a delay between up-regulated expression and translation into increased MMP-10 activity.

MMP-12 gene expression was only observed to be up-regulated at 0.1 and 10 µg/mL EBC-46 and EBC-211, respectively; at 24 h (Proteinases/Proteinase Inhibitor-Related Genes, Supplementary Data Tables). Following the aforementioned trend of delayed increases in activity, no significant differences were observed at any EBC-46 or EBC-211 concentrations analysed, at 24 h; compared to their respective TGF-β_1-positive, compound-free controls (all *p = >0.05*; Figure 5.7A and 5.7B, respectively). This was also the case at 72 h, except at 0.1 µg/mL and 10 µg/mL of EBC-46 and EBC-211, respectively; which exhibited significant increases in MMP-12 activity, compared to their respective TGF-β_1-positive, compound-free controls (*p = <0.05* and *p = <0.01* in Figure 5.7A and 5.7B, respectively).

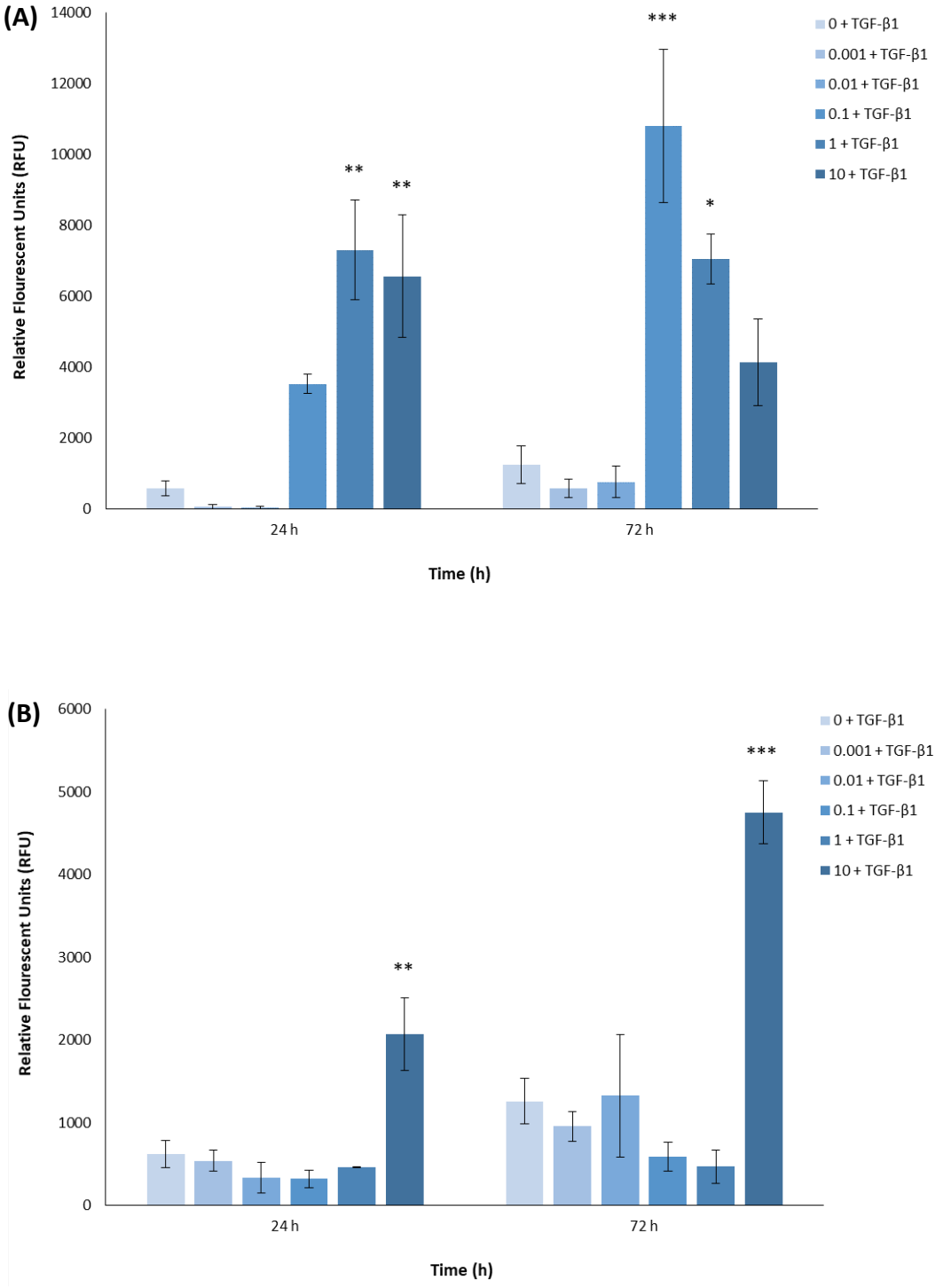

Figure 5.6. MMP-10 activity levels in DFs, cultured with either EBC-46 (A) or EBC-211 (B), at 0.001 µg/mL, 0.01 µg/mL, 0.1 µg/mL, 1 µg/mL and 10 µg/mL, in the presence of TGF-β_1 (10 ng/mL); for 24 and 72 h. TGF-β_1-positive, non-compound controls were also included at each time-point (*n = 3*, mean±SEM; *p = *<0.05, **<0.01, ***<0.001,* versus TGF-β_1-positive controls).

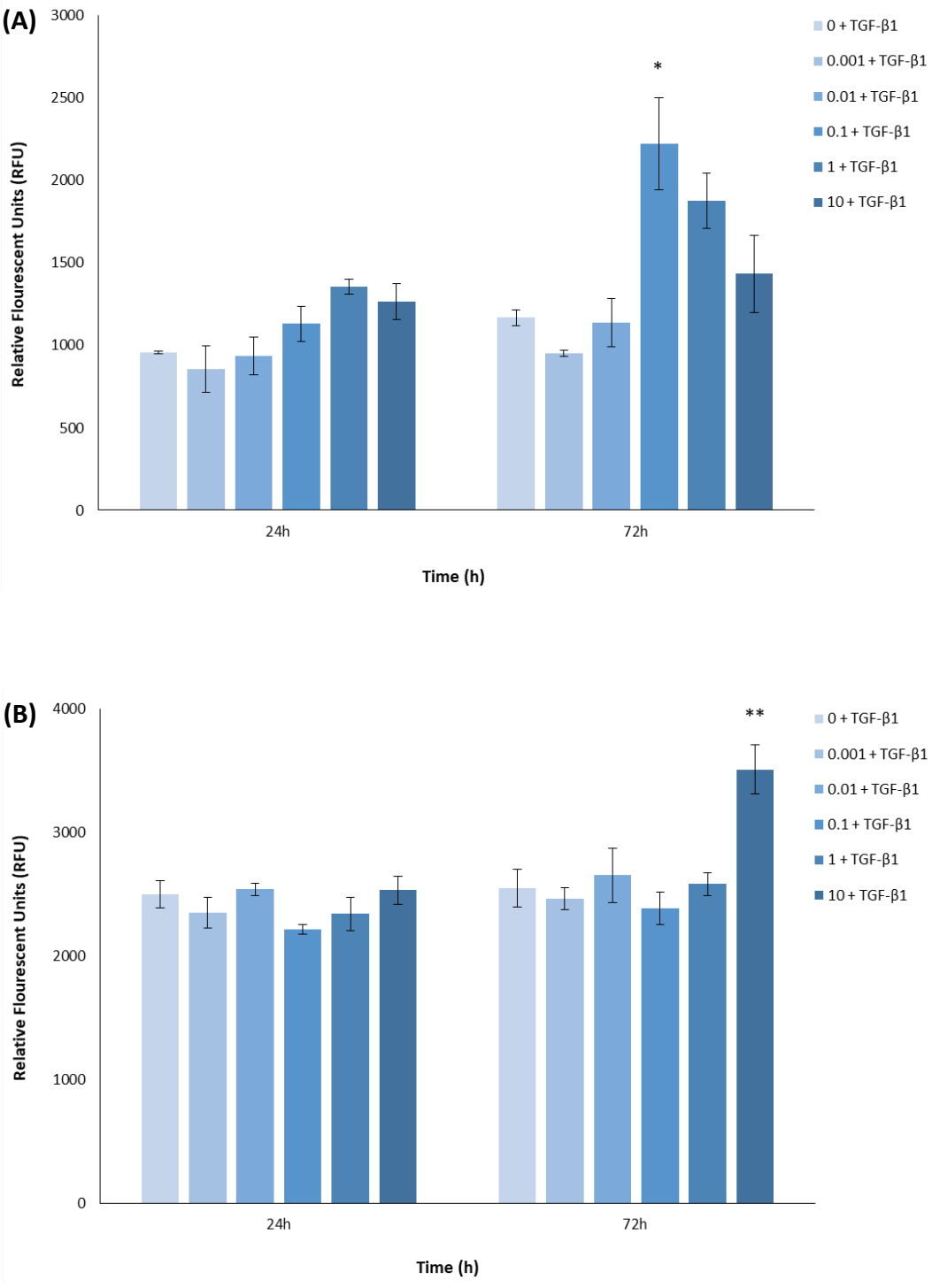

Figure 5.7. MMP-12 activity levels in DFs, cultured with either EBC-46 (A) or EBC-211 (B), at 0.001 µg/mL, 0.01 µg/mL, 0.1 µg/mL, 1 µg/mL and 10 µg/mL, in the presence of TGF-β_1 (10 ng/mL); for 24 and 72 h. TGF-β_1-positive, non-compound controls were also included at each time-point (*n = 3*, mean±SEM; *p = *<0.05*, ***<0.01* versus TGF-β_1-positive controls).

5.5 Discussion

The present Chapter focused on analysing the global gene expression profiles of DFs /myofibroblasts post treatment with EBC-46 and EBC-211 at 24 h and 72 h; compared to TGF-β_1-positive, compound-free controls. Microarray studies performed aimed to distinguish differentially expressed genes and subsequently identify which genes contribute to the beneficial DF wound healing responses observed; during *in vitro* studies (Chapters 3 and 4) and during *in vivo* studies performed by QBiotics Group. As discussed previously (Chapter 5.1), there are a number of differentially expressed genes involved in mediating preferential (ie. oral mucosal repair and early-gestational healing) or detrimental (i.e. hypertrophic and keloid scars), wound healing responses (Sayah *et al*. 1999; Colwell *et al*. 2008; Seifert *et al*. 2008; Chen *et al*. 2010; Hahn *et al*. 2013; Turabelidze *et al*. 2014; Huang *et al*. 2015; Tan *et al*. 2015). As such, these studies were undertaken in order to identify any potential gene expression changes induced by EBC-46 and EBC-211, related to the preferential DF responses and scarless healing overall. It was envisaged that undertaking such studies may provide further information regarding the underlying mechanisms of the responses observed after EBC-46 and EBC-211 treatment (Chapters 3 and 4), including the inhibition of DF-myofibroblast differentiation and the preferential modulation of ECM constituents at specific concentrations. Furthermore, global gene analysis allowed any genes of interest to be investigated further by protein-based validation (Chapters 5.4.2 and 5.4.3).

Evident in Tables 5.1 and 5.2, there were a plethora of genes differentially expressed following EBC-46 and EBC-211 treatment, across all concentrations and time-points. As aforementioned (Chapter 5.4.1), at both 24 h and 72 h, greater differences in the numbers of differentially expressed genes were induced between the epoxy-tigliane concentrations, than those observed between the two analogues themselves; which possess similar gene expression profiles overall. Furthermore, there were a greater number of genes differentially expressed at the higher concentrations of EBC-46 and EBC-211 (0.1 μg/mL and 10 μg/mL, respectively), at both time-points. In addition, the highest fold-changes (≥ 5-fold and ≥ 10-fold) were generally found at 24 h, rather

than 72 h. Moreover, there were a higher number of fold-changes in gene expression following 24 h treatment for both epoxy-tiglianes, versus the 72 h time-point. Overall, these results lend support to findings of the previous Chapters, which demonstrated significant differences between epoxy-tigliane concentrations; yet highlighted similar responses despite 100-fold differences in EBC-46 and EBC-211 concentrations (0.1 µg/mL and 10 µg/mL, respectively). Thus, it appears that the epoxy-tiglianes induce biphasic, concentration-dependent effects upon cellular behaviour and activities; hypothesised as being a consequence of the contrasting activation, distribution and localisation of protein kinase C (PKC) isoforms (Boyle *et al*. 2014).

Due to the large number of genes analysed only, those differentially expressed ≥ 2-fold were further categorised based upon their function in the wound repair process and analysed accordingly (Supplementary Data Tables). Therefore, each gene has been allocated into one category only, for the purpose of succinctly displaying the findings from this study. Additionally, genes and categories discussed herein do not represent an exhaustive list, but focus on those of particular interest with regards to fibroblasts, excessive dermal fibrosis and/or scarless healing situations.

5.5.1 Myofibroblast Formation-Related Genes

In the Myofibroblast Formation-Related Gene category, 19 genes (6 up-regulated, 13 down-regulated), were differentially expressed between epoxy-tigliane-treated DFs and the TGF-β_1-positive, compound-free controls. All the genes were differentially expressed between 2 - 7.6-fold; the up-regulated genes of particular interest include chromosome 5, open reading frame 13 (C5ORF13), TRAF3 interacting protein 2, transcript variant 2 (TRAF3IP2), sphingosine kinase 1, transcript variant 1 (SPHK1) and S100 calcium binding protein A4, transcript variant 2 (S100A4). Of these four genes, only SPHK1 was shown to be up-regulated at every EBC-46 concentration and at both time-points (2.1 - 3.1-fold); whereas for EBC-211, this was only the case for TRAF3IP2 (2.3 - 3.2-fold). Generally, the highest up-regulations were found at 0.1 µg/mL and 10 µg/mL of EBC-46 and EBC-211, respectively. Interestingly, within Chapter 3, these concentrations were shown to inhibit DF-myofibroblast differentiation. However,

these appear to increase the expression of certain genes reported to be involved in promoting myofibroblastic differentiation. C5ORF13 (or P311) expression has been shown to be associated with an induction of the myofibroblast phenotype, albeit with reduced TGF-β_1 and -β_2 expression, as well as the inhibition of TGF-β receptor$_2$ (TGF-βR_2) and MMP-2/MMP-9 activities; resulting in decreased type I and type III collagen expression (Pan *et al*. 2002; Paliwal *et al*. 2004). In addition, C5ORF13 binds to the TGF-β_1 latency associated protein (LAP), resulting in the formation of TGF-β_1-independent, non-fibrogenic myofibroblasts. P311-induced myofibroblasts have also been demonstrated to migrate in an ameboid, rather than mesenchymal, pattern; characterised by a lack of focal adhesions (FAs) and stress fibres, absence of integrins, and MMP activation, resulting in increased cell motility. Thus, C5ORF13 is thought to promote a phenotype adapted to rapidly populate the initial wound matrix (Pan *et al*. 2002; Paliwal *et al*. 2004; Shi *et al*. 2006). In contrast, C5ORF13 has also been identified to be up-regulated in both keloid and hypertrophic fibroblasts; with normal DFs, transfected with C5ORF13 (P311), expressing increased α-smooth muscle actin (αSMA), TGF-β_1 and type I collagen expression (Naitoh *et al*. 2005; Tan *et al*. 2010; Cheng *et al*. 2017).

Increased TRAF3IP2 expression has been shown to induce the expression of multiple pro-fibrotic and pro-inflammatory mediators, inducing fibrosis in murine hearts. Silencing TRAF3IP2 resulted in the inhibition of MMP and tissue inhibitor of MMP-1 (TIMP-1) activation, inflammatory cytokine expression, collagen synthesis/deposition and the proliferation/migration of cardiac fibroblasts. As such, TRAF3IP2 is believed to play causal roles in chronic inflammatory and fibro-proliferative diseases (Valente *et al*. 2013; Somanna *et al*. 2015; Yariswamy *et al*. 2016; Das *et al*. 2018). Regarding SPHK1, it is known to catalyse sphingosine-1-phosphate phosphorylation; involved in the regulation of cellular proliferation, migration, adhesion, survival and cytoskeletal architecture (Alemany *et al*. 2007). In addition, SPHK1 up-regulation has been found to promote fibrosis-related processes, including TGF-β_1 signalling, DF-myofibroblast differentiation, TIMP-1 expression and collagen production (Yamanaka *et al*. 2004; Kono *et al*. 2007; Gellings Lowes *et al*. 2009; Albinet *et al*. 2014). Lastly, S100A4 was

shown to be increased at 0.1 µg/mL and 10 µg/mL EBC-46 and EBC-211, respectively; at both time-points. S100A4 has been demonstrated as dramatically elevated in various fibrotic diseases, modulating cardiac fibrosis through cell proliferation and collagen expression and amplifying TGF-β-induced fibroblast activation in systemic sclerosis (Tamaki *et al*. 2013; Tomcik *et al*. 2015). However, this protein has also been shown to enhance angiogenesis, cell survival and motility; the latter seemingly mediated by changes to the cellular organisation of actin (Goh Then Sin *et al*. 2011).

Of the down-regulated genes, those of particular interest include Krüppel-like factor 4 (KLF4), cyclin-dependent kinase inhibitor 2B (CDKN2B), GLI pathogenesis-related 2 (GLIPR2), cysteine-rich, angiogenic inducer 61 (CYR61), integrin α_{11} (ITGA11), growth arrest-specific 6 (GAS6), maternally expressed 3 (MEG3), tribbles homolog 3 (TRIB3) and glutaminase (GLS). As demonstrated with the up-regulated genes, the greatest down-regulations were exhibited at 0.1 µg/mL and 10 µg/mL of EBC-46 and EBC-211, respectively. In comparison to the number of up-regulated myofibroblast formation-related genes, double the number were found to be down-regulated. KLF4 has been found to play a crucial role in angiotensin II-induced cardiac fibroblast-myofibroblast differentiation and ECM synthesis through the transcriptional up-regulation of TGF-β_1. Elevated KLF4 expression was exhibited to increase αSMA and type I/III collagen expression; acting as a promoter of fibroblast-myofibroblast differentiation. As such, KLF4 down-regulation may represent a novel therapy in the prevention/treatment of cardiac fibrosis (Zhang *et al*. 2014). KLF4 knockout has also been seen to significantly reduce pulmonary metastasis, which was accompanied by decreased populations of fibrocytes, fibroblasts and myofibroblasts in the lung (Shi *et al*. 2014). Furthermore, following a loss of KLF4 expression, αSMA, fibronectin (FN) and type I collagen gene expression levels have been found to be decreased in foetal and neonatal lung; specifically in lung myofibroblasts (Jean *et al*. 2013). Similarly to KLF4, CDKN2B was down-regulated across most conditions analysed. However, loss of CDKN2B has been shown to promote fibroblast-myofibroblast differentiation in idiopathic pulmonary fibrosis (Scruggs *et al*. 2018). As demonstrated post-24 h treatment with both epoxy-tiglianes, GLIPR2 down-regulation is likely beneficial as it has been found to be up-

regulated in kidney fibrosis. In GLIPR2-transfected cells, extracellular signal-regulated kinases 1 and 2 (ERK1/2) activation was increased, leading to elevated αSMA gene expression (Huang *et al*. 2013b). CYR61, GLS and ITGA11 were found to be down-regulated at 0.1 μg/mL and 10 μg/mL EBC-46 and EBC-211, respectively; at both time-points. CYR61 appears to up-regulate the expression of numerous genes in DFs, which are involved in inflammation, angiogenesis and ECM remodelling; and is highly induced in granulation tissue DFs during cutaneous wound repair (Chen *et al*. 2001). Regarding GLS, silencing its expression has been found to abrogate TGF-β_1-induced expression of pro-fibrotic markers (Bernard *et al*. 2018). ITGA11, which was the most highly down-regulated gene in this category, has been exhibited to co-localise with αSMA-positive myofibroblasts and its expression is correlated with fibrogenesis in human fibrotic organs. Knockdown of ITGA11 in liver myofibroblasts reduced TGF-β-induced differentiation and altered the myofibroblast phenotype; indicated by the loss of protrusions, impaired contractility of type I collagen matrices and attenuated adhesion/migration (Bansal *et al*. 2017). GAS6 was also found to be strongly induced in rat liver myofibroblasts; while GAS6-deficient mice showed reduced inflammation and myofibroblast activation, in addition to decreased expression of TGF-β and type I gene expression (Lafdil *et al*. 2006; Fourcot *et al*. 2011). Lastly, the down-regulation of TRIB3 and MEG3 appear favourable as silencing the former has been exhibited to attenuate renal fibrosis in rodents, accompanied by decreased ERK phosphorylation (Ding *et al*. 2014). TRIB3 knockdown has also been shown to reduce the pro-fibrotic effects of TGF-β and decrease collagen synthesis. In contrast, TRIB3 over-expression has been demonstrated to stimulate canonical TGF-β signalling and induce activated phenotypes in resting fibroblasts (Tomcik *et al*. 2016). MEG3 has been shown to be up-regulated in idiopathic pulmonary fibrosis; whereas its inhibition *in vivo* resulted in the prevention of MMP-2 induction, leading to reduced cardiac fibrosis (Piccoli *et al*. 2017; Gokey *et al*. 2018).

In summary, although certain genes relating to myofibroblast formation were found to be up-regulated (including C5ORF13, TRAF3IP2, SPHK1 and S100A4), over double the number of genes were down-regulated (including KLF4, CDKN2B, GLIPR2, CYR61,

ITGA11, GAS6, MEG3, TRIB3 and GLS). Thus, these findings corroborate those of the previous Chapters; demonstrating that the epoxy-tiglianes collectively suppress DF genes associated with myofibroblast formation. Indeed, as the greatest expression changes occur at 0.1 μg/mL and 10 μg/mL EBC-46 and EBC-211, respectively; these are likely to contribute to the lack of myofibroblast formation observed at these concentrations (Chapter 1); and the minimal scarring responses observed *in vivo*.

5.5.2 Growth Factor-Related Genes

In the Growth Factor-Related Gene category, 43 genes and 40 genes (14 up-regulated /29 down-regulated and 12 up-regulated/28 down-regulated for EBC-46 and EBC-211, respectively), were differentially expressed between epoxy-tigliane-treated DFs and the TGF-β_1-positive, non-compound controls. All of the genes were differentially expressed between 2 - 42.4-fold and as found in many other categories, the greatest fold-changes were generally demonstrated at 0.1 μg/mL and 10 μg/mL EBC-46 and EBC-211, respectively. Many of the genes in this category were either TGF-β family members or are associated with TGF-β signalling pathways. The up-regulated genes of particular interest, included bone morphogenetic protein 2 (BMP2), gremlins (GREM1/GREM2) and FK506 binding protein 1A (FKBP1A). Of the four genes, only GREM1 and GREM2 were up-regulated at every EBC-46 concentration and at both time-points (between 2.7 - 7.3-fold). BMP2 and FKBP1A were up-regulated at 0.1 and 10 μg/mL EBC-46 and EBC-211, respectively; at both time-points.

BMPs are members of the TGF-β superfamily, defined as homo- and hetero-dimeric proteins linked by disulphide bonds (Miyazawa *et al*. 2002; Botchkarev and Sharov, 2004). BMP-2, -4, -6, and -7 are all expressed in wound tissue by keratinocytes and DFs; with increased BMP signalling implicated in various fibrotic disorders. Thus, an up-regulation of BMP2 would, theoretically, promote fibrosis (Wankell *et al*. 2001; Russell *et al*. 2010). Indeed, exogenous BMP2 application has been shown to induce scar formation in early-gestational wounds, which normally heal scarlessly (Stelnicki *et al*. 1998). However, simultaneous up-regulation of BMP antagonists, GREM1 and GREM2, would likely exert potent inhibitory actions on various BMPs via binding to

BMPs; thereby preventing ligand-receptor interaction and subsequent downstream signalling (Wordinger *et al*. 2008). As the GREM up-regulations are greater than the BMP2 up-regulation, the balance appears to favour BMP inhibition via GREM activity. GREM1 and GREM2 may also exert effects upon cell function via BMP-independent mechanisms, such as endothelial cell modulation; which subsequently results in the modulation of angiogenesis (Wordinger *et al*. 2008). Also related to BMP regulation, FKBP1A (also called FKBP-12), acts to bind and stabilise the inactive conformations of all TGF-β/BMP type I receptors (Kaplan *et al*. 2009). When bound, FKBP1A prevents the 'promiscuous' or 'leaky' activation of these receptors, in the absence of ligands (Wang *et al*. 1996; Chen *et al*. 1997; Huse *et al*. 1999). Upon ligand stimulation, the FKBP-12 is released in order to fully propagate the signal (Yamaguchi *et al*. 2006). In addition, FKBP1A serves as a docking protein for SMAD complexes, which modulate the internalisation and degradation of all BMP type I receptors (Ebisawa *et al*. 2001; Yamaguchi *et al*. 2006; Kaplan *et al*. 2009). Thus, FKBP1A is thought to regulate the steady state concentration of cell membrane BMP receptors and act as an inhibitor of TGF-β signalling (Kaplan *et al*. 2009).

Of those down-regulated genes, those of particular interest include BMP and activin membrane-bound inhibitor (BAMBI), BMP6, connective tissue growth factor (CTGF), fibroblast growth factor 2 (FGF2), follistatin-like 1 (FSTL1), insulin-like growth factor binding protein 3 (IGFBP3), SMAD6 and TGF-β receptor$_3$ (TGF-βR_3). Of these genes, BAMBI and CTGF were down-regulated specifically at 0.1 μg/mL and 10 μg/mL EBC-46 and EBC-211, respectively; at both time-points. BAMBI has been shown to inhibit TGF-β, BMP and activin signalling; acting as a negative regulator (Onichtchouk *et al*. 1999; Shangguan *et al*. 2012). However, conversely, aberrant elevation of BAMBI has been found to lead to tumorigenic responses; with BAMBI over-expression found in a number of cancers (Sekiya *et al*. 2004; Zhou *et al*. 2013). More favourable is the CTGF down-regulation, which upon TGF-β_1 treatment alone, is found to be increased (Igarashi *et al*. 1993; Frazier *et al*. 1996). CTGF is a potent inducer of ECM synthesis, through its synergistic effects upon TGF-β_1 activity; enhancing receptor binding and inhibiting the TGF-β_1 antagonists, the BMPs (Frazier *et al*. 1996; Abreu *et al*. 2002;

Gressner and Gressner, 2008). Synergism between TGF-β_1 and CTGF is also apparent by CTGF's enhancement of SMAD2 phosphorylation and TGFβ_1-driven expression of pro-fibrotic genes (Abreu *et al*. 2002). Thus, such synergism promotes persistent and heightened TGF-β_1/SMAD signalling, increasing the likelihood of a sustained fibrotic response. Indeed, CTGF is over-expressed in fibrotic lesions (Leask, 2004). It is highly up-regulated in fibroblasts derived from systemic sclerosis, scleroderma, keloid and hypertrophic scars; amongst others (Shi-wen *et al*. 2000; Holmes *et al*. 2001; Leask, 2004; Colwell *et al*. 2005; Smith *et al*. 2008). Knockdown of CTGF has been shown to attenuate experimental liver fibrosis; whilst anti-fibrotic agents, such as pirfenidine, partly act via the suppression of CTGF expression (Hewitson *et al*. 2001; Gressner and Gressner, 2008). Thus, CTGF down-regulation by epoxy-tiglianes is highly desirable.

BMP6, IGFBP3 and TGF-βR_3 were all down-regulated at all concentrations and time-points, for both epoxy-tiglianes; with the greatest down-regulations observed at 0.1 and 10 µg/mL EBC-46 and EBC-211, respectively. Interestingly, BMP6 deficiency has been shown to aggravate renal fibrosis through a lack of inhibition of inflammatory genes (Dendooven *et al*. 2011). Conversely, enhanced expression appears to inhibit hepatic fibrosis via inhibition of hepatic stellate cell activation and reduction of pro-inflammatory and pro-fibrogenic gene expression in those already activated (Arndt *et al*. 2014). Regarding IGFBP3, the greatest down-regulations in the category were demonstrated following 72 h treatment with 0.1 µg/mL and 10 µg/mL of EBC-46 and EBC-211, respectively. IGFBP3 has been exhibited to be essential to TGF-β_1-driven differentiation and although not sufficient to stimulate differentiation alone. IGFBP3 synergistically potentiated TGF-β_1-driven stromal remodelling by human prostatic cells (Sampson *et al*. 2013). Moreover, hypertrophic scar-derived fibroblasts have also been shown to express more IGFBP3 than normal DFs (Hathaway *et al*. 1996). Although they do not play direct roles in TGF-β signalling, type III TGF-β receptors (known as betaglycans), are believed to facilitate binding of TGF-β to type II receptors (López-Casillas *et al*. 1993; Webber *et al*. 2010). Certain cancer-derived exosomes have been shown to trigger fibroblast-myofibroblast differentiation, due to their expression of betaglycan. Exosomes expressing low betaglycan levels have low TGF-

β levels and do not induce differentiation; whereas those with higher surface levels possess sufficient levels of TGF-β to drive differentiation. Furthermore, the loss of exosomal betaglycan expression has been shown to decrease exosomal TGF-β levels and attenuate their capacities to stimulate fibroblast-myofibroblast differentiation (Webber *et al*. 2010, 2015). Thus, down-regulation of betaglycan may contribute to the inhibition of DF-myofibroblast differentiation found at 0.1 μg/mL and 10 μg/mL EBC-46 and EBC-211, respectively (Chapter 3).

FGF2, FSTL1 and SMAD6 were all down-regulated at 0.1 μg/mL and 10 μg/mL EBC-46 and EBC-211, respectively, at both time-points; as well as at 0.01 μg/mL and 1 μg/mL EBC-46 and EBC-211, respectively, following 72 h treatment. FGF2 is up-regulated in the acute wound and plays roles in the formation of granulation tissue, keratinocyte re-epithelialisation and ECM remodelling (Powers *et al*. 2000). Interestingly, previous studies have demonstrated the ability of exogenously administered FGF2 to act as a cutaneous anti-fibrotic agent (Carroll *et al*. 2002; Ono *et al*. 2007; Nunes *et al*. 2016). FGF2 has been found to inhibit DF-myofibroblast differentiation; resulting in greater numbers of rapidly proliferating, spindle-shaped cells (Dolivo *et al*. 2017). Therefore, this suggests that epoxy-tiglianes mediate their inhibition of differentiation by FGF2-independent means. Conversely, FSTL1 down-regulation is a favourable response, as it is a pro-fibrotic glycoprotein found to be up-regulated in fibrotic lung tissue. It has been demonstrated to promote fibrogenesis by facilitating TGF-β_1/SMAD signalling; whereas FSTL1 haplodeletion has been found to attenuate pulmonary fibrosis (Dong *et al*. 2015; Zheng *et al*. 2017; Chen *et al*. 2018; Jin *et al*. 2018). Moreover, knockdown of FSTL1 attenuated hepatic stellate cell activation through suppression of the TGF-β_1/ SMAD3 signalling pathway; reducing the levels of αSMA and type I collagen in the TGF β_1 treated cells (Shang *et al*. 2017). In contrast, the reduced SMAD6 expression appears unfavourable as keloid-derived fibroblasts demonstrate reduced expression (Yu *et al*. 2006). However, overall, the epoxy-tigliane-induced responses described in this section indicate the down-regulation of TGF-β/BMP receptor binding and growth factors relating to the downstream activation of SMAD-dependent or -independent pathways. Such findings complement those of prior Chapters, as if the TGF-β_1/BMP

signalling pathways are suppressed, DF-myofibroblast differentiation is halted. This suggests that the underlying mechanism of action of the minimal scarring responses observed in epoxy-tigliane treated skin is, at least partly, mediated by alterations to the canonical TGF-β and BMP signalling pathways.

5.5.3 Cell Signalling-Related Genes

In the Cell Signalling-Related Gene category, 83 and 90 genes (37 up-regulated/46 down-regulated and 37 up-regulated/53 down-regulated with EBC-46 and EBC-211, respectively), were differentially expressed between epoxy-tigliane-treated DFs and the TGF-β_1-positive, non-compound controls. All genes were differentially expressed between 2 - 9.3-fold and as found in many of the other categories, the greatest fold-changes were found at 0.1 μg/mL and 10 μg/mL EBC-46 and EBC-211, respectively. Regarding the signalling mechanisms underlying DF-myofibroblast differentiation, as detailed previously (Chapter 1), TGF-β_1 is considered the most potent stimulator. It is well-established that TGF-β_1 modulates DF-myofibroblast differentiation through two co-operating pathways: the SMAD and HA-mediated CD44/EGFR pathways; both of which are required for differentiation to take place (Schiller *et al*. 2004; Simpson *et al*. 2010; Meran *et al*. 2011). TGF-β_1 has also been shown to mediate such effects via the activation of Rho GTPases/Rho-associated kinases (ROCK) and mitogen activated protein kinase (MAPK) signalling pathways (p38, ERK and c-Jun N-terminal kinases; JNK; Moustakas and Heldin, 2005; Kardassis *et al*. 2009). Many of the genes differentially expressed within this category are Ras superfamily members, as well as Rac and Rho GTPase sub-family members.

Members of the Rho GTPase family are vital to the regulation of signal transduction cascades from extracellular stimuli to the cell's nucleus and cytoskeleton. They have crucial roles in the regulation of intracellular actin dynamics, including actin filament organisation; thus influencing cellular migration and differentiation (Ren *et al*. 1998; Aspenström *et al*. 2004). Rho GTPase activating protein 22 (ARHGAP22) is increased following epoxy-tigliane treatment at both time-points, at 0.1 μg/mL and 10 μg/mL EBC-46 and EBC-211, respectively. ARHGAP22 has been shown to be a key mediator,

which suppresses Ras-related C3 botulinum toxin substrate 1 (RAC1), downstream of Ras homolog gene family, members A (RHOA); and is involved in the amoeboid movement of melanoma cells (Croft and Olsen, 2008; Sanz-Moreno *et al*. 2008). Additionally, ARHGAP22 has been shown to regulate the actin cytoskeleton and cell morphology through Rac inactivation. Forced ARHGAP22 expression blocked cellular spreading and lamellae formation, whereas knockdown stimulated cell spreading (Mori *et al*. 2014). Also up-regulated at the same conditions, RAC2 encodes a GTPase capable of regulating the formation of actin filaments and lamellipodia, related to cell growth, cytoskeletal reorganisation and protein kinase activation (Aspenström *et al*. 2004). Additional up-regulated genes of interest include the essential components of the MAPK pathway, MAP4K2 and MAPK13. Both were up-regulated following 24 h treatment, at 0.1 µg/mL and 10 µg/mL EBC-46 and EBC-211, respectively. MAPKs are involved in directing cellular responses to an array of stimuli, including pro-inflammatory cytokines (Pearson *et al*. 2001). Galanin propeptide (GAL) was also up-regulated at the above-mentioned time and concentrations; and is found to be up-regulated during dermal wound repair, possessing roles in inflammation and cellular proliferation (Bauer *et al*. 2010).

Of the down-regulated genes, those of particular interest include Rho/Rac guanine nucleotide exchange factor (GEF) 2 (ARHGEF2), RHOB and Rho-related BTB domain containing 3 (RHOBTB). Rho proteins cycle between inactive, guanosine diphosphate (GDP)-bound states and active, guanosine triphosphate (GTP)-bound states. The Rho activation is modulated by GEFs, which promote GDP to GTP exchange (Arthur *et al*. 2002). ARHGEF2, which activates RHOA, is attached to the microtubule network and sequestered in an inhibited state. ARHGEF2 phosphorylation and RHOA activation is required for formation of stress fibres and FAs, as well as organised cell architecture in 3D-culture (Sandi *et al*. 2017). ARHGEF2 down-regulation and lack of differentially expressed RHOA may contribute to the inhibition of DF-myofibroblast differentiation at 0.1 and 10 µg/mL EBC-46 and EBC-211, respectively. RHOBTB gene expression was also down-regulated at these concentrations after 72 h treatment, whereas RHOB's greatest down-regulation were observed at 0.1 µg/mL and 10 µg/mL EBC-46 and EBC-

211, respectively. RHOA/B-dependent signalling regulates TGF-β-stimulated actin expression, reorganisation and myofibroblast formation; with RHOB mediating the regulation of long-term actin remodelling via SMAD2/SMAD3 (Vardouli *et al*. 2008). Lastly, a number of genes from the G protein-coupled receptor (GPCR) family were contrastingly expressed during the Microarray studies. GPER and GPR1 were down-regulated, while GPR177 and GPR68 were increased. GPR177 is a Wnt transcriptional target, activated to assist sub-cellular Wnt distribution in a feedback regulatory loop. GPR177 has been demonstrated to be expressed during embryonic development and embryos with deficient GPR177 exhibit defects in establishment of body axis (Fu *et al*. 2009; Yu *et al*. 2010). GPR177 is also expressed in a variety of tissues and cell types during organogenesis; thus, it may contribute to the regenerative phenotype of the epoxy-tigliane treated skin *in vivo* (Yu *et al*. 2010).

In summary, as found with the previous categories, there were a greater number of down-regulated genes following epoxy-tigliane treatment, than those up-regulated. Those highlighted indicate that the Rho signalling pathway may be suppressed. This would affect the regulation of actin dynamics, including αSMA expression and fibre organisation. Ultimately, this would affect the DF/myofibroblast cytoskeleton and, in combination with the down-regulations in myofibroblast formation-related genes, may contribute to the inhibition of myofibroblast development observed at certain epoxy-tigliane concentrations.

5.5.4 Cytoskeleton-Related Genes

Within the Cytoskeleton-Related Gene category, 66 and 65 genes (38 up-regulated/30 down-regulated and 35 up-regulated/32 down-regulated for EBC-46 and EBC-211, respectively), were differentially expressed between epoxy-tigliane-treated DFs and the TGF-β_1-positive, compound-free controls. All genes were differentially expressed between 2 - 9.7-fold and as found in many of the other categories, the greatest fold-changes were generally demonstrated at 0.1 μg/mL and 10 μg/mL EBC-46 and EBC-211, respectively. Many genes differentially expressed in this category are related to actin-based cytoskeletal organisation/assembly and were shown to be contrastingly

up- or down-regulated based on epoxy-tigliane concentration; supporting the other concentration-dependent effects demonstrated throughout the Chapters. Actins, in particular, αSMA, are major components of the DF/myofibroblast cytoskeleton and contractile apparatus; involved in both cellular motility and ECM contraction (Hinz *et al*. 2001a; Pellegrin and Mellor, 2007; Sandbo and Dulin, 2011). Whilst the α isoform is transiently expressed during wound healing, the β and γ isoforms are constituents of both the DF and myofibroblast cytoskeleton; all acting to define morphology and drive cellular function (Sappino *et al*. 1990; Sandbo and Dulin, 2011). Indeed, the up-regulation of actin isoform gene expression is a characteristic of fibrotic skin, as well as keloid fibroblasts (Vozenin *et al*. 1998; Satish *et al*. 2006). Early-gestational foetal wounds, in contrast, show down-regulated actin-related gene expression and do not possess myofibroblasts (Estes *et al*. 1994; Cowin *et al*. 2003; Kathju *et al*. 2006). Oral mucosal fibroblasts are resistant to TGF-β_1-driven differentiation also, unlike normal DFs (Meran *et al*. 2007, 2008; Dally *et al*. 2017). Thus, alterations in actin-associated gene and protein expression in pathological and preferential scenarios suggests that modulation of the DF/myofibroblast cytoskeleton is a critical determinant of healing outcome.

Following the Microarray studies, actin α (ACTC1) and actin α_2 (ACTA2) were shown to be decreased by certain epoxy-tigliane concentrations. Corroborating the findings of Chapter 1, the gene encoding αSMA (ACTA2) was down-regulated at both 0.1 µg/mL and 10 µg/mL EBC-46 and EBC-211, respectively. However, unlike the results of the qPCR studies, this was only found to be the case following 24 h treatment; rather than at both time-points. This discrepancy is likely due to the high-throughput nature of the Microarray; whereas the probes utilised in the qPCR studies are more sensitive. With regards to ACTC1, similar down-regulations in gene expression were observed at the same concentrations as ACTA2; but also following 72 h treatment. In contrast, ACTC1 expression was up-regulated at 0.01 µg/mL and 1 µg/mL EBC-46 and EBC-211, respectively; at both time-points. No difference or up-regulated expression of these actin-related genes at the lower epoxy-tigliane concentrations analysed, compared to TGF-β_1-positive compound-free controls, corroborates the findings of

previous Chapters; as these concentrations generally exhibited either no change or synergistic effects with TGF-β_1. Conversely, 0.1 µg/mL and 10 µg/mL of EBC-46 and EBC-211, respectively, exhibited more 'anti-fibrotic' responses which are reflected in their down-regulation of ACTC1 and ACTA2. The latter responses are more analogous to those demonstrated during scarless healing scenarios (Estes *et al*. 1994; Kathju *et al*. 2006).

The higher concentrations of EBC-46 and EBC-211 were also found to down-regulate ectodermal-neural cortex (ENC1), LIM domain and actin binding 1 (LIMA1), solute carrier family 3, member 2 (SLC3A2) and tropomyosin α_1 (TPM1) genes, at both time-points. ENC1 encodes an actin-binding protein, which plays a role in reorganisation of the cytoskeleton during cellular differentiation (Kim *et al*. 2009). LIMA1, or EPLIN, expression has been found to increase the number and size of actin stress fibres and inhibits membrane ruffling. Moreover, EPLIN binds to actin monomers and filaments, bundling them and inhibiting actin filament depolymerisation. Thus, EPLIN is thought to promote the formation of stable actin structures and thus, down-regulated EPLIN expression may contribute to cell motility (Maul and Chang, 1999; Maul *et al*. 2003). TPM1 is also an actin-binding protein, required to provide stability to actin filaments (Lin *et al*. 2008). TPM1 over-expression has been identified in keloid fibroblasts; and in contrast, knockdown studies have demonstrated that fibroblasts lacking specific tropomyosin isoforms fail to stably incorporate αSMA into stress fibres upon TGF-β_1 treatment (Satish *et al*. 2006; Prunotto *et al*. 2015). Finally, SLC3A2 is a membrane protein found to be involved in exertion of force on the ECM, through its interaction with integrins; resulting in RhoA-driven contractility (Féral *et al*. 2007).

Other genes down-regulated at the higher concentrations of EBC-46 and EBC-211, albeit only following 24 h treatment, were caldesmon 1 (CALD1), microtubule-actin crosslinking factor 1 (MACF1) and the tubulin sub-units, tubulin β_2A (TUBB2A) and β_2B (TUBB2B). Caldesmon binds/stabilises actin filaments and regulates actomyosin interactions, as well as stimulating actin binding of tropomyosin; which was also down-regulated at these concentrations (Mayanagi and Sobue, 2011). MACF1 is also

a filamentous actin (F-actin) binding protein, which acts to cross-link F-actin to other cytoskeletal proteins. MACF1-deficiency compromises the targeting of microtubules along F-actin to FAs (Ning *et al*. 2016; Miao *et al*. 2017). Down-regulation of tubulin sub-units by the epoxy-tiglianes was also significant, given their key roles in bundling and binding of microtubules (Ludueňa, 1998). Indeed, over-expression of tubulin has been identified in keloid fibroblasts (Satish *et al*. 2006). Other genes down-regulated by the epoxy-tiglianes include actin filament associated protein 1 (AFAP1), filamin B (FLNB), filamin C (FLNC) and EH domain binding protein 1 (EHBP1). AFAP1 represents an Src binding partner, thought to be a mediator of actin filament integrity. Previous reports have demonstrated that it is capable of binding and altering actin filaments (Qian *et al*. 2000; Baisden *et al*. 2001). EHBP1 links clathrin-mediated endocytosis to the actin cytoskeleton and its high expression has been shown to mediate extensive actin reorganisation (Guilherme *et al*. 2004). Finally, the filamins cross-link filaments of actin and contribute to anchoring membrane proteins to the cytoskeleton. Mouse embryonic fibroblasts depleted of filamin demonstrate decreased adhesion stability, manifesting as reduced FA size, transient traction forces and decreased stress fibres (Lynch *et al*. 2011). Furthermore, specific FLNB-deficiency in these fibroblasts results in increased MMP-9 proteolytic activity and cell invasion, modulated by the RAS/ERK pathway (Bandaru *et al*. 2014).

With regards to up-regulated genes, those of particular interest include podoplanin (PDPN), leupaxin (LPXN), shroom (SHRM) and shroom family member 3 (SHROOM3), myosin light chain kinase (MYLK) and syncoilin (SYNC1). Of those listed above, PDPN is the only gene up-regulated at all concentrations and time-points, for both epoxy-tiglianes. However, 0.1 and 10 µg/mL EBC-46 and EBC-211, respectively, display the greatest up-regulations. PDPN is a transmembrane glycoprotein, whose interactions with cluster of differentiation 44 (CD44) promotes directional migration in epithelial cells and tumour cells (Martín-Villar *et al*. 2010). *In vitro*, primary DFs readily express PDPN in response to inflammatory stimuli, whereas PDPN gene expression in cancer-associated fibroblasts is correlated with the progression of tumours (Kan *et al*. 2014; Nazari *et al*. 2016). LPXN, which was also more greatly increased at 0.1 µg/mL and 10

μg/mL of EBC-46 and EBC-211, respectively; is a member of the paxillin family of FA proteins and contributes to cell migration, spreading and adhesion regulation. With regards to cell adhesion, it acts as a negative regulator in integrin-mediated adhesion processes (Chen and Kroog, 2010). In contrast, SHRM, SHROOM3 and MYLK were more highly expressed at the lower epoxy-tigliane concentrations. SHROOM3 has previously been associated with kidney fibrosis, acting to facilitate canonical TGF-β_1 signalling and up-regulate type I collagen, α_1 chain (COL1α_1) expression. In contrast, SHROOM3 knockdown was shown to markedly abrogate interstitial fibrosis (Menon *et al*. 2015). Regarding MYLK, contraction of the granulation tissue by myofibroblasts has been shown to be dependent on Rho/Rho kinase/MYLK activity (Tomasek *et al*. 2006). SYNC1 was also up-regulated at lower epoxy-tigliane concentrations, but following 72 h treatment only. Syncoilin has been shown to be strongly up-regulated by hepatic stellate cells after their activation *in vitro*. Upon activation, they change to myofibroblast-like cells with contractile properties and syncoilin was found to co-localise with αSMA, β-actin and α-tubulin (Van Rossen *et al*. 2014).

Overall, down-regulation of cytoskeletal-related genes at the higher concentrations of epoxy-tiglianes, versus the up-regulations at lower concentrations, corroborates the conclusions of the previous Chapters; in which 0.1 μg/mL and 10 μg/mL EBC-46 and EBC-211, respectively, were found to induce 'anti-fibrotic' responses, while 0.01 μg/mL and 1 μg/mL EBC-46 and EBC-211, respectively, stimulated more 'pro-fibrotic' responses. Such findings further corroborate the theory that the epoxy-tiglianes exert biphasic, concentration-dependent effects on cellular activities and behaviour.

5.5.5 Cell Adhesion/Migration-Related Genes

In the Cell Adhesion/Migration-Related Gene category, 38 genes and 37 genes (12 up-regulated/26 down-regulated and 12 up-regulated/25 down-regulated for EBC-46 and EBC-211, respectively), were differentially expressed between epoxy-tigliane-treated DFs and the TGF-β_1-positive, compound-free controls. All of the genes were differentially expressed between 2 - 8.1-fold and as found in many other categories, the greatest fold-changes were demonstrated at 0.1 μg/mL and 10 μg/mL EBC-46 and

EBC-211, respectively. Up-regulated genes of interest include transglutaminase 2 (TGM2) and integrin α_2 (ITGA2). TGM2 was the only gene of the category to exhibit up-regulation at all epoxy-tigliane concentrations and time-points analysed (except at 1 µg/mL EBC-211 at 72 h). ITGA2 only showed up-regulations at 0.1 µg/mL and 10 µg/mL EBC-46 and EBC-211, respectively; post-24 h treatment. However, the two exhibited the greatest up-regulations of the category. TGM2 catalyses the cross-linking of ECM and intracellular proteins, including collagen and FN; acting to increase ECM stability (Lorand and Graham, 2003; Agah *et al*. 2005). Strong TGM2 activity has been shown in placental fibroblasts, where it supports cell adhesion and plays a role in FN cross-linking (Robinson *et al*. 2006). Additionally, it is thought that TGM2 is involved in stabilisation of tissue inflammation and apoptotic cells, prior to clearance (Nanda *et al*. 2001; Quan *et al*. 2005). TGM2 inhibition has also been found to lead to reduced ECM compaction during early wound remodelling (up to 48 h; Simon *et al*. 2014). In contrast, however, TGM2 has also been implicated in the development of fibrosis; with the inhibition of TGM2 activity resulting in an attenuation of cardiac fibrosis (Wang *et al*. 2018). With regards to ITGA2, its encoded protein forms an α/β heterodimeric, cell surface glycoprotein receptor for cellular adhesion to various ECM ligands (Barczyk *et al*. 2010). Integrin α_2 has been demonstrated to influence DF-myofibroblast differentiation, as the up-regulation of collagen receptor, integrin $\alpha_2\beta_1$, has been exhibited to down-regulate αSMA synthesis/expression (Ehrlich *et al*. 1998). Also, integrin $\alpha_2\beta_1$ was found to up-regulate MMP-1 expression; mediated by changes in the balance of collagen receptors (Znoyko *et al*. 2006). Such differential expression is found in early-gestational foetal skin, with foetal fibroblasts expressing higher integrin α_2 than adult fibroblasts (Moulin and Plamondon, 2002).

Of the down-regulated genes, those of particular interest include cadherin-2 (CDH2), FAT tumour suppressor homolog 1 (FAT1) and integrin β-like$_1$ (ITGBL1). For each of these genes, the fold-changes occurred at both time-points; at 0.1 µg/mL and 10 µg/mL of EBC-46 and EBC-211, respectively. Following EBC-211 treatment at both 24 h and 72 h, FAT1 was also down-regulated at 1 µg/mL. Cadherin-2, also known as N-cadherin, is a member of the cadherin transmembrane receptor family that modulate

calcium-dependent cell-cell adhesion (Lefort *et al*. 2001). N-cadherin is the dominant family member expressed by fibroblasts, acting to mediate the adherens junctions. These N-cadherin-dependent junctions play crucial roles in cellular migration, differentiation and embryonic development (El Sayegh *et al*. 2007). N-cadherin has also been shown to be over-expressed in disease states, including oral squamous carcinoma and Crohn's disease (Burke *et al*. 2011; Walker *et al*. 2014). In two oral squamous carcinoma cell lines, N-cadherin over-expression increased cell motility, invasive capacity and MMP-9 synthesis (Walker *et al*. 2014). Fibroblasts in Crohn's disease express increased N-cadherin and thus, show enhanced migration (Burke *et al*. 2011). Also a member of the cadherin family, FAT1 is mainly expressed in proliferating epithelial tissues and plays a key role in cellular polarisation, migration and modulation of cell-cell contact (Tanoue and Takeichi, 2005). In murine models of chronic liver injury and in cirrhotic livers of patients, FAT1 expression has been shown to be up-regulated (Valletta *et al*. 2012). In contrast, knockdown of FAT1 has been found to result in disorganisation of cell junction-associated filamentous actin (F-actin) and other actin fibres, decreased fibroblast adhesion/migration, inhibition of wound margin cellular polarity and cell-cell contact disturbance (Tanoue and Takeichi, 2004; Gee *et al*. 2016). Lastly, ITGBL1 has been demonstrated to promote hepatic stem cell activation, and differentiation into myofibroblast-like cells, by up-regulating TGF-β_1. Thus, ITGBL1 promotes hepatic fibrosis and acts as a key regulator of fibrogenesis (Wang *et al*. 2017).

5.5.6 Extracellular Matrix-Related Genes

In the ECM-Related Gene category, 58 and 56 genes (21 up-regulated/37 down-regulated and 19 up-regulated/37 down-regulated for EBC-46 and EBC-211, respectively), were differentially expressed between epoxy-tigliane-treated DFs and the TGF-β_1-positive compound-free controls. All of the genes were differentially expressed between 2 - 53.7-fold and as observed in many of the other categories, the greatest fold-changes were generally found at 0.1 µg/mL and 10 µg/mL EBC-46 and EBC-211, respectively. Many genes differentially expressed within this category are collagen isoforms; most of which were down-regulated. Down-regulated collagens

include type IV (COL4α_1), type V (COL5α_1/α_2), type VI (COL6α_3), type VIII (COL8α_1/α_2), type XII (COL12α_1), type XV (COL15α_1) and type XVI (COL16α_1); all of which were down-regulated by both of the epoxy-tiglianes. Type IV collagen is a non-fibrillar isoform and a major basement membrane component. In lung fibroblasts, COL4α_1 and α_2 expression was enhanced following TGF-β_1 stimulation; whilst knockdown of these chains increased migration, with increased phosphorylation of focal adhesion kinase (FAK; Urushiyama *et al*. 2015). With regards to the epoxy-tiglianes, following TGF-β_1 stimulation, the COL4α_1 expression decreased at both time-points. However, only at 0.1 µg/mL and 10 µg/mL of EBC-46 and EBC-211, respectively; opposing the results found in lung fibroblasts and DFs treated with TGF-β_1 alone. This was also found to be the case with type VIII and type XII collagens. Type VIII collagen is a short chain family member present in basement membranes and a variety of matrices. It is involved in up-regulating smooth muscle cellular migration and maintaining the phenotype. Therefore, COL8α_1/α_2 are associated with differentiation and fibrosis (Shuttleworth, 1997). In mice, knockout of COL8α_1/α_2 has been shown to attenuate production of the ECM and fibrosis, as well as reduce the number of interstitial myofibroblasts (Loeffler *et al*. 2012). Furthermore, neonatal fibroblasts from COL8-knockout mice expressed lower levels of TGF-β and αSMA; thus, a lack of type VIII collagen has been found to inhibit myofibroblast differentiation (Skrbic *et al*. 2015). Type XII collagen has been found to be associated with type I collagen; which is believed to modify the interactions between type I collagen fibrils and the ECM. In Chapter 4, COL1α_1 was also exhibited to be decreased at the same concentrations as COL4α_1, COL8α_1/α_2 and COL12α_1 after 72 h treatment; however, this was not found to be the case during the Microarray studies, as expression was only down-regulated by EBC-46 and EBC-211 between 1.4 - 1.9-fold over 72 h culture. This discrepancy is likely a result of the high-throughput nature of the Microarray; while the probes used in the qPCR studies are more sensitive. As well as its association with type I collagen, type XII collagen is over-expressed in human and mouse corneal scars (Massoudi *et al*. 2012). It has also been found to be highly expressed in the desmoplastic stroma and around αSMA-positive cancer-associated fibroblasts (Karagiannis *et al*. 2012).

The remaining down-regulated collagen genes were differentially expressed at times and concentrations that varied. The α_1 isoform of type V collagen was decreased at 0.1 μg/mL and 10 μg/mL of EBC-46 and EBC-211, respectively, at both time-points; but also following 0.01 μg/mL and 1 μg/mL of EBC-46 and EBC-211, respectively, at 72 h. In contrast, the α_2 isoform was down-regulated following 72 h treatment with 0.1 μg/mL EBC-46 alone; but at both time-points for 10 μg/mL of EBC-211. Type V collagen is fibrillar and found to be highly expressed during tissue development and wound repair; thought to play a modulating role in contraction. However, increased type V collagen content is also a feature of many inflammatory and fibroproliferative diseases (Berendsen *et al*. 2006; Breuls *et al*. 2009). COL6α_3 expression was only observed to be decreased post-72 h treatment with 0.01 μg/mL and 1 μg/mL EBC-46 and EBC-211, respectively. Type VI collagen has been demonstrated to facilitate the differentiation of cardiac fibroblasts to myofibroblasts and regulate dermal ECM assembly (Naugle *et al*. 2006; Theocharidis *et al*. 2016). COL15α_1 expression was down-regulated at both concentrations of the two epoxy-tiglianes following 72 h treatment. Conversely, TGF-β_1 treatment alone has been shown to enhance COL15α_1 expression in human DFs (Kivirikko *et al*. 1999). Finally, COL16α_1 is the only gene of the down-regulated collagens that was found to be differentially expressed across all concentrations and time-points for both epoxy-tiglianes. Interestingly, as found with COL15α_1, TGF-β treatment alone increases the COL16α_1 gene expression in human DFs. Type XVI collagen also demonstrates higher expression in fibrotic skin diseases (Grässel *et al*. 1998; Akagi *et al*. 1999). In addition to the prior two family members, TGF-β is also a potent stimulator of types I, IV, V and VI collagen; all of which are down-regulated by the epoxy-tiglianes (Grässel *et al*. 1998). This suggests that certain concentrations of the epoxy-tiglianes modulate, and potentially reverse, the normal effects of TGF-β_1 upon DFs/myofibroblasts.

Other down-regulated genes of particular interest include cartilage oligomeric matrix protein (COMP), dermatopontin (DPT), fibrillin (FBN1 and FBN2), lysyl oxidase (LOX), EGF-containing fibulin-like ECM protein 1 (EFEMP1), fibulin (FBLN2 and FBLN5), pro-collagen-lysine 2-oxoglutarate 5-dioxygenase 2 (PLOD2), versican (VCAN), tenascin C

(TNC) and osteopontin (SPP1). Of these genes, COMP possessed the greatest change in gene expression, following treatment with 0.1 µg/mL and 10 µg/mL EBC-46 and EBC-211, respectively; at both time-points (down-regulated between 7.9 - 24.6-fold). COMP is a constitutive cutaneous ECM component and is strongly up-regulated in fibrosis. It is capable of high-affinity binding to type I and XII collagens; both of which were also down-regulated by the epoxy-tiglianes. Lack of COMP-collagen interaction within the ECM has been exhibited to lead to changes in collagen fibril morphology and density (Halper and Kjaer, 2014; Schulz *et al*. 2016). Furthermore, it has been demonstrated that COMP also plays an important role in assisting efficient collagen secretion, such collagens were retained in the endoplasmic reticulum of COMP-null mice fibroblasts. Therefore, COMP-null mice displayed greatly attenuated fibrotic responses in skin (Schulz *et al*. 2016). Within the skin, dermatopontin has been found to be chiefly located on the surface of collagen fibres; acting to accelerate collagen fibril formation. It is also thought to mediate DF adhesion to the ECM and interacts with TGF-β_1, enhancing its activity (Okamoto and Fujiwara, 2006; Kato *et al*. 2011). Interestingly, treatment with TGF-β_1 only up-regulates DPT gene/protein expression in skin fibroblasts (Kuroda *et al*. 1999). However, co-treatment with the epoxy-tiglianes, at certain concentrations, decreases its expression; indicating a reversal of its usual effects on DPT post-epoxy-tigliane treatment.

EFEMP1, LOX and PLOD2 were all down-regulated at 0.1 µg/mL and 10 µg/mL EBC-46 and EBC-211 alone, respectively; at both time-points. EFEMP1 is an EGF-related protein that binds EGFR and its over-expression has been shown to promote tumour growth (Camaj *et al*. 1999). Lysyl oxidase cross-links collagen and elastin, playing key roles in ECM maturation and regulating their promoters; inducing their activity (Oleggini *et al*. 2007). Consequently, LOX genes are generally up-regulated in keloid fibroblasts; whereas early-gestational fibroblasts possess less lysyl oxidase activity, resulting in decreased collagen cross-linking in foetal wounds (Lovvorn *et al*. 1999; Colwell *et al*. 2006; Satish *et al*. 2006). PLOD2 is also associated with collagen fibrillogenesis and assembly of elastin fibres; encoding lysyl hydroxylase 2, which catalyses hydroxylation of the lysyl residues in collagen-like peptides. The resulting

hydroxy-lysyl groups are attachment sites for the carbohydrates in collagen and thus, are crucial for cross-link stability (Kagan and Li, 2003; van der Slot *et al*. 2003). Such alterations in cross-linking are related to the irreversible collagen accumulation in fibrotic tissues, with PLOD2 demonstrating consistent up-regulation in several forms of fibrosis, including systemic sclerosis. PLOD2 gene expression is highly increased in skin fibroblasts from these patients, whereas in normal human DFs, TGF-β_1 increases PLOD2 expression (van der Slot *et al*. 2003, 2005). Thus, the down-regulation of the aforementioned cross-linking mediators by the epoxy-tiglianes may lead to increased collagen susceptibility to proteolytic degradation by proteinases, several of which were up-regulated after epoxy-tigliane treatment (Chapter 5.5.7).

As previously described, fibulins (FBLN2 and FBLN5) and fibrillins (FBN1 and FBN2) were also down-regulated by the epoxy-tiglianes. The fibulins are elastin-associated ECM components. In particular, fibulin-5 possesses crucial roles in the assembly and maturation of elastic fibres by organising tropoelastin and the cross-linking enzymes onto microfibrils (Hirai *et al*. 2007). Interestingly, FBLN5 expression was found to be induced in endothelial and smooth muscle cells in response to injury and was found to stimulate substantial collagen expression within dermal wounds (Lee *et al*. 2004). In addition, FBLN5-null mice exhibit notable elastinopathy as a result of disorganised elastic fibres (Nakamura *et al*. 2002; Yanagisawa *et al*. 2002). Also linked with elastic fibre development, fibrillin is secreted by fibroblasts and becomes incorporated into microfibrils, which provide a scaffold for tropoelastin deposition (Kielty *et al*. 2002). Fibrillin microfibrils are also engaged in cell-ECM interactions, including with TGF-β, BMPs and integrins, with fibrillin-2 co-localising with fibulin-2 in the skin (Jensen and Handford, 2016). Within the superficial and deep dermis, fibrillin-1 volume density is decreased in normal, keloid and hypertrophic scars; versus normal skin (Amadeu *et al*. 2004). SPP1, TNC and VCAN were also differentially expressed by epoxy-tiglianes, the former two genes were decreased at both concentrations of the epoxy-tiglianes at 72 h alone, whilst VCAN was down-regulated at these conditions, as well as at 0.1 µg/mL EBC-46 following 24 h treatment. Decreased SPP1 expression is favourable as osteopontin has been demonstrated as necessary for myofibroblast differentiation

(Lenga *et al*. 2008). Osteopontin-deficient mice displayed less dermal fibrosis, in comparison to wild-type mice, in a bleomycin-induced fibrosis model (Wu *et al*. 2012). Furthermore, down-regulated osteopontin levels at the wound site have been shown to accelerate healing and reduce scarring (Mori *et al*. 2008). With regards to TNC, its levels are normally elevated during wound healing and it has been shown to be increased at the wound edges and throughout the granulation tissue after injury (Mackie *et al*. 1998). Post-wound contraction, TNC expression levels regress and it is undetectable in scar tissue (Jones and Jones, 2000). Exposed to TGF-β_1 only, human DFs are stimulated to express TNC. However, keloid-derived fibroblasts express even greater levels (Dalkowski *et al*. 1999; Jinnin *et al*. 2004). Lastly, VCAN is a chondroitin sulphate proteoglycan (PG) that, under normal conditions, is increased during wound repair (Wang *et al*. 2000). Indeed, VCAN over-expression has been shown to induce myofibroblast phenotypes in murine fibroblasts (Carthy *et al*. 2015). As observed following epoxy-tigliane treatment, VCN down-regulation may potentially contribute to inhibition of DF-myofibroblast differentiation observed at certain concentrations of the compounds; as both hyaladherins, VCAN and TNF-stimulated gene-6 (TSG6), are promoters of the HA-mediated CD44/EGFR differentiation pathway (Meran *et al*. 2007, 2008; Martin *et al*. 2016). TSG6 gene expression was also demonstrated to be down-regulated by the epoxy-tiglianes (Chapter 1). However, such differential expression changes were not reflected in the Microarray studies. This discrepancy is likely a result of the high-throughput nature of the Microarray; while the probes used in the qPCR studies are more sensitive.

Of the up-regulated genes in the category, those of particular interest include elastin (ELN), HA synthases (HAS2 and HAS3), HA-mediated motility receptor (HMMR) and KIAA1199. ELN was only shown to be up-regulated at both time-points, at the lower concentrations of those analysed. This corroborated the results of the prior Chapter, in which ELN was significantly up-regulated at 0.01 µg/mL and 1 µg/mL EBC-46 and EBC-211, respectively; post-72 h treatment. As detailed previously (Chapter 4), ELN is a fibrous protein involved in ECM homeostasis; providing structural integrity and tissue resilience (Klingberg *et al*. 2013). It is generally understood that production of

elastin by DFs is low after injury, which partly accounts for the rigidity and breaking strength of scar tissue, in comparison to that of intact connective tissue (Schultz and Wysocki, 2009; Klingberg *et al*. 2013). However, several studies have shown that ELN production by fibroblasts is increased after tissue damage, in response to cytokines including TGF-β_1 (Liu and Davidson, 1988; Kähäri *et al.* 1992). With regards the HASs, the greatest fold-changes in HAS2 expression were observed at both time-points for 0.1 μg/mL and 10 μg/mL EBC-46 and EBC-211, respectively; whereas HAS3 was only observed to be up-regulated at 0.01 μg/mL and 1 μg/mL EBC-46 and EBC-211, respectively; post-72 h treatment. Such findings corroborate those found previously (Chapter 4); however, the qPCR studies also found HAS3 to be increased at the aforementioned concentrations at 24 h and 48 h. As detailed previously (Chapters 1 and 4), HAS2 is the primary isoform expressed by DFs and interestingly, increased HAS2 expression in normal DFs would indicate a pro-fibrotic phenotype (Meran *et al.* 2007; Albeiroti *et al*. 2015). However, prior work has demonstrated (Chapters 3 and 4) that at these concentrations, there is an inhibition of myofibroblast formation. HAS2 is also known to be essential to embryonic and early-gestational development; an environment in which fibroblasts are resistant to developing scarring phenotypes. In such situations, elevated and persistent HA synthesis stimulates cell migration and invasiveness in a preferential manner (Longaker *et al*. 1989; Mast *et al*. 1995; Camenisch *et al*. 2000). The HAS3 findings also complement the prior findings; as at the concentrations that HAS3 was demonstrated to be up-regulated, myofibroblast formation was observed (Chapter 3). HAS3 also produces low-molecular weight HA, which is associated with more pro-fibrotic repair responses (David-Raoudi *et al.* 2008; Huang *et al.* 2009). In addition to the HAS up-regulation, the HA receptor, HMMR (also known as RHAMM), was also found to be up-regulated. Interestingly, HMMR up-regulation is correlated with fibroplasia and decreased HA content, whereas less expression of HA receptors is associated with scarless healing in early-gestational wounds (Lovvorn *et al.* 1998). However, a balance appears to be necessary as RHAMM knockout fibroblasts fail to re-surface scratch wounds and fail to invade HA-supplemented collagen gels; leading to defective wound repair (Tolg *et al*. 2006). Finally, KIAA1199 was shown to be up-regulated at 24 h alone, at both concentrations

of the epoxy-tiglianes; with greater fold-changes demonstrated at the lower concentrations. KIAA1199 is also a binding protein for HA, playing a key role in its depolymerisation in the skin, in a CD44/hyaluronidase (HYAL)-independent manner (Yoshida *et al*. 2013). TGF-β_1 is known to decrease KIAA1199 expression, contributing to the accumulation of HA. However, in scenarios where KIAA1199 is increased, high molecular weight HA is depolymerised to lower molecular weight fragments, which are pro-inflammatory and pro-fibrotic (Nagaoka *et al*. 2015; Soroosh *et al*. 2016). Therefore, higher KIAA1199 expression at the lower epoxy-tigliane concentrations would support the pro-fibrotic responses previously shown at these concentrations; whereas the lesser increases at the higher concentrations may be favourable *in vivo*, as HA fragments are also capable of enhancing cell migration and neovascularisation.

Corroborating the findings of the previous Chapter 4, the Microarray studies further evidence the abilities of the epoxy-tiglianes to modulate ECM component synthesis. With the down-regulation of numerous collagens and associated genes (COMP, DPT, LOX and PLOD2), amongst other pro-fibrotic genes (SPP1, TNC and VCAN), it appears that the epoxy-tiglianes may induce a more 'anti-fibrotic' matrix environment. Also, the changes stimulated may encourage a more regenerative environment, with up-regulations in the HASs and ELN. In particular, up-regulations in HAS expression not only corroborate the previous Chapter's findings, but also indicate gene expression changes akin to those of scarless healing scenarios; such as early-gestational foetal wound repair.

5.5.7 Proteinases/Proteinase Inhibitor-Related Genes

In the Proteinases/Proteinase Inhibitor-Related Gene category, 34 and 35 genes (22 up-regulated/12 down-regulated and 22 up-regulated/13 down-regulated for EBC-46 and EBC-211, respectively), were differentially expressed between epoxy-tigliane-treated DFs and the TGF-β_1-positive, compound-free controls. All of the genes were differentially expressed between 2 - 62.7-fold and unlike the other gene categories, the most notable observation was the magnitude of differential expression for many of the proteinase/proteinase inhibitor genes. In particular, this was apparent with a

number of MMPs, which exhibited major increases in gene expression; especially at 0.1 µg/mL and 10 µg/mL EBC-46 and EBC-211, respectively. MMP-1 demonstrated a much higher fold-change in expression, in comparison to the other MMPs; and was found to be up-regulated at all concentrations and time-points analysed. However, the greatest changes were observed post-24 h exposure (49.7-fold and 62.7-fold for EBC-46 and EBC-211, respectively). These were followed by MMP-10 (29.1-fold and 26.3-fold for EBC-46 and EBC-211, respectively) and MMP-3 (19.1-fold and 18.2-fold for EBC-46 and EBC-211, respectively). MMP-12 was also up-regulated at 0.1 µg/mL and 10 µg/mL EBC-46 and EBC-211, respectively; but only at 24 h (9.5-fold and 7.8-fold, respectively). At the same concentrations, MMP-11 was increased by 4.2-fold and 4.8-fold, respectively; but only following 72 h treatment.

Such changes in favour of ECM turnover may be enhanced through epoxy-tigliane-induced down-regulation of TIMP-3 expression; due to the function of TIMP-3 in the predominant inhibition of MMP-1, -2, -3, -9 and -13 (Apte *et al*. 1995; Brew and Nagase, 2010). In contrast, the tissue factor pathway inhibitor 2 (TFPI-2) proteinase inhibitor, capable of inhibiting MMP activity to a lesser extent than the TIMPs, was found to be up-regulated at 24 h (Chand *et al*. 2005). Nevertheless, given the overall levels of MMP gene expression, versus the extent of differentially expressed genes in other categories, it is apparent that MMP up-regulation and the subsequently heightened ECM turnover is a crucial mechanism through which the epoxy-tiglianes induce their enhanced wound healing responses (Campbell *et al*. 2014, 2017; Reddell *et al*. 2014).

This conclusion was further supported by validation of the changes in MMP gene expression, at the protein level. Reflecting the expression differences between the concentrations of both EBC-46 and EBC-211, significant up-regulations in MMP-1 activity were only found at 0.1 µg/mL EBC-46 and above, and at 10 µg/mL EBC-211; at both time-points. This corroborated the Microarray and qPCR findings (Chapter 4), in which large differences in gene expression were found between 0.01 µg/mL and 0.1 µg/mL EBC-46 and 1 µg/mL and 10 µg/mL EBC-211, respectively. These results

support the other concentration-dependent effects shown throughout the Chapters. MMP-3 and MMP-12 activities were also exhibited to be significantly increased at 0.1 μg/mL and 10 μg/mL EBC-46 and EBC-211, respectively; after 72 h treatment alone. Higher fold-changes in gene expression found at 24 h, but greater activity at 72 h, indicates that there may be a delay between up-regulated MMP expression and its translation into increased activity. This was also exhibited to be the case with MMP-10, with the greatest activity demonstrated post-72 h.

The importance of MMP-modulated ECM turnover has been emphasised previously (Chapters 1 and 4); due to their abilities to collectively degrade mostly all major ECM components, including collagens, PGs and FN (Parks, 1999; Caley *et al*. 2015). Due to such properties, correlations between the expression and activities of various MMPs and the extent of scarring/fibrosis are now well-established. MMP-1 plays key roles in the cleavage and degradation of collagen, particularly types I and III (Beanes *et al*. 2003; Do and Eming, 2016). MMP-1 up-regulation and degradation aids keratinocyte migration into the wound site and subsequent re-epithelialisation. Thus, the epoxy-tigliane-induced MMP-1 increase in DFs may facilitate keratinocyte migration *in vivo*; contributing to the rapid re-epithelialisation found in treated skin (Dasu *et al*. 2003; Visse and Nagase, 2003; Moses, 2016). In situations characterised by scarless repair, there is a greater MMP activity than TIMP activity; which favours earlier remodelling and more rapid collagen turnover (Dang *et al*. 2003; Yagi *et al*. 2016; Moore *et al.* 2018). Elevated MMP-1 and -3 inductions have been exhibited in foetal wounds, occurring more rapidly and present at greater levels than in scarring wounds, whilst increased TIMP-3 expression has been shown in scarring wounds alone (Peled *et al*. 2002; Dang *et al*. 2003). However, in wounds of the oral mucosa, MMP-1 and MMP-10 have a reduced presence versus dermal wounds; but show higher MMP-2 levels, likely as a result of reduced TIMP activity (Stephens *et al*. 2001; Chen *et al*. 2010). In contrast, a lack of MMP activity can lead to excessive scar development via collagen accumulation (Fineschi *et al*. 2006; Giménez *et al*. 2017). MMP-1 has been shown to be down-regulated in pathological scarring, such as keloid and hypertrophic scarring (Lee *et al*. 2015). Keloid fibroblasts have also been shown to down-regulate MMP-3

expression (Russell *et al*. 2010). Conversely, however, some studies have found keloid fibroblasts to express greater MMP-1 and -2 expression than normal DFs; thought to allow the fibrotic response to extend beyond the wound margin, via the degradation of collagen (Fujiwara *et al*. 2005; Shih *et al*. 2010).

As performed with the greatest up-regulated genes in the category, validation at the protein level was carried out for the greatest down-regulated gene. PI16 was down-regulated at all concentrations analysed for both EBC-46 and EBC-211 at both time-points; with much higher fold-changes observed at 0.1 µg/mL and 10 µg/mL EBC-46 and EBC-211, respectively. At 24 h, 23.3 and 23.9-fold decreases were shown for 0.1 µg/mL and 10 µg/mL EBC-46 and EBC-211, respectively; while at 72 h, 12.5 and 12.7-fold decreases were shown, respectively. Western blot analyses corroborated these changes, with undetectable protein levels demonstrated between 0.01 - 10 µg/mL EBC-46 and at 10 µg/mL EBC-211 at both time-points. Despite the evident decreases in PI16 induced by the epoxy-tiglianes, little is known on PI16's role within skin. PI16 is abundant in mouse skin and has been shown to be up-regulated in damaged human heart tissue; particularly in the hypertrophic and failing myocardium (Frost and Engelhardt, 2007; Gibbs *et al*. 2008). Thus, PI16 is thought to have a role in ECM remodelling during heart failure, predominantly expressed by cardiac fibroblasts. In addition, recombinant PI16 has been shown to efficiently inhibit cathepsin K (CTSK; Regn *et al*. 2016). Consequently, the epoxy-tigliane-induced down-regulation of PI16 may contribute to the CTSK up-regulation also observed post-72 h treatment. Within the dermis, CTSK is only expressed under certain circumstances, such as scarring or inflammation. Cultured DFs and neonatal fibroblasts have been exhibited to express CTSK in their lysosomes; consistent with the intracellular degradation of internalised collagen (Garnero *et al*. 1998; Rünger *et al*. 2007; Quintanilla-Dieck *et al*. 2009). As the most potent and versatile collagen-degrading protease, CTSK over-expression is associated with decreased type I collagen deposition and reduced fibrosis (Bühling *et al*. 2004; Rünger *et al*. 2007; Srivastava *et al*. 2008; Quintanilla-Dieck *et al*. 2009).

A number of serpin peptidase inhibitors (SERPINs) were also shown to be expressed differentially following epoxy-tigliane treatment. SERPINB2, SERPINB7 and SERPINF1 were all up-regulated between 2 - 7.6-fold, whereas SERPINE1 was down-regulated between 2.5 - 3-fold. Generally, these differences were observed at 72 h across both concentrations of the two epoxy-tiglianes. SERPINB2 displayed the greatest increase of the three up-regulated genes and is known to be a key inhibitor of urokinase-type plasminogen activator (uPA). Also known as plasminogen activator inhibitor (PAI-2), SERPINB2 expression is associated with reduced metastasis and has been shown as required by stromal cells for normal collagen remodelling; regulating the interaction and engagement of fibroblasts with the collagen in the contracting ECM (Harris *et al*. 2017). PAI-2 has also shown higher expression in keloid scars, compared to normal skin and hypertrophic scars (Suarez *et al*. 2013, 2015). SERPINB7 is believed to inhibit MMP-2 and -9 activities, whilst SERPINF1 has been shown to contribute to wound resolution by inducing blood vessel regression and stimulating maturation of the vascular microenvironment; promoting a return to homeostasis following injury (Ohtomo *et al*. 2008; Wietecha *et al*. 2015). SERPINE1, also known as PAI-1, has also been found to be down-regulated in early-gestational foetal skin; as well as following epoxy-tigliane treatment (Huang *et al*. 2002; Li *et al*. 2006). Furthermore, knockout mice for PAI-1 possess accelerated skin wound closure (Chan *et al*. 2001). PAI-1 also acts as a urokinase-type plasminogen activator (PLAU) inhibitor, which might explain why PLAU and its receptor are up-regulated following epoxy-tigliane treatment.

In addition to MMPs and SERPINs, other proteinases were down-regulated by epoxy-tigliane treatment, such as members of the disintegrin and metalloproteinases with thrombospondin (TS) motifs (ADAMTSs) families: ADAMTS1 and ADAMTS5. The two are capable of ECM degradation through the cleavage of PG core proteins and both are inhibited by TIMP-3 (Toriseva and Kähäri, 2009; Shiomi *et al*. 2010). Thus, down-regulation in TIMP-3 expression induced by epoxy-tigliane treatment would result in a reduction of ADAMTS expression and activity. Furthermore, low concentrations of ADAMTS1 have been shown to promote fibroblast migration and ADAMTS1 itself is a potent inhibitor of angiogenesis (Krampert *et al*. 2015). With regards to ADAMTS5,

DFs lacking the proteinase demonstrated reduced versican proteolysis (shown to be down-regulated after epoxy-tigliane treatment also), altered cell shapes, enhanced αSMA expression, bigger pericellular matrices and increased contractility within 3D collagen gels. Thus, differential expression of ADAMTS5 may be capable of regulating the phenotypic continuum between DFs and myofibroblasts (Hattori *et al*. 2011).

Reflecting the results of the prior Chapter, the Microarray and subsequent validation studies further demonstrate the capabilities of the epoxy-tiglianes to mediate ECM turnover and remodelling. Highly up-regulated MMP expression and resulting MMP activity, combined with the reduced collagen levels (Chapter 5.5.6) and up-regulated HA levels (Chapter 4), would favour a more pliable, hydrated ECM subjected to more rapid proteolytic turnover. Further complemented by inhibition of DF-myofibroblast differentiation (Chapter 1), which appears to be at least partly modulated by down-regulation of myofibroblast formation-related genes (Section 5.5.1) and cytoskeletal-related genes (Chapter 5.5.4); as well as changes in genes and growth factors relating to TGF-β and BMP signalling pathways. In conclusion, these findings provide further evidence and clarification on the preferential wound healing responses observed *in vivo* following epoxy-tigliane treatment; including rapid development of granulation tissue, rapid wound resolution and minimal scarring (Reddell *et al.* 2014; Campbell *et al.* 2017; Hansen *et al.* 2018). However, further protein level validation is required in order to confirm the involvement of many of certain genes; as genotypic changes are not always evident at a phenotypic level, due to post-translational modifications preventing translation to protein expression/activity level changes. Furthermore, as prior work has shown that the anti-cancer effects of the epoxy-tiglianes are induced via classical PKC activation (Boyle *et al*. 2014), PKC involvement in mediating epoxy-tigliane effects upon DFs and myofibroblasts were next investigated; as described in Chapter 6.

Chapter 6

Role of Protein Kinase C Isoforms in Mediating Epoxy-Tigliane Effects on Dermal Fibroblast-Myofibroblast Responses

Chapter 6 - Role of Protein Kinase C Isoforms in Mediating Epoxy-Tigliane Effects on Dermal Fibroblast-Myofibroblast Responses

6.1 Introduction

The previous studies performed have shown that the epoxy-tiglianes are capable of inhibiting TGF-β_1-driven dermal fibroblast (DF)-myofibroblast differentiation (Chapter 3) in a biphasic, concentration-dependent manner; as well as altering the gene and protein expression of key extracellular matrix (ECM) components, such as type I and III collagens, elastin and matrix metalloproteinase-1 (MMP-1). Inhibition of collagen synthesis and up-regulated MMP-1 expression/activity favour an environment which is characterised by greater proteolytic ECM remodelling and faster collagen turnover and degradation. Also, the observed increases in HA synthesis and production would favour a more pliable, hydrated ECM akin to those found in scarless wound healing scenarios, such as early-gestational, foetal and oral mucosal repair (Chapter 4). The findings of these Chapters were further complimented by Microarray studies, which demonstrated that the aforementioned alterations appear to be modulated by down -regulation of myofibroblast formation-related and cytoskeletal-related genes; along with promotion of an 'anti-fibrotic' ECM environment via collagen down-regulation, and down-regulated 'pro-fibrotic' genes (Chapter 5). Furthermore, alterations in the genes relating to transforming growth factor-β (TGF-β)/bone morphogenetic protein (BMP) signalling pathways indicate that epoxy-tiglianes preferentially modulate pro-fibrotic signalling pathways (Chapter 5).

However, despite these studies, little is known on the cellular signalling mechanisms by which the epoxy-tiglianes exert their preferential effects on wound healing. With regards to their anti-cancer properties, previous work has found that EBC-46-induced tumour destruction is modulated through protein kinase C (PKC) activation (Boyle *et al*. 2014). As described previously (Chapter 1), EBC-46 co-injection with the pan-PKC inhibitor, bisindolylmaleimide-1 (BIM-1), significantly reduced efficacy of treatment

in tumour-bearing mouse models. Furthermore, BIM-1 pre-treatment prevented *in vitro* endothelial cell dye uptake; indicating that EBC-46's ability to induce vascular permeability is PKC-dependent. In particular, exposure to EBC-46 resulted in a high number of cells demonstrating translocation of PKC-βI and -βII isoforms (Boyle *et al*. 2014). In the context of wound healing, recent studies conducted by our group have exhibited that EBC-46 and EBC-211 induce enhanced keratinocyte healing responses and re-epithelialisation by PKC activation; principally the α and β isoforms (*currently unpublished data*). Together, the above studies have inspired the hypothesis that the pathways underpinning the compound effects upon DFs and myofibroblasts involve PKC activation. Given the findings of previous Chapters, greater understanding of the underlying mechanism of action is necessary to pursue EBC-46 and EBC-211 as novel wound healing agents.

The PKC family are ubiquitous serine-threonine kinases which upon their activation, translocate to membranes and regulate diverse downstream processes; such as cell proliferation, migration and differentiation (Nishizuka, 1992; Battaini and Mochly-Rosen, 2007; Boyle *et al*. 2014). Existence of multiple PKC isoforms has led scientists to question whether each isoform has a specific function. Indeed, variations in PKC isoform structures and substrate requirements have led to the family being divided into three groups (Way *et al*. 2000; Leask *et al*. 2008). Conventional PKC isoforms (α, βI, βII and γ) are calcium-dependent and activated by diacylglycerol (DAG); while the novel isoforms (δ, ε, η and θ) are calcium-independent. However, they require DAG for their activation. Finally, the atypical PKC isoforms (ι and ζ) are insensitive to both calcium and DAG, but are activated by distinct lipids and protein-protein interactions (Coussens *et al*. 1986; Ono *et al*. 1988; Boyle *et al*. 2014). Cells involved in the dermal wound repair process have been demonstrated to possess calcium-dependent and -independent PKC isozymes; with PKC-α existing as the most abundant isoform in the epidermis (Papp *et al*. 2004; Breitkreutz *et al*. 2007; Jerome-Morais *et al*. 2009). Yet, despite elucidation of the presence of PKC isoforms within the skin, with regards to research into the modulatory effects of PKC upon the downstream functions of DFs and keratinocytes, the field remains in its infancy. Despite some pioneer studies on

the involvement of PKC signalling in regenerative mechanisms carried out >20 years ago, the roles of PKC isoforms in tissue repair have only been studied in-depth over recent years (Joyce and Meklir, 1992; Rui *et al*. 2017). However, regarding reparation and prevention of tissue damage, PKC activation and the subsequent stimulation of downstream pathways has steadily gained in relevance. Recent literature has shown that PKC-α and -δ isoforms are those predominantly involved in the repair processes; particularly associated with chronic wounds, exacerbated by conditions like diabetes (Thomason *et al*. 2012; Khamaisi *et al*. 2016; Rui *et al*. 2017). Thus, PKC isoforms are increasingly being shown to be valuable targets in the promotion of scarless healing and/or tissue regeneration; with novel wound healing agents, selectively modulating specific isoforms of PKC, representing innovative clinical treatments for conditions characterised by aberrant healing (Rui *et al*. 2017).

6.2 Chapter Aims

As detailed previously (Chapter 6.1), studies have shown that the anti-cancer effects of EBC-46 are induced via PKC activation; particularly the classical isoforms (α, βI, βII and γ; Boyle *et al*. 2014). Thus, it was hypothesised that this may be the mechanism by which EBC-46 and EBC-211 mediate the preferential DF responses demonstrated in previous Chapters. Thus, the aim of this Chapter was to assess whether beneficial DF responses stimulated by EBC-46 and EBC-211 treatments are modulated via PKC signalling pathways. BIM-1 and Gö6976 (pan- and α-/βI-PKC inhibitors, respectively) were used to elucidate the roles of PKC isoforms in TGF-β_1-driven DF-myofibroblast differentiation; particularly, whether the inhibitory effects stimulated by the epoxy-tiglianes at certain concentrations are modulated by the PKCs. These studies would provide greater insight into the underlying mechanisms of action regarding how the compounds stimulate the preferential healing outcomes shown *in vivo* (Reddell *et al.* 2014; Campbell *et al.* 2017; Hansen *et al.* 2018).

6.3 Materials and Methods

DFs were sourced, cultured and counted as previously described (Chapters 2.2.1 and 2.2.2). Following determination of cell density and viability (Chapter 2.2.2), DFs were

seeded into 8-well chamber slides for immunocytochemical analysis (Chapter 2.10.2) or 6-well plates for quantitative polymerase chain reaction (qPCR) analysis (Chapter 2.10.3) at $2.5x10^4$ cells/mL. Seeding, serum-starvation and treatment volumes were 250 µL and 2 mL for chamber slides and 6-well plates, respectively. DFs were kept in a 37 °C humidified incubator with 5 % CO_2/95 % air atmosphere for the experiment duration, as previously detailed (Chapter 2.2.1). After growth arrest (Chapter 2.2.1), DFs were treated with either EBC-46 or EBC-211 at the forthcoming concentrations: 0 µg/mL, 0.001 µg/mL, 0.01 µg/mL, 0.1 µg/mL, 1 µg/mL or 10 µg/mL (Chapter 2.1.1); in the presence or absence of TGF-β_1 (10 ng/mL; Chapter 2.1.2) and either 1 µM BIM-1 or Gö6976 (Chapter 2.10.1; pan- and α-/βI-PKC inhibitors, respectively). Following 72 h treatment, immunocytochemistry (ICC) was used to visualise αSMA stress fibre formation and localisation (Chapter 2.10.2); and qPCR was utilised to analyse αSMA gene expression (Chapter 2.10.3). Statistical analyses were performed, as previously described (Chapter 2.11).

6.4 Results

6.4.1 Effects of BIM-1 on αSMA Stress Fibre Formation

To determine whether pan-PKC inhibition altered the effects of EBC-46 and EBC-211 upon DF-myofibroblast differentiation (Chapter 3); αSMA stress fibre formation was visualised by ICC. Analysis was performed on DFs cultured with EBC-46 or EBC-211 at all aforementioned concentrations (Chapter 6.3), with TGF-β_1 (10 ng/mL) and BIM-1 (1 µM), over 72 h in culture. Representative images are shown in Figures 6.1 and 6.2. Non-compound controls with/without TGF-β_1, in the absence and presence of BIM-1 (Figures 6.1 and 6.2A - D), were further included for comparative purposes. Primary antibody-free controls were included to confirm the absence of non-specific binding (Figures 6.1 and 6.2J). As reported prior, TGF-β_1-driven differentiation was indicated via positive αSMA staining and stress fibre formation, coupled with polygonal cellular morphologies (Jenkins *et al.* 2004; Meran *et al.* 2007; Webber *et al.* 2009). TGF-β_1-negative control DFs exhibited elongated, spindle-shaped morphologies with lack of stress fibre formation (Figures 6.1A and 6.2A); no obvious differences were found on BIM-1 inclusion (Figures 6.1B and 6.2B). As found previously upon TGF-β_1 treatment

(Chapter 3), the aforementioned stress fibre formation and polygonal morphologies were observed (Figures 6.1C and 6.2C). In contrast, BIM-1 co-treatment with TGF-β_1 appeared to abrogate differentiation to a degree; with fewer DFs demonstrating the aforementioned characteristic myofibroblast features (Figures 6.1D and 6.2D).

Cells cultured with EBC-46 (0.001 - 10 µg/mL), in the presence of TGF-β_1 (10 ng/mL) and BIM-1 (1 µM; Figure 6.1E - I), exhibited similar characteristics to those observed following TGF-β_1 treatment alone (Figure 6.1C). Cells at all concentrations displayed comparable αSMA localisation and stress fibre formation, coupled with polygonal DF morphologies (Figure 6.1E - I); as shown in the TGF-β_1-positive control (Figure 6.1C). Findings were consistent with those shown in Chapter 3, following EBC-46 treatment with the same concentrations, in the presence of TGF-β_1, but without BIM-1 (Figure 3.1C - D and F - G); barring at 0.1 µg/mL (Figure 3.1E). BIM-1 co-treatment with TGF-β_1 and EBC-46 at 0.1 µg/mL abrogated the inhibitory effect demonstrated previously at this concentration (Figure 3.1E); with the DFs showing myofibroblast phenotypes (Figure 6.1G), similar to those found in TGF-β_1-positive controls (Figure 6.1C) and at all other EBC-46 concentrations (Figure 6.1E - F and H - I).

Similar results were found when DFs were cultured with EBC-211 (0.001 - 10 µg/mL), in the presence of TGF-β_1 (10 ng/mL) and BIM-1 (1 µM; Figure 6.2E - I). At all EBC-211 concentrations, DFs displayed comparable αSMA localisation, stress fibre formation and polygonal morphologies (Figure 6.2E - I); to the TGF-β_1-positive controls (Figure 6.2C). Results were consistent with those obtained post-EBC-211 treatment with the same EBC-211 concentrations, in the presence of TGF-β_1, but without BIM-1 (Figure 3.2C - F); barring at 10 µg/mL (Figure 3.2G). BIM-1 co-treatment with TGF-β_1 and 10 µg/mL EBC-211 abrogated the inhibitory effect previously seen at this concentration (Figure 3.2G); with DFs showing myofibroblast phenotypes (Figure 6.2I), comparable to those observed in TGF-β_1-positive controls (Figure 6.2C) and at all other EBC-211 concentrations (Figure 6.2E - H).

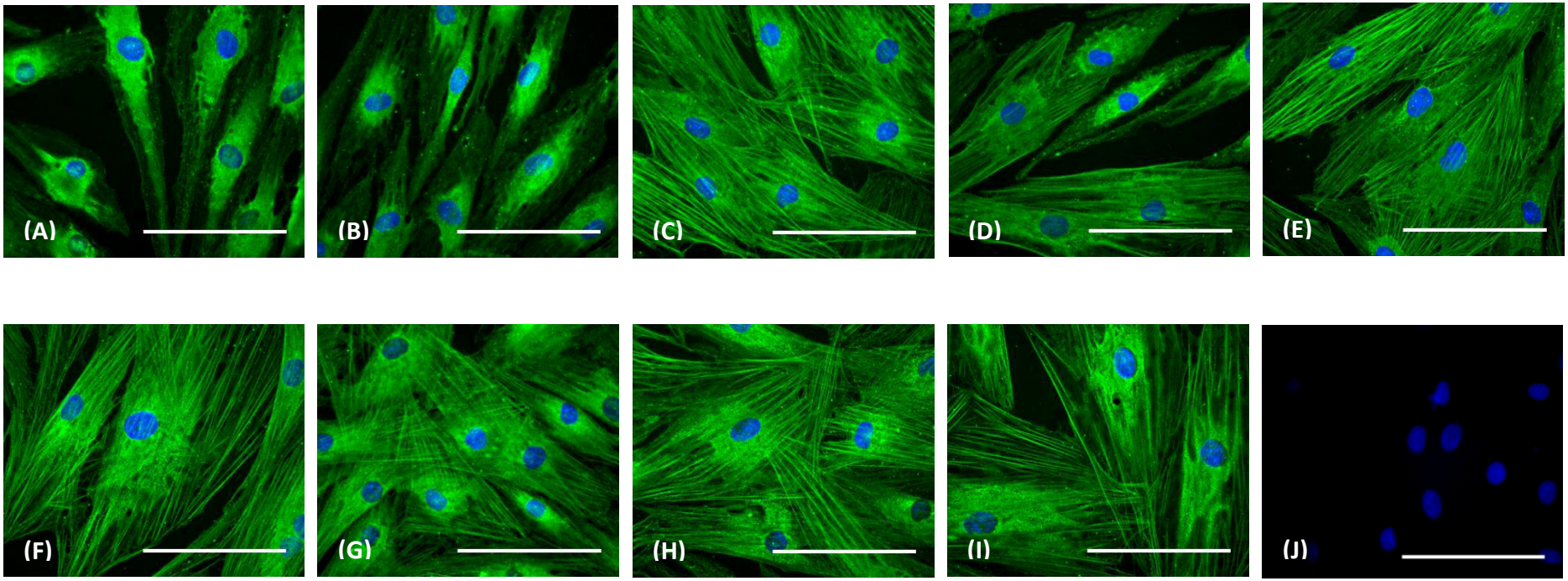

Figure 6.1. ICC analysis of DF-myofibroblast differentiation via visualisation of αSMA localisation and stress fibre formation (green), following treatment with (E) 0.001 µg/mL, (F) 0.01 µg/mL, (G) 0.1 µg/mL, (H) 1 µg/mL and (I) 10 µg/mL EBC-46; in the presence of TGF-β_1 (10 ng/mL) and BIM-1 (1 µM), for 72 h. TGF-β_1-negative and TGF-β_1-positive compound-free controls, in the absence of BIM-1 (A and C, respectively), were also included; as well as TGF-β_1-negative and TGF-β_1-positive compound-free controls, in the presence of BIM-1 (B and D, respectively). Additionally, primary antibody-free controls (J) were included and nuclei were visualised by Hoechst stain (blue). Images shown represent *n = 3* independent experiments captured at x400 magnification (scale bar = 100 µm).

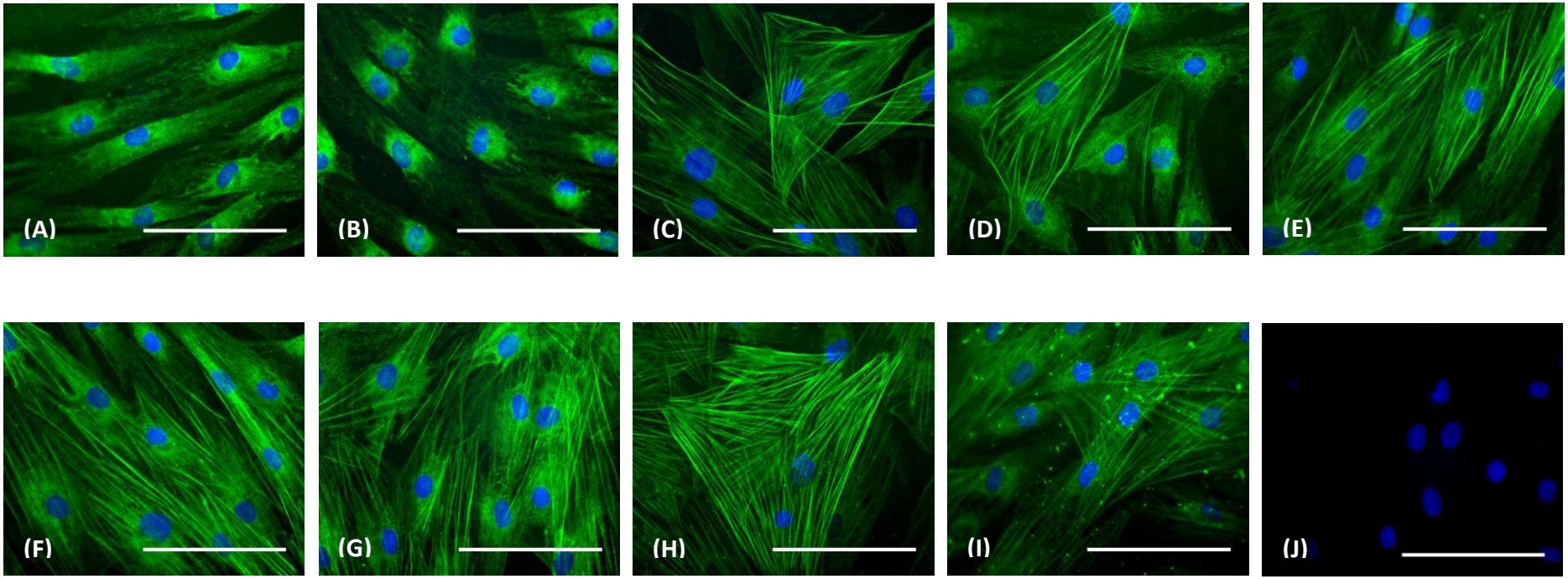

Figure 6.2. ICC analysis of DF-myofibroblast differentiation via visualisation of αSMA localisation and stress fibre formation (green), following treatment with (E) 0.001 µg/mL, (F) 0.01 µg/mL, (G) 0.1 µg/mL, (H) 1 µg/mL and (I) 10 µg/mL EBC-211; in the presence of TGF-β_1 (10 ng/mL) and BIM-1 (1 µM), for 72 h. TGF-β_1-negative and TGF-β_1-positive compound-free controls, in the absence of BIM-1 (A and C, respectively), were also included; as well as TGF-β_1-negative and TGF-β_1-positive compound-free controls, in the presence of BIM-1 (B and D, respectively). Additionally, primary antibody-free controls (J) were included and nuclei were visualised by Hoechst stain (blue). Images shown represent *n = 3* independent experiments captured at x400 magnification (scale bar = 100 µm).

6.4.2 Effects of BIM-1 on αSMA Gene Expression

Following the ICC studies (Chapter 6.4.1), qPCR analysis was performed to determine the effects of pan-PKC inhibition upon αSMA gene expression levels. Quantification was performed on DFs cultured with either EBC-46 (0.01 and 0.1 µg/mL) or EBC-211 (1 and 10 µg/mL); in the presence of TGF-β_1 (10 ng/mL), and with/without BIM-1 (1 µM), after 72 h culture (Figures 6.3A and B). Compound-free controls with/without TGF-β_1, in the absence or presence of BIM-1, were further included for comparative purposes (Figures 6.3A and B). As reported previously, TGF-β_1-driven differentiation was genotypically indicated via an up-regulation of αSMA gene expression, peaking between 48 - 72 h in culture (Meran *et al.* 2007; Webber *et al.* 2009). Findings were consistent with the previous studies, as approximately 23-fold and 26-fold increases in αSMA gene expression were seen following TGF-β_1 treatment (Figure 6.3A and B, respectively); versus TGF-β_1-negative controls. In addition, BIM-1 treatment did not have any significant effects upon αSMA expression in TGF-β_1-negative DFs (*p = >0.05* for Figure 6.3A and B). However, BIM-1 co-treatment with TGF-β_1 decreased αSMA expression by 2-fold and 3.6-fold (*p = >0.05* and *p = <0.001* for Figures 6.3A and B, respectively); versus TGF-β_1-positive controls.

Cells cultured with EBC-46 (0.01 - 0.1 µg/mL), in the presence of TGF-β_1 (10 ng/mL) and BIM-1 (1 µM), exhibited varying increases in αSMA gene expression; compared to their respective BIM-1-negative counterparts (Figure 6.3A). Following BIM-1 co-treatment, 0.01 µg/mL EBC-46 demonstrated an approximate 1.3-fold up-regulation in αSMA gene expression; versus the expression induced by 0.01 µg/mL EBC-46 and TGF-β_1 treatment only. However, this change was not deemed statistically significant (*p = >0.05*; Figure 6.3A). In contrast, the 3.5-fold increase induced at 0.1 µg/mL EBC-46 following BIM-1 inclusion was considered significant (*p = <0.001*); in comparison to the expression induced by 0.1 µg/mL EBC-46 and TGF-β_1 treatment alone (Figure 6.3A). Such up-regulation corroborated the prior ICC data, in which BIM-1 inclusion abrogated the inhibitory effect of 0.1 µg/mL of EBC-46 on αSMA expression (Figure 3.1E); allowing αSMA stress fibre formation and thus, TGF-β_1-driven, myofibroblast differentiation to occur (Figure 6.1G).

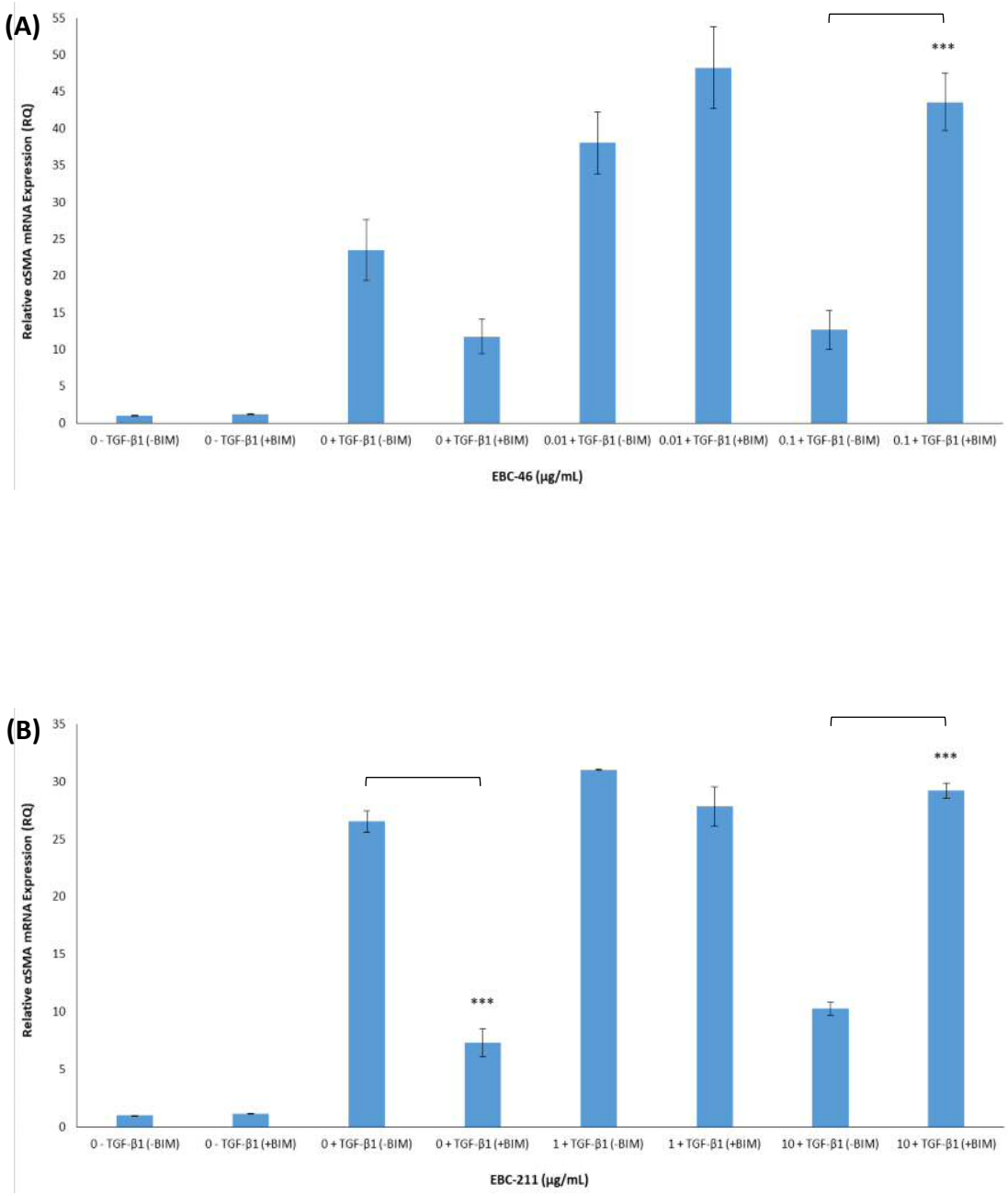

Figure 6.3. Analysis of DF-myofibroblast differentiation via quantification of αSMA gene expression by qPCR; following treatment with (A) EBC-46 (0.01 and 0.1 µg/mL) and (B) EBC-211 (1 and 10 µg/mL), in the presence of TGF-β_1 (10 ng/mL) and ± BIM-1 (1 µM), for 72 h. Compound-free controls ± TGF-β_1 and ± BIM-1 were also included (*n = 3*, mean±SEM; *p = ***<0.001* versus each respective BIM-1-negative control).

DFs cultured with EBC-211 (1 - 10 µg/mL), in the presence of TGF-β_1 (10 ng/mL) and BIM-1 (1 µM), also demonstrated contrasting responses regarding αSMA expression; compared to their respective BIM-1-negative counterparts (Figure 6.3B). After BIM-1 co-treatment, 1 µg/mL EBC-211 showed an approximate 1.1-fold down-regulation in αSMA gene expression; versus the expression induced by 1 µg/mL EBC-211 and TGF-β_1 alone. However, this difference was not deemed statistically significant (*p = >0.05*; Figure 6.3B). In contrast, significant 2.9-fold up-regulation was induced at 10 µg/mL EBC-211 post-BIM-1 and TGF-β_1 co-treatment (*p = <0.001*); versus αSMA expression stimulated by 10 µg/mL EBC-211 and TGF-β_1 alone (Figure 6.3B). This increase again reflected the prior ICC data, in which BIM-1 inclusion abrogated the inhibitory effect of 10 µg/mL EBC-211 on αSMA expression (Figure 3.2G); allowing TGF-β_1-driven DF-myofibroblast differentiation to occur (Figure 6.1I).

6.4.3 Effects of Gö6976 on αSMA Stress Fibre Formation

To determine whether classical-PKC (α and βI isoforms) inhibition altered the effects of EBC-46 and EBC-211 on myofibroblast differentiation (Chapter 3), similar studies to those described previously (Chapter 6.4.1) were performed with Gö6976, instead of BIM-1. Representative images obtained are exhibited in Figures 6.4 and 6.5. Non-compound controls with/without TGF-β_1, in the absence/presence of Gö6976, were also included for comparison purposes (Figures 6.4 and 6.5A - D); as well as primary antibody-free controls Figures 6.4J and 6.5J). As previously (Chapter 6.4.1), TGF-β_1-negative control DFs exhibited elongated, spindle-shaped morphologies with lack of stress fibre formation (Figures 6.4A and 6.5A); no obvious differences were observed upon Gö6976 inclusion (Figures 6.4B and 6.5B). As displayed previously upon TGF-β_1 treatment (Chapter 6.4.1), stress fibre formation and polygonal morphologies were observed (Figures 6.4 and 6.5C). This was also the case for Gö6976/TGF-β_1-positive cells (Figures 6.4D and 6.5D).

Cells cultured with EBC-46 (0.001 - 10 µg/mL), in the presence of TGF-β_1 (10 ng/mL) and Gö6976 (1 µM; Figure 6.4E - I), exhibited similar characteristics to those shown by cells following both TGF-β_1- and TGF-β_1/Gö6976-positive treatment (Figure 6.4C

and D, respectively). Cells at all EBC-46 concentrations demonstrated similar αSMA localisation, stress fibre formation and polygonal morphology (Figure 6.4E - I) to DFs observed in the aforementioned controls (Figure 6.4C and D). Findings were similar to those found following treatment with the same concentrations of EBC-46, in the presence of TGF-β_1, without Gö6976 inclusion (Figure 3.1C - D and F - G); barring at 0.1 µg/mL (Figure 3.1E). Gö6976 co-treatment with TGF-β_1 and EBC-46 at 0.1 µg/mL abrogated the inhibitory effects found previously at this concentration (Figure 3.1E); with cells displaying myofibroblast morphologies (Figure 6.4G), comparable to those observed in both TGF-β_1-only and TGF-β_1/Gö6976-positive controls (Figure 6.4C and D, respectively), as well as all other EBC-46 concentrations (Figure 6.4E - F and H - I).

Similar results were found when DFs were cultured with EBC-211 (0.001 - 10 µg/mL), in the presence of TGF-β_1 (10 ng/mL) and Gö6976 (1 µM; Figure 6.5E - I). At all EBC-211 concentrations, cells demonstrated comparable αSMA localisation, stress fibre formation and polygonal morphologies (Figure 6.5E - I) to DFs observed in both TGF-β_1-alone and TGF-β_1/Gö6976-positive controls (Figure 6.5C and D, respectively). The findings were consistent with those observed following EBC-211 treatment with the same concentrations, in the presence of TGF-β_1, and absence of Gö6976 (Figure 3.2C - F); barring at 10 µg/mL EBC-211 (Figure 3.2G). Gö6976 co-treatment with 10 µg/mL EBC-211 and TGF-β_1 abrogated the inhibitory effect shown previously (Figure 3.2G). DFs exhibited myofibroblast phenotypes (Figure 6.5I), similar to those found in both TGF-β_1-alone and TGF-β_1/Gö6976-positive controls (Figure 6.5C and D, respectively), as well as the other EBC-211 concentrations (Figure 6.5E - H).

6.4.4 Effects of Gö6976 on αSMA Gene Expression

As with BIM-1 studies, following the ICC studies (Chapter 6.4.3), qPCR was performed to determine the effects of classical PKC inhibition on αSMA gene expression. Similar studies to those described previously (Chapter 6.4.2) were performed with Gö6976, instead of BIM-1 (Figures 6.6A and B). Epoxy-tigliane-free controls, in the absence or presence of TGF-β_1, and with/without Gö6976, were further included for comparison purposes (Figures 6.6A and B). As previously (Chapter 6.4.2), results were consistent

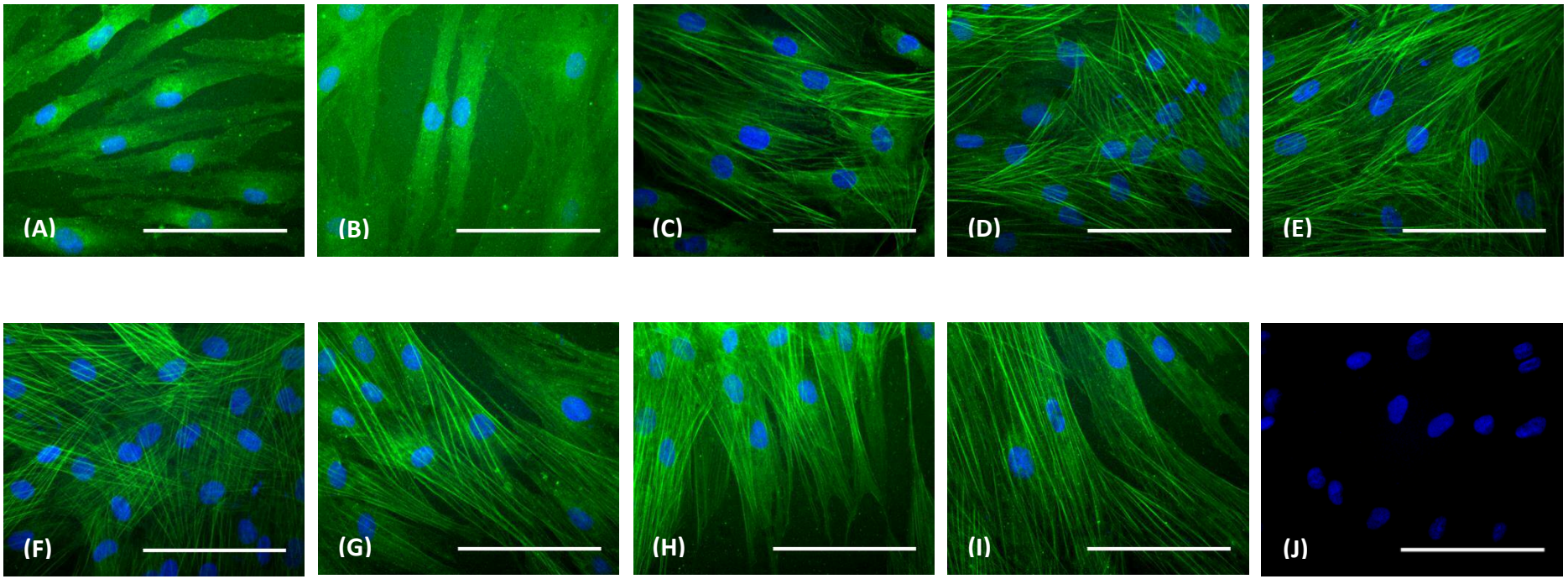

Figure 6.4. ICC analysis of DF-myofibroblast differentiation via visualisation of αSMA localisation and stress fibre formation (green), following treatment with (E) 0.001 µg/mL, (F) 0.01 µg/mL, (G) 0.1 µg/mL, (H) 1 µg/mL and (I) 10 µg/mL EBC-46; in the presence of TGF-β_1 (10 ng/mL) and Gö6976 (1 µM), for 72 h. TGF-β_1-negative and TGF-β_1-positive compound-free controls, in the absence of Gö6976 (A and C, respectively), were included; as well as TGF-β_1-negative and TGF-β_1-positive compound-free controls, in the presence of Gö6976 (B and D, respectively). Moreover, primary antibody-free controls (J) were included and nuclei were visualised by Hoechst stain (blue). Images shown represent *n = 3* independent experiments captured at x400 magnification (scale bar = 100 µm).

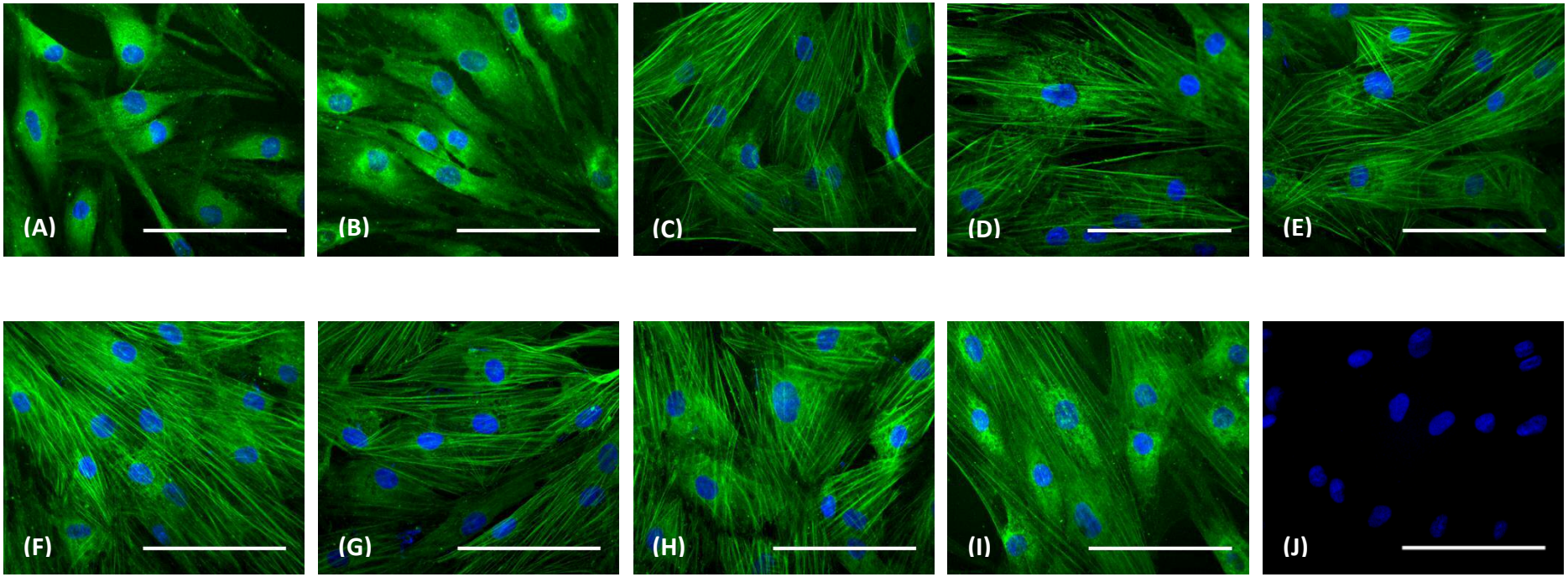

Figure 6.5. ICC analysis of DF-myofibroblast differentiation via visualisation of αSMA localisation and stress fibre formation (green), following treatment with (E) 0.001 µg/mL, (F) 0.01 µg/mL, (G) 0.1 µg/mL, (H) 1 µg/mL and (I) 10 µg/mL EBC-211; in the presence of TGF-β_1 (10 ng/mL) and Gö6976 (1 µM), for 72 h. TGF-β_1-negative and TGF-β_1-positive compound-free controls, in the absence of Gö6976 (A and C, respectively), were included; as well as TGF-β_1-negative and TGF-β_1-positive compound-free controls, in the presence of Gö6976 (B and D, respectively). Moreover, primary antibody-free controls (J) were included and nuclei were visualised by Hoechst stain (blue). Images shown represent *n = 3* independent experiments captured at x400 magnification (scale bar = 100 µm).

with reported studies, as approximately 28-fold up-regulations in αSMA expression were demonstrated after TGF-β_1 treatment alone (Figure 6.6A and B, respectively); versus the TGF-β_1-negative controls. In addition, Gö6976 treatment did not have any significant effects upon αSMA gene expression in TGF-β_1-negative DFs (*p = >0.05* for Figure 6.6A and B). However, Gö6976 co-treatment with TGF-β_1 up-regulated αSMA expression by approximately 1.2-fold and 1-fold (*p = <0.05* and *p = >0.05* for Figure 6.6A and B, respectively); versus TGF-β_1-positive controls.

Cells cultured with EBC-46 (0.01 - 0.1 µg/mL), in the presence of TGF-β_1 (10 ng/mL) and Gö6976 (1 µM), demonstrated varying up-regulations in αSMA gene expression; compared to their respective Gö6976-negative counterparts (Figure 6.6A). Following Gö6976 treatment, 0.01 µg/mL EBC-46 exhibited an approximate 1.2-fold significant increase in αSMA gene expression; in comparison to the expression induced by 0.01 µg/mL and TGF-β_1 treatment alone (*p = <0.001*; Figure 6.6A). Furthermore, a greater increase was induced at 0.1 µg/mL EBC-46 following Gö6976 treatment (2.5-fold; *p = <0.001*); versus the expression induced by 0.1 µg/mL and TGF-β_1 treatment alone (Figure 6.6A). This increase is consistent with previous ICC studies, in which Gö6976 inclusion was found to abrogate the inhibitory effect displayed by 0.1 µg/mL EBC-46 previously (Figure 3.1E); allowing the formation of αSMA stress fibres and thus, TGF-β_1-driven, myofibroblast differentiation to occur (Figure 6.4G).

Comparable results to those induced by EBC-46 were demonstrated when DFs were cultured with EBC-211 (1 - 10 µg/mL), in the presence of both TGF-β_1 (10 ng/mL) and Gö6976 (1 µM). After Gö6976 treatment, 1 µg/mL EBC-211 exhibited approximately 1.2-fold significant increase in αSMA expression; versus gene expression induced by EBC-211 1 µg/mL and TGF-β_1 alone (*p = <0.001*; Figure 6.6B). Furthermore, a greater increase was induced at 10 µg/mL of EBC-211 after Gö6976 treatment (1.7-fold; *p = <0.001*); versus the αSMA expression observed post-10 µg/mL and TGF-β_1 treatment alone (Figure 6.6B). This up-regulation is consistent with the findings of previous ICC studies, in which Gö6976 was found to abrogate the inhibitory effect demonstrated previously by 10 µg/mL EBC-211 (Figure 3.2G); allowing αSMA stress fibre formation

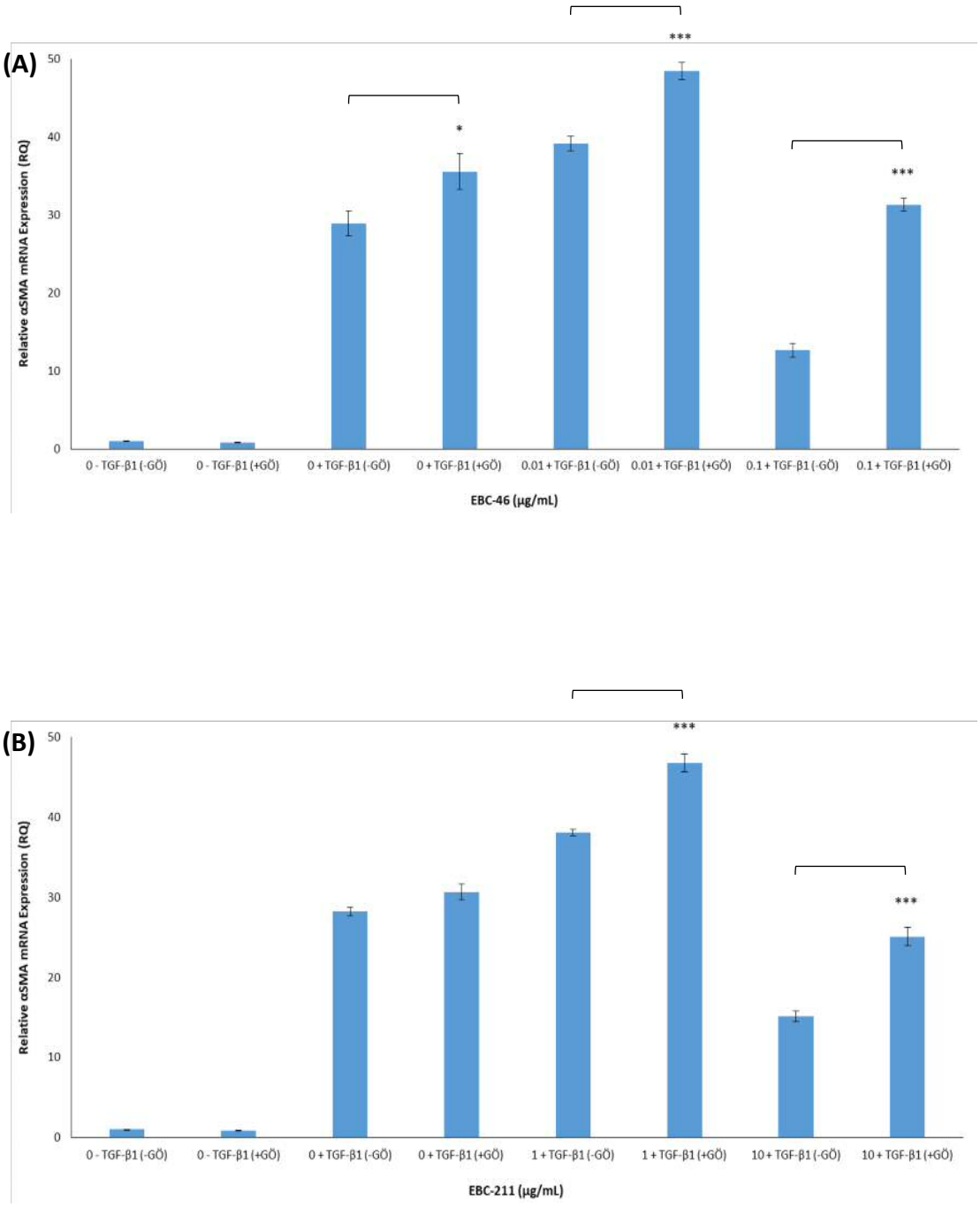

Figure 6.6. Analysis of DF-myofibroblast differentiation via quantification of αSMA gene expression by qPCR; following treatment with (A) EBC-46 (0.01 and 0.1 µg/mL) and (B) EBC-211 (1 and 10 µg/mL), in the presence of TGF-β_1 and ± Gö6976 (1 µM), for 72 h. Compound-free controls ± TGF-β_1 (10 ng/mL) and ± Gö6976 were included (*n = 3*, mean±SEM; *p = *<0.05, ***<0.001* versus each respective Gö6976-negative control).

and thus, TGF-β_1-driven, DF-myofibroblast differentiation to occur (Figure 6.5I).

6.5 Discussion

The present Chapter focused upon assessing whether the preferential modulation of the DF/myofibroblast genotype and phenotype induced by certain concentrations of the epoxy-tiglianes, EBC-46 and EBC-211; were mediated through PKC activation and downstream signalling pathways. As previously described (Chapter 6.1), EBC-46 has been demonstrated to induce its anti-cancer properties primarily through the PKC-β isoforms; and via PKC-α and -γ to a lesser degree (Boyle *et al*. 2014). As such, it was hypothesised that the wound repair responses exhibited both *in vivo* and *in vitro* are modulated via PKC signalling also; particularly via the classical PKC isoforms (Reddell *et al*. 2014). Given such findings and those of previous Chapters, it was hypothesised that the epoxy-tigliane effects on TGF-β_1-driven differentiation involve PKC activation and modulation of downstream signalling pathways. Greater understanding of the underlying epoxy-tigliane mechanisms of action on DFs/myofibroblasts is necessary to pursue EBC-46 and EBC-211 as novel wound healing agents and to facilitate their progression towards human clinical trials.

It has been well-documented that signal transduction networks regulate conversion of environmental prompts into cellular actions. Protein kinases are among the main influencers within such networks, acting to acutely and reversibly modulate protein functions; and subsequently affecting cellular events (Rosse *et al*. 2010). As detailed prior (Chapter 6.1), members of the PKC family have been increasingly implicated in cell signalling and propagation; with examples of their orchestration becoming more apparent, concerning the regulation of diverse downstream processes, including cell migration and differentiation (Battaini and Mochly-Rosen, 2007; Rosse *et al*. 2010). These conclusions have fuelled research interest regarding the possible involvement of PKC isoforms in wound repair; gaining greater attention over the last ten years, in particular. However, as an emerging field, deeper understanding and clarification of the roles of specific PKC isoforms in cells critical to wound closure is required (Rui *et al*. 2017). Various studies have contributed to delineating whether PKCs are involved

in both keratinocyte and DF responses; with many using PKC inhibitors to elucidate which isoforms may contribute to cell-specific functions, such as re-epithelialisation and wound contraction (Leask *et al*. 2008; Thomason *et al*. 2012). BIM-1, a pan-PKC ligand, is endowed with high affinity towards different isoforms and possesses good selectivity for PKC over other kinases. Additionally, Gö6976 has emerged as a potent and selective inhibitor of the conventional PKC isozymes (Martiny-Baron *et al*. 1993; Davies *et al*. 2000; Bain *et al*. 2007; Anastassiadis *et al*. 2011; Rui *et al*. 2017). Thus, BIM-1 and Gö6976 were utilised to determine whether PKCs are involved in TGF-β_1-driven DF-myofibroblast differentiation; and particularly, whether inhibitory effects induced by EBC-46 and EBC-211 at certain concentrations are modulated by PKCs.

As the initial studies undertaken (Chapter 3) demonstrated that the epoxy-tiglianes are capable of modulating αSMA gene expression and stress fibre formation, similar studies were performed, in the presence of BIM-1 or Gö6976, to determine whether PKC signalling is fundamental to the modulatory effects of EBC-46 and EBC-211 upon DF-myofibroblast genotype/phenotype and formation. Following co-treatment with TGF-β_1 and BIM-1, cells cultured with EBC-46 or EBC-211 (0.001 - 10 μg/mL) showed no major changes in αSMA localisation or stress fibre development to those treated with TGF-β_1 alone. This was also shown to be the case with the comparable studies, after co-treatment with Gö6976 at the same concentrations. At each concentration, cells showed bundles of parallel αSMA-positive stress fibres, coupled with polygonal morphologies; typically observed post-stimulation with TGF-β_1 (Gabbiani *et al.* 1971; Sandbo and Dulin, 2011). In contrast, as evident in Chapter 3, cells in the absence of PKC inhibitors, and presence of TGF-β_1, at 72 h displayed a lack of αSMA stress fibre formation at 0.1 μg/mL and 10 μg/mL EBC-46 and EBC-211, respectively; exhibiting elongated, spindle-shaped morphologies. Thus, both BIM-1 and Gö6976 treatment was shown to abrogate the concentration-specific inhibitory effects of both EBC-46 and EBC-211 on myofibroblast formation; allowing DF-myofibroblast differentiation to take place. These observations were validated via qPCR studies, which displayed significant increases in αSMA gene expression at both 0.1 μg/mL and 10 μg/mL EBC-46 and EBC-211, respectively; following co-treatment with TGF-β_1 and BIM-1; versus their respective BIM-1-negative counterparts. In contrast, no significant differences

were found at the other doses investigated. Regarding EBC-211, significant increases in αSMA gene expression were demonstrated for all concentrations of EBC-46 (0.01 - 0.1 μg/mL) and EBC-211 (1 - 10 μg/mL) post-TGF-β_1/Gö6976 treatment; compared to their respective Gö6976-negative counterparts. Therefore, together, such findings suggest that the anti-fibrotic effects of the epoxy-tiglianes are PKC-dependent. Also, the Gö6976 studies suggest that such effects are modulated by the activation of the classical PKC isoforms (α, βI, βII and γ).

With regards to the role of classical PKC isoforms in regulating DF and myofibroblast responses, little is known despite PKC-α's identification as the predominant isoform in human DFs (Choi *et al*. 1998). However, PKC-α's role in fibroblasts/myofibroblasts at other anatomical sites is more well-known. Differentiation of adventitial fibroblasts to myofibroblasts, after TGF-β_1 treatment, has been shown to be PKC-α-dependent. TGF-β_1 stimulation increased PKC-α gene expression and activity; whereas calphostin C, a PKC inhibitor, inhibited TGF-β_1-induced αSMA expression (Gao *et al*. 2003; Zhou *et al*. 2010). PKC-α has also been found to drive fibroblast activation and subsequent kidney fibrosis; with Gö6976 treatment shown to abrogate this activation (Xue *et al*. 2018). Another classical PKC isoform, PKC-β, has been demonstrated to be involved in a signalling pathway with extracellular signal-regulated kinase (ERK)1/2, resulting in cardiac fibrosis (Su *et al*. 2014).

Unlike research into the classical isoforms, studies into the role of novel and atypical isoforms have been more prevalent. Of the former group, PKC-ε has been shown to be involved in cutaneous wound repair; with PKC-$\varepsilon^{-/-}$ mice exhibiting delayed wound closure and reduced numbers of myofibroblasts, versus wild-type littermates (Leask *et al*. 2008). Moreover, in both the absence and presence of TGF-β_1, DFs from PKC-$\varepsilon^{-/-}$ mice have impaired abilities regarding formation of 'super-mature' focal adhesions (FAs) and αSMA stress fibre formation. PKC's contribution to FA development is not fully understood, yet their formation is associated with PKC stimulation (Woods and Couchman, 1992; Leask *et al*. 2008). Thrombin-induced contractile activities of lung myofibroblasts have also been exhibited to be mediated by PKC-ε (Bogatkevich *et al*.

2003). PKC-$\varepsilon^{-/-}$ mice DFs demonstrated inhibited contractile, adhesive and migratory abilities; and impaired SMAD3 phosphorylation and pro-fibrotic protein production (αSMA, type I collagen, β_1 and α_4 integrins, CCN2 and paxillin); in response to TGF-β_1 (Leask *et al*. 2008). Together, these findings imply that PKC-ε loss significantly affects TGF-β_1 signalling cascades; leading to inhibition of myofibroblast formation/function. Inhibited pro-fibrotic gene/protein expression and DF-myofibroblast differentiation are similar responses to those induced by 0.1 μg/mL and 10 μg/mL EBC-46 and EBC-211, respectively; indicating potential compound-induced reduction in PKC-ε activity. Thus, selectively targeting PKC-ε may be beneficial in clinical situations characterised by excessive dermal fibrosis, such as hypertrophic and keloid scarring.

Another novel isozyme, PKC-δ, has also been linked with DF migratory responses via the stimulation of signal transducer and activator of transcription 3 (STAT3). During wound healing, the Janus-activated kinase (JAK)/STAT3 pathway contributes to cell migration and differentiation; with cytokines aiding in the activation of STAT3 (Sano *et al*. 1999; Tokumaru *et al*. 2005; Song *et al*. 2017). One of these cytokines, platelet-derived growth factor (PDGF), induces the translocation and leading-edge clustering of PKC-δ in DFs. In contrast, the inhibition of endogenous PKC-δ signalling has been shown to inhibit PDGF-induced activation of STAT3 and therefore, DF migration (Fan *et al*. 2006). Additionally, PKC-δ has also been shown to up-regulate fibronectin (FN) expression in DFs post-activation by epidermal growth factor (EGF). This increase in FN was inhibited following treatment with PKC inhibitors, Calphostin C and Rottlerin (Mimura *et al*. 2004). As detailed prior (Chapter 1), FN is an essential component of the wound healing process, promoting cell migration, attachment and spreading; as well as clot formation, development of granulation tissue/extracellular matrix (ECM) and re-epithelialisation (Grinnell *et al*. 1981; Grinnell, 1984). Regarding the synthesis and turnover of ECM, PKC-δ has been implicated in collagen gene regulation in DFs; in both the absence and presence of TGF-β_1. Rottlerin was shown to inhibit type I/III collagen gene expression in normal human DFs; with optimal concentrations leading to 70 - 90 % inhibition of type I collagen production and over 70 % reduction in type III collagen gene expression (Jimenez *et al*. 2001; Jinnin *et al*. 2005). Furthermore, a

study by Moriya *et al*. (2011) implicated PKC-δ in the positive regulation of MMP-13 expression. Activity of the atypical isoform, PKC-ζ, was also shown to increase MMP-1 gene expression in primary human DFs when grown in collagen gels. This induction was abrogated by the PKC inhibitors, BIM-1 and Calphostin C (Xu and Clark, 1997). In conclusion, these activation and inhibition studies into PKC signalling and the role of various isoforms in DF/myofibroblast function, highlight the potential for selectively targeting specific PKC isoforms for clinical benefit. However, greater insight into the roles of classical PKC isoforms in DF/myofibroblast modulation is needed. Regarding the epoxy-tigliane mechanism of action, future PKC inhibition studies will be used to determine the impact of PKC activity, post-compound treatment, upon the gene and protein levels of key ECM components and differentially expressed genes; identified during microarray analysis. Moreover, as the TGF-β_1/SMAD pathway is crucial to DF-myofibroblast differentiation, future research will focus on delineating whether this signalling pathway is modulated by the epoxy-tiglianes; as found with PKC.

Overall, findings from this Chapter indicate that the concentration-specific effects of the epoxy-tiglianes, described in prior Chapters, are PKC-dependent and modulated through their downstream signalling pathways. This also provides evidence towards the hypothesis that the epoxy-tiglianes stimulate common pathways in different cell types; as previous studies have exhibited that the anti-cancer responses induced by EBC-46 are modulated via PKC activation, inducing endothelial cell permeability and subsequent tumour destruction (Boyle *et al*. 2014). Also, through investigating both EBC-211 and EBC-46, the findings suggest that different EBC analogues may activate similar, if not identical, PKC isoforms. If this is the case, this may indicate a potential opportunity for development of a panel of epoxy-tigliane clinical treatments, with a wider therapeutic range; based on analogue activity and potency. However, further research is required utilising a spectrum of selective PKC inhibitors to target specific isoforms. This would aid in clarifying whether PKC activation by the epoxy-tiglianes is group-specific, or whether the effects on DFs are mediated by activation of a sole member of the conventional sub-group. Furthermore, as highlighted by Boyle *et al*. (2014), there is a possibility that other known targets of DAG analogues other than

PKC isoforms, or DAG itself, may be affected by the compounds. Thus, future studies would aim to assess whether EBC-46 and EBC-211 similarly activate molecules other than PKC family members. In conclusion, initial studies suggest that the anti-fibrotic responses induced by the epoxy-tiglianes are PKC-dependent; with modulation likely occurring through activation of the classical isoforms (α, βI, βII and γ). These findings highlight the potential for further development of the compounds as a novel class of therapeutics for clinical situations characterised by excessive scar formation and/or impaired wound contraction; stimulating scarless or potentially regenerative healing outcomes.

Chapter 7

General Discussion

Chapter 7 - General Discussion

7.1 Overview

This PhD study aimed to assess the effects of the naturally occurring epoxy-tiglianes, EBC-46 and EBC-211, upon dermal fibroblast (DF) and myofibroblast wound healing responses *in vitro*. This was performed through culturing DFs with such novel epoxy-tiglianes and observing the effects upon key wound healing responses, including DF-myofibroblast differentiation, extracellular matrix (ECM) component synthesis and turnover and DF/myofibroblast global gene expression. Furthermore, the study also aimed to determine whether the activation of protein kinase C (PKC) contributes to the underlying epoxy-tigliane mechanism of action; as the anti-cancer effects of EBC-46 have been exhibited to occur through classical PKC activation, in particular, the β isoforms (Boyle *et al*. 2014). Also, the enhanced human keratinocyte cell line of skin origin (HaCaT) responses, induced by both epoxy-tiglianes *in vitro,* are mediated by classical PKC activation (currently unpublished data). Thus, it was hypothesised that any preferential effects exerted by the epoxy-tiglianes would involve PKC activation.

Previously undertaken *in vivo* animal studies and veterinary clinical trials performed by the QBiotics Group have demonstrated the exceptional wound healing responses induced after epoxy-tigliane treatment; with treated skin showing rapid granulation tissue development, keratinocyte re-epithelialisation, wound resolution and closure; as well as minimal scar formation (Campbell *et al*. 2014, 2017; Reddell *et al*. 2014). Such findings highlighted the necessity to determine how the novel epoxy-tiglianes influence two of the primary cell types involved in wound repair: keratinocytes and DFs. EBC-46 and EBC-211 have been demonstrated to stimulate HaCaT proliferation and migration (Moses, 2016); however, little was known on how the epoxy-tiglianes exert their anti-scarring properties. As DFs and myofibroblasts are key mediators of ECM synthesis/turnover, wound contraction and scarring, they represented feasible targets for the modulatory actions of the epoxy-tiglianes; especially due to the anti-fibrotic effects demonstrated in *in vivo*. Consequently, it was hypothesised that the

novel epoxy-tiglianes, EBC-46 and EBC-211, may induce a more regenerative healing response; versus the normal adult reparative process, which often culminates in scar formation.

7.2 Effects on Dermal Fibroblast-Myofibroblast Differentiation

Post-DF culture with 0.001 - 10 μg/mL EBC-46 or EBC-211, in the presence of TGF-β_1, inhibition of DF-myofibroblast differentiation was evident at certain concentrations of EBC-46 (0.1 μg/mL) and EBC-211 (10 μg/mL); shown through a lack of stress fibre formation and myofibroblast morphology (Desmoulière *et al*. 1993; Gabbiani, 2003; Desmoulière *et al*. 2005). Significantly reduced α-smooth muscle actin (αSMA) gene expression was also exhibited at these concentrations; further confirming the lack of DF-myofibroblast differentiation as, under normal circumstances, TGF-β_1 treatment induces an up-regulation of αSMA expression and its incorporation into stress fibres (Desmoulière *et al*. 1993; Malmström *et al.* 2004). Conversely, other concentrations either showed no difference or the synergistic up-regulation of αSMA expression; as well as the associated phenotypic changes characteristic of differentiation (i.e. αSMA -positive stress fibres and polygonal morphology; Desmoulière *et al*. 1993; Gabbiani, 2003; Desmoulière *et al*. 2005). Accompanying changes in filamentous actin (F-actin) organisation were also found at these concentrations (0.1 μg/mL and 10 μg/mL EBC-46 and EBC-211, respectively). DFs showed less prominent cytoskeletal organisation and despite the presence of polymerised F-actin, cells retained elongated, spindle-shaped morphologies; with less apparent fibres, localised more prominently around the cell periphery. These responses are akin to those demonstrated by oral mucosal fibroblasts (OMFs) following exposure to TGF-β_1 stimulation; and these cells possess an inherent resistance to TGF-β_1-driven differentiation (Meran *et al.* 2007; Dally *et al.* 2017). In contrast, other concentrations exhibited no major differences in F-actin re-organisation versus the TGF-β_1-positive control; exhibiting prominent cytoskeletal re-arrangement and larger, polygonal morphologies. The above investigations were also performed in the absence of TGF-β_1; however, no major differences were found in αSMA stress fibre formation/gene expression or F-actin re-arrangement across all concentrations; versus the TGF-β_1-negative controls. Due to the lack of modulatory

effects in the absence of TGF-β_1, it was decided that only TGF-β_1-stimulated studies would be taken forward. Inhibition of DF-myofibroblast differentiation at 0.1 μg/mL and 10 μg/mL EBC-46 and EBC-211, respectively, following 72 h treatment, was also found to be present at earlier time-points; indicating the complete inhibition, rather than reversal, of the myofibroblast phenotype. Yet, extra domain-A-fibronectin (EDA-FN) gene expression was shown to be up-regulated at every concentration analysed over the course of 72 h; however, greater expression was still exhibited at the lower concentrations (0.01 μg/mL and 1 μg/mL EBC-46 and EBC-211, respectively). Finally, no major differences were discerned across all concentrations of EBC-46 or EBC-211 (0.001 - 10 μg/mL) analysed; with regards to cluster of differentiation 44 (CD44) and epidermal growth factor receptor (EGFR) expression. However, all concentrations of both EBC-46 and EBC-211 demonstrated a down-regulation of TNF-stimulated gene-6 (TSG6) gene expression.

Alterations in normal DF and myofibroblast function are evident in both preferential and detrimental healing processes, such as early-gestational foetal and oral mucosal wound repair or excessive scarring situations, respectively (Shih *et al*. 2010; Glim *et al.* 2014). The findings summarised above support the preferential healing outcomes demonstrated post-epoxy-tigliane treatment during the *in vivo* veterinary trials and studies; during which the wounds healed with minimal scar formation (Campbell *et al*. 2014, 2017; Reddell *et al*. 2014). These characteristics are also exhibited in early-gestational and oral mucosal healing scenarios, indicating the potential of analogous responses following epoxy-tigliane treatment. It is well-established that phenotypic differences exist between adult DFs and those present within the above-mentioned preferential tissues (Lee and Eun, 1999; Mak *et al*. 2009; Yagi *et al.* 2016). Before the end of the second trimester of gestation, scarless healing has been demonstrated to occur following foetal injury; resulting in normal skin architecture at the wound site (Lorenz *et al*. 1992; Lorenz and Adzick, 1993; Larson *et al*. 2010). Foetal wounds heal rapidly, and with a lack of scar formation, due to the fibroblast population exhibiting increased migratory and proliferative abilities (Lorenz *et al.* 1993; Larson *et al.* 2010). Furthermore, it is currently thought that myofibroblasts are either negligibly present

or absent in foetal wounds (Larson *et al*. 2010). With regards to oral mucosal wound repair, as briefly aforementioned, OMFs are intrinsically resistant to TGF-β_1-induced differentiation. Following TGF-β_1 stimulation, they exhibit a lack of αSMA stress fibre development and αSMA gene expression (Meran *et al*. 2007; Dally *et al*. 2017). Such responses are comparable to those observed post-treatment with 0.1 μg/mL and 10 μg/mL EBC-46 and EBC-211, respectively. Despite lacking contractile cells, wounds of the oral mucosa still heal; which may be similar to what takes place following epoxy-tigliane treatment *in vivo*, resulting in reduced scarring (Campbell *et al*. 2014, 2017; Reddell *et al*. 2014).

Regarding the biphasic, concentration-dependent effects epoxy-tiglianes induce on DF-myofibroblast differentiation, it is not yet fully understood why these inhibitory responses only occur at 0.1 μg/mL and 10 μg/mL EBC-46 and EBC-211, respectively, but not at the other concentrations; hypothesised as due to contrasting activation, distribution and localisation of PKC isoforms. Also, it would be of interest to identify the comparable concentrations used during the *in vivo* studies. This is of particular interest due to the narrow concentration range at which both of the epoxy-tiglianes produce these 'anti-fibrotic' responses *in vitro*.

7.3 Effects on Extracellular Matrix Composition

Concentration-dependent effects were also evident after epoxy-tigliane treatment, with regards to the gene/protein expression of key ECM components. Following 0.1 μg/mL and 10 μg/mL EBC-46 and EBC-211 treatment, respectively; type I and type III collagen gene and protein expression was reduced, while matrix metalloproteinase-1 (MMP1) gene expression was highly up-regulated. At all other concentrations, the gene and protein expression levels of type I collagen either showed no difference or synergistic up-regulation; versus the TGF-β_1 positive control. No major differences in type III collagen gene expression were induced across all other concentrations also (except at 0.001 μg/mL EBC-46); though reduced type III collagen protein detection levels were apparent over a wider range of epoxy-tigliane concentrations, and were time-dependent (0.1 - 10 μg/mL EBC-46 at 24 h and 0.1 - 10 μg/mL EBC-211 at 72 h).

Lastly, though MMP-1 expression was found to be up-regulated at all epoxy-tigliane concentrations, only the increases exhibited at 0.1 μg/mL and 10 μg/mL EBC-46 and EBC-211, respectively; were significant. Regarding elastin, across all concentrations of both epoxy-tiglianes, the gene expression was up-regulated. However, these were only significant at the lower concentrations of EBC-46 (0.001 - 0.01 μg/mL) and at all EBC-211 concentrations; except 10 μg/mL. Interestingly, the lowest increases in ELN expression were seen at 0.1 μg/mL and 10 μg/mL EBC-46 and EBC-211, respectively. Conversely, no clear differences in protein detection were discerned following EBC-46 treatment at either 24 or 72 h; whereas with EBC-211, comparable protein levels were shown at most concentrations (0.001 - 0.1 μg/mL) after 24 h, with lower levels observed at 1 - 10 μg/mL. Due to the inconsistent nature of the antibody detection, further work into elastin quantification would be required to fully elucidate whether responses observed at the genotypic level are translated to the phenotypic level.

Regarding hyaluronan (HA) synthesis, hyaluronan synthase (HAS2) gene expression was up-regulated at all concentrations of both epoxy-tiglianes, at every time-point. However the greatest and most significant increases were shown at 0.1 μg/mL and 10 μg/mL EBC-46 and EBC-211, respectively. In contrast, HAS3 expression was only significantly up-regulated at 0.01 and 1 μg/mL EBC-46 and EBC-211, respectively; at each time-point. Overall, the most significant increases by the epoxy-tiglianes were with HAS2 expression; whereas HAS1 was mostly down-regulated or unaffected and HAS3 up-regulation was concentration-dependent. Total HA protein production was found to be up-regulated at all concentrations (0.001 - 10 μg/mL) following EBC-46 and EBC-211 treatment. However, such increases were only significant at 0.1 μg/mL EBC-46 and 1 - 10 μg/mL EBC-211. Lastly, the cells at all concentrations of the epoxy-tiglianes (except at 0.1 and 10 μg/mL EBC-46 and EBC-211, respectively) appeared to possess larger HA coats. However, despite the inhibition of differentiation evident at 0.1 and 10 μg/mL EBC-46 and EBC-211, respectively, cells showed HA coat formation; this indicates the presence of cells with intermediate phenotypes between DFs and myofibroblasts.

The results summarised above corroborate the previous findings (Section 7.2), which indicate that specific epoxy-tigliane concentrations inhibit differentiation. Previous studies support this as normally, TGF-β_1 triggers a transcriptional programme which favours collagen deposition via up-regulation of type I collagen gene expression and down-regulation of MMP-1 gene expression (Bujor *et al.* 2008; Fineschi *et al*. 2006; Goffin *et al.* 2010). The findings detailed here demonstrate that both epoxy-tiglianes inhibit collagen synthesis and induce MMP expression; potentially leading to greater proteolytic ECM remodelling and faster collagen degradation/turnover, which would promote an anti-fibrotic wound environment. Conversely, excessive dermal fibrosis is characterised by excessive accumulation of ECM components (Ehrlich *et al.* 1994; Gauglitz *et al.* 2011). Keloid and hypertrophic scars exhibit exacerbations of normal DF phenotypes; subsequently leading to excessive collagen synthesis (Schmid *et al.* 1998; Lee *et al.* 1999). Hypertrophic and keloid-derived fibroblasts have been found to possess reduced MMP-1 expression and demonstrate a lack of responsiveness to cytokines typically found to stimulate MMP-1 expression (Ghahary *et al.* 1996; Dasu *et al.* 2004; Smith *et al.* 2008; Eto *et al.* 2012). However, in early-gestational wounds and oral mucosal wounds, cells positive for type I collagen were significantly reduced (Wong *et al*. 2009; Glim *et al*. 2013). Furthermore, as found following epoxy-tigliane treatment, there is greater MMP activity than tissue inhibitor of MMP (TIMP) activity in scarless healing scenarios; favouring earlier tissue remodelling and faster collagen turnover (Dang *et al*. 2003; Yagi *et al*. 2016; Moore *et al.* 2018). In addition, elevated and more persistent HA synthesis has been shown in early-gestational wounds, as a result of up-regulated HAS expression (Longaker *et al*. 1989; Mast *et al*. 1995; West *et al*. 1997). Therefore, the effects upon key ECM components following treatment with certain epoxy-tigliane concentrations appear analogous to those demonstrated by cells of scarless healing tissues. Also, the responses appear to support those seen in vivo, including rapid granulation tissue formation and re-formation of appendages (Campbell *et al*. 2014, 2017; Reddell *et al*. 2014). The latter is also noted to occur in early-gestational repair, but absent following adult dermal repair (Lorenz *et al*. 1993; Leung *et al*. 2012).

7.4 Genotypic and Phenotypic Responses

Following the beneficial responses observed in previous Chapters on key DF wound healing responses, it was essential to determine the genotypic responses following epoxy-tigliane treatment. There were a plethora of genes differentially expressed at both 24 h and 72 h; with bigger differences in the amount of differentially expressed genes between the epoxy-tigliane concentrations, than those observed between the two analogues themselves; which possess similar gene expression profiles overall. In addition, there were a greater number of genes differentially expressed at 0.1 μg/mL and 10 μg/mL EBC-46 and EBC-211, respectively, at both time-points; corroborating the previous findings of the 'anti-fibrotic' nature of these concentrations. There are numerous differentially expressed genes involved in producing preferential (i.e. oral mucosal healing and early-gestational healing) or detrimental (i.e. hypertrophic and keloid scars) wound healing responses (Sayah *et al*. 1999; Colwell *et al*. 2008; Seifert *et al*. 2008; Chen *et al*. 2010; Hahn *et al*. 2013; Turabelidze *et al*. 2014; Huang *et al*. 2015; Tan *et al*. 2015). As such, these studies were undertaken to elucidate potential gene expression changes relating to preferential DF responses.

The main areas of interest with regards to the differentially expressed genes include myofibroblast formation-related genes, growth factor-related genes, cell signalling-related genes, cytoskeleton-related genes, cell adhesion/migration-related genes, ECM-related genes and proteinases/proteinase inhibitor-related genes. In particular, the differentially expressed genes in the myofibroblast-related, cytoskeleton-related, ECM-related and protease/protease inhibitor-related gene categories corroborated the findings of previous Chapters. Epoxy-tiglianes were generally found to suppress DF genes associated with myofibroblast formation; with the greatest changes taking place at 0.1 μg/mL and 10 μg/mL of EBC-46 and EBC-211, respectively. Cytoskeletal-related genes were generally contrastingly differentially expressed; with inhibitions at the higher concentrations and increases at lower concentrations. Such differences corroborate the findings of Chapter 3, in which 0.1 and 10 μg/mL of EBC-46 and EBC-211, respectively, were found to induce 'anti-fibrotic' responses; whereas 0.01 and 1 μg/mL EBC-46 and EBC-211, respectively, induced 'pro-fibrotic' responses. Reflecting

the findings of Chapter 4, numerous collagens and collagen-linked genes were down-regulated, among other pro-fibrotic genes; with up-regulated HASs and elastin. The differentially expressed genes of the proteases/protease inhibitor-related category complemented such findings, as various proteases were up-regulated and inhibitors down-regulated. The highly up-regulated MMPs were of particular interest and their genotypic changes were found to translate into highly up-regulated activity levels.

The aforementioned increases in MMP expression and subsequent activity can result in beneficial or detrimental responses. MMPs are crucial in allowing the migration of both DFs and keratinocytes into the wound site; which then synthesise/remodel the ECM and establish the epidermal barrier, respectively (Woodley *et al*. 1985; Werner *et al*. 2007). However, if MMP expression is prolonged or excessive, this can lead to detrimental responses; such as those observed in chronic wounds (Cook *et al*. 2000; Caley *et al*. 2015). Through the *in vivo* studies performed by the QBiotics Group, we are aware of the efficacy of the epoxy-tiglianes in veterinary wounds, and it appears that MMP levels are optimal; as evidenced by the lack of chronic wounds instigated following treatment. Optimal MMP levels are also found in early-gestational wounds, as detailed prior (Section 7.3). Overall, highly increased MMP activity, in combination with reduced collagen expression and up-regulated HA levels, would favour a more pliable, hydrated ECM subjected to more rapid proteolytic turnover. This situation is further complemented by the evident inhibition of DF-myofibroblast differentiation, which appears to be, at least partly, modulated by down-regulation of myofibroblast formation-related and cytoskeletal-related genes; as well as alterations in genes and growth factors relating to the TGF-β and BMP signalling pathways. Collectively, such differences are reminiscent of those exhibited in early-gestational and oral mucosal healing scenarios; providing further clarification of the underlying DF/myofibroblast mechanisms of action within epoxy-tigliane treated skin.

7.5 Protein Kinase C Involvement in Epoxy-Tigliane-Induced Responses

As the epoxy-tigliane-stimulated anti-cancer effects and the aforementioned HaCaT responses have been shown to occur through classical PKC activation (β isoforms, in

particular), it was theorised that any beneficial effects exerted by the epoxy-tiglianes upon DFs/myofibroblasts would involve PKC activation (Boyle *et al*. 2014). Inhibitors of PKC were utilised to assess the importance of PKC activity/signalling upon epoxy-tigliane-induced responses; specifically, DF-myofibroblast differentiation. Following DF culture with 0.001 - 10 μg/mL EBC-46 or EBC-211, in the presence of TGF-β_1 and bisindolylmaleimide-1 (BIM-1; pan-PKC inhibitor), cells showed no major differences across all concentrations; versus the TGF-β_1-positive, BIM-1-negative controls. Cells at each concentration displayed αSMA stress fibre formation coupled with polygonal morphologies; typically observed following stimulation with TGF-β_1 alone (Gabbiani *et al.* 1971; Sandbo and Dulin, 2011). This was also the case in similar studies carried out using Gö6976 (α-/βI-PKC inhibitor). Therefore, BIM-1 and Gö6976 were found to abrogate the concentration-specific inhibitory effects of the epoxy-tiglianes upon DF-myofibroblast differentiation (0.1 and 10 μg/mL EBC-46 and EBC-211, respectively). Such observations were validated at the genotypic level, which exhibited significant increases in αSMA gene expression at both 0.1 μg/mL EBC-46 and 10 μg/mL EBC-211 post-72 h co-exposure to TGF-β_1 and BIM-1 or Gö6976; compared to their respective inhibitor-negative counterparts. The other concentrations analysed either displayed no difference or the synergistic up-regulation of αSMA expression upon the inclusion of inhibitor. Together, such studies suggest that the anti-fibrotic effects of the epoxy -tiglianes are PKC-dependent; in particular, modulated via activation of the classical isoforms (α, βI, βII and γ).

As detailed prior (Chapter 6), the PKC family are ubiquitous serine-threonine kinases which upon activation, translocate to membranes and regulate diverse downstream processes; such as cell proliferation, migration and differentiation (Nishizuka, 1992; Battaini and Mochly-Rosen, 2007; Boyle *et al*. 2014). PKC isoform involvement within tissue repair has only been studied in-depth over recent years and little is known on how the PKCs influence DFs/myofibroblasts (Joyce and Meklir, 1992; Rui *et al*. 2017). However, PKC-$\varepsilon^{-/-}$ mice DFs have been found to show inhibited contractile, adhesive and migratory abilities; as well as impaired SMAD3 phosphorylation and pro-fibrotic protein production; following TGF-β_1 treatment (Leask *et al*. 2008). These responses

are similar to those induced by 0.1 and 10 μg/mL EBC-46 and EBC-211, respectively; in response to TGF-β_1. As such, selectively targeting PKC may be beneficial in clinical situations characterised by excessive dermal fibrosis.

7.6 Significance to Regenerative Medicine

The benefit of previously performed *in vivo* veterinary studies and clinical trials was the provision of indications that novel epoxy-tigliane treatment induced preferential wound healing responses; such as rapid granulation tissue formation, wound closure and contraction; in addition to minimal scarring (Campbell *et al*. 2014, 2017; Reddell *et al*. 2014). However, for these epoxy-tiglianes to progress as novel pharmaceutical agents for the clinical treatment of excessive scarring conditions, or to enhance the repair process, a more comprehensive understanding of DF responses to the epoxy-tiglianes and their underlying mechanism of action was required. Of great interest, a number of differentially expressed genes and proteins post-epoxy-tigliane treatment are associated with preferential healing responses; supporting the enhanced wound repair responses observed during the *in vitro* and *in vivo* studies (Colwell *et al*. 2008; Rolfe and Grobbelaar, 2012; Campbell *et al*. 2014, 2017; Reddell *et al*. 2014). As aforementioned, it is hypothesised that the epoxy-tiglianes stimulate a regenerative wound healing response; more reminiscent of early-gestational foetal wound repair or oral mucosal healing (Leung *et al*. 2012; Rolfe and Grobbelaar, 2012; Yates *et al*. 2012). Encouraging the induction of more regenerative healing responses is an area of immense interest and importance; and the potential shown by the epoxy-tiglianes in stimulating more anti-fibrotic DF responses would be of great benefit in excessive scarring situations, such as hypertrophic and keloid scarring (Alster and Tanzi, 2003; Gauglitz *et al*. 2011; Gauglitz, 2013).

As described prior (Chapter 1), despite the wide array of treatment options available for fibrotic disease, it still presents a huge clinical and economic burden; and there is yet a gold-standard therapy available (Atiyeh, 2007; Huang *et al*. 1013; Kaplani *et al*. 2018). Current wound care strategies are clinically unsatisfactory with regards to the treatment of excessive scarring situations, such as hypertrophic and keloid scarring;

as a result, patients may suffer physical, aesthetic and psychological consequences (Dorfmüller, 1995; Taal and Faber, 1998; Robert *et al*. 1999). Indeed, most currently utilised therapies are used for both scar types (Chike-Obi *et al*. 2009; Gauglitz, 2013). Thus, there is an urgent clinical need to develop novel treatment modalities and the novel epoxy-tiglianes show great promise in enhancing wound resolution and easing the impact upon both patients and healthcare providers (Guest *et al*. 2015; Harding, 2015).

Currently, the *in vivo* veterinary studies and clinical trials have only involved EBC-46, as oppose to EBC-211. From the *in vitro* studies, it appears that both analogues exert their responses by the same mechanism; albeit at different concentrations. Thus, it is theorised that EBC-211 would also induce preferential healing outcomes *in vivo*. The former analogue is considered to be of 'lesser activity', and has been demonstrated to possess reduced cytotoxicity, compared to EBC-46. As such, it is possible that EBC-211 could be deemed a more promising therapeutic than EBC-46. However, despite the exceptional responses observed throughout the *in vitro* studies, numerous other cell types are present within the dermal and epidermal layers; including a variety of stem cell and immune cell populations. These also impact the overall healing process and their responses to epoxy-tigliane treatment have not yet been investigated.

7.7 Future Research

With a view to building upon the research performed during this PhD study, further validation of the differentially expressed genes found during the Microarray studies would be beneficial. As genotypic changes are not always evident at the phenotypic level, this would provide further clarification of the proteins influencing the epoxy-tigliane-induced wound healing responses. Moreover, as the epoxy-tiglianes appear to inhibit TGF-β_1-driven DF-myofibroblast differentiation at specific concentrations, it would be pertinent to investigate the effects of the compounds upon the TGF-β_1/ SMAD pathway; the major co-operating pathway to the HA-modulated CD44/EGFR signalling pathway. This would further clarify the effects of the epoxy-tiglianes upon the mechanisms underlying DF-myofibroblast differentiation. Also, although findings

have demonstrated the involvement of PKC activity in the epoxy-tigliane mechanism of action in DFs/myofibroblasts, further studies are required to elucidate the effects of PKC inhibitors, BIM-1 and Gö6976, on the differentially expressed genes discussed during this study. It would be beneficial to carry out a comparative Microarray study, following the inclusion of such inhibitors, to determine the impact of PKC activity on global gene expression. It would be particularly interesting to see whether a reversal effect would be demonstrated. Furthermore, a number of mechanistic studies could identify the impact of specific PKC isoforms upon the responses previously observed. Such analysis could focus on the downstream signalling pathways of PKCs, including MAPK/ERK kinase (MEK)1/2, extracellular signal-regulated kinase (ERK)1/2, mitogen activated protein kinase (MAPK)1/2, janus kinase/signal transducers and activators of transcription (JAK-STAT), Akt, phosphatidylinositide 3-kinase (PI3K) and SMAD. In order to determine the impact on these downstream signalling pathway genes and proteins, quantitative polymerase chain reaction (qPCR) and Western blot analyses would be performed, respectively; using specific pathway inhibitors.

In addition to investigating the effects of the epoxy-tiglianes on DFs, *in vitro* studies could also be performed upon keloid- and hypertrophic scar-derived fibroblasts; to determine whether epoxy-tigliane treatment can induce anti-fibrotic responses in these abnormal cell types, which are fundamental to excessive scarring pathologies (Bran *et al*. 2009; Gauglitz *et al*. 2011). Concerning normal DFs and keratinocytes, it would be of interest to co-culture the cells through use of a 3D organotypic culture system. This could provide insights into how epoxy-tiglianes induce their responses on each cell type, but with incorporation of a strong paracrine feedback system that can be found between these cells. However, this model does not incorporate all cell types involved during wound repair (Maas-Szabowski *et al*. 1999; Lee and Cho, 2005; Sriram *et al*. 2015). More advanced studies could also be performed through the use of animal wound healing models; to determine the histology and tensile strength of the repaired skin tissue after epoxy-tigliane treatment (Davidson, 1998; Ansell *et al*. 2012). Limited availability of animal models for pathological scarring has delayed the elucidation of the underlying cellular and molecular basis of keloid and hypertrophic

scars (Morris *et al*. 1997; van den Broek *et al*. 2014). However, a nude mouse model has been developed, which allows the grafting of full-thickness human skin onto the mouse (Alrobaiea *et al*. 2016). This model will hopefully assist in providing a greater understanding of excessive dermal fibrosis, as keloid or hypertrophic skin could also be grafted onto the mouse (Alrobaiea *et al*. 2016). Wound closure ability and rate at which this occurs can be calculated following experimental treatment modalities via these models; as well as histological assessments of the underlying dermis, in order to elucidate ECM composition and organisation (Alrobaiea *et al*. 2016).

As well as the potential future research opportunities regarding EBC-46 and EBC-211, research is currently ongoing on over 70 different natural and semi-synthetic epoxy-tigliane analogues. Proof-of-efficacy testing is being carried out on many, along with more advanced *in vitro* studies using others. Unlike the narrow concentration ranges of action demonstrated by EBC-46 and EBC-211, other novel analogues have shown anti-fibrotic efficacy and induction of preferential responses over a broader range of concentrations. Examples of two analogues with differing modifications are found in Figure 7.1. EBC-1040 is an analogue with modification of the epoxy group and B ring, whereas EBC-1013 has chain modifications at C12/C13; both of which have exhibited

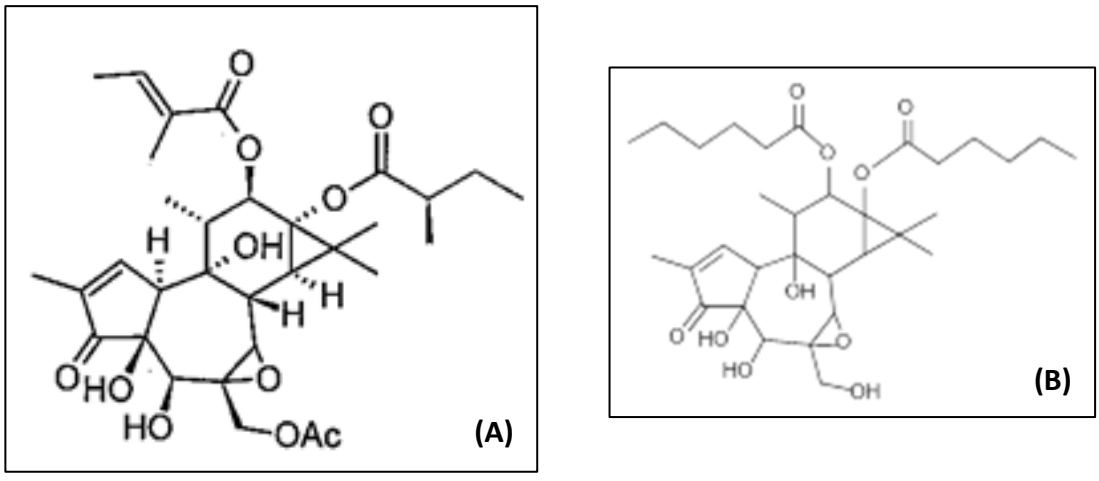

Figure 7.1. The chemical structures of the analogues EBC-1040 (A) and EBC-1013 (B) (QBiotics Group, Yungaburra, Australia).

broader range efficacy during the preliminary studies performed by members of our group, in partnership with the QBiotics Group.

The aims of undertaking the above-mentioned further research would be to further elucidate the underlying mechanism(s) of action of these novel epoxy-tiglianes and determine the dermal composition following treatment. This knowledge would aid in the progression of these epoxy-tiglianes, or similar analogues with wider efficacy ranges, to clinical trials; for the treatment of excessive dermal fibrosis, such as keloid and hypertrophic scarring.

Bibliography

Aarabi, S. *et al*. 2007. Mechanical load initiates hypertrophic scar formation through decreased cellular apoptosis. *FASEB Journal* 21(12), pp. 3250-3261. doi: 10.1096/fj.07-8218com

Abreu, J. *et al*. 2002. Connective-tissue growth factor (CTGF) modulates cell signalling by BMP and TGF-β. *Nature: Cell Biology* 4(8), pp. 599-604. doi: 10.1038/ncb826

Agah, A. *et al*. 2005. Proteolysis of cell-surface tissue transglutaminase by matrix metalloproteinase-2 contributes to the adhesive defect and matrix abnormalities in thrombospondin-2-null fibroblasts and mice. *American Journal of Pathology* 167(1), pp. 81-88. doi: 10.1016/s0002-9440(10)62955-0

Akagi, A. *et al*. 1999. Expression of type XVI collagen in human skin fibroblasts: enhanced expression in fibrotic skin diseases. *Journal of Investigative Dermatology* 113(2), pp. 246-250. doi: 10.1046/j.1523-1747.1999.00663.x

al-Khateeb, T. *et al*. 1997. An investigation of preferential fibroblast wound repopulation using a novel *in vitro* wound model. *Journal of Periodontology* 68(11), pp. 1063-1069. doi: 10.1902/jop.1997.68.11.1063

Alaish, S. *et al*. 1994. Biology of foetal wound healing: hyaluronate receptor expression in foetal fibroblasts. *Journal of Pediatric Surgery* 29(8), pp. 1040-1043.

Albeiroti, S. *et al*. 2015. Hyaluronan's role in fibrosis: a pathogenic factor or a passive player? *BioMed Research International* 2015(1), pp. 1-10. doi: 10.1155/2015/790203

Albinet, V. *et al*. 2014. Dual role of sphingosine kinase-1 in promoting the differentiation of dermal fibroblasts and the dissemination of melanoma cells. *Oncogene* 33(26), pp. 3364-3373. doi: 10.1038/onc.2013.303

Alemany, R. *et al*. 2007. Regulation and functional roles of sphingosine kinases. *Naunyn-Schmiedeberg's Archives of Pharmacology* 374(5-6), pp. 413-428. doi: 10.1007/s00210-007-0132-3

Alonso, L. and Fuchs, E. 2003. Stem cells of the skin epithelium. *Proceedings of the National Academy of Sciences of the USA* 100(1), pp. 11830-11835. doi: 10.1073/pnas.1734203100

Alrobaiea, S. *et al*. 2016. A novel nude mouse model of hypertrophic scarring using scratched full thickness human skin grafts. *Advances in Wound Care* 5(7), pp. 299-313. doi: 10.1089/wound.2015.0670

Alster, T. and Handrick, C. 2000. Laser treatment of hypertrophic scars, keloids, and striae. *Seminars in Cutaneous Medicine and Surgery* 19(4), pp. 287-292. doi: 10.1053/sder.2000.18369

Alster, T. and Tanzi, E. 2003. Hypertrophic scars and keloids: aetiology and management. *American Journal of Clinical Dermatology* 4(4), pp. 235-243. doi: 10.2165/00128071-200304040-00003

Alster, T. and Williams, C. 1995. Treatment of keloid sternotomy scars with 585 nm flashlamp-pumped pulsed-dye laser. *Lancet* 345(8959), pp. 1198-1200.

Amadeu, T. *et al*. 2004. Fibrillin-1 and elastin are differentially expressed in hypertrophic scars and keloids. *Wound Repair and Regeneration* 12(2), pp. 169-174. doi: 10.1111/j.1067-1927.2004.012209.x

Anastassiadis, T. *et al*. 2011. Comprehensive assay of kinase catalytic activity reveals features of

kinase inhibitor selectivity. *Nature Biotechnology* 29(11), pp. 1039-1045. doi: 10.1038/nbt.2017

Ansell, D. *et al*. 2012. Animal models of wound repair: are they cutting it? *Experimental Dermatology* 21(8), pp. 581-585. doi: 10.1111/j.1600-0625.2012.01540.x

Apte, S. *et al*. 1995. The gene structure of tissue inhibitor of metalloproteinases (TIMP)-3 and its inhibitory activities define the distinct TIMP gene family. *Journal of Biological Chemistry* 270(24), pp. 14313-14318.

Arda, O. *et al*. 2014. Basic histological structure and functions of facial skin. *Clinics in Dermatology* 32(1), pp. 3-13. doi: 10.1016/j.clindermatol.2013.05.021

Arndt, S. *et al*. 2015. Enhanced expression of BMP6 inhibits hepatic fibrosis in non-alcoholic fatty liver disease. *Gut* 64(6), pp. 973-981. doi: 10.1136/gutjnl-2014-306968

Arno, A. *et al*. 2014. Up-to-date approach to manage keloids and hypertrophic scars: a useful guide. *Burns* 40(7), pp. 1255-1266. doi: 10.1016/j.burns.2014.02.011

Arthur, W. *et al*. 2002. XPLN, a guanine nucleotide exchange factor for RhoA and RhoB, but not RhoC. *Journal of Biological Chemistry* 277(45), pp. 42964-42972. doi: 10.1074/jbc.M207401200

Asilian, A. *et al*. 2006. New combination of triamcinolone, 5-Fluorouracil, and pulsed-dye laser for treatment of keloid and hypertrophic scars. *Dermatologic Surgery* 32(7), pp. 907-915. doi: 10.1111/j.1524-4725.2006.32195.x

Aspenstrom, P. *et al*. 2004. Rho GTPases have diverse effects on the organisation of the actin filament system. *Biochemical Journal* 377(2), pp. 327-337. doi: 10.1042/bj20031041

Atiyeh, B. 2007. Non-surgical management of hypertrophic scars: evidence-based therapies, standard practices, and emerging methods. *Aesthetic Plastic Surgery* 31(5), pp. 468-494. doi: 10.1007/s00266-006-0253-y

Atmatzidis, D. *et al*. 2017. Langerhans cell: exciting developments in health and disease. *Journal of the European Academy of Dermatology and Venereology* 31(11), pp. 1817-1824. doi: 10.1111/jdv.14522

Badley, R. *et al*. 1980. Cytoskeleton changes in fibroblast adhesion and detachment. *Journal of Cell Science* 43, pp. 379-390.

Badylak, S. 2002. The extracellular matrix as a scaffold for tissue reconstruction. *Seminars in Cell and Developmental Biology* 13(5), pp. 377-383.

Bagabir, R. *et al*. 2012. Site-specific immunophenotyping of keloid disease demonstrates immune up-regulation and the presence of lymphoid aggregates. *British Journal of Dermatology* 167(5), pp. 1053-1066. doi: 10.1111/j.1365-2133.2012.11190.x

Bain, J. *et al*. 2007. The selectivity of protein kinase inhibitors: a further update. *The Biochemical Journal* 408(3), pp. 297-315. doi: 10.1042/bj20070797

Bainbridge, P. 2013. Wound healing and the role of fibroblasts. *Journal of Wound Care* 22(8), pp. 407-412. doi: 10.12968/jowc.2013.22.8.407

Baisden, J. *et al*. 2001. The intrinsic ability of AFAP-110 to alter actin filament integrity is linked with its ability to also activate cellular tyrosine kinases. *Oncogene* 20(45), pp. 6607-6616. doi: 10.1038/sj.onc.1204802

Balasubramani, M. *et al*. 2001. Skin substitutes: a review. *Burns* 27(5), pp. 534-544.

Balza, E. *et al*. 1988. Transforming growth factor-β regulates the levels of different fibronectin isoforms in normal human cultured fibroblasts. *FEBS Letters* 228(1), pp. 42-44.

Bandaru, S. *et al*. 2014. Targeting filamin B induces tumor growth and metastasis via enhanced activity of matrix metalloproteinase-9 and secretion of VEGF-A. *Oncogenesis* 3, pp. 1-9. doi: 10.1038/oncsis.2014.33

Bansal, R. *et al*. 2017. Integrin α_{11} in the regulation of the myofibroblast phenotype: implications for fibrotic diseases. *Experimental and Molecular Medicine* 49(11), pp. 1-16. doi: 10.1038/emm.2017.213

Barara, M. *et al*. 2012. Cryotherapy in treatment of keloids: evaluation of factors affecting treatment outcome. *Journal of Cutaneous and Aesthetic Surgery* 5(3), pp. 185-189. doi: 10.4103/0974-2077.101376

Barczyk, M. *et al*. 2010. Integrins. *Cell and Tissue Research* 339(1), pp. 269-280. doi: 10.1007/s00441-009-0834-6

Barnett, C. *et al*. 2018. Optimising intratumoral treatment of head and neck squamous cell carcinoma models with the diterpene ester, Tigilanol Tiglate. *Investigational New Drugs*, pp. 1-8. doi: 10.1007/s10637-018-0604-y

Baroni, A. *et al*. 2012. Structure and function of the epidermis related to barrier properties. *Clinics in Dermatology* 30(3), pp. 257-262. doi: 10.1016/j.clindermatol.2011.08.007

Barrick, B. *et al*. 1999. Leukocyte proteinases in wound healing: roles in physiologic and pathologic processes. *Wound Repair and Regeneration* 7(6), pp. 410-422.

Barrientos, S. *et al*. 2008. Growth factors and cytokines in wound healing. *Wound Repair and Regeneration* 16(5), pp. 585-601. doi: 10.1111/j.1524-475X.2008.00410.x

Bassino, E. *et al*. 2017. Dermal-epidermal cross-talk: differential interactions with microvascular endothelial cells. *Journal of Cellular Physiology* 232(5), pp. 897-903. doi: 10.1002/jcp.25657

Battaini, F. and Mochly-Rosen, D. 2007. Happy birthday protein kinase C: past, present and future of a superfamily. *Pharmacological Research* 55(6), pp. 461-466. doi: 10.1016/j.phrs.2007.05.005

Bauer, J. *et al*. 2010. Galanin family of peptides in skin function. *EXS* 102(1), pp. 51-59.

Bayat, A. *et al*. 2003. Skin scarring. *British Medical Journal* 326(7380), pp. 88-92.

Bayat, A. *et al*. 2005. Keloid disease: clinical relevance of single versus multiple site scars. *British Journal of Plastic Surgery* 58(1), pp. 28-37. doi: 10.1016/j.bjps.2004.04.024

Beanes, S. *et al*. 2002. Confocal microscopic analysis of scarless repair in the foetal rat: defining the transition. *Plastic and Reconstructive Surgery* 109(1), pp. 160-170.

Beanes, S. *et al*. 2003. Skin repair and scar formation: the central role of TGF-β. *Expert Reviews in Molecular Medicine* 5(8), pp. 1-22. doi: doi:10.1017/S1462399403005817

Bella, J. and Hulmes, D. 2017. Fibrillar Collagens. *Sub-Cellular Biochemistry* 82, pp. 457-490. doi: 10.1007/978-3-319-49674-0_14

Bennett, N. and Schultz, G. 1993. Growth factors and wound healing: Part II. Role in normal and chronic wound healing. *American Journal of Surgery* 166(1), pp. 74-81.

Berendsen, A. *et al*. 2006. Collagen type V enhances matrix contraction by human periodontal

ligament fibroblasts seeded in three-dimensional collagen gels. *Matrix Biology* 25(8), pp. 515-522. doi: 10.1016/j.matbio.2006.07.006

Berman, B. and Duncan, M. 1989. Short-term keloid treatment *in vivo* with human interferon alfa-2b results in a selective and persistent normalisation of keloidal fibroblast collagen, glycosaminoglycan, and collagenase production *in vitro*. *Journal of the American Academy of Dermatology* 21(4), pp. 694-702.

Bernard, K. *et al*. 2018. Glutaminolysis is required for transforming growth factor-β_1-induced myofibroblast differentiation and activation. *Journal of Biological Chemistry* 293(4), pp. 1218-1228. doi: 10.1074/jbc.RA117.000444

Bershadsky, A. *et al*. 2006. Assembly and mechanosensory function of focal adhesions: experiments and models. *European Journal of Cell Biology* 85(3-4), pp. 165-173. doi: 10.1016/j.ejcb.2005.11.001

Bertheim, U. and Hellstrom, S. 1994. The distribution of hyaluronan in human skin and mature, hypertrophic and keloid scars. *British Journal of Plastic Surgery* 47(7), pp. 483-489.

Bettinger, D. *et al*. 1996. The effect of TGF-β on keloid fibroblast proliferation and collagen synthesis. *Plastic and Reconstructive Surgery* 98(5), pp. 827-833.

Birk, D. and Trelstad, R. 1986. Extracellular compartments in tendon morphogenesis: collagen fibril, bundle, and macroaggregate formation. *Journal of Cell Biology* 103(1), pp. 231-240.

Blanpain, C. and Fuchs, E. 2006. Epidermal stem cells of the skin. *Annual Review of Cell and Developmental Biology* 22(1), pp. 339-373. doi: 10.1146/annurev.cellbio.22.010305.104357

Blumenberg, M. and Tomic-Canic, M. 2007. Gene profiling: implications in dermatology. *Expert Review of Dermatology* 2(6), pp. 763-768. doi: 10.1586/17469872.2.6.763

Bochaton-Piallat, M. *et al*. 2016. The myofibroblast in wound healing and fibrosis: answered and unanswered questions. *F1000Research* 26(5), pp. 1-8. doi: 10.12688/f1000research.8190.1

Bock, O. *et al*. 2005. Studies of transforming growth factors-β 1-3 and their receptors I and II in fibroblast of keloids and hypertrophic scars. *Acta Dermato-Venereologica* 85(3), pp. 216-220. doi: 10.1080/00015550410025453

Bogatkevich, G. *et al*. 2003. Contractile activity and smooth muscle α-actin organisation in thrombin-induced human lung myofibroblasts. *American Journal of Physiology: Lung Cellular and Molecular Physiology* 285(2), pp. 334-343. doi: 10.1152/ajplung.00417.2002

Boissy, R. 2003. Melanosome transfer to, and translocation in, the keratinocyte. *Experimental Dermatology* 12(2), pp. 5-12.

Bombaro, K. *et al*. 2003. What is the prevalence of hypertrophic scarring following burns? *Burns* 29(4), pp. 299-302.

Borsi, L. *et al*. 1990. Transforming growth factor-β regulates the splicing pattern of fibronectin messenger RNA precursor. *FEBS Letters* 261(1), pp. 175-178.

Botchkarev, V. and Sharov, A. 2004. BMP signalling in the control of skin development and hair follicle growth. *Differentiation* 72(9), pp. 512-526. doi: 10.1111/j.1432-0436.2004.07209005.x

Bottcher-Haberzeth, S. *et al*. 2010. Tissue engineering of skin. *Burns* 36(4), pp. 450-460. doi: 10.1016/j.burns.2009.08.016

Boulais, N. and Misery, L. 2008. The epidermis: a sensory tissue. *European Journal of Dermatology*

18(2), pp. 119-127. doi: 10.1684/ejd.2008.0348

Boutli-Kasapidou, F. *et al*. 2005. Hypertrophic and keloidal scars: an approach to polytherapy. *International Journal of Dermatology* 44(4), pp. 324-327. doi: 10.1111/j.1365-4632.2004.02570.x

Boyce, D. *et al*. 2001. Inflammatory-cell subpopulations in keloid scars. *British Journal of Plastic Surgery* 54(6), pp. 511-516. doi: 10.1054/bjps.2001.3638

Boyle, G. *et al*. 2014. Intra-lesional injection of the novel PKC activator EBC-46 rapidly ablates tumours in mouse models. *PLoS One* 9(10), pp. 1-12. doi: 10.1371/journal.pone.0108887

Bran, G. *et al*. 2009. Keloids: current concepts of pathogenesis. *International Journal of Molecular Medicine* 24(3), pp. 283-293.

Braverman, I. and Fonferko, E. 1982. Studies in cutaneous ageing: the elastic fibre network. *Journal of Investigative Dermatology* 78(5), pp. 434-443.

Breitkreutz, D. *et al*. 2007. Protein kinase C family: on the crossroads of cell signalling in skin and tumour epithelium. *Journal of Cancer Research and Clinical Oncology* 133(11), pp. 793-808. doi: 10.1007/s00432-007-0280-3

Breitkreutz, D. *et al*. 2013. Skin basement membrane: the foundation of epidermal integrity. BM functions and diverse roles of bridging molecules, nidogen and perlecan. *BioMed Research International* 2013(1), pp. 1-16. doi: 10.1155/2013/179784

Brem, H. *et al*. 2007. Molecular markers in patients with chronic wounds to guide surgical debridement. *Molecular Medicine* 13(1), pp. 30-39. doi: 10.2119/2006-00054.Brem

Breuls, R. *et al*. 2009. Collagen type V modulates fibroblast behaviour dependent on substrate stiffness. *Biochemical and Biophysical Research Communications* 380(2), pp. 425-429. doi: 10.1016/j.bbrc.2009.01.110

Brew, K. and Nagase, H. 2010. The tissue inhibitors of metalloproteinases (TIMPs): an ancient family with structural and functional diversity. *Biochimica et Biophysica Acta* 1803(1), pp. 55-71. doi: 10.1016/j.bbamcr.2010.01.003

Brodsky, B. and Persikov, A. 2005. Molecular structure of the collagen triple helix. *Advances in Protein Chemistry* 70(1), pp. 301-339. doi: 10.1016/s0065-3233(05)70009-7

Brohem, C. *et al*. 2011. Artificial skin in perspective: concepts and applications. *Pigment Cell and Melanoma Research* 24(1), pp. 35-50. doi: 10.1111/j.1755-148X.2010.00786.x

Broughton, G. *et al*. 2006. Wound healing: an overview. *Plastic and Reconstructive Surgery* 117(7), pp. 1-32. doi: 10.1097/01.prs.0000222562.60260.f9

Brown, J. and Bayat, A. 2009. Genetic susceptibility to raised dermal scarring. *British Journal of Dermatology* 161(1), pp. 8-18. doi: 10.1111/j.1365-2133.2009.09258.x

Buhling, F. *et al*. 2004. Pivotal role of cathepsin K in lung fibrosis. *American Journal of Pathology* 164(6), pp. 2203-2216. doi: 10.1016/s0002-9440(10)63777-7

Bujor, A. *et al*. 2008. Akt blockade down-regulates collagen and up-regulates MMP1 in human dermal fibroblasts. *Journal of Investigative Dermatology* 128(8), pp. 1906-1914. doi: 10.1038/jid.2008.39

Burd, A. and Huang, L. 2005. Hypertrophic response and keloid diathesis: two very different forms of scar. *Plastic and Reconstructive Surgery* 116(7), pp. 150-157.

Burke, J. *et al*. 2011. N-cadherin is over-expressed in Crohn's stricture fibroblasts and promotes intestinal fibroblast migration. *Inflammatory Bowel Diseases* 17(8), pp. 1665-1673. doi: 10.1002/ibd.21543

Calderon, M. *et al*. 1996. Increased proliferation in keloid fibroblasts wounded *in vitro*. *Journal of Surgical Research* 61(2), pp. 343-347. doi: 10.1006/jsre.1996.0127

Caley, M. *et al*. 2015. Metalloproteinases and wound healing. *Advances in Wound Care* 4(4), pp. 225-234. doi: 10.1089/wound.2014.0581

Camaj, P. *et al*. 2009. EFEMP1 binds the EGF receptor and activates MAPK and Akt pathways in pancreatic carcinoma cells. *Biological Chemistry* 390(12), pp. 1293-1302. doi: 10.1515/bc.2009.140

Camenisch, T. *et al*. 2000. Disruption of hyaluronan synthase-2 abrogates normal cardiac morphogenesis and hyaluronan-mediated transformation of epithelium to mesenchyme. *Journal of Clinical Investigation* 106(3), pp. 349-360. doi: 10.1172/jci10272

Campbell, J. *et al*. 2014. Exceptional *in vivo* wound healing following destruction of cutaneous and subcutaneous tumours in domesticated animals treated with the novel epoxy-tigliane drug, EBC-46. *Wound Repair and Regeneration* 22(76), pp. 73-100.

Campbell, J. *et al*. 2017. Using triamcinolone in combination with the investigational anti-cancer agent EBC-46 (Tigilanol Tiglate) in the local treatment of a canine subcutaneous mast cell tumour. *Centre for Veterinary Education: Control and Therapy Series* 5598(286), pp. 11-17.

Candi, E. *et al*. 2005. The cornified envelope: a model of cell death in the skin. *Nature Reviews: Molecular Cell Biology* 6(4), pp. 328-340. doi: 10.1038/nrm1619

Carlier, M. *et al*. 2015. Control of polarised assembly of actin filaments in cell motility. *Cellular and Molecular Life Sciences* 72(16), pp. 3051-3067. doi: 10.1007/s00018-015-1914-2

Carroll, L. *et al*. 2002. Triamcinolone stimulates bFGF production and inhibits TGF-β_1 production by human dermal fibroblasts. *Dermatologic Surgery* 28(8), pp. 704-709.

Carthy, J. *et al*. 2015. Versican V_1 over-expression induces a myofibroblast-like phenotype in cultured fibroblasts. *PLoS One* 10(7), pp. 1-16. doi: 10.1371/journal.pone.0133056

Chan, J. *et al*. 2001. Accelerated skin wound healing in plasminogen activator inhibitor-1-deficient mice. *American Journal of Pathology* 159(5), pp. 1681-1688. doi: 10.1016/s0002-9440(10)63015-5

Chand, H. *et al*. 2005. Structure, function and biology of tissue factor pathway inhibitor-2. *Thrombosis and Haemostasis* 94(6), pp. 1122-1130. doi: 10.1160/th05-07-0509

Chang, H. *et al*. 2002. Diversity, topographic differentiation, and positional memory in human fibroblasts. *Proceedings of the National Academy of Sciences of the USA* 99(20), pp. 12877-12882. doi: 10.1073/pnas.162488599

Charles, C. *et al*. 2008. A gene signature of non-healing venous ulcers: potential diagnostic markers. *Journal of the American Academy of Dermatology* 59(5), pp. 758-771. doi: 10.1016/j.jaad.2008.07.018

Chen, C. *et al*. 2001. The angiogenic factor Cyr61 activates a genetic program for wound healing in human skin fibroblasts. *Journal of Biological Chemistry* 276(50), pp. 47329-47337. doi: 10.1074/jbc.M107666200

Chen, J. *et al*. 2011. Multiphoton microscopy study of the morphological and quantity changes of collagen and elastic fibre components in keloid disease. *Journal of Biomedical Optics* 16(5), pp. 1-6.

doi: 10.1117/1.3569617

Chen, L. *et al*. 2010. Positional differences in the wound transcriptome of skin and oral mucosa. *BMC Genomics* 11(471), pp. 1-15. doi: 10.1186/1471-2164-11-471

Chen, P. and Kroog, G. 2010. Leupaxin is similar to paxillin in focal adhesion targeting and tyrosine phosphorylation but has distinct roles in cell adhesion and spreading. *Cell Adhesion and Migration* 4(4), pp. 527-540. doi: 10.4161/cam.4.4.12399

Chen, W. and Abatangelo, G. 1999. Functions of hyaluronan in wound repair. *Wound Repair and Regeneration* 7(2), pp. 79-89.

Chen, W. *et al*. 1989. Differences between adult and foetal fibroblasts in the regulation of hyaluronate synthesis: correlation with migratory activity. *Journal of Cell Science* 94(3), pp. 577-584.

Chen, Y. *et al*. 1997. Mechanism of TGF-β receptor inhibition by FKBP12. *The EMBO Journal* 16(13), pp. 3866-3876. doi: 10.1093/emboj/16.13.3866

Chen, Z. *et al*. 2018. Haplodeletion of follistatin-like 1 attenuates radiation-induced pulmonary fibrosis in mice. *International Journal of Radiation Oncology, Biology and Physics* 103(1), pp. 208-216. doi: 10.1016/j.ijrobp.2018.08.035

Cheng, T. *et al*. 2017. Neuronal protein 3.1 deficiency leads to reduced cutaneous scar collagen deposition and tensile strength due to impaired transforming growth factor-β_1 to -β_3 translation. *American Journal of Pathology* 187(2), pp. 292-303. doi: 10.1016/j.ajpath.2016.10.004

Chike-Obi, C. *et al*. 2009. Keloids: pathogenesis, clinical features and management. *Seminars in Plastic Surgery* 23(3), pp. 178-184. doi: 10.1055/s-0029-1224797

Chin, G. *et al*. 2001. Differential expression of transforming growth factor-β receptors I and II and activation of SMAD3 in keloid fibroblasts. *Plastic and Reconstructive Surgery* 108(2), pp. 423-429.

Choi, S. *et al*. 1998. Protein kinase C-α levels are inversely associated with growth rate in cultured human dermal fibroblasts. *Journal of Dermatological Science* 18(1), pp. 54-63.

Cichorek, M. *et al*. 2013. Skin melanocytes: biology and development. *Postepy Dermatologii I Alergologii* 30(1), pp. 30-41. doi: 10.5114/pdia.2013.33376

Clark, R. *et al*. 1982. Fibronectin and fibrin provide a provisional matrix for epidermal cell migration during wound re-epithelialisation. *Journal of Investigative Dermatology* 79(5), pp. 264-269.

Clark, R. 1990. Fibronectin matrix deposition and fibronectin receptor expression in healing and normal skin. *Journal of Investigative Dermatology* 94(6), pp. 128-134.

Clark, R. 1993. Regulation of fibroplasia in cutaneous wound repair. *American Journal of Medical Sciences* 306(1), pp. 42-48.

Clore, J. *et al*. 1979. Quantitative assay of types I and III collagen synthesised by keloid biopsies and fibroblasts. *Biochimica et Biophysica Acta* 586(2), pp. 384-390.

Cole, J. *et al*. 2001. Early gene expression profile of human skin to injury using high-density cDNA microarrays. *Wound Repair and Regeneration* 9(5), pp. 360-370.

Colwell, A. *et al*. 2005. Hypertrophic scar fibroblasts have increased connective tissue growth factor expression after transforming growth factor-β stimulation. *Plastic and Reconstructive Surgery* 116 (5), pp. 1387-1390.

Colwell, A. *et al*. 2006. Early-gestation foetal scarless wounds have less lysyl oxidase expression. *Plastic and Reconstructive Surgery* 118(5), pp. 1125-1131. doi: 10.1097/01.prs.0000221056.27536.db

Colwell, A. *et al*. 2008. Identification of differentially regulated genes in foetal wounds during regenerative repair. *Wound Repair and Regeneration* 16(3), pp. 450-459. doi: 10.1111/j.1524-475X.2008.00383.x

Conway, K. *et al*. 2006. The molecular and clinical impact of hepatocyte growth factor, its receptor, activators, and inhibitors in wound healing. *Wound Repair and Regeneration* 14(1), pp. 2-10. doi: 10.1111/j.1743-6109.2005.00081.x

Cook, H. *et al*. 2000. Defective extracellular matrix reorganisation by chronic wound fibroblasts is associated with alterations in TIMP-1, TIMP-2, and MMP-2 activity. *Journal of Investigative Dermatology* 115(2), pp. 225-233. doi: 10.1046/j.1523-1747.2000.00044.x

Corbett, S. *et al*. 1997. Covalent cross-linking of fibronectin to fibrin is required for maximal cell adhesion to a fibronectin-fibrin matrix. *Journal of Biological Chemistry* 272(40), pp. 24999-25005.

Costa, A. *et al*. 1999. Mechanical forces induce scar remodelling: study in non-pressure-treated versus pressure-treated hypertrophic scars. *American Journal of Pathology* 155(5), pp. 1671-1679. doi: 10.1016/s0002-9440(10)65482-x

Coussens, L. *et al*. 1986. Multiple, distinct forms of bovine and human protein kinase C suggest diversity in cellular signalling pathways. *Science* 233(4766), pp. 859-866.

Cowin, A. *et al*. 2003. Differential effect of wounding on actin and its associated proteins, paxillin and gelsolin, in foetal skin explants. *Journal of Investigative Dermatology* 120(6), pp. 1118-1129. doi: 10.1046/j.1523-1747.2003.12231.x

Cowin, A. 2005. Differential expression of F-actin in *in utero* foetal wounds. *European Journal of Dermatology* 15(3), pp. 133-139.

Croce, M. *et al*. 2001. Hyaluronan affects protein and collagen synthesis by *in vitro* human skin fibroblasts. *Tissue and Cell* 33(4), pp. 326-331. doi: 10.1054/tice.2001.0180

Croft, D. and Olson, M. 2008. Regulating the conversion between rounded and elongated modes of cancer cell movement. *Cancer Cell* 14(5), pp. 349-351. doi: 10.1016/j.ccr.2008.10.009

Cruz, N. and Korchin, L. 1994. Inhibition of human keloid fibroblast growth by isotretinoin and triamcinolone acetonide *in vitro*. *Annals of Plastic Surgery* 33(4), pp. 401-405.

Csoka, A. *et al*. 2001. The six hyaluronidase-like genes in the human and mouse genomes. *Matrix Biology* 20(8), pp. 499-508.

D'Orazio, J. *et al*. 2013. UV radiation and the skin. *International Journal of Molecular Sciences* 14(6), pp. 12222-12248. doi: 10.3390/ijms140612222

Daley, W. *et al*. 2008. Extracellular matrix dynamics in development and regenerative medicine. *Journal of Cell Science* 121(3), pp. 255-264. doi: 10.1242/jcs.006064

Dalkowski, A. *et al*. 1999. Increased expression of tenascin C by keloids *in vivo* and *in vitro*. *British Journal of Dermatology* 141(1), pp. 50-56.

Dally, J. *et al*. 2017. Hepatocyte growth factor mediates enhanced wound healing responses and resistance to transforming growth factor-β_1-driven myofibroblast differentiation in oral mucosal fibroblasts. *International Journal of Molecular Sciences* 18(9), pp. 1-15. doi: 10.3390/ijms18091843

Dang, C. *et al*. 2003. Scarless foetal wounds are associated with an increased matrix metalloproteinase-to-tissue-derived inhibitor of metalloproteinase ratio. *Plastic and Reconstructive Surgery* 111(7), pp. 2273-2285. doi: 10.1097/01.prs.0000060102.57809.da

Darby, I. *et al*. 1990. Alpha-smooth muscle actin is transiently expressed by myofibroblasts during experimental wound healing. *Laboratory Investigation* 63(1), pp. 21-29.

Darby, I. *et al*. 2014. Fibroblasts and myofibroblasts in wound healing. *Clinical, Cosmetic and Investigational Dermatology* 7(1), pp. 301-311. doi: 10.2147/ccid.s50046

Darlenski, R. *et al*. 2011. Skin barrier function: morphological basis and regulatory mechanisms. *Journal of Clinical Medicine* 4(1), pp. 36-45.

Das, N. *et al*. 2018. TRAF3IP2 mediates TWEAK/TWEAKR-induced pro-fibrotic responses in cultured cardiac fibroblasts and the heart. *Journal of Molecular and Cellular Cardiology* 121(1), pp. 107-123. doi: 10.1016/j.yjmcc.2018.07.003

Dasu, M. *et al*. 2003. Matrix metalloproteinase expression in cytokine-stimulated human dermal fibroblasts. *Burns* 29(6), pp. 527-531.

Dasu, M. *et al*. 2004. Gene expression profiles from hypertrophic scar fibroblasts before and after IL-6 stimulation. *Journal of Pathology* 202(4), pp. 476-485. doi: 10.1002/path.1539

David-Raoudi, M. *et al*. 2008. Differential effects of hyaluronan and its fragments on fibroblasts: relation to wound healing. *Wound Repair and Regeneration* 16(2), pp. 274-287. doi: 10.1111/j.1524-475X.2007.00342.x

Davidson, J. 1998. Animal models for wound repair. *Archives for Dermatological Research* 290(1), pp. 1-11.

Davies, S. *et al*. 2000. Specificity and mechanism of action of some commonly used protein kinase inhibitors. *The Biochemical Journal* 351(1), pp. 95-105.

Day, A. and Prestwich, G. 2002. Hyaluronan-binding proteins: tying up the giant. *Journal of Biological Chemistry* 277(7), pp. 4585-4588. doi: 10.1074/jbc.R100036200

de Felice, B. *et al*. 2007. Differential p63 and p53 expression in human keloid fibroblasts and hypertrophic scar fibroblasts. *DNA and Cell Biology* 26(8), pp. 541-547. doi: 10.1089/dna.2007.0591

de Oliveira, G. *et al*. 2001. Silicone versus non-silicone gel dressings: a controlled trial. *Dermatologic Surgery* 27(8), pp. 721-726.

Debelle, L. and Tamburro, A. 1999. Elastin: molecular description and function. *International Journal of Biochemistry and Cell Biology* 31(2), pp. 261-272.

Deed, R. *et al*. 1997. Early-response gene signalling is induced by angiogenic oligosaccharides of hyaluronan in endothelial cells: inhibition by non-angiogenic, high-molecular-weight hyaluronan. *International Journal of Cancer* 71(2), pp. 251-256.

Dendooven, A. *et al*. 2011. Loss of endogenous bone morphogenetic protein-6 aggravates renal fibrosis. *American Journal of Pathology* 178(3), pp. 1069-1079. doi: 10.1016/j.ajpath.2010.12.005

Deo, P. and Deshmukh, R. 2018. Pathophysiology of keratinisation. *Journal of Oral and Maxillofacial Pathology* 22(1), pp. 86-91. doi: 10.4103/jomfp.JOMFP_195_16

Desmouliere, A. *et al*. 1993. Transforming growth factor-β_1 induces alpha-smooth muscle actin expression in granulation tissue myofibroblasts and in quiescent and growing cultured fibroblasts.

Journal of Cell Biology 122(1), pp. 103-111.

Desmouliere, A. *et al*. 1995. Apoptosis mediates the decrease in cellularity during the transition between granulation tissue and scar. *American Journal of Pathology* 146(1), pp. 56-66.

Desmouliere, A. *et al*. 2005. Tissue repair, contraction and the myofibroblast. *Wound Repair and Regeneration* 13(1), pp. 7-12. doi: 10.1111/j.1067-1927.2005.130102.x

Ding, W. *et al*. 2014. Protection from renal fibrosis: putative role of TRIB3 gene silencing. *Experimental and Molecular Pathology* 96(1), pp. 80-84. doi: 10.1016/j.yexmp.2013.12.003

Do, N. and Eming, S. 2016. Skin fibrosis: models and mechanisms. *Current Research in Translational Medicine* 64(4), pp. 185-193. doi: 10.1016/j.retram.2016.06.003

Dolivo, D. *et al*. 2017. FGF2-mediated attenuation of myofibroblast activation is modulated by distinct MAPK signaling pathways in human dermal fibroblasts. *Journal of Dermatological Science* 88(3), pp. 339-348. doi: 10.1016/j.jdermsci.2017.08.013

Dong, L. *et al*. 2008. Structure and absolute stereochemistry of the anti-cancer agent EBC-23 from the Australian rainforest. *Journal of the American Chemical Society* 130(46), pp. 15262-15263. doi: 10.1021/ja807133p

Dong, L. *et al*. 2009. Anti-cancer agents from the Australian tropical rainforest: spiroacetals EBC-23, 24, 25, 72, 73, 75 and 76. *Chemistry* 15(42), pp. 11307-11318. doi: 10.1002/chem.200901525

Dong, Y. *et al*. 2015. Blocking follistatin-like 1 attenuates bleomycin-induced pulmonary fibrosis in mice. *Journal of Experimental Medicine* 212(2), pp. 235-252. doi: 10.1084/jem.20121878

Dorfmuller, M. 1995. Psychological management and after-care of severely burned patients. *Der Unfallchirurg* 98(4), pp. 213-217.

Duca, L. *et al*. 2004. Elastin as a matrikine. *Critical Reviews in Oncology/Hematology* 49(3), pp. 235-244. doi: 10.1016/j.critrevonc.2003.09.007

Dugina, V. *et al*. 2001. Focal adhesion features during myofibroblastic differentiation are controlled by intracellular and extracellular factors. *Journal of Cell Science* 114(8), pp. 3285-3296.

Durani, P. and Bayat, A. 2008. Levels of evidence for the treatment of keloid disease. *Journal of Plastic, Reconstructive and Aesthetic Surgery* 61(1), pp. 4-17. doi: 10.1016/j.bjps.2007.05.007

Ebisawa, T. *et al*. 2001. Smurf1 interacts with transforming growth factor-β type I receptor through SMAD7 and induces receptor degradation. *Journal of Biological Chemistry* 276(16), pp. 12477-12480. doi: 10.1074/jbc.C100008200

Eckes, B. *et al*. 2010. Cell-matrix interactions in dermal repair and scarring. *Fibrogenesis and Tissue Repair* 3(4), pp. 1-11. doi: 10.1186/1755-1536-3-4

Eckhart, L. *et al*. 2013. Cell death by cornification. *Biochimica et Biophysica Acta* 1833(12), pp. 3471-3480. doi: 10.1016/j.bbamcr.2013.06.010

Ehrlich, H. *et al*. 1994. Morphological and immunochemical differences between keloid and hypertrophic scar. *American Journal of Pathology* 145(1), pp. 105-113.

Ehrlich, H. *et al*. 1998. The expression of $\alpha_2\beta_1$ integrin and alpha smooth muscle actin in fibroblasts grown on collagen. *Cell Biochemistry and Function* 16(2), pp. 129-137. doi: 10.1002/(SICI)1099-0844(199806)16:2<129::AID-CBF780>3.0.CO;2-6

El Sayegh, T. *et al*. 2007. Beyond the epithelium: cadherin function in fibrous connective tissues. *FEBS Letters* 581(2), pp. 167-174. doi: 10.1016/j.febslet.2006.12.029

Ellis, I. *et al*. 1992. Antagonistic effects of TGF-β_1 and MSF on fibroblast migration and hyaluronic acid synthesis: possible implications for dermal wound healing. *Journal of Cell Science* 102(3), pp. 447-456.

Ellis, I. and Schor, S. 1996. Differential effects of TGF-β_1 on hyaluronan synthesis by foetal and adult skin fibroblasts: implications for cell migration and wound healing. *Experimental Cell Research* 228(2), pp. 326-333. doi: 10.1006/excr.1996.0332

Eming, S. *et al*. 2007. Inflammation in wound repair: molecular and cellular mechanisms. *Journal of Investigative Dermatology* 127(3), pp. 514-525. doi: 10.1038/sj.jid.5700701

Eming, S. *et al*. 2010. Differential proteomic analysis distinguishes tissue repair biomarker signatures in wound exudates obtained from normal healing and chronic wounds. *Journal of Proteome Research* 9(9), pp. 4758-4766. doi: 10.1021/pr100456d

Eming, S. *et al*. 2014. Wound repair and regeneration: mechanisms, signalling and translation. *Science: Translational Medicine* 6(265), pp. 1-36. doi: 10.1126/scitranslmed.3009337

Enoch, S. and Leaper, D. 2005. Basic science of wound healing. *Surgery (Oxford)* 23(2), pp. 37-42. doi: 10.1383/surg.23.2.37.60352

Enoch, S. *et al*. 2009. Increased oral fibroblast lifespan is telomerase-independent. *Journal of Dental Research* 88(10), pp. 916-921. doi: 10.1177/0022034509342979

Enoch, S. *et al*. 2010. 'Young' oral fibroblasts are geno/phenotypically distinct. *Journal of Dental Research* 89(12), pp. 1407-1413. doi: 10.1177/0022034510377796

Erickson, J. and Echeverri, K. 2018. Learning from regeneration research organisms: the circuitous road to scar free wound healing. *Developmental Biology* 433(2), pp. 144-154. doi: 10.1016/j. ydbio.2017.09.025

Escarmant, P. *et al*. 1993. The treatment of 783 keloid scars by iridium 192: interstitial irradiation after surgical excision. *International Journal of Radiation Oncology, Biology and Physics* 26(2), pp. 245-251.

Espana, A. *et al*. 2001. Bleomycin in the treatment of keloids and hypertrophic scars by multiple needle punctures. *Dermatologic Surgery* 27(1), pp. 23-27.

Estes, J. *et al*. 1994. Phenotypic and functional features of myofibroblasts in sheep foetal wounds. *Differentiation* 56(3), pp. 173-181.

Eto, H. *et al*. 2012. Therapeutic potential of fibroblast growth factor-2 for hypertrophic scars: up-regulation of MMP-1 and HGF expression. *Laboratory Investigation* 92(2), pp. 214-223. doi: 10.1038 /labinvest.2011.127

Eyden, B. 1993. Brief review of the fibronexus and its significance for myofibroblastic differentiation and tumour diagnosis. *Ultrastructural Pathology* 17(6), pp. 611-622.

Fan, C. *et al*. 2015. Shikonin reduces TGF-β_1-induced collagen production and contraction in hypertrophic scar-derived human skin fibroblasts. *International Journal of Molecular Medicine* 36(4), pp. 985-991. doi: 10.3892/ijmm.2015.2299

Fan, D. *et al*. 2012. Oxymatrine inhibits collagen synthesis in keloid fibroblasts via inhibition of transforming growth factor-β_1/SMAD signalling pathway. *International Journal of Dermatology* 51(4),

pp. 463-472. doi: 10.1111/j.1365-4632.2011.05234.x

Fan, J. *et al*. 2006. PKC-delta clustering at the leading edge and mediating growth factor-enhanced, but not ECM-initiated, dermal fibroblast migration. *Journal of Investigative Dermatology* 126(6), pp. 1233-1243. doi: 10.1038/sj.jid.5700149

Feng, X. and Derynck, R. 2005. Specificity and versatility in TGF-β signalling through SMADs. *Annual Review of Cell and Developmental Biology* 21, pp. 659-693. doi: 10.1146/annurev.cellbio. 21.022404.142018

Feral, C. *et al*. 2007. CD98hc (SLC3A2) participates in fibronectin matrix assembly by mediating integrin signalling. *Journal of Cell Biology* 178(4), pp. 701-711. doi: 10.1083/jcb.200705090

Fineschi, S. *et al*. 2006. Proteasome blockade exerts an anti-fibrotic activity by coordinately down-regulating type I collagen and tissue inhibitor of metalloproteinase-1 and up-regulating metalloproteinase-1 production in human dermal fibroblasts. *FASEB Journal* 20(3), pp. 562-564. doi: 10.1096/fj.05-4870fje

Fitzpatrick, R. 1999. Treatment of inflamed hypertrophic scars using intralesional 5-FU. *Dermatologic Surgery* 25(3), pp. 224-232.

Fourcot, A. *et al*. 2011. Gas6 deficiency prevents liver inflammation, steatohepatitis, and fibrosis in mice. *American Journal of Physiology: Gastrointestinal and Liver Physiology* 300(6), pp. 1043-1053. doi: 10.1152/ajpgi.00311.2010

Frantz, C. *et al*. 2010. The extracellular matrix at a glance. *Journal of Cell Science* 123(24), pp. 4195-4200. doi: 10.1242/jcs.023820

Fraser, J. *et al*. 1997. Hyaluronan: its nature, distribution, functions and turnover. *Journal of Internal Medicine* 242(1), pp. 27-33.

Frazier, K. *et al*. 1996. Stimulation of fibroblast cell growth, matrix production, and granulation tissue formation by connective tissue growth factor. *Journal of Investigative Dermatology* 107(3), pp. 404-411.

Friedman, D. *et al*. 1993. Regulation of collagen gene expression in keloids and hypertrophic scars. *Journal of Surgical Research* 55(2), pp. 214-222. doi: 10.1006/jsre.1993.1132

Fries, K. *et al*. 1994. Evidence of fibroblast heterogeneity and the role of fibroblast subpopulations in fibrosis. *Clinical Immunology and Immunopathology* 72(3), pp. 283-292.

Frost, R. and Engelhardt, S. 2007. A secretion trap screen in yeast identifies protease inhibitor 16 as a novel anti-hypertrophic protein secreted from the heart. *Circulation* 116(16), pp. 1768-1775. doi: 10.1161/circulationaha.107.696468

Fu, J. *et al*. 2009. Reciprocal regulation of Wnt and Gpr177/mouse Wntless is required for embryonic axis formation. *Proceedings of the National Academy of Sciences of the USA* 106(44), pp. 18598-18603. doi: 10.1073/pnas.0904894106

Fu, J. and Hsu, W. 2013. Epidermal Wnt controls hair follicle induction by orchestrating dynamic signalling cross-talk between the epidermis and dermis. *Journal of Investigative Dermatology* 133(4), pp. 890-898. doi: 10.1038/jid.2012.407

Fu, X. and Sun, X. 2009. Can haematopoietic stem cells be an alternative source for skin regeneration? *Ageing Research Reviews* 8(3), pp. 244-249. doi: 10.1016/j.arr.2009.02.002

Fuchs, E. and Raghavan, S. 2002. Getting under the skin of epidermal morphogenesis. *Nature*

reviews: Genetics 3(3), pp. 199-209. doi: 10.1038/nrg758

Fuchs, E. 2007. Scratching the surface of skin development. *Nature* 445(7130), pp. 834-842. doi: 10.1038/nature05659

Fujiwara, M. *et al*. 2005. Keloid-derived fibroblasts show increased secretion of factors involved in collagen turnover and depend on matrix metalloproteinase for migration. *British Journal of Dermatology* 153(2), pp. 295-300. doi: 10.1111/j.1365-2133.2005.06698.x

Funayama, E. *et al*. 2003. Keratinocytes promote proliferation and inhibit apoptosis of the underlying fibroblasts: an important role in the pathogenesis of keloid. *Journal of Investigative Dermatology* 121(6), pp. 1326-1331. doi: 10.1111/j.1523-1747.2003.12572.x

Gabbiani, G. *et al*. 1971. Presence of modified fibroblasts in granulation tissue and their possible role in wound contraction. *Experientia* 27(5), pp. 549-550.

Gabbiani, G. 2003. The myofibroblast in wound healing and fibrocontractive diseases. *Journal of Pathology* 200(4), pp. 500-503. doi: 10.1002/path.1427

Gao, F. *et al*. 2010. Hyaluronan oligosaccharides promote excisional wound healing through enhanced angiogenesis. *Matrix Biology* 29(2), pp. 107-116. doi: 10.1016/j.matbio.2009.11.002

Gao, P. *et al*. 2003. Differentiation of vascular myofibroblasts induced by transforming growth factor-β_1 requires the involvement of protein kinase C-α. *Journal of Molecular and Cellular Cardiology* 35(9), pp. 1105-1112.

Garnero, P. *et al*. 1998. The collagenolytic activity of cathepsin K is unique among mammalian proteinases. *Journal of Biological Chemistry* 273(48), pp. 32347-32352.

Gauglitz, G. *et al*. 2011. Hypertrophic scarring and keloids: pathomechanisms and current and emerging treatment strategies. *Molecular Medicine* 17(1), pp. 113-125. doi: 10.2119/molmed. 2009.00153

Gauglitz, G. 2013. Management of keloids and hypertrophic scars: current and emerging options. *Clinical, Cosmetic and Investigational Dermatology* 6(1), pp. 103-114. doi: 10.2147/ccid.s35252

Gee, H. *et al*. 2016. FAT1 mutations cause a glomerulotubular nephropathy. *Nature Communications* 7(1), pp. 1-11. doi: 10.1038/ncomms10822

Gellings Lowe, N. *et al*. 2009. Sphingosine-1-phosphate and sphingosine kinase are critical for transforming growth factor-β-stimulated collagen production by cardiac fibroblasts. *Cardiovascular Research* 82(2), pp. 303-312. doi: 10.1093/cvr/cvp056

Gelse, K. *et al*. 2003. Collagens - structure, function, and biosynthesis. *Advanced Drug Delivery Reviews* 55(12), pp. 1531-1546.

Ghahary, A. *et al*. 1996. Collagenase production is lower in post-burn hypertrophic scar fibroblasts than in normal fibroblasts and is reduced by insulin-like growth factor-1. *Journal of Investigative Dermatology* 106(3), pp. 476-481.

Gibbs, G. *et al*. 2008. The CAP superfamily: cysteine-rich secretory proteins, antigen 5, and pathogenesis-related 1 proteins: roles in reproduction, cancer, and immune defense. *Endocrine Reviews* 29(7), pp. 865-897. doi: 10.1210/er.2008-0032

Gimenez, A. *et al*. 2017. Dysregulated collagen homeostasis by matrix stiffening and TGF-β_1 in fibroblasts from idiopathic pulmonary fibrosis patients: role of FAK/Akt. *International Journal of Molecular Sciences* 18(11), pp. 1-18. doi: 10.3390/ijms18112431

Glim, J. *et al*. 2013. Detrimental dermal wound healing: what can we learn from the oral mucosa? *Wound Repair and Regeneration* 21(5), pp. 648-660. doi: 10.1111/wrr.12072

Glim, J. *et al*. 2014. Extracellular matrix components of oral mucosa differ from skin and resemble that of foetal skin. *Archives of Oral Biology* 59(10), pp. 1048-1055. doi: 10.1016/j.archoralbio. 2014.05.019

Goel, A. and Shrivastava, P. 2010. Post-burn scars and scar contractures. *Indian Journal of Plastic Surgery* 43(1), pp. 63-71. doi: 10.4103/0970-0358.70724

Goffin, J. *et al*. 2006. Focal adhesion size controls tension-dependent recruitment of alpha-smooth muscle actin to stress fibres. *Journal of Cell Biology* 172(2), pp. 259-268. doi: 10.1083/jcb.200506179

Goffin, L. *et al*. 2010. Transcriptional regulation of matrix metalloproteinase-1 and collagen I α_2 explains the anti-fibrotic effect exerted by proteasome inhibition in human dermal fibroblasts. *Arthritis Research and Therapy* 12(2), pp. 1-14. doi: 10.1186/ar2991

Goh Then Sin, C. *et al*. 2011. S100A4 downregulates filopodia formation through increased dynamic instability. *Cell Adhesion and Migration* 5(5), pp. 439-447. doi: 10.4161/cam.5.5.17773

Gokey, J. *et al*. 2018. MEG3 is increased in idiopathic pulmonary fibrosis and regulates epithelial cell differentiation. *JCI Insight* 3(17), pp. 1-16. doi: 10.1172/jci.insight.122490

Gonzalez, A. *et al*. 2016. Wound healing: a literature review. *Anais Brasileiros De Dermatologia* 91(5), pp. 614-620. doi: 10.1590/abd1806-4841.20164741

Gordon, M. and Hahn, R. 2010. Collagens. *Cell and Tissue Research* 339(1), pp. 247-257. doi: 10.1007/s00441-009-0844-4

Grassel, S. *et al*. 1998. Collagen type XVI expression is modulated by basic fibroblast growth factor and transforming growth factor-β. *FEBS Letters* 436(2), pp. 197-201.

Gressner, O. and Gressner, A. 2008. Connective tissue growth factor: a fibrogenic master switch in fibrotic liver diseases. *Liver International* 28(8), pp. 1065-1079. doi: 10.1111/j.1478-3231.2008. 01826.x

Grinnell, F. *et al*. 1981. Distribution of fibronectin during wound healing *in vivo*. *Journal of Investigative Dermatology* 76(3), pp. 181-189.

Grinnell, F. 1984. Fibronectin and wound healing. *Journal of Cellular Biochemistry* 26(2), pp. 107-116. doi: 10.1002/jcb.240260206

Grinnell, F. 2000. Fibroblast-collagen-matrix contraction: growth-factor signalling and mechanical loading. *Trends in Cell Biology* 10(9), pp. 362-365.

Guest, J. *et al*. 2015. Health economic burden that wounds impose on the National Health Service in the UK. *BMJ Open* 5(12), pp. 1-8. doi: 10.1136/bmjopen-2015-009283

Guilherme, A. *et al*. 2004. EHD2 and the novel EH domain binding protein EHBP1 couple endocytosis to the actin cytoskeleton. *Journal of Biological Chemistry* 279(11), pp. 10593-10605. doi: 10.1074 /jbc.M307702200

Guix, B. *et al*. 2001. Treatment of keloids by high-dose-rate brachytherapy: a seven-year study. *International Journal of Radiation Oncology, Biology & Physics* 50(1), pp. 167-172.

Guo, S. and Dipietro, L. 2010. Factors affecting wound healing. *Journal of Dental Research* 89(3), pp. 219-229. doi: 10.1177/0022034509359125

Gurtner, G. *et al*. 2008. Wound repair and regeneration. *Nature* 453(7193), pp. 314-321. doi: 10.1038/nature07039

Hahn, J. *et al*. 2013. Keloid-derived keratinocytes exhibit an abnormal gene expression profile consistent with a distinct causal role in keloid pathology. *Wound Repair and Regeneration* 21(4), pp. 530-544. doi: 10.1111/wrr.12060

Haisa, M. *et al*. 1994. Elevated levels of PDGF-alpha receptors in keloid fibroblasts contribute to an enhanced response to PDGF. *Journal of Investigative Dermatology* 103(4), pp. 560-563.

Halper, J. and Kjaer, M. 2014. Basic components of connective tissues and extracellular matrix: elastin, fibrillin, fibulins, fibrinogen, fibronectin, laminin, tenascins and thrombospondins. *Advances in Experimental Medicine and Biology* 802(1), pp. 31-47. doi: 10.1007/978-94-007-7893-1_3

Hansen, N. *et al*. 2018. Progressive cutaneous viral pigmented plaques in three Hungarian Vizslas and the response of lesions to topical Tigilanol Tiglate gel. *Veterinary Medicine and Science* 4(1), pp. 53-62. doi: 10.1002/vms3.85

Har-Shai, Y. *et al*. 2003. Intra-lesional cryotherapy for enhancing the involution of hypertrophic scars and keloids. *Plastic and Reconstructive Surgery* 111(6), pp. 1841-1852. doi: 10.1097/01.prs.0000056868.42679.05

Harada, H. and Takahashi, M. 2007. CD44-dependent intracellular and extracellular catabolism of hyaluronic acid by hyaluronidase-1 and -2. *Journal of Biological Chemistry* 282(8), pp. 5597-5607. doi: 10.1074/jbc.M608358200

Harding, K. 2015. Innovation and wound healing. *Journal of Wound Care* 24(4), pp. 7-13. doi: 10.12968/jowc.2015.24.Sup4b.7

Harris, N. *et al*. 2017. SerpinB2 regulates stromal remodelling and local invasion in pancreatic cancer. *Oncogene* 36(30), pp. 4288-4298. doi: 10.1038/onc.2017.63

Hathaway, C. *et al*. 1996. Differential expression of IGFBPs by normal and hypertrophic scar fibroblasts. *Journal of Surgical Research* 60(1), pp. 156-162. doi: 10.1006/jsre.1996.0025

Hattori, N. *et al*. 2011. Pericellular versican regulates the fibroblast-myofibroblast transition: a role for ADAMTS5 protease-mediated proteolysis. *Journal of Biological Chemistry* 286(39), pp. 34298-34310. doi: 10.1074/jbc.M111.254938

He, S. *et al*. 2012. Compound *Astragalus* and *Salvia miltiorrhiza* extract inhibits cell proliferation, invasion and collagen synthesis in keloid fibroblasts by mediating transforming growth factor-β/SMAD pathway. *British Journal of Dermatology* 166(3), pp. 564-574. doi: 10.1111/j.1365-2133.2011.10674.x

Heldin, C. *et al*. 1997. TGF-β signalling from cell membrane to nucleus through SMAD proteins. *Nature* 390(6659), pp. 465-471. doi: 10.1038/37284

Helmo, F. *et al*. 2013. Foetal wound healing biomarkers. *Disease Markers* 35(6), pp. 939-944.

Hewitson, T. *et al*. 2001. Pirfenidone reduces *in vitro* rat renal fibroblast activation and mitogenesis. *Journal of Nephrology* 14(6), pp. 453-460.

Hinz, B. *et al*. 2001a. Alpha-smooth muscle actin expression up-regulates fibroblast contractile activity. *Molecular Biology of the Cell* 12(9), pp. 2730-2741. doi: 10.1091/mbc.12.9.2730

Hinz, B. *et al*. 2001b. Mechanical tension controls granulation tissue contractile activity and myofibroblast differentiation. *American Journal of Pathology* 159(3), pp. 1009-1020. doi: 10.

1016/s0002-9440(10)61776-2

Hinz, B. *et al*. 2003. Alpha-smooth muscle actin is crucial for focal adhesion maturation in myofibroblasts. *Molecular Biology of the Cell* 14(6), pp. 2508-2519. doi: 10.1091/mbc.e02-11-0729

Hinz, B. 2006. Masters and servants of the force: the role of matrix adhesions in myofibroblast force perception and transmission. *European Journal of Cell Biology* 85(3-4), pp. 175-181. doi: 10.1016 /j.ejcb.2005.09.004

Hirai, M. *et al*. 2007. Fibulin-5/DANCE has an elastogenic organiser activity that is abrogated by proteolytic cleavage *in vivo*. *Journal of Cell Biology* 176(7), pp. 1061-1071. doi: 10.1083/jcb. 200611026

Hoffman, M. and Monroe, D. 2005. Re-thinking the coagulation cascade. *Current Haematology Reports* 4(5), pp. 391-396.

Holick, M. *et al*. 1987. Skin as the site of vitamin D synthesis and target tissue for 1,25-dihydroxyvitamin D3: use of calcitriol (1,25-dihydroxyvitamin D3) for treatment of psoriasis. *Archives of Dermatology* 123(12), pp. 1677-1683.

Holmes, A. *et al*. 2001. CTGF and SMADs: maintenance of scleroderma phenotype is independent of SMAD signalling. *Journal of Biological Chemistry* 276(14), pp. 10594-10601. doi: 10.1074/jbc. M010149200

Hu, M. *et al*. 2014. Gene expression in foetal murine keratinocytes and fibroblasts. *Journal of Surgical Research* 190(1), pp. 344-357. doi: 10.1016/j.jss.2014.02.030

Huang, C. *et al*. 2013a. Keloids and hypertrophic scars: update and future directions. *Plastic and Reconstructive Surgery* 1(4), pp.1-7. doi: 10.1097/GOX.0b013e31829c4597

Huang, E. *et al*. 2002. Differential expression of urokinase-type plasminogen activator and plasminogen activator inhibitor-1 in early and late gestational mouse skin and skin wounds. *Wound Repair and Regeneration* 10(6), pp. 387-396.

Huang, L. *et al*. 2009. A reappraisal of the biological effects of hyaluronan on human dermal fibroblasts. *Journal of Biomedical Materials Research* 90(4), pp. 1177-1185. doi: 10.1002/jbm.a.32173

Huang, L. *et al*. 2015. Screening of differentially expressed genes in pathological scar tissues using expression microarray. *Genetics and Molecular Research* 14(3), pp. 10743-10751. doi: 10.4238 /2015.September.9.13

Huang, S. *et al*. 2013b. GLIPR-2 over-expression in HK-2 cells promotes cell EMT and migration through ERK1/2 activation. *PLoS One* 8(3), pp. 1-9. doi: 10.1371/journal.pone.0058574

Huse, M. *et al*. 1999. Crystal structure of the cytoplasmic domain of the type I TGF-β receptor in complex with FKBP12. *Cell* 96(3), pp. 425-436.

Igarashi, A. *et al*. 1993. Regulation of connective tissue growth factor gene expression in human skin fibroblasts and during wound repair. *Molecular Biology of the Cell* 4(6), pp. 637-645.

Inman, G. *et al*. 2002. Nucleocytoplasmic shuttling of SMADs 2, 3, and 4 permits sensing of TGF-β receptor activity. *Molecular Cell* 10(2), pp. 283-294.

Iocono, J. *et al*. 1998. Repeated additions of hyaluronan alters granulation tissue deposition in sponge implants in mice. *Wound Repair and Regeneration* 6(5), pp. 442-448.

Iozzo, R. 1998. Matrix proteoglycans: from molecular design to cellular function. *Annual Review of*

Biochemistry 67, pp. 609-652. doi: 10.1146/annurev.biochem.67.1.609

Iozzo, R. 2005. Basement membrane proteoglycans: from cellar to ceiling. *Nature Reviews: Molecular Cell Biology* 6(8), pp. 646-656. doi: 10.1038/nrm1702

Itano, N. *et al*. 1999. Three isoforms of mammalian hyaluronan synthases have distinct enzymatic properties. *Journal of Biological Chemistry* 274(35), pp. 25085-25092.

Itoh, Y. 2015. Membrane-type matrix metalloproteinases: their functions and regulations. *Matrix Biology* 44(46), pp. 207-223. doi: 10.1016/j.matbio.2015.03.004

Jalali, M. and Bayat, A. 2007. Current use of steroids in management of abnormal raised skin scars. *Surgeon* 5(3), pp. 175-180.

Jarvelainen, H. *et al*. 2009. Extracellular matrix molecules: potential targets in pharmacotherapy. *Pharmacological Reviews* 61(2), pp. 198-223. doi: 10.1124/pr.109.001289

Jean, J. *et al*. 2013. Transcription factor KLF4, induced in the lung by oxygen at birth, regulates perinatal fibroblast and myofibroblast differentiation. *PLoS One* 8(1), pp. 1-13. doi: 10.1371 /journal.pone.0054806

Jenkins, R. *et al*. 2004. Myofibroblastic differentiation leads to hyaluronan accumulation through reduced hyaluronan turnover. *Journal of Biological Chemistry* 279(40), pp. 41453-41460. doi: 10. 1074/jbc.M401678200

Jensen, S. and Handford, P. 2016. New insights into the structure, assembly and biological roles of 10-12 nm connective tissue microfibrils from fibrillin-1 studies. *Biochemical Journal* 473(7), pp. 827-838. doi: 10.1042/bj20151108

Jerome-Morais, A. *et al*. 2009. Role for protein kinase C-alpha in keratinocyte growth arrest. *Journal of Investigative Dermatology* 129(10), pp. 2365-2375. doi: 10.1038/jid.2009.74

Jiang, D. *et al*. 2006. The role of toll-like receptors in non-infectious lung injury. *Cell Research* 16(8), pp. 693-701. doi: 10.1038/sj.cr.7310085

Jimenez, S. *et al*. 1984. Selective inhibition of human diploid fibroblast collagen synthesis by interferons. *Journal of Clinical Investigation* 74(3), pp. 1112-1116. doi: 10.1172/jci111480

Jimenez, S. *et al*. 2001. Role of protein kinase C-delta in the regulation of collagen gene expression in scleroderma fibroblasts. *Journal of Clinical Investigation* 108(9), pp. 1395-1403. doi: 10.1172/ jci12347

Jin, Y. *et al*. 2018. Follistatin-like 1 promotes bleomycin-induced pulmonary fibrosis through the transforming growth factor-β_1/mitogen-activated protein kinase signalling pathway. *Chinese Medical Journal* 131(16), pp. 1917-1925. doi: 10.4103/0366-6999.238151

Jinnin, M. *et al*. 2004. Tenascin-C up-regulation by transforming growth factor-β in human dermal fibroblasts involves SMAD3, Sp1 and Ets1. *Oncogene* 23(9), pp. 1656-1667. doi: 10.1038/sj. onc.1207064

Jinnin, M. *et al*. 2005. Alpha$_2$(I) collagen gene regulation by protein kinase C signalling in human dermal fibroblasts. *Nucleic Acids Research* 33(4), pp. 1337-1351. doi: 10.1093/nar/gki275

Jones, F. and Jones, P. 2000. The tenascin family of ECM glycoproteins: structure, function, and regulation during embryonic development and tissue remodelling. *Developmental Dynamics* 218(2), pp. 235-259. doi: 10.1002/(SICI)1097-0177(200006)218:2<235::AID-DVDY2>3.0.CO;2-G

Jones, P. and Watt, F. 1993. Separation of human epidermal stem cells from transit amplifying cells on the basis of differences in integrin function and expression. *Cell* 73(4), pp. 713-724.

Joyce, N. and Meklir, B. 1992. Protein kinase C activation during corneal endothelial wound repair. *Investigative Ophthalmology and Visual Science* 33(6), pp. 1958-1973.

Jumper, N. *et al*. 2015. Functional histopathology of keloid disease. *Histology and Histopathology* 30(9), pp. 1033-1057. doi: 10.14670/hh-11-624

Kagan, H. and Li, W. 2003. Lysyl oxidase: properties, specificity, and biological roles inside and outside of the cell. *Journal of Cellular Biochemistry* 88(4), pp. 660-672. doi: 10.1002/jcb.10413

Kahari, V. *et al*. 1992. Transforming growth factor-β up-regulates elastin gene expression in human skin fibroblasts: evidence for post-transcriptional modulation. *Laboratory Investigation* 66(5), pp. 580-588.

Kahari, V. and Saarialho-Kere, U. 1997. Matrix metalloproteinases in skin. *Experimental Dermatology* 6(5), pp. 199-213.

Kan, S. *et al*. 2014. Podoplanin expression in cancer-associated fibroblasts predicts aggressive behaviour in melanoma. *Journal of Cutaneous Pathology* 41(7), pp. 561-567. doi: 10.1111/cup.12322

Kaplan, F. *et al*. 2009. The FOP metamorphogene encodes a novel type I receptor that dysregulates BMP signalling. *Cytokine and Growth Factor Reviews* 20(5-6), pp. 399-407. doi: 10.1016/j. cytogfr.2009.10.006

Kaplani, K. *et al*. 2018. Wound healing-related agents: ongoing research and perspectives. *Advanced Drug Delivery Reviews* 129(1), pp. 242-253. doi: 10.1016/j.addr.2018.02.007

Karagiannis, G. *et al*. 2012. Proteomic signatures of the desmoplastic invasion front reveal collagen type XII as a marker of myofibroblastic differentiation during colorectal cancer metastasis. *Oncotarget* 3(3), pp. 267-285. doi: 10.18632/oncotarget.451

Kardassis, D. *et al*. 2009. Control of transforming growth factor-β signal transduction by small GTPases. *FEBS Journal* 276(11), pp. 2947-2965. doi: 10.1111/j.1742-4658.2009.07031.x

Kathju, S. *et al*. 2006. Identification of differentially expressed genes in scarless wound healing utilising polymerase chain reaction-suppression subtractive hybridisation. *Wound Repair and Regeneration* 14(4), pp. 413-420. doi: 10.1111/j.1743-6109.2006.00140.x

Kato, A. *et al*. 2011. Dermatopontin interacts with fibronectin, promotes fibronectin fibril formation and enhances cell adhesion. *Journal of Biological Chemistry* 286(17), pp. 14861-14869. doi: 10.1074 /jbc.M110.179762

Kendall, R. and Feghali-Bostwick, C. 2014. Fibroblasts in fibrosis: novel roles and mediators. *Frontiers in Pharmacology* 5(1), pp. 1-13. doi: 10.3389/fphar.2014.00123

Kennedy, C. *et al*. 2000. Pro-inflammatory cytokines differentially regulate hyaluronan synthase isoforms in foetal and adult fibroblasts. *Journal of Paediatric Surgery* 35(6), pp. 874-879. doi: 10. 1053/jpsu.2000.6869

Khamaisi, M. *et al*. 2016. PKC-delta inhibition normalises the wound-healing capacity of diabetic human fibroblasts. *Journal of Clinical Investigation* 126(3), pp. 837-853. doi: 10.1172/jci82788

Khatri, K. *et al*. 2011. Laser scar revision: a review. *Journal of Cosmetic and Laser Therapy* 13(2), pp. 54-62. doi: 10.3109/14764172.2011.564625

Kielty, C. *et al*. 2002. Elastic fibres. *Journal of Cell Science* 115(14), pp. 2817-2828.

Kim, S. *et al*. 2009. Expression of ectodermal neural cortex 1 and its association with actin during the ovulatory process in the rat. *Endocrinology* 150(8), pp. 3800-3806. doi: 10.1210/en.2008-1587

Kivirikko, S. *et al*. 1999. Cytokine modulation of type XV collagen gene expression in human dermal fibroblast cultures. *Experimental Dermatology* 8(5), pp. 407-412.

Klaus, S. 1969. Pigment transfer in mammalian epidermis. *Archives of Dermatology* 100(6), pp. 756-762.

Klingberg, F. *et al*. 2013. The myofibroblast matrix: implications for tissue repair and fibrosis. *Journal of Pathology* 229(2), pp. 298-309. doi: 10.1002/path.4104

Knox, P. *et al*. 1986. Role of fibronectin in the migration of fibroblasts into plasma clots. *Journal of Cell Biology* 102(6), pp. 2318-2323.

Knox, S. and Whitelock, J. 2006. Perlecan: how does one molecule do so many things? *Cellular and Molecular Life Sciences* 63(21), pp. 2435-2445. doi: 10.1007/s00018-006-6162-z

Kohan, M. *et al*. 2010. EDA-containing cellular fibronectin induces fibroblast differentiation through binding to $\alpha_4\beta_7$ integrin receptor and MAPK/ERK 1/2-dependent signalling. *FASEB Journal* 24(11), pp. 4503-4512. doi: 10.1096/fj.10-154435

Kohda, D. *et al*. 1996. Solution structure of the link module: a hyaluronan-binding domain involved in extracellular matrix stability and cell migration. *Cell* 86(5), pp. 767-775.

Kondo, T. and Ishida, Y. 2010. Molecular pathology of wound healing. *Forensic Science International* 203(1), pp. 93-98. doi: 10.1016/j.forsciint.2010.07.004

Kono, Y. *et al*. 2007. Sphingosine kinase 1 regulates differentiation of human and mouse lung fibroblasts mediated by TGF-β_1. *American Journal of Respiratory Cell and Molecular Biology* 37(4), pp. 395-404. doi: 10.1165/rcmb.2007-0065OC

Kopecki, Z. and Cowin, A. 2016. The role of actin remodelling proteins in wound healing and tissue regeneration. *Wound Healing - New insights into Ancient Challenges* 1(1) pp. 1-20. doi: 10.5772/64673

Krafts, K. 2010. Tissue repair: the hidden drama. *Organogenesis* 6(4), pp. 225-233. doi: 10.4161/org.6.4.12555

Krampert, M. *et al*. 2005. ADAMTS1 proteinase is up-regulated in wounded skin and regulates migration of fibroblasts and endothelial cells. *Journal of Biological Chemistry* 280(25), pp. 23844-23852. doi: 10.1074/jbc.M412212200

Kresse, H. and Schonherr, E. 2001. Proteoglycans of the extracellular matrix and growth control. *Journal of Cellular Physiology* 189(3), pp. 266-274. doi: 10.1002/jcp.10030

Krieg, T. and Aumailley, M. 2011. The extracellular matrix of the dermis: flexible structures with dynamic functions. *Experimental Dermatology* 20(8), pp. 689-695. doi: 10.1111/j.1600-0625.2011.01313.x

Krummel, T. *et al*. 1988. Transforming growth factor-β induces fibrosis in a foetal wound model. *Journal of Paediatric Surgery* 23(7), pp. 647-652.

Kucich, U. *et al*. 1997. Stabilisation of elastin mRNA by TGF-β: initial characterisation of signalling pathway. *American Journal of Respiratory Cell and Molecular Biology* 17(1), pp. 10-16. doi: 10.

1165/ajrcmb.17.1.2816

Kuo, Y. *et al*. 2005. Suppressed TGF-β_1 expression is correlated with the up-regulation of matrix metalloproteinase-13 in keloid regression after flashlamp pulsed-dye laser treatment. *Lasers in Surgery and Medicine* 36(1), pp. 38-42. doi: 10.1002/lsm.20104

Kurkinen, M. *et al*. 1980. Sequential appearance of fibronectin and collagen in experimental granulation tissue. *Laboratory Investigation* 43(1), pp. 47-51.

Kuroda, K. *et al*. 1999. Dermatopontin expression is decreased in hypertrophic scar and systemic sclerosis skin fibroblasts and is regulated by transforming growth factor-β_1, IL-4 and matrix collagen. *Journal of Investigative Dermatology* 112(5), pp. 706-710. doi: 10.1046/j.1523-1747.1999.00563.x

Kwiatkowska, D. and Kwiatkowska-Korczak, J. 1999. Adhesive glycoproteins of the extracellular matrix. *Postepy Higieny i Medycyny Doswiadczalnej* 53(1), pp. 55-74.

Lafdil, F. *et al*. 2006. Induction of Gas6 protein in CCL4-induced rat liver injury and anti-apoptotic effect on hepatic stellate cells. *Hepatology* 44(1), pp. 228-239. doi: 10.1002/hep.21237

Lamalice, L. *et al*. 2007. Endothelial cell migration during angiogenesis. *Circulation Research* 100(6), pp. 782-794. doi: 10.1161/01.RES.0000259593.07661.1e

Lamont, R. *et al*. 2016. Population genetic analysis of a medicinally significant Australian rainforest tree, *Fontainea picrosperma* C.T. White (*Euphorbiaceae*): biogeographic patterns and implications for species domestication and plantation establishment. *BMC Plant Biology* 16(1), pp. 1-12. doi: 10.1186/s12870-016-0743-2

Langevin, H. *et al*. 2011. Fibroblast cytoskeletal remodelling contributes to connective tissue tension. *Journal of Cellular Physiology* 226(5), pp. 1166-1175. doi: 10.1002/jcp.22442

Larson, B. *et al*. 2010. Scarless foetal wound healing: a basic science review. *Plastic and Reconstructive Surgery* 126(4), pp. 1172-1180. doi: 10.1097/PRS.0b013e3181eae781

Laurent, T. *et al*. 1996. The structure and function of hyaluronan: an overview. *Immunology and Cell Biology* 74(2), pp. 1-7. doi: 10.1038/icb.1996.32

Layton, A. *et al*. 1994. A comparison of intra-lesional triamcinolone and cryosurgery in the treatment of acne keloids. *British Journal of Dermatology* 130(4), pp. 498-501.

Leask, A. 2004. Transcriptional profiling of the scleroderma fibroblast reveals a potential role for connective tissue growth factor (CTGF) in pathological fibrosis. *The Keio Journal of Medicine* 53(2), pp. 74-77.

Leask, A. and Abraham, D. 2004. TGF-β signalling and the fibrotic response. *FASEB Journal* 18(7), pp. 816-827. doi: 10.1096/fj.03-1273rev

Leask, A. *et al*. 2008. Loss of protein kinase C-epsilon results in impaired cutaneous wound closure and myofibroblast function. *Journal of Cell Science* 121(20), pp. 3459-3467. doi: 10.1242/jcs.029215

LeBleu, V. *et al*. 2007. Structure and function of basement membranes. *Experimental Biology and Medicine* 232(9), pp. 1121-1129. doi: 10.3181/0703-mr-72

Lee, D. and Cho, K. 2005. The effects of epidermal keratinocytes and dermal fibroblasts on the formation of cutaneous basement membrane in three-dimensional culture systems. *Archives of Dermatological Research* 296(7), pp. 296-302. doi: 10.1007/s00403-004-0529-5

Lee, D. *et al*. 2015. High-mobility group box protein-1, matrix metalloproteinases, and vitamin D in

keloids and hypertrophic scars. *Plastic and Reconstructive Surgery* 3(6), pp. 1-9. doi: 10.1097/gox.0000000000000391

Lee, H. and Eun, H. 1999. Differences between fibroblasts cultured from oral mucosa and normal skin: implication to wound healing. *Journal of Dermatological Science* 21(3), pp. 176-182.

Lee, M. *et al*. 2004. Fibulin-5 promotes wound healing *in vivo*. *Journal of the American College of Surgeons* 199(3), pp. 403-410. doi: 10.1016/j.jamcollsurg.2004.04.021

Lee, S. *et al*. 2006. An update of the defensive barrier function of skin. *Yonsei Medical Journal* 47(3), pp. 293-306. doi: 10.3349/ymj.2006.47.3.293

Lee, T. *et al*. 1999. Expression of transforming growth factor-β_1, -β_2 and -β_3 proteins in keloids. *Annals of Plastic Surgery* 43(2), pp. 179-184.

Lefort, C. *et al*. 2011. N-cadherin cell-cell adhesion complexes are regulated by fibronectin matrix assembly. *Journal of Biological Chemistry* 286(4), pp. 3149-3160. doi: 10.1074/jbc.M110.115733

Lenga, Y. *et al*. 2008. Osteopontin expression is required for myofibroblast differentiation. *Circulation Research* 102(3), pp. 319-327. doi: 10.1161/circresaha.107.160408

Leung, A. *et al*. 2012. Foetal wound healing: implications for minimal scar formation. *Current Opinion in Pediatrics* 24(3), pp. 371-378. doi: 10.1097/MOP.0b013e3283535790

Li, J. *et al*. 2007. Pathophysiology of acute wound healing. *Clinics in Dermatology* 25(1), pp. 9-18. doi: 10.1016/j.clindermatol.2006.09.007

Li, M. *et al*. 2017. Theoretical and practical aspects of using foetal fibroblasts for skin regeneration. *Ageing Research Reviews* 36(1), pp. 32-41. doi: 10.1016/j.arr.2017.02.005

Li, W. *et al*. 2006. Transforming growth factor-β_3 affects plasminogen activator inhibitor-1 expression in foetal mice and modulates fibroblast-mediated collagen gel contraction. *Wound Repair and Regeneration* 14(5), pp. 516-525. doi: 10.1111/j.1743-6109.2006.00158.x

Lin, J. *et al*. 2008. Human tropomyosin isoforms in the regulation of cytoskeleton functions. *Advances in Experimental Medicine and Biology* 644, pp. 201-222.

Liu, J. and Davidson, J. 1988. The elastogenic effect of recombinant transforming growth factor-β on porcine aortic smooth muscle cells. *Biochemical and Biophysical Research Communications* 154(3), pp. 895-901.

Loeffler, I. *et al*. 2012. Collagen VIII influences epithelial phenotypic changes in experimental diabetic nephropathy. *American Journal of Physiology: Renal Physiology* 303(5), pp. 733-745. doi: 10.1152/ajprenal.00212.2012

Longaker, M. *et al*. 1989. Studies in foetal wound healing. IV. Hyaluronic acid-stimulating activity distinguishes foetal wound fluid from adult wound fluid. *Annals of Surgery* 210(5), pp. 667-672.

Longaker, M. *et al*. 1994. Adult skin wounds in the foetal environment heal with scar formation. *Annals of Surgery* 219(1), pp. 65-72.

Lopez-Casillas, F. *et al*. 1993. Betaglycan presents ligand to the TGF-β signalling receptor. *Cell* 73(7), pp. 1435-1444.

Lorand, L. and Graham, R. 2003. Transglutaminases: cross-linking enzymes with pleiotropic functions. *Nature Reviews: Molecular Cell Biology* 4(2), pp. 140-156. doi: 10.1038/nrm1014

Lorencini, M. *et al*. 2014. Active ingredients against human epidermal ageing. *Ageing Research Reviews* 15(1), pp. 100-115. doi: 10.1016/j.arr.2014.03.002

Lorenz, H. *et al*. 1992. Scarless wound repair: a human foetal skin model. *Development* 114(1), pp. 253-259.

Lorenz, H. *et al*. 1993. Foetal wound healing: the ontogeny of scar formation in the non-human primate. *Annals of Surgery* 217(4), pp. 391-396.

Lorenz, H. and Adzick, N. 1993. Scarless skin wound repair in the foetus. *Western Journal of Medicine* 159(3), pp. 350-355.

Love, P. and Kundu, R. 2013. Keloids: an update on medical and surgical treatments. *Journal of Drugs in Dermatology* 12(4), pp. 403-409.

Lovvorn, H. *et al*. 1998. Hyaluronan receptor expression increases in foetal excisional skin wounds and correlates with fibroplasia. *Journal of Pediatric Surgery* 33(7), pp. 1062-1069.

Lovvorn, H. *et al*. 1999. Relative distribution and cross-linking of collagen distinguish foetal from adult sheep wound repair. *Journal of Pediatric Surgery* 34(1), pp. 218-223.

Lu, L. *et al*. 2005. The temporal effects of anti-TGF-β_1, -β_2, and -β_3 monoclonal antibody on wound healing and hypertrophic scar formation. *Journal of the American College of Surgeons* 201(3), pp. 391-397. doi: 10.1016/j.jamcollsurg.2005.03.032

Lucero, H. and Kagan, H. 2006. Lysyl oxidase: an oxidative enzyme and effector of cell function. *Cellular and Molecular Life Sciences* 63(19), pp. 2304-2316. doi: 10.1007/s00018-006-6149-9

Luduena, R. 1998. Multiple forms of tubulin: different gene products and covalent modifications. *International Review of Cytology* 178, pp. 207-275.

Lynch, C. *et al*. 2011. Filamin depletion blocks endoplasmic spreading and destabilises force-bearing adhesions. *Molecular Biology of the Cell* 22(8), pp. 1263-1273. doi: 10.1091/mbc.E10-08-0661

Maas-Szabowski, N. *et al*. 1999. Keratinocyte growth regulation in fibroblast co-cultures via a double paracrine mechanism. *Journal of Cell Science* 112(12), pp. 1843-1853.

Macintyre, L. and Baird, M. 2006. Pressure garments for use in the treatment of hypertrophic scars - a review of the problems associated with their use. *Burns* 32(1), pp. 10-15. doi: 10.1016/j. burns.2004.06.018

Mackie, E. *et al*. 1988. Induction of tenascin in healing wounds. *Journal of Cell Biology* 107(6), pp. 2757-2767.

Madden, J. and Peacock, E. 1971. Studies on the biology of collagen during wound healing: dynamic metabolism of scar collagen and remodelling of dermal wounds. *Annals of Surgery* 174(3), pp. 511-520.

Mak, K. *et al*. 2009. Scarless healing of oral mucosa is characterised by faster resolution of inflammation and control of myofibroblast action compared to skin wounds in the red Duroc pig model. *Journal of Dermatological Science* 56(3), pp. 168-180. doi: 10.1016/j.jdermsci.2009.09.005

Malmstrőm, J. *et al*. 2004. Transforming growth factor-β_1 specifically induce proteins involved in the myofibroblast contractile apparatus. *Molecular and Cellular Proteomics* 3(5), pp. 466-477. doi: 10. 1074/mcp.M300108-MCP200

Mancini, R. and Quaife, J. 1962. Histogenesis of experimentally produced keloids. *Journal of*

Investigative Dermatology 38(1), pp. 143-181.

Marieb, E. and Hoehn, K. 2010. *Human anatomy and physiology*. 8th ed. California: Pearson-Benjamin Cummings.

Marneros, A. and Krieg, T. 2004. Keloids - clinical diagnosis, pathogenesis, and treatment options. *Journal of the German Society of Dermatology* 2(11), pp. 905-913.

Martin, J. *et al*. 2016. Tumour necrosis factor-stimulated gene 6 (TSG-6)-mediated interactions with inter-alpha-inhibitor heavy chain 5 facilitate tumour growth factor-β_1 (TGF-β_1)-dependent fibroblast to myofibroblast differentiation. *Journal of Biological Chemistry* 291(26), pp. 13789-13801. doi: 10.1074/jbc.M115.670521

Martin, P. and Leibovich, S. 2005. Inflammatory cells during wound repair: the good, the bad and the ugly. *Trends in Cell Biology* 15(11), pp. 599-607. doi: 10.1016/j.tcb.2005.09.002

Martin-Villar, E. *et al*. 2010. Podoplanin associates with CD44 to promote directional cell migration. *Molecular Biology of the Cell* 21(24), pp. 4387-4399. doi: 10.1091/mbc.E10-06-0489

Martiny-Baron, G. *et al*. 1993. Selective inhibition of protein kinase C isozymes by the indolocarbazole, Gő6976. *Journal of Biological Chemistry* 268(13), pp. 9194-9197.

Massague, J. and Wotton, D. 2000. Transcriptional control by the TGF-β/SMAD signalling system. *The EMBO Journal* 19(8), pp. 1745-1754. doi: 10.1093/emboj/19.8.1745

Massague, J. *et al*. 2005. SMAD transcription factors. *Genes and Development* 19(23), pp. 2783-2810. doi: 10.1101/gad.1350705

Massoudi, D. *et al*. 2012. NC1 long and NC3 short splice variants of type XII collagen are over-expressed during corneal scarring. *Investigative Ophthalmology and Visual Science* 53(11), pp. 7246-7256. doi: 10.1167/iovs.11-8592

Mast, B. *et al*. 1995. Hyaluronic acid degradation products induce neovascularisation and fibroplasia in foetal rabbit wounds. *Wound Repair and Regeneration* 3(1), pp. 66-72. doi: 10.1046/j.1524-475X.1995.30112.x

Maul, R. and Chang, D. 1999. EPLIN - epithelial protein lost in neoplasm. *Oncogene* 18(54), pp. 7838-7841. doi: 10.1038/sj.onc.1203206

Maul, R. *et al*. 2003. EPLIN regulates actin dynamics by cross-linking and stabilising filaments. *Journal of Cell Biology* 160(3), pp. 399-407. doi: 10.1083/jcb.200212057

Mayanagi, T. and Sobue, K. 2011. Diversification of caldesmon-linked actin cytoskeleton in cell motility. *Cell Adhesion and Migration* 5(2), pp. 150-159.

McCauley, R. *et al*. 1992. Altered cytokine production in black patients with keloids. *Journal of Clinical Immunology* 12(4), pp. 300-308.

McKeown, S. *et al*. 2007. Matrix metalloproteinase-3 differences in oral and skin fibroblasts. *Journal of Dental Research* 86(5), pp. 457-462. doi: 10.1177/154405910708600513

McMillan, J. *et al*. 2003. Epidermal basement membrane zone components: ultrastructural distribution and molecular interactions. *Journal of Dermatological Science* 31(3), pp. 169-177.

Mehta, M. *et al*. 2016. The evidence for natural therapeutics as potential anti-scarring agents in burn-related scarring. *Burns and Trauma* 4(1), pp. 1-12. doi: 10.1186/s41038-016-0040-1

Menon, G. 2002. New insights into skin structure: scratching the surface. *Advanced Drug Delivery Reviews* 54(1), pp. 3-17.

Menon, M. *et al*. 2015. Intronic locus determines SHROOM3 expression and potentiates renal allograft fibrosis. *Journal of Clinical Investigation* 125(1), pp. 208-221. doi: 10.1172/jci76902

Meran, S. *et al*. 2007. Involvement of hyaluronan in regulation of fibroblast phenotype. *Journal of Biological Chemistry* 282(35), pp. 25687-25697. doi: 10.1074/jbc.M700773200

Meran, S. *et al*. 2008. Hyaluronan facilitates TGF-β_1-mediated fibroblast proliferation. *Journal of Biological Chemistry* 283(10), pp. 6530-6545. doi: 10.1074/jbc.M704819200

Meran, S. *et al*. 2011. Hyaluronan facilitates transforming growth factor-β_1-dependent proliferation via CD44 and epidermal growth factor receptor interaction. *Journal of Biological Chemistry* 286(20), pp. 17618-17630. doi: 10.1074/jbc.M111.226563

Merkel, J. *et al*. 1988. Type I and type III collagen content of healing wounds in foetal and adult rats. *Proceedings of the Society for Experimental Biology and Medicine* 187(4), pp. 493-497.

Meyer, L. *et al*. 2000. Reduced hyaluronan in keloid tissue and cultured keloid fibroblasts. *Journal of Investigative Dermatology* 114(5), pp. 953-959. doi: 10.1046/j.1523-1747.2000.00950.x

Miao, Z. *et al*. 2017. Microtubule actin cross-linking factor 1, a novel potential target in cancer. *Cancer Science* 108(10), pp. 1953-1958. doi: 10.1111/cas.13344

Midgley, A. *et al*. 2013. Transforming growth factor-β_1 (TGF-β_1)-stimulated fibroblast-myofibroblast differentiation is mediated by hyaluronan (HA)-facilitated epidermal growth factor receptor (EGFR) and CD44 co-localisation in lipid rafts. *Journal of Biological Chemistry* 288(21), pp. 14824-14838. doi: 10.1074/jbc.M113.451336

Midgley, A. 2014. *Cellular mechanisms of myofibroblast differentiation and dysfunctions in wound healing.* Cardiff University.

Midwood, K. and Schwarzbauer, J. 2002. Elastic fibres: building bridges between cells and their matrix. *Current Biology* 12(8), pp. 279-281.

Milner, C. and Day, A. 2003. TSG-6: a multi-functional protein associated with inflammation. *Journal of Cell Science* 116(10), pp. 1863-1873. doi: 10.1242/jcs.00407

Milstone, L. 2004. Epidermal desquamation. *Journal of Dermatological Science* 36(3), pp. 131-140. doi: 10.1016/j.jdermsci.2004.05.004

Mimura, Y. *et al*. 2004. Epidermal growth factor induces fibronectin expression in human dermal fibroblasts via protein kinase C delta signalling pathway. *Journal of Investigative Dermatology* 122(6), pp. 1390-1398. doi: 10.1111/j.0022-202X.2004.22618.x

Mishell, B. and Shiigi, S. 1982. Selected methods in cellular immunology. *Biochemistry and Molecular Biology Education* 10(1), pp. 486-486. doi: 10.1016/0307-4412(82)90061-9

Miyazawa, K. *et al*. 2002. Two major SMAD pathways in TGF-β superfamily signalling. *Genes to Cells* 7(12), pp. 1191-1204.

Moll, I. *et al*. 2005. Human Merkel cells - aspects of cell biology, distribution and functions. *European Journal of Cell Biology* 84(2), pp. 259-271. doi: 10.1016/j.ejcb.2004.12.023

Monzon, M. *et al*. 2010. Reactive oxygen species and hyaluronidase 2 regulate airway epithelial hyaluronan fragmentation. *Journal of Biological Chemistry* 285(34), pp. 26126-26134. doi: 10.1074

/jbc.M110.135194

Moore, A. *et al*. 2018. Scarless wound healing: transitioning from foetal research to regenerative healing. *Wiley Reviews: Developmental Biology* 7(2), pp. 1-19. doi: 10.1002/wdev.309

Mori, M. *et al*. 2014. ARHGAP22 localises at endosomes and regulates actin cytoskeleton. *PLoS One* 9(6), pp. 1-13. doi: 10.1371/journal.pone.0100271

Mori, R. *et al*. 2008. Molecular mechanisms linking wound inflammation and fibrosis: knockdown of osteopontin leads to rapid repair and reduced scarring. *Journal of Experimental Medicine* 205(1), pp. 43-51. doi: 10.1084/jem.20071412

Morioka, S. *et al*. 1987. Migrating keratinocytes express urokinase-type plasminogen activator. *Journal of Investigative Dermatology* 88(4), pp. 418-423.

Moriya, C. *et al*. 2011. Expression of matrix metalloproteinase-13 is controlled by IL-13 via PI3K/Akt3 and PKC-delta in normal human dermal fibroblasts. *Journal of Investigative Dermatology* 131(3), pp. 655-661. doi: 10.1038/jid.2010.361

Morris, D. *et al*. 1997. Acute and chronic animal models for excessive dermal scarring: quantitative studies. *Plastic and Reconstructive Surgery* 100(3), pp. 674-681.

Moseley, R. *et al*. 2004. Extracellular matrix metabolites as potential biomarkers of disease activity in wound fluid: lessons learned from other inflammatory diseases? *British Journal of Dermatology* 150(3), pp. 401-413. doi: 10.1111/j.1365-2133.2004.05845.x

Moses, R. 2016. *Evaluation of the stimulatory effects of EBC-46 on dermal fibroblast and keratinocyte wound healing responses in vitro and correlation to preferential healing in vivo.* Cardiff University.

Mosser, D. and Edwards, J. 2008. Exploring the full spectrum of macrophage activation. *Nature reviews: Immunology* 8(12), pp. 958-969. doi: 10.1038/nri2448

Moulin, V. and Plamondon, M. 2002. Differential expression of collagen integrin receptor on foetal versus adult skin fibroblasts: implication in wound contraction during healing. *British Journal of Dermatology* 147(5), pp. 886-892.

Moustakas, A. and Heldin, C. 2005. Non-SMAD TGF-β signals. *Journal of Cell Science* 118(16), pp. 3573-3584. doi: 10.1242/jcs.02554

Muir, I. 1990. On the nature of keloid and hypertrophic scars. *British Journal of Plastic Surgery* 43(1), pp. 61-69.

Muiznieks, L. and Keeley, F. 2013. Molecular assembly and mechanical properties of the extracellular matrix: a fibrous protein perspective. *Biochimica et Biophysica Acta* 1832(7), pp. 866-875. doi: 10. 1016/j.bbadis.2012.11.022

Muller, M. *et al*. 2008. Matrix metalloproteinases and diabetic foot ulcers: the ratio of MMP-1 to TIMP-1 is a predictor of wound healing. *Diabetic Medicine* 25(4), pp. 419-426. doi: 10.1111/j.1464-5491.2008.02414.x

Muro, A. *et al*. 2003. Regulated splicing of the fibronectin EDA exon is essential for proper skin wound healing and normal lifespan. *Journal of Cell Biology* 162(1), pp. 149-160. doi: 10.1083/ jcb.200212079

Murray, J. 1994. Keloids and hypertrophic scars. *Clinics in Dermatology* 12(1), pp. 27-37.

Murray, P. and Wynn, T. 2011. Protective and pathogenic functions of macrophage subsets. *Nature reviews: Immunology* 11(11), pp. 723-737. doi: 10.1038/nri3073

Mustoe, T. *et al*. 2002. International clinical recommendations on scar management. *Plastic and Reconstructive Surgery* 110(2), pp. 560-571.

Mustoe, T. 2008. Evolution of silicone therapy and mechanism of action in scar management. *Aesthetic Plastic Surgery* 32(1), pp. 82-92. doi: 10.1007/s00266-007-9030-9

Mutalik, S. 2005. Treatment of keloids and hypertrophic scars. *Indian Journal of Dermatology, Venereology and Leprology* 71(1), pp. 3-8.

Mutsaers, S. *et al*. 1997. Mechanisms of tissue repair: from wound healing to fibrosis. *International Journal of Biochemistry and Cell Biology* 29(1), pp. 5-17.

Nagaoka, A. *et al*. 2015. Regulation of hyaluronan (HA) metabolism mediated by HYBID (hyaluronan-binding protein involved in HA depolymerisation, KIAA1199) and HA synthases in growth factor-stimulated fibroblasts. *Journal of Biological Chemistry* 290(52), pp. 30910-30923. doi: 10.1074/jbc.M115.673566

Naitoh, M. *et al*. 2005. Gene expression in human keloids is altered from dermal to chondrocytic and osteogenic lineage. *Genes to Cells* 10(11), pp. 1081-1091. doi: 10.1111/j.1365-2443.2005.00902.x

Nakamura, T. *et al*. 2002. Fibulin-5/DANCE is essential for elastogenesis *in vivo*. *Nature* 415(6868), pp. 171-175. doi: 10.1038/415171a

Nakamura, T. *et al*. 2011. Hepatocyte growth factor twenty years on: much more than a growth factor. *Journal of Gastroenterology and Hepatology* 26(1), pp. 188-202. doi: 10.1111/j.1440-1746.2010.06549.x

Nanda, N. *et al*. 2001. Targeted inactivation of Gh/tissue transglutaminase II. *Journal of Biological Chemistry* 276(23), pp. 20673-20678. doi: 10.1074/jbc.M010846200

Natarajan, V. *et al*. 2014. Multi-faceted pathways protect human skin from UV radiation. *Nature: Chemical Biology* 10(7), pp. 542-551. doi: 10.1038/nchembio.1548

Naugle, J. *et al*. 2006. Type VI collagen induces cardiac myofibroblast differentiation: implications for post-infarction remodelling. *American Journal of Physiology: Heart and Circulatory Physiology* 290(1), pp. 323-330. doi: 10.1152/ajpheart.00321.2005

Nauta, A. *et al*. 2011. Wound healing and regenerative strategies. *Oral Diseases* 17(6), pp. 541-549. doi: 10.1111/j.1601-0825.2011.01787.x

Nazari, B. *et al*. 2016. Altered dermal fibroblasts in systemic sclerosis display podoplanin and CD90. *American Journal of Pathology* 186(10), pp. 2650-2664. doi: 10.1016/j.ajpath.2016.06.020

Neame, P. *et al*. 2000. Independent modulation of collagen fibrillogenesis by decorin and lumican. *Cellular and Molecular Life Sciences* 57(5), pp. 859-863. doi: 10.1007/s000180050048

Nedelec, B. *et al*. 2001. Myofibroblasts and apoptosis in human hypertrophic scars: the effect of interferon-$\alpha_2\beta$. *Surgery* 130(5), pp. 798-808. doi: 10.1067/msy.2001.116453

Neely, A. *et al*. 1999. Gelatinase activity in keloids and hypertrophic scars. *Wound Repair and Regeneration* 7(3), pp. 166-171.

Newman, A. *et al*. 2011. The requirement for fibroblasts in angiogenesis: fibroblast-derived matrix proteins are essential for endothelial cell lumen formation. *Molecular Biology of the Cell* 22(20), pp.

3791-3800. doi: 10.1091/mbc.E11-05-0393

Niessen, F. *et al*. 1999. On the nature of hypertrophic scars and keloids: a review. *Plastic and Reconstructive Surgery* 104(5), pp. 1435-1458.

Ning, W. *et al*. 2016. The CAMSAP3-ACF7 complex couples non-centrosomal microtubules with actin filaments to coordinate their dynamics. *Developmental Cell* 39(1), pp. 61-74. doi: 10.1016/j.devcel.2016.09.003

Nishizuka, Y. 1992. Intracellular signalling by hydrolysis of phospholipids and activation of protein kinase C. *Science* 258(5082), pp. 607-614.

Nunes, Q. *et al*. 2016. Fibroblast growth factors as tissue repair and regeneration therapeutics. *PeerJ* 4(1535), pp. 1-31. doi: 10.7717/peerj.1535

Nurden, A. 2011. Platelets, inflammation and tissue regeneration. *Thrombosis and Haemostasis* 105(1), pp. 13-33. doi: 10.1160/ths10-11-0720

Nystrom, A. and Bruckner-Tuderman, L. 2018. Matrix molecules and skin biology. *Seminars in Cell and Developmental Biology* 18(1), pp. 30104-30106. doi: 10.1016/j.semcdb.2018.07.025

O'Brien, L. and Pandit, A. 2006. Silicone gel sheeting for preventing and treating hypertrophic and keloid scars. *Cochrane Database of Systematic Reviews* 1(1), pp. 1-49. doi: 10.1002/14651858.CD003826.pub2

O'Brien, L. and Jones, D. 2013. Silicone gel sheeting for preventing and treating hypertrophic and keloid scars. *Cochrane Database of Systematic Reviews* (9), pp. 1-80. doi: 10.1002/14651858.CD003826.pub3

Ogawa, R. *et al*. 2011. Clinical applications of basic research that shows reducing skin tension could prevent and treat abnormal scarring: the importance of fascial/subcutaneous tensile reduction sutures and flap surgery for keloid and hypertrophic scar reconstruction. *Journal of Nippon Medical School* 78(2), pp. 68-76.

Ohtomo, S. *et al*. 2008. The role of megsin, a serine protease inhibitor, in diabetic mesangial matrix accumulation. *Kidney International* 74(6), pp. 768-774. doi: 10.1038/ki.2008.302

Okamoto, O. and Fujiwara, S. 2006. Dermatopontin, a novel player in the biology of the extracellular matrix. *Connective Tissue Research* 47(4), pp. 177-189. doi: 10.1080/03008200600846564

Oksala, O. *et al*. 1995. Expression of proteoglycans and hyaluronan during wound healing. *Journal of Histochemistry and Cytochemistry* 43(2), pp. 125-135.

Oleggini, R. *et al*. 2007. Regulation of elastin promoter by lysyl oxidase and growth factors: cross-control of lysyl oxidase on TGF-β_1 effects. *Matrix Biology* 26(6), pp. 494-505. doi: 10.1016/j.matbio.2007.02.003

Onichtchouk, D. *et al*. 1999. Silencing of TGF-β signalling by the pseudoreceptor, BAMBI. *Nature* 401(6752), pp. 480-485. doi: 10.1038/46794

Ono, I. *et al*. 2007. Basic fibroblast growth factor reduces scar formation in acute incisional wounds. *Wound Repair and Regeneration* 15(5), pp. 617-623. doi: 10.1111/j.1524-475X.2007.00293.x

Ono, Y. *et al*. 1988. The structure, expression, and properties of additional members of the protein kinase C family. *Journal of Biological Chemistry* 263(14), pp. 6927-6932.

Overall, C. *et al*. 1989. Independent regulation of collagenase, 72-kDa progelatinase, and

metalloendoproteinase inhibitor expression in human fibroblasts by transforming growth factor-β. *Journal of Biological Chemistry* 264(3), pp. 1860-1869.

Pakyari, M. *et al*. 2013. Critical role of transforming growth factor-β in different phases of wound healing. *Advances in Wound Care* 2(5), pp. 215-224. doi: 10.1089/wound.2012.0406

Paliwal, S. *et al*. 2004. P311 binds to the latency associated protein and down-regulates the expression of TGF-β_1 and TGF-β_2. *Biochemical and Biophysical Research Communications* 315(4), pp. 1104-1109. doi: 10.1016/j.bbrc.2004.01.171

Pan, D. *et al*. 2002. P311 induces a TGF-β_1-independent, non-fibrogenic myofibroblast phenotype. *Journal of Clinical Investigation* 110(9), pp. 1349-1358. doi: 10.1172/jci15614

Pang, C. *et al*. 2017. An overview of the therapeutic potential of regenerative medicine in cutaneous wound healing. *International Wound Journal* 14(3), pp. 450-459. doi: 10.1111/iwj.12735

Papp, H. *et al*. 2004. Opposite roles of protein kinase C isoforms in proliferation, differentiation, apoptosis, and tumorigenicity of human HaCaT keratinocytes. *Cellular and Molecular Life Sciences* 61(9), pp. 1095-1105. doi: 10.1007/s00018-004-4014-2

Parekh, A. and Hebda, P. 2017. The contractile phenotype of dermal foetal fibroblasts in scarless wound healing. *Current Pathobiology Reports* 5(3), pp. 271-277. doi: 10.1007/s40139-017-0149-3

Parks, W. 1999. Matrix metalloproteinases in repair. *Wound Repair and Regeneration* 7(6), pp. 423-432.

Peacock, E. *et al*. 1970. Biologic basis for the treatment of keloids and hypertrophic scars. *Southern Medical Journal* 63(7), pp. 755-760.

Peake, M. *et al*. 2014. Identification of a transcriptional signature for the wound healing continuum. *Wound Repair and Regeneration* 22(3), pp. 399-405. doi: 10.1111/wrr.12170

Pearson, G. *et al*. 2001. Mitogen-activated protein (MAP) kinase pathways: regulation and physiological functions. *Endocrine Reviews* 22(2), pp. 153-183. doi: 10.1210/edrv.22.2.0428

Peled, Z. *et al*. 2002. Matrix metalloproteinases and the ontogeny of scarless repair: the other side of the wound healing balance. *Plastic and Reconstructive Surgery* 110(3), pp. 801-811.

Pellegrin, S. and Mellor, H. 2007. Actin stress fibres. *Journal of Cell Science* 120(20), pp. 3491-3499. doi: 10.1242/jcs.018473

Pepper, M. 2001. Role of the matrix metalloproteinase and plasminogen activator-plasmin systems in angiogenesis. *Arteriosclerosis, Thrombosis and Vascular Biology* 21(7), pp. 1104-1117.

Phan, T. *et al*. 2003. Dietary compounds inhibit proliferation and contraction of keloid and hypertrophic scar-derived fibroblasts *in vitro*: therapeutic implication for excessive scarring. *Journal of Trauma* 54(6), pp. 1212-1224. doi: 10.1097/01.ta.0000030630.72836.32

Piccoli, M. *et al*. 2017. Inhibition of the cardiac fibroblast-enriched lncRNA Meg3 prevents cardiac fibrosis and diastolic dysfunction. *Circulation Research* 121(5), pp. 575-583. doi: 10.1161/ circresaha.117.310624

Piek, E. *et al*. 1999. Specificity, diversity and regulation in TGF-β superfamily signalling. *FASEB Journal* 13(15), pp. 2105-2124.

Plonka, P. *et al*. 2009. What are melanocytes really doing all day long? *Experimental Dermatology* 18(9), pp. 799-819. doi: 10.1111/j.1600-0625.2009.00912.x

Poochareon, V. and Berman, B. 2003. New therapies for the management of keloids. *Journal of Craniofacial Surgery* 14(5), pp. 654-657.

Powers, C. *et al*. 2000. Fibroblast growth factors, their receptors and signalling. *Endocrine-Related Cancer* 7(3), pp. 165-197.

Prehm, P. 1984. Hyaluronate is synthesised at plasma membranes. *The Biochemical Journal* 220(2), pp. 597-600.

Proksch, E. *et al*. 2008. The skin: an indispensable barrier. *Experimental Dermatology* 17(12), pp. 1063-1072.

Prunotto, M. *et al*. 2015. Stable incorporation of alpha-smooth muscle actin into stress fibres is dependent on specific tropomyosin isoforms. *Cytoskeleton* 72(6), pp. 257-267. doi: 10.1002/cm. 21230

Pullmann, H. *et al*. 1977. Disturbance of DNA synthesis in early psoriasis. *Archives for Dermatological Research* 258(2), pp. 211-218.

Qian, Y. *et al*. 2000. The carboxy terminus of AFAP-110 modulates direct interactions with actin filaments and regulates its ability to alter actin filament integrity and induce lamellipodia formation. *Experimental Cell Research* 255(1), pp. 102-113. doi: 10.1006/excr.1999.4795

Quan, G. *et al*. 2005. TGF-β_1 up-regulates transglutaminase 2 and fibronectin in dermal fibroblasts: a possible mechanism for the stabilisation of tissue inflammation. *Archives of Dermatological Research* 297(2), pp. 84-90. doi: 10.1007/s00403-005-0582-8

Quintanilla-Dieck, M. *et al*. 2009. Expression and regulation of cathepsin K in skin fibroblasts. *Experimental Dermatology* 18(7), pp. 596-602. doi: 10.1111/j.1600-0625.2009.00855.x

Ragoowansi, R. *et al*. 2003. Treatment of keloids by surgical excision and immediate post-operative single-fraction radiotherapy. *Plastic and Reconstructive Surgery* 111(6), pp. 1853-1859. doi: 10.1097/01.prs.0000056869.31142.de

Reddell, P. and Gordon, V. 2007. *Tiglien-3-one derivatives.* [Patent].

Reddell, P. *et al*. 2014. *Methods and compositions for wound healing.* [Patent].

Regn, M. *et al*. 2016. Peptidase inhibitor 16 is a membrane-tethered regulator of chemerin processing in the myocardium. *Journal of Molecular and Cellular Cardiology* 99, pp. 57-64. doi: 10. 1016/j.yjmcc.2016.08.010

Reiken, S. *et al*. 1997. Control of hypertrophic scar growth using selective photothermolysis. *Lasers in Surgery and Medicine* 21(1), pp. 7-12.

Reinke, J. and Sorg, H. 2012. Wound repair and regeneration. *European Surgical Research* 49(1), pp. 35-43. doi: 10.1159/000339613

Reish, R. and Eriksson, E. 2008. Scars: a review of emerging and currently available therapies. *Plastic and Reconstructive Surgery* 122(4), pp. 1068-1078. doi: 10.1097/PRS.0b013e318185d38f

Ren, Y. *et al*. 1998. Cloning and characterisation of GEF-H1, a microtubule-associated guanine nucleotide exchange factor for Rac and Rho GTPases. *Jour* 273(52), pp. 34954-34960.

Reno, F. *et al*. 2001. Effects of mechanical compression on hypertrophic scars: prostaglandin E2 release. *Burns* 27(3), pp. 215-218.

Ricard-Blum, S. *et al*. 2018. Molecular and tissue alterations of collagens in fibrosis. *Matrix Biology* 68(1), pp. 122-149. doi: 10.1016/j.matbio.2018.02.004

Ries, C. and Petrides, P. 1995. Cytokine regulation of matrix metalloproteinase activity and its regulatory dysfunction in disease. *Biological Chemistry Hoppe-Seyler* 376(6), pp. 345-355.

Robert, R. *et al*. 1999. Disfiguring burn scars and adolescent self-esteem. *Burns* 25(7), pp. 581-585.

Robinson, N. *et al*. 2006. Tissue transglutaminase expression and activity in placenta. *Placenta* 27(2), pp. 148-157. doi: 10.1016/j.placenta.2005.01.008

Rolfe, K. and Grobbelaar, A. 2012. A review of foetal scarless healing. *ISRN Dermatology* 2012(1), pp. 1-9. doi: 10.5402/2012/698034

Romberger, D. 1997. Fibronectin. *International Journal of Biochemistry and Cell Biology* 29(7), pp. 939-943.

Rosenbloom, J. *et al*. 1993. Extracellular matrix 4: the elastic fibre. *FASEB Journal* 7(13), pp. 1208-1218.

Rosse, C. *et al*. 2010. PKC and the control of localised signal dynamics. *Nature Reviews: Molecular Cell Biology* 11(2), pp. 103-112. doi: 10.1038/nrm2847

Rudolph, R. 1979. Location of the force of wound contraction. *Surgery, Gynecology and Obstetrics* 148(4), pp. 547-551.

Rui, M. *et al*. 2017. PKC in regenerative therapy: new insights for old targets. *Pharmaceuticals* 10(2), pp. 1-14. doi: 10.3390/ph10020046

Runger, T. *et al*. 2007. Role of cathepsin K in the turnover of the dermal extracellular matrix during scar formation. *Journal of Investigative Dermatology* 127(2), pp. 293-297. doi: 10.1038/sj.jid. 5700535

Ruoslahti, E. 1988. Structure and biology of proteoglycans. *Annual Review of Cell Biology* 4(1), pp. 229-255. doi: 10.1146/annurev.cb.04.110188.001305

Rusciani, L. *et al*. 1993. Use of cryotherapy in the treatment of keloids. *Journal of Dermatologic Surgery and Oncology* 19(6), pp. 529-534.

Russell, S. *et al*. 2010. Epigenetically altered wound healing in keloid fibroblasts. *Journal of Investigative Dermatology* 130(10), pp. 2489-2496. doi: 10.1038/jid.2010.162

Saarialho-Kere, U. *et al*. 1992. Distinct localisation of collagenase and tissue inhibitor of metalloproteinases expression in wound healing associated with ulcerative pyogenic granuloma. *Journal of Clinical Investigation* 90(5), pp. 1952-1957. doi: 10.1172/jci116073

Sakai, T. *et al*. 2001. Plasma fibronectin supports neuronal survival and reduces brain injury following transient focal cerebral ischemia, but is not essential for skin wound healing and haemostasis. *Nature Medicine* 7(3), pp. 324-330. doi: 10.1038/85471

Sallstrom, K. *et al*. 1989. Treatment of keloids with surgical excision and post-operative X-ray radiation. *Scandinavian Journal of Plastic, Reconstructive and Hand Surgery* 23(3), pp. 211-215.

Sampson, N. *et al*. 2013. Stromal insulin-like growth factor binding protein 3 (IGFBP3) is elevated in the diseased human prostate and promotes *ex vivo* fibroblast-myofibroblast differentiation. *Endocrinology* 154(8), pp. 2586-2599. doi: 10.1210/en.2012-2259

Sandbo, N. and Dulin, N. 2011. Actin cytoskeleton in myofibroblast differentiation: ultrastructure defining form and driving function. *Translational Research* 158(4), pp. 181-196. doi: 10.1016/j.trsl.2011.05.004

Sandi, M. *et al*. 2017. MARK3-mediated phosphorylation of ARHGEF2 couples microtubules to the actin cytoskeleton to establish cell polarity. *Science Signalling* 10(503), pp. 1-22. doi: 10.1126/scisignal.aan3286

Sang, Q. 1998. Complex role of matrix metalloproteinases in angiogenesis. *Cell Research* 8(3), pp. 171-177. doi: 10.1038/cr.1998.17

Sano, S. *et al*. 1999. Keratinocyte-specific ablation of Stat3 exhibits impaired skin remodelling, but does not affect skin morphogenesis. *The EMBO Journal* 18(17), pp. 4657-4668. doi: 10.1093/emboj/18.17.4657

Sanz-Moreno, V. *et al*. 2008. Rac activation and inactivation control plasticity of tumour cell movement. *Cell* 135(3), pp. 510-523. doi: 10.1016/j.cell.2008.09.043

Sappino, A. *et al*. 1990. Differentiation repertoire of fibroblastic cells: expression of cytoskeletal proteins as marker of phenotypic modulations. *Laboratory Investigation* 63(2), pp. 144-161.

Sarrazy, V. *et al*. 2011. Mechanisms of pathological scarring: role of myofibroblasts and current developments. *Wound Repair and Regeneration* 19(1), pp. 10-15. doi: 10.1111/j.1524-475X.2011.00708.x

Satish, L. *et al*. 2006. Gene expression patterns in isolated keloid fibroblasts. *Wound Repair and Regeneration* 14(4), pp. 463-470. doi: 10.1111/j.1743-6109.2006.00135.x

Sayah, D. *et al*. 1999. Down-regulation of apoptosis-related genes in keloid tissues. *Journal of Surgical Research* 87(2), pp. 209-216. doi: 10.1006/jsre.1999.5761

Schaefer, L. and Iozzo, R. 2008. Biological functions of the small leucine-rich proteoglycans: from genetics to signal transduction. *Journal of Biological Chemistry* 283(31), pp. 21305-21309. doi: 10.1074/jbc.R800020200

Schaefer, L. and Schaefer, R. 2010. Proteoglycans: from structural compounds to signalling molecules. *Cell and Tissue Research* 339(1), pp. 237-246. doi: 10.1007/s00441-009-0821-y

Schiller, M. *et al*. 2004. TGF-β-induced SMAD signalling and gene regulation: consequences for extracellular matrix remodelling and wound healing. *Journal of Dermatological Science* 35(2), pp. 83-92. doi: 10.1016/j.jdermsci.2003.12.006

Schmid, P. *et al*. 1998. Enhanced expression of transforming growth factor-β type I and type II receptors in wound granulation tissue and hypertrophic scar. *American Journal of Pathology* 152(2), pp. 485-493.

Schrementi, M. *et al*. 2008. Site-specific production of TGF-β in oral mucosal and cutaneous wounds. *Wound Repair and Regeneration* 16(1), pp. 80-86. doi: 10.1111/j.1524-475X.2007.00320.x

Schultz, G. and Wysocki, A. 2009. Interactions between extracellular matrix and growth factors in wound healing. *Wound Repair and Regeneration* 17(2), pp. 153-162. doi: 10.1111/j.1524-475X.2009.00466.x

Schulz, J. *et al*. 2016. COMP-assisted collagen secretion - a novel intracellular function required for fibrosis. *Journal of Cell Science* 129(4), pp. 706-716. doi: 10.1242/jcs.180216

Schwartz, M. and Horwitz, A. 2006. Integrating adhesion, protrusion and contraction during cell

migration. *Cell* 125(7), pp. 1223-1225. doi: 10.1016/j.cell.2006.06.015

Sciubba, J. *et al*. 1978. A fine structural comparison of the healing of incisional wounds of mucosa and skin. *Journal of Oral Pathology* 7(4), pp. 214-227.

Scruggs, A. *et al*. 2018. Loss of CDKN2B promotes fibrosis via increased fibroblast differentiation rather than proliferation. *American Journal of Respiratory Cell and Molecular Biology* 59(2), pp. 200-214. doi: 10.1165/rcmb.2017-0298OC

Seifert, A. *et al*. 2012. Skin regeneration in adult axolotls: a blueprint for scar-free healing in vertebrates. *PLoS One* 7(4), pp. 1-19. doi: 10.1371/journal.pone.0032875

Seifert, O. *et al*. 2008. Identification of unique gene expression patterns within different lesional sites of keloids. *Wound Repair and Regeneration* 16(2), pp. 254-265. doi: 10.1111/j.1524-475X. 2007.00343.x

Sekiya, T. *et al*. 2004. Identification of BMP and activin membrane-bound inhibitor (BAMBI), an inhibitor of transforming growth factor-β signalling, as a target of the β-catenin pathway in colorectal tumour cells. *Journal of Biological Chemistry* 279(8), pp. 6840-6846. doi: 10.1074/ jbc.M310876200

Sen, C. *et al*. 2009. Human skin wounds: a major and snowballing threat to public health and the economy. *Wound Repair and Regeneration* 17(6) pp. 763-771. doi: 10.1111/j.1524-475X.2009. 00543.x.

Serini, G. *et al*. 1998. The fibronectin domain ED-A is crucial for myofibroblastic phenotype induction by transforming growth factor-β_1. *Journal of Cell Biology* 142(3), pp. 873-881.

Serini, G. and Gabbiani, G. 1999. Mechanisms of myofibroblast activity and phenotypic modulation. *Experimental Cell Research* 250(2), pp. 273-283. doi: 10.1006/excr.1999.4543

Shang, H. *et al*. 2017. Knockdown of Fstl1 attenuates hepatic stellate cell activation through the TGF-β_1/SMAD3 signalling pathway. *Molecular Medicine Reports* 16(5), pp. 7119-7123. doi: 10.3892/ mmr.2017.7445

Shangguan, L. *et al*. 2012. Inhibition of TGF-β/SMAD signalling by BAMBI blocks differentiation of human mesenchymal stem cells to carcinoma-associated fibroblasts and abolishes their pro-tumour effects. *Stem Cells* 30(12), pp. 2810-2819. doi: 10.1002/stem.1251

Shannon, D. *et al*. 2006. Phenotypic differences between oral and skin fibroblasts in wound contraction and growth factor expression. *Wound Repair and Regeneration* 14(2), pp. 172-178. doi: 10.1111/j.1743-6109.2006.00107.x

Shi, J. *et al*. 2006. P311-induced myofibroblasts exhibit ameboid-like migration through RalA activation. *Experimental Cell Research* 312(17), pp. 3432-3442. doi: 10.1016/j.yexcr.2006.07.016

Shi, Y. *et al*. 2014. Deficiency of Kruppel-like factor KLF4 in myeloid-derived suppressor cells inhibits tumour pulmonary metastasis in mice accompanied by decreased fibrocytes. *Oncogenesis* 3(1), pp. 1-7. doi: 10.1038/oncsis.2014.44

Shi-wen, X. *et al*. 2000. Autocrine over-expression of CTGF maintains fibrosis: RDA analysis of fibrosis genes in systemic sclerosis. *Experimental Cell Research* 259(1), pp. 213-224. doi: 10.1006/ excr.2000.4972

Shih, B. *et al*. 2010. Molecular dissection of abnormal wound healing processes resulting in keloid disease. *Wound Repair and Regeneration* 18(2), pp. 139-153. doi: 10.1111/j.1524-475X.2009.00553.x

Shih, B. and Bayat, A. 2010. Genetics of keloid scarring. *Archives of Dermatological Research* 302(5), pp. 319-339. doi: 10.1007/s00403-009-1014-y

Shiomi, T. *et al*. 2010. Matrix metalloproteinases, a disintegrin and metalloproteinases, and a disintegrin and metalloproteinases with thrombospondin motifs in non-neoplastic diseases. *Pathology International* 60(7), pp. 477-496. doi: 10.1111/j.1440-1827.2010.02547.x

Shiraha, H. *et al*. 2000. Ageing fibroblasts present reduced epidermal growth factor (EGF) responsiveness due to preferential loss of EGF receptors. *Journal of Biological Chemistry* 275(25), pp. 19343-19351. doi: 10.1074/jbc.M000008200

Shuttleworth, C. 1997. Type VIII collagen. *International Journal of Biochemistry and Cell Biology* 29(10), pp. 1145-1148.

Sidgwick, G. *et al*. 2013. Altered expression of hyaluronan synthase and hyaluronidase mRNA may affect hyaluronic acid distribution in keloid disease compared with normal skin. *Experimental Dermatology* 22(5), pp. 377-379. doi: 10.1111/exd.12147

Simon, D. *et al*. 2014. Tissue transglutaminase, not lysyl oxidase, dominates early calcium-dependent remodelling of fibroblast-populated collagen lattices. *Cells Tissues Organs* 200(2), pp. 104-117. doi: 10.1159/000381015

Simpson, C. *et al*. 2011. Deconstructing the skin: cytoarchitectural determinants of epidermal morphogenesis. *Nature Reviews: Molecular Cell Biology* 12(9), pp. 565-580. doi: 10.1038/nrm3175

Simpson, R. *et al*. 2010. Ageing fibroblasts resist phenotypic maturation because of impaired hyaluronan-dependent CD44/epidermal growth factor receptor signalling. *American Journal of Pathology* 176(3), pp. 1215-1228. doi: 10.2353/ajpath.2010.090802

Singer, A. and Clark, R. 1999. Cutaneous wound healing. *The New England Journal of Medicine* 341(10), pp. 738-746. doi: 10.1056/nejm199909023411006

Skalli, O. *et al*. 1986. A monoclonal antibody against alpha-smooth muscle actin: a new probe for smooth muscle differentiation. *Journal of Cell Biology* 103(6), pp. 2787-2796.

Skrbic, B. *et al*. 2015. Lack of collagen VIII reduces fibrosis and promotes early mortality and cardiac dilatation in pressure overload in mice. *Cardiovascular Research* 106(1), pp. 32-42. doi: 10.1093 /cvr/cvv041

Slemp, A. and Kirschner, R. 2006. Keloids and scars: a review of keloids and scars, their pathogenesis, risk factors and management. *Current Opinion in Paediatrics* 18(4), pp. 396-402. doi: 10.1097/01. mop.0000236389.41462.ef

Smith, J. *et al*. 2008. Gene profiling of keloid fibroblasts shows altered expression in multiple fibrosis-associated pathways. *Journal of Investigative Dermatology* 128(5), pp. 1298-1310. doi: 10.1038/ sj.jid.5701149

Smith, L. *et al*. 1986. Collagen types I, III and V in human embryonic and foetal skin. *American Journal of Anatomy* 175(4), pp. 507-521. doi: 10.1002/aja.1001750409

Smith-Mungo, L. and Kagan, H. 1998. Lysyl oxidase: properties, regulation and multiple functions in biology. *Matrix Biology* 16(7), pp. 387-398.

Somanna, N. *et al*. 2015. Aldosterone-induced cardiomyocyte growth, and fibroblast migration and proliferation, are mediated by TRAF3IP2. *Cellular Signalling* 27(10), pp. 1928-1938. doi: 10.1016/ j.cellsig.2015.07.001

Song, H. *et al*. 1997. *In vivo* MR microscopy of the human skin. *Magnetic Resonance in Medicine* 37(2), pp. 185-191.

Song, Q. *et al*. 2017. JAK/STAT3 and SMAD3 activities are required for the wound healing properties of *Periplaneta americana* extracts. *International Journal of Molecular Medicine* 40(2), pp. 465-473. doi: 10.3892/ijmm.2017.3040

Soo, C. *et al*. 2000. Differential expression of matrix metalloproteinases and their tissue-derived inhibitors in cutaneous wound repair. *Plastic and Reconstructive Surgery* 105(2), pp. 638-647.

Soroosh, A. *et al*. 2016. Crohn's disease fibroblasts overproduce the novel protein KIAA1199 to create pro-inflammatory hyaluronan fragments. *Cellular and Molecular Gastroenterology and Hepatology* 2(3), pp. 358-368. doi: 10.1016/j.jcmgh.2015.12.007

Sotiropoulou, P. and Blanpain, C. 2012. Development and homeostasis of the skin epidermis. *Cold Spring Harbour: Perspectives in Biology* 4(7), pp. 1-19. doi: 10.1101/cshperspect.a008383

Sottile, J. and Hocking, D. 2002. Fibronectin polymerisation regulates the composition and stability of extracellular matrix fibrils and cell-matrix adhesions. *Molecular Biology of the Cell* 13(10), pp. 3546-3559. doi: 10.1091/mbc.e02-01-0048

Sparber, F. 2014. Langerhans cells: an update. *Journal of the German Society of Dermatology* 12(12), pp. 1107-1111. doi: 10.1111/ddg.12506

Spicer, A. and McDonald, J. 1998. Characterisation and molecular evolution of a vertebrate hyaluronan synthase gene family. *Journal of Biological Chemistry* 273(4), pp. 1923-1932.

Sriram, G. *et al*. 2015. Fibroblast heterogeneity and its implications for engineering organotypic skin models *in vitro*. *European Journal of Cell Biology* 94(11), pp. 483-512. doi: 10.1016/ j.ejcb.2015.08.001

Srivastava, M. *et al*. 2008. Over-expression of cathepsin K in mice decreases collagen deposition and lung resistance in response to bleomycin-induced pulmonary fibrosis. *Respiratory Research* 9(54), pp. 1-12. doi: 10.1186/1465-9921-9-54

Stadelmann, W. *et al*. 1998. Physiology and healing dynamics of chronic cutaneous wounds. *American Journal of Surgery* 176(2), pp. 26-38.

Stelnicki, E. *et al*. 1998. Bone morphogenetic protein-2 induces scar formation and skin maturation in the second trimester foetus. *Plastic and Reconstructive Surgery* 101(1), pp. 12-19.

Stephens, P. *et al*. 1996. A comparison of the ability of intra-oral and extra-oral fibroblasts to stimulate extracellular matrix reorganisation in a model of wound contraction. *Journal of Dental Research* 75(6), pp. 1358-1364. doi: 10.1177/00220345960750060601

Stephens, P. *et al*. 2001. Skin and oral fibroblasts exhibit phenotypic differences in extracellular matrix reorganisation and matrix metalloproteinase activity. *British Journal of Dermatology* 144(2), pp. 229-237.

Stern, R. and Maibach, H. 2008. Hyaluronan in skin: aspects of ageing and its pharmacologic modulation. *Clinics in Dermatology* 26(2), pp. 106-122. doi: 10.1016/j.clindermatol.2007.09.013

Su, Z. *et al*. 2014. Up-regulated HMGB1 in EAM directly led to collagen deposition by a PKC-β/ERK1/2-dependent pathway: cardiac fibroblast/myofibroblast might be another source of HMGB1. *Journal of Cellular and Molecular Medicine* 18(9), pp. 1740-1751. doi: 10.1111/jcmm.12324

Suarez, E. *et al*. 2013. Up-regulation of tension-related proteins in keloids: knockdown of Hsp27,

$\alpha_2\beta_1$-integrin and PAI-2 shows convincing reduction of extracellular matrix production. *Plastic and Reconstructive Surgery* 131(2), pp. 158-173. doi: 10.1097/PRS.0b013e3182789b2b

Suarez, E. *et al*. 2015. Identification of biomarkers involved in differential profiling of hypertrophic and keloid scars versus normal skin. *Archives of Dermatological Research* 307(2), pp. 115-133. doi: 10.1007/s00403-014-1512-4

Sudo, T. *et al*. 2013. Expression of mesenchymal markers vimentin and fibronectin: the clinical significance in esophageal squamous cell carcinoma. *Annals of Surgical Oncology* 20(3), pp. 324-335. doi: 10.1245/s10434-012-2418-z

Sund, B. 2000. *New developments in wound care*. London: PBJ Publications.

Suter, M. *et al*. 2009. The keratinocyte in epidermal renewal and defence. *Veterinary Dermatology* 20(5), pp. 515-532. doi: 10.1111/j.1365-3164.2009.00819.x

Swee, M. *et al*. 1995. Developmental regulation of elastin production - expression of tropoelastin pre-mRNA persists after down-regulation of steady-state mRNA levels. *Journal of Biological Chemistry* 270(25), pp. 14899-148906.

Szpaderska, A. *et al*. 2003. Differential injury responses in oral mucosal and cutaneous wounds. *Journal of Dental Research* 82(8), pp. 621-626. doi: 10.1177/154405910308200810

Taal, L. and Faber, A. 1998. Post-traumatic stress and maladjustment among adult burn survivors 1-2 years post-burn. Part II: the interview data. *Burns* 24(5), pp. 399-405.

Takeo, M. *et al*. 2015. Wound healing and skin regeneration. *Cold Spring Harbour: Perspectives in Medicine* 5(1), pp. 1-13. doi: 10.1101/cshperspect.a023267

Tamaki, Y. *et al*. 2013. Metastasis-associated protein, S100A4, mediates cardiac fibrosis potentially through the modulation of p53 in cardiac fibroblasts. *Journal of Molecular and Cellular Cardiology* 57(1), pp. 72-81. doi: 10.1016/j.yjmcc.2013.01.007

Tan, J. *et al*. 2010. Investigating the role of P311 in the hypertrophic scar. *PLoS One* 5(4), pp. 1-6. doi: 10.1371/journal.pone.0009995

Tan, J. *et al*. 2015. iTRAQ-based proteomic profiling reveals different protein expression between normal skin and hypertrophic scar tissue. *Burns and Trauma* 3(13), pp. 1-8. doi: 10.1186/s41038-015-0016-6

Tan, K. *et al*. 2011. Characterisation of hyaluronan and TSG-6 in skin scarring: differential distribution in keloid scars, normal scars and unscarred skin. *Journal of Dermatology and Venereology* 25(3), pp. 317-327. doi: 10.1111/j.1468-3083.2010.03792.x

Tandara, A. and Mustoe, T. 2011. MMP and TIMP secretion by human cutaneous keratinocytes and fibroblasts - impact of co-culture and hydration. *Journal of Plastic, Reconstructive and Aesthetic Surgery* 64(1), pp. 108-116. doi: 10.1016/j.bjps.2010.03.051

Tanoue, T. and Takeichi, M. 2004. Mammalian FAT1 cadherin regulates actin dynamics and cell-cell contact. *Journal of Cell Biology* 165(4), pp. 517-528. doi: 10.1083/jcb.200403006

Tanoue, T. and Takeichi, M. 2005. New insights into FAT cadherins. *Journal of Cell Science* 118(11), pp. 2347-2353. doi: 10.1242/jcs.02398

Theocharidis, G. *et al*. 2016. Type VI collagen regulates dermal matrix assembly and fibroblast motility. *Journal of Investigative Dermatology* 136(1), pp. 74-83. doi: 10.1038/jid.2015.352

Thomason, H. *et al*. 2012. Direct evidence that PKC-α positively regulates wound re-epithelialisation: correlation with changes in desmosomal adhesiveness. *Journal of Pathology* 227(3), pp. 346-356. doi: 10.1002/path.4016

Tokumaru, S. *et al*. 2005. SOCS3/CIS3 negative regulation of STAT3 in HGF-induced keratinocyte migration. *Biochemical and Biophysical Research Communications* 327(1), pp. 100-105. doi: 10.1016/j.bbrc.2004.11.145

Tolg, C. *et al*. 2006. Rhamm-/- fibroblasts are defective in CD44-mediated ERK1/2 motogenic signalling, leading to defective skin wound repair. *Journal of Cell Biology* 175(6), pp. 1017-1028. doi: 10.1083/jcb.200511027

Tolg, C. *et al*. 2014a. Hyaluronan and RHAMM in wound repair and the "cancerisation" of stromal tissues. *BioMed Research International* 2014(1), pp. 1-18. doi: 10.1155/2014/103923

Tolg, C. *et al*. 2014b. Specific sizes of hyaluronan oligosaccharides stimulate fibroblast migration and excisional wound repair. *PLoS One* 9(2), pp. 1-10. doi: 10.1371/journal.pone.0088479

Tomasek, J. *et al*. 1997. Gelatinase A activation is regulated by the organisation of the polymerised actin cytoskeleton. *Journal of Biological Chemistry* 272(11), pp. 7482-7487.

Tomasek, J. *et al*. 2002. Myofibroblasts and mechanoregulation of connective tissue remodelling. *Nature Reviews: Molecular Cell Biology* 3(5), pp. 349-363. doi: 10.1038/nrm809

Tomasek, J. *et al*. 2006. Contraction of myofibroblasts in granulation tissue is dependent on Rho/Rho kinase/myosin light chain phosphatase activity. *Wound Repair and Regeneration* 14(3), pp. 313-320. doi: 10.1111/j.1743-6109.2006.00126.x

Tomcik, M. *et al*. 2015. S100A4 amplifies TGF-β-induced fibroblast activation in systemic sclerosis. *Annals of Rheumatic Diseases* 74(9), pp. 1748-1755. doi: 10.1136/annrheumdis-2013-204516

Tomcik, M. *et al*. 2016. Tribbles homologue 3 stimulates canonical TGF-β signalling to regulate fibroblast activation and tissue fibrosis. *Annals of Rheumatic Diseases* 75(3), pp. 609-616. doi: 10.1136/annrheumdis-2014-206234

Toole, B. 1990. Hyaluronan and its binding proteins, the hyaladherins. *Current Opinion in Cell Biology* 2(5), pp. 839-844.

Toole, B. 2002. Hyaluronan promotes the malignant phenotype. *Glycobiology* 12(3), pp. 37-42.

Toriseva, M. and Kahari, V. 2009. Proteinases in cutaneous wound healing. *Cellular and Molecular Life Sciences* 66(2), pp. 203-224. doi: 10.1007/s00018-008-8388-4

Tracy, L. *et al*. 2016. Extracellular matrix and dermal fibroblast function in the healing wound. *Advances in Wound Care* 5(3), pp. 119-136. doi: 10.1089/wound.2014.0561

Tredget, E. *et al*. 1997. Hypertrophic scars, keloids and contractures: the cellular and molecular basis for therapy. *Surgical Clinics of North America* 77(3), pp. 701-730.

Trengove, N. *et al*. 1999. Analysis of the acute and chronic wound environments: the role of proteases and their inhibitors. *Wound Repair and Regeneration* 7(6), pp. 442-452.

Tsatmali, M. *et al*. 2002. Melanocyte function and its control by melanocortin peptides. *Journal of Histochemistry and Cytochemistry* 50(2), pp. 125-133. doi: 10.1177/002215540205000201

Tsou, R. *et al*. 2000. Analysis of hypertrophic and normal scar gene expression with cDNA microarrays. *Journal of Burn Care and Rehabilitation* 21(6), pp. 541-550.

Tsukazaki, T. *et al*. 1998. SARA, a FYVE domain protein that recruits SMAD2 to the TGF-β receptor. *Cell* 95(6), pp. 779-791.

Turabelidze, A. *et al*. 2014. Intrinsic differences between oral and skin keratinocytes. *PLoS One* 9(9), pp. 1-10. doi: 10.1371/journal.pone.0101480

Uchida, G. *et al*. 2003. Tretinoin reverses up-regulation of matrix metalloproteinase-13 in human keloid-derived fibroblasts. *Experimental Dermatology* 12(2), pp. 35-42.

Uitto, J. *et al*. 1985. Altered steady-state ratio of type I/III procollagen mRNAs correlates with selectively increased type I procollagen biosynthesis in cultured keloid fibroblasts. *Proceedings of the National Academy of Sciences of the USA* 82(17), pp. 5935-5939.

Urushiyama, H. *et al*. 2015. Role of α_1 and α_2 chains of type IV collagen in early fibrotic lesions of idiopathic interstitial pneumonias and migration of lung fibroblasts. *Laboratory Investigation* 95(8), pp. 872-885. doi: 10.1038/labinvest.2015.66

Vaalamo, M. *et al*. 1996. Patterns of matrix metalloproteinase and TIMP-1 expression in chronic and normally healing human cutaneous wounds. *British Journal of Dermatology* 135(1), pp. 52-59.

Valente, A. *et al*. 2013. TRAF3IP2 mediates interleukin-18-induced cardiac fibroblast migration and differentiation. *Cellular Signalling* 25(11), pp. 2176-2184. doi: 10.1016/j.cellsig.2013.07.013

Valletta, D. *et al*. 2012. Expression and function of the atypical cadherin FAT1 in chronic liver disease. *Biochemical and Biophysical Research Communications* 426(3), pp. 404-408. doi: 10.1016/j.bbrc. 2012.08.104

van den Broek, L. *et al*. 2014. Human hypertrophic and keloid scar models: principles, limitations and future challenges from a tissue engineering perspective. *Experimental Dermatology* 23(6), pp. 382-386. doi: 10.1111/exd.12419

van der Rest, M. *et al*. 1991. Structure and function of the fibril-associated collagens. *Biochemical Society Transactions* 19(4), pp. 820-824.

van der Rest, M. and Garrone, R. 1991. Collagen family of proteins. *FASEB Journal* 5(13), pp. 2814-2823.

van der Slot, A. *et al*. 2003. Identification of PLOD2 as telopeptide lysyl hydroxylase, an important enzyme in fibrosis. *Journal of Biological Chemistry* 278(42), pp. 40967-40972. doi: 10.1074/ jbc.M307380200

van der Slot, A. *et al*. 2005. Elevated formation of pyridinoline cross-links by pro-fibrotic cytokines is associated with enhanced lysyl hydroxylase 2b levels. *Biochimica et Biophysica Acta* 1741(1), pp. 95-102. doi: 10.1016/j.bbadis.2004.09.009

van der Veer, W. *et al*. 2009. Potential cellular and molecular causes of hypertrophic scar formation. *Burns* 35(1), pp. 15-29. doi: 10.1016/j.burns.2008.06.020

van Rossen, E. *et al*. 2014. Syncoilin is an intermediate filament protein in activated hepatic stellate cells. *Histochemistry and Cell Biology* 141(1), pp. 85-99. doi: 10.1007/s00418-013-1142-5

van Smeden, J. *et al*. 2014. The important role of stratum corneum lipids for the cutaneous barrier function. *Biochimica et Biophysica Acta* 1841(3), pp. 295-313. doi: 10.1016/j.bbalip.2013.11.006

Vardouli, L. *et al*. 2008. A novel mechanism of TGF-β-induced actin reorganisation mediated by SMAD proteins and Rho GTPases. *FEBS Journal* 275(16), pp. 4074-4087. doi: 10.1111/j.1742-4658. 2008.06549.x

Varga, J. *et al*. 1987. Transforming growth factor-β (TGF-β) causes a persistent increase in steady-state amounts of type I and type III collagen and fibronectin mRNAs in normal human dermal fibroblasts. *The Biochemical Journal* 247(3), pp. 597-604.

Venkataraman, L. and Ramamurthi, A. 2011. Induced elastic matrix deposition within 3D collagen scaffolds. *Tissue Engineering* 17(21), pp. 2879-2889. doi: 10.1089/ten.TEA.2010.0749

Verhaegen, P. *et al*. 2009. Differences in collagen architecture between keloid, hypertrophic scar, normotrophic scar, and normal skin: an objective histopathological analysis. *Wound Repair and Regeneration* 17(5), pp. 649-656. doi: 10.1111/j.1524-475X.2009.00533.x

Vigetti, D. *et al*. 2014. Hyaluronan: biosynthesis and signalling. *Biochimica et Biophysica Acta* 1840(8), pp. 2452-2459. doi: 10.1016/j.bbagen.2014.02.001

Visse, R. and Nagase, H. 2003. Matrix metalloproteinases and tissue inhibitors of metalloproteinases: structure, function and biochemistry. *Circulation Research* 92(8), pp. 827-839. doi: 10.1161/01.res.0000070112.80711.3d

Vozenin, M. *et al*. 1998. The myofibroblast markers, α-smooth muscle actin and β-actin, are differentially expressed in 2 and 3D culture models of fibrotic and normal skin. *Cytotechnology* 26(1), pp. 29-38. doi: 10.1023/a:1007992824966

Wagenseil, J. and Mecham, R. 2007. New insights into elastic fibre assembly. *Birth Defects Research* 81(4), pp. 229-240. doi: 10.1002/bdrc.20111

Walker, A. *et al*. 2014. The cytoplasmic domain of N-cadherin modulates MMP9 induction in oral squamous carcinoma cells. *International Journal of Oncology* 45(4), pp. 1699-1706. doi: 10.3892/ijo.2014.2549

Wall, I. *et al*. 2008. Fibroblast dysfunction is a key factor in the non-healing of chronic venous leg ulcers. *Journal of Investigative Dermatology* 128(10), pp. 2526-2540. doi: 10.1038/jid.2008.114

Walmsley, G. *et al*. 2015. Scarless wound healing: chasing the holy grail. *Plastic and Reconstructive Surgery* 135(3), pp. 907-917. doi: 10.1097/prs.0000000000000972

Wang, H. *et al*. 2001. Focal adhesion kinase is involved in mechanosensing during fibroblast migration. *Proceedings of the National Academy of Sciences of the USA* 98(20), pp. 11295-11300. doi: 10.1073/pnas.201201198

Wang, J. *et al*. 2000. Molecular and cell biology of skin wound healing in a pig model. *Connective Tissue Research* 41(3), pp. 195-211.

Wang, M. *et al*. 2017. Characterisation of gene expression profiles in HBV-related liver fibrosis patients and identification of ITGBL1 as a key regulator of fibrogenesis. *Scientific Reports* 7(1), pp. 1-13. doi: 10.1038/srep43446

Wang, T. *et al*. 1996. The immunophilin FKBP12 functions as a common inhibitor of the TGF-β family type I receptors. *Cell* 86(3), pp. 435-444.

Wang, Z. *et al*. 2018. Cardiac fibrosis can be attenuated by blocking the activity of transglutaminase 2 using a selective small-molecule inhibitor. *Cell Death and Disease* 9(6), pp. 1-12. doi: 10.1038/s41419-018-0573-2

Wankell, M. *et al*. 2001. Impaired wound healing in transgenic mice over-expressing the activin antagonist, follistatin in the epidermis. *The EMBO Journal* 20(19), pp. 5361-5372. doi: 10.1093/emboj/20.19.5361

Way, K. *et al*. 2000. Identification of PKC isoform-specific biological actions using pharmacological approaches. *Trends in Pharmacological Sciences* 21(5), pp. 181-187.

Webb, A. *et al*. 2004. Location and phenotype of human adult keratinocyte stem cells of the skin. *Differentiation* 72(8), pp. 387-395. doi: 10.1111/j.1432-0436.2004.07208005.x

Webber, J. *et al*. 2009a. Modulation of TGF-β_1-dependent myofibroblast differentiation by hyaluronan. *American Journal of Pathology* 175(1), pp. 148-160. doi: 10.2353/ajpath.2009.080837

Webber, J. *et al*. 2009b. Hyaluronan orchestrates transforming growth factor-β_1-dependent maintenance of myofibroblast phenotype. *Journal of Biological Chemistry* 284(14), pp. 9083-9092. doi: 10.1074/jbc.M806989200

Webber, J. *et al*. 2010. Cancer exosomes trigger fibroblast to myofibroblast differentiation. *Cancer Research* 70(23), pp. 9621-9630. doi: 10.1158/0008-5472.can-10-1722

Webber, J. *et al*. 2015. Differentiation of tumour-promoting stromal myofibroblasts by cancer exosomes. *Oncogene* 34(3), pp. 290-302. doi: 10.1038/onc.2013.560

Weigel, P. *et al*. 1986. A model for the role of hyaluronic acid and fibrin in the early events during the inflammatory response and wound healing. *Journal of Theoretical Biology* 119(2), pp. 219-234.

Weigel, P. and DeAngelis, P. 2007. Hyaluronan synthases: a decade-plus of novel glycosyltransferases. *Journal of Biological Chemistry* 282(51), pp. 36777-36781. doi: 10.1074/jbc. R700036200

Weinstein, G. and Boucek, R. 1960. Collagen and elastin of human dermis. *Journal of Investigative Dermatology* 35(1), pp. 227-229.

Wells, A. *et al*. 2016. Skin tissue repair: matrix microenvironmental influences. *Matrix Biology* 49, pp. 25-36. doi: 10.1016/j.matbio.2015.08.001

Wendling, J. *et al*. 2003. 5-fluorouracil blocks transforming growth factor-β-induced α_2 type I collagen gene (COL1α_2) expression in human fibroblasts via c-Jun NH2-terminal kinase/activator protein-1 activation. *Molecular Pharmacology* 64(3), pp. 707-713. doi: 10.1124/mol.64.3.707

Werner, S. and Grose, R. 2003. Regulation of wound healing by growth factors and cytokines. *Physiological Reviews* 83(3), pp. 835-870. doi: 10.1152/physrev.2003.83.3.835

Werner, S. *et al*. 2007. Keratinocyte-fibroblast interactions in wound healing. *Journal of Investigative Dermatology* 127(5), pp. 998-1008. doi: 10.1038/sj.jid.5700786

West, D. *et al*. 1997. Fibrotic healing of adult and late gestation foetal wounds correlates with increased hyaluronidase activity and removal of hyaluronan. *International Journal of Biochemistry and Cell Biology* 29(1), pp. 201-210.

Whitby, D. and Ferguson, M. 1991. Immunohistochemical localisation of growth factors in foetal wound healing. *Developmental Biology* 147(1), pp. 207-215.

Wietecha, M. *et al*. 2015. Pigment epithelium-derived factor as a multi-functional regulator of wound healing. *American Journal of Physiology: Heart and Circulatory Physiology* 309(5), pp. 812-826. doi: 10.1152/ajpheart.00153.2015

Wilgus, T. *et al*. 2013. Neutrophils and wound repair: positive actions and negative reactions. *Advances in Wound Care* 2(7), pp. 379-388. doi: 10.1089/wound.2012.0383

Wise, S. and Weiss, A. 2009. Tropoelastin. *International Journal of Biochemistry and Cell Biology*

41(3), pp. 494-497. doi: 10.1016/j.biocel.2008.03.017

Wong, J. *et al*. 2009. Wound healing in oral mucosa results in reduced scar formation as compared with skin: evidence from the red Duroc pig model and humans. *Wound Repair and Regeneration* 17(5), pp. 717-729. doi: 10.1111/j.1524-475X.2009.00531.x

Woodley, D. *et al*. 1985. Cutaneous wound healing: a model for cell-matrix interactions. *Journal of the American Academy of Dermatology* 12(2), pp. 420-433.

Woods, A. and Couchman, J. 1992. Protein kinase C involvement in focal adhesion formation. *Journal of Cell Science* 101(2), pp. 277-290.

Woods, E. 2016. *Hyaluronan and CD44 control of cell fate.* Cardiff University.

Wordinger, R. *et al*. 2008. Focus on molecules: gremlin. *Experimental Eye Research* 87(2), pp. 78-79. doi: 10.1016/j.exer.2007.11.016

Wrana, J. *et al*. 1992. TGF-β signals through a heteromeric protein kinase receptor complex. *Cell* 71(6), pp. 1003-1014.

Wu, M. *et al*. 2012. Osteopontin in systemic sclerosis and its role in dermal fibrosis. *Journal of Investigative Dermatology* 132(6), pp. 1605-1614. doi: 10.1038/jid.2012.32

Wulff, B. *et al*. 2013. Novel differences in the expression of inflammation-associated genes between mid- and late-gestational dermal fibroblasts. *Wound Repair and Regeneration* 21(1), pp. 103-112. doi: 10.1111/j.1524-475X.2012.00860.x

Wysocki, A. *et al*. 1993. Wound fluid from chronic leg ulcers contains elevated levels of metalloproteinases, MMP-2 and MMP-9. *Journal of Investigative Dermatology* 101(1), pp. 64-68.

Xu, J. and Clark, R. 1997. A 3D collagen lattice induces protein kinase C-zeta activity: role in α_2 integrin and collagenase mRNA expression. *Journal of Cell Biology* 136(2), pp. 473-483.

Xue, M. *et al*. 2006. Targeting matrix metalloproteases to improve cutaneous wound healing. *Expert Opinion on Therapeutic Targets* 10(1), pp. 143-155. doi: 10.1517/14728222.10.1.143

Xue, X. *et al*. 2018. Protein kinase C-α drives fibroblast activation and kidney fibrosis by stimulating autophagic flux. *Journal of Biological Chemistry* 293(28), pp. 11119-11130. doi: 10.1074/jbc. RA118.002191

Yager, D. and Nwomeh, B. 1999. The proteolytic environment of chronic wounds. *Wound Repair and Regeneration* 7(6), pp. 433-441.

Yagi, L. *et al*. 2016. Human foetal wound healing: a review of molecular and cellular aspects. *European Journal of Plastic Surgery* 39(4), pp. 239-246. doi: 10.1007/s00238-016-1201-y

Yamada, Y. *et al*. 2004. Differential regulation by IL-1β and EGF of expression of three different hyaluronan synthases in oral mucosal epithelial cells, fibroblasts and dermal fibroblasts: quantitative analysis using real-time RT-PCR. *Journal of Investigative Dermatology* 122(3), pp. 631-639. doi: 10.1111/j.0022-202X.2004.22332.x

Yamaguchi, T. *et al*. 2006. FKBP12 functions as an adaptor of the SMAD7-Smurf1 complex on activin type I receptor. *Journal of Molecular Endocrinology* 36(3), pp. 569-579. doi: 10.1677/jme.1.01966

Yamaguchi, Y. and Yoshikawa, K. 2001. Cutaneous wound healing: an update. *Journal of Dermatology* 28(10), pp. 521-534.

Yamanaka, M. *et al*. 2004. Sphingosine kinase 1 (SPHK1) is induced by transforming growth factor-β and mediates TIMP-1 up-regulation. *Journal of Biological Chemistry* 279(52), pp. 53994-54001. doi: 10.1074/jbc.M410144200

Yanagisawa, H. *et al*. 2002. Fibulin-5 is an elastin-binding protein essential for elastic fibre development *in vivo*. *Nature* 415(6868), pp. 168-171. doi: 10.1038/415168a

Yariswamy, M. *et al*. 2016. Cardiac-restricted over-expression of TRAF3 interacting protein 2 (TRAF3IP2) results in spontaneous development of myocardial hypertrophy, fibrosis and dysfunction. *Journal of Biological Chemistry* 291(37), pp. 19425-19436. doi: 10.1074/jbc.M116.724138

Yates, C. *et al*. 2012. Skin wound healing and scarring: foetal wounds and regenerative restitution. *Birth Defects Research* 96(4), pp. 325-333. doi: 10.1002/bdrc.21024

Yoshida, H. *et al*. 2013. KIAA1199, a deafness gene of unknown function, is a new hyaluronan binding protein involved in hyaluronan depolymerisation. *Proceedings of the National Academy of Sciences of the USA* 110(14), pp. 5612-5617. doi: 10.1073/pnas.1215432110

Yosipovitch, G. *et al*. 2001. A comparison of the combined effect of cryotherapy and corticosteroid injections versus corticosteroids and cryotherapy alone on keloids: a controlled study. *Journal of Dermatological Treatment* 12(2), pp. 87-90. doi: 10.1080/095466301317085363

Younai, S. *et al*. 1994. Modulation of collagen synthesis by transforming growth factor-β in keloid and hypertrophic scar fibroblasts. *Annals of Plastic Surgery* 33(2), pp. 148-151.

Yu, H. *et al*. 2006. Decreased expression of inhibitory SMAD6 and SMAD7 in keloid scarring. *Journal of Plastic, Reconstructive and Aesthetic Surgery* 59(3), pp. 221-229.

Yu, H. *et al*. 2010. Expression of Gpr177, a Wnt trafficking regulator, in mouse embryogenesis. *Developmental Dynamics* 239(7), pp. 2102-2109. doi: 10.1002/dvdy.22336

Yurchenco, P. *et al*. 2004. Basement membrane assembly, stability and activities observed through a developmental lens. *Matrix Biology* 22(7), pp. 521-538. doi: 10.1016/j.matbio.2003.10.006

Zaki, T. and Choate, K. 2018. Recent advances in understanding inherited disorders of keratinisation. *F1000Research* 7(1), pp. 1-6. doi: 10.12688/f1000research.14514.1

Zeng, G. *et al*. 2013. Resveratrol-mediated reduction of collagen by inhibiting proliferation and producing apoptosis in human hypertrophic scar fibroblasts. *Bioscience, Biotechnology and Biochemistry* 77(12), pp. 2389-2396. doi: 10.1271/bbb.130502

Zhang, Y. *et al*. 2013. Kruppel-like factor 4 transcriptionally regulates TGF-β_1 and contributes to cardiac myofibroblast differentiation. *PLoS One* 8(4), pp. 1-10. doi: 10.1371/journal.pone.0063424

Zheng, Q. *et al*. 2006. Normal wound healing in mice deficient for fibulin-5, an elastin binding protein essential for dermal elastic fibre assembly. *Journal of Investigative Dermatology* 126(12), pp. 2707-2714. doi: 10.1038/sj.jid.5700501

Zheng, X. *et al*. 2017. TGF-β_1 induces Fstl1 via the SMAD3/c-Jun pathway in lung fibroblasts. *American Journal of Physiology: Lung Cellular and Molecular Physiology* 313(2), pp. 240-251. doi: 10.1152/ajplung.00523.2016

Zhou, H. *et al*. 2010. The PDE1A-PKC-α signalling pathway is involved in the up-regulation of alpha-smooth muscle actin by TGF-β_1 in adventitial fibroblasts. *Journal of Vascular Research* 47(1), pp. 9-15. doi: 10.1159/000231716

Zhou, L. *et al*. 2013. The over-expression of BAMBI and its involvement in the growth and invasion of

human osteosarcoma cells. *Oncology Reports* 30(3), pp. 1315-1322. doi: 10.3892/or.2013.2569

Zhou, Z. *et al*. 2004. Impaired angiogenesis, delayed wound healing and retarded tumour growth in perlecan heparan sulfate-deficient mice. *Cancer Research* 64(14), pp. 4699-4702. doi: 10.1158/0008-5472.can-04-0810

Znoyko, I. *et al*. 2006. Collagen binding $\alpha_2\beta_1$ and $\alpha_1\beta_1$ integrins play contrasting roles in regulation of Ets-1 expression in human liver myofibroblasts. *Molecular and Cellular Biochemistry* 282(1), pp. 89-99. doi: 10.1007/s11010-006-1400-0